# 25th Annual Combustion Research Conference

U.S. Department of Energy
Office of Basic Energy Sciences

Airlie Conference Center
Warrenton, Virginia
June 1 – June 4, 2004

FOREWORD

The achievement of National goals for energy conservation and environmental protection will rely on technology more advanced than we have at our disposal today. Combustion at present accounts for 85% of the energy generated and used in the U.S. and is likely to remain a dominant source of energy for the coming decades. Achieving energy conservation while minimizing unwanted emissions from combustion processes could be greatly accelerated if accurate and reliable means were at hand for quantitatively predicting process performance.

The reports appearing in this volume present work in progress in basic research contributing to the development of a predictive capability for combustion processes. The work reported herein is supported by the Department of Energy's Office of Basic Energy Sciences (BES) and in large measure by the chemical physics program. The long-term objective of this effort is the provision of theories, data, and procedures to enable the development of reliable computational models of combustion processes, systems, and devices.

The development of reliable models for combustion requires the accurate knowledge of chemistry, turbulent flow, and the interaction between the two at temperatures and pressures characteristic of the combustion environment. In providing this knowledge, the research supported by BES addresses a wide range of continuing scientific issues of long standing.

➢ For even the simplest fuels, the chemistry of combustion consists of hundreds of reactions. Key reaction mechanisms, the means for developing and testing these mechanisms and the means for determining which of the constituent reaction rates are critical for accurate characterization are all required.

➢ For reactions known to be important, accurate rates over wide ranges of temperature, pressure and composition are required. To assess the accuracy of measured reaction rates or predict rates that would be too difficult to measure, theories of reaction rates and means for calculating their values are needed. Of particular importance are reactions involving open shell systems such as radicals and excited electronic states.

➢ To assess the accuracy of methods for predicting chemical reaction rates, the detailed, state-specific dynamics of prototypical reactions must be characterized.

➢ Methods for observing key reaction species in combustion environments, for interpreting these observations in terms of species concentrations, and for determining which species control the net reactive flux are all required

➢ Energy flow and accounting must be accurately characterized and predicted.

➢ Methods for reducing the mathematical complexity inherent in hundreds of reactions, without sacrificing accuracy and reliability are required. Methods for reducing the computational complexity of computer models that attempt to address turbulence, chemistry, and their interdependence and also needed.

Although the emphasis in this list is on the development of mathematical models for simulating the gas phase reactions characteristic of combustion, such models, from the chemical dynamics of a single molecule to the performance of a combustion device,

require validation by experiment. Hence, the DOE program represented by reports in this volume supports the development and application of new experimental tools in chemical dynamics, kinetics, and spectroscopy.

The success of this research effort will be measured by the quality of the research performed, the profundity of the knowledge gained, as well as the degree to which it contributes to goals of resource conservation and environmental stewardship. In fact, without research of the highest quality, the application of the knowledge gained to practical problems will not be possible.

The emphasis on modeling and simulation as a basis for defining the objectives of this basic research program has a secondary but important benefit. Computational models of physical processes provide the most efficient means for ensuring the usefulness and use of basic theories and data. The importance of modeling and simulation remains well recognized in the Department of Energy and is receiving support through the Scientific Discovery through Advanced Computing (SciDAC) initiative; several work-in-progress reports funded through SciDAC are included in this volume.

During the past year, the Chemical Physics program has benefited from the involvement of Dr. William Kirchhoff, program manager for Chemical Physics, Dr. Eric Rohlfing, team leader for the Fundamental Interactions programs, and Dr. Richard Hilderbrandt, who recently joined DOE as a program manager in Chemical Physics and in Computational and Theoretical Chemistry. Bill Kirchhoff recently retired after 40 years of Federal Service, and his many contributions to the scientific programs described herein are well known and greatly appreciated. Sadly, this volume will be the first in many years lacking a contribution from Professor Richard Bersohn, an insightful scientist and gracious gentleman who passed away in November, 2003. Finally, the efforts of Sophia Kitts, Andreene Witt, and Rachel Smith of the Oak Ridge Institute for Science Education and Karen Talamini of the Division of Chemical Sciences, Geosciences, and Biosciences, Office of Basic Energy Sciences in the arrangements for the meeting are also much appreciated.

Frank P. Tully, SC-141
Division of Chemical Sciences, Geosciences, and Biosciences
Office of Basic Energy Sciences

June 1, 2004

25th Annual Combustion Research Conference
U. S. Department of Energy
Office of Basic Energy Sciences

Agenda

Tuesday, June 1, 2004

3:00 pm   *Registration*

7:00 pm   *Dinner and Reception*

Wednesday, June 2, 2004
Morning Session

Timothy S. Zwier, Chair

8:15 am   *Welcome and Introduction*, Frank P. Tully

8:30 am   *"Producing and Using Vibrationally Excited Molecules,"* Thomas R. Rizzo

9:30 am   *"International Scientific Research and U.S. Foreign Policy in the 21st Century,"* George H. Atkinson

10:30 am   *Break*

10:45 am   *"Spectroscopic and Dynamical Studies of Highly Energized Small Polyatomic Molecules,"* Robert W. Field...85

11:15 am   *"Spectroscopy and Dynamics of Transient Species,"* Trevor J. Sears... 261

11:45 am   *"High-Resolution Spectroscopic Probes of Chemical Dynamics,"* Gregory E. Hall...111

12:15 pm   *Lunch*

5:00 pm   *Dinner*

Wednesday, June 2, 2004
Evening Session

Stephen B. Pope, Chair

Thursday, June 3, 2004
Morning Session

Graham P. Glass, Chair

Thursday, June 3, 2004
Afternoon and Evening Session

Richard L. Hilderbrandt, Chair

Friday, June 4, 2004
Morning Session

F. Fleming Crim, Chair

Table of Contents

Photoelectron Photoion Coincidence Studies: Heats of Formation of Ions, Molecules, and Free Radicals

Tomas Baer (baer@unc.edu)
Department of Chemistry
University of North Carolina
Chapel Hill, NC 27599-3290
DOE Grant DE-FG02-97ER14776

Program Scope

The photoelectron photoion coincidence (PEPICO) technique is utilized to investigate the dissociation dynamics and thermochemistry of energy selected medium to large organic molecular ions. Extensive modeling of the dissociation rate constant using the RRKM theory or variational transition state theory (VTST) is used in order to determine the dissociation limits of energy selected ions. These studies are carried out with the aid of molecular orbital calculations of both ions and the transition states connecting the ion structure to their products. The results of these investigations yield accurate heats of formation of ions and free radicals. In addition, they provide information about the potential energy surface that governs the dissociation process. Isomerization reactions prior to dissociation are readily inferred from the PEPICO data.

The PEPICO Experiment

The threshold photoelectron photoion coincidence (TPEPICO) experiment in Chapel Hill is carried out with a laboratory H_2 discharge light source. Threshold electrons are collected by focusing them into a 1.5 mm hole that discriminate against electrons with perpendicular velocity components. The TPEPICO spectrometer incorporates a velocity focusing detector for threshold electrons and a separate detector for hot electrons so that two TPEPICO spectra are simultaneously collected. The ion TOF is either a linear version or a reflectron for studying H loss processes. This apparatus is now producing beautiful results. The purpose of the reflectron is to permit us to look at slower ion dissociation rates. The electrons provide the start signal for measuring the ion time of flight distribution. When ions dissociate in the microsecond time scale, their TOF distributions are asymmetric. The dissociation rate constant can be extracted by modeling the asymmetric TOF distribution. A high-resolution version of this experiment is currently being constructed using an imaging detector for the electrons at the Chemical Dynamics Beamline of the ALS. When combined with coincidence ion detection, the results permit the measurement of ion dissociation limits to within 1 meV or 0.1 kJ/mol.

Recent Results

The Heats of Formation of the Acetyl radical and Ion obtained by Threshold Photoelectron Photoion Coincidence

The dissociative photoionization onsets for the production of $CH_3CO^+ + CH_3^\bullet$ from acetone and $CH_3CO^+ + CH_3CO^\bullet$ from 2,3-butanedione have been measured by threshold photoelectron photoion coincidence (TPEPICO) in which time of flight (TOF) mass spectra are obtained as a function of the ion internal energy. The use of velocity focusing for threshold electrons and the subtraction of "hot" electrons from the TPEPICO signal allows the 0K dissociation onset to be measured with a precision of 10 meV (1 kJ/mol). The measured onsets

for $CH_3^\bullet$ loss from CH_3COCH_3 was measured to be 10.563 ± 0.010 eV and the onset for $CH_3CO^\bullet$ loss from $CH_3COCOCH_3$ was found to be 10.101 ± 0.010 eV. A 298 K heat of formation of the CH_3CO^+ of 659.4 ± 2 kJ/mol is obtained by combining the measured dissociation onset with the well established heats of formation of acetone and the methyl radical. A 298 K heat of formation of the $CH_3CO^\bullet$ radical of -8.9 ± 2 kJ/mol is obtained by combining the measured dissociation onset with the well known heat of formation of 2,3-butanedione, and the measured heat of formation of CH_3CO^+. The ionization energies of acetone are measured to be 9.708 ± 0.004 eV and 9.30 ± 0.05 eV, respectively.

Neutral Cobalt–Carbonyl Bond Energy By Combined Threshold Photoelectron Photoion Coincidence and He(I) Photoelectron Spectroscopy

Ultraviolet Photoelectron (PE) spectroscopic experiments were carried out on cyclopentadienyl cobalt dicarbonyl $CpCo(CO)_2$ (I) using a pyrolysis inlet system. Above a certain temperature this molecule loses a carbonyl group resulting in the 16-electron molecule $CpCoCO$ (II). By subtracting the PE spectrum of (I) from the mixed experimental spectrum, the PES of (II) was obtained. Adiabatic and vertical ionization energies (IEs) were also determined. By using a thermodynamic cycle, which included the appearance energy of $CpCoCO^+$ determined in an earlier threshold photoelectron photoion coincidence (TPEPICO) experiment, the dissociation energy of $CpCoCO\cdots CO$ was obtained to be 1.91 ± 0.05 eV. Quantum-chemical calculations were also carried out to help the reassignment of the photoelectron spectrum of (I) and to help establish a reliable value of the adiabatic IE of (II).

The heats of formation of t-butyl isocyanide and other alkyl isocyanides by photoelectron photoion coincidence spectroscopy

Threshold photoelectron photoion coincidence (TPEPICO) spectroscopy has been used to investigate the dissociation energy of t-butyl isocyanide (t-$C_4H_9NC^+$) ion. The 0 K dissociation limit of $NC + C_4H_9^+$ (10.943 ± 0.010 eV) is determined from the breakdown diagram. The ionization energy of t-butyl isocyanide is measured by threshold photoelectron spectra (TPES) and found to be 10.757 ± 0.005 eV. These values are used to obtain the 298 K heat of formation of t-butyl isocyanide molecule (84.5 ± 2 kJ/mol). The 298 K heats of formation of CH_3CH_2NC and $(CH_3)_2CHNC$ are found to be 141.4 ± 8 kJ/mol and 114.1 ± 8 kJ/mol, respectively by a linear interpolation between the heats of formation of CH_3NC and t-C_4H_9NC. These experimental results are in excellent agreement with density functional and *ab initio* theoretical values obtained from isomerization energies between the alkyl cyanides and the isocyanide heats of formation. Aside from CH_3NC, these are the first experimental heats of formation for the alkyl isocyanide molecules.

Ethylene Glycol Ions Dissociate by Tunneling through an H-atom transfer Barrier: A DFT and TPEPICO Study

Density functional theory (DFT) and threshold photoelectron-photoion coincidence spectroscopy (TPEPICO) have been used to investigate the dissociation dynamics of the ethylene glycol ion. Thirteen isomers of the ethylene glycol ion ($C_2H_6O_2^{+\bullet}$) and the transition states connecting them were obtained at the B3LYP/6-31G(d) level. The TPEPICO experimental results show that the $CH_3OH_2^+$ ion, produced by a double hydrogen transfer, and the CH_2OH^+ ion, produced by direct C-C bond cleavage, are the two dominant products. The H_2O loss channel, the lowest dissociation energy channel according to the DFT calculations, is suppressed because of a high barrier leading to its formation. The time-of-flight distributions of the $CH_3OH_2^+$ ion at low energies are asymmetric, which indicates that this ion is produced from a slowly dissociating (metastable) parent ion. A two-well-two-channel model is proposed to

describe the isomerization and dissociation process. The simulations combined with RRKM theory suggest that the production of the $CH_3OH_2^+$ ion involves a hydrogen-bridged reaction intermediate and tunneling through the isomerization barrier causes its slow production. This mechanism is supported by data for deuterated ethylene glycol. The 0 K appearance energy for the CH_2OH^+ ion is determined to be 11.08 ± 0.04 eV, from which the 298 K heat of formation of the ethylene glycol molecule is determined to be -383.1 ± 4.5 kJ/mol, in agreement with other experimental values.

Continued Involvement at the Chemical Dynamics Beamline at the ALS

We are currently involved in constructing the velocity focusing TPEPICO experiment at the ALS. This will incorporate an imaging plate for the electrons so that a full photoelectron spectrum between 0 and 1 eV can be obtained and all of the ions in coincidence with these electrons will be recorded. This experiment will permit for the first time to measure the distribution of zero energy electrons in Franck-Condon gaps, a problem that has been unresolved since it's discovery some 20 years ago. In addition, we will be able to collect TPES with a resolution of 1 meV. The experimental set-up will be available for all people interested in carrying out TPEPICO experiments at the ALS.

We are also working with the ALS on an aerosol experiment, which will permit us to study gas-surface reactions on superfine aerosol particles that cannot be studied with pulsed lasers. However, this project is outside the scope of the DOE project.

Future Plans

The TPEPICO experiment with subtraction of hot electron PEPICO counts is working well now, as are the reflectron and linear TOF MS. Having begun the study on the acetyl radical and ion, we will continue with these reactions, by studying the following systems that should yield accurate heats of formation of the propanyl ion and radical.

$$\textbf{CH}_3\textbf{CH}_2\textbf{COCH}_3 \rightarrow \textit{CH}_3\textit{CH}_2\textit{CO}^+ + \textbf{CH}_3^\bullet \qquad (1a)$$

$$\rightarrow CH_3CO^+ + C_2H_5^\bullet \qquad (1b)$$

$$\textbf{CH}_3\textbf{CH}_2\textbf{COCOCH}_3 \rightarrow CH_3CO^+ + \textit{CH}_3\textit{CH}_2\,\textit{CO}^\bullet \qquad (2)$$

$$\textit{C}_2\textit{H}_5\textit{COCOC}_2\textit{H}_5 \rightarrow \textit{C}_2\textit{H}_5\textit{CO}^\bullet + C_2H_5CO^+ \rightarrow \textit{C}_2\textit{H}_5\textit{CO}^\bullet + \textbf{CH}_2\textbf{CH}_2^+ + \textbf{CO} \qquad (3)$$
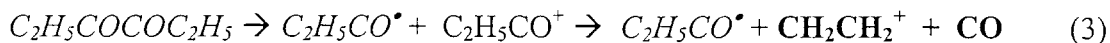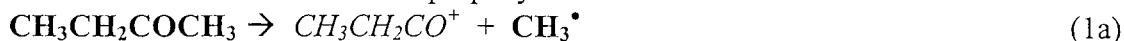
The molecules or ions in bold are those known well in the literature. The ones listed in italics will be derived from our TPEPICO data. The net result is that we can determine the heats of formation of CH_3CO^+, $CH_3CO^\bullet$, $C_2H_5CO^+$, and $C_2H_5CO^\bullet$.

We have found that the heats of formation of the series of ethyl phosphenes, H_nPEth_{3-n}, n = 0, 1, and 2 are completely unknown. To determine these by TPEPICO, we use the sequential nature of the ethyl phosphene ion dissociation:

$$PEth_3^+ \rightarrow HPEth_2^+ + C_2H_4 \rightarrow H_2PEth^+ + 2\,C_2H_4 \rightarrow H_3P^+ + 3C_2H_4$$
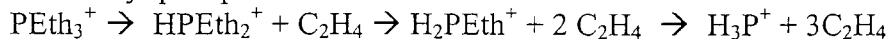
This means that if we dissociatively ionize the triethyl- diethyl-, and mono-ethyl-phosphene all the way to $H_3P^+ + 3C_2H_4$, whose heats of formation are well known, we can determine the heats of formation of all three of the ethyl phosphenes. Unfortunately, our photon source does not go to a sufficiently high energy dissociate the tri-ethyl phosphene ion all the way to the final products. However, by starting out with the di-ethyl and the mono-ethyl phosphene, we can accomplish the same goal.

Research Publications Resulting from DOE grant 2002 – 2003

Y.Li and T. Baer, Threshold photoelectron-photoion coincidence spectroscopy: Dissociation of the 1-chloroadamantane ion and the heat of formation of the 1-adamantyl cation, *J.Phys.Chem. A*, **106** 272-278 (2002)

F. Qi, L. Sheng, M. Ahmed, D.S. Peterka, and T. Baer, Exclusive production of excited state sulfur (^1D) from 193 nm photolysis of thietane, *Chem.Phys. Lett.* **357 204-208 (2002)

Y.Li, J.E. McGrady, and T. Baer, Metal-benzene and metal-CO bond energies in neutral and ionic $C_6H_6Cr(CO)_3$ studied by threshold photoelectron photoion coincidence spectroscopy and DFT theory, *J. Am. Chem. Soc.*, **124** 4487-4494 (2002)

Y. Li and T. Baer, Neutral and ionic bond energies in $(C_6H_6)_2Cr$ studied by threshold photoelectron photoion coincidence spectroscopy, *J. Phys. Chem. A*. **106** 9820-9826 (2002)

T. Baer and Y. Li, Threshold photoelectron spectroscopy with velocity focusing: An ideal match for coincidence studies, *Int. J. Mass Spectrom.* **219** 381-389 (2002)

Y. Li, B. Sztaray, and T. Baer, The dissociation kinetics of energy selected Cp_2Mn^+ ions studied by threshold photoelectron photoion coincidence spectroscopy, *J.Am.Chem.Soc.* **124** 5843-5849 (2002)

B. Sztáray, L. Szepes, and T. Baer, Neutral Cobalt–Carbonyl Bond Energy By Combining Threshold Photoelectron Photoion Coincidence Spectroscopy with He(I) Photoelectron Spectroscopy, *J.Phys.Chem.A*. **107** 9486-9490 (2003)

Y. Li and T. Baer, Theoretical studies on the isomerization and dissociation of the acrolein ions, *Int. J. Mass Spectrom* **218** 19-37 (2002).

Y. Li and T. Baer, The Dissociation Dynamics and Thermochemistry of the Acrolein Ion Studied by Threshold Photoelectron-Photoion Coincidence Spectroscopy, *Int. J. Mass Spectrom.* **218** 37-48 (2002)

Y. Li and T. Baer, Dissociation dynamics of ethylene glycol ions studied by photoelectron photoion coincidence, *J.Phys.Chem.A* **106** 8658-8666 (2002)

B. Sztaray and T. Baer, Consecutive and parallel dissociation of energy selected $Co(CO)_3NO^+$ ions, *J. Phys. Chem.A* **106** 8046-8053 (2002)

B. Sztaray and T. Baer, The suppression of hot electron in threshold photoelectron photoion coincidence spectroscopy using velocity focusing optics, *Rev. Sci. Instrum.* **74** 3763-3768 (2003)

X.M. Qian, T. Zhang, C. Chang, P. Wang, C.Y. Ng, Y-H Chiu, D.J. Levandier, S.Miller, R.A. Dressler, T. Baer, and D.S. Peterka, High-resolution state-selected ion-molecule reaction studies using pulsed field ionization photoelectron-secondary ion coincidence method, *Rev. Sci. Instrum.* **74 4096-4109 (2003)

W.K. Lewis, B.E. Applegate, J. Sztáray, B. Sztáray, T. Baer, R.J. Bemish, and R.E. Miller, Electron impact ionization in helium nanodroplets: Controlled fragmentation by active cooling of molecular ions, *J. Am. Chem. Soc.* (2003) submitted

E.A. Fogleman, H. Koizumi, J. Kercher, B. Sztaray, and T. Baer, The Heats of Formation of the Acetyl radical and Ion obtained by Threshold Photoelectron Photoion Coincidence, *J. Phys. Chem.* (2003) submitted

** Based on experiments at the Chemical Dynamics Beamline (ALS)

Turbulence-Chemistry Interactions in Reacting Flows

Robert S. Barlow
Combustion Research Facility
Sandia National Laboratories, MS 9051
Livermore, California 94551
barlow@ca.sandia.gov

Program Scope

This program is directed toward achieving a more complete understanding of turbulence-chemistry interactions in flames. Experiments are conducted in the Turbulent Combustion Laboratory at the CRF. Simultaneous line imaging of spontaneous Raman scattering, Rayleigh scattering, and two-photon laser-induced fluorescence (LIF) of CO is applied in hydrocarbon flames to obtain spatially and temporally resolved measurements of temperature, the concentrations of all major species, and mixture fraction (ξ), as well as gradients in these quantities. The instantaneous three-dimensional orientation of the turbulent reaction zone is also measured by imaging of OH LIF in two crossed planes, which intersect along the laser axis for the multiscalar measurements. These combined data characterize both the thermo-chemical state and the instantaneous flame structure, such that the influence of turbulent mixing on flame chemistry may be quantified. Our experimental work is closely coupled with international collaborative efforts to develop and validate predictive models for turbulent combustion. This is accomplished through our visitor program and through an ongoing series of workshops on Turbulent Nonpremixed Flames (TNF). Recent work has focused on measurements of scalar dissipation, which is a central concept in combustion theory and an important modeled quantity for several computational approaches.

Recent Progress

Fine Scale Structure of Turbulent Jet Flames

We have investigated spatial resolution requirements and spatial averaging effects in measurements of scalar variance and scalar dissipation. This was done by applying successive spatial filters to measured instantaneous profiles of mixture fraction obtained at various locations in three piloted CH$_4$/air jet flames (Sandia flames C, D, and E). The scalar variance, ξ''^2, was observed to decrease linearly with increasing filter width, while the variance of scalar dissipation rate followed an exponential dependence. In both cases, the observed functional dependence was used to extrapolate to zero filter width, yielding estimates of the "fully resolved" profiles of measured quantities. Here, the radial component of the scalar dissipation rate, $\chi_r = 2D_\xi (\partial \xi / \partial r)^2$, along each instantaneous profile was calculated *after* spatial filtering of the mixture fraction profile. Length scales associated with fluctuations in mixture fraction and scalar dissipation were also extracted from the spatial filtering analysis and compared with those obtained from spatial autocorrelations. Results show that the direct (unfiltered) measurements of scalar variance resolve more than 90% of the estimated "fully resolved" values at most locations in these flames. The length scale, L_{90_ξ}, corresponding to 90% resolution of the scalar variance is roughly constant across the center of the jet flame and within the reaction zone, but it increases toward the edge of the jet flame. The Favre average scalar dissipation rate is not significantly affected by spatial filtering, indicating that the present system has sufficient spatial resolution to

accurately measure scalar dissipation in these flames. The "fully resolved" values of the variance of scalar dissipation, $\chi_r''^2$, were obtained from exponential fitting of the measured variance vs. filter width at each location. The corresponding length scale, L_{90_χ}, for 90% resolution of $\chi_r''^2$ varied from about 90 μm at x/d=7.5 in flame E to about 260 μm at x/d=30 in flame C. These results represent a significant step forward with respect to the availability of experimental data for validation of models for scalar dissipation and scalar variance, including LES subgrid models for these quantities.

Three-Dimensional Measurements

We applied crossed-planar LIF imaging of OH in the same series of turbulent piloted CH_4/air jet flames in order to measure the instantaneous three-dimensional orientation of the reaction zone as it intersects the axis for multiscalar line-imaged measurements. For realizations without localized extinction, isosurfaces in OH are assumed to align with isosurfaces in mixture fraction, such that the flame normal vector, $\vec{n} \equiv -\nabla \xi / |\nabla \xi|$, is aligned with the OH normal vector determined from the crossed PLIF images. The full, three-dimensional, flame-normal scalar dissipation rate is then estimated from its projection onto the measured line segment. With increasing Reynolds number and increasing downstream distance, the angular distribution of the flame normal becomes broader, reflecting the enhanced turbulent character of the flame, and differences between the pdf's of the radial scalar dissipation, χ_r, and full (three-dimensional) scalar dissipation, χ, become larger.

Turbulence-Chemistry Interactions Illuminated by Doubly Conditional Statistics

Our multiscalar diagnostic system yields simultaneous measurements of temperature, mass fractions of the major species (N_2, O_2, CH_4, H_2O, CO_2, H_2, CO), mixture fraction, and scalar dissipation. Therefore, we can explore in detail the joint statistics of these quantities. Figure 1 shows mean values of the mass fractions of CO_2, H_2O, CO, and H_2 in piloted flame E conditional on both mixture fraction and the local instantaneous scalar dissipation rate. Here we have conditionally averaged the data using the directly measured radial component of scalar dissipation, χ_r, and have used data from all measurement locations in flame E. Flame E has a significant probability of localized extinction, so this data set samples a wide range of conditions. At the lowest scalar dissipation rates (below 1 s^{-1}) the species mass fractions approach equilibrium values. Reaction progress decreases, on average, as local scalar dissipation increases, particularly for the intermediates, CO and H_2. The highest measured scalar dissipation rates are above the steady laminar extinction limit.

High-Fidelity LES of Piloted CH_4/Air Flames

In collaboration with Joe Oefelein (Sandia) we have initiated a project to apply high-fidelity LES to our experimental flames, starting with the piloted CH_4/air jet flames described above. Unlike most other LES approaches, the present framework closes the filtered energy and chemical source terms directly, using a moment-based reconstruction methodology similar to that of Sarkar and coworkers. The LES grid uses between 3.5 and 6 million nodes (depending on the flame Reynolds number). High-fidelity LES and detailed experiments are complementary tools for fundamental scientific investigations of turbulent combustion phenomena in well-characterized laboratory-scale flames.
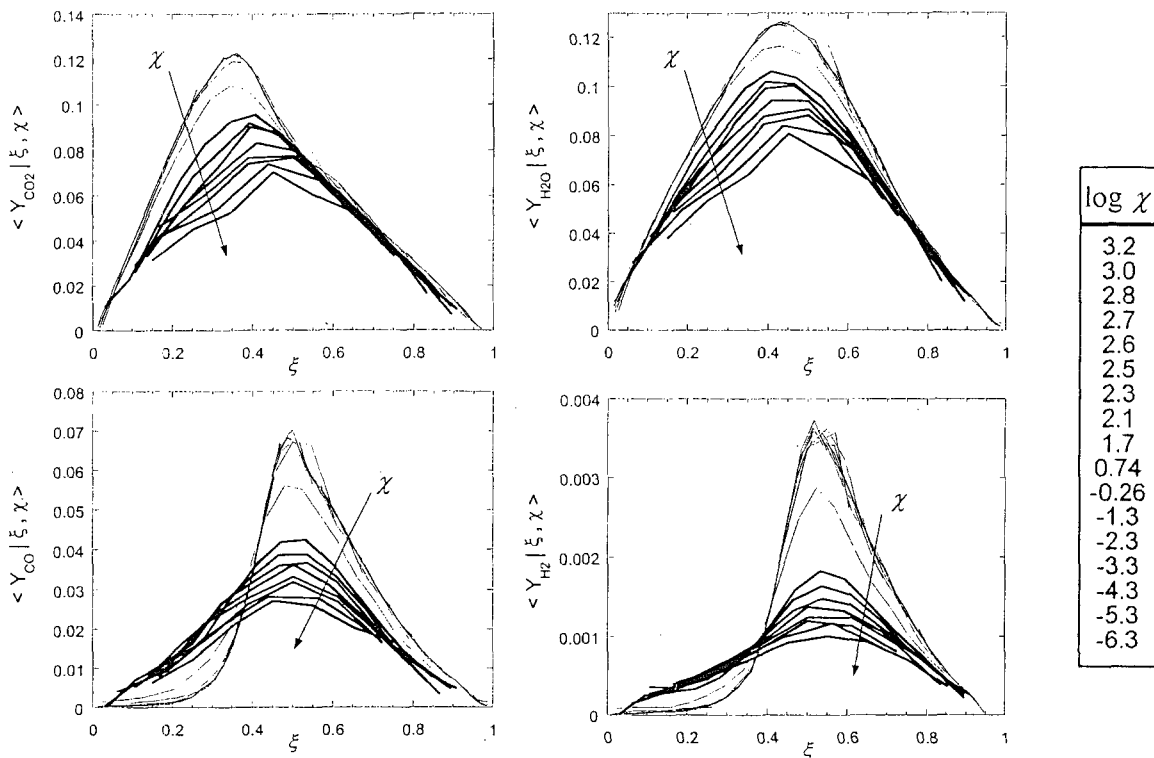
Fig. 1. Average species mass fractions in piloted flame E doubly conditioned on both mixture fraction and local scalar dissipation, χ_r. The table shows center values of the non-uniformly spaced bins.

Future Plans

Experiments are in progress on a series of piloted CH_4/H_2/air jet flames, which can be pushed to higher Reynolds numbers than the CH_4/air flames without running into the complication of localized extinction. This will allow better characterization of the scaling behavior of the scalar dissipation and more rigorous evaluation of scalar dissipation models. Measurements of scalar dissipation and related quantities are also planned in other TNF Workshop target flames. These will be carried out in collaboration with visiting researchers from corresponding institutions, including Sydney University, TU Darmstadt, DLR-Stuttgart, and Imperial College. We are also collaborating with Beth Anne Bennett and Mitch Smooke of Yale University and with Jonathan Frank (Sandia) to perform detailed measurements and simulations of steady laminar partially-premixed CH_4/air jet flames. The motivation from the experimental side is that well-characterized reference flames are needed to better understand error sources in measurements of scalar dissipation. We will continue to pursue highly-resolved LES as a complement to detailed experiments. Once validated to a sufficient degree, such LES results may serve as computational benchmarks for evaluating LES and RANS modeling approaches that are less computationally expensive.

Two laboratory enhancements are planned. The first is to add hardware for line imaging of NO LIF. The second is to allow for crossed planar LIF imaging of CH. This will be applied as an alternative to OH imaging in the determination of local flame structure (orientation and

7

curvature). CH imaging is expected to be more useful for experiments on edge flames and turbulent lifted flames.

BES Supported Publications (2002 - present)

1. R.S. Barlow, C.D. Carter, and R.W. Pitz, "Multiscalar Diagnostics in Turbulent Flames," in *Applied Combustion Diagnostics*, J.B. Jeffries and K. Kohse-Hoeinghaus, eds., Taylor & Francis, 2002.

2. A.N. Karpetis and R.S. Barlow, "Measurements of Scalar Dissipation in a Turbulent Piloted Methane/Air Jet Flame," *Proc. Comb. Inst.* **29**, 1929-1936 (2002).

3. R. Cabra, T. Myhrvold, J.-Y. Chen, R.W. Dibble, A.N. Karpetis, and R.S. Barlow, "Simultaneous Laser Raman-Rayleigh-LIF Measurements and Numerical Modeling Results of a Lifted Turbulent H2/N2 Jet Flame in a Vitiated Coflow," *Proc. Comb. Inst.* **29**, 1881-1888 (2002).

4. B.B. Dally, A.R. Masri, R.S. Barlow, and G.J. Fiechtner, "Two-Photon Laser-Induced Fluorescence Measurements of CO in Turbulent Nonpremixed Bluff Body Flames," *Combust. Flame* **132**, 272-274 (2002).

5. B.B. Dally, A.N. Karpetis, and R.S. Barlow, "Structure of Turbulent Nonpremixed Jet Flames in a Dilute Hot Coflow," *Proc. Comb. Inst.* **29**, 1147-1154 (2002).

6. P.A.M. Kalt, Y.M. Al-Abdeli, A.R. Masri, and R.S. Barlow, "Swirling Turbulent Nonpremixed Flames of Methane: Flowfield and Compositional Structure," *Proc. Comb. Inst.* **29**, 1913-1919 (2002).

7. A.N. Karpetis and R.S. Barlow, "Measurements of Scalar Dissipation in a Turbulent Piloted Methane/Air Jet Flame," *Proc. Comb. Inst.* **29**, 1929-1936 (2002)

8. X.L. Zhu, J.P. Gore, A.N. Karpetis, and R.S. Barlow, "The Effects of Self-Absorption of Radiation on an Opposed Flow Partially Premixed Flame," *Combust. Flame* **129**, 342-345 (2002).

9. Y. Zheng, R.S. Barlow, and J.P. Gore, "Measurements and Calculations of Spectral Radiative Intensities for Turbulent Non-Premixed and Partially Premixed Flames," *ASME J. Heat Transfer*, **125**, 678-696 (2003).

10. Y. Zheng, R S. Barlow, and J.P. Gore, "Spectral Radiative Properties of Turbulent Partially Premixed Flames," *ASME J. Heat Transfer*, **125**, 1065-1073 (2003).

11. A.N. Karpetis, T.B. Settersten, R.W. Schefer, and R.S. Barlow, "Laser Imaging System for Determination of Three-Dimensional Scalar Gradients in Turbulent Flames," *Optics Let.* **29**, 355-357 (2004).

12. A.R. Masri, P.A.M. Kalt, and R.S. Barlow, "The compositional structure of swirl-stabilized turbulent nonpremixed flames," *Combust. Flame* **137**, 1-37 (2004).

13. R.S. Barlow and A.N. Karpetis, "Measurements of Scalar Variance, Scalar Dissipation, and Length Scales in Turbulent Piloted Methane/Air Jet Flames," *Flow Turb. Combust.*, (accepted).

14. R.S. Barlow and A.N. Karpetis, "Scalar Length Scales and Spatial Averaging Effects in Turbulent Piloted Methane/Air Jet Flames," *Proc. Combust. Inst.* (accepted).

15. A.N. Karpetis and R.S. Barlow, "Measurements of Flame Orientation and Scalar Dissipation in Turbulent Partially Premixed Methane Flames," *Proc. Combust. Inst.* (accepted).

16. K. Kohse-Hoeinghaus, R. S. Barlow, M. Alden, J. Wolfrum, "Combustion at the Focus: Laser Diagnostics and Control," *Proc. Combust. Inst.* (invited plenary paper for the 30th Combustion Symposium, 2004).

Web-Based Information

http://www.ca.sandia.gov/CRF/staff/barlow.html   Research Page
http://www.ca.sandia.gov/TNF   TNF Workshop

Theoretical Studies of Combustion Dynamics

Joel M. Bowman
Cherry L. Emerson Center for Scientific Computation and
Department of Chemistry, Emory University
Atlanta, GA 30322,
jmbowma@emory.edu

Program Scope

The research funded by the Department of Energy is a theoretical and computational program to develop and apply rigorous quantum dynamical methods to chemical processes of importance in gas-phase combustion. These include quantum calculations of bimolecular and unimolecular reactions and the *ab initio*-based potentials that govern these processes. Recent work has focused a new global potential energy surface for H_2CO dissociation and reaction, and the quantum dynamics of the $O(^3P)+HCl$ reaction. We have made major progress in both projects.

Recent Progress

A full global potential energy surface for H_2CO

The photodissociation dynamics of formaldehyde has been of long-standing interest, both experimentally[1-4] and theoretically.[5-9] Previous theoretical work has included high quality *ab initio* calculations of various stationary points of the potential. Potential surfaces have been developed, which however, do not describe the H+HCO radical channel. Classical dynamics have been done on these surfaces, and "direct-classical dynamics" have aso been performed with the focus on the product distributions of the CO and H_2 molecular products.

We recently completed a global potential surface for H_2CO, in collaboration with
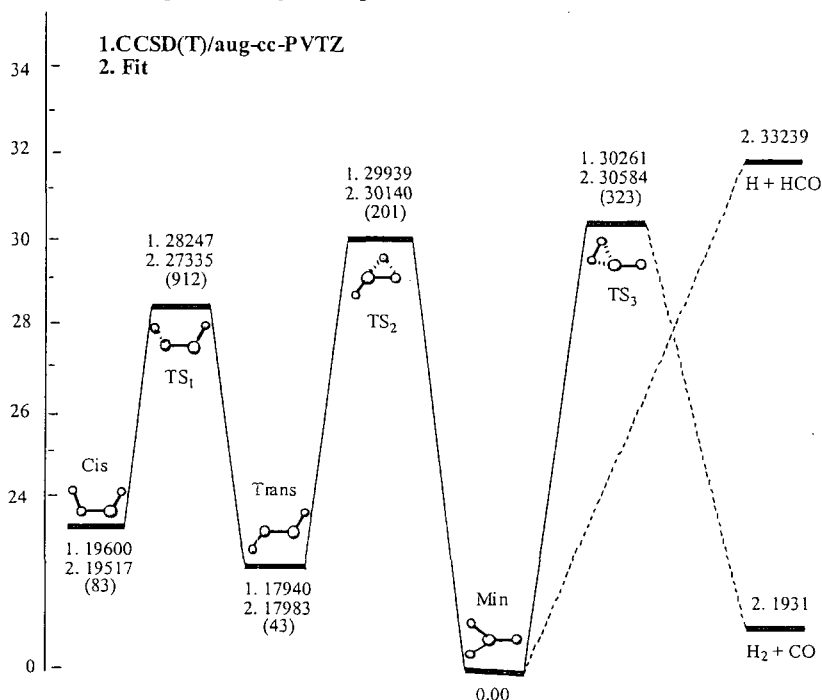
L.B. Harding.[10] This surface describes both the molecular and H+HCO radical channels, as well as the cis and trans isomers HCOH. The surface is a combination of six local fits joined smoothly by five switching functions. The fits are to roughly 80000 CCSD(T)/aug-cc-PVTZ and 53000 and MR-CI/aug-cc-PVTZ calculations of electronic energies. A comparsion of the *ab initio* energies (cm^{-1}) and those from the fit are shown above. The fit is quite precise and smooth and can be used in detailed dynamics studies of both the unimolecular dissociation to the H_2+CO and H+HCO channels and the bimolecular reaction H+HCO, which has not been studied theoretically prior to the present work.

$O(^3P)$+HCl reaction on $^3A''$ and $^3A'$ potential energy surfaces

We have completed quantum reactive scattering studies of this reaction on both the $^3A''$ and $^3A'$ potential energy surfaces. These are very new potentials obtained by Ramachandran and Peterson.[11] Rate constants on both potentials have been calculated and (finally) good agreement with experiment is found, except at temperatures above 2000 K, where there is disagreement with new experiments of Lee and co-workers.[12] The $^3A''$ surface contains significant van der Waals wells, which influence the rate constant at low temperatures and which appear to be the major source of disagreement with the ICVT/μOMT rate constant obtained using 'POLYRATE'[13] at temperatures below 500 K.

Stimulated by the low-energy resonances in the exact reaction probability, we have developed a new model for tunneling which contains the effect of low-energy resonances due to pre and post-barrier wells.[14] This expression can be applied to any activated reaction with van der Waals or hyrdrogen-bonded wells. The key component of the theory is the energy and lifetime of the quasibound states supported by these wells.

Future Plans

We plan to carry out extensive dynamics calculations with the new H_2CO potential surface. These will include calculations of the molecular channel, starting at the transition state for that channel, as others have done.[5,8] In addition we will investigate the radical channel, H + HCO. Unfortunately, there is currently no detailed mechanism of the radiationless transition that leads from S_1 to S_0 and so in the absence of that understanding, assumptions about initial conditions will have to be made. We will consider several possible reasonable choices and investigate the dynamics based on these choices. We will also study the (unambiguous) bimolecular reaction H+HCO $\rightarrow$ H_2+CO. One very interesting aspect of these calculations will be the extent to which this reaction proceeds via direct abstraction of H versus H_2CO complex formation and subsequent decay to form the molecular products.

Another major project we will initiate is an approach to combine *ab initio* direct-dynamics with potential fitting for several combustion reactions. This success of this approach has been demonstrated for the vibrational motion of CH_5^+[15] and we are confident it will work for reactions. We have begun this work for the challenging $O(^3P)$ + C_3H_3 reaction, which contains numerous minima, saddle points, and reaction products.

References

1. For a review up to 1983, see, C. B. Moore and J. C. Weisshaar, Ann. Rev. Phys. Chem. **34**, 525 (1983).
2. (a) T. J. Butenhoff, K. L. Carteton and C. B. Moore, J. Chem. Phys. **92**, 377 (1990); (b) W. F. Polik, D. R. Guyer and C. B. Moore, J. Chem. Phys. **92**, 3453 (1990); (c) R. D. Zee, M. F. Foltz, and C. B. Moore, J. Chem. Phys. **99**, 1664 (1993).
3. A. C. Terentis and S. H. Kable, Chem. Phys. Lett. **258**, 626 (1996).
4. L. R. Valachovic, M. F. Tuchler, M. Dulligan, Th., Droz-George, M., Zyrianov, A. Kolessov, H. Reisler, and C. J. Wittig, J. Chem. Phys. **112**, 2752 (2000).
5. Y. Chang, C. Minichino, and W. H. Miller, J. Chem. Phys. **96**, 4341 (1992).
6. Y. Yamaguchi , S. S. Wesolowski, T. J. Huis, H. F. Shaefer , J. Chem. Phys. **108**, 5281 (1998).
7. D. Feller, M. Dupuis, and B. C. Garrett, J. Chem. Phys. **113**, 218 (2000).
8. (a) X. Li, J. M. Millam and H. B. Schlegel , J. Chem. Phys. **113**, 10062 (2000); (b) W. Chen, W. L Hase. and H. B. Schlegel, Chem. Phys. Lett. **228**, 436 (1994).
9. T. Yonehara and S., J. Kato Chem. Phys. **117**, 11131 (2002).
10. X. Zhang, S. Zou, L. B. Harding, and J. M. Bowman, J. Phys. Chem. A, submitted.
11. B. Ramachandran, and K. A. Peterson, J. Chem. Phys. **119**, 9590 (2003).
12. C. C. Hsiao, Y. P. Lee, N. S. Wang, J. H. Wang, and M. C. Lin, J. Chem. Phys. **106**, 10231 (2002).
13. Y.-Y. Chuang, *et al.* POLYRATE-version 8.4.1, University of Minnesota, MN, 1998.
14. J. M. Bowman, Enhancement of tunneling due to resonances in pre-barrier wells in chemical reactions, Chem. Phys., in press.
15. A. Brown, B. J. Braams, K. M. Christoffel, Z. Jin, and J. M. Bowman, J. Chem. Phys. **119**, 8790 (2003).

PUBLICATIONS SUPPORTED BY THE DOE (2002-present)

The challenge of high resolution dynamics: Rotationally mediated unimolecular dissociation of HOCl, J. M. Bowman, in <u>Accurate Description of Low-Lying Electronic States</u>, edited by M. Hoffman (ACS, Washington, DC, 2002).

A quasiclassical trajectory study of $O(^1D)+HCl$ reactive scattering on an improved *ab initio* surface, K. M. Christoffel and J. M. Bowman, J. Chem. Phys. **116**, 4842 (2002).

Reduced dimensionality quantum calculations of acetylene   vinylidene isomerization, S.-L. Zou and J. M. Bowman, J. Chem. Phys. **116**, 6667 (2002).

Resonances in the $O(^3P)+HCl$ reaction due to Van der Waals minima, T. Xie, D. Wang, J. M.

Bowman, and D. E. Manolopoulos, J. Chem. Phys. **116**, 7461 (2002).

Overview of reduced dimensionality quantum approaches to reactive scattering, J. M. Bowman, Theor. Chem. Acc. **108**, 125 (2002).

Full dimensionalty quantum calculations of acetylene   vinylidene isomerization, S. Zou and J. M. Bowman, J. Chem. Phys. **117**, 5507 (2002).

A new *ab initio* potential energy surface describing acetylene/vinylidene isomerization, S. Zou and J. M. Bowman, Chem. Phys. Lett. **368**, 421 (2003).

Full-dimensionality quantum calculations of acetylene   vinylidene isomerization, S.-L. Zou, J. M. Bowman, and A. Brown, J. Chem. Phys. **118**, 10012 (2003).

A scaled *ab initio* potential energy surface for acetylene and vinylidene, D. Xu, H. Guo, S.-L. Zou, and J. M. Bowman, Chem. Phys. Lett. **377**, 582 (2003).

Quantum calculations of the rate constant for the O(3P) + HCl reaction on new ab initio 3A" and [3]A' surfaces, T. Xie, J. M. Bowman, K. A. Peterson, and B. Ramachandran, J. Chem. Phys. **119**, 9601 (2003).

Enhancement of tunneling due to resonances in pre-barrier wells in chemical reactions, J. M. Bowman, Chem. Phys. in press.

Very High Pressure Single Pulse Shock Tube Studies of Aromatic Species

Kenneth Brezinsky (PI)
Department of Mechanical Engineering (M/C 251),
University of Illinois at Chicago,
2039, Engineering Research Facility,
842 W. Taylor St.,
Chicago, IL 60607.
Kenbrez@uic.edu
www.uic.edu/~kenbrez/

Program Scope

This program focuses on understanding the oxidation and pyrolysis chemistry of aromatic molecules and radicals with the aim of developing a comprehensive model at conditions that are relevant to practical combustion devices. The experimental approach uses a very high pressure single pulse shock tube, HPST, equipped with GC-FID/TCD and GC/MS analyses, to obtain experimental data over the pressure range 5-1000 atm at pre-flame temperatures and a broad spectrum of equivalence ratios. Subsequent simulations of the experimental data from the HPST and data from other laboratories (if available) using kinetic models are used to improve and develop a comprehensive model that can describe aromatics oxidation and pyrolysis over a wide range of experimental conditions.

Recent Progress

The primary focus in this reporting period was in the development of a comprehensive model for toluene oxidation which is the first step in our program of aromatics oxidation and pyrolysis. The challenges faced in simulating the fuel rich experimental data have suggested deficiencies in the pyrolytic routes and a detailed experimental and modeling study on the pyrolysis of benzene and the phenyl radical was initiated. The experimental and modeling study performed in this period falls under two broad categories, the oxidation of toluene and the pyrolysis of benzene.

Toluene Oxidation

The abundance of toluene in current fuels has suggested it to be one of the primary representatives around which detailed kinetic mechanisms need to be constructed to best reflect aromatic chemistry[1]. In view of its relevance, the oxidation of toluene was studied in the HPST. Experiments were performed behind the reflected shock over a wide range of pressures from 25-610 bars for the first time, in the temperature range from 1200-1500 K at nominal reaction times of 1.5 ms. Experiments were performed for stoichiometric oxidation $\Phi=1$ as well as fuel rich oxidation $\Phi=5$. More than 75 experiments comprising six data sets were performed over the wide range of experimental conditions[2]. Dilute reagent mixtures with initial toluene concentrations from 8-85 ppm were used in these experiments. Reaction temperatures were obtained from prior temperature calibration work[3] at each of the reaction pressures. The analytical techniques used in the HPST are GC/FID-TCD and GC/MS. Samples of the pre-shock and post-shock gases were collected for each experiment and the stable species were identified and quantified. The primary intermediates and products observed and quantified in these experiments in addition to the fuel, toluene, were benzene, CO, C_2H_2, CO_2, C_4H_2 and C_2H_4. Trace species observed in these experiments include C_2H_6, C_3H_6, C_3H_4, 1, 3 C_4H_6, C_4H_8, cyclopentadiene, ethylbenzene and xylene.

The experimental data was simulated using current literature models for toluene oxidation: the KBG Model[4] and the Dagaut et al. model[5]. Preliminary modeling[2] indicated that

the KBG model[4] which is based on our prior work forms a good starting point for the development of a more comprehensive model valid over a wide range of conditions. The KBG model[4] is able to simulate well the lower temperature HPST data, but there are large discrepancies at the higher temperatures. This is not very surprising since the KBG model was optimized against flow reactor data at lower temperatures (< 1200 K) and at 1 atm. A more detailed discussion of the experimental data and the model simulations is available in our recently submitted paper[2].

The HPST experimental data formed the basis of a more detailed modeling study[6]. The conventional tools of sensitivity analyses and reaction path analyses were used to identify the major contributors to fuel decay and intermediates growth at such high pressures. Several modifications were made to the KBG model[4] to better reflect the HPST experimental data. Rate parameters for a few key reactions were updated and also a number of new reactions were included in the modified model[6]. A summarized discussion of the changes is presented below.

In general, at the higher pressures and lower temperatures of our experimental study the fuel decay was dominated by oxidation reactions, viz. reactions of the benzyl radical with HO_2, OH and O atom and that of the phenyl radical with O_2 and O atom. The rate parameters for a number of these reactions were updated based on new experimental measurements of their rates as well as theoretical estimates. At the lower pressures and higher temperatures ring rupture reactions specifically of the benzyl radical and the phenyl radical play an increasingly dominant role in describing the toluene decay as well as buildup of C_6H_6 and C_2H_2 even in stoichiometric oxidation. The base KBG model[4] which was developed against data obtained at much lower temperatures than the current study does not include the high temperature ring rupture reactions of the benzyl and phenyl radical. These reactions were included in the modified version of the KBG model[6]. The inclusion of an alternate pathway in the reaction between C_6H_5 and O_2 to form p-$C_6H_4O_2$ (p-benzoquinone) and H also had a significant effect in describing the fuel decay as well as CO buildup. A total of nine changes were made to rate parameters in the KBG model[4] and also nine new reactions were included in the modified model[6].

The modified model[6] is able to describe well the stoichiometric oxidation data obtained in the HPST over the entire pressure and temperature range. The model describes well the toluene decay as well as the primary intermediates CO, C_2H_2 and C_6H_6 profiles. The model was also tested against data obtained from other laboratories, specifically, ignition delay data obtained by Burcat and co-workers[7] as well as the original flow reactor data against which the base KBG model[4] was developed. Burcat et al.[7] obtained the most comprehensive data for ignition delay times for toluene and benzene mixtures with oxygen in argon. The data spans temperature ranges from 1200-1800 K and pressures from 2-8 atm. The modified model is able to do a good job in describing Burcat et al.'s[7] ignition delay data both for a stoichiometric $\Phi=1$ as well as fuel lean $\Phi=0.33$ data set over the wide temperature range and at relatively low pressures around 3 atm. Simulations performed with the modified model to describe the lower temperature, 1 atm flow reactor data were also successful with predictions being no more than 20% off from the experimental data at short reaction times. There was better agreement between the data and the model predictions at longer reaction times and the model does a very good job in describing the CO and C_2H_2 profiles from the flow reactor. The modified model is able to simulate the fuel lean as well as stoichiometric oxidation data over a wide range of temperatures and pressures thereby confirming and validating the oxidation routes as well as their associated rates in the model. However one drawback of this model is its inability to simulate the fuel rich $\Phi=5$ HPST data. To better understand the fuel rich chemistry, the high temperature pyrolysis of toluene and benzene was initiated.

Benzene Pyrolysis

As the first part of the pyrolysis study benzene pyrolysis experiments[8] were performed in the HPST. Experiments were performed at 50 atm over a wide temperature range from 1200-2100K. The reaction times for these experiments were in the range 1.3-1.5 ms. The primary species identified and quantified in these experiments other than the fuel, benzene, were C_2H_2 and C_4H_2. The experimental data was simulated using the modified KBG model[6] as well as two mechanisms that were developed to describe the high temperature pyrolysis of benzene, the Laskin-Lifshitz[9] mechanism and the Wang et al.[10] mechanism. The modified model does the best job among the three models in describing the decay of benzene. However there are large discrepancies between the data and all model predictions for the two primary intermediates C_2H_2 and C_4H_2. The formation of these species is thought to occur by the breakdown of the C_6H_5 radical and a detailed modeling study is in progress on investigating the routes for their formation from the decay of the C_6H_5 radical.

Future Plans

Recently, heating systems have been installed which allow the entire sampling rig as well as mixture rig to be maintained at temperatures in excess of $100^\circ C$. This would permit not only the use of richer starting fuel concentrations but also facilitate more accurate measurements for the heavy species as well as species formed in very small amounts.

Currently work is in progress on experiments at high pressures involving the pyrolysis of nitrosobenzene which is a high temperature source for the phenyl radical. The phenyl pyrolysis experiments and their modeling in combination with the complementary benzene pyrolysis modeling should help to gain a better understanding of the decay of the phenyl radical and should be able to explain the intermediates formation under high pressure, high temperature conditions. Experiments are proposed to be performed on the pyrolysis of toluene as well as the oxidation of benzene to obtain a wider experimental data base for benzene and toluene combustion for which currently experimental data is scarce. The performance of the recently developed model[6] can be tested against this experimental database to develop a more comprehensive aromatics combustion model.

References

1. Farrell J. T., *Workshop on Combustion Simulation Databases for Real Transportation Fuels,* NIST, Gaithesburg, Maryland, September 4-5, 2003.
2. Sivaramakrishnan R., Tranter R. S., Brezinsky K., "High Pressure, High Temperature Oxidation of Toluene", Submitted, Combustion and Flame, March 2004.
3. Tranter R. S., Sivaramakrishnan R., Srinivasan N. and Brezinsky K., Int. J. Chem. Kinet., 33 (11) 722-731 (2001).
4. Klotz S. D., Brezinsky K., Glassman I., Proc. Combust. Inst., 27 (1) 337-344 (1998).
5. Dagaut P., Pengloan G., Ristori A., Phys. Chem. Chem. Phys., 4, 1846-1854 (2002).
6. Sivaramakrishnan R., Tranter R. S., Brezinsky K., "A High Pressure Model for the Oxidation of Toluene", Accepted for Publication, 30th International Symposium on Combustion, 2004.
7. Burcat A., Snyder C., Brabbs T., *Ignition Delay Times of Benzene and Toluene with Oxygen in Argon Mixtures,* NASA TM 87312, NASA 1986.
8. Sivaramakrishnan R., Vasudevan H., Raju A. S. K., Tranter R. S., Brezinsky K., "A High Pressure Model for Aromatics Oxidation and Pyrolysis", Proceedings of the 2004 Technical Meeting of the Central States Section of the Combustion Institute, March 2004, Austin, Texas.
9. Laskin A. and Lifshitz A., Proc. Combust. Inst., 26, 669-675 (1996).

10. Wang H., Laskin A., Moriarty N. W., Frenklach M., Proc. Combust. Inst., 28, 1545-1555 (2000).

Publications based on the DOE supported work (2002 - Current):

Tranter R.S., Sivaramakrishnan R., Brezinsky K., Allendorf M.D., High Pressure, High Temperature Shock Tube Studies of Ethane Pyrolysis and Oxidation", Phys. Chem., Chem. Phys. 4, 2001-2010, 2002.

Tranter R.S., Ramamoorthy H., Raman A., Brezinsky K., Allendorf M.D., "High Pressure Single Pulse Shock Tube Investigation of Rich and Stoichiometric Ethane Oxidation", Proc. Combust. Inst., 29, 1267-1275, 2002.

Sivaramakrishnan R., Tranter R. S., Brezinsky K., "A High Pressure Model for the Oxidation of Toluene", Accepted for Publication, 30th International Symposium on Combustion, 2004.

Tranter R. S., Raman A., Sivaramakrishnan R., Brezinsky K., "Ethane Oxidation and Pyrolysis from 5 bar to 1000 bar: Experiments and Simulation", Submitted, Int. J. Chem. Kin., February 2004.

Sivaramakrishnan R., Tranter R. S., Brezinsky K., "High Pressure, High Temperature Oxidation of Toluene", Submitted, Combustion and Flame, March 2004.

Presentations based on the DOE supported work (2002 - Current):

Tranter R.S., Ramamoorthy H., Raman A., Sivaramakrishnan, R. and Brezinsky K., "Shock Tube Investigations of Hydrocarbon Oxidation and Pyrolysis Over Very Wide Pressure Ranges", Proceedings of the 2002 Technical Meeting of the Central States Section of the Combustion Institute, April 2002, Knoxville, Tennessee.

Tranter R.S., Sivaramakrishnan R. and Brezinsky K., "High Pressure Shock Tube Studies of Aromatics", AIChE Annual Meeting, November 2002, Indianapolis, Indiana.

Brezinsky K., Tranter R.S., Sivaramakrishnan R., Durgam S. and Vasudevan H., "High Temperature, High Pressure Oxidation of Toluene", Third Joint Meeting of the U.S. Sections of The Combustion Institute, March, 2003.

Sivaramakrishnan R., Tranter R. S., Brezinsky K., "High Pressure Oxidation of Toluene", Paper 544h, AIChE Annual Meeting, November 21 2003, San Francisco, CA.

Sivaramakrishnan R., Vasudevan H., Raju A. S. K., Tranter R. S., Brezinsky K., "A High Pressure Model for Aromatics Oxidation and Pyrolysis", Proceedings of the 2004 Technical Meeting of the Central States Section of the Combustion Institute, March 2004, Austin, Texas.

COMBUSTION CHEMISTRY

Principal Investigator: Nancy J. Brown

Environmental Energy Technologies Division

Lawrence Berkeley National Laboratory

Berkeley, California, 94720

510-486-4241

NJBrown@lbl.gov

PROJECT SCOPE

Combustion processes are governed by chemical kinetics, energy transfer, transport, fluid mechanics, and their complex interactions. Understanding the fundamental chemical processes offers the possibility of optimizing combustion processes. The objective of our research is to address fundamental issues of chemical reactivity and molecular transport in combustion systems. Our long-term research objective is to contribute to the development of reliable combustion models that can be used to understand and characterize the formation and destruction of combustion-generated pollutants. We emphasize studying chemistry at both the microscopic and macroscopic levels. To contribute to the achievement of this goal, our current activities are concerned with three tasks: Task 1) developing models for representing combustion chemistry at varying levels of complexity to use with models for laminar and turbulent flow fields to describe combustion processes; Task 2) developing tools to probe chemistry fluid interactions; and Task 3) modeling and analyzing combustion in multi-dimensional flow fields. A theme of our research is to bring new advances in computing, and, in particular, parallel computing to the study of important and computationally intensive combustion problems.

RECENT PROGRESS

Task 1: Developing models for representing combustion chemistry at varying levels of complexity to use with models for laminar and turbulent flow fields to describe combustion processes (with Shaheen R. Tonse and Marcus Day) The dominant computational cost in modeling turbulent combustion phenomena numerically with high fidelity chemical mechanisms is the time required to solve the ordinary differential equations (ODEs) associated with the chemical kinetics. To develop models that describe pollutant formation in combustion, the computational burden attributable to chemistry must be reduced. We have pursued an approach that can contribute to this problem, PRISM (Piecewise Reusable Implementation of Solution Mapping). PRISM has been developed as an economical strategy for implementing complex kinetics into high fidelity fluids codes. This approach to mechanism reduction draws upon factorial design, statistics and numerics, caching strategies, data structures, and long term reuse of chemical kinetic calculations. A solution-mapping procedure is applied to parameterize the solution of the initial-value ordinary differential equation system as a set of algebraic polynomial equations.

We have made progress on extending PRISM to CH_4/air combustion. The factorial designs produced by the GOSSET approach provide better accuracy than orthogonal fractional designs, and require approximately half the ODE calls, thereby improving the efficiency of polynomial construction by a factor of two. Since the designs are not orthogonal, a full

matrix inversion at the polynomial construction stage is required; however, this cost is easily offset by the reduced number of ODE calls. The high dimensionality remains a problem and to address this we have developed a dynamical dimensional reduction method which we designate the "Fast and Low" method (). The approach is to separate chemical species into two classes, those that have both fast time scales and low concentrations, (FnL species), and those that do not. Once the FnL species are identified, the dimensionality of the system is reduced to that of the number of non-FnL species, making hypercube construction less costly. The inspiration comes from the steady-state approximation and Intrinsic Low Dimensional Manifold (ILDM) concepts in which concentrations of fast species tend to depend on the concentrations of slow species. The degree of the reduction is dynamic, and it varies from hypercube to hypercube because the properties of chemical composition space vary.

Evaluations of the FnL method were conducted with a 22-species reduced methane mechanism, DRM-19, based upon the 32-species GRI-Mech 1.2. DRM-19 was constructed by a manual examination of the chemical rates and species concentrations and subsequent removal of species based upon their low concentrations and low reaction rates. We observed a reduction in dimensionality from 22 species to approximately 12-15 with our automated process thus removing an additional 7-10 species. This is because of the dynamic nature of our approach which allows for different reductions in different regions of chemical composition space. This approach was extended to the 32-species GRI-Mech 1.2 mechanism, that is a 34-dimensional system in the PRISM context. A reduction in dimensionality from 34 to 12-15 was observed verifying the attractive nature of the dynamic approach.

The FnL process has three key parameters: the fast-time vs. slow-time partitioning parameter, the high concentration vs. low concentration partitioning parameter, and the perturbation parameter used to determine a species' time-scale. Optimum values of the three parameters were determined that resulted in dramatic reductions in dimensionality, which in some cases were as low as 4. Figure 1. is a histogram showing the distribution of reduced dimensionality observed for the dynamic reduction of the GRI-Mech 1.2 chemical mechanism. It is particularly encouraging that very low dimensionality was observed quite frequently during dynamic reduction.
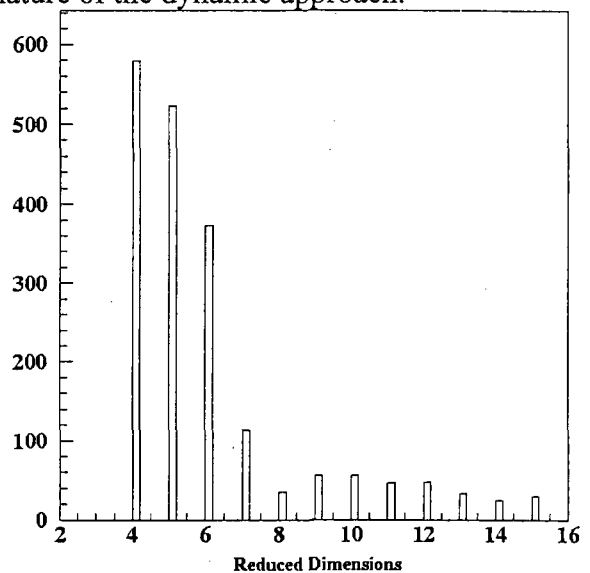
Figure 1 Distribution of Reduced Dimensionality

PRISM was interfaced with the Adaptive Mesh Refinement code of Bell and colleagues (Day and Bell, 2000). The accuracy and efficiency of using the FnL approach with PRISM for CH4/Air combustion with GRI-Mech 1.2 is being evaluated for a premixed laminar flame, and two cases of vortex-flame interactions that differ in the strength of the imposed vortex. The total CPU time spent in the chemistry portion of simulations that use PRISM, and simulations that use an ODE solver are compared. Results indicate that the total chemistry

CPU time is reduced by a factor of 3 for the laminar flame, by a factor of 2 for the flame with the weaker vortex, and a factor of 1.5 for the flame interacting with the stronger vortex.

A large fraction of the CPU time is devoted to solving the ODEs in PRISM because polynomials are not constructed for a hypercube until it is determined that its reuse will be sufficient to recoup the construction cost. Our previous studies have developed criteria that determine *a priori* a hypercubes's degree of reuse. As a result of applying the criteria, polynomials are constructed for approximately 2% of the hypercubes in the 34-dimensional methane system,. During the course of a simulation approximately 70% of the calls made to the chemistry module were evaluated with polynomials associated with 2% of the hypercubes, for which polynomials were evaluated. The remaining 30% of ODE calls were addressed by the remaining 98% hypercubes, which did not meet the criteria for polynomial construction, and for which the ODE solver was called. When a CPU profiler was used to disaggregate the CPU costs, it was observed that 90% of the CPU time was used for the 30% (ODE) calls, while only 10% of the time was devoted to the 70% ODE calls that resulted in polynomial evaluations. This indicates that the polynomial evaluations are about 20 times faster than the ODE calls, but that ODE calls still dominate the total chemistry cost. We are currently investigating an approach for remedying this situation that will ultimately result in mean reuse increases and more efficient polynomial construction.

Task 2: Developing tools to facilitate building and validating chemical mechanisms (with Kenneth Revzan): Sensitivity to transport and molecular properties was investigated in C_2H_4/air, CO/H_2/air, and H_2/air flames using the Sandia codes for transport properties (Tranlib) and our transport codes that are based upon work of Mason and colleagues (Mason and Uribe, 1996). A paper describing this work is in internal review. Since we use measured flame velocities, temperature profiles, and species concentration profiles to validate chemical mechanisms, we focus on the sensitivity of these variables to chemical and transport parameterizations. Sensitivities of several transport properties are comparable in magnitude to those associated with the kinetic parameters. Normalized sensitivities were considered significant if they were greater than 0.1. The importance of individual transport properties and their underlying parameterizations depends upon the specific dependent variable being considered and the combustion conditions investigated. Sensitivity coefficients of observables with respect to diffusion coefficients of select species are the same size as those associated with Arrhenius A factors. Sensitivities to pure species thermal conductivities of N_2, O_2, and the fuel are among the largest observed. Sensitivities to thermal diffusion ratios for H_2/N_2 and H/N_2 are also important. These observations are true for many dependent variables examined: flame speeds, temperatures, and species concentrations, and for both approaches to the calculation of transport properties. First order flame speed sensitivities to the Lennard-Jones collision diameter and its counterpart in the exponential repulsive potential, the length scaling parameter are especially significant for H, N_2, H_2, CO, O_2, C_2H_4, O, H_2O, CO_2, and OH. Sensitivities to well depths were most frequently an order of magnitude less than those for collision diameters, but under some circumstances for N_2, H_2O, CO_2, H, and CO were significant. Analysis also revealed that the sensitivity to dipole moments, polarizabilities, and rotational relaxation collision numbers is not significant.

Task 3: Modeling combustion in multi-dimensional flow fields (with John Bell, Robert Cheng, Marcus Day, and Shaheen Tonse): This is a coordinated effort to investigate fundamental processes of chemistry/turbulence interactions covering a large range of well controlled quasi-steady fluid motions and mixture conditions. By performing experiments,

simulations, and application of analysis tools, we will deduce useful information regarding the suitability of the chemical and transport parameters used in simulations of complex turbulent flames. Previous studies of quasi-steady laminar flames have shown that the thermal-diffusive effects can be attenuated at frequencies that are comparable to the characteristic flame time. The frequencies are in the range of 200 to 600 sec^{-1} for typical methane premixed flames, and can occur even at moderate turbulence levels. The local flame speed would not be highly sensitive to turbulent stretch for flames propagating at higher turbulence levels,. Flame models based on instability modes that contribute to enhancement or attenuation of flame surface area must capture these changes. The purpose of our collaborative study of H_2, CH_4, and C_3H_8 flames is to gain insight into this phenomenon that has yet to be systematically explored. Research accomplished to data involves planning of experiments and simulations.

REFERENCES

Day, M.S. and Bell, J.B., Numerical Simulation of Laminar Reacting Flows with Complex Chemistry. Combust. Theory and Modelling, 4(4), pp. 535-556 (2000). Also LBNL Report 44682.

Smith, G.P., Golden, D.M., Frenklach, M., Moriarty, N.W., Eiteneer, B., Goldenberg, M., Bowman, C.T., Hanson, R.K., Song, S., Gardiner, W.C., Lissianski, V.V., and Qin. Z. http://www.me.berkeley, edu/gri_mech/

Mason, E.A. and Uribe, F.J., The Corresponding-States Principle: Dilute Gases. Millat J, Dymond J.H., and Nieto de Castro CA, eds. Transport Properties of Fluids. Cambridge University Press, Cambridge, 1996.

PUBLICATIONS

Tonse, S.R., Moriarty, N.W., Frenklach, M., and Brown, N.J., "Computational Economy Improvements in PRISM." Intl. J. Chem. Kin. Vol. 35, pp 438-452 (2003). Also Lawrence Berkeley National Laboratory Report No. LBNL-48858.

Tonse, S.R. and Brown, N.J., "Dimensionality Estimate of the Manifold in Chemical Composition Space for a Turbulent Premixed H2+air flame," Intl. J. Chem. Kin. Vol. 36, pp. 326-336 (2004).Also Lawrence Berkeley National Laboratory Report No. LBNL-52058.

Tonse, S.R. and Brown, N.J., "Computational Economy Improvements in PRISM." Proceedings The 3rd Joint Symposium of the U.S. Sections of the Combustion Inst. Paper-B36 (2003). Also Lawrence Berkeley National Laboratory Report No. LBNL-48858.

Tonse, S.R, Day, M.S.,. and Brown, N.J., "PRISM: Dynamical Dimensional Reduction Applied to CH4 Flame Simulations. (2004), Abstract submitted to the 30th International Symposium on Combustion.

Brown, N.J. and Tonse, S. R., "PRISM: Piecewise Reusable Implementation of Solution Mapping to Improve Computational Economy, 2004 Abstract 755011 American Chemical Society National Meeting.

Molecular Beam Studies of Radical Combustion Intermediates

Laurie J. Butler

The University of Chicago, The James Franck Institute
5640 South Ellis Avenue, Chicago, IL 60637
L-Butler@uchicago.edu

I. Program Scope

Polyatomic radical intermediates play a key role in a wide range of combustion processes. Our recent DOE-supported work[1-7] not only investigates competing product channels in photodissociation processes used to generate radical intermediates important in combustion, but also utilize a new technique developed in my lab to investigate the unimolecular dissociation and isomerization channels of the nascent radicals. The technique allows us to generate selected polyatomic radical isomers with a well-defined internal energy distribution in the ground electronic state and then resolve the branching between dissociation and isomerization channels of the radical as a function of the radical's internal energy. In contrast to other methodologies which produce the radicals in a molecular beam source and then access the dissociation channels of the radical by exciting it with a UV photon, this method does not require one to electronically excite the radical, so offers a more direct probe of the radical's ground electronic state dissociation dynamics. The data provides a direct measure, based on energy conservation and the velocity of the lowest energy dissociation products, of the energetic onsets (barrier heights) for polyatomic radical dissociation reactions for both the lowest barrier dissociation channel and any other C-H, O-H or N-H bond fission channel competing at higher energy. We have also been developing experiments to probe radical intermediates important along bimolecular reaction coordinates. Dispersing the radical intermediates by velocity and thus by internal energy, and then measuring the velocity of the reaction products, allowing us to identify the product branching as a function of internal energy in the radical intermediate for energies that span the lowest energy product channels. Our experimental studies use a combination of techniques including analysis of product velocity and angular distributions in a crossed laser-molecular beam apparatus, emission spectroscopy of dissociating molecules, high-n Rydberg H atom time-of-flight spectroscopy (HRTOF), and, most recently, velocity map imaging of the dissociation products. Much of the work also serves to test and develop our fundamental understanding of chemical reaction dynamics. We focus on testing the range of applicability of two fundamental assumptions used in calculating reaction cross sections and the branching between energetically-allowed product channels: the assumption of complete intramolecular vibrational energy redistribution often used in transition state theories and the assumption of electronic adiabaticity invoked in many quantum scattering calculations and assumed in most statistical transition state estimates of reaction rates. The influence of angular momentum on product branching is also of increasing interest.

II. Recent Progress

Our work in the last year included: 1) completing and publishing[5] our experiments on d-2 allyl iodide to investigate the marked stability of the CH_2CDCH_2 radical as compared to the CH_2CHCH_2 radical due to centrifugal effects in the dissociation to H (or D) + allene; 2) writing up work[6] on the unimolecular dissociation channels of the CH_2CHCO radical product and the CH_2CCO molecular product of the C-Cl bond fission and HCl elimination channels, respectively, of the acryloyl chloride photolytic precursor; 3) completing and publishing our work[7] on the unimolecular dissociation of the CH_3CH_2CO radical produced in the photodissociation of propionyl chloride and the competing C-Cl fission and HCl elimination channels of the precursor; and 4) initiating and analyzing the first data on experiments to resolve the branching between the allyl + $Cl(^2P_{3/2})$ and the allyl + $Cl(^2P_{1/2})$ photodissociation channels of allyl chloride.

A. Centrifugal Effects in the Unimolecular Dissociation of the Allyl Radical: Comparing the CH_2CDCH_2 radical with the CH_2CHCH_2 radical

Prior work in my group on the dissociation dynamics of the nascent allyl radicals produced from the photodissociation of allyl iodide at 193 nm dissociation showed that a substantial fraction of the allyl radicals from the I ($^2P_{1/2}$) channel formed with internal energies as high as 15 kcal/mol above the 60 kcal/mol barrier were stable to H atom loss.[3] We attributed the stability to centrifugal effects caused by significant rotational energy imparted to the allyl radical during the precursor photolysis and the small impact parameter and reduced mass characterizing the loss of an H atom from an allyl radical to form allene + H. In the new experiments begun in early 2003 and written up for publication later this past year,[5] we sought to probe the relative stability of the CH_2CDCH_2 radical as compared to the CH_2CHCH_2 radical. Using d-2 allyl iodide we synthesized, modifying the synthesis used by P. Chen, our data at the Chemical Dynamics Beamline at the Berkeley ALS dispersed the CH_2CDCH_2 radicals from the I ($^2P_{1/2}$) + CH_2CDCH_2 channel to determine which of the radicals were formed stable to direct dissociation to allene + D (and to isomerization to 2-propenyl and subsequent dissociation.) As in our prior work on CH_2CHCH_2 radicals, a large fraction of the radical with higher internal energy than the barrier to C-D bond fission were stable to C-D bond fission due to centrifugal effects. The data we took evidences the differences in the survival probability of highly rotationally excited CH_2CDCH_2 radicals as compared to CH_2CHCH_2 radicals. The competing effects evidence the profound effect that conservation of total angular momentum ($|L_{allyl}| = |L_{allene}| + \mu v_{rel}b$) can have on the dissociation of allyl radicals. The centrifugal barrier and the resulting stability of highly internally excited d-2 allyl versus undeuterated allyl radicals depends on 1) the reduced mass μ for C-D fission in CH_2CDCH_2 is almost 2 times higher than for C-H fission in CH_2CHCH_2 radicals; 2) the amplitude of the C-D bending and wagging motion is more restricted in the zero point level at the transition state than the amplitude of C-H bending and wagging, so the range of impact parameters accessed by the deuterated radical is smaller; and 3) the zero-point correction to the barrier results in the barrier to C-D fission in CH_2CDCH_2 being slightly higher than the barrier to C-H fission in CH_2CHCH_2. The latter two effects suggest the d-2 allyl radicals with high internal energies will show even a larger probability of surviving secondary dissociation. This is what our data evidences; the CH_2CDCH_2 radicals are stable to C-D fission at even higher internal energies than CH_2CHCH_2 radicals despite similar partitioning of rotational energy to these radicals in the photolytic step.

B. The competing dissociation channels of the acryloyl chloride at 193 nm and the unimolecular dissociation channels of the nascent CH_2CHCO radical product

The work[6] used photofragment translational spectroscopy to investigate the primary and secondary dissociation channels of acryloyl chloride ($CH_2=CHCOCl$) excited at 193 nm. (Fei Qi had taken extensive data on acryloyl chloride photodissociation at 193 nm on Endstation 1 at the ALS and asked us to analyze the data for him.) The data evidenced three primary photodissociation channels. Two C-Cl fission channels occur, one producing fragments with high kinetic recoil energies and the other producing fragments with low translational energies. These channels produced nascent CH_2CHCO radicals with internal energies ranging from 23 to 66 kcal/mol for the high-translational-energy channel and 50 to 68 kcal/mol for the low-translational-energy channels. We found that all nascent CH_2CHCO radicals were unstable to CH_2CH + CO formation, in agreement with our G3//B3LYP barrier height of 22.4 kcal/mol to within experimental and computational uncertainties. Interestingly, though, the CH_2CHCO radicals from the high translational energy C-Cl fission channel in the precursor (an electronic predissociation) partioned more energy to relative kinetic energy when they underwent C-C fision to form vinyl +

CO than did the CH₂CHCO radicals from the low translational energy C-Cl fission channel. This suggests that while the internal conversion C-Cl fission channel in the precursor produced ground state CH₂CHCO radicals that dissociated statistically while the nascent radicals from the C-Cl channel that proceeded by a curve crossing with a repulsive state did not. The third primary channel is HCl elimination. All of the nascent CH₂CCO co-products were found to have enough internal energy to dissociate, producing CH₂C: + CO, in qualitative agreement with the G3//B3LYP barrier of 39.5 kcal/mol. We derive from the experimental results an upper limit of 23 ± 3 kcal/mol for the zero-point-corrected barrier to the unimolecular dissociation of the CH₂CHCO radical to form CH₂CH + CO.

C. Unimolecular dissociation channels of the CH₃CH₂CO radical and the primary photodissociation channels of the propionyl chloride photolytic precursor

While the unimolecular dissociation dynamics of the acetyl radical, CH₃CO, has been extensively investigated, the unimolecular dissociation of the CH₂CHCO radical is much less well studied. Two kinetics experiments in the 1960's indicated the barrier for propionyl radicals to dissociate to CH₃CH₂+ CO is 14.6 (14.7) kcal/mol, but more recent computations have favored a barrier near 17 kcal/mol based on the sum of the endoergicity (13 kcal/mol) and the barrier height to the reverse reaction (4.8 kcal/mol).

Our experiments this year on the unimolecular dissociation of the CH₃CH₂CO radical produced from photodissociation of propionyl chloride show that the dominant unimolecular decomposition channel of the radical is C-C fission to form ethyl + CO; the C-H fission channel to form methyl ketene (CH₃HC=C=O) + H does not compete with C-C fission in the radical. Our data on the stable radicals formed from the 248 nm photodissociation propionyl chloride (analyzed by acknowledging that both spin-orbit states of the Cl atom co-product are produced in such electronic predissociation channels) arrive at a barrier to the dissociation of the CH₃CH₂CO radical of 16.3 +/- 1 kcal/mol, in agreement with the more recent estimates based on adding the exoergicity to the experimentally measured barrier to the reverse reaction. Our work also investigates the competing C-Cl fission channel and HCl elimination channel of the propionyl chloride photolytic precursor.

D. Branching between allyl + Cl(²P₃/₂) and allyl + Cl(²P₁/₂) products in the two C-Cl bond fission photodissociation channels of allyl chloride at 234 nm

The 193 nm and 234 nm photodissociation of allyl chloride evidence a minor C-Cl fission channel that is assigned to internal conversion and a major channel that proceeds via electronic predissociation by a state repulsive in the C-Cl bond. We have just completed experiments which resolve the spin-orbit state of the Cl atom product in each of these two dissociation channels. Resolving the recoil velocities of the Cl atom product and, simultaneously, the Cl spin orbit state using 2+1 REMPI detection in our new velocity map imaging apparatus, gave some interesting results that showed prior measurements on this system by Park et al. were in error. While the minor internal conversion channel evidences exclusively Cl(²P₃/₂) products, the electronic predissociation channel resulting in high kinetic energy Cl atoms produces Cl atoms in both spin orbit states, and with very similar velocity distributions. We interpret the results as follows. The branching between the two Cl atom spin-orbit states from the electronic predissociation pathway most likely results from angular momentum recoupling at long C-Cl internuclear distances, similar to the recoupling that produced a branching between the two spin-orbit states of the Cl atom product in prior HCl photodissociation studies by Orr-Ewing et al. Indeed, the fraction of Cl atoms produced in the excited spin orbit state in our electronic predissociation channel is 43%. This is in very close agreement with the yield of spin-orbit excited state Cl atoms from HCl photodissociation observed by Orr-Ewing et al and predicted by their theoretical collaborators.

That branching resulted from angular momentum recoupling at long internuclear distances on the repulsive electronic state(s). We are currently investigating this spin-orbit branching ratio in similar systems to assess the validity of the high recoil energy models of this recoupling by Singer and Freed.

III. Future Plans

This summer we plan to collaborate with Dr. Jim Lin and Y. T. Lee to take data at the Taiwan Light Source on the dissociation channels of the CH_3OCO radical intermediate of the $CH_3O + CO \rightarrow CH_3 + CO_2$ reaction. This system is analogous to the HOCO intermediate of the important $OH + CO \rightarrow H + CO_2$ reaction. We plan to measure the quantum yield of the $CH_3O + CO$ products (detecting CH_3O at the CHO^+ ion it forms upon photoionization), calibrating the detection efficiency of CH_3O by using the relative signal from the 1:1 production of CH_3O and Cl fragments from CH_3OCl photodissociation and correcting for the appropriate Jacobian factors. We plan to produce the nascent CH_3OCO radicals from the UV photodissociation of methyl chloroformate, determining the internal energy distribution of the nascent radical intermediates by measuring the Cl atom velocity distribution and accounting for energy conservation. This study thus uses the radical intermediate to access both the entrance channel and the exit channel of the corresponding bimolecular reaction.

IV. Publications Acknowledging DE-FG02-92ER14305 (2002 or later)

1. C-Cl Bond Fission, HCl Elimination, and Secondary Radical Decomposition in the 193 nm Photodissociation of Allyl Chloride, M. L. Morton, L. J. Butler, T. A. Stephenson, and F. Qi,, J. Chem. Phys. 116, 2763-75 (2002).

2. Theoretical Investigation of the Transition States Leading to HCl Elimination in 2-Chloropropene, B. F. Parsons, L. J. Butler, and B. Ruscic, Molecular Physics 100, 865-74 (2002).

3. Primary and Secondary Dissociation of Allyl Iodide Excited at 193 nm: Centrifugal Effects in the Unimolecular Dissociation of the Allyl Radical, D. E. Szpunar, M. L. Morton, L. J. Butler, and P. M. Regan, J. Phys. Chem. B 106, 8086-8095 (2002).

4. Photodissociation Dynamics of Ethyl Ethynyl Ether: A new ketenyl radical precursor, M. J. Krisch, J. L. Miller, L. J. Butler, H. Su, R. Bersohn, and J. Shu, J. Chem. Phys. 119, 176-186 (2003).

5. Photodissociation of allyl-d_2 iodide excited at 193 nm: Stability of highly rotationally excited H_2CCDCH_2 radicals to C-D fission, D. E. Szpunar, Y. Liu, M. McCullagh, L. J. Butler, and J. Shu, J. Chem. Phys. 119, 5078-5084 (2003).

6. The 193 nm photodissociation of acryloyl chloride to probe the unimolecular dissociation of CH_2CHCO radicals and CH_2CCO, D. E. Szpunar, J. L. Miller, L. J. Butler and F. Qi,, J. Chem. Phys. 120, 4223-30 (2004).

7. Competing pathways in the 248 nm photodissociation of propionyl chloride and the barrier to dissociation of the propionyl radical, L. R. McCunn, M. J. Krisch, K. Takematsu, L. J. Butler, and J. Shu, J. Phys. Chem. A, in revision (2004).

Independent Generation and Study of Key Radicals in Hydrocarbon Combustion
(DE-FG02-98ER14857)

PI: Barry K. Carpenter
Department of Chemistry and Chemical Biology
Cornell University
Ithaca, NY 14853-1301
E-mail: bkc1@cornell.edu

Experimental Studies Related to the Phenyl+O_2 Reaction.
We have proposed that a mechanism similar to that for the formation of CHO and CH_2O from vinyl + O_2 might apply also to phenyl + O_2. Subsequent extensive DFT and *ab initio* studies by other groups have supported that suggestion. However, experimental evidence is still lacking. The most plausible distinguishing signature that would differentiate our mechanism from the original one for phenyl oxidation is the formation of the 2-oxepinoxy radical.
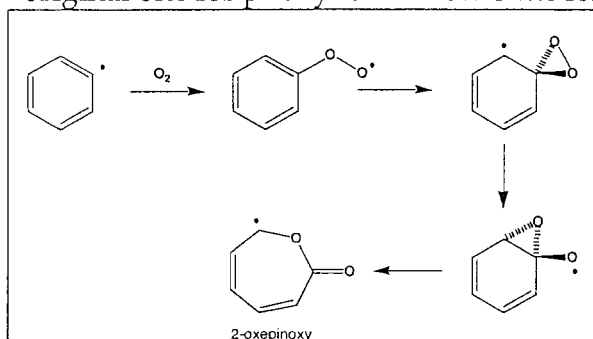
2-oxepinoxy

All unimolecular reactions of this radical that have been investigated computationally are found to have barriers of ≥ 25 kcal/mol. Detection of 2-oxepinoxy would provide strong support for the new mechanism, since it does not appear in the pathway originally proposed for oxidative cleavage of the aromatic ring:

(phenylperoxy —> phenoxy + O —> cyclopentadienyl + CO). Our goal has been to prepare a precursor to 2-oxepinoxy that could be used to determine its heat of formation, infrared spectrum, and unimolecular chemistry. Since 2-oxepinoxy is a resonantly stabilized radical, it could be prepared in principle by formal hydrogen atom removal any one of four isomeric precursors:

Somewhat surprisingly, none of these compounds is known, and so our first task has been to prepare one or more of them. Two routes were explored but found to be unacceptable. The route that eventually proved to be successful is shown on the next page.

2-(5*H*)-oxepinone   2-(3*H*)-oxepinone   2-(7*H*)-oxepinone   2-oxepinoxy   2-hydroxyoxepin
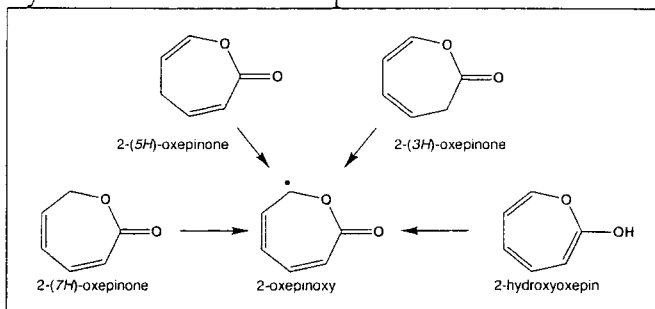
It has been demonstrated to have the robustness and reproducibility needed for a "production-line" synthesis. As it turns out, two of the four precursors to 2-oxepinoxy readily interconvert in solution, with the one on the left of the diagram (2-(3*H*)- oxepinone) being strongly favored. There is no detectable amount of the other two isomers at equilibrium. The precursors are now being

used for direct physical measurements, and will also be synthetically elaborated, for reasons described below.
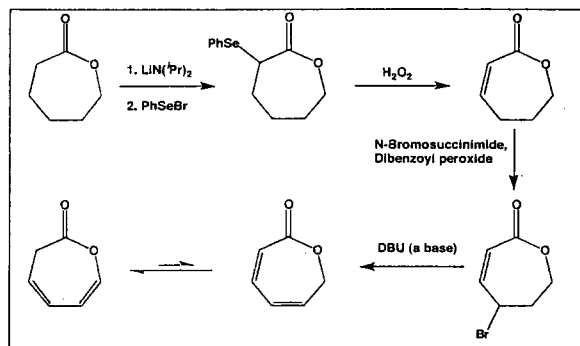
The first order of business is to determine the experimental enthalpy and entropy differences between the 2-(*3H*)- and 2-(*7H*)-oxepinone isomers. This is necessary because the gas-phase acidity measurements described below are being made under conditions where equilibration of these isomers is expected. Direct determination of the gas-phase equilibrium constant is difficult, but solution-phase determination is easy (by a simple van't Hoff plot from variable-temperature ^{1}H nmr). We do not expect the *differential* solvation of the two isomers to be significant, but that is being checked by determining the thermodynamic parameters in a variety of solvents. If, as we expect, there turns out to be negligible solvent dependence, then the extrapolation to the gas phase could be made with confidence. As a further check, we can compare our results with the predictions of high-level *ab initio* calculations. For example, CBS-QB3 calculations predict $\Delta H° = 3.8$ kcal/mol and $\Delta S° = 0.19$ cal/(mol K), with the equilibrium constant favoring the 2-(*3H*)- isomer, in the gas phase.

In parallel with this study we have just initiated a collaboration with Professor Christopher Hadad at The Ohio State University to generate the 2-oxepinoxy anion in a flowing afterglow. The purpose is to determine the gas-phase acidities of 2-(*3H*)-oxepinone and 2-(*7H*)-oxepinone. What is not known at this stage is whether gas-phase F$^-$ will reversibly deprotonate 2-(*3H*)- and 2-(*7H*)-oxepinone. Simple DFT calculations suggest that it should, but those calculations cannot anticipate all of the possible side reactions. Should the reversible deprotonation not prove feasible, the "bracketing" technique, using a variety of bases of known basicity, will be employed.

At the end of June, 2004, the PI finishes his term as Department Chair, and will then be on sabbatical leave. Part of that leave, beginning in January 2005, will be spent at the University of Colorado at Boulder with Professor G. Barney Ellison. The intention will be again to generate the 2-oxepinoxy anion, but this time to photodetach it in a negative-ion photoelectron spectrometer in order to determine its ionization potential(s). For this experiment an irreversible generation of the anion is preferred, and so a modified precursor may be necessary. A plausible candidate is 2-trimethylsiloxy-oxepin, which should be readily available from the 2-(*3H*)- and 2-(*7H*)-oxepinones that we have already prepared.
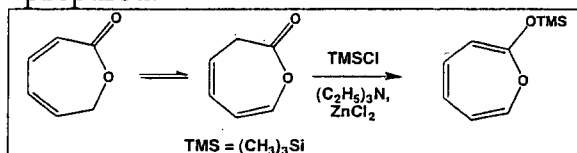
Good precedent suggests that its treatment with F$^-$ in the gas phase will result in irreversible formation of the desired anion plus $(CH_3)_3SiF$.

The negative ion photoelectron spectrum, in combination with the gas-phase acidity measurement and some standard calorimetry on the precursors will

allow us to determine an experimental heat of formation for the ground state of the 2-oxepinoxy radical, and possibly for any low-lying excited states that may be accessible in the photodetachment experiment.

Investigation of the Role of Nonstatistical Dynamics in Combustion Reactions.

Over the past several years, this laboratory has been conducting NSF-sponsored experimental and computational research into the role of nonstatistical dynamics in the behavior of thermally generated reactive intermediates. Early on, we thought that these phenomena were restricted to relatively exotic intermediates, such as singlet biradicals, that sit on energetic plateaus on the PE surface. There is little reason to believe that intermediates of that kind have much relevance to combustion chemistry. However, more recently we have found evidence for nonstatistical behavior of intermediates that sit in local minima as much as 20 kcal/mol deep.[1-3] That discovery greatly broadens the potential range of reactions that could be affected by this phenomenon, and brings many of the elementary reactions of combustion into play.

The principal experimental evidence in support of the nonstatistical picture comes from studying reactions in which the intermediate sits on an effective symmetry element of the PE surface. However, it is important to emphasize that the presence of the symmetry element is not required for the nonstatistical behavior – it merely makes its experimental detection easier. When there are two exit channels from the intermediate that are related to each other by a symmetry operation, the prediction of a product ratio becomes trivial for any statistical model – it is unity. In reality, however, product ratios as high as 10:1 have been found for such systems. The 10:1 ratio was found for a molecule with 24 atoms, and so the argument that the high density of vibrational states in polyatomic systems ensures statistical behavior also seems not to be universally valid.

Recently[4] we have begun to develop an analytical model for the nonstatistical dynamics revealed by the experiments and simulations. It is currently being further elaborated. Its key feature is that it reproduces the findings from quasiclassical trajectory simulations, which show that formation of products from thermally generated reactive intermediates is often not well described by single-exponential functions, and can sometimes have oscillatory components as illustrated in the graph below. The function $y(t)$ describes the excess product per unit time formed in two symmetry-related exit channels from an intermediate generated in a thermal reaction of an asymmetric reactant.
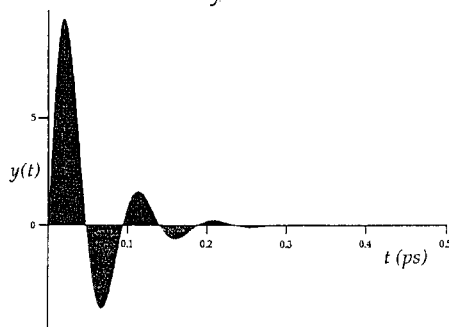
The decay of the oscillations is due both to product formation and to IVR.

We believe that the nonstatistical dynamics of thermally generated reactive intermediates has potentially important consequences for the modeling of combustion reactions because its occurrence implies that the branching ratio from such intermediates could not be accurately predicted by statistical kinetic models even if an exact PE surface were available.

With the increasing availability of inexpensive, high-performance computers, it is starting to become feasible to run direct-dynamics calculations using *ab initio* or DFT models for the PE surface. We would like to explore the use of such methods for a reaction of importance in atmospheric chemistry. We have selected it because the size of the molecular species makes the calculations tractable, and their chemical structures are very similar to those of intermediates that are of importance in combustion. Furthermore, the reaction in question has many steps, with multiple possible branches at several of the steps – just as one sees in combustion. If we find that nonstatistical dynamical effects are important in this model study, we can begin to think about how they might play a role in combustion kinetics. The reaction in question is of ozone with ethylene. It is known that atmospheric ozone reacts with alkenes to generate OH, but the mechanism is unclear. For example, Anderson *et al.* have shown that ozone react with ethylene to make OH. Their mechanism for the reaction is shown below:

carbonyl oxide
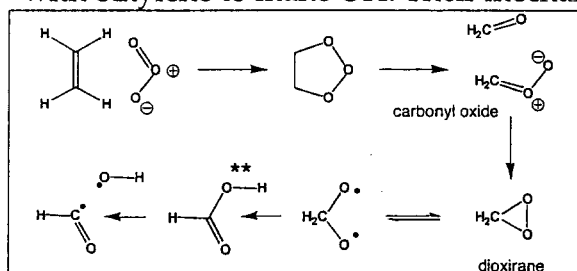
dioxirane

Perhaps the most controversial feature of this mechanism is the conversion of dioxirane, via a biradical, to vibrationally hot formic acid, which then breaks the C–O bond to generate OH. It is certainly true that the exothermicity of the conversion of the biradical to formic acid is enough (estimated 140 kcal/mol) to break the C–O bond (dissociation enthalpy 110 kcal/mol). However, formic acid has available to it at least two other reaction channels with lower barriers than C–O scission: formation of CO and H_2O is calculated to have a barrier of 69 kcal/mol, and formation of CO_2 and H_2 is found to have a barrier of 73 kcal/mol. Furthermore, the biradical intermediate has a very low-barrier reaction for extrusion of H_2 to form CO_2. So, if the Anderson mechanism is correct, there must be some dynamically interesting phenomena that lead to an unexpectedly high efficiency for the formation of OH. We would like to understand what those are, not only because the reaction itself is of importance in atmospheric chemistry, but also because there may well be lessons learned in this exercise that could be transferable to combustion chemistry.

References
(1) Reyes, M.B.; Lobkovski, E.B.; Carpenter, B.K. *J. Am. Chem. Soc.* **2002**, *124*, 641.
(2) Debbert, S.L.; Carpenter, B.K.; Hrovat, D.A.; Borden, W.T. *J. Am. Chem. Soc* **2002**, *124*, 7896.
(3) Nummela, J.A.; Carpenter, B.K. *J. Am. Chem. Soc.* **2002**, *124*, 8512.
(4) Carpenter, B.K. *J. Phys. Org. Chem.* **2003**, *16*, 858.

Ion Imaging Studies of Chemical Dynamics

David W. Chandler

Combustion Research Facility, mail Stop 9054, Sandia National Laboratories,
Livermore, CA 94551-0969
chand@sandia.gov

Scope of Program

The goal of this program is to develop and utilize advanced imaging techniques for the study of chemical processes. The processes to be studied range from bimolecular process such as rotational, vibrational and electronic energy transfer and reactive collsions to unimolecular photochemistry. Of present interest have been electronic non-adiabatic collision processes, non-adiabatic photo-dissociation of van der Waals molecules, production of ultra-cold molecules by inelastic collisions and near threshold photo-dissociation of van der Waals molecules. These studies are carried out under molecular beam conditions and, when possible, the results are compared to state-of-the-art calculations.

Progress Report

Bimolecular Processes

Cl ($^2P_{3/2}$ or $^2P_{1/2}$) + D_2 Reaction

The chlorine plus D_2 reaction has been the subject of considerable controversy over the last several years. Kopin Liu published a crossed molecular beam study of this reaction and found that the non-adiabatic channel, $Cl^*(^2P_{1/2}) + D_2$, channel was more reactive than the adiabatic, $Cl(^2P_{3/2}) + D_2$, channel even at energies where both channels were open. Millard Alexander has performed high quality scattering calculations on this system and finds that the non-adiabatic channel is on the order of 5% as reactive as the adiabatic channels under the same condition as the experiments. This has been referred to as one of the biggest outstanding discrepancies between theory and experiment for small molecule chemistry. In order for the non-adiabatic channel to be highly reactive, the curve crossing between the channels must be of sufficient probability. In order to determine an upper limit to the probability of curve crossing we are investigating the non-adiabatic scattering of Cl from D_2 to produce $Cl^* + D_2$. The curve crossing is calculated to be far out in the entrance channel and therefore as Cl collides with D_2 it will hop surfaces long before the chlorine atom interacts with the repulsive core of the D_2 molecule and scatters. By imaging both the Cl and Cl^* products we should be able to observe, on different parts of the images, elastic scattering of Cl from D_2 as well as the elastic scattering of Cl^* and the non-adiabatic inelastic scattering of Cl to produce Cl^*. In Figure 1 below we show the images of an atomic beam of 95% ground state Cl atoms and 5% Cl^* atoms after scattering from a molecular beam of D_2. Note the elastic scattering is predominantly forward scattered and the Cl^* image looks identical to the image of the Cl. If there was significant curve crossing from the Cl surface to the Cl^*

surface with the corresponding loss of ~800 cm^{-1} of translational energy then a small ring in the center of the Cl* image would be visible. From the lack of any visible signature of curve crossing and knowing the ratio of Cl to Cl* in our molecular beam we can estimate that the curve crossing cross section is at least 3000 times smaller than the elastic scattering cross section. We are continuing with this study to push this limit even lower.
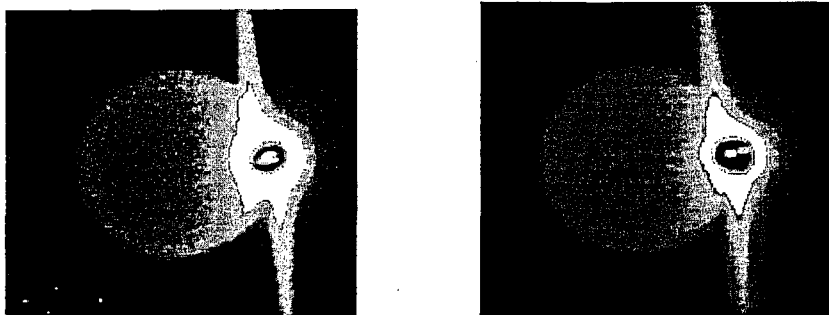
Figure 1 Images of Cl (^{2}P$_{3/2}$) and Cl(^{2}P$_{1/2}$) in collision with D$_2$. The rings represent elastic scattering.

NO + Ar

The radical nature of the NO molecule has made it an important molecule for scattering studies. The inelastic scattering system of NO collision with Ar has become a benchmark system because of the excellent potential energy surface for this system and the amount of high level calculations that have been performed upon it. In performing inelastic energy transfer experiments on this and other systems we have noticed that the intensity patterns that we observe are asymmetric and more intense at velocities that are small in the laboratory reference frame. This is because the slower moving molecules in the laboratory frame tend to be more localized at the point where the lasers intersect the scattering and create ions. We have investigated this single collision process in crossed molecular beams for the slowing (or cooling) of gas phase molecules. We have found that by controlling a collision between a nitric oxide (NO) molecule and an argon (Ar) atom we are able to slow the NO molecules to speeds that correspond to temperatures of less than 400 millikelvin (0.4K), or speeds less than 15 meters/sec. For our experimental conditions this speed distribution is only obtained for one particular rotational quantum state of the NO molecule, NO(j=7.5). This quantum state has the proper energy such that its recoil speed is equal to that of the center-of-mass speed of the collision pair and some of those scattered into this state are traveling opposite in direction to the center of mass of the system and are therefore slowed or "cooled" in the laboratory reference frame. For other collision energies or collision partners the particular quantum state that will be "cooled" in the laboratory reference frame will be different.

We believe that this measured speed distribution represents an upper limit and that in reality we have made a distribution of molecules with an effective temperature of 40 millikelvin (~4 m/s). We believe this due to extensive modeling of this collision system. Figure 2 is an image of the NO(j=7.5) that is produced by collision with Ar along with

the speed distribution that is measured for the slowly moving molecules in the bright spot at the top of the image. This work was done in collaboration with Professor James Valentini of Columbia University.
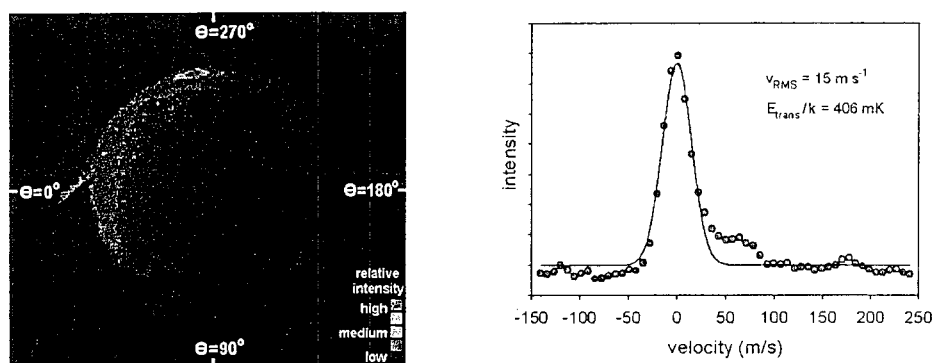
Figure 2. Image of NO(j=7.5) collision product showing slowly moving molecules and the speed distribution of the molecules that are slowed in the laboratory reference frame.

Unimolecular Reactions

Cyclohexane / X_2 (X = Cl or O) Dimers

We have investigated dissociation from the charge transfer state of van der Waals clusters after excitation through a strong absorption band in the ultraviolet. Based on a simple model and low level *ab initio* calculations, the location of the charge transfer absorption for a Cl_2-cyclohexane cluster is predicted and the dissociation of this cluster leading to $Cl^*(^2P_{1/2})$ and $Cl(^2P_{3/2})$ was investigated. The translational energy distribution, $P(E_T)$ for each cluster is analyzed in terms of two possible dissociation mechanisms. The dissociation may be considered to proceed on the initially accessed charge transfer state through a harpooning type mechanism. Alternatively, the dissociation may proceed following a non-adiabatic electronic transition to the neutral excited states of the diatomic subunit of the cluster. For O_2-cyclohexane, the $P(E_T)$ is consistent with the second dissociation mechanism. We determine from the available data that the likely structure for the vdW complex is analogous to the resting structure of I_2-benzene with the O_2 bond axis lying above the cyclohexane ring. For Cl_2-cyclohexane, we analyze the velocity dependence of the Cl recoil anisotropy and find it increases from nearly isotropic ($\beta \sim 0$) to distinctly anisotropic ($\beta \sim 1.7$-2). The fast, anisotropic Cl atoms result from dissociation of the cluster on the neutral excited states of Cl_2. The slow, isotropic Cl atoms likely result from secondary dissociation of the product Cl-cyclohexane cluster. We determine a $Cl^*(^2P_{1/2})/Cl(^2P_{3/2})$ branching ratio of 0.53 ± 0.05 and estimate that ~19% of the observed Cl atoms result from primary dissociation on the initially accessed charge transfer state. The data suggests that the Cl_2-cyclohexane cluster has an axial like structure following absorption of a photon. Finally, the rapid non-adiabatic hop from the charge transfer state to the neutral excited states of the diatomic can be explained in terms of coupling of the states though a one-electron change.

31

Future Directions

The collisional cooling of molecules to millikelvin temperatures represents a new way of creating single quantum states of translationally cold molecules. We propose to further investigate this technique for cooling molecules and will attempt to trap the molecules in either an intense off resonant laser field or an electric field Stark trap. We believe that by picking the appropriate mass combination of molecule and atom for collision that we can push the speed distribution into the microkelvin range. If this is possible many molecules can be trapped for the performance of high-resolution spectroscopy or collisonal studies at very low collision energies.

In the area of reactive scattering we would like to extend our study of the electronically non-adiabatic scattering to the observation directly of the non-adiabatic reaction products. In the case of the reaction above, Cl or Cl* + D_2 the product is DCl. By measuring the velocity distribution of a single quantum state of the DCl product we hope to determine the contributions to that product channel from the Cl and the Cl* channels. This will require further refinements to the existing apparatus.

Publications:

1) E. A. Wade, J. I. Cline, K. T. Lorenz, C. C. Hayden and D. W. Chandler, "Direct measurement of the binding energy of the NO dimer ", J. Chem.. Phys. V 116(12) 4755 (2002).

2) D. W. Chandler and J. I. Cline, "Ion Imaging Applied to the Study of Chemical Dynamics" in Advanced Series in Physical Chemistry, World Scientific Publishing ed. K.P. Liu and X Yang. (2002).

3) D. W. Chandler and C. C. Hayden, "Ion Imaging Techniques for the Measurement of Ion Velocities" Encyclopedia of Mass Spectrometry, Vol 5, ed P. B. Armentrout (2002).

4) K. T. Lorenz, D. W. Chandler and G. C. McBane, "State to State differential cross sections for rotational excitation of CO by Ne by velocity mapping." J. Phys Chem. A , v. 106(#7) pp. 1144-1151(2002).

5) M. Elioff, and D. W. Chandler, "State-to-state differential cross sections for spin multiplet-changing collisions of NO($X\,^2P_{3/2}$) with argon" JCP, v. 117, P6455-6462 (2002).

6) B. F. Parsons and D. W. Chandler, "On the Dissociation of van der Waals Clusters of X2-cyclohexane (X=O, Cl) Following Charge Tranfer Excitation in the Ultraviolet" J. Phys. Chem. A, V. 107, p. 10544 (2003).

7) E. A. Wade, K.T. Lorenz, J. L. Springfield, and D. W. Chandler, "Collisions of HCl with Rare Gas and Molecular Colliders" J. Phys. Chem. A, V. 107, p. 4976 (2003).

8) M. Elioff, J. J. Valentini and D. W. Chandler, "Production of cold molecules by crossed molecular beam scattering" Science, vol. 302, p 1940 (2003).

9) Raarup, MK; Chandler, DW; Olsthoorn, RCL; Schmidt, T "Single Molecule FRET microscopy of conformational changes in the RNA of Alfalfa mosaic virus." Biophyics Journal v. 84, p. 299A (2003).

Direct Numerical Simulation and Modeling of Turbulent Combustion

Jacqueline H. Chen, Evatt Hawkes, Shiling Liu, and James Sutherland
Sandia National Laboratories, Mail Stop 9051
Livermore, California 94551-0969
Email: jhchen@sandia.gov

Program Scope

The goal of this research program is to gain fundamental insight into unsteady flow/chemistry interactions that occur in turbulent combustion, and to develop and validate combustion models required in various engineering CFD approaches including Reynolds Averaged Navier-Stokes (RANS) and Large-eddy simulation (LES). In this work a high-fidelity numerical approach known as direct numerical simulation (DNS), which resolves all of the scales in the scalar and velocity fluctuations, is used to efficiently investigate fine-grained physical phenomena associated with interactions between convective and diffusive transport with detailed chemistry in the combustion of hydrogen and hydrocarbon fuels.

Recent Progress

In the past couple of years we have extended the DNS approach to explore new parameter spaces, enabled by improvements in numerical boundary condition treatment [6] and high-order implicit time integration of chemically stiff systems [7]. The former improvement enables exploration of laboratory experimental configurations with detailed chemistry in which fully-developed grid turbulence interacts with a flame in the computational domain (e.g. jet flames, Bunsen and V-flame, counterflow). In this manner the statistically stationary behavior of a flame can now be studied with DNS, without the previous limitations of decaying velocity fluctuations in isotropic turbulence. The additive Runge-Kutta method has enabled the integration of stiff chemical kinetics, e.g. autoignition in large hydrocarbon fuels like n-heptane. These improvements along with a new efficient F90 MPP modular construction of the 3D DNS code, S3D, have enabled us to pursue new research thrusts described below.

Ignition Front Propagation in a Constant Volume at High Pressure With Temperature Inhomogeneities

At present, the combustion mode in HCCI engines is not well understood, as both volumetric and front-like combustion modes can occur. A major challenge posed by this method of combustion is to control the heat release rate, and in particular, to provide a means to spread it out over several crank angle degrees, suppressing the occurrence of damaging engine knock. We have used DNS to explore the influence of temperature inhomogeneities on characteristics of ignition and subsequent combustion in an HCCI environment. We simulated the evolution of autoignition from an initial temperature fluctuation spectrum of "hot spots" at high pressure using two-dimensional direct numerical simulations (DNS) with a detailed hydrogen/air reaction mechanism [13,14]. One of the primary objectives in this study was to develop systematic and rational methods to identify and analyze different regimes of ignition and subsequent combustion processes. The theoretical basis stems from an earlier study by Zel'dovich, who described ignition of a nonuniform mixture in three distinct regimes of propagation: deflagration, spontaneous ignition front propagation, and detonation. He further showed that the spontaneous ignition front speed is inversely proportional to the initial temperature gradient, suggesting a characterization of ignition regimes based on the speed of the ignition front. The concept has been applied to identifying ignition regimes in various one-dimensional configurations. We extended the idea to more realistic two-dimensional ignition problems, where multi-dimensional aspects including wrinkling and mutual interaction of fronts are fully accounted for.

To obtain the speed of the advancing combustion wave, we defined an ignition delay time for a given fluid parcel as the time for a scalar to reach a critical level, resulting in the unambiguous identification of the ignition front speed with the iso-surface displacement speed, s_d^*, that has been used in previous studies. We further identified the role of molecular diffusional effects including heat conduction and mass diffusion on ignition propagation. Ignition front propagation evolution during constant volume combustion was monitored by evaluating the surface mean of the ratio of the local front speed to the local deflagration speed. This local measure was also used to distinguish front propagation in the different regimes and was applied to several different initial temperature fields characterized by the standard deviation and skewness of the temperature fluctuation. The results compared favorably with a volumetric measure based on a critical temperature gradient.

The Effects of Strain Rate on High-Pressure Nonpremixed N-Heptane Autoignition in Counterflow

Ignition processes are an integral part of combustion in many practical systems including, for example, diesel engines. Ignition in diesel engines typically occurs while strong fuel-air and temperature inhomogeneities exist, making the study of ignition in non-premixed configurations with compressed reactants particularly valuable. N-heptane has a cetane number similar to diesel fuel, and it is widely used as a model fuel to study the ignition process. Research into n-heptane ignition in homogeneous systems, where kinetics is best studied, is mature, but there have been few fundamental studies of inhomogeneous mixtures at conditions relevant to diesel ignition. We studied the effect of steady strain on the transient autoignition of n-heptane at high pressure numerically with detailed chemistry and transport in a counterflow configuration. Using a skeletal mechanism developed for ignition at high pressure by Professor H. Pitsch at Stanford University [9] we studied the effect of strain on multistage n-heptane ignition, first, by imposing a uniform temperature for both the fuel and oxidizer streams. Second, we imposed a temperature gradient between the fuel and oxidizer streams. We were able to capture the global effect of strain on ignition by defining a Damköhler number based on either heat release rate or the characteristic chain branching rate as we have done in earlier studies [3].

We discovered that for multi-stage ignition, negative temperature coefficient behavior does not exist for high scalar dissipation rate. The reason for this behavior is the self-generated temperature gradient associated with the transition from low-temperature to intermediate-temperature chemistry. This gradient is steep and results in significant diffusive losses that inhibit second stage intermediate-temperature chemistry. Moreover, we found that the imposition of an overall temperature gradient further inhibited ignition because reaction zones for key branching reactions with large activation energies are narrowed. For a fixed oxidizer temperature that is not sufficiently high, a higher fuel temperature resulted in a shorter ignition delay provided that the heptyl radicals are mainly oxidized by low-temperature chemistry. As expected, we found that an increase in pressure significantly increased reaction rates and reduced ignition delay time. However, with increasing pressure there is a shift towards single-stage low-temperature dominated ignition, which serves to delay ignition. Similar to homogeneous conditions, we discovered that the pressure dependence of the ignition delay can be fit to a power relation.

Ignition of Hydrogen in Unsteady Non-premixed Flows – Comparison of experiment and computation

We investigated the effects of unsteady strain on hydrogen ignition in non-premixed flows with both experimental measurements and numerical counterflow computations [15]. These experiments and computations represent the first attempt at quantifying the effect of strain, both steady and unsteady, on the evolution of radicals during ignition through to the formation of a flame. Comparisons between computations and experiments were made for the evolution of OH during autoignition both for steady and unsteady strain. We used the computations to evaluate the performance of selected hydrogen/air mechanisms for ignition in the presence of transport, and also to aid in the interpretation of experimental

results. Previous evaluation of chemical mechanisms for ignition were conducted in homogeneous systems, e.g. flow reactors in the absence of diffusive transport. Similar to the experiments, we triggered ignition computationally by introducing a Gaussian profile of O atoms at a fixed location. We found that for both steady and unsteady strain, the transient one-dimensional counterflow ignition simulations of hydrogen/nitrogen against heated air showed excellent agreement with the experiment in terms of predicting ignition delays and the rate of OH accumulation during the induction period. The computations also captured the super-equilibrium OH during the transition to the formation of a steady flame, although not to the degree observed experimentally.

To better understand the cause of the super-equilibrium OH we performed 2D DNS of the steady counterflow ignition configuration. The 2D simulations reveal the formation of an edge flame propagating radially outward from the ignition kernel following thermal-runaway. Because the edge flame is in a strain field, the three branches of the triple flame are collapsed on one another and there exists substantial preferential diffusion at the leading edge of the highly curved propagating front. Preferential diffusion of H_2 results in enhanced radical production and fuel consumption rates locally. Peak intensity of OH LIF was also observed at the radial edges in the experiment following ignition. Because the hydroxyl radical recombines slowly it can diffuse back to the centerline where the measurements of the superequilibrium OH were observed.

Influence of Hydrogen Blending on Lean Premixed Methane-Air Flames

Lean premixed combustion in gas turbines offers the potential to produce power with low NO_x emissions but can suffer from poor combustion stability, resulting in poor combustion efficiency, higher emissions of CO and unburned hydrocarbons, and (potentially) mechanical damage. The replacement of small amounts of the fuel with hydrogen offers the opportunity to increase flame stability, and thus reduce emissions. We investigated the effect of hydrogen blending on lean premixed methane-air flames using the DNS approach coupled with a reduced chemical mechanism [8]. Two flames were compared with respect to stability and pollutant formation characteristics - one a pure methane flame close to the lean limit, and one enriched with hydrogen.

The stability of the flame was quantified in terms of the turbulent flame speed. A higher speed was observed for the hydrogen-enriched flame consistent with extended blow-off stability limits found in measurements. The greater flame speed is a result of a combination of higher laminar flame speed, enhanced area generation, and greater burning rate per unit area. Preferential diffusion of hydrogen coupled with shorter flame time scales account for the enhanced flame surface area. In particular the enriched flame is less diffusive-thermally stable and more resistant to quenching than the pure methane flame resulting in a greater flame area generation. The burning rate per unit area correlated strongly with curvature as a result of preferential diffusion effects focusing fuel at positive cusps. Lower CO emissions per unit fuel consumption were observed for the enriched flame, consistent with experimental data. CO production was greatest in regions that undergo significant downstream interaction where the enriched flame exhibits faster oxidation rates as a result of higher levels of OH concentration. NO emissions were increased for the enriched flame as a result of locally higher temperature and radical concentrations found in cusp regions.

Future Plans

Ignition Front Propagation DNS and Model Development

Recent DNS of lean hydrogen-air ignition at high pressure at constant volume with temperature inhomogeneities showed the dual significance of scalar dissipation- first, limiting the minimum attainable ignition front speed, and second, modulating the initial spectrum of temperature gradients, thereby

promoting spontaneous front propagation rather than deflagration. We will investigate this latter effect in greater detail by simulating over a wider range of turbulence and initial temperature distributions for H2/air mixtures and then extend this study to consider differential compressive heating in multi-stage autoignition of hydrocarbon fuels. We anticipate that larger initial integral length scales of the temperature field that are more representative of HCCI combustion will favor the spontaneous ignition front mode of propagation. We will develop a unified theoretical basis for predicting the front speed fully accounting for cumulative compressive heating. In the model, the turbulent DNS ignition data will be used to provide a probabilistic description of the evolution of the initial temperature and mixture fluctuations. We are also planning to use the transported pdf approach to describe compression ignition in a turbulent environment.

Unsteady Strain Effects on Autoignition of N-Heptane in Counterflow

Results from our recent study of steady strain effects on the transient autoignition of n-heptane at high pressure showed that, for multi-stage ignition, strain has an unequal effect on low-temperature and intermediate-temperature chemistry. In particular, it was shown that, at sufficiently high strain or scalar dissipation rate, intermediate-stage chemistry is inhibited such that negative temperature coefficient behavior ceases to exist. We plan to further investigate the effect of unsteady strain, both monochromatic oscillation as well as impulsive forcing, on the behavior of transient n-heptane ignition at high pressure. We are especially interested in determining whether alternate chemical pathways to multi-stage ignition exist in situations where an ignition kernel encounters scalar dissipation rates comparable to critical characteristic branching rates, which may inhibit normal pathways to ignition.

BES Publications (2002-2004)

1. H. G. Im and J. H. Chen, "Direct Numerical Simulation of Turbulent Premixed Flame Interaction," *Combust. Flame*, 131:246-258 (2002).
2. S. D. Mason, J. H. Chen, H.G. Im, "Effects of Unsteady Scalar Dissipation Rate on Ignition of Non-premixed Hydrogen/Air Mixtures in Counterflow," *Proceedings of the Combustion Institute,* 29, (2002), pp. 1629-1636.
3. T. Echekki and J. H. Chen, "High-Temperature Combustion in Autoigniting Non-Homogeneous Hydrogen-Air Mixtures", *Proceedings of the Combustion Institute,* 29, (2002), pp. 2061-2068.
4. T. Echekki and J. H. Chen, "Direct Numerical Simulation of Autoignition in Non-homogeneous Hydrogen-Air Mixtures," *Combust. Flame*, 134:169-191. (2003).
5. J. C. Sutherland and C. A. Kennedy, "Improved Boundary Conditions for Viscous, Reacting, Compressible Flows," *J. Comp. Phys.* 191:502-524 (2003).
6. C. A. Kennedy and M. H. Carpenter, "Additive Runge-Kutta Schemes for Convective-Diffusion-Reaction Equations," *Appl. Num. Math.* 44:139-181 (2003).
7. S. Liu, J. C. Hewson, J. H. Chen, and H. Pitsch, "Effects of Strain Rate on High-Pressure Nonpremixed N-Heptane Autoignition in Counterflow," *Combust. Flame*, 137:320-339 (2004).
8. E. R. Hawkes and J. H. Chen, "Direct Numerical Simulation of Hydrogen Enriched Lean Premixed Methane/Air Flames," in press *Combust. Flame*, (2004).
9. E. R. Hawkes and J. H. Chen, "Evaluation of Models for Flame Stretch in the Thin Reaction Zones Regime," to appear in *Proceedings of the Combustion Institute*, 30, (2004).
10. R. Sankaran, H. G. Im, E. R. Hawkes, and J. H. Chen, "The Effects of Nonuniform Temperature Distribution on the Ignition of a Lean Homogeneous Hydrogen-Air Mixture," to appear in *Proceedings of the Combustion Institute*, 30, (2004).
11. R. Seiser, J. H. Frank, S. Liu, J. H. Chen, R. J. Sigurdsson, and K. Seshadri, "Ignition of Hydrogen in Unsteady Nonpremixed Flows," to appear in *Proceedings of the Combustion Institute*, 30, (2004).

Turbulent Combustion

Robert K. Cheng
Environmental Energy Technologies Div.
Lawrence Berkeley National Laboratory
70 –109, 1 Cyclotron Rd.
Berkeley, CA 94720

E-mail : rkcheng@lbl.gov

Larry Talbot
Dept. of Mechanical Engineering
University of California at Berkeley
6173 Etcheverry Hall
Berkeley, CA 94720-1740

E-mail : Talbot@cmsa.Berkeley

Scope

This research program focuses on lean premixed combustion: an advanced low emission energy technology for heating and power systems. Combustion processes in these systems are turbulent and are not sufficiently well characterized or understood to guide turbulent combustion theories and computational methods. Our objective is to investigate experimentally the coupling of turbulence with burning rate, flame stability, extinction and pollutant formation. The goal is to provide for energy technologies the chemical and fluid mechanical scientific underpinnings that can be captured in models and simulations that will become accurate and reliable tools for predicting combustion process performance. This effort is responsive to DOE's mission to "foster a secure and reliable energy system that is environmentally and economically sustainable." Our approach is to conduct detailed measurements of the spatial structures of the turbulent scalar and velocity fields of laboratory flames over a wide range of fuel/air ratios, flow velocities and turbulence intensities. The analysis and interpretation are guided by a theoretical concept of classifying premixed flames according to the initial turbulence and thermo-chemical conditions. Specific goals for FY 05-07 will be (1) to obtain experimental data and analyses to support the development of 3D time dependent numerical simulations with comprehensive chemistry at the local scale ($O(1$ cm$)$) and at the devise scale ($O(10$ cm$)$), and (2) elucidate the fundamental processes in turbulent premixed flames at very high flame speeds (> 15 m/s) and/or at elevated initial pressures and temperatures.

Recent Progress

With the implementation of a Particle Image Velocity (PIV) system in FY03, we have extended our capability to measure instantaneous 2D velocity vectors within a relatively large field of view (13cm^2) for comparison with results from computational methods such as Large Eddy Simulation (LES), and 3D time dependent direct numerical simulations using Adaptive Mesh Refinement (AMR). Our PIV system has a dual synchronized YAG-laser system interfaced with a PC- controlled frame grabber and a 2048 by 2048 pixel digital camera. Data acquisition and analysis software is provided by NASA Glenn Research Center. The PIV system has been used to obtain a large set of data for our collaboration with LBNL's Center for Computational Science and Engineering at LBNL. The CCSE group lead by John Bell is developing discretization methodology for low Mach number flows using compressible second order Navier-Stokes equations. AMR is one of their major areas of research for time dependent 3D simulations of premixed turbulent combustion. We selected two experimental configurations. The first is a plane symmetric v-flame that is one of the basic configurations for fundamental studies. The

second is an air-jet low-swirl burner (LSB) that is more complex but is a critical test-bed for assessing the simulation method and the flame and species transport models.

For the v-flame, experiment and simulation conditions are CH_4/air at $\phi = 0.7$, $U_o = 3$ m/s, u' = 7%, and, v' = 5%. The conditions are chosen to be compatible with the current capability of the simulation. Velocity measurements on 2D plans perpendicular and parallel to the rod-stabilizer have been made to infer the 3D flowfield features. Both non-reacting and reacting flow data have been obtained and analyzed. The non-reacting data was necessary to establish the initial conditions for the simulation and to verify the intensity, isotropy and length-scale of the simulated turbulent inflow. The reacting flow was computed by a 3D AMR method using a time-dependent low Mach number algorithm that conserves both species mass and total enthalpy. It incorporates detailed chemical kinetics and a mixture model for differential species diffusion. Methane chemistry and transport are modeled using the DRM-19 (20-species, 84-reaction) mechanism derived from the GRI-Mech 1.2 mechanism along with its associated thermodynamics and transport databases. AMR dynamically resolves the flame and turbulent structures.

A primary objective of our first study was to determine, by direct comparison with PIV data, the refinement levels necessary to predict the overall scalar field (flame brush) and flowfields (mean and rms velocities). The simulation was carried out in two parts. Inflow conditions were generated in a separate nonreacting simulation of the upstream turbulent flow produced by a perforated plate in a circular nozzle. For the reacting flow region, a $(12 \text{ cm})^3$ domain was used. It was found that, with the low Mach number implementation, a 3-level adaptive grid hierarchy, with a finest-level grid spacing, $\Delta x = 312.5$ µm, was capable of predicting with remarkable fidelity the major features of the experimental results. The results confirm that the AMR low Mach number implementation is well-suited for our laboratory flames. It is expected that a higher level of mesh refinement will improve the fidelity of the computation and resolve the internal structures of the flamelets.

We also applied PIV to an LSB flames that is being simulated by AMR. The conditions also involve relatively low velocity and turbulence (CH_4/air at $\phi = 0.8$, $U_o = 5$ m/s, u' = 7%, and v' = 5%). However, the field of view provided by PIV showed that the LSB flames have some features that have yet to be fully characterized. For some cases, stagnation points are found downstream of the flame brushes indicating the formation of flow recirculation in the products. To further understand the significance, role, and influence of the downstream recirculation on other flame processes we conducted an extensive study on the effects of heat release, flow Reynolds number and swirl number on the flowfield dynamics of the LSB. Nine CH_4/air flames and their corresponding non-reacting flows were measured. At a fixed swirl rate, the non-reacting flows show that the recirculation zones were formed only when $U_o > 5$ m/s. With combustion, the flames were all stabilized upstream of the recirculation and gas expansion in the products pushed the recirculation zone downstream. To characterize the recirculation strength, we calculated the local mass flux of the recirculating fluid, M_r and normalized by the total axial mass flux M_o. The results show that the maximum values of M_r/M_o were < 1%. These levels are about an order of magnitude lower than in conventional high-swirl burners where the recirculation zone is critical to flame stabilization. As the flame brushes are situated upstream of the weak recirculation zone, flow reversal in the farfield has no significant impact on most aspect

of the turbulent flame brushes but is a distinct characteristic of the LSB flowfield. The prediction of location and strength of the weak recirculation zone can be an additional test criterion for computation methods.

Our studies have concentrated thus far on CH_4 flames where the local speed of the flame fronts are not highly sensitive to flame curvature, compression or strain. This is not the case for H_2 and C_3H_8 flames where aerodynamic stretch and flame curvature are coupled to flame front instability modes that contribute to enhance or reduce flame surface area. This is the thermal-diffusive effect due to nonuniform species diffusion that either generates cellular flame structures in lean H_2/air flames with Lewis number Le $<<$ 1 or dampens the formation of wrinkles in lean C_3H_8/air flames with Le $>>$ 1. This self-turbulizing and laminarizing nature has a direct impact on turbulent burning rate but remains relatively unexplored by experiments and analyses. Recent experimental and numerical studies on unsteady laminar flames have shown that these flame instability effects may be attenuated at higher turbulence intensities.

To determine whether or not the relative influences of thermal-diffusion effects decrease with increasing turbulence, we initiated a series of studies of H_2/air, CH_4/air and C_3H_8/air flames using an air-jet LSB. We varied Le by the use of mixtures of H_2 (Le = 0.33, ϕ = 0.3), CH_4 (Le $\approx$ 1, ϕ = 0.8) and C_3H_8 (Le = 1.85, ϕ = 0.75) having the same laminar flame speed, s_L, of 0.3 m/s. Their flame regime parameters (i.e., Ka, Da) are also the same for a given level of turbulence. The test matrix consists of U_o at 5, 10 and 15 m/s all with S = 0.8. We plan a comprehensive study using OH-PLIF and PIV to measure the scalar and velocity statistics. The conditioned and unconditioned PIV measurements are complete and the OH-PLIF measurements are in progress. The flame wrinkled structures shown on PIV raw images seem to suggest the Le effects persist even at higher turbulence. This effect will be quantifiable by analyzing the flame curvature statistics from OH-PLIF measurements.

Relative to the experimental efforts, our research on computational method is more modest. From the onset, our focus has been to develop Largragian time-dependent methods with infinite rate chemistry that can capture the turbulent flame flowfield properties and simulate evolving processes such as flow deflection, turbulence production and dissipation, and flame wrinkling. We focus on the use of 2D discrete vortex simulation to study v-flames. Though other more elaborate numerical approaches, such as LES and AMR, have been developed, the discrete vortex method provides a useful and very economic alternative to resolve the salient features of the time-dependent dynamic flowfield. In collaboration with Prof. C. K. Chan of the Hong Kong Polytechnic University our recent achievements include improvement in the simulation of the complex flame fronts by a novel numerical technique called Contour Advection with Surgery (CAS) [35]. We found that CAS can be extended to other combustion geometries, such as stagnation flame, when the reaction sheet model is employed.

At the 8th International Workshop on Premixed Turbulent Flames, we offered to lead the development of a website for disseminating experimental data published in archival journals. The collective recommendation was to group the experiments into three categories (1) oblique flames, e.g. v-flames (2) envelop flames e.g. Bunsen type conical flames, and (3) detached flames, e.g. LSB flames. Each category will have a separate website offering a description of their attributes, definitions of the flame properties and a list of papers. Data and supplemental

data for the papers can be accessed through DOE's Collaboratory for Multi-scale Chemical Science (CMCS) web portal. We are working with Bill Pitz of Lawrence Livermore Nat'l Lab and David Leahy of Sandia Nat'l Lab to design and test the sites. A preview is currently available at (http://eetd.lbl.gov/aet/combustion/workshop/Database/flame-config.html).

4. Summary of Planned Research

Our longer term goal is to develop the experimental capabilities to characterize 3D velocity statistics and flame structures. The tasks for FY 05 – 07 are:

1. Collaborate on the development of computational methods with (1) LBNL-CCSE group on Low Reynolds number AMR simulations of v-flame and LSB flame, (2) Georgia Tech on LES simulation of LSB flames, (3) Sandia National Lab CRF on direct numerical simulation of small turbulent v-flames, and (4) Hong Kong Poly. Univ on discrete vortex method of laboratory turbulent v-flames.
2. Investigate the role of thermal-diffusive effects on flame/turbulence interactions to determine a possible attenuation of the thermal/diffusive instability with increasing turbulence.
3. Develop an unsteady laminar flame configuration as a fundamental theoretical and experimental test-bed for developing robust species transport models that can be used in flame models with detailed chemistry (Collaborate with N. J. Brown and LBNL-CCSE).
4. Investigation of premixed turbulent flames at high velocities.
5. Studies of turbulent flames at high initial pressures and/or temperatures
6. Experimental database for premixed turbulent flames

Publications

1. Bell, J.B., M.S. Day, I.G. Shepherd, M.R. Johnson, R.K. Cheng, V.E. Beckner, M.J. Lijewski, and J.F. Grcar, *Numerical Simulation of a Laboratory-Scale Turbulent V-Flame.* Submitted to Proc. Comb. Inst., 2004. **30.**
2. J. S. L. Lam, C. K. Chan, L. Talbot, and I. G. Shepherd, "On the High-resolution Modelling of a Turbulent Premixed Open V-flame," *Combustion Theory and Modelling,* 7, 1-28, (2003).
3. Shepherd, I. G. and Cheng, R. K. "Premixed Flame Front Structure in Intense Turbulence" Proceedings of the Combustion Institute, 29, p. 1833-1840 (2002).
4. Shepherd, I. G., Cheng R. K., Plessing T., Kortschik C., and Peters N., "Premixed Flame Front Structure in Intense Turbulence," *Proc. Comb. Inst.,* vol. 29, 2002.

ELECTRONIC STRUCTURE STUDIES OF GEOCHEMICAL AND PYROLYTIC FORMATION OF HETEROCYCLIC COMPOUNDS IN FOSSIL FUELS

J.Cioslowski, Department of Chemistry and Biochemistry, Florida State University, Tallahassee, FL 32306
jerzy.csit.fsu.edu, (850) 644-8274

Program scope

This research program has as its objective uncovering of the reaction mechanisms responsible for the formation of various heteroatom-containing combustion emittants. As such, it holds the promise of guiding the practitioners of applied science and engineering in their efforts to significantly reduce the pyrolytic production of carcinogens and other hazardous substances. At the same time, it is slated to test practical limits of the predictive power of modem quantum-chemical methods and shed light on mechanisms of many reactions that are commonly employed in organic syntheses.

Recent progress

The research funded by this grant has thus far yielded 20 papers with the P.I. as the main author or a co-author (see the enclosed list for the 11 publications that appeared in years 2001-2003). In addition, several papers were published by the co-P.I. (Dr. D. Moncrieff) who has since departed from the research program. Five research projects resulted in papers published in 2003.

1. When calibrated against the available experimental data for didehydrobenzenes, RB3LYP/cc-pVTZ, QCISD/cc-pVTZ, CCSD(T)/cc-pVTZ, and G3 electronic structure calculations were found to provide reliable predictions of standard enthalpies and singlet-triplet splittings in all possible isomers of didehydroazines, which (with a possible exception of 2,6-didehydropyridine) possess singlet ground states [3]. Singlet didehydroazines with larger numbers of nitrogen atoms turned out to be more prone to ring opening, as indicated by the fact that out of the 6, 11, 6, and 3 possible didehydropyridines, didehydrodiazines, didehydrotriazines, and didehydrotetrazines,respectively, 5, 7, 2, and none were actually found. Immediate proximity of the nitrogen atom to the formally triple carbon-carbon bond confers decreased thermodynamic stabilities and smaller singlet-triplet plittings on the species of the 1,2-didehydro type. Some of the aza-analogs of singlet 1,3-didehydrobenzene are as stable as their 1,2-didehydro counterparts. The only existing aza-analog of singlet 1,4-didehydrobenzene is 2,5-didehydropyrazine, which is particularly stable and possesses a large singlet-triplet splitting, making it a feasible synthetic target. Our calculations indicated that the experimental standard enthalpies of formation of pyrimidine and pyrazine are in error.

2. Test G3 calculations on 2,3-didehydronaphthalene confirmed the reliability of the additive correction scheme in the prediction of properties of annelated analogs of 1,2-didehydrobenzene. Such a scheme opens an avenue to facile electronic structure calculations on didehydrogenation reactions of polycondensed heterocyclic compounds with six-membered rings [4].

41

3. B3LYP/6-311G* electronic structure calculations revealed that the dependence of the complexation energy $E_{cmpl}(z)$ on the longitudinal displacement z of the guest in endohedral complexes of the Na^+ cation with capped [5,5] armchair single-walled carbon nanotubes stems from an interplay between the polarization of the host by the electric field of the guest and the guest-host steric repulsion [6]. Overall, $E_{cmpl}(z)$ is characterized by the presence of a periodic pattern of local minima and maxima that reflect the discrete nature of the tube and of a pair of global minima located at fixed distances from the tube termini. Because of the large barrier height to zero-point energy ratio, the endohedral motion of the Na^+ cation at T = 0 [K] is largely confined to a surface that internally follows the contour of the tube. Vibrations perpendicular to the surface give rise to transitions in the vicinity of 100 [cm^{-1}], whereas the unimpeded motions within the surface result in a plethora of transitions with onsets as low as 0.1 [cm^{-1}].

4. Analysis of the HF/6-31G** and B3LYP/6-311G** relative energies of 25 unbranched catacondensed benzenoid hydrocarbons with six rings revealed a well-pronounced dependence of their thermodynamic stabilities on the presence of simple structural motifs [7]. In particular, the energy contribution due to steric overcrowding is proportional to the number of pairs of adjacent angular annelations of the same helicity, whereas the contribution due to conjugation effects is related to the number and mutual position of linear annelations. Although the arrangement of linear annelations also uniquely determines the number of Kekulé structures, the latter does not correlate directly with the non-steric energy component. This study also demonstrated the uselessness of the simple additive nodal increment model in accurate prediction of thermodynamic stabilities of PAHs.

5. In a continuing effort to design new electronic structure methods, a model system of three electrons in a harmonic oscillator potential was thoroughly investigated [11].

Future plans

1. The Wellington mechanism of chlorine/hydrogen elimination. The completion of the reactions that lead from elementary sulfur and alkenes, alkynes, or their chloro-derivatives to (chloro) thiophenes requires elimination of hydrogen/chlorine from the 2 and 5 positions of the thiophene ring. Since no evolution of H_2S is observed in such transformations, a free-radical mechanism is unlikely in this case. On the other hand, the concerted elimination that is operational in the well-known unimolecular decompositions of 2,5-dihydroheterocycles to their parent species and H_2 may be involved. In order to either confirm or discard this possibility, electronic structure calculations on the relevant Wellington eliminations are being carried out. In the case of unsubstituted species, the computed activation enthalpies will be compared with the experimental values of 54.8, 44.6, and 48.5 [kcal/mol] for the S, NH, and 0 heteroatoms, respectively. Stereochemistry of the reaction will be established and the preferential elimination of H_2 over CH_4 in 2-methyl-2,5-dihydrofuran will be explained.

2. Thermochemistry and kinetics of rearrangements of azynes to aza analogs of cyclopentadienylidenecarbene. The electronic factors affecting the barriers and energetics of these rearrangements are being investigated by analyzing the data produced by G3 and CCSD(T) calculations on didehydroazines and the respective carbene isomers. Stabilities of the latter species with respect to fragmentation are being assessed.

3. The mechanism of thermal decomposition of quinoline and isoquinoline. Pyrolysis of quinoline and isoquinoline produces a large number of products that arise from fragmentation of both the benzene

and pyridine moieties. The decomposition pathways of these two species appear to share several intermediates, the most important of which is the 1-indeneimine radical. The following issues concerning these reactions are being addressed:

a) The positional dependence of the energetics of the C-H bond scissions in quinoline and isoquinoline are being studied. Electronic factors affecting stabilities of the resulting radicals are being determined.
b) Kinetic and thermodynamic viabilities of various fragmentation patterns of the quinydyl and isoquinydyl radicals are being evaluated. Possible equilibration among the radicals and/or their fragmentation products is being studied.
c) The viability of the conjectured equilibria among the intermediates involved in these reactions are being investigated.

The aforedescribed theoretical work will furnish a wealth of data of importance to experimental research. Kinetic models of thermal decompositions of nitrogen-containing heterocyclic compounds will be verified and corrected/augmented if necessary. Mechanistic hypotheses for several reactions will be either proved or rejected, advancing the knowledge of pyrolytic processes.

Publications resulting from the DOE sponsored research (2002-2004)

[1] J.Cioslowski, A.Szarecka, and D.Moncrieff; Mol.Phys. **100** (2002) 1559; Conformations and Thermodynamic Properties of Sulfur Homocycles: II. The Fluxional S_8^+ Radical Cation

[2] J.Cioslowski, A.Szarecka, and D.Moncrieff; Int.J.Quant.Chem. **90** (2002) 1049; Conformations of the S_5^+ and S_6^+ Homocyclic Radical Cations

[3] J.Cioslowski, A.Szarecka, and D.Moncrieff; Mol.Phys. **101** (2003) 839; Energetics, Electronic Structures, and Geometries of Didehydroazines

[4] J.Cioslowski, A.Szarecka, and D.Moncrieff; Mol.Phys. **101** (2003) 1221; Energetics, Electronic Structures, and Geometries of Naphthalene, Quinoline, and Isoquinoline Analogs of 1,2-Didehydrobenzene

[5] J.Cioslowski, N.Rao, and D.Moncrieft; J.Amer.Chem.Soc. **124** (2002) 8485; Electronic Structures and Energetics of [5,5] and [9,0] Single-Walled Carbon Nanotubes

[6] J.Cioslowski, N.Rao, K.Pernal, and D.Moncrieff; J.Chem.Phys. **118** (2003) 4456; Endohedral Motions Inside Capped Single-Walled Nanotubes

[7] J.Cioslowski and J.C.Dobrowolski; Chem.Phys. Letters **371** (2003) 317; Structural Dependence of Thermodynamic Stability of Unbranched Catacondensed Benzenoid Hydrocarbons

[8] J.Cioslowski and K.Pernal; J.Chem.Phys. **116** (2002) 4802; Density Matrix Theory of Weak Intermolecular Interactions

[9] J.Cioslowski, K.Pernal, and P.Ziesche; J.Chem.Phys. **117** (2002) 9560; Systematic Construction of Approximate 1-Matrix Functionals for the Electron-Electron Repulsion Energy

[10] J.Cioslowski and K.Pernal; J.Chem.Phys. **117** (2002) 67; Variational Density Matrix Functional Theory Calculations with the Lowest-Order Yasuda Functional

[11] M.Taut, K.Pernal, J.Cioslowski, and V.Staemmler; J.Chem.Phys. **118** (2003) 4861; Three Electrons in a Harmonic Oscillator Potential: Pairs vs. Single Particles

Dynamics and Energetics of Elementary Combustion Reactions and Transient Species
Grant DE-FG03-98ER14879

Robert E. Continetti
Department of Chemistry and Biochemistry
University of California San Diego
9500 Gilman Drive
La Jolla, CA 92093-0340
April 12, 2004

Program Scope and Direction

This research program uses photodetachment and dissociative photodetachment of negative ions to carry out studies of the energetics and dynamics of combustion-relevant radicals and the transition state dynamics of hydroxyl radical reactions. Negative ion photodetachment allows the preparation of both stable radical species and unstable neutral complexes in the vicinity of the transition state for bimolecular reactions. The energetics and spectroscopy of these species can be probed using the well-established method of photodetachment photoelectron spectroscopy, and uniquely in our laboratory, the subsequent dissociation dynamics of unstable neutrals can be determined using photoelectron-photofragment coincidence spectroscopy.

The studies of radicals in the last year have focused on oxygenated organic radicals. A study of the branching between a minor channel yielding stable acetyloxyl radicals and the dissociative photodetachment to $CH_3 + CO_2 + e^-$ has been completed and submitted for publication. Complementary experiments on progressively larger carboxylate anions, to illustrate the probable trend towards more stable radicals as size increases, are planned in the near future. In addition, experiments on the photodetachment of alkynoxide and substituted acetylide species have been completed and should be submitted for publication in the near future. In the last year a significant effort to demonstrate vacuum ultraviolet (VUV) photodetachment of negative ions was made, however, this has not yielded results as of the date of this report. If this experiment is successful, it will enable studies of higher excited states of hydrocarbon radicals and other species than has been possible previously using the photoelectron-photofragment coincidence technique.

The transition state dynamics of hydroxyl radical reactions continues to be an important focus of this research program. Following previous work on the OH + OH, OH + H_2O and OH + CO reactions, we have obtained results on the O + HF reaction at a photon energy of 4.80 eV. Given the large electron affinity of this system (≈ 3.3 eV), only the three lowest HF vibrational states are accessible at this wavelength, and there is not enough energy available to reach the OH + F channel. Nonetheless, given the previous studies of this system,[1] including theoretical studies of the dissociative photodetachment of OHF$^-$ by Dixon and Tachikawa,[2] this is an important system for studying in the present effort to characterize hydroxyl radical reactions. To complete our studies of triatomic hydroxyl radicals, we have also made efforts to develop an ion source capable of generating intense beams of OHCl$^-$ and OH-H_2^- at the kHz repetition rates required in the coincidence experiment to permit studies of the OH + Cl and OH + H_2 reactions, respectively. These efforts have yet to be successful, however. Currently we are working on synthesis of the OH$^-$(CH$_3$) anion to prepare the OH + CH$_3$ reaction transition state. These efforts, including a study of the deuterated DOCO$^-$ anion to follow up our earlier studies of HOCO$^-$, will continue through the end of this grant.

Recent Progress

1. Energetics and Dynamics of Oxygenated Organic Radicals

1.1. Dissociative Photodetachment of the Acetate Anion: Energetics and Stability of the Acetyloxyl Radical

Oxygenated organic radicals are important combustion intermediates and also have a significant role in other applications in chemistry. Carboxylate anions and carboxyl radicals, for example, play an important role synthetically in decarboxylation reactions. Expanding on our previous studies of HCO_2 we have carried out a study of the acetyloxyl radical, CH_3CO_2, by photodetachment of the acetate anion at 355, 340 and 258 nm. These experiments have shown that at all of these wavelengths, $\approx 90\%$ of the nascent radicals dissociate to $CH_3 + CO_2$ radicals, with a large kinetic energy release, peaking at $E_T = 0.65$ eV for 355 nm excitation. The EA of the CH_3CO_2 radical is found to be 3.47 eV, yielding a near-threshold photoelectron spectrum in the 355 nm data with two resolved features. Deuteration yields a nearly identical photoelectron spectrum, indicating that the observed features do not involve C-H excitation, and suggesting that these features correspond to two low-lying electronic states of this radical. The 258 nm data reveals evidence for two higher-lying electronic states, consistent with the complicated electronic structure predicted for this free radical. The next step in this project is to study the energetics and stability of slightly larger carboxyl radicals by photodetachment of species including the propanoate ($CH_3CH_2CO_2^-$) and benzoate ($C_6H_5CO_2^-$) anions.

1.2. Photodetachment Imaging of Alkynoxides and Substituted Acetylides

In the last year we completed our initial studies of alkynoxides, substituted acetylides and the corresponding neutral free radicals. In these systems, no dissociative photodetachment was observed, so the experiments focus on photodetachment imaging studies of the photoelectron spectra for propynoxide, the butynoxides and 4-pentyn-1-oxide. Generation of anions both by proton abstraction from the corresponding alcohol with O^- and by electron impact on the corresponding nitrite precursors has allowed us to prepare only the alkynoxide species, or, when the ethynyl moiety is terminal in the carbon chain, the substituted acetylides as well. We find that the electron affinities of the alkynoxide radicals are ≈ 2 eV, while the acetylides have electron affinities of ≈ 3.2 eV. Two manuscripts describing these experiments are currently in preparation, one focusing on the propynoxide and butynoxide species, and the second one focusing on substituent effects on the gas-phase acidity of the alkynol precursors.

1.3. VUV Photodetachment

In the past year we have made two attempts to demonstrate photodetachment of negative ions with VUV radiation, but have not been successful yet. The combination of the relatively low peak power available from our 1 kHz regenerative amplifier (120 mW at 386 nm in a 1.8 ps pulse) and the low anion number densities ($10^5 - 10^6$ cm^{-3}) of course make this a difficult experiment. The proof of principle experiments have focused on Br$^-$ and I$^-$ atomic anions, however we have yet to demonstrate spatio-temporal overlap of the atomic and VUV beams. The ultimate goal of this effort is to study the energetics and dissociative excited states of a number

of small hydrocarbon radicals, including vinylidene, allyl and cyclopentadienyl radicals by photodetachment of the corresponding anions.

2. Transition State Dynamics of Hydroxyl Radical Reactions

2.1. Probing the O + HF reaction by dissociative photodetachment of OHF⁻

The O + HF → OH + F reaction is another simple bimolecular reaction involving the hydroxyl radical, providing another benchmark system for study by dissociative photodetachment of the OHF⁻ anion. Neumark and co-workers[1] and have previously studied this system by photoelectron spectroscopy, and Dixon and Tachikawa[2] have followed up these experiments by carrying out wavepacket dynamics calculations on this system. One aspect of this experiment that makes it more difficult for us to study is the high electron affinity (3.3 eV), and the significant endothermicity of the OH + F reaction channel. In our experiments on the DPD of OHF⁻ at 258 nm, we cannot access the OH + F channel, and only access the three lowest vibrational states of HF. The results obtained at 258 nm do reveal some vibrationally resolved structure in the correlated photoelectron-photofragment kinetic energy spectra, indicating that photodetachment to a repulsive region of the surface in the vicinity of the transition state is occurring. To extend this study to OH + F exit channel as well will require higher energy photons, potentially either the VUV source discussed above or by anti-Stokes Raman shifting in H_2.

2.2. Probing the transition state for the OH + CH₃ radical-radical reaction by photodetachment of the OH⁻(CH₃) complex

Recently Johnson and co-workers have characterized the OH⁻(CH₃) radical using infrared spectroscopy, revealing that it is best described as a hydroxide anion interacting with a methyl radical.[3] We have been working on producing this anion in significant quantities in a new source involving the interaction of a beam of O⁻ produced in a pulsed discharge of N_2O with a secondary beam of CH_4. If these experiments yield results, we will gain insights into the dynamics of the radical-radical reaction OH + CH₃. It is hoped that by the time of the contractor's meeting, interesting new results on this system will be available.

2.3. Continued efforts on other hydroxyl radical systems

In the final months of the current grant we also hope to revisit our earlier study of the HOCO⁻ anion by forming the deuterated DOCO⁻ species. This anion can be synthesized by the reaction of OH⁻ or OH with CO in the supersonic expansion, however, this will be rather expensive since CD_4/N_2O gas mixtures are required. We have obtained some CD_4, however, so we will carry out this study in the near future. The OH + H_2 reaction remains of considerable interest. In the case of DPD of the OH⁻(H_2) complex, this is a system for which the photoelectron-photofragment coincidence (PPC) experiment has already been predicted by Mick Collins and co-workers.[4] Thus, this remains a high priority. The O + HCl reaction, beginning with the O⁻(HCl) precursor is also a system of great interest owing to the detailed potential energy surfaces available for this species. We have had difficulty making either one of these anions in our 1 kHz or continuous ion sources in the densities required to carry out the PPC experiment

Publications: 2002 – Present

1. T.G. Clements, R.E. Continetti and J.S. Francisco, "Exploring the OH + CO $\rightarrow$ H + CO$_2$ potential surface via dissociative photodetachment of (HOCO)$^-$," J. Chem. Phys. **117**, 6478-6488 (2002).
2. R.E. Continetti and C.C. Hayden, "Coincidence imaging techniques," in <u>Modern Trends in Reaction Dynamics</u>, ed. X. Yang and K. Liu, World Scientific (Singapore), 2004.

Literature Cited

[1] S.E. Bradforth, D.W. Arnold, R.B. Metz, A. Weaver and D.M. Neumark, J. Phys. Chem. **95**, 8066 (1991).

[2] R.N. Dixon and H. Tachikawa, Mol. Phys. **97**, 195 (1999).

[3]. M.A. Johnson, private communication.

[4]. D.H. Zhang, M.Yang, M.A. Collins, S.-Y. Lee, Proc. Nat. Acad. Sci. **99**, 11579 (2002).

Flame Sampling Photoionization Mass Spectrometry

Terrill A. Cool
School of Applied and Engineering Physics
Cornell University, Ithaca, New York 14853
tac13@cornell.edu

Project Scope

Direct measurements of the absolute concentrations of combustion intermediates in carefully controlled and documented laboratory flames are required for the development of kinetic models for the combustion of ethylene, ethane, propene, propane, ethanol, propanol, and higher hydrocarbons. These models are used in current efforts to minimize environmental pollution associated with hydrocarbon combustion.

Time-of-flight molecular beam photoionization mass spectrometry (PIMS), applied to the selective detection of flame species is a powerful new approach for studies of flame chemistry [1]. Measurements of the absolute concentrations of flame species are possible with PIMS when species photoionization cross sections are known [1-3]. A flame-sampling time-of-flight mass spectrometer (TOFMS), recently designed and constructed for use with a synchrotron radiation light source [1] [LBNL Advanced Light Source (ALS)] provides significant improvements over previous facilities that have employed tunable VUV laser sources. These include superior signal-to-noise, soft ionization, and photon energies readily tunable over the 8 to 17 eV range required for comprehensive flame species concentration measurements.

The new instrument is routinely used for measurements of concentration profiles and photoionization efficiency (PIE) curves for species sampled from well-characterized low-pressure laminar flames. Both stable and radical intermediates are detectable at mole fractions as low as 10^{-6}. Individual isomeric species may often be selectively detected and identified; this is one of the most important advantages of VUV PIMS. The work described here is part of a collaborative effort between investigators at Cornell, the Sandia Combustion Research Facility, and the University of Massachusetts. A further description of recent achievements of this collaboration appears in Craig Taatjes' abstract.

Recent Progress

Flame studies: Species mole fraction profiles, temperature profiles and species PIE curves were measured for several reaction systems to assist in kinetic model development. Complete data sets were obtained for each system for both stoichiometric and fuel-rich conditions. The flame systems studies were:

- propane/oxygen/argon
- ethane/oxygen/argon
- ethylene/oxygen/argon

- allene-doped ethylene/oxygen/argon
- ethanol/oxygen/argon
- n-propanol/oxygen/argon
- isopropanol/oxygen/argon
- hydrogen/oxygen/argon
- glyoxal/hydrogen/oxygen/argon
- formic acid/hydrogen/oxygen/argon
- glyoxal/hydrogen/nitrogen dioxide/oxygen/argon
- formic acid/hydrogen/nitrogen dioxide/oxygen/argon

Work currently in progress includes a comparison of the results for the ethylene, propane, propene, and ethanol systems with kinetic modeling calculations.

Measurement of absolute photoionization cross sections for reaction intermediates: Knowledge of absolute cross sections for photoionization is required for measurements of flame species mole fractions. In our work we measure photoionization cross sections for "target" species by comparing ion signals recorded from a binary mixture of the target with a "standard" species of known photoionization cross section. We have completed cross section measurements for 10 key reaction intermediates found in the combustion of simple hydrocarbons. Preliminary measurements for 10 more intermediates are available; final measurements will be completed during the upcoming June-July ALS beam cycle.
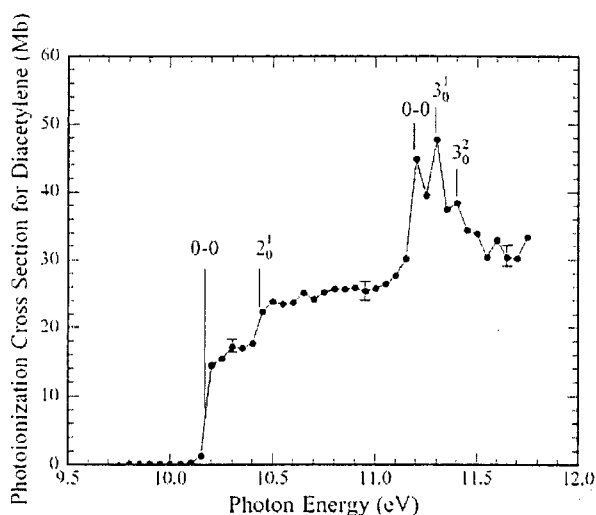
Fig. 1. Photoionization cross sections for diacetylene
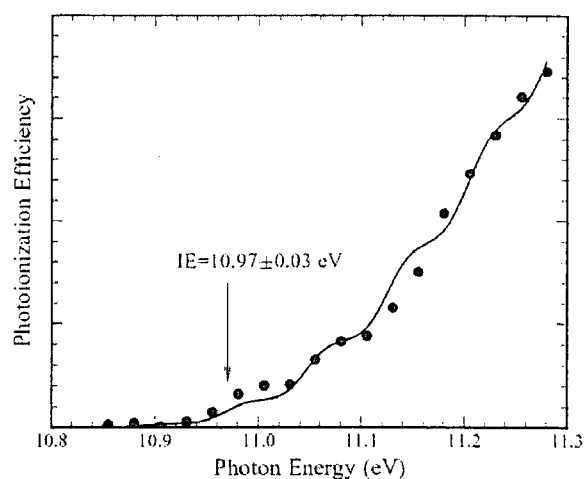
Fig. 2. Photoionization Efficiency for *trans*-HONO

Highlighted in Fig. 1 are absolute cross section measurements for diacetylene. Both absorption and photoelectron spectroscopy have been used to study the spectrum of diacetylene in the region between the first (10.17 eV) and second (12.62 eV) ionization potentials. The vacuum ultraviolet spectrum of diacetylene was first recorded by Price and Walsh [4], and later by Smith [5]. No previous studies of photoionization efficiency have been undertaken. The cross section data of Fig. 1 show the adiabatic ionization threshold at 10.17 eV and the origin band of an autoionizing resonance at 11.19 eV.

The step at 10.43 eV arises from excitation of the ν_2 C≡C (2177 cm^{-1}) symmetric stretch of the $C_4H_2^+$ ground state. The origin band at 11.19 eV (90250 cm^{-1}) is accompanied by the first two members of a progression with a vibrational spacing of 0.1 eV (807 cm^{-1}). This spacing is identical to the frequency of the ν_3 C-C symmetric vibration of the $A^2\Pi_u$ state (second ionization potential) of the ion [6,7], which suggests that these bands are vibronic components of an autoionized member of a Rydberg series leading to the $A^2\Pi_u$ state.

The photoionization efficiency of HONO: Nitrous acid, HONO, is an important chemical reaction intermediate in the combustion of solid propellants. Both NO_2 and HONO play key roles in the ignition and combustion of the nitramine-based propellants HMX and RDX and propellant formulations containing the nitrate esters nitroglycerine and nitrocellulose. Despite the well-studied roles of HONO in combustion and atmospheric chemistry, the ionization energy of HONO has, until now, never been directly measured. As a result the currently accepted heat of formation for the *trans*-HONO cation is based primarily on bracketing measurements of proton-transfer reactions [8,9] that yield indirect estimates of the proton affinity of NO_2.

Our measurements of the near-threshold ionization efficiency (PIE) of *trans*-HONO are presented in Fig. 2. These data were obtained using molecular beam sampling to observe the spatial profiles of HONO and NO_2 very near the burner face of a low pressure (20 Torr) premixed $NO_2/O_2/H_2/Ar$ flame.

In order to analyze the shape of the PIE curve near threshold, Franck-Condon factors were calculated for the photoionization of *trans*- HONO by Craig Taatjes and David Osborn. The calculations were based on force constant matrices and frequencies for both neutral and cationic *trans*-HONO calculated at the B3LYP/6-311++G(3*df*,2*pd*) level using the Gaussian98 quantum chemistry suite. The results are in agreement with the B3LYP/6-311++G(3*df*,2*pd*) calculations reported by Sengupta et al.[10]. A PIE spectrum was simulated using a Franck-Condon envelope calculated with a 400 K thermal population among initial states, convolved with a Gaussian photon energy distribution with a 40 meV FWHM corresponding to our measured energy resolution. The result (solid curve) is compared with the experimental PIE measurements (dark circles) in Fig. 2. The solid curve represents the best fit between experiment and calculation using the adiabatic ionization energy as a variable parameter. The fitting yields IE=10.97± 0.03 eV. Recent *ab initio* calculations of 10.86 eV (DFT) and 10.98 eV (G2) [10] are in excellent agreement with the present experimental value. Our IE value, combined with the known heat of formation of *trans*-HONO (-78.83±1.34 kJ mol^{-1})[11] yields $\Delta H^0_{f,298K}$ (HONO$^+$) = 979.6±3.2 kJ mol^{-1}, and a derived value for the proton affinity of NO_2, PA(NO_2) = 583.5±3.3 kJ mol^{-1}. These values are in good agreement with respective values of 977 kJ mol^{-1} and 585.8±8.4 kJ mol^{-1} based on the bracketing measurements. The present measurement provides a direct benchmark for the thermochemistry of the HONO cation, and the results are consistent with existing thermochemical estimates for HONO and NO_2.

Future Directions

Of particular interest will be continuing studies of the chemistry of the formation and destruction of ethenol (vinyl alcohol) a novel combustion intermediate, detected for the first time in our recent studies of fuel-rich ethylene/oxygen flames [1]. The ethenol and acetaldehyde isomers of C_2H_4O (m/e=44) are easily distinguished with VUV PIMS because of their differing ionization energies (9.33 and 10.23 eV, respectively). We find that the fraction of the m/e=44 ion signal attributable to ethenol increases monotonically from about 10% in the preheat zone to greater than 60% near the end of the primary flame zone where both isomers are consumed. Ethenol is also observed in significant concentrations in ethanol, propanol and 1,3-butadiene flames. Formation mechanisms under consideration are sequential H-atom abstraction from ethanol and reactive decomposition of the $HO \bullet C_2H_4$ adduct formed by the addition of OH to ethylene at the C=C double bond [12].

A collaborative kinetic modeling effort will be pursued in analysis of extensive data accumulated on the several hydrocarbon flames studied in the past two beam cycles at the ALS. We will also initiate new studies of several fuel-rich hydrocarbon and oxygenated hydrocarbon flames directed toward a better understanding of reaction mechanisms leading to the formation of polycyclic aromatic pollutants. Finally, measurements of absolute photoionization cross sections will be continued for many additional reaction intermediates of importance in hydrocarbon combustion.

References

1. T. A. Cool, K. Nakajima, T. A. Mostefaoui, F. Qi, A. McIlroy, P. R. Westmoreland, M. E. Law, L. Poisson, D. S. Peterka, and M. Ahmed, *J. Chem. Phys.,* **119** (2003) 8356-8365.
2. T. A. Cool, K. Nakajima, C. A. Taatjes, A. McIlroy, P. R. Westmoreland, M. E. Law and A. Morel, *Thirtieth Symposium (International) on Combustion,* The Combustion Institute, Pittsburgh, PA. (2004), accepted.
3. J. C. Robinson, N. E. Sveum, and D. M. Neumark, *J. Chem. Phys.* **119** (2003) 5311-5314.
4. W. C. Price and A. D. Walsh, *Trans. Faraday Soc.* **41** (1945) 381.
5. W. L. Smith, *Proc. Roy. Soc. A.* **300** (1967) 519-533.
6. V. E. Bondybey and J. H. English, J. Chem. Phys. **71** (1979) 777-782.
7. J. P. Maier and F. Thommen, J. Chem. Phys. **73** (1980) 5616-5619.
8. E. P. L. Hunter and S. G. Lias, *J. Phys. Chem. Ref. Data* **27** (1998) 413.
9. C. W. Polley and B. Munson, *Int. J. Mass Spectrom. Ion Processes* **59** (1984) 333-337.
10. D. Sengupta, R. Sumathi, and S. D. Peyerimhoff, *Chem. Phys.* **248** (1999) 147-159.
11. M. W. Chase, Jr., NIST-JANAF Thermochemical Tables, Fourth Edition, *J. Phys. Chem. Ref. Data,* Monograph No. 9 (1998).
12. F. P. Tully, *Chem. Phys. Letters* **143**, 510 (1988); **96**, 148 (1983).

DOE Publications

1. T. A. Cool, K. Nakajima, T. A. Mostefaoui, F. Qi, A. McIlroy, P. R. Westmoreland, M. E. Law, L. Poisson, D. S. Peterka, and M. Ahmed, *J. Chem. Phys.,* 119 (2003) 8356-8365.
2. T. A. Cool, K. Nakajima, C. A. Taatjes, A. McIlroy, P. R. Westmoreland, M. E. Law and A. Morel, "Studies of a fuel-rich propane flame with photoionization mass spectrometry" *Thirtieth Symposium (International) on Combustion,* The Combustion Institute, Pittsburgh, PA. (2004), submitted and accepted.
3. T. A. Cool, K. Nakajima, C. A. Taatjes, and A. McIlroy, "Photoionization cross sections for reaction intermediates in hydrocarbon combustion", *J. Chem. Phys.,* submitted.
4. C. A. Taatjes, D. L. Osborn, T. A. Cool, and K. Nakajima, "Synchrotron Photoionization Measurements of Combustion Intermediates: The Photoionization Efficiency of HONO", *Chem. Phys. Letters,* submitted.
5. T. A. Cool, A. McIlroy, F. Qi, P. R. Westmoreland, L. Poisson, D. S. Peterka and M. Ahmed, "A photoionization mass spectrometer for studies of flame chemistry with a synchrotron light source", *Rev. Sci. Instr.,* submitted.

STATE CONTROLLED PHOTODISSOCIATION OF VIBRATIONALLY EXCITED

MOLECULES AND HYDROGEN BONDED DIMERS

F.F. Crim
Department of Chemistry
University of Wisconsin–Madison
Madison, Wisconsin 53706
fcrim@chem.wisc.edu

Our research investigates the chemistry of vibrationally excited molecules. The properties and reactivity of vibrationally energized molecules are central to processes occurring in environments as diverse as combustion, atmospheric reactions, and plasmas and are at the heart of many chemical reactions. The goal of our work is to unravel the behavior of vibrationally excited molecules and to exploit the resulting understanding to determine molecular properties and to control chemical processes. A unifying theme is the preparation of a molecule in a specific vibrational state using one of several excitation techniques and the subsequent photodissociation of that prepared molecule. Because the initial vibrational excitation often alters the photodissociation process, we refer to our double resonance photodissociation scheme as *vibrationally mediated photodissociation*. In the first step, fundamental or overtone excitation prepares a vibrationally excited molecule and a second photon, the photolysis photon, excites the molecule to an electronically excited state. Vibrationally mediated photodissociation provides new vibrational spectroscopy, measures bond strengths with high accuracy, alters dissociation dynamics, and reveals the properties of and couplings among electronically excited states.

Several recent measurements illustrate the scope of the approach and point to new directions. We have completed an extensive study the spectroscopy and non-adiabatic dissociation dynamics of ammonia (NH_3) and have new results on the vibrationally mediated photodissociation of methanol (CH_3OH). In each case, the goals are understanding and exploiting vibrations in the ground electronic state, studying the vibrational structure of the electronically excited molecule, and probing and controlling the dissociation dynamics of the excited state.

Ammonia (NH_3)

Ammonia is a famously well-studied molecule that holds interesting opportunities for vibrationally mediated photodissociation experiments because it has both a nonadiabatic dissociation to yield ground state $NH_2 + H$ and an adiabatic dissociation to form excited state $NH_2^* + H$. We have used vibrationally mediated photodissociation spectroscopy to observe the symmetric N-H stretching vibration (v_1), the antisymmetric N-H stretching vibration (v_3), and the first overtone of the bending vibration ($2v_4$), obtaining simplified spectra originating in the lowest few rotational states. In addition, we have observed combination bands with the umbrella vibration (v_2) for each of these states, (v_1+v_2), (v_2+v_3), and (v_2+2v_4). The action spectra come from observing the production of the excited state NH_2^* from photolysis well above the threshold energy for its formation. We observe the first hint of the effect of vibrational excitation on the dissociation dynamics in these experiments, finding that the relative yield of excited products is *lower* for photodissociation of molecules containing a quantum of the symmetric stretching vibration in the ground state compared to those with

antisymmetric stretching or bending excitation. This differential dissociation disappears completely upon addition of a quantum of the umbrella vibration in the ground state.

The electronic spectroscopy available through vibrationally mediated photodissociation is particularly informative. Because the initial vibrational excitation of NH_3 molecules cooled in a supersonic expansion selects single rotational states of vibrationally excited molecules, both the Franck-Condon factors and positions of the transitions change from the one-photon spectra. By using this extra dimension, we are able for the first time to identify unambiguously the progression in the excited state bending vibration (v_4), the combination bands between the bending and excited state umbrella vibration (v_2+v_4), and the origin of the excited state symmetric stretch vibration (v_1). The resulting new harmonic frequencies and anharmonicities are $\omega_2^0 = 881 \pm 12$ cm^{-1}, $x_{22} = 6 \pm 2$ cm^{-1}, $\omega_4^0 = 910 \pm 23$ cm^{-1}, $x_{44} = 9 \pm 6$ cm^{-1}, $g_{44} = 16 \pm 7$ cm^{-1}, and $x_{24} = 56 \pm 13$ cm^{-1}. The values for the umbrella vibration (v_2) agree well with those previously determined by Vaida, and the large off-diagonal anharmonicity between the umbrella and bending vibrations is consistent with their near degeneracy, which prevented the direct observation of v_4 in the past. Our necessarily less precise estimate of the origin of the broad excited state symmetric stretch vibration (v_1) is $\omega_1^0 \approx 2360$ cm^{-1}

Information about the excited state structure makes it possible to investigate the dynamics of the dissociation of electronically excited molecules with different vibrations excited. The experiments use resonant enhanced multiphoton ionization to perform Doppler spectroscopy on the H atom fragment. In agreement with previous measurements, we observe both slow and fast components in the distribution of recoil velocities upon excitation of different excited state umbrella vibrations. The excited state bending vibrations behave similarly with a slightly larger fraction of fast hydrogen atoms. The dramatic different is in the stretching vibrations, which we can excite unambiguously for the first time. Dissociation from the state containing one quantum of symmetric stretch (v_1) produces a distribution with both fast and slow components that are similar to that for the origin. Dissociation from the antisymmetric N-H stretch state (v_3), however, produces dramatically different results. It forms *only* slow hydrogen atoms, likely reflecting preferential decomposition to make solely the excited state product. New calculations by D. Yarkony (private communication) seem consistent with molecules having excited asymmetric N-H stretching vibrations preferentially remaining on the excited state surface, avoiding the conical intersection.

Methanol (CH$_3$OH)

Our first explorations of the vibrationally mediated photodissociation of methanol allowed us to obtain spectra of the second and third overtone of the O-H stretching vibration in the cooled molecules that agreed well with other measurements. We have also obtained similar spectra in the fundamental region of the O-H stretch and made the first measurements of the vibrationally mediated photodissociation dynamics detecting the H-atom product in order to obtain the ultraviolet spectra of the vibrationally excited molecules. The electronic excitation spectrum of vibrationally excited methanol begins about 2600 cm^{-1} lower in total excitation energy than that for ground vibrational state methanol. A simple model using a one-dimensional vibrational wavefunction mapped onto a dissociative excited electronic state surface recovers the qualitative features of the spectrum. Using *ab initio* calculations of portions of the ground and excited potential energy surfaces, we calculate vibrational wavefunctions and simulate the electronic excitation spectra using the overlap integral for the bound and dissociative vibrational wavefunctions on the two surfaces. The qualitative agreement of the cal-

culation with the measurement suggests that, at the energy of the fundamental vibration, the O-H stretch is largely uncoupled from the rest of the molecule during the dissociation.

FUTURE DIRECTIONS

The two near term goals of the project are to study of the dissociation of vibrationally excited methanol and its dimers. Both studies are likely to involve the addition of ion imaging capabilities to our apparatus. Ion imaging detection will also allow a more incisive study of the striking result on vibrational control of the passage through the conical intersection in ammonia. The subsequent step is to investigate the dimers of other well characterized systems to determine how simple complexation influences these well-understood dissociation dynamics.

PUBLICATIONS SINCE 2002 ACKNOWLEDGING DOE SUPPORT

Vibrational Spectroscopy and Photodissociation of Jet-Cooled Ammonia. Andreas Bach, J. Matthew Hutchison, Robert J. Holiday, and F. Fleming Crim, J. Chem. Phys. **116**, 4955 (2002).

Vibronic Structure and Photodissociation Dynamics of the A State of Jet–cooled Ammonia. Andreas Bach, J. Matthew Hutchison, Robert J. Holiday, and F. Fleming Crim, J. Chem. Phys. **116**, 9315 (2002).

Competition between Adiabatic and Nonadiabatic Pathways in the Photodissociation of Vibrationally Excited Ammonia. Andreas Bach, J. Matthew Hutchison, Robert J. Holiday, and F. Fleming Crim, J. Phys. Chem. A, **107**, 10490 (2003).

Photodissociation of Vibrationally Excited Ammonia: Rotational Excitation in the NH_2 Product. Andreas Bach, J. Matthew Hutchison, Robert J. Holiday, and F. Fleming Crim, J. Chem. Phys. **118**, 7144 (2003).

Action spectroscopy and photodissociation of vibrationally excited methanol. J. Matthew Hutchison, Robert J. Holiday, Andreas Bach, Shizuka Hsieh, and F. Fleming Crim, J. Phys. Chem. (*in press*).

INFRARED ABSORPTION SPECTROSCOPY AND CHEMICAL KINETICS OF FREE RADICALS

Robert F. Curl and Graham P. Glass
Department of Chemistry and Rice Quantum Institute
Rice University, Houston, TX 77251
(713)348-4816 (713)348-3285
rfcurl@rice.edu gglass@rice.edu

PROGRAM SCOPE

This research is directed at the detection, monitoring, and study of the chemical kinetic behavior by infrared absorption spectroscopy of small free radical species thought to be important intermediates in combustion. In the last year, work on the reaction of OH with acetaldehyde has been completed and published. In the course of our investigation of branching ratios of the reactions of $O(^1D)$ with acetaldehyde and methane, we discovered that hot atom chemistry effects are not negligible at the gas pressures (13 Torr) initially used. Branching ratios of the reaction of $O(^1D)$ with CH_4 have been measured at a tenfold higher He flow and fivefold higher pressure. The measurements of branching ratios in the reaction of $O(^1D)$ with acetaldehyde must now be measured under the higher pressure condition.

PRODUCT YIELDS IN THE REACTION OF OH WITH ACETALDEHYDE

The reaction of OH with acetaldehyde in the gas phase has been studied by tunable infrared laser kinetic spectroscopy. As expected the main channel is the production of water (~100%). An upper bound of 5% was placed on the yield of CH_3, and the yield of H is estimated as 5±5%. A rate constant of $1.67(10)\times10^{-11}$ molecules^{-1} cm^3 s^{-1} is obtained for the title reaction in good agreement with previous measurements. The major product of the reaction, CH_3CO, reacts with O_3 producing CH_3, CO_2 and O_2 in one channel with a rate constant of $1.4(5)\times10^{-11}$ molecules^{-1}cm^3 s^{-1} and producing CH_3CO_2 and O_2 in the other channel with a rate constant of $3.3(5)\times10^{-11}$ molecules^{-1} cm^3 s^{-1}. Thus the reaction between OH and acetaldehyde is primarily an H atom abstraction. Any contribution at room temperature from addition channels is small.

HOT ATOM EFFECTS IN O(^{1}D) REACTIONS

After beginning work with $O(^1D)$ in its reaction with acetaldehyde, we decided that we needed to develop our understanding of the application of our infrared kinetic spectroscopy approach to $O(^1D)$ reactions. Our primary interest is in the determination of branching ratios, but we do have the capability of measuring relative rates by competition for $O(^1D)$. A good test for our procedures was to measure the rate constant of $O(^1D)$ + H_2 (reaction 1) relative to $O(^1D)$ + N_2O (reaction 2). The expected OH absorbance (base e) upon photolysis of a mixture of H_2 and N_2O with a small amount of NO added to relax vibrationally excited OH can be expressed as

$$A(OH) = \sigma L \frac{k_1 [H_2]}{k_1[H_2] + k_2[N_2O] + k_3[NO]} [\,O(^1D)]_0$$

where σ is the OH absorption cross-section, L is the pathlength, and the other quantities are rate constants and concentrations. This can be rearranged to

$$\frac{1}{A(OH)} = \frac{1}{\sigma L[\,O(^1D)]_0} \left(1 + \frac{k_2[N_2O] + k_3[NO]}{k_1}[H_2]^{-1}\right)$$

Thus if $1/A(OH)$ is plotted vs $1/[H_2]$, a straight line is expected with the ratio of the slope to intercept being $k_2[N_2O]/k_1$. Figure 1a shows such a Stern-Volmer plot in a system where the partial pressure of N_2O is 362.8 mTorr and the partial pressure of the helium buffer gas is 12 Torr. The straight line on this graph is the best fit to the data adjusting only the quantity $\sigma L[O(^1D)]_0$ with k_1 and k_2 fixed to the literature values of 1.1×10^{-10} and 1.15×10^{-10} cm^{3}sec^{-1} respectively. Clearly the data of Fig. 1a strongly disagrees with the ratio of the accepted rate constants.

It occurred to us that the disagreement might be the result of hot atom chemistry. The photolysis of N_2O at 193 nm can produce $O(^1D)$ with a maximum translational energy of 166 kJ/mol. We estimate using a hard sphere collision model a fractional translational energy loss per collision with He of about 1/3. As many as one in ten collisions will be with H_2 at the highest H_2 pressures used so that some effects caused by translationally hot $O(^1D)$ seem quite possible. Fig 1b shows a Stern-Volmer plot of the same system with the helium flow rate raised tenfold with the flow rates of the reagents fixed. The agreement with the literature results is excellent.

BRANCHING IN THE REACTION OF $O(^1D)$ WITH METHANE

Since our methodology had not been previously tested, we decided to study a reaction system, $O(^1D) + CH_4$, which had been studied by several previous investigators using different methods. Even this simple reaction has several open channels:

$$O(^1D) + CH_4 \rightarrow CH_3 + OH \qquad \Delta H = -179 \text{kJ/mol} \qquad (1a)$$
$$\rightarrow CH_2OH + H \qquad \Delta H = -172 \text{kJ/mol} \qquad (1b)$$
$$\rightarrow CH_3O + H \qquad \Delta H = -128 \text{kJ/mol} \qquad (1c)$$
$$\rightarrow H_2CO + H_2 \qquad \Delta H = -473 \text{kJ/mol} \qquad (1d)$$
$$\rightarrow H_2CO + 2H \qquad \Delta H = -37 \text{kJ/mol} \qquad (1e)$$
$$\rightarrow {}^1CH_2 + H_2O \qquad \Delta H = -176 \text{kJ/mol} \qquad (1f)$$
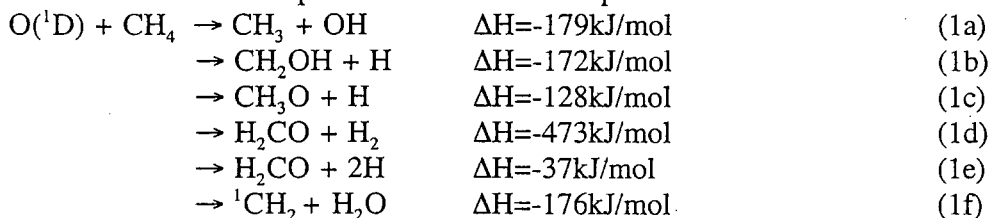
With regard to the branching ratios, the recent JPL compilation[1] summarizes previous work and lists channel (1a) as 75±15%, (1b)+(1c) as 20±7% and (1d) as 5±5% and is silent concerning channels (1e) and (1f).

To measure the branching into channel (1a), we divide the intercept of the Stern-Volmer plot of the OH absorbance from $O(^1D) + H_2$ by the intercept of the Stern-Volmer plot of the OH absorbance from $O(^1D) + CH_4$ and obtain 70% for channel 1a. To measure the sum of channels (1d)+(1e), we compare the formaldehyde absorbance to the OH absorbance under the same conditions

$$\frac{(1d)+(1e)}{(1a)} = \frac{\sigma(H_2CO)}{\sigma(OH)} \frac{S(H_2CO)}{S(OH)}$$

using the HITRAN integrated absorption cross-section and the measured linewidths at the elevated He pressure of 66 Torr to calculate the σ's. The resulting total fraction into (1d)+(1e) is 6±2%.

To our knowledge, channel (1f) has never been observed previously. We observed that when N_2O is photolyzed in the presence of a mixture of CH_4 and CD_4 infrared absorptions of H_2O and D_2O, but not of HDO appear. This is compelling evidence for channel (1f). Because of H_2O background absorptions, measuring this yield for the normal system does not seem feasible. We measure the branching ratio into (1f) by dividing the D_2O signal in the N_2O and CD_4 system (at high pressures of CD_4) by the D_2O signal obtained with the same partial pressure of N_2O in a system flooded with D_2 containing sufficient CD_3CDO to convert all the

OD produced by $O(^1D) + D_2 \rightarrow OD + D$ is converted into D_2O through reaction with CD_3CDO (see the first section). This gives the branching into (1f) for the D system of 7±2%.

To measure the sum (1c) + (1d) + 2(1e), we determine the total OH yield with NO_2 as the source of $O(^1D)$ using the same Stern-Volmer intercept approach making use of the reactions

$$O(^1D) + H_2 \rightarrow OH + H \qquad\qquad (2)$$
$$H + NO_2 \rightarrow OH + NO \qquad\qquad (3)$$
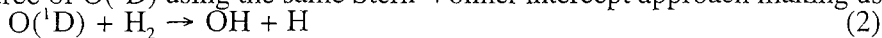
to obtain

$$(1a) + (1b) + (1c) + 2(1e) = \frac{2*(\text{SV intercept of OH from } H_2)}{\text{SV intercept from } CH_4}$$

The sum (1a) + (1b) + (1c) + 2(1e) resulting is about 98±10%.

Summarizing all our measurements, we have (1a)+(1d)+(1e)+(1f) = 83% from direct measurements assuming that the D_2O yield of 7% for (1f) is applicable to the H_2O system. Assuming no other channels are present, (1b)+(1c)=17%. Substituting this last result together with (1a)=70%, we have 2(1e)=(98-70-17)%=11% or (1e)=5.5%. Since (1d)+(1e) = 6%, we conclude that we can account for all the observations without a need for (1d), i.e. the production of H_2, but (1e) is definitely needed. Because the uncertainties are large, whether (1d) is actually absent is unclear.

A final interesting observation is that the yield of CH_2O when NO_2 is photolyzed to produce $O(^1D)$ is three times higher than obtained when N_2O is photolyzed with the extra CH_2O being produced at longer reaction times (10-100 μsec). We have verified reports that the reaction of CH_3O with NO_2 produces some, but not very much CH_2O (probably less than 10% of the total CH_3O); apparently an adduct of NO_2 with CH_3O is the major product. We believe most of the additional CH_2O results from the reaction of CH_2OH with NO_2 suggesting that (1b)>>(1c).

PRODUCT YIELDS IN THE REACTION OF $O(^1D)$ WITH ACETALDEHYDE

Last year we were involved in measuring the yields into the following reaction channels:

$O(^1D) + CH_3CHO \rightarrow CH_3 + CO_2 + H$	$\Delta H = -262.6$ kJ/mol	(2a)
$\rightarrow CH_3 + HCO_2$	$\Delta H = -281.2$ kJ/mol	(2b)
$\rightarrow CH_3 + HOCO$	$\Delta H = -350.1$ kJ/mol	(2c)
$\rightarrow CH_2OH + HCO$	$\Delta H = -261.8$ kJ/mol	(2d)
$\rightarrow CH_3O + HCO$	$\Delta H = -213.7$ kJ/mol	(2e)
$\rightarrow OH + CH_3CO$	$\Delta H = -258.4$ kJ/mol	(2f)
$\rightarrow CH_4 + CO_2$	$\Delta H = -741.4$ kJ/mol	(2g)
$\rightarrow H + CH_2OHCO$	$\Delta H = ?$	(2h)
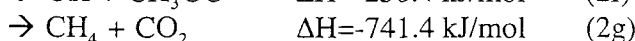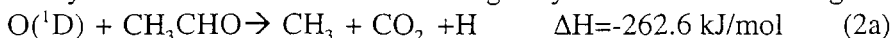
At pressures of 13 Torr (mostly He buffer), we observed infrared absorption lines of CH_3, HCO, OH, CH_4 and CO_2 from this reaction, but were unable to observe any transient absorption signals at the known frequencies of the strongest lines of the HOCO OH stretch fundamental. We observed H indirectly through the NO_2 precursor method described above. Our qualitative observations were that H is a major product and HCO, OH, CH_4 and CO_2 are relatively minor products. Now that we have found that hot atom chemistry is significant at 13 Torr, we must redo these measurements at 66 Torr to quantify the reaction channels under thermalized conditions.

FUTURE PLANS

We propose to measure the branching ratios of $O(^1D)$ + CH_3CHO at He buffer gas pressures of >60 Torr in order to minimize hot atom effects.

Reference
1. Sander, S. P.; Friedl, R. R.; Golden, D. M.; Hampson, R. F.; Kurylo, M. J.; Huie, R.E.; Orkin, V.L.; Moortgat, G. K.; Ravishankara, A. R.; Kolb, C. E.; Molina, M. J.; Finlayson-Pitts, B. J. "Chemical kinetics and photochemical data for use in stratospheric modeling. Evaluation number 14," JPL Publication, California Institute of Technology, 2002.
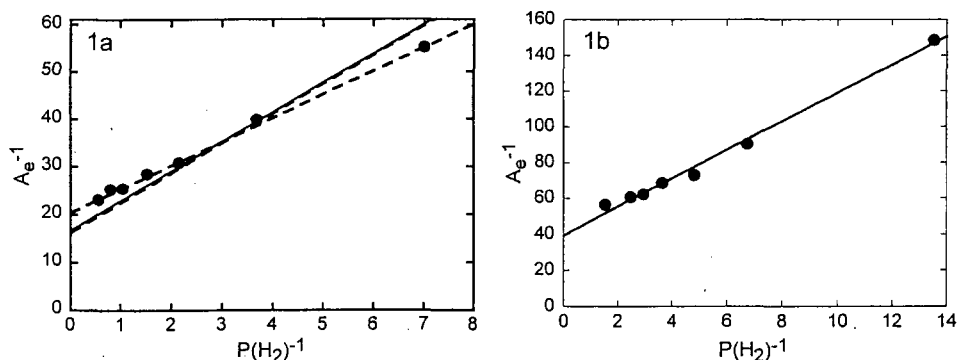
Fig. 1. In Fig. 1a, F(He)=1000 sccm; P(He)=12 torr; F(N$_2$O)=30 sccm; F(NO)=6 sccm; F(H$_2$)~10; 20; 35;50;75;100;150 sccm. The solid straight line assumes k(H$_2$)=1.1x10^{-10}, k(N$_2$O)=1.15x10^{-10}, k(NO)=0.6x10^{-10} cm^{3}s^{-1}. The dashed line is the best linear fit of the points. In Fig. 1b, F(He)=10000 sccm; P(He)=63.22 torr; the other flows are essentially the same. The solid straight line assumes the rate constants above. The best straight line through the points is indistinguishable from the model line.

Publications

1. "High-resolution infrared spectra of jet-cooled allyl radical (CH$_2$-CH-CH$_2$): ν_2, ν_3, and ν_{14} C-H stretch vibrations," J-X. Han, Yu. Utkin, H-B. Chen, N. T. Hunt, and R. F. Curl, *J. Chem. Phys.* **116**, 6505-6512 (2002).

2. "A kinetic study of the reaction of acetaldehyde with OH," Jinjin Wang, Hongbing Chen, Graham P. Glass and R. F. Curl, *J. Phys. Chem. A.* **107**, 10834-10844 (2003).

Spectroscopy and Dynamics of Vibrationally Excited Transient Radicals

Hai-Lung Dai
Department of Chemistry, University of Pennsylvania
Philadelphia, PA 19104-6323; dai@sas.upenn.edu

I. Introduction

With the goals of characterizing the spectroscopy and structure of unknown transient radicals that are important in combustion processes, we have applied a newly developed approach based on nanosecond time resolved Fourier Transform IR Emission Spectroscopy (TR-FTIRES) to the investigating of several unknown radicals: deuterated-vinyl and OCCN, in addition to the previously reported vinyl and cyanovinyl. The transient radical species is produced with high vibrational excitation through UV photolysis of a precursor molecule. The IR emission from the highly excited species through its IR active vibrational modes is detected with fast time resolution using the TR-FTIR technique. A new two-dimensional cross-spectra correlation technique has been developed for analyzing the time-resolved FTIR emission spectra. This analysis enables the common set of emission bands from the same target radical in the emission spectra obtained using different precursors. The spectroscopic approach also allows the reactions of the excited radical and the photolysis reaction of the precursor molecules to be characterized. All these information are fundamentally important to the understanding of chemical dynamics of radicals as well as the combustion processes. A brief description of the progress is presented below.

II. Vibrational Bands of Vinyl-d_3

In 2000 we reported the detection of the fundamental transitions of all nine vibrational modes of the vinyl radial, for which only one mode was reported previously. To confirm the assignment of the IR emission bands from the vinyl radical, we have performed isotope substitution experiment. Comparing the ratio of the experimentally observed frequencies for the deuterated and non-deuterated vinyl radical with the theoretically predicted ratio allows the assignments to be examined. Deuterated vinyl bromide was used a precursor for the production of the vinyl-d_3 radical. The photodissociation reaction of vinyl bromide proceeds via two main channels and the IR emission peaks can be assigned to known frequencies of the photofragments, acetylene-d_3, DBr and Br*, in addition to peaks that are due to vinyl-d_3. Four bands are attributed to vinyl-d_3. The most intense band is at 984 cm^{-1} (CD bend). Peaks in the CD stretching region at 2420 (CD stretch), 2346 (CD$_2$ asym. stretch) and 2264 (CD$_2$ sym. Stretch) cm^{-1} also have considerable intensity. The corresponding bands of the hydrogenated vinyl have all been identified. The correlation between the bands from the deuterated vinyl with those from the non-deuterated vinyl is established by a comparison of the peak shape, frequency and intensity. For instance, the most intense feature in the non-deuterated vinyl spectrum at 1277 cm^{-1} corresponds to the most intense peak of vinyl-d_3 that has shifted to 984 cm^{-1}.

III. The ν_1 and ν_2 Vibrational Bands of The OCCN Radical

The vibrational modes of the small but important cyanooxomethyl radical, OCCN, in the electronic ground state has, until this work, remained unreported despite the significant role of this radical in the atmospheric medium. OCCN is an important dissociation product of many substituted carbonyls with the general structure NC(CO)X, a class of carbonyl containing compounds that are major constituents of urban atmospheric pollution related to motor vehicles.

The OCCN radical is produced through 193 nm photodissociation of carbonyl cyanide, CO(CN)$_2$, pivaloyl cyanide, CO(CN)(CH$_3$)$_3$, and methyl cyanoformate, CO(CN)(OCH$_3$). The time resolved spectra following photodissocaition of carbonyl cyanide is shown in Fig. 1. Since all three precursor molecules

all result in OCCN as the only common product in their dissociation, their emission spectra should reveal common features that can be assigned to OCCN. Fig. 2 shows the emission spectra from the three different precursors. The assignment of the emission features, however, is not straightforward. The CN stretch (v_2) at 2093 cm^{-1} is the mode with the strongest transition intensity and can be readily identified in the emission spectra from all three precursors. The CO stretch (v_1) at 1774 cm^{-1} is more than one order of magnitude weaker and not as apparent as the strongest mode in the emission spectra but can be identified after the two-dimensional cross-spectra correlation analysis, described below, of the spectra. *Ab initio* calculation results confirm the reasonableness of the assignment of both the frequency and relative intensity of the two modes.

IV. Two Dimensional Cross-Spectra Correlation Analysis of Time-Resolved FT Emission Spectra

The 2-D correlation analysis, commonly used to unraveling the spectral features with the same phase characteristics within the same spectrum, has been applied to the identification of the emission bands from the same radical in the time-resolved FT emission spectra obtained with different precursor molecules. Each individual set of time-resolved emission spectra, recorded following the photolysis of a particular precursor molecule, contains bands from the radical of interest. When different precursor molecules are used for generating the same radical, all the corresponding emission spectra obtained should contain the same set of emission bands from this radical. These bands share similar time-evolution in their relative intensity and frequency shift, resulted from collision quenching of the vibrational excitation of the radical by ambient gases. The time-dependence in intensity provides the phase information needed for the correlation analysis. A 2-D correlation analysis across two different spectra allows the bands with identical time-dependence to be revealed.

We have developed the theoretical basis for analyzing spectral peaks phase correlations among different spectra. The effectiveness of this "2-D cross-spectra correlation analysis" is demonstrated on the OCCN radical, which can be generated from using three different precursors mentioned above. Figure 2 shows the longer time emission spectra (10 μs after the photolysis pulse in a sample with about 0.1 Torr precursor in 4 Torr Ar) from experiments using the three different precursors. Emission peaks in the longer time spectra mimic more of the fundamental transitions of the vibrational modes. Figure 3 shows the spectra after correlation treatment among all three spectra. All peaks are assignable to the OCCN radical and other common products of secondary reactions following the photolysis. [The student who worked on this project, William McNavage, presented this new 2-D cross-spectra analysis in the Columbus International Symposium on Molecular Spectroscopy in 2003 and received the Rao Prize for the best paper presented by a student.]

V. Plans for Next Year
A). Collision Energy Transfer from Vibrationally Excited Radicals

In the high temperature environment of a combustion chamber, it is expected that the transient intermediates and reaction products are excited with high internal energies. The internal excitation will have an effect on the reaction rates that needs to be characterized for the understanding of reaction mechanisms in combustion. The other important aspect of understanding the reaction mechanism in a combustion environment is the characterization of the collision energy transfer rates of the excited species. The collision energy transfer rate is deterministic of the thermalization of the reaction exothermicity and gravely affects the amount of energy available in promoting the reactions of the excited species.

We have used time-resolved IR emission from vibrationally excited molecules during collision quenching process to measure the collision energy transfer rates of highly excited stable polyatomic molecules. The IR emission spectrum at a specific time following the excitation laser pulse can be used to reveal the vibrational energy distribution at that time. This information allows the deduction of the

average energy of the excited molecules as a function of the number of collisions with the ambient gas after the initial excitation and the determination of the average energy transferred per collision.

To determine the energy distribution from the IR emission bands of vibrationally excited molecules we need to know the vibrational anharmonicity of at least a few modes. This information is available for many stable small/medium size molecules for which detailed spectroscopic studies have been performed. This is in general not the case for radicals. On the other hand, both information- the anharmonicity and the energy distribution- is inherently contained in the spectra. Previous studies have conformed that a Gaussian function can be effectively used to describe the energy distribution which can be characterized by the average energy and the width. The range and behavior of anharmonicity has also been known and can be approximately described for a specific mode. We propose that a model can be set up with the anharmonicity and the Gaussian characteristics as variables to be determined from fitting of the multiple time-resolved spectra for the radicals. Collision energy transfer behavior of radicals can thus be investigated.

B). The Ketenyl Radical (HCCO)

The ketenyl radical is an important intermediate in hydrocarbon combustion. Previous works by Hirota and Endo have determined HCCO as a near prolate symmetric top with a large A constant. The strongest vibrational band, the v_2 (CCO antisymmetric stretch) was found by Curl, Glass and coworkers to be at 2022.644 cm^{-1}. The $\tilde{B}^2\Pi - \tilde{X}^2 A''$ system origin was found by Rolfing and coworkers to be at 33,424 cm^{-1} and the v_5 CCH (cis) bend was reported at 494 cm^{-1}. Other vibrational modes including the v_1 CH stretch and the v_3 sym. CCO str. have yet to be detected spectroscopically although many theoretical results, such as those by Schaffer and coworkers, have been reported. It should be mentioned that a recent work by Osborn using time resolved Fourier transform infrared emission spectroscopy has successfully monitored the reaction between HCCO and O_2. The formation of CO and CO_2 was detected, lending validity to the mechanisms proposed for the consumption of HCCO in combustion flame.

Given the lack of characterization of the vibrational modes of the HCCO radical, we have chosen UV dissociation of ethyl ethynyl ether, characterized by Butler and coworkers, as a clean source of HCCO and monitor the time resolved infrared emission from all photoproducts using FTIR Emission Spectroscopy following the precursor photolysis. Preliminary results indicate the detection of electronically and vibrationally excited HCCO from the precursor dissociation.

VI. Publications since 2002 acknowledging support from this grant
Structure and Vibrational Modes of the Cyanovinyl Radical: A Study by Time-Resolved FTIR Emission Spectroscopy
    J. Phys. Chem. A, 106, 12035-40 (2002), L. T. Letendre and H. L. Dai
Experimental and Theoretical Studies of the Effect of Collision and Magnetic Field of Quantum Beat
    Mol. Phys., 100, 1117-1128 (2002), C. H. Chang, C. K. Ni, C. L. Huang, H. L. Dai, M. Hayashi, K. K. Liang, and S. H. Lin
The v_1 and v_2 Vibrational Bands of The OCCN Radical Detected Through Time-Resolved Fourier Transform IR Emission Spectroscopy
    Can. J. Chem. [Herzberg Memorial Issue], (2004) W. McNavage, W. Dailey and H. L. Dai
Two-Dimensional Cross-Spectra Correlation Analysis of Time-Resolved Fourier Transform IR Emission Spectra
    J. Chem. Phys., submitted, W. McNavage and H. L. Dai

Figure 1.
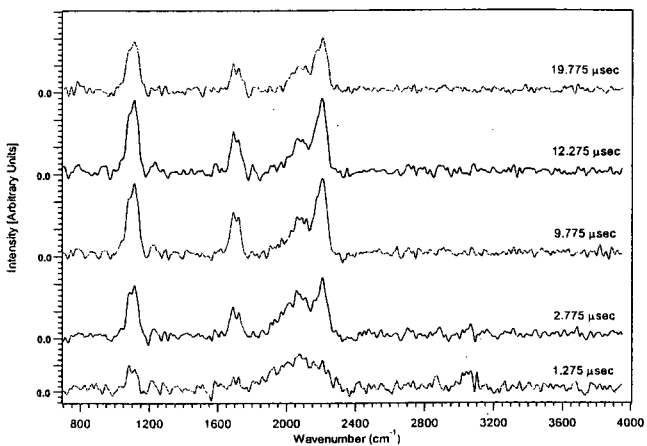
Figure 2.
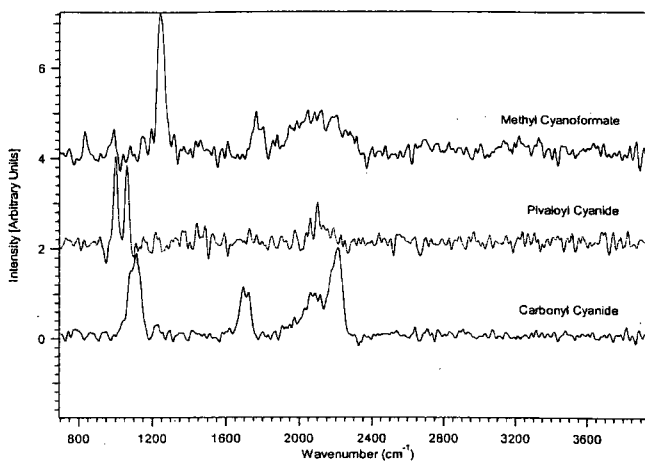
Figure 3.
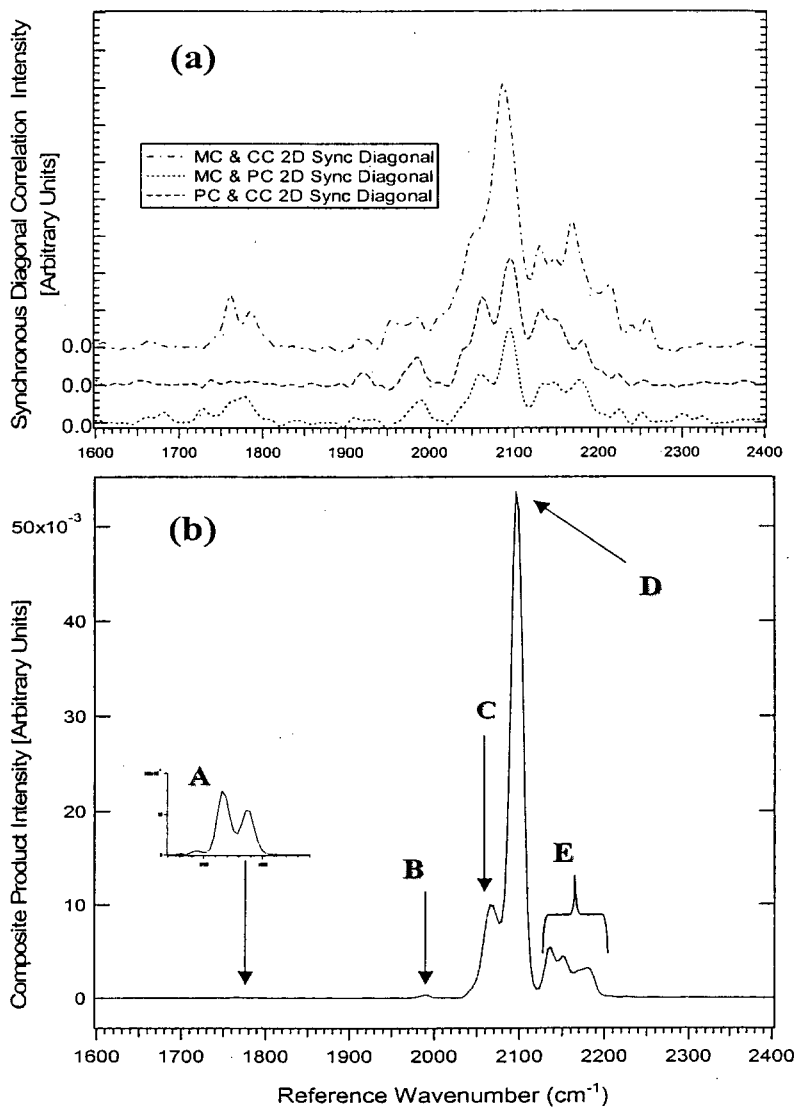
Bimolecular Dynamics of Combustion Reactions

H. Floyd Davis
Department of Chemistry and Chemical Biology
Baker Laboratory, Cornell University, Ithaca NY 14853-1301
hfd1@Cornell.edu

I. Program Scope:

The aim of this project is to better understand the mechanisms and product energy disposal in bimolecular reactions fundamental to combustion chemistry. Using the crossed molecular beams method, a molecular beam containing highly reactive free radicals is crossed at right angles with a second molecular beam. The angular and velocity distributions of the products from single reactive collisions are measured, primarily using the Rydberg tagging method.

II. Recent Progress:

During the first year of this grant, which started July 1, 2003, we have continued studies of the reaction of OH radicals with hydrogen and deuterium, with an emphasis on the question of how different kinds of reactant energy (*e.g.*, translational, electronic, and vibrational) promotes the chemical reaction. We have also made progress towards an investigation of the reaction H + $O_2 \rightarrow$ OH +O(^{3}P), using O atom Rydberg time-of-flight spectroscopy, a method recently developed in our laboratory.[1]

i. Studies of Reactive Quenching: OH(A$^2\Sigma^+$) + $D_2 \rightarrow$ HOD + D.

It has been known for many years that electronically excited OH radicals are quenched by collisions with small molecules. Although quenching rate constants for many molecules have been measured as functions of temperature, until quite recently, the possible role of reactions, rather than simple physical quenching, has remained unexplored.[2] The reaction of ground state OH with D_2 proceeds over a substantial potential energy barrier with a small reaction cross section.[3] On the other hand, the reactive quenching process involving electronically excited OH is highly exothermic, and is believed to proceed without any potential energy barrier.[2]

Our experimental configuration was similar to that used in our earlier study of the reaction of ground state OH.[3] We produce a beam of OH radicals by photodissociation of HNO$_3$ at 193 nm, and have added a laser in the near UV to electronically excite OH to the (A$^2\Sigma^+$) state as the radicals cross the D_2 beam. To ensure the D atoms observed in our experiment resulted from reaction of OH (A$^2\Sigma^+$), data was collected with the laser tuned to the peak of an OH absorption line, as well as with the laser tuned off resonance. The D atom angular distribution was found to be very broad, with products scattered at all laboratory angles. The time-of-flight and laboratory angular distributions led us to the CM translational energy, P(E), and angular distribution, T(θ), shown in
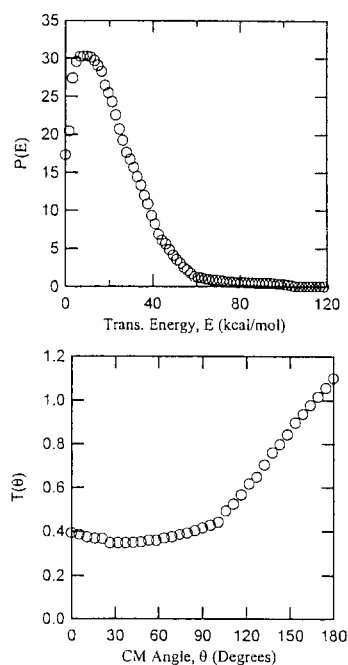
Fig. 1: Translational energy and CM angular distribution for OH(A) + $D_2 \rightarrow$ HOD + D reactive quenching process.

Fig. 1. The product flux contour diagram is shown in Fig. 2. The data suggests formation of a short lived collision complex that survives a fraction of a rotational period before decaying to products. From the translational energy release, the most probable level of vibrational excitation in the HOD is $\approx$ 90 kcal/mol.

We believe that the transient complex results from the presence of an adiabatic well resulting from the crossing of diabatic surfaces correlating to the ground and electronically excited states of OH + D_2. Chemical reaction results from a nonadiabatic transition mediated by a conical intersection formed by these interacting surfaces.

10,000 m/s

Fig. 2. D atom product flux contour map from OH(A) + $D_2 \rightarrow$ HOD + D reactive quenching process.

In this experiment, and in other studies, the experimental signal to noise ratio (S/N) was not as high as we would have liked. We have therefore reconfigured the source chambers, allowing us to move each nozzle to a distance of about one half of that in previous studies. Since the density of each beam scales as r^{-2}, this will increase the overall signal level by a factor of about 16. We have also upgraded the vacuum system to reduce the partial pressures of interfering species (primarily oil vapor) by approximately an order of magnitude. We have had the apparatus remachined, allowing us to introduce the VUV needed in the Rydberg tagging schemes more efficiently. At the same time, we relocated the apparatus to a newly renovated and much more spacious laboratory, and experiments have resumed as of April 2004.

ii. Progress towards Studies of H + $O_2 \rightarrow$ OH ($^2\Pi$) + O (^3P_J) using Rydberg Time-of-Flight Spectroscopy.

We have recently extended the hydrogen atom Rydberg time-of-flight (HRTOF) method, used previously in our laboratory and elsewhere, to the detection of ground state oxygen atoms, O (^3P_J). An article describing this method has now appeared.[1] A particular spin-orbit state of oxygen is "tagged" by a double-resonance two-photon excitation to high-n Rydberg states, and the Rydberg O atoms fly to a detector where they are field ionized and collected.

This method is well-suited for studies of the reaction H + $O_2 \rightarrow$ OH ($^2\Pi$) + O (^3P_J), in which the OH fragment is preferentially formed in high-N levels at collision energies above the reaction endoergicity. This reaction is very important in combustion processes. Our ultimate goal is to study this reaction using a true crossed beams configuration involving fast photolytic H atoms produced by photodissociation of HI at 248 nm. In order to assess the feasibility of this experiment using ORTOF, we have started by carrying out a simpler "single beam" experiment involving a mixture of 5% HI and 30% O_2 in He. The HI is photolyzed by the residual 212 nm light used for VUV generation, and the resulting H atoms react with O_2 producing OH + O. These experiments have been encouraging, and we have definitively observed the OH + O channel using ORTOF, demonstrating the feasibility of the experiments. We believe with the recent improvements made to our apparatus (discussed in section i), our proposed study will be successful.
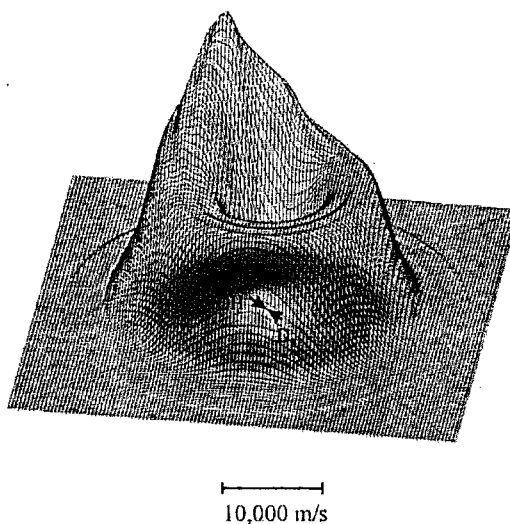
iii. Progress Towards Studies of OH + D$_2$ (v=1) → HOD + D

Recently, calculations on the reaction OH + D$_2$ (v=1) → HOD + D have been carried out. [4] An experimental study in which the HOD product vibrational distribution is measured as a function of scattering angle would provide an important test of the PES. In this experiment, the D$_2$ is pumped to v = 1 by stimulated Raman pumping using two laser beams (532 nm and 633 nm, produced by Raman shifting in D$_2$). Although this method has been demonstrated by several groups to be efficient, we have found that we were unable to pump a sufficient fraction of the D$_2$ molecules using our existing Nd:YAG laser, due to its broad linewidth (1 cm^{-1}). As part of our funding for year 1, we were able to upgrade our laser by addition of an injection seeder. We plan to use this laser to carry out an experimental study of the title reaction during the next year.

III. Future Plans:

Currently, our apparatus is configured to study the reaction H + O$_2$ → OH ($^2\Pi$) + O (^3P_J) at E_{coll} = 1.84eV. The experiment is presently under way. During the summer, we plan to return to the OH + D$_2$ system, first by revisiting the reactive quenching process OH(A$^2\Sigma^+$) + D$_2$ → HOD + D, but instead looking at reaction of v = 0 (rather than v = 1) of the electronically excited OH reactant. We are also planning to investigate the H atom channel, OH(A$^2\Sigma^+$) + D$_2$ → DOD + H, seen in the previous work by the Lester group. [2] Following that study, we plan to pursue the study of OH + D$_2$ (v=1) → HOD + D using our newly refurbished Nd:YAG laser. Along the way, we plan to compare the efficiency for production of D$_2$ (v=1) using two alternative approaches to generate the 633 nm light necessary for stimulated Raman pumping: either by Raman shifting of the second harmonic of the Nd:YAG (532 nm) in liquid nitrogen cooled D$_2$ gas, or by using a dye laser.

IV. Publications since 2002:

1. Oxygen Atom Rydberg Time-of-Flight Spectroscopy- ORTOF, C. Lin, M.F. Witinski, and H. Floyd Davis, *J. Chem. Phys.* **119**, 251 (2003).

V. References:

1. C. Lin, M.F. Witinski, and H. Floyd Davis, *J. Chem. Phys.* **119**, 251 (2003).

2. M.W. Todd, D.T. Anderson, and M.I Lester, a) *J. Phys. Chem. A.* **105**, 10031 (2001); b) *J. Chem. Phys.* **110**, 11117 (1999).

3. B. Strazisar, C. Lin and H.F. Davis, *Science* **290**, 958 (2000).

4. M. J. Lakin, D. Troya, G. Lendvay, M. Gonzalez and G.C. Schatz, *J. Chem. Phys.* **115**, 5160 (2001).

Multiple–time–scale kinetics

Michael J. Davis

Chemistry Division
Argonne National Laboratory
Argonne, IL 60439
Email: davis@tcg.anl.gov

Research in this program focuses on three interconnected areas. The first involves the study of intramolecular dynamics, particularly of highly excited systems. The second area involves the use of nonlinear dynamics as a tool for the study of molecular dynamics and complex kinetics. Recently, this work has been extended to spatially distributed systems (reaction-diffusion equations). The third area is the study of the classical/quantum correspondence for highly excited systems, particularly systems exhibiting classical chaos.

Recent Progress

Work on model Boltzmann equations has continued, but almost all recent progress has been on the reduction of nonlinear partial differential equations. Some of this work is in collaboration with Skodje and involves hyperbolic partial differential equations, but most of the work has been on dissipative parabolic systems: reaction-diffusion equations. This work is in collaboration with Zagaris and Kaper (Mathematics Department, Boston University).

The main focus of the reduction has been on the study and the generation of low-dimensional manifolds. There are three kinds of manifolds that we have studied: 1) chemical-kinetic manifolds, 2) diffusional manifolds, and 3) inertial manifolds. This order reflects the time range at which the manifolds are important (shorter to longer). Chemical-kinetic manifolds are the generalization of low-dimensional manifolds from the zero-dimensional pure chemical-kinetic system. They are usually only slightly modified from the zero-dimensional problem by diffusion. The diffusional manifolds result from the breakdown of constants of the motion that exist in the pure chemical-kinetic problem. These manifolds can be thought of as modifications of the hypersurface of equilibrium points. In cases where they are present, inertial manifolds describe the longest time motion. While the first two types of manifolds reduce the number of partial differential equations, inertial manifolds describe a reduction from a set of partial differential equations to a few ordinary differential equations.

The study of the reaction-diffusion systems employs numerical, analytical, and asymptotic techniques. It combines the study of phenomenology and the development of numerical methods. In particular, we have developed a method to generate chemical-kinetic and diffusional manifolds for reaction-diffusions systems that includes the full reaction-diffusion dynamics. For inertial manifolds, the techniques used for ordinary differential equations are employed.

Four aspects of low-dimensional manifolds for dissipative reaction-diffusion systems are now highlighted from our research.

1) *Global Representation of low-dimensional manifolds for nonlinear partial differential equations.* The most general form for chemical-kinetic and diffusional manifolds is in function space and maps functions to functions. We have studied such representations and have developed an algorithm for generating manifolds that is similar to the Maas-Pope algorithm for ordinary differential equations. It is convenient to represent this manifold spectrally. Representations using a grid of

points are also straightforward. If one considers the distributions for each species as expansions in a basis set:

$$y_1(x,t) = \sum_n a_n^1(t)\, \Phi_n(x) \text{ and } y_2(x,t) = \sum_n a_n^2(t)\, \Phi_n(x),$$

the manifold is defined as:

$$a_n^2 = F(\{a_i^1\})$$

The figure shows distributions along such a manifold for a system with an exact nonlinear manifold plotted as a solid line. The dashed line on the left panel shows the results of our method for a case in which the time scale separation is small and the right panel shows the results for a case with much larger time-scale seperation as a set of dots. These plots demonstrate that the method can be very accurate but will breakdown if the time-scale separation is not large.
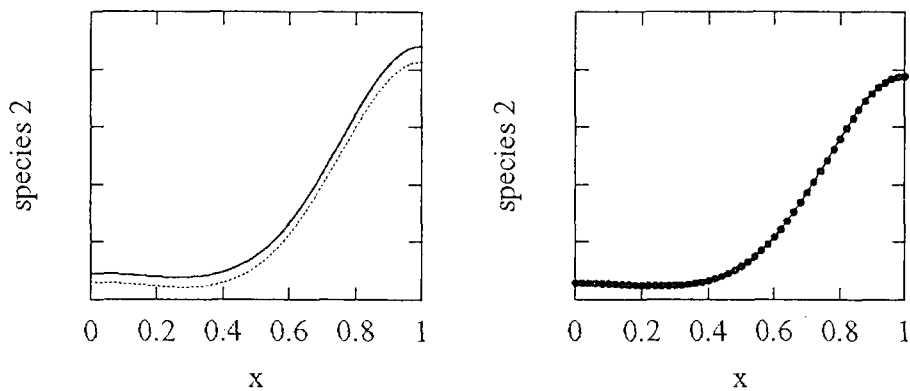
2) *Local representations.* It is possible to develop local representations of manifolds as expansions. A typical example is shown below for a chemical-kinetic manifold. The pure chemical-kinetic manifold is shown as a solid line and a manifold corrected for diffusion is shown as a dotted line:,

species 1
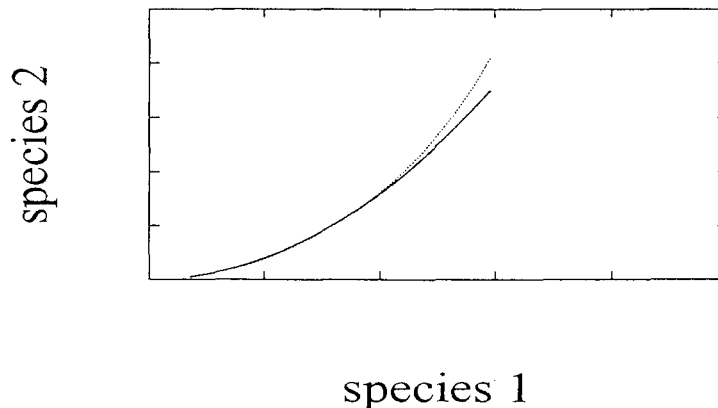
The corrected manifold in the figure above has this typical form:

$$y_2 = G(y_1) + H(\frac{\partial y_1}{\partial x}, \frac{\partial^2 y_1}{\partial x^2}) + \ldots$$

3) *Inertial manifolds*. We have studied inertial manifolds for the reaction-diffusion systems. They appear to be a generic consequence of diffusional manifolds. They reduce the system of partial differential equations to a finite-dimensional system. The enclosed figure shows the consequences of a one-dimensional inertial manifold. The center plot in the figure has a single point. The presence of a one-dimensional inertial manifold means that a single point on the distribution for any species defines the full distribution for that species and the distributions for all other species. This is what is shown by the arrows in the figure which point to two full distributions.
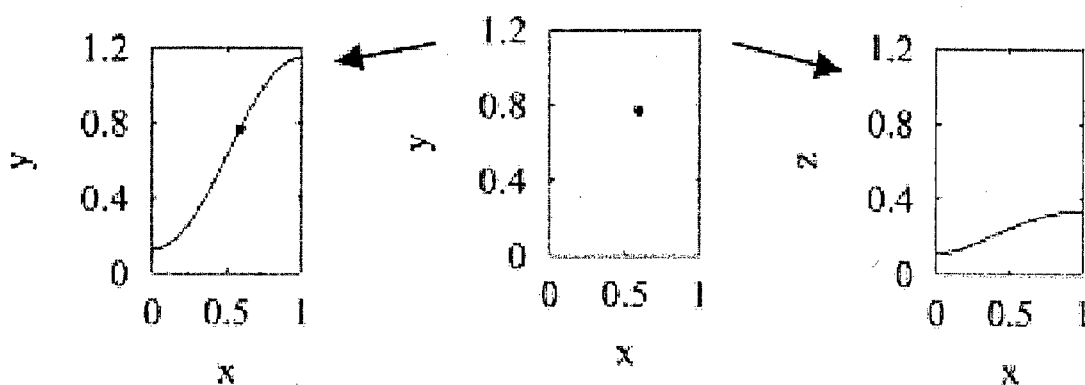
Inertial manifolds are more straightforward to calculate than the other two types of manifolds, requiring the same techniques that have been developed for systems of ordinary differential equations.

4) *Spatial low-dimensional manifolds*. Another aspect of our work on low-dimensional manifold for reaction-diffusion systems has been the study of spatial low-dimensional manifolds in the steady states of these systems. Generally, stiffness in chemical kinetics and a separation between diffusion and kinetic time scales leads to multiple length scales that may dissipate away from the boundary. We are developing methods to generate these low-dimensional manifolds. The plot below shows a series of "spatial trajectories"(dotted lines) that approach the solid line that is the low-dimensional manifold. The progress variable in the figure is spatial, rather than temporal. Some extra care has to be used to generate the manifold compared to other manifolds, because of the boundary conditions.

68

species 1
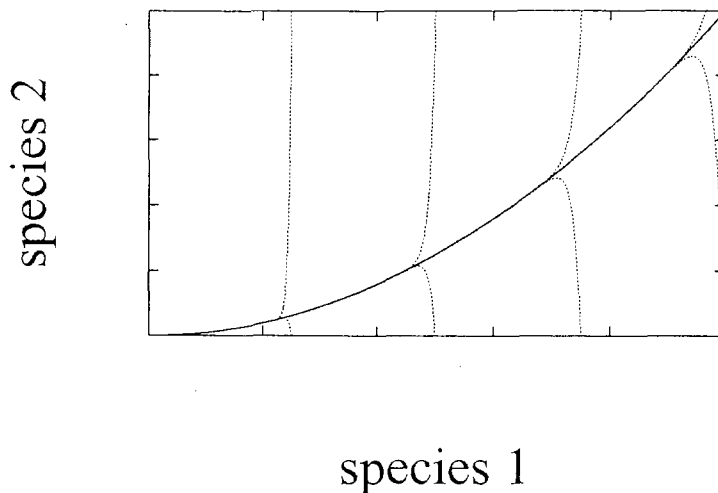
Future Plans

The project on the Boltzmann equation will continue. However, the major plans are for continuation of the work on nonlinear partial differential equations. The work will be extended in two ways. In collaboration with Zagaris and Kaper, new methods of calculating low-dimensional manifolds in nonlinear partial differential will be developed and tested on the systems studied in the past year. In collaboration with Tomlin (Leeds), the study of manifolds in nonlinear partial differential equations will be extended to systems of higher spatial dimension as well as more complex systems of spatial dimension one.

Publications

M. J. Davis and J. H. Kiefer, "Modeling of nonlinear vibrational relaxation of large molecules in shock waves with a nonlinear, temperature-varying master equation", J. Chem. Phys. **116**, 7814 (2002),

M. J. Davis, "Dynamics of a nonlinear master equation: Low-dimensional manifolds and the nature of vibrational relaxation:, J. Chem. Phys. **116**, 7828 (2002).

M. J. Davis and S. J. Klippenstein, "Geometric investigation of association/dissociation kinetics with an application to the master equation for $CH_3 + CH_3 \leftrightarrow C_2H_6$", J. Phys. Chem. A **106**, 5860 (2002)

COMPREHENSIVE MECHANISMS FOR COMBUSTION CHEMISTRY: EXPERIMENT, MODELING, AND SENSITIVITY ANALYSIS

Frederick L. Dryer
Department of Mechanical and Aerospace Engineering
Princeton University, Princeton, New Jersey 08544-5263
fldryer@princeton.edu

Program Scope

Experiments conducted in a Variable Pressure Flow Reactor (VPFR) at pressures from 0.3 to 20 atm and temperatures from 500 K to 1200 K, with observed reaction times from 0.5×10^{-2} to 2 seconds, and laminar flame speed measurements at atmospheric pressure are combined with literature data and numerical studies to develop and validate chemical kinetic reaction mechanisms and to determine important elementary rates. Continuing efforts are: (1) utilizing the perturbations of the H_2/O_2 and $CO/H_2O/Oxidant$ reaction systems by the addition of small amounts of other species to further clarify elementary reaction properties; (2) further elucidating the reaction mechanisms for the pyrolysis and oxidation of hydrocarbons (alkanes, olefins) and oxygenates (aldehydes, alcohols, and ethers).

Recent Progress

Comprehensive mechanisms have been further advanced for hydrogen oxidation, oxidation systems involving species containing a single carbon atom (excluding methane), and for ethanol. New methodology has been demonstrated to identify the windows of temperature over which temperature dependent properties in flames result in larger sensitivities for laminar flame propagation. Progress is briefly summarized below.

Comprehensive Kinetic Mechanism for Hydrogen Oxidation (*submitted to Int. J. Chem. Kinet. 2004*)

We have developed an updated H_2/O_2 chemical kinetic mechanism based on Mueller et al. (Int. J. Chem. Kinet. 1999, 31). Major issues addressed include:

1. The Enthalpy of Formation of OH was changed to that recommended by Ruscic et al. (J. Phys. Chem. A, 2002, 106, 2727).
2. The rate expression for $H + O_2 = OH + O$, (R1), developed in the recent analyses of Hessler (J. Phys. Chem. A, 1998, 102, 4517) was adopted to predict both high temperature results and the low temperatures measurements of Pirraglia et al. (J. Phys. Chem. 1989, 93, 282).
3. The rate expression for $H + O_2 + M = HO_2 + M$, (R2), was developed using the Troe formulation with the high-pressure-limit rate constant used in Mueller et al. and the low-pressure-limit results reported in Michael et al. (J. Phys. Chem. A, 2002, 106, 5297).
4. Adjustment of the A factor for $H + OH + M = H_2O + M$, (R3), within experimental uncertainty.

The revised mechanism predicts a wide range of experimental observations found in shock tubes, flow reactors, and laminar premixed flames, including new results published subsequent to the work of Mueller et al., particularly high pressure laminar flame speed and shock tube ignition results. The reaction $H+OH+M$ is found to be primarily significant only to laminar flame speed propagation predictions at high pressure. As a result of the uncertainty in the rate and third body efficiency data for this reaction, available experimental observations can be adequately fit using any of the standard transport models available in the literature for the hydrogen oxygen system simply by adjusting the rate parameters for this reaction within the present uncertainties.

Comprehensive Kinetic Mechanisms for C_1 Species (*submitted to Int. J. Chem. Kinet. 2004*)

In the hierarchical development of kinetic mechanisms for large hydrocarbons, the reaction systems involving C_1 species represent the next level of complexity beyond the H_2/O_2 reaction system discussed above. Encompassing the above update of the H_2/O_2 reaction system, we have revisited the $CO/H_2/O_2$, CH_2O/O_2, and CH_3OH/O_2 systems, considering recent kinetic and thermochemical results. The mechanisms were tested using new experimental targets as well as those originally employed in our earlier publications. The most important revisions to our prior published mechanisms involve the rate constant descriptions for $CO + OH = CO_2 + H$, (R4), and $HCO + M = H + CO + M$, (R5). Recently, Golden et al. (J. Phys. Chem. A, 1998, 102, 8598), Troe (Proc. Combust. Inst., 1998, 27, 167) and Senesiain et al. (Int. J. Chem. Kinet., 2003, 35, 464) all performed RRKM calculations to model the temperature and pressure dependence of reaction (R4). The rate constant expressions universally predict values higher than experimental measurements at low to intermediate temperatures (see Fig. 1). A weighted least squares fitting of literature experimental data for (R1) yields $k_{4f} = 2.23 \times 10^5 \, T^{1.89} \exp(-583/T)$ which lies within 6% at 800-3500 K of the expression of Yu et al. (Eastern States Sectional Fall Meeting 1991), within 10% at 800-2000K of the predictions of Troe, and about 20% lower than the result presented in Senesiain et al. (at 1 atm).

The decomposition reaction (R5) and the abstraction reaction, $HCO + O_2 = HO_2 + CO$, (R6), are the main pathways to generating CO during the high temperature combustion of hydrocarbons. Recent results of Friedrichs et al. (Phys. Chem. Chem. Phys., 2002, 4, 5778) for 835-1230 K determine k_{5f} to be about a factor of two lower than reported by Timonen et al. (J. Phys. Chem., 1987, 91, 5325). DeSain et al. (Chem. Phys. Lett., 2001, 347, 79) reported k_{6f} at 296-673 K to be nearly temperature-independent and about two times lower than the results of Timonen et al. (J. Phys. Chem., 1988, 92, 651) at 1000 K. The uncertainties of the new rate measurements are sufficiently small to exclude the earlier work.

Premixed flame speeds of small-hydrocarbon oxygenate/air mixtures (methanol, dimethyl ether, ethanol) are particularly sensitive to (R5) and (R6), and the new expressions result in significantly degraded flame speed predictions for these systems. Our studies reported below show that flame speeds are most sensitive to the values of R5 and R6 in the temperature ranges 1350-2000 K and 1200-1900 K, respectively, well above the range of conditions of the more recent measurements. It is likely that the rate constant for (R5) is in fact non-Arrhenius, and as a result, we adopted a weighted least squares fitting of literature data (k_{5f} = 4.75 × 10^{11} $T^{0.66}$ exp(-7485/T)) spanning the appropriate temperatures (see Fig. 2). Because there are few experimental measurements at high temperatures (NIST kinetics database, 2004) for k_{6f}, the recommendation of Timonen et al. was adopted as in our earlier models (Hochgreb and Dryer, 1992; Held and Dryer, 1998).

For the CH_2O/O_2 system, review of other reactions led us to adopt the recommendations of Friedrichs et al. (Int. J. Chem. Kinet., 2004, 36, 157), Eiteneer et al. (J. Phys. Chem. A., 1998, 102, 5196), and Irdam et al. (1993) for the formaldehyde decomposition reactions and abstraction reaction with HO_2 and H, respectively. The result of Irdam et al. (Int. J. Chem. Kinet., 1993, 25, 285-303) is in excellent agreement with the more recent direct measurements of Friedrichs et al. (Phys. Chem. Chem. Phys., 2002, 4, 5778).

Methanol combustion is also very sensitive to the fuel abstraction and decomposition reactions, and we have adopted the rate constants for CH_3OH decomposition reactions from GRI-3.0 obtained from a 5-channel RRKM fit to several sets of experimental data published from 1984 to 1994. The value of the rate constant for CH_3OH (+M) = CH_3 + OH (+M) agrees reasonably well (within 50%) with the recent experiment measurements of Koike et al. (Int. J. Chem. Kinet., 2000, 32, 1). Jimenez et al. (*J. of Photochemistry and Photobiology A: Chemistry*, 2003, 157, 237) derived experimentally the total rate constants for the abstraction reaction, CH_3OH + OH → products, at 235-360 K. The total rate constants agree within 20% with those of Bott and Cohen (*Int. J. Chem. Kinet.*, 1991, 23, 1075), which are used in the current updated mechanism.

The present C_1/O_2 mechanism has been compared against a wide range of experimental conditions (300-3000 K, 0.15-9.6 atm, ϕ = 0.4-6.1 for CO oxidation; 300-2150 K, 0.03-12.0 atm, ϕ = 0.005 to pyrolysis for CH_2O; 300-2200 K, 1.0-20 atm, ϕ = 0.05-6.0 for CH_3OH oxidation) and for laminar-premixed flame speeds, shock tube ignition delay, and flow reactor species time history experiments. Very good agreement of the model predictions with the experimental measurements was achieved in all comparisons, e.g. see Figs. 3, 4.

Experimental and Numerical Study on Ethanol Oxidation *(In preparation for Publication)*

In recent published works (Li et al., 3rd Joint Meeting of the U.S. Sections of the Combustion Institute, Chicago, IL, 2003), our laboratory has produced new pyrolysis data, and we have produced new rate determinations for ethanol unimolecular decomposition reactions (Li et al, submitted to J. Phys. Chem. A, April, 2004). We also performed a series of ethanol oxidation experiments in a flow reactor at high pressures (initial temperature at 800-950K and pressure 3-12atm). The time histories of stable species concentrations were measured using Fourier Transformed Infrared Spectrometry techniques. The new oxidation experiments are poorly described by predictions using the recently published mechanism of Marinov (Int. J. Chem. Kinet., 1999, 31, 183).

A detailed mechanism for ethanol pyrolysis and oxidation has been developed hierarchically, based upon the recent work on small-molecule chemistry described above. The C_2 sub-mechanism was assembled from the C_2 model of Wang et al (Eastern States Section of the Combustion Institute Technical Meeting, Raleigh, NC, 1999) and the acetaldehyde and ethanol sub-mechanisms of Marinov, with the following revisions:

1. H_2/O_2 sub-mechanism. The entire subset was replaced with the updated version described above
2. C_1/O_2 sub-mechanism. The CO, CH_2O, and CH_3OH subsets were replaced with the updated mechanisms described above.
3. CH_3HCO sub-mechanism. The present subset encompasses an acetaldehyde decomposition reaction, (missing in Marinov's mechanism), and updates the rate constants of abstraction reactions by OH based upon the extensive literature review of Atkinson et al. (J. Phys. Chem. Ref. Data, 1997, 26, 521).
4. C_2H_5OH (+M) = C_2H_4 + H_2O (+M) and C_2H_5OH (+M) = CH_3 + CH_2OH (+M). The rate expressions for the main decomposition reactions of ethanol are those developed by our laboratory (Li et al, submitted to J. Phys. Chem. A, 2004).
5. C_2H_5OH + OH → products. The reaction rates and branching ratios for the each of the three specific H-atom abstraction sites in ethanol were estimated using the same empirical procedure as in Marinov (1999).
6. The rate coefficients of methyl abstraction reactions are adopted from Bott and Cohen (Int. J. Chem. Kinet., 1991, 23, 1075).

Predictions using the ethanol mechanism described above compare favorably against VPFR experiments for the major stable species (C_2H_5OH, O_2, H_2O, and CO), representing a significant improvement over comparisons using the Marinov mechanism. Model predictions for other species are reasonable, but can be further improved, with mechanism elements involving acetaldehyde being least satisfactory. The predictions of the shock tube ignition delay time for $C_2H_5OH/O_2/Ar$ system deviate by amounts comparable to those shown by Marinov, while the predictions of laminar flame speeds are considerably improved.

Temperature-Dependent Feature Sensitivity Analysis of Flames *(Submitted to ACS Annual Meeting)*

Typically, sensitivity studies are performed by perturbing the *A*-factor for individual reaction rate coefficients and monitoring the effect of these perturbations on the observable(s) of interest. The sensitivity coefficients

obtained in this manner do not contain any information on possible temperature dependence effects. In many combustion processes, e.g. in premixed flames, the system undergoes substantial temperature changes, and the importance of individual reaction rates may be confined to specific ranges of temperature within the flame structure itself. In this work, temperature dependent sensitivity characteristics for key reaction rates and for binary diffusion coefficients on laminar flame speed were determined by perturbing the most sensitive specific reaction rates or the binary diffusion coefficients by small values at multiple points in the flame temperature profile. A Gaussian function perturbation profile was utilized, where the center of the Gaussian profile moves with the assigned temperature of interest. Numerical experiments were used to test the effects of the value and width of the perturbation profile on the obtained sensitivity parameters and exemplar applications of the technique were demonstrated using hydrogen, carbon monoxide, methanol and propane flames. Different reaction models were used for different fuels based primarily on the ability of each model to accurately predict the flame speeds over the entire equivalence ratio range.

Fig. 5 shows the sensitivity spectrum of reaction (R1) in the updated H_2 kinetic model described above at different pressures for a range of equivalence ratios. The bars in the figure indicate the temperature range where the sensitivity is larger than 10% of the maximum value. The sensitivity of the flame speed is dominated by values of (R1) in the relatively narrow temperature range $850 - 1550$ K, with a shift in this temperature "window" to higher values with increasing system pressure. Differences in rate expressions outside this temperature range have very little effect on predicted flame speeds. The selected diluent species and concentration are found to influence the temperature window size and location, being broadened by helium substitution for nitrogen and shifted toward lower temperatures as overall dilution is increased. As a result, kinetic models verified against flame speed data with one diluent condition may yield disparities at other diluent conditions, based entirely on the temperature dependent characteristics of an important reaction. A similar investigation of the importance of (R4) on CO/H_2 flame speed at atmospheric pressure shows that the most sensitivity to this reaction is at temperatures lower than 1900 K. We utilized this information in developing the updated C_1 mechanism described above. Similar studies were performed to investigate the importance of reactions R5 and R6 described above. The use of the newly determined reaction rate improves the prediction of flame speed (Figs. 3, 4). Similar temperature dependent sensitivity analyses can be applied to other reactions in analyzing flame speeds of higher hydrocarbon fuels.

The temperature dependent sensitivity features of binary diffusion coefficients on laminar flame speed were also demonstrated using hydrogen air flames. Fig. 6 shows temperature dependent sensitivity of H/He binary diffusion coefficient on the predicted $H_2/O_2/He$ laminar flame speed. The shape of the presented curve is a result of complex reaction/transport interactions within the flame structure. At lower temperatures, an increase in the diffusion coefficient causes an enhanced transport of H atoms toward the cold region where they do not contribute to chain branching kinetics (primarily, via R1). Consequently, the sensitivity with respect to of H/He binary diffusion coefficient is *negative*. As the temperature increases, the H/He diffusion sensitivity becomes positive and peaks close to the point where the sensitivity with respect to R1 has its maximum. Here, the diffusion flux brings H atoms to the regions where chain branching is active, resulting in an increase in the flame speed. At even higher temperatures, the sensitivity with respect to the H/He binary diffusion coefficient goes through zero again (around the point where H concentration has its peak, indicative of directional change in H diffusion flux). From this point, the diffusion flux carries H atoms away from the chain-branching region toward the post-flame zone, and the sensitivity becomes negative again. Non-monotonic behavior of binary diffusion coefficient sensitivity with respect to temperature has significant implications for detailed flame modeling. For example, Middha et al. (Proc. Combust. Inst., 2002, 29, 1361) recently reported improved values of H/He binary diffusion coefficient which are generally higher than those computed with the CHEMKIN II database over the entire temperature range of interest. However, it was also reported that the resulting flame speeds did not change significantly. The present study shows that the difference in binary diffusion coefficient may be compensated by the sensitivity sign change with the temperature, resulting in a minor difference in predicted flame speed.

Plans

Reaction systems of present interest over the coming year, include continued efforts on the pyrolyses and oxidations of acetaldehyde, methyl formate, and toluene, all over a range of pressures and temperatures similar to our previous work.

Publications, 2002 – Present

1. T. Carriere, P.R. Westmoreland, A. Kazakov, A., Y.S. Stein, and F.L. Dryer, "Modeling Ethylene Combustion From Low To High Pressure", Proc. Int. Comb. Ins. 29, 1257-1266 (2002).
2. Z. Zhao, A. Kazakov, J. Li, and F.L. Dryer, "Initial Temperature And N_2 Dilution Effect On The Laminar Flame Speed Of Propane/Air Mixtures", Combust. Sci. and Tech. (2004) *In Press.*

Papers Submitted for Review

1. J. Li, A. Kazakov, and F.L. Dryer, "Experimental And Numerical Studies of Ethanol Decomposition Reactions", J. Phys. Chem. (2004) *Submitted.*
2. J. Li, Z. Zhao, A. Kazakov, and F.L. Dryer, "An Updated Comprehensive Kinetics Model of H_2 Combustion", Int. J. Chem. Kin. (2004) *Submitted.*
3. Z. Zhao, J. Li, A. Kazakov, S. P. Zeppieri, and F.L. Dryer, "Burning Velocities Of N-Decane A High Temperature Skeletal Kinetic Model For N-Decane-Air Mixtures", Combust. Sci. and Tech. (2004) *Submitted.*
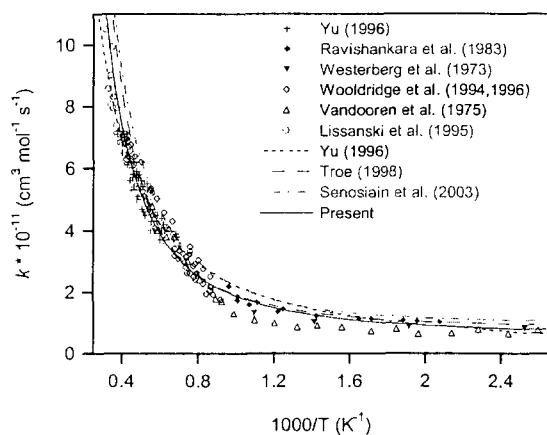
Fig.1. Rata constant of reaction CO + OH → CO$_2$ + H. Symbols are experimental results available in literature, and lines are model predictions at 1 atm.

Fig. 2. Rata constant of reaction HCO + M → H + CO + M. Symbols and lines with symbols are literature experimental results, and lines are model predictions.
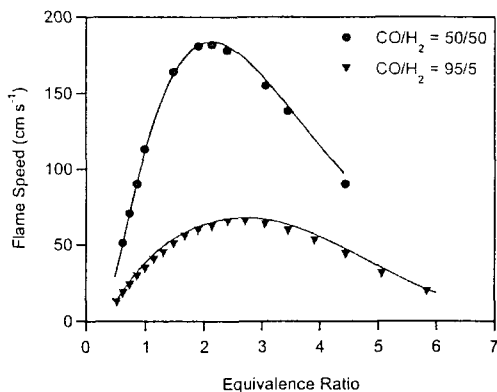
Fig. 3. Laminar flame speed of CO/H$_2$/air mixtures at 298 K and 1 atm for two fuel compositions (95% CO + 5% H$_2$ or 50% CO + 50% H$_2$). Symbols represent the experimental data (McLean et al., *Proc. Combust.* Inst., 1994, 25, 749), and lines are predictions of present CO/H$_2$/O$_2$ mechanism.

Fig. 4. Atmospheric laminar flame speed of CH$_3$OH/air mixtures at different initial temperature (318, 340, and 368 K). Symbols represent the experimental data of Egofopoulos et al. (*Combust. Sci. and Tech.*, 1992, 83, 33), and lines are predictions of present CH$_3$OH/O$_2$ mechanism.
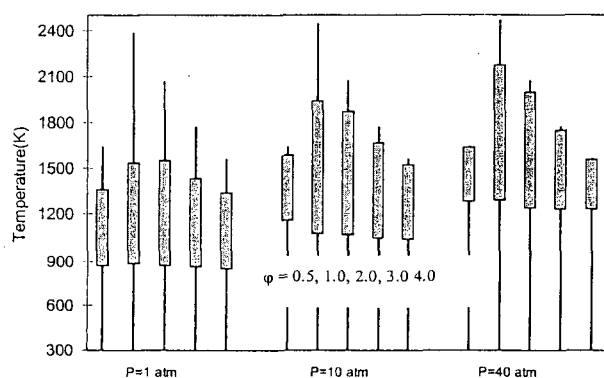
Fig. 5. Sensitivity temperature window for reaction rate of H + O$_2$ → OH + O for an H$_2$/air flame, 298 K, 1 atm pressure.
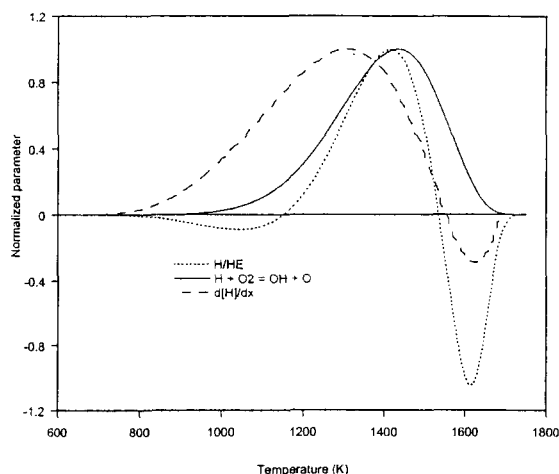
Fig. 6. Normalized sensitivity of H/He binary diffusion coefficient and the H + O$_2$ → OH + O reaction plotted with the H concentration gradient for H$_2$/He/O$_2$ (He/O$_2$ = 23/2) flame at equivalence ratio 1.5 and 20 atm.

73

LASER PHOTOELECTRON SPECTROSCOPY OF IONS

G. Barney Ellison
Department of Chemistry & Biochemistry
University of Colorado
Boulder, CO 80309-0215
Email: barney@JILA.colorado.edu

1. Ion-Radical Reactions.

Ions and radicals are energetic and reactive species. Over the last decades, molecular beam and flow tube techniques have been used to explore the spectroscopy and bimolecular chemistry of these species. Thousands of ion reactions have been studied with stable neutrals and with some atomic radicals in the gas phase,[1] with the aim of understanding the fundamental chemical reaction dynamics as well as the chemistry of the earth's upper atmosphere, interstellar medium, lasers, and other plasma phenomena.[2]

Ion-organic radical reactions are also expected to be important in several environments, including in combustion processes. Here, the elevated temperatures generate high densities of energetic species which react rapidly to spawn a myriad of combustion products. In oxy-acetylene flames,[3] HCO^+, $C_3H_3^+$, H_3O^+, HC_2^-, O_2^-, CN^-, and HO^- have been identified as major ions at densities of $10^8 - 10^{10}$ cm^{-3}. Experimental studies of ion-organic radical reactions are challenging primarily because of the difficulty in generating the radicals cleanly and in high densities. In a flowing afterglow-selected ion flow tube (FA-SIFT) instrument, the reaction time in the flow tube is roughly 10 ms. In order to generate detectable amount of product ions, the density of the radicals in the FA-SIFT reaction flow tube must to be at least 10^9 radicals cm^{-3}. Reactant ions and radicals may be lost easily, before their mutual encounter, by reactions with their chemical precursors and by radical-radical reactions.

We have employed a new approach that combines a supersonic pyrolysis nozzle[4] with the FA-SIFT instrument.[5] Thermal decomposition of a variety of organic compounds in a pulsed supersonic nozzle produces clean and intense beams of organic radicals or diradicals;[6] typical nozzle temperatures range from $300 - 1800$ K and the residence time of radicals in the nozzle is about 30 μsec. The SIFT instrument is used to generate mass-selected ions in a helium buffer gas (0.5 Torr) free from their chemical precursors. The high-pressure flow tube environment allows *both* the ions and radicals to be thermally equilibrated (≈ 300 K) and contained for a moderately long reaction time (≈ 10 ms).

We reported[7] the first observation of ion reactions with hydrocarbon radicals and diradicals using the flowing afterglow technique. A simple radical, allyl (CH_2CHCH_2), and a diradical, *ortho*-benzyne (o-C_6H_4) are produced in a hyperthermal nozzle.[6]

$$CH_2=CH-CH_2I + \Delta \longrightarrow \text{(allyl radical)} + I\cdot \qquad (1)$$

benzoyl chloride $+ \Delta \longrightarrow$ benzyne $+ CO + HC\ell$ (2)
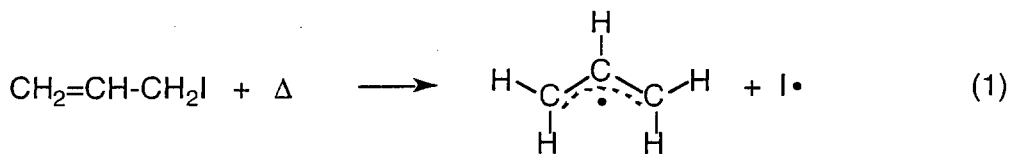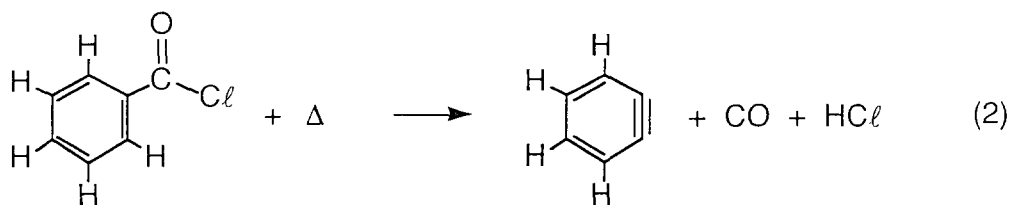
We demonstrate that these radicals react with simple gas phase ions, hydronium cation (H_3O^+) and hydroxide anion (HO^-).

$$CH_2CHCH_2 + H_3O^+ \rightarrow C_3H_6^+ + H_2O \qquad (3)$$
$$CH_2CHCH_2 + HO^- \rightarrow \text{no product ions} \qquad (4)$$
$$o\text{-}C_6H_4 + H_3O^+ \rightarrow C_6H_5^+ + H_2O \qquad (5)$$
$$o\text{-}C_6H_4 + HO^- \rightarrow C_6H_3^- + H_2O \qquad (6)$$
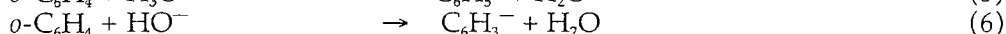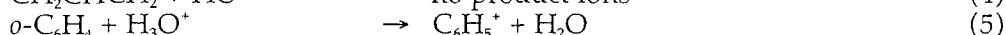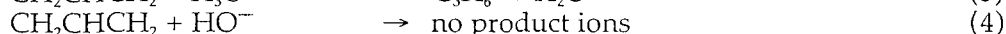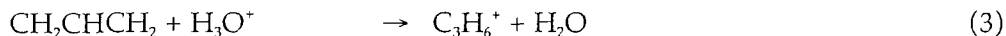
The proton transfer reactions with H_3O^+ occur at nearly every collision ($k^{II} \cong 10^{-9}$ cm^3 s^{-1}). An unexpected result has been obtained for $o\text{-}C_6H_4 + HO^-$; the exothermic proton abstraction is significantly slower than the collision rate by nearly an order of magnitude ($k_6^{II} \cong 10^{-10}$ cm^3 s^{-1}). This observation has been rationalized by competing associative detachment: $o\text{-}C_6H_4 + HO^- \rightarrow C_6H_5O + e^-$. No charged products have been observed for $CH_2CHCH_2 + HO^-$, presumably because of similar detachment pathways.

2. Vibrational Spectroscopy and Reaction Dynamics of Propargyl, $HC\equiv C\text{-}CH_2$.

Beams of the propargyl radical have been produced by thermal dissociation of $HC\equiv C\text{-}CH_2Br$ and $HC\equiv C\text{-}CH_2CH_2ONO$ in a hyperthermal nozzle. The presence of the $HC\equiv C\text{-}CH_2$ radical was verified with a photoionization mass spectrometer: $HC\equiv C\text{-}CH_2 + \hbar\omega_{118.2nm} \rightarrow HC\equiv C\text{-}CH_2^+$ (m/z 39). Samples of propargyl were collected on a 10 K cold CsI window and the polarized infrared absorption spectrum of the propargyl radical was measured.[8] We have detected nine of the twelve possible fundamental vibrational modes of propargyl: $\Gamma_{vib}(HC\equiv C\text{-}CH_2) = 5a_1 \oplus 3b_1 \oplus 4b_2$. The experimental $HC\equiv C\text{-}CH_2 \; \tilde{X} \; ^2B_1$ frequencies (cm^{-1}) and polarizations follow: a_1 modes — 3308, 3028, 1935, 1369, 1061; b_1 modes — 686, 483; b_2 modes — 1017, 620. The linear dichroism was measured with photooriented samples to yield experimental polarizations of the vibrational modes. When beams of $HC\equiv C\text{-}CH_2$ and O_2 are co-deposited at 10 K, a chemical reaction is observed to produce the propargyl peroxyl radical: $HC\equiv C\text{-}CH_2 \; \tilde{X} \; ^2B_1 + O_2 \rightarrow HC\equiv C\text{-}CH_2OO \; \tilde{X} \; ^2A''$.

References

[1] Y. Ikezoe, S. Matsuoka, M. Takebe, and A. Viggiano, *Gas Phase Ion-Molecule Reaction Rate Constants Through 1986.* (Maruzen, Tokyo, 1987).

[2] *The Encyclopedia of Mass Spectrometry*, edited by M. L. Gross and R. Capriori (Elsevier, Amsterdam, 2003), Vol. 1; *Theory and Ion Chemistry*.

[3] A. N. Hayhurst and D. B. Kittelson, Combust. Flame **31**, 37 (1978).

[4] J. A. Blush, H. Clauberg, D. W. Kohn, D. W. Minsek, X. Zhang, and P. Chen, Acc. Chem. Res. **25**, 385 (1992).

[5] J. M. Van Doren, S. E. Barlow, C. H. DePuy, and V. M. Bierbaum, Int. J. Mass Spectrom. Ion Processes **81**, 85 (1987).

[6] X. Zhang, A. V. Friderichsen, S. Nandi, G. B. Ellison, D. E. David, J. T. McKinnon, T. G. Lindeman, D. C. Dayton, and M. R. Nimlos, Rev. Sci. Instrum. **74**, 3077 (2003).

[7] X. Zhang, V. M. Bierbaum, G. B. Ellison, and S. Kato, J. Chem. Phys. **120**, 3531 (2004).

[8] E. B. Jochnowitz, X. Zhang, M. R. Nimlos, M. E. Varne, J. F. Stanton, and G. B. Ellison, J. Phys. Chem. A **(to be submitted)** (2004).
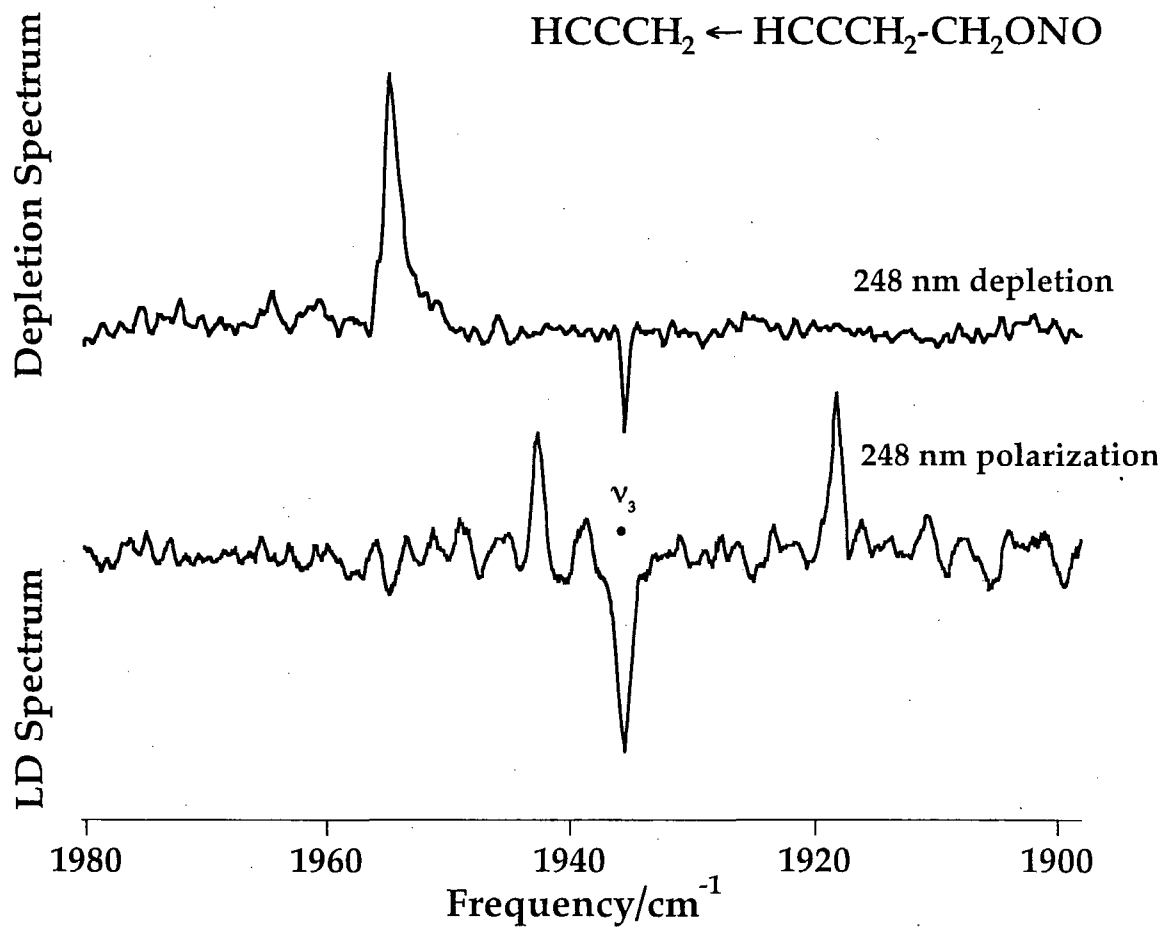
Vibrational Spectrum of ν_3 of the $HC{\equiv}C\text{-}CH_2$ $\tilde{X}$ $^2B_1$ radical in an argon matrix at 20 K; $\nu_3(HC{\equiv}CCH_2) = 1935$ cm^{-1}. The linear dichrosim spectrum demonstrates that $\nu_3(HC{\equiv}CCH_2)$ has a_1 symmetry. Other $-C{\equiv}C-$ stretching frequencies are: ($HC{\equiv}CH$, 1974 cm^{-1}) and ($HC{\equiv}C\text{-}CH_3$, 2142 cm^{-1}).

Jon C. Rienstra-Kiracofe, G. S. Tschumper, Henry F. Schaefer III, Sreela Nandi and G. Barney Ellison, "Atomic and Molecular Electron Affinities: Photoelectron Experiments and Theoretical Computations," *Chem. Revs.*, **102**, 231-282 (2002).

S. Nandi, S. R. Blanksby, X. Zhang, M. R. Nimlos, D. R. Dayton and G. B. Ellison, "Polarized Infrared Absorption Spectra of Matrix-Isolated Methylperoxyl Radicals, $CH_3OO \tilde{X}\,^2A'''$", J. Phys. Chem. A, **106**, 7547-7556 (2002).

M. R. Nimlos, G. E. Davico, C. M. Geise, P. G. Wenthold, W. C. Lineberger, S. J. Blanksby, C. M. Hadad, G. A. Petersson, G. B. Ellison, "Photoelectron spectroscopy of $HCCN^-$ and $HCNC^-$ reveals the quasilinear triplet carbenes, HCCN and HCNC," J. Chem. Phys., **117**, 4323-4339 (2002).

S. J. Blanksby, S. Kato, V. M. Bierbaum, G. B. Ellison, "Ion Induced Fragmentation of Alkylhydroperoxides," *J. Am. Chem. Soc.* **2002**, *124*, 3196-3197 (2002).

T. M. Ramond, S. J. Blanksby, S. Kato, V. M. Bierbaum, G. E. Davico, R. L. Schwartz, W. C. Lineberger and G. B. Ellison, "The Heat of Formation of the Hydroperoxyl Radical HOO *via* Negative Ions", J. Phys. Chem. A, **106**, 9641-9647 (2002).

M. R. Nimlos, S. J. Blanksby, G. B. Ellison, R. J. Evans, , "Enhancement of 1,2-dehydration of alcohols by alkali cations and protons: a model for dehydration of carbohydrates", *J. Anal. Appl. Pyrolysis* **2003**, *66*, 3-27.

Stephen J. Blanksby and G. Barney Ellison, "Bond Dissociation Energies of Organic Molecules," Acct. Chem. Res., **36**, 255-263 (2003).

X. Zhang, A. V. Friderichsen, S. Nandi, G. B. Ellison, D. E. David, J. T. McKinnon, T. G. Lindeman, D. C. Dayton, and M. R. Nimlos, "An Intense, Hyperthermal Source of Organic Radicals for Matrix-Isolation Spectroscopy" Rev. Sci. Instrum. **74**, 3077-3086 (2003).

Stephen J. Blanksby, Veronica M. Bierbaum, G. Barney Ellison, and Shuji Kato, "Fragmentations of Deprotonated Alkyl Hydroperoxides (ROO^-) Upon Collisional Activation: A Combined Experimental and Computational Study, Aust. J. Chem., **56**, 459-472 (2003).

G. Barney Ellison, "Photoelectron Spectroscopy of Negative Ion Beams: Measurements of Electron Affinities", 390-398. in *The Encyclopedia of Mass Spectroscopy*, **Vol. 1** *Theory and Ion Chemistry* Ed. Peter B. Armentrout, Elsevier Amsterdam (2003).

Xu Zhang, Veronica M. Bierbaum, G. Barney Ellison, and Shuji Kato, "Gas-Phase Reactions of Organic Radicals and Diradicals with Ion", J. Chem. Phys., **120**, 3531-3534 (2004).

Thermochemistry of Hydrocarbon Radicals:
Guided Ion Beam Studies

Kent M. Ervin
Department of Chemistry/216
University of Nevada, Reno
Reno, Nevada 89557
Telephone: 775-784-6676
E-mail: ervin@chem.unr.edu

Project Scope

Gas phase negative ion chemistry methods are employed to determine enthalpies of formation of hydrocarbon radicals that are important in combustion processes and to investigate the dynamics of ion–molecule reactions. Using guided ion beam tandem mass spectrometry, we measure collisional threshold energies of endoergic proton transfer and hydrogen atom transfer reactions of hydrocarbon molecules with negative reagent ions. The measured reaction threshold energies for proton transfer yield the relative gas phase acidities. In an alternative methodology, competitive collision-induced dissociation of proton-bound ion–molecule complexes provides accurate gas phase acidities relative to a reference acid. Combined with the electron affinity of the R· radical, the gas phase acidity yields the RH bond dissociation energy of the corresponding neutral molecule, or equivalently the enthalpy of formation of the R· organic radical. The threshold energy for hydrogen abstraction from a hydrocarbon molecule yields its hydrogen atom affinity relative to the reagent anion, providing the RH bond dissociation energy directly. Electronic structure calculations are used to evaluate the possibility of potential energy barriers or dynamical constrictions along the reaction path, and as input for RRKM and phase space theory calculations. In newer experiments, we have measured the product velocity distributions to obtain additional information on the energetics and dynamics of the reactions.

Recent Progress

O–H Bond Dissociation Energy of Phenol

Recent work using competitive threshold collision-induced dissociation techniques has centered on determination of the bond dissociation energy of phenol, $D(C_6H_5O-H)$, for which recent literature determinations are not in complete agreement. We have produced proton-bound heterodimers such as $[C_6H_5O..H..CN]^-$, which upon collisional activation dissociates as shown in the figure on the next page into either $C_6H_5O^- + HCN$ or $C_6H_5OH + CN^-$. The higher threshold energy for the latter channel qualitatively implies that phenol is a stronger gas phase acid than HCN. Using statistical rate theories, we quantitatively model the branching ratio between these
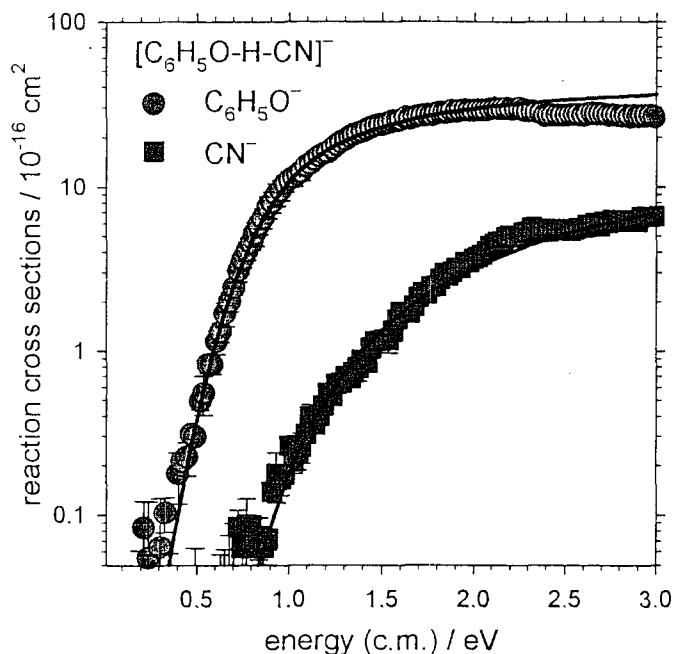
two product channels as a function of the available energy. Our preliminary results suggest that $D(C_6H_5-H)$ is moderately, but significantly, smaller than the values reported from proton transfer energy thresholds by both our group $(Cl^- + C_6H_5OH)$[1] and the Scott Anderson group at the University of Utah $(ND_3 + C_6H_5OH^+)$.[2] We are now extending our experimental work on the phenol system by using additional reference acids besides HCN, namely H_2S and substituted phenols, to create a gas-phase acidity ladder for a more precise determination.

In conjunction with this work, we have continued a collaboration with P. B. Armentrout (University of Utah) on the CRUNCH program[3] for fitting cross section data with statistical rate theory. In particular, we have extended the models to include phase space theory in addition to RRKM theory, and have incorporated an approximate treatment of the permanent dipoles of the neutral product for orbiting transition states. The CRUNCH program is in use by about 25 gas-phase ion chemistry research groups internationally.

Electron Affinity of O_2

Recently published reports by Chen and Chen[4,5] have claimed that the electron affinities of several molecules, including the diatomics O_2 and NO, are widely different than the previously accepted values obtained by photoelectron spectroscopy. Chen and Chen further claim that the anions observed in photoelectron spectra are actually electronically excited anions. In collaboration with W. C. Lineberger (University of Colorado, Boulder) and J. Simons (University of Utah), we presented[6] overwhelming spectroscopic and theoretical evidence that the electron affinity is $EA_0(O_2)$ is 0.448 ± 0.006 eV, in agreement with photoelectron spectra reported by a number of groups since the early 1980s, and that the only stable electronic state of the anion is the O_2^- ($^2\Pi$) ground state. This implies that there are serious flaws in the Electron Capture Detector experiments and analysis methods used by Chen and Chen to obtain their reported value of $EA(O_2) = 1.07 \pm 0.07$ eV.

As part of this work, we revised our program for fitting the Franck-Condon vibrational profiles of photoelectron spectra, PESCAL.[7] Ten groups have requested copies of this program in the last three years.

Product Velocity Distribution Measurements

   The velocity distributions of the products of ion molecule reactions provide information on the energy partitioning in the reactions. We have modified our guided ion beam tandem mass spectrometer to perform time-of-flight measurements on product ions, which can be transformed into axial product velocity distributions. We have published[8] the product velocity distributions for hydrogen atom transfer reactions of S^- with H_2, CH_4, and C_2H_6. We had previously investigated the collision energy dependence of the total reaction cross sections for these reactions with the hope of using the threshold energies to obtain the radical product enthalpies of formation. Although this worked well for the hydrogen reaction,[9] for the hydrocarbons we observed large reverse activation energy barriers. Ab initio potential energy surfaces show either no (H_2) or low (CH_4, C_2H_6) energy barriers along the reaction path, but these latter barriers are not high enough to explain the elevated threshold energies. Examining the product velocities provides a handle on the dynamics of the reactions. Near threshold, the SH^- product is back-scattered, consistent with direct collisions with low impact parameters needed to drive the endoergic reaction. At higher energies, a forward scattered feature becomes dominant. The distributions indicate that the reactions are direct, with inefficient translational to vibrational energy transfer accounting for the excess threshold energies.

Future Directions

We plan on continuing our competitive threshold collision-induced dissociation measurements for obtaining gas-phase acidities, targeting larger molecules important in combustion systems that remain challenging for theoretical energy calculations. We are particularly interested in oxygenated species, as well as molecules with aromatic rings and CC triple bonds. A major part of this project is the application of more advanced statistical rate models of the dissociation processes. We will also further pursue the application of proton transfer and hydrogen atom transfer reactions for determination of neutral radical thermochemistry.

References

[1] V. F. DeTuri and K. M. Ervin, Int. J. Mass Spectrom. **175**, 123 (1998).

[2] H.-T. Kim, R. J. Green, J. Qian, and S. L. Anderson, J. Chem. Phys. **112**, 5717 (2000).

[3] P. B. Armentrout and K. M. Ervin, CRUNCH, Fortran program, version 5.04 (2004).

[4] E. S. Chen, W. E. Wentworth, and E. C. M. Chen, J. Mol. Struct. **606**, 1 (2002).

[5] E. S. Chen and E. C. M. Chen, J. Phys. Chem. A **2002**, 6665 (2002).

[6] K. M. Ervin, I. Anusiewicz, P. Skurski, J. Simons, and W. C. Lineberger, J. Phys. Chem. A **107**, 8521 (2003).

[7] K. M. Ervin and , PESCAL, Fortran program, 2003.

[8] L. A. Angel, M. K. Dogbevia, K. M. Rempala, and K. M. Ervin, J. Chem. Phys. **199**, 8996 (2003).

[9] K. Rempala and K. M. Ervin, J. Chem. Phys. **112**, 4579 (2000).

Publications, 2002–present

"Anchoring the gas-phase acidity scale", K. M. Ervin and V. F. DeTuri, *J. Phys. Chem. A*, **106**, 9947-9956 (2002).

"Dynamics of the gas-phase reactions of chloride ions with fluoromethane", L. A. Angel, S. P. Garcia, and K. M. Ervin, *J. Am. Chem. Soc.* **124**, 336-345 (2002).

"Microcanonical analysis of the kinetic method. The meaning of the 'apparent entropy'", K. M. Ervin, *J. Am. Soc. Mass Spectrom.* **13**, 435-452 (2002).

"Experimental techniques in gas phase ion thermochemistry" (Erratum), K. M. Ervin, *Chem. Rev.*, **102**, 855 (2002).

"Gas-phase S_N2 and bromine abstraction reactions of chloride ion with bromomethane: Reaction cross sections and energy disposal into products", L. A. Angel and K. M. Ervin, *J. Am. Chem. Soc.* **125**, 1014-1027 (2003).

"Thermochemistry: Definitions and Tabulations" Ervin, K. M.; Armentrout, P. B. In The Encyclopedia of Mass Spectrometry. Volume 1: Theory and Ion Chemistry, Armentrout, P. B., Ed.; (Elsevier: Amsterdam, 2003) pp. 309-315.

"The only stable state of O_2^- is the $X\,{}^2\Pi_g$ ground state and it (still!) has an electron detachment energy of 0.45 eV", K. M. Ervin, I. Anusiewicz, P. Skurski, J. Simons, and W. C. Lineberger, *J. Phys. Chem. A.*, **107**, 8521-8529 (2003).

"Gas-phase hydrogen abstraction reactions of S^- with H_2, CH_4, and C_2H_6", L. A. Angel, M. K. Dogbevia, K. M. Rempala, and K. M. Ervin, *J. Chem. Phys.* **199**, 8996-9007 (2003).

PESCAL, Fortran program for Franck-Condon analysis of photoelectron spectra, K. M. Ervin, (revised 2003).

CRUNCH, Fortran program for analysis of reaction cross sections with RRKM and PST models, K. M. Ervin and P. B. Armentrout, version 5.004 (2004).

"Systematic and random errors in ion affinities and activation entropies from the extended kinetic method", K. M. Ervin and P.B. Armentrout, *J. Mass Spectrom.* (accepted 2004).

Experimental Kinetics and Mechanistic Investigations of Hydrocarbon Radicals Relevant to Combustion Modeling

Askar Fahr*
Chemistry Department
American University
Washington, D.C. 20899-8382
askarfahr@hotmail.com

*Guest Scientist at: Physical & Chemical Properties Division
National Institute of Standards and Technology
Gaithersburg, MD 20899-8382
askar.fahr@nist.gov, 301-975-2511

SCOPE OF THE PROGRAM

The objective of this research program is to determine, experimentally, kinetic parameters, the nature and yields of reaction products, and mechanistic data for several key elementary radical-radical and radical-molecule reactions involving C2 and C3 hydrocarbon radicals. Small hydrocarbon radicals, such as vinyl (C_2H_3) and propargyl ($HCCCH_2$) are believed to play pivotal roles in the formation of aromatic and polyaromatic hydrocarbons and in the inception of soot. There are either very limited or no reported experimental or computational results on reactions of these radicals.

Methods employed for our studies include, excimer-laser photolysis for generating the radicals, time-resolved UV-absorption spectroscopy for direct kinetic studies, GC/MS methods for identification and quantification of final reaction products as well as for comparative rate determinations. Detailed kinetic modeling is used for data analysis and interpretations. For a better understanding of the reaction mechanisms emphasis is given to determination of the isomeric nature of the products and on examining the effects of pressure and temperature on product channels and on the nature and yields of the reaction products.

RECENT PROGRESS
a. Product Channels and Kinetics of the $C_2H_3 + C_2H_4$ Reaction
The reaction of vinyl radical with ethylene has been studied at various temperature (523 K to 723 K) and pressure (~20 mbar to 950 mbar) conditions. Vinyl radicals were generated by photolysis of C_2H_3I at 248 nm. Final product studies indicated the formation of 1-butene, 1,3-butadiene, 1,5-hexadiene, cyclohexene and 1,7-octadiene. The relative yields of final products show significant and complex pressure and/or temperature dependences. For example, the yield of 1-butene at 523 K increases rapidly with pressure, reaching a maximum at around 200 mbar then the yield decreases as the

pressure is increased. Also the yield of 1-butene decreases as the temperature is increased. The yield of 1,3-butadiene and cyclohexene increase with temperature while the yield of 1,5-hexadiene decreases as temperature is increased. The product studies and a detailed kinetic modeling of the reaction system suggest a large array of reactions occurring in the system including dissociation and isomerization of certain intermediates or products leading to reactive species not initially present in the reaction system.

Direct kinetic studies of the $C_2H_3+C_2H_4$ reaction have been performed (and will continue) in collaboration with Dr. Craig Taatjes at CRF. Time profiles of vinyl radicals are probed directly at 230 nm region (at NIST) or 420 nm, using a multipass Herriott-type cell (CRF). Preliminary kinetic results for the $C_2H_3+C_2H_4$ reaction, determined at 100 mbar suggest a rate constant of $\sim 2.5 \times 10^{-14}$ cm^3 molecule^{-1} s^{-1}.

b. Review of Reactions and Kinetics of Unsaturated C_2 Hydrocarbon Radicals
The chemistry associated with small unsaturated hydrocarbon radicals has direct relevance to a host of combustion processes, catalytic reactions and fundamental organic chemistry. Accurate reaction rate constants as well as detailed product analysis for radical reactions are required to realistically interpret and model macroscopic hydrocarbon reaction systems and to determine the factors affecting the efficiency of the hydrocarbon growth and abundance of various molecular and radical species. During the past 20 years, as a result of significant advances in both new experimental approaches and *ab initio* theory a significant amount of data on properties of these species; their spectroscopy, electronic structure, as well as their reactions and kinetics have become available. In a review article we have compiled and evaluated the available reaction kinetic and mechanistic data on C_2 unsaturated hydrocarbon radicals including ethynyl (C_2H), vinylidene ($H_2C=C$), and vinyl (C_2H_3) radicals. In addition, the thermochemistry, spectroscopy, means of production and detection of these radical species and results of the relevant computational studies have been discussed and preferred rate parameters are presented.

FUTURE PLANS
Our future work will include continuation of the kinetics and product studies of the vinyl and propargyl radical reactions. We will expand our investigations of the radical-radical and radical-molecule reactions and examine effects of pressure and temperature on the vinyl + propargyl and propargyl + acetylene reactions. The reaction $C_3H_3+C_2H_2$ is an important process and can yield cyclopentadienyl. An interesting issue is the pressure dependence of the process.

Once again, the emphasis of the studies will be on the nature and yields of the final products as a function of temperature and pressure. Particular attention will be given to see if any of the products will undergo isomerization and/or cyclization.

Publications Supported by DOE

1. Howe, P. T. and Fahr, A. "Pressure and Temperature Effects on Product Channels of the Propargyl (HC≡CCH$_2$) Combination Reaction and the Formation of Benzene"

J. Phys. Chem. A, **2003**, *107*, 9603.

2.   Howe, P. T.; Fahr, A. and Laufer, A. H., "Effect of Water Vapor on the Combination and Disproportionation of Ethyl Radicals in the Gas Phase" *J. Phys. Chem. A*, **2004**, *108*, 1639.

3.   Laufer, A. H. and Fahr, A. "Review of Reactions and Kinetics of Unsaturated C_2 Hydrocarbon Radicals" *Chemical Reviews*, **2004** (accepted, in press).

4.   Striebel, F., Jusinski, L. E., Fahr, A., Halpern, J. B., Klippenstein, S. J.' and Taatjes, C. A; "Kinetics of the Reaction of Vinyl Radicals with NO: Ab Initio Theory, Master Equation Predictions, and Laser Absorption Measurements" *Phys. Chem.. Chem. Phys.* **2004,** 6 (accepted, in press).

Spectroscopic and Dynamical Studies of Highly Energized Small Polyatomic Molecules

Robert W. Field
Massachusetts Institute of Technology
Cambridge, MA 02139
rwfield@mit.edu

<u>Program Definition:</u> Our research program is centered on the development and application of experimental and theoretical methods for studying the dynamics (Intramolecular Vibrational Redistribution and Isomerization) and kinetics of combustion species. The primary focus is the dynamics of small molecules at internal energies above the barrier to bond-breaking isomerization. Two systems are currently under study: the S_0 ($\tilde{X}\,^1\Sigma_g^+$) state of C_2H_2 near the acetyelene $\leftrightarrow$ vinylidene isomerization barrier, and the S_0 ($\tilde{X}\,^1\Sigma^+$) state of HCN near the hydrogen cyanide $\leftrightarrow$ hydrogen isocyanide isomerization barrier.

Recent Progress

Our current research is driven by efforts to selectively populate and to conclusively assign the vibrational levels in the vicinity of the acetyelene $\leftrightarrow$ vinylidene isomerization transition state. In order to achieve significant population transfer into these target states, we have devised a scheme that exploits a "local-bender pluck" by using the half-linear turning point of the antisymmetric in-plane bend (ν_6) in the $\tilde{A}$ state in order to drop down onto the half-linear acetylene $\leftrightarrow$ vinylidene isomerization barrier in the ground state. Once a suitable intermediate state has been located, SEP spectra of ^{13}C-acetylene will reveal permutation tunneling splittings, allowing an unprecedentedly complete description of the anharmonic couplings in the vicinity of the transition state.

Because the intermediate states crucial to achieving a "local-bender pluck" for use in a double resonance spectrum are not Franck-Condon allowed but rather are illuminated by anharmonic and Coriolis interactions with the FC bright states, their appearance in the spectrum is often weak and fragmentary. Additionally, their appearance in the spectrum is often obscured by the more intense hot bands that originate from ground state vibrational levels with excitation in the *trans*-bending mode. Thus it is necessary to develop both new experimental methods to uncover and isolate the spectral features due to transitions into these states and to develop new methods of assignment of these bands in the absence of complete rotational information. The hallmark of this effort has been the development of several multispectral techniques that can be used to sort excitation spectra according to the character of the observed eigenstates.

We have refined a technique to extract only the "cold band" features from the LIF excitation spectrum recorded in a static gas cell. LIF spectra are simultaneously recorded in two attached sample cells. One cell is heated to ~ 75°C and the other is cooled to ~ 0°C. The ratio of intensities for each feature in these Differential Temperature-Laser Induced Fluorescence (DT-LIF) spectra reveals the degree of excitation of the initial state. The spectra can therefore be processed by a computer algorithm to remove all but bands originating from the zero-point level of the ground electronic state. A paper describing this technique has been submitted to the journal *Chemical Physics* and is currently undergoing revision.

The use of another multispectral technique, simultaneous Surface Electron Ejection by Laser Excited Metastables (SEELEM) and LIF recorded in a supersonic molecular beam source has led to the first assignment of all three symmetry-allowed components of the $4\nu_{bend}$ polyad, of which at least one member strongly perturbs the $3\nu_3$ vibrational level of the $\tilde{A}$ state and has been used as an intermediate in SEP experiments with the hope that its character is dominated by the antisymmetric in-plane bend (ν_6). The assignments indicate the primary perturbation is $2\nu_4 + 2\nu_6$, and therefore unlikely to give the desired access to the isomerization transition state. The two additional members of the $4\nu_{bend}$ polyad are only observed in the recorded SEELEM+UV-LIF spectrum in their $K=0$ sublevels, which are obscured in the static cell LIF by the strong unperturbed $3\nu_3$ lines. In order to predict the locations of the $K=1$ sublevels of the $4\nu_4$ and $4\nu_6$ bands, the available data have been fit to an effective Hamiltonian model incorporating the strong anharmonic and Coriolis interactions expected to exist between members of the polyad.

These perturbed bands are likely to require a great deal of spectroscopic detective work to uncover. A new technique, Filtered Fluorescence Cross Correlation (FFCC), has been developed to quickly sort LIF spectra on the basis of the number of quanta of excitation in the *trans*-bending mode (v_3), and therefore be able to identify, among other weak features, those lines that are due to eigenstates containing no excitation in the *trans* bend. This technique is based on the differential detectivity of the eigenstates due to gross features of the fluorescence spectrum. States with non-zero quanta of vibration in the *trans*-bend have emission spectra that are dominated by two classical turning points: one nearly linear and one very bent. The near-linear turning point radiates primarily to ground state levels that contain less than 15,000 cm^{-1} of vibrational excitation. In contrast, the very bent turning point radiates to highly vibrationally excited states (> 20,000 cm^{-1} of vibrational excitation). We can exploit the two lobes of Franck-Condon activity to characterize the eigenstates observed in a spectrum. This can be accomplished by simultaneously recording two LIF spectra with the light filtered to accept only the emission to the low-lying levels (<400 nm) onto one detector and filtered to accept only emission to high lying levels (>475 nm) onto the other detector. Unlike all other eigenstates, the important states containing zero quanta of *trans*-bending vibration do not have multiple turning points and are easily separated from the other states based on their negligible emission onto the long-wavelength detector.
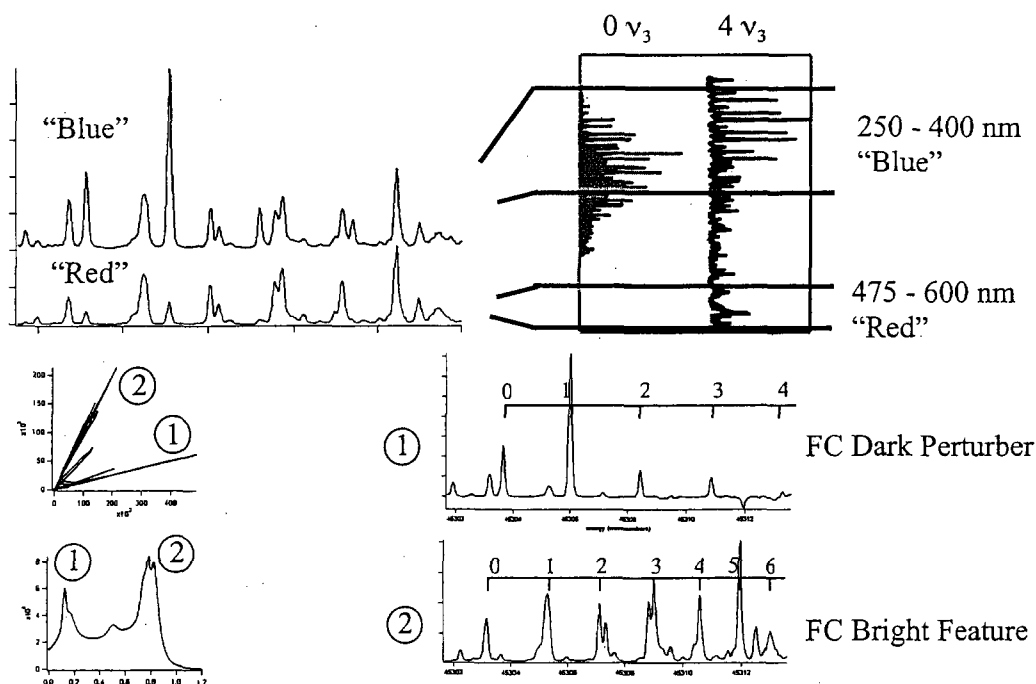
Figure 1: Filtered Fluorescence Cross Correlation (FFCC) used to separate a Franck-Condon bright state from a Franck-Condon dark perturber state. The two spectra ("Blue" and "Red") are simultaneously recorded with filter combinations used to select gross features of the Dispersed Fluorescence spectra as demonstrated by spectra from the origin band and from $4v_3$. An XCC-like algorithm is used to generate a recursion map and merit function that reveal two well-defined patterns in the spectrum. The first pattern corresponds to the perturbing state. The second pattern corresponds to the Franck-Condon bright state. The second pattern also contains features from the nearby triplet states, which, since they have emission spectra identical to the features from which they borrow intensity, cannot be separated by this technique.

It should be possible, using this technique, to locate the $K=1$ levels of $4v_4$ and $4v_6$ as predicted by the effective Hamiltonian model, and further to extend to higher energies the search for perturbing states that contain zero or one quanta of excitation in the *trans*-bend. We are working with an *ab initio* quantum chemist,

John Stanton, to develop a reduced dimension model of the acetylene emission to semi-quantitatively model the ratio of intensities from the two turning points as a function of number of quanta of excitation in the *trans*-bend. We also are extending the use of multispectral detection by incorporating direct absorption (cavity ringdown) and photoacoustic spectroscopies.

Future Plans

Since the success of this approach hinges on the use of the of $\tilde{A} \leftrightarrow \tilde{X}$ electronic transition in both excitation and emission, knowledge of the both the transition moment and intensity sharing mechanisms in the $\tilde{A}$ state are crucial. Despite the relative simplicity of the acetylene molecule, the intensity sharing mechanisms among vibrational levels of the $\tilde{A}$ state elude description by a simple, two level 'bright state-dark state' interaction. Neither can the intensity be modeled by a multiresonant effective Hamiltonian that incorporates only anharmonic interactions that are near resonance. We are currently developing an effective Hamiltonian that incorporates large but off-resonance matrix elements that cannot be treated through second order perturbation theory. The results of these calculations will be compared to variational calculations performed by our collaborators John Stanton (University of Texas) and Joel Bowman (Emory University).

The importance of spectroscopic perturbations in the acetylene isomerization problem has led us to renew our interest in HCN $\leftrightarrow$ HNC isomerization, where the lack of inversion symmetry obviates reliance on perturbations as a means to reach the transition state. Rather, the bending mode is strongly active in both the excitation and in the emission spectra. Because the system contains only three atoms, there is also a considerable benefit in terms of the reduced density of states at high energy and therefore in our ability to make reliable assignments.

Unlike previous SEP-based studies of the HCN $\leftrightarrow$ HNC system, we plan to initiate excitation from molecules with a HNC rather than HCN geometry. Upon excitation from the $\tilde{X}$ state to the $\tilde{A}$ state, the HNC geometry is stabilized in relation to the HCN geometry, resulting in a considerably lower electronic transition frequency. The $\tilde{A} \leftarrow \tilde{X}$ transition has not been observed despite the simplicity of this HNC. This is likely due to pervasive predissociation of the Franck-Condon accessible $\tilde{A}$ state vibrational levels, which is also observed in HCN. In order to access the lowest, and likely least predissociated levels, we will use an IR-UV double resonance scheme exploiting an intermediate level that is excited in the CN-stretching mode. Our scheme for recording the excitation spectrum is to excite the HNC while using another laser to record an action spectrum of the CN photofragments. This necessitates a clean preparation of HNC, free of CN background, which should be achievable through the use of a pyrolysis jet source in which an organic precursor (formamide or acrylonitrile) is decomposed by passing it rapidly through a resistively heated SiC tube. We are currently preparing such a source based on original designs by Peter Chen as modified by Hanna Reisler and Barney Ellison. We plan to use millimeter wave absorption spectroscopy to optimize the source conditions for the production of HNC.

SEP spectra will be recorded the using the CN photofragment fluorescence dip to monitor the HNC population transferred to the lower electronic state before the parent molecule dissociates. These experiments will provide information complementary to the known vibrational level structure of HCN and will give a complete picture of the HCN $\leftrightarrow$ HNC isomerization dynamics on the $\tilde{X}$ state. As in acetylene, we seek methods to definitively assign those eigenstates that are delocalized over multiple isomeric minima. One observable through which we can gain information related to the character of nuclear motion is the charge distribution of the molecule in a given vibrational state. In particular, the bending mode of HCN/HNC has been calculated to have a profound effect on the molecular dipole moment. As the bending degree of freedom leads to delocalization and eventually free rotation of the hydrogen atom around the CN core, the oppositely signed HCN and HNC dipole moments are essentially averaged out, while the dipole moment of an eigenstate of comparable excitation energy confined near linearity will give only a small shift from the equilibrium value of the dipole moment.

Once the vibrational states in the HNC $\tilde{X}$ state have been located, direct and precise measurements of their dipole moments will be obtained by SEP-millimeter-wave Stark spectroscopy. In this technique an additional resonant step is added to induce a pure rotational transition within the highly vibrationally excited (HVE) ground state level accessed by a SEP transition. Subsequent to their sudden transfer into the HVE

state, the molecules undergo transient nutation in the millimeter-wave field if the field is resonant with the rotational transition. A variable DC field introduced perpendicular to the molecular beam will induce a quadratic Stark shift in the frequency of the rotational transition, the magnitude of which can be used to directly determine the magnitude of the dipole moment.
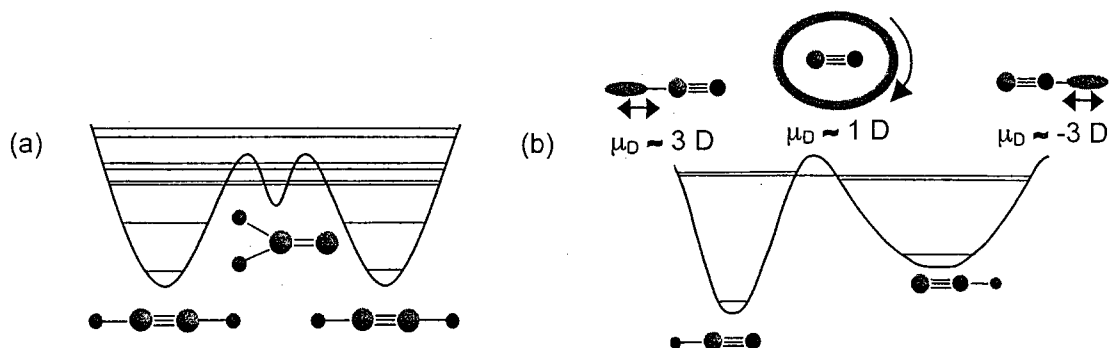
Figure 2: Unconventional observables used to assign vibrational states delocalized over multiple potential wells. In (a), the symmetric double minumum potential (acetylene), evolution of the permutation splitting is a sensitive probe of the barrier height and location of nearby vinylidene-localized levels. In (b), the asymmetric double minimum (HCN/HNC), the character of the nuclear wavefunction, as monitored by the Stark effect, provides a gauge of the delocalization across both potential wells.

We are also investigating alternative methods for assigning highly vibrationally excited states. In collaboration with Friedrich Temps of the University of Kiel, we are planning to carry out velocity map imaging photoelectron spectroscopy of HVE molecules near an isomerization barrier. Since the photoelectron spectrum projects the ground state vibrational wavefunction onto an ionic potential energy surface, states that are "chemically delocalized" should show the photoelectron signatures of both configurations over which they are delocalized.

We are exploring theoretical methods to extract information about chemical barriers from permutation tunneling splittings in floppy molecules, such as acetylene. We are currently collaborating with Jon Hougen (NIST) to fit Michael McCarthy's (Harvard Smithsonian Astrophysical Observatory) microwave spectrum of silicon trimer (Si_3) to an effective Hamiltonian that incorporates the ability of this isosceles triangular molecule to shift its apex position through large amplitude pseudorotation, which leads to shifting of the energy levels away from their asymmetric rotor positions. These tools, once developed, will be brought to bear upon the analysis of the permutation doublets anticipated in the SEP spectra of ^{13}C-acetylene.

Recent DOE-supported Publications (Since 2002)

1. M.L. Silva, M.P. Jacobson, Z. Duan, and R.W. Field, "Unexpected simplicity in the $S_1 - S_0$ Dispersed Fluorescence spectra of $^{13}C_2H_2$," J. Chem. Phys. 116, 93 (2002).

2. Z.-H. Loh and R.W. Field, "Contrasting origins of the isomerization barriers for vinylidene, fluorovinylidene, and difluorovinylidene," J. Chem. Phys. 118, 4037 (2003).

3. A.J. Merer, N. Yamakita, S. Tsuchiya, J.F. Stanton, Z. Duan, and R.W. Field," New vibrational assignments in the $\tilde{A} \, ^1A_u \leftarrow \tilde{X} \, ^1\Sigma_g^+$ electronic transition of acetylene, C_2H_2: the ν_1 frequency," Mol. Phys. 101, 663 (2003).

Scanning Tunneling Microscopy Studies of Chemical Reactions on Graphite Surfaces

George Flynn, Department of Chemistry, Columbia University
Mail Stop 3109, 3000 Broadway, New York, New York 10027
flynn@chem.columbia.edu

Introduction and Overview

Our Department of Energy sponsored work was for many years involved with the study of vibrational energy transfer in the gas phase using laser pump and probe techniques. Most recently this work focused on the quenching of molecules with chemically significant amounts of vibrational energy, an aspect of combustion chemistry in which vibrational energy transfer plays a critical role. We have concluded this phase of our program and launched a new effort to study chemical reactions on graphite surfaces using the Scanning Tunneling Microscope as an analytical tool to probe single molecule and single site surface processes.

This new work is focused on fundamental chemical events taking place on graphite surfaces with the intent of shedding light on the role of these surfaces in mediating the formation of polycyclic aromatic hydrocarbons (PAHs) and the growth of soot particles.[1-11] Interest in soot is ultimately driven by the environmental and health implications arising from its formation in combustion reactions (particularly those involving heavier, diesel fuels), which are nearly ubiquitous throughout our society.[1] There is also some practical interest in high temperature graphite chemistry due to the existence of graphite nuclear reactors.[12,13] Like any set of experiments designed to investigate fundamental chemical combustion processes, the systems being studied here represent a compromise between simple models (with their well defined conditions) and exact replicas of real combustion reactors (with their inherent complexity). Of the four phases of soot formation,[3,4] the work being pursued here is focused on surface reactions that lead to growth and oxidation of these particles. Our experimental system employs Scanning Tunneling Microscopy and other surface science techniques to study a well defined graphite surface (rather than the more complex soot particle) interacting with vapor phase or adsorbed molecules.

Scanning tunneling microscopy, with its ability to identify surface defects and step edges, as well as to resolve and probe individual molecules on surfaces, provides a powerful tool with which to follow the behavior of such reaction processes on surfaces and complements gas phase spectroscopic studies of PAH formation.[1-11] One of the principal focuses of our STM work over the past few years has been concerned with the identification and use of STM "chemical marker groups" to interpret patterns of molecular ordering and conformation of individual molecules adsorbed at the liquid-solid and vacuum-solid interface.[14-16] "Marker groups" are chemical functional groups that exhibit unusual contrast in the STM images relative to the rest of the atoms in a molecule; the thiol end group (-SH) provides a vivid example of such a marker.[14,15] The unusual contrast of these marker groups can be attributed to a combination of factors related to the electronic structure, size, and spatial orientation of the chemical functionality.[17,18] In particular with STM, molecules having C=C double and C≡C triple bonds can be distinguished from those having C-C single bonds and aromatic structures when these molecules are adsorbed on a surface.[19] This ability to distinguish chemical functional groups and carbon bond types on surfaces is extraordinarily useful when tracing the mechanistic pathways in the formation of PAH's from small molecule carbon precursors reacting on model graphite surfaces.

The experimental program that we are pursuing can be divided into two parts. First, we plan to deposit small to medium sized molecules and simple PAH moieties on a relatively cool (25-400 K) graphite surface in an ultrahigh vacuum system, trigger reaction between different chemical species, and use STM and other surface techniques to probe both the pre-reaction and post-reaction species. Minimally, we expect such studies to provide fundamental information about the reactions of hydrocarbons on graphite surfaces, the role of surface defects and step edges in mediating these reactions, and the effect of temperature on the chemical mechanisms of importance for such reactions. Second, by taking advantage of the high temperature capability of our UHV STM, we plan to heat graphite to high temperatures (800-1200 K), characterize the surface with STM, and impinge potential PAH/soot precursor molecules onto the graphite. The surface will then be re-characterized with STM after growth of carbonaceous material is initiated in order to identify the species forming at the graphite-vacuum interface. Our expectation is that experiments such as these will contribute to an understanding of the mechanism for formation of PAH's on surfaces as well as the route by which small PAH's grow into larger ones.

Results:
A key feature of these experiments involves the identification of adsorbates on the surface using temperature tunable, ultra-high-vacuum Scanning Tunneling Microscopy. We have begun our efforts on this project by depositing chrysene and other PAH molecules on a graphite surface that was pre-cleaned by heating to >700 K. Because of the low vapor pressure of chrysene, we have used a vacuum evaporation oven in conjunction with a quartz-crystal microbalance to deposit molecules on the surface at mono-layer or sub-mono-layer coverage. STM topographs of the chrysene covered graphite surface, taken at 80 K, show arrays of well ordered dimers. At the tunneling conditions used (nominally 2 volts and 100 pA) the chrysene can be clearly seen sitting on top of the graphite surface. Though the molecules on the surface form well ordered arrays, they pack flat in a two dimensional low density arrangement on the surface. Wide "empty spaces" can be clearly seen between the chrysene dimers, and the carbon atoms on the graphite surface are easily resolved in the voids.

When the sample is held at a positive voltage, the image of a chrysene molecule is different from that obtained when the sample is negative. The positive sample image shows a tunneling pattern over an individual chrysene molecule that resembles the shape of the chrysene π-LUMO electronic wavefunction while the tunneling pattern with negative sample bias resembles the π-HOMO electronic state wavefunction. (Wavefunctions were calculated in vacuum without the influence of the graphite surface using DFT.) This suggests that the tunneling process for electrons moving from tip to surface is predominantly mediated by the empty LUMO state, while tunneling from surface to tip is dominated by the filled HOMO orbital. Though such behavior is somewhat unusual for non-conjugated hydrocarbons on graphite, it is likely to be typical of highly conjugated systems such as PAH's. Molecules of this type have relatively small HOMO-LUMO gaps and ionization potentials, which taken together, place the HOMO and LUMO levels of the adsorbates near in energy to the surface Fermi level. When this happens, tunneling into the surface tends to be dominated by the empty LUMO while tunneling out of the surface tends to be dominated by the filled HOMO level.

While flat chrysene, having no carbon sp^3 hybridized bonds, is achiral in 3 dimensions, when adsorbed flat on the surface it becomes pro-chiral. Essentially, in two dimensions the mirror image of a chrysene molecule cannot be superimposed on itself without lifting the molecule up and flipping it over. As might be expected for our relatively high temperature deposition conditions, the arrays of chrysene molecules on the surface show equal numbers (within $[N]^{1/2}$) of "left" and "right" handed species. These mirror image molecules appear

90

to be intermixed in a random fashion, neither separating into chiral domains nor forming regular arrays of side by side chirally alternating species. Eventually, we hope to probe whether the prochiral nature of the chrysene affects its reactivity.

Present and Future Experimental Program

We plan to continue our efforts to identify small and large PAH molecules and their precursors on graphite surfaces. These identification studies are necessary before investigations of surface chemical reactions are begun. The STM techniques described above will be supplemented with Scanning Tunneling Spectroscopy methods that allow the electronic energies of the adsorbate molecular states to be determined relative to the graphite Fermi level. The spectroscopic "signatures", especially for different conjugated molecules, are expected to be quite distinct, thereby providing another means of identifying individual molecules on the surface. Once a number of individual species have been so probed and their STM and STS signatures determined, we plan to study mixtures of several PAH's to determine if specific molecules can be located on the surface in a 2-dimensional mixture.

Our variable temperature STM allows us to image surfaces at temperatures as high as 1200 K in order to characterize both the pre- and post-reaction landscapes. Since acetylene appears to be the principal fuel that drives the surface reactions that lead to soot growth (H abstraction-C_2H_2-addition or "HACA" mechanism),[3,4] in the first high temperature experiment we plan to spray acetylene onto a hot graphite surface to see if there is any growth in the surface carbon layers, particularly near step edges and defects. While simple acetylene (C_2H_2) is the most appealing candidate for the fuel in this case (because it is thought to be the "active ingredient" for soot growth in combustion systems),[3,4] we can also use substituted acetylenes (e.g. C_2HI or C_2HBr), which are more likely to produce radicals such as C_2H upon striking the hot surface. In experiments of this type, it should also be possible to co-deposit or spray both acetylene and small to medium sized PAH molecules on the surface simultaneously. The STM can then be used to test for new structures formed at step edges in the presence of the PAH/acetylene combination.

Studies of clean graphite itself will also be undertaken to search for defects and step edges. Low and high temperature STM images of graphite can be obtained to see if these structures are stable on the surface. Following this, we plan to add oxygen to our chamber to determine the reactivity of defects and step edges by probing the change in surface STM images before and after the addition of oxygen.

References

1. J. A. Miller and G. A. Fisk, "Combustion Chemistry", Chem. & Eng. News, 65 (35), 22-46, August 31, 1987
2. C. S. McEnally, A. G. Robinson, L. D. Pfefferle and T. S. Zwier, "Aromatic Hydrocarbon Formation in Nonpremixed Flames Doped with Diacetylene, Vinylacetylene, and Other Hydrocarbons: Evidence for Pathways Involving C4 Species", Combustion and Flame 123, 344-357 (2000)
3. M. Frenklach, "Reaction mechanism of soot formation in flames", Phys. Chem. Chem. Phys. 4, 2028-2037 (2002)
4. M. Frenklach and H. Wang, "Detailed modeling of soot particle nucleation and growth", Proc. Combust. Inst. 23, 1559-1566 (1991)
5. H. Richter and J. B. Howard, "Formation of Polycyclic Aromatic Hydrocarbons and their Growth to Soot – A Review of Chemical Reaction Pathways", Prog. Energy and Combust. Sci. 26, 565-608 (2000)
6. C. F. Melius, M. E. Colvin, N. M. Marinov, W. J. Pitz and S. M. Senkan, "Reaction mechanisms in aromatic hydrocarbon formation involving the C_5H_5 cyclopentadienyl moiety", Proc. Combust. Inst. 26, 685-692 (1996)

7. P. R. Westmoreland, A. M. Dean, J. B. Howard and J. P. Longwell, "Forming benzene in flames by chemically activated isomerization", J. Phys. Chem. 93, 8171-8180 (1989)

8. M. Frenklach, N. W. Moriarty and N. J. Brown, "Hydrogen migration in polyaromatic growth", Proc. Combust. Inst. 27, 1655-1661 (1998)

9. M. Frenklach, "On surface growth mechanism of soot particles", Proc. Combust. Inst. 26, 2285-2293 (1996)

10. C. A. Arrington, C. Ramos, A. D. Robinson and T. S. Zwier, "Aromatic ring-forming reactions of metastable diacetylene with 1, 3-butadiene", J. Phys. Chem. A 102, 3315-3322 (1998)

11. N. M. Marinov, W. J. Pitz, C. K. Westbrook, M. J. Castaldi and S. M. Senkan, "Modeling of aromatic and polycyclic aromatic hydrocarbon formation in premixed methane and ethane flames", Combust. Sci. Technol. 116, 211-287 (1996)

12. R. Backreedy, J. M. Jones, M. Pourkashanian and A. Williams, "A study of the reaction of oxygen with graphite: Model chemistry", Faraday Discuss. 119, 385-394 (2001)

13. Forrest Stevens, Lisa A. Kolodny, and Thomas P. Beebe, Jr. "Kinetics of Graphite Oxidation: Monolayer and Multilayer Etch Pits in HOPG Studied by STM" J. Phys. Chem. B, 102, 10799-10804 (1998)

14. B. Venkataraman, G. W. Flynn, J. Wilbur, J. P. Folkers, G. M. Whitesides, "Differentiating Functional Groups with the Scanning Tunneling Microscope", Journal of Physical Chemistry, 99, 8684-8689 (1995).

15. D. M. Cyr, B. Venkataraman, G. W. Flynn, A. Black, and G. M. Whitesides, "Functional Group Identification in Scanning Tunneling Microscopy of Molecular Adsorbates", Journal of Physical Chemistry, 100, 13747-13759 (1996).

16. Thomas Müller, George Flynn, Anna T. Mathauser and Andrew Teplyakov, "Temperature Programmed Desorption Studies of n-Alkane Derivatives on Graphite: Desorption Energetics and the Influence of Functional Groups on Adsorbate Self-Assembly", Langmuir, 19, 2812-2821 (2003)

17. Leanna C. Giancarlo and George W. Flynn, "Scanning Tunneling and Atomic Force Microscopy Probes of Self-Assembled, Physisorbed Monolayers: Peeking at the Peaks", Annu. Rev. Phys. Chem., 49, 297-336 (1998)

18. L.C. Giancarlo and G. W. Flynn, "Raising Flags: Applications of Chemical Marker Groups to Study Self-Assembly, Chiralty, and Orientation of Interfacial Films by Scanning Tunneling Microscopy", Accts. Chem. Res., 33, 491-501 (2000)

19. M. Hibino, A. Sumi, and I. Hatta, "Atomic Images of Saturated and Unsaturated Fatty Acids at Liquid/Graphite Interface and Difference of Tunneling Currents between Them Observed by Scanning Tunneling Microscopy", Jap. J. Appl. Phys., 34, 610-614 (1995).

DOE Publications: (2002-2004)

1. George W. Flynn, Encyclopedia of Chemical Physics and Physical Chemistry, Volume III: Applications, Part C3 Chemical Kinetics and Dynamics, "Energy Transfer in Gases", John Moore and Nicholas Spencer, Eds., Institute of Physics Publishing, Bristol and Philadelphia, pp 2681-2700, (2002)

2. Natalie Seiser, Kavita Kannappan, George Flynn, "Long Range Collisional Energy Transfer from Highly Vibrationally Excited Pyrazine to CO Bath Molecules: Excitation of the v=1 CO Vibrational Level", J. Phys. Chem., 107, 8191-97, (2003)

3. Gina M. Florio, Tova L. Werblowsky, Thomas Mueller, Bruce J. Berne, and George W. Flynn, "The Self-Assembly of Small Polycyclic Aromatic Hydrocarbons on Graphite: A Combined STM and Theoretical Approach, in preparation.

Gas-Phase Molecular Dynamics: Radical-Radical Reaction Kinetics

Christopher Fockenberg and Jack M. Preses

Chemistry Department, Brookhaven National Laboratory, Upton, NY 11973-5000

fknberg@bnl.gov, preses@bnl.gov

The purpose of this program is to explore the kinetics of chemical reactions resulting from molecular collisions in the gas phase. The goal of this work is a fundamental understanding of chemical processes related to combustion. We are interested in the microscopic factors affecting the structure, dynamics and reactivity of short-lived intermediates such as free radicals in gas-phase reactions. Molecular species are studied using both experimental and theoretical tools including high-resolution spectroscopic probes, time-of-flight mass spectrometry, *ab initio* electronic structure calculations and both time-dependent and time-independent quantum calculations of nuclear motion. The synergy between the experimental and theoretical components of the research is an important element in achieving the goals of the program.

Recent Progress

Kinetics studies of the CH_3 + OH reactions

Current research is focused on measuring the kinetics and especially the product distribution of the methyl-hydroxyl radical reaction at low pressures and temperatures around 620 K:

$$
\begin{aligned}
CH_3 + OH \quad &\rightarrow CH_3OH & (1a)\\
&\rightarrow {}^1CH_2 + H_2O & (1b)\\
&\rightarrow CH_2O + H_2 & (1c)\\
&\rightarrow HCOH + H_2 & (1d)\\
&\rightarrow CH_3O + H & (1e)\\
&\rightarrow CH_2OH + H. & (1f)
\end{aligned}
$$
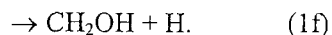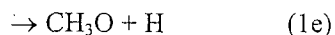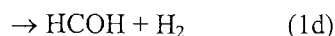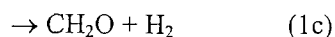
According to *ab initio* calculations carried out in our group, the energies of almost all transition states lie within a few kcal/mol of the entrance channel making the product distribution very sensitive to pressure and temperature.

Particular attention is placed on channel (1d), the transition state for which lies below the energy of the reactants, and, therefore, should be able to compete at low pressures and/or high temperatures with channel (1b) that lies energetically above the entrance channel. We believe the lifetime of the hydroxymethylene radical to be short due to fast isomerization to formaldehyde. To distinguish the formaldehyde from the ethane signal, ^{13}C-labeled acetone is used leading to a separation of $^{13}C_2H_6$ (*m/e* = 32) from $^{13}CH_2O$ (*m/e* = 31). The complex nature of the chemistry involved makes it necessary to analyze the experiments by simulation calculations, for which will make use of our new computer program based on the Chemkin program package employing genetic and simplex algorithms. The current version allows several different types of parameters, such as rate constants and their temperature dependencies, signal-to-concentration conversion factors, initial concentrations, and signal offsets to be fitted to the complete data set.

OH radicals are generated in the reaction of singlet oxygen atoms, $O(^1D)$, with hydrogen molecules or water, which also serves as collision partner for OH thermalizing the vibrational hot distribution quickly. $O(^1D)$ atoms are produced by the photolysis of nitrous oxide at 193 nm. The relatively small absorption coefficient of N_2O limits the amount of hydroxyl radicals that can be produced in these experiments, which, however, reduces secondary chemistry involving OH radicals. Unfortunately, OH radicals are not

observable with the current apparatus so that their existence has to be inferred from their reaction products. Nevertheless, experiments undertaken at room temperature and 620 K, show the increasing yield of CH_2O with increasing temperature (see Fig. 1).
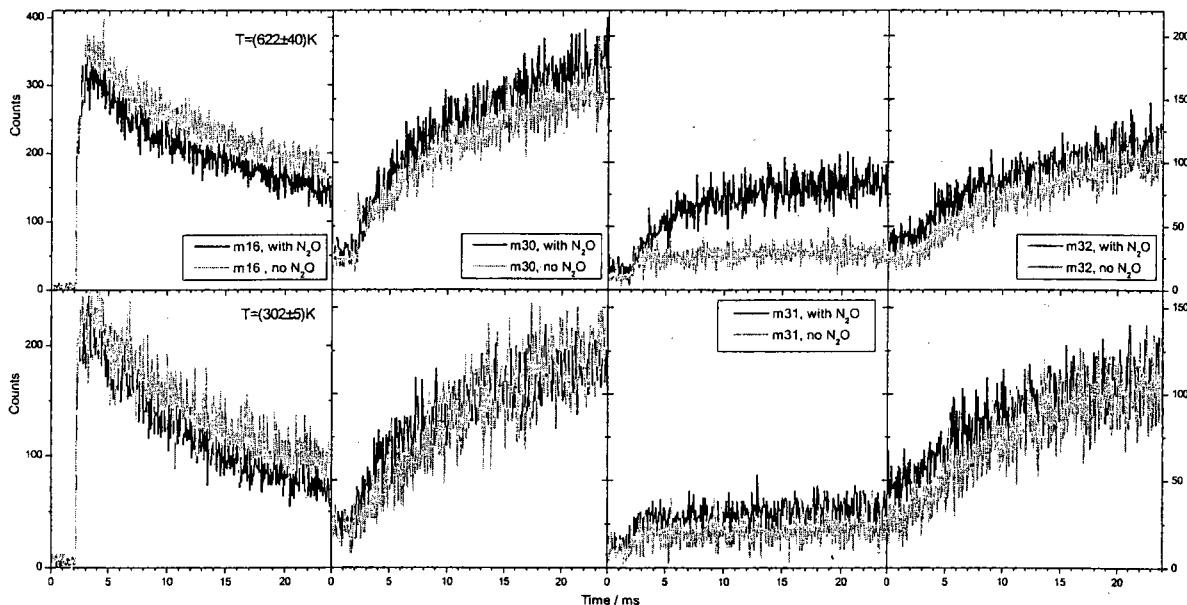
Figure 1. Signal traces observed for the $^{13}CH_3$+OH reaction at masses 16 ($^{13}CH_3$), 30,31, and 32 ($^{13}C_2H_4$, $^{13}C_2H_6$, $^{13}CH_2O$) at room temperature (lower row) and 622 K (upper row). Black and gray coloring indicates differences between traces obtained with OH radicals present (black) and absent (gray).

Mid-IR Diode laser absorption studies of the reaction of CH_3 and OH

The TOF experiments described above suggest a minor channel in the reaction of CH_3 and OH radicals ultimately producing CH_2O (perhaps *via* a CHOH intermediate that cannot be differentiated from CH_2O in the TOF experiment). In order to confirm the production of CH_2O, we use mid-IR diode laser absorption to detect CH_2O unequivocally.

As in any mid-IR diode laser experiment, the first decision is the choice of wavelength to use: an intense diode may not be available where strong molecular transitions occur or *vice versa*. The C–H stretching region near 3 μm is a natural choice, but diodes are generally poor at this wavelength, and the broad spread of the wavelengths of C–H stretching transitions means that an individual diode covers absorptions of few molecules. An excellent second choice of diode wavelength turns out to be the C–H bending region near ~1450 cm^{-1}. An intense diode was obtained, and C–H bending transitions from different molecules are much more narrowly distributed in wavelength than in the C–H stretching region, so that a single diode covers absorptions of several molecules, such as CH_2O, CH_3OH, H_2O, C_2H_6, and C_3H_3Cl, absorptions from which have been confirmed using this diode. The potential to observe absorptions of other molecules using this diode, such as other hydrocarbons is likely.

CH_3 and OH radicals were prepared as in the TOF experiment using the reaction scheme explained above. Pressures were chosen so that [CH_3] was greatly in excess of [OH], and overall reactant pressures were kept sufficiently low to minimize "dark" reactions between radicals and molecules between laser pulses. The diode was ramped over a wavelength range covering a strong CH_2O absorption line without interference from a C_2H_6 absorption line (C_2H_6 is the major product). Lines were verified using authentic samples of CH_2O and C_2H_6. Other possible accidental interferences from molecules such as H_2O were carefully ruled out. Absorption was detected after single excimer laser pulses, and product concentration

94

was monitored following generation of the radicals as a function of the number of excimer laser pulses in order to reveal the role of secondary chemistry. Preliminary results confirm that secondary chemistry is not a problem. Confirmation of the presence of CH_2O and quantification of the yield is presently underway.

Another application of diode absorption involves the reaction of propargyl radicals and H atoms. Propargyl, C_3H_3, appears to be *the* important species in the formation of early aromatic rings leading to the formation of soot.[1,2] We have undertaken a TOF study of the reaction of C_3H_3 with H atoms using propargyl chloride as a radical precursor. Analysis of the reaction scheme has turned out to be more complex than expected. Our TOF experiments confirmed that allene, $H_2C=C=CH_2$ is one product of the reaction between C_3H_3 and H atoms, and we wanted to make a precise determination of the allene yield. We have undertaken a series of diode laser absorption experiments to determine the allene yield by comparing the loss of propargyl radicals with the appearance of allene. The reaction scheme involves 193-nm production of propargyl from propargyl chloride, and H-atoms from H_2S, velocity modulated with He.

The flowing reaction mixture contained excess H_2, and among the products is allene. Assuming that the only photolysis products are as above, measuring the loss of propargyl chloride determines the initial concentration of propargyl radicals. Measurement of allene concentration then permits the determination of the allene yield. Allene absorptions are identified by comparison with authentic allene sample using the allene v_2 CH_2 scissors-mode absorption near 1440 cm^{-1}.

Allene is a stable molecule whose structure has long been known. Its detailed IR spectroscopy, however, is much less well known, and many of its rovibrational transitions have not been analyzed in detail. In connection with this work, we obtained a high-resolution allene v_6 absorption spectrum from S. Sharpe (PNNL) in order to calibrate our 1957 cm^{-1} diode (initial experiments were performed using a v_6 transition) and to identify allene absorption features. We are currently working toward assigning this transition and determining the molecular constants in the v_6 state. The opportunity to perform this work is a good indicator of the advantages of the combined expertise that our group brings to bear on scientific problems, and it demonstrates the utility of cooperation between programs at different National Laboratories.

Future Work

TOFMS study of ketene photolysis at 193 nm

Time permitting, we will investigate the photolysis of ketene at 193 nm. Recent studies show significant discrepancies in the photolytic yields for singlet *vs.* triplet methylene as well as ketenyl radicals. By exchanging hydrogen for helium as bath gas or by adding water we hope to determine the relative amount of singlet to total methylene produced by observing changes in the CH_2 and CH_3 signals. Based on these results we can work on answering specific questions, such as temperature dependence, of physical compared to reactive quenching of $^1CH_2$ by H_2 or O_2.

References

1. J. A. Miller, C. F. Melius, *Combust. Flame* **91**, 21 (1992).
2. R. D. Kern, H. Chen, J. H. Kiefer, P. S. Mudpalli, *Combust. Flame* **100**, 177 (1995).

Publications since 2002

1. R. A. Holroyd and J. M. Preses, *Radiation Chemical Effects of X-Rays on Liquids*, in *Chemical Applications of Synchrotron Radiation*. 2002, World Scientific Publishing: Singapore.
2. B. Wang, H. Hou, L. Yoder, J. T. Muckerman and C. Fockenberg, *Experimental and Theoretical Investigations on the Methyl-Methyl Recombination Reaction*. J. Phys. Chem. *A* **107**, 11414 (2003).

Acknowledgment

Quantitative Imaging Diagnostics for Reacting Flows

Jonathan H. Frank
Combustion Research Facility
Sandia National Laboratories, MS 9051
Livermore, CA 94551
jhfrank@ca.sandia.gov

Program Scope

The primary objective of this project is the development and application of laser-based imaging diagnostics for studying reacting flows. Imaging diagnostics provide temporally and spatially resolved measurements of species, temperature, and velocity distributions over a wide range of length scales. Multi-dimensional measurements are necessary to determine spatial correlations, scalar and velocity gradients, flame orientation, curvature, and connectivity. Our current efforts focus on planar laser-induced fluorescence (PLIF) and Rayleigh scattering techniques for probing the detailed structure of both isolated flow-flame interactions and turbulent flames. The investigation of flow-flame interactions is of fundamental importance in understanding the coupling between transport and chemistry in turbulent flames. These studies require the development of a new suite of imaging diagnostics to measure key species in the hydrocarbon-chemistry mechanism as well as to image rates of reaction and scalar dissipation.

Recent Progress

Recent research has continued to emphasize the development and application of diagnostics for probing the detailed structure of reaction zones during flow-flame interactions. The coupling of measurements with simulations also remains an essential element of this program. Research activities have included the following: i) Interference-free PLIF measurements of atomic oxygen with picosecond excitation, ii) An investigation of the interaction between flow transients and ignition kernels, iii) Reaction-rate imaging with CO and OH PLIF in edge flames.

Atomic oxygen imaging We have demonstrated the use of picosecond lasers to reduce photolytic interference in two-photon O-atom LIF imaging. Quantitative 2-D measurements of atomic oxygen concentrations in flames are needed to better understand the coupling between transport and combustion chemistry and in particular, nitric oxide formation. Two-photon LIF can provide sensitive detection of atomic oxygen in flames. However, previous studies using nanosecond pulsed lasers have shown that photolytically produced O-atoms cause a significant interference to measurements of the naturally occurring oxygen. We conducted a comparison of O-atom LIF line imaging with ps- and ns-laser excitation at 226 nm ($3p^3P \leftarrow \leftarrow 2p^3P$) and detection at 845 nm ($3p^3P \rightarrow 2s^3S$) in premixed methane and hydrogen flames. Our measurements indicated that thermally excited CO_2 is the dominant precursor to photolytically produced atomic oxygen in hydrocarbon flames. This result is contrary to the conventional belief that vibrationally excited O_2 is the primary photolytic precursor. We measured the photolytically produced atomic oxygen directly using a ns and a ps laser in a pump/probe configuration in both hydrogen and methane flames. In this configuration, the ns laser was tuned off the O-atom resonance, and the ps laser was tuned on resonance to measure the photolytically produced O-atom. In lean premixed H_2/O_2 flames, interference from O_2 photolysis was negligible compared to the LIF signal from the native O-atoms. Consequently, interference-free LIF measurements were obtained in the H_2/O_2 flame using either the ns or the ps laser. In lean ($\phi=0.70$) methane flames, however, the ns laser produced significant photolytic interference, and the interference increased dramatically with the addition of CO_2 as a diluent.

The ps laser offers an advantage because at 226 nm the O-atom excitation is a two-photon process, and the photolysis is a single-photon process. Because the two-photon LIF signal depends quadratically on laser *intensity*, while the photolysis process depends linearly (or sublinearly) on laser *energy*, we reduced the interference by an order of magnitude when exciting LIF with a 55-ps pulse instead of 3.5-ns pulse. The extension of two-photon LIF measurements to two dimensions is complicated by relatively weak absorption cross sections and the nonlinear dependence of the LIF signal on laser intensity. To facilitate 2-D imaging, we added an amplification stage to the ps dye laser. Using the modified ps laser, we demonstrated two-dimensional interference-free O-atom LIF measurements. Our results of O-atom LIF imaging in an acoustically forced Bunsen flame illustrate the feasibility of investigating O-atom distributions during a flow-flame interaction. This project is conducted in collaboration with Tom Settersten (Sandia).

Interaction of flow transients and ignition kernels We have investigated the effects of transient flows on hydrogen ignition kernels in a nonpremixed counterflow. The ultimate goal of this effort is to develop the capability of accurate predictions for hydrocarbon fuel ignition in transient flows. In this initial study, hydrogen flames provided a good testbed because the chemical mechanism is relatively simple. Experiments were performed in collaboration with Kal Seshadri (UCSD), and Jackie Chen (Sandia) conducted an accompanying computational study. In the experiments, we measured the temporal evolution of OH during the ignition of a hydrogen flame in steady and unsteady laminar opposed flows. Prior to ignition, a mixing layer was established with heated air flowing from one side of the burner and a N_2-diluted H_2 mixture ($X_{H2}=0.08$) flowing from the opposite side. Ignition was initiated by photodissociating molecular oxygen in the heated air flow with an ArF laser ($\lambda=193nm$), thereby producing a sheet of $O(^3P)$ atoms. The impact of the laser-initiated ignition was minimized by setting the temperature of the oxidizer flow to 3K below the autoignition temperature and using the minimum laser fluence that reliably ignited the flame. This laser-initiated ignition was sufficiently repeatable that we could record the temporal evolution of the ignition kernel by measuring OH PLIF over multiple ignition events while varying the time delay between the ArF laser and the OH-PLIF laser.

For ignition in a steady strained counterflow, the OH exhibited a 60% overshoot relative to a steady diffusion flame. This peak value was attained at 6 ms after the ignition laser pulse. To study the effects of unsteady strain, the fuel flow was pulsed at different times after the initiation of ignition. The survival of the flame kernel was highly dependent on the time history of the flow. For a time delay of 3.9 ms, the kernel extinguished and never recovered. For time delays of 4.5 ms and 5.5 ms, the transient flow increased the induction time and decreased the amount of OH overshoot. These results indicate the complexity of modeling localized extinction and ignition processes in turbulent flows.

The measured temporal evolution of the peak centerline OH for the different cases was compared with unsteady 1-D laminar flame calculations. The simulations captured the extinction of the 3.9-ms case as well as the delayed ignition and reduced OH overshoot of the 4.5-ms and 5.5-ms cases. However, the computations predicted a smaller OH overshoot than was observed experimentally. Multi-dimensional effects may need to be included, and 2-D direct numerical simulations are under way. To better understand the factors contributing to the increased ignition delay with impulsive straining, we examined the time history of an instantaneous Damköhler number, based on the net ratio of the net reaction rate of OH to the diffusion of OH. This measure showed partial (4.5-ms case) or complete quenching (3.9-ms case) of the kernel attributed to excessive scalar dissipation rate encountered during the initial phases of chemical induction.

Reaction-rate imaging in edge flames The investigation of edge-flame behavior is important for understanding diffusion-flame stabilization as well as local extinction/ignition phenomena in highly strained turbulent flames. In collaboration with Alessandro Gomez (Yale) and Mitchell Smooke (Yale), we have conducted an initial study of edge-flame propagation during extinction and ignition of a

counterflow methane-air flame using simultaneous CO/OH PLIF to determine the forward reaction rate of CO+OH = CO_2+H. This reaction represents the primary pathway for the formation of CO_2 in a methane-air flame. The basic concept of the diagnostic involves using the product of simultaneous OH and CO PLIF measurements to obtain an image with a signal proportional to the reaction rate. Results showed that the reaction-rate did not increase significantly near the tip of the strained edge flame. In contrast, previous simulations of unstrained edge flames predicted a significant increase in the reaction rate near the tip. The relative velocity of the reactants and the flame was determined from particle image velocimetry (PIV) measurements in Sandia's Turbulent Combustion Laboratory. The results indicated that the extinction edge flame was advected by the mean flow, and we found no evidence of a negative propagation velocity. These experimental results will be coupled with 2-D simulations performed at Yale University.

Future Plans

Reaction-rate imaging We plan to continue the development and application of diagnostics that provide imaging measurements of reaction-rates. The new capability of O-atom LIF imaging will be used to develop a technique for measuring the spatial distribution of the forward reaction rate of the N_2+O = N + NO reaction, which is the rate-limiting step for the Zeldovich, or 'thermal', mechanism of NO production.

Mixture fraction imaging We plan to expand our initial demonstration of simultaneous 2-D mixture-fraction and temperature measurements by implementing the technique in a wider range of turbulent jet flames and repeatable flow-flame interactions. Further developments are needed to determine the uncertainty of the scalar dissipation rates and to extend the technique to flames having localized extinction. A portion of this effort will be conducted in collaboration with Marshall Long (Yale).

C_2-Species diagnostic We are developing a laser-induced fragmentation fluorescence (LIFF) technique for probing vinyl (C_2H_3) and acetylene (C_2H_2) in premixed flames. As part of the development, we will conduct a series of low-pressure flame experiments to quantify the temperature dependence of the LIFF signal by combining LIFF measurements with photoionization mass spectrometry in a low-pressure flame. The mass spectrometer will provide quantitative measurements of the vinyl and acetylene profiles in the flames. Measurements will be performed on the Chemical Dynamics Beamline of the Advanced Light Source (ALS) at Lawrence Berkeley National Laboratory in collaboration with David Osborn (Sandia), Craig Taatjes (Sandia), Terrill Cool (Cornell), and Stephen Leone (Berkeley).

Effects of unsteady flow on premixed flames In collaboration with Habib Najm (Sandia), a joint numerical and experimental investigation will be conducted in an acoustically forced axisymmetric Bunsen flame. This burner configuration provides advantages over the previously studied V-flame burner. Our continually expanding suite of imaging diagnostics will be applied to study the transient response of axisymmetric flames. Initial O-atom LIF measurements were already performed in this burner. We are particularly interested in studying the response of NO formation to unsteady flows.

Two-photon LIF imaging: O-atom and H-atom We plan to build upon our recent progress in interference-free imaging of two-photon O-atom LIF and refine the diagnostic technique through continued collaboration with Tom Settersten. The proposed activities include measurements of the O-atom yields from photolysis of CO_2, determination of the temperature-dependent quenching cross-sections of atomic oxygen, and the development of an *in situ* calibration technique for absolute O-atom measurements. To take full advantage of our new capability for interference-free O-atom LIF imaging, we propose to add O-atom LIF measurements to the suite of imaging diagnostics that is currently

available in the Advanced Imaging Laboratory (AIL). This effort will involve the construction of a tunable picosecond dye laser system in the AIL facility.

Atomic hydrogen is another key radical in combustion chemistry that is challenging to measure without photolytic interference. We plan to investigate H-atom LIF detection with ps lasers as a possible means to obtain H-atom measurements without photolytic interference. In two-photon H-atom LIF, ground-state atomic hydrogen is excited at 205 nm via the $3d\,^2D\leftarrow\leftarrow1s\,^2S$ transition, and fluorescence is detected from the $3d\,^2D\rightarrow2p\,^2P$ transition at 656 nm. Single-photon photodissociation of CH_3 and thermally excited water molecules is a significant source of photolytic interference for 205-nm excitation. Since H-atom LIF excitation is a two-photon process while the photolytic interference is a single-photon process, ps-laser excitation may provide a significant advantage over ns lasers.

Adequacy of CH laser-induced fluorescence as a marker of heat release rate The CH radical is frequently used as a flame marker because it is relatively short lived, is present over a narrow region in flames, and can be measured by LIF. Discontinuities in the CH LIF signal along a flame front are often interpreted as localized extinction of the flame. However, the adequacy of CH LIF as a flame marker is questionable. To resolve this issue, we will conduct a detailed study of the correlation between CH LIF and heat release rate in steady and unsteady flames. Simultaneous OH and CH_2O LIF measurements will be used to determine variations in the forward reaction rate of $CH_2O+OH \rightarrow HCO + H_2O$, which is highly correlated with the rate of heat release in premixed methane/air flames.

Ignition processes in transient flows We plan to investigate a broader range of conditions for hydrogen ignition and study the edge-flame propagation that occurs as the ignition kernel spreads. In addition, measurements of other key species will be performed. We will extend the ignition and edge-flame studies to include hydrocarbon fuels. This effort will be conducted in collaboration with Jackie Chen (Sandia) and Kal Seshadri (UCSD).

DOE Supported Publications (2002 – present)

1. J. H. Frank, S. A. Kaiser, and M. B. Long, "Reaction-rate, Mixture Fraction, and Temperature Imaging in Turbulent Methane/Air Jet Flames," *Proc. Combust. Inst.* 29:2687 (2002).

2. J. Fielding, J. H. Frank, S. A. Kaiser, M. D. Smooke, and M. B. Long, "Polarized/Depolarized Rayleigh Scattering for Determining Fuel Concentrations in Flames," *Proc. Combust. Inst.* 29:2703 (2002).

3. C. M. Vagelopoulos and J. H. Frank, "Effects of Flow and Chemistry on OH Levels in Premixed Flame-Vortex Interactions," *Proc. Combust. Inst.* 29:1721 (2002).

4. J.H. Frank, X. Chen, B.D. Patterson, T.B. Settersten, "Comparison of Nanosecond and Picosecond Excitation for Two-Photon LIF Imaging of Atomic Oxygen in Flames," *Appl. Opt.*, in press (2004).

5. J.H. Frank and T.B. Settersten, "Two-photon LIF Imaging of Atomic Oxygen in Flames with Picosecond Excitation," *Proc. Combust. Inst. 30,* in press (2004).

6. C.M. Vagelopoulos and J.H. Frank, "An Experimental and Numerical Study on the Adequacy of CH as a Flame Marker in Premixed Methane Flames," *Proc. Combust. Inst. 30,* in press (2004).

7. R. Seiser, J.H. Frank, S. Liu, J.H. Chen, R.J. Sigurdsson, and K. Seshadri, "Ignition of Hydrogen in Unsteady Nonpremixed Flows," *Proc. Combust. Inst. 30,* in press (2004).

8. G. Amantini, J.H. Frank, and A. Gomez, "Experiments on Standing and Traveling Edge Flames around Flame Holes in Both Ignition and Extinction Modes," *Proc. Combust. Inst. 30,* in press (2004).

MECHANISM AND DETAILED MODELING OF SOOT FORMATION

Principal Investigator:Michael Frenklach

Department of Mechanical Engineering
The University of California
Berkeley, CA 94720-1740
Phone: (510) 643-1676; E-mail: myf@me.berkeley.edu

Project Scope: Soot formation is one of the key environmental problems associated with operation of practical combustion devices. Mechanistic understanding of the phenomenon has advanced significantly in recent years, shifting the focus of discussion from conceptual possibilities to specifics of reaction kinetics. However, along with the success of initial models comes the realization of their shortcomings. This project focuses on fundamental aspects of physical and chemical phenomena critical to the development of predictive models of soot formation in the combustion of hydrocarbon fuels, as well as on computational techniques for the development of predictive reaction models and their economical application to CFD simulations. The work includes theoretical and numerical studies of gas-phase chemistry of gaseous soot particle precursors, soot particle surface processes, particle aggregation into fractal objects, and development of economical numerical approaches to reaction kinetics.

Recent Progress:

Homogeneous Nucleation of Carbon Nanoparticles (with S. C. Schuetz)

We completed molecular dynamics (MD) simulations with on-the-fly quantum forces investigating collisions of different-size aromatics. It is widely accepted that polycyclic aromatic hydrocarbons (PAH) are the precursors to soot particles. However, the mechanisms that transform gaseous PAH molecules into solid phase soot particles are still unclear. In the previous study, we performed molecular dynamics simulations that demonstrated how binary collisions of pyrene molecules could form van der Waals dimers, under practical flame conditions. The results indicated that during collisions, the constituent PAH monomers of the dimer develop internal free rotors. These internal rotors absorb and trap a portion of the collisional energy, resulting in dimers with lifetimes sufficient to evolve into soot nuclei.

Our previous study focused on the dimerization of pyrene because of the species exceptional stability and suggested role in initiating particle nucleation. In the present study, we investigated the effects of monomer size on the dynamics of PAH collisions to further explore the phenomena of PAH dimerization and the roll it may play in soot nucleation. We examined binary collisions of coronene, to see if increasing monomer size would interfere with the development of internal rotors. Then we examined collisions of different sized PAHs, with collisions of coronene-pyrene, coronene-anthracene, and coronene-napthalene. Additionally, we explored the effect of radicals on PAH dimerization with collisions between pyrene and its radical.

The MD simulations were successful in producing dimers of coronene-coronene, coronene pyrene, and coronene-anthracene with substantial collision frequency and lifetimes far exceeding the equilibrium-based predictions. Dimers of coronene with naphthalene and pyrene with its radical were also examined, yet dimers with long lifetimes were not observed in these runs. The principal finding of the present study is the forming dimers are stabilized by the development of internal rotors. It was observed that smaller molecules developed internal rotations more quickly

than large molecules; yet, all of the species examined effectively trapped collisional energy in rotational modes.

The combined results of this and the previous study form a general understanding of how binary collisions of PAH molecules can form dimers, with significant collision frequency and lifetime, under typical combustion conditions. Consistent with our previous study, the principal findings of the performed numerical simulations is that the constituent PAH monomers of the dimer develop internal free rotors, and this phenomenon translates into substantially increased dimer lifetimes. The implication is that physical clustering is a phenomena common to a range of small and midsized PAH species, and that PAH clusters are likely to survive long enough to evolve into soot nuclei.

Soot Particle Surface Reactions (with S. C. Schuetz and J. Ping)

We completed initial sterically-resolved Monte Carlo simulations investigating the migration mechanism of aromatic-edge growth. A new reaction pathway is suggested for the five-member ring migration along a graphene edge. The migration sequence is initiated by H-atom addition to the adsorbed cyclopentha group. The elementary steps of the migration pathway were analyzed using quantum ab initio calculations. Based on the obtained energetics, the dynamics of the system were investigated by solving master equations. The reaction rates show values sufficiently high to compete with, and even dominate, other surface reactions. The kinetics results indicate that the rate-limiting step of the migration sequence is the β-scission of the five-member ring after the addition of H atom, with the rest of the steps reaching partial equilibrium at higher temperatures. Employing the new migration kinetics along with adsorption, desorption, and growth steps sterically resolved kinetic Monte Carlo simulations were carried out at conditions typical of soot growth in hydrocarbon flames. The simulation results provide further support to the critical role of the five-member ring migration in the growth of graphene layers. The evolving surface morphology and ensuing growth rate are determined by the competition between migration of five-member rings and "nucleation" of six-member rings at surface corners. An important implication of this migration phenomenon is that while five-member rings are being constantly formed on the growing edge, they do not accumulate; rather they are converted to six-member rings.

The molecular structures produced in the present Monte Carlo simulations are consistent with recent spectroscopic observations of PAH species in interstellar clouds.

Particle Aggregation with Simultaneous Surface Growth: the Effect of a Realistic Particle Size Distribution (with M. Balthasar)

Transformation of gas into particulate matter is at the core of a variety of natural phenomena and industrial processes; examples may include formation of atmospheric fog, combustion soot, interstellar dust, carbon black, and commodity ceramics like fumed silica and pigmentary titania. Conventional description of the particulate inception begins with homogeneous nucleation of precursors in the gas phase, leading to the appearance of the first recognizable particles. These *primary* particles are assumed to be spherical and collisions among them coalescent, i.e., forming larger spherical particles. In the case of solid particulates, the collected samples often exhibit characteristics of fractal-like aggregates. It is understood therefore that the initial period of coalescent growth must transition to particle aggregation. Surface deposition also contributes to particle growth. Gas phase species attach themselves to the surface of the particles during both

the coalescent and aggregation stages of formation. This adds a layer of mass on the particle surface.

While the formation of particle aggregates is well documented and their fractal-like appearance is well characterized, the transition between the formation of primary particles and chain-like aggregates is not well understood. In the past few years, we investigated this transition using dynamic Monte-Carlo simulations and on the basis of these results developed a formulation that captures the essential physics but in a form that allowed us to incorporate the aggregation phenomena into the method of moments. The latter was coupled with our detailed chemical kinetic mechanism of soot formation. The combined model was applied to ensemble-average simulations of a number of burner stabilized premixed laminar flames and the results were validated against experimental observations of soot yields and particle sizes.

During the past year, we completed Monte-Carlo simulations of soot particle coagulation and aggregation whose objective was to investigate further the key notion of the prior studies—the critical role of the small particles on the transition from coalescent to aggregate growth. Specifically, we focused on the effect of a realistic particle size distribution on the sphericity of primary particles. The particle distribution was treated explicitly and use was made of the transition location predicted by the simulations with the method of moments with interpolative closure. Using this approach, shapes of individual primary particles and integral quantities describing the state of the particle ensemble were investigated.

The evolution of the soot particle morphology was investigated in a laminar premixed flame of ethylene with the emphasis on the effect of a realistic particle size distribution. The flame was divided into a nucleation-dominated zone early in the flame and a post-nucleation zone governed by surface growth and aggregation. The transition between the two zones was taken from the results of our prior study. In the nucleation zone of the flame, particles were allowed to grow by coagulation and surface growth while only surface growth was applied in the post-nucleation zone. This is motivated by the fact that coagulation in the second part of the flame does not affect the shape of primary particles but merely determines the final fractal nature of aggregates.

The candidate particles available for coagulation were obtained from a size distribution of particles calculated from the Smoluchowski master equations with additional source terms for surface growth and nucleation. It was found that the particle size distribution in the nucleation zone of the flame can be divided into two parts: the newly incepted particles that dominate the distribution and a small fraction of larger particles formed by coagulation. The evolution of these larger particles was simulated by a time-dependent Monte-Carlo method.

In the first part of the flame, the larger particles coagulate almost exclusively with small particles due to a higher coagulation probability forming slightly aggregated particles. The use of a realistic size distribution reduces the mean size of candidate particles selected for coagulation and hence the degree of aggregation of primary particles at the point of transition. Once nucleation has ceased, the small particles are rapidly scavenged by the large particles and transition occurs. From this point in the flame onward, the larger particles can be regarded as primary particles. It was found that surface growth acting on the particles in the post-nucleation zone was able to recover the spherical shape of the primary particles.

The present results provide further support to the mechanism of transition from coalescent coagulation to fractal-like growth identified in our previous studies and exhibit the significance of small particles on the formation of spherical primary particles.

Future Plans

Pre-nucleation Chemistry: In collaboration with William Lester's group we have continued ab initio quantum-chemical analysis of reactions that are critical to the development of kinetic models of aromatic growth. Our current attention is on QMC analysis of small aliphatic unsaturated C_2-C_5 radicals, and the A and B states of the cyclopentadienyl radical.

Developing Models for Representing Combustion Chemistry at Varying Levels of Complexity to Use with Models for Laminar and Turbulent Flow Fields to Describe Combustion Processes: We have an ongoing collaboration with the Sandia group of Habib Najm on developing and testing the CSP-PRISM ultra-economical approach to modeling of reactive flows with realistic chemical kinetics.

Soot Particle Aggregation: We will continue development and analysis of soot particle aggregation phenomena. Of immediate interest is the analysis of aggregate-aggregate collisions at a detailed level. Thus far, we examined the trajectories of a single aggregate particle colliding with surrounding spherical particles and simultaneous surface growth, and aggregate-aggregate collisions treated in a lumped manner. Our present objective is to perform Monte Carlo simulations with aggregate-aggregate collisions resolved explicitly.

Homogeneous Nucleation of Carbon Nanoparticles: We will continue molecular dynamics simulations with on-the-fly quantum forces. Our next objective is to examine formation and behavior of PAH clusters larger than dimers.

Graphene Structure Growth: Our primary objective, as the next step in this direction, is to develop a more versatile computer code that will allow us to explore the new reaction pathways, identified in the initial phase of this investigation. The code will be written in an object-based manner, so that to allow a quick addition of (arbitrary) reactions. Likewise, it will allow consideration of a three-dimensional growth rather than limited to a surface layer. In this way, we will be able to explore not just the growth of a graphene surface layer, but also the development of the curvature in the aromatic structures.

Publications

1. "Reaction Mechanism of Soot Formation in Flames," *Phys. Chem. Chem.* **4**, 2028–2037 (2002).
2. "Method of Moments with Interpolative Closure," *Chem. Eng. Sci.* **57**, 2229–2239 (2002).
3. "On the Formation of the First Aromatic Ring," N. W. Moriarty, X. Krokidis, W. A. Lester Jr., and M. Frenklach, *Preprints of the 224th ACS National Meeting*, Vol. 47, No. 2, 2002, pp. 769–770.
4. "Nucleation of Soot: Molecular Dynamics Simulations of Pyrene Dimerization," C. A. Schuetz and M. Frenklach, *Proc. Combust. Inst.* **29**, 2307–2314 (2002).
5. "Computational Economy Improvements in PRISM," S. R. Tonse, N. W. Moriarty, M. Frenklach, and N. J. Brown, *Int. J. Chem. Kinet.* **35**, 438–452 (2003).
6. "Particle Aggregation with Simultaneous Surface Growth," P. Mitchell and M. Frenklach, *Phys. Rev. E* **67**, 061407 (2003).
7. "Geometry Optimization in Quantum Monte Carlo with Solution Mapping: Application to Formaldehyde," C. A. Schuetz, M. Frenklach, A. C. Kollias, and W. A. Lester, Jr., *J. Chem. Phys.* **119**, 9386–9392 (2003).
8. "On the Role of Surface Migration in Growth and Structure of Graphene Layers," M. Frenklach and J. Ping, *Carbon '03, International Conference on Carbon*, 2003, ISBN 84-607-8305-7.
9. "Coupling Reaction Chemistry with Fluid Dynamics: Methods and Applications," M. Frenklach, *19th International Colloquium on the Dynamics of Explosions and Reactive Systems*, 2003, ISBN4-9901744-1-0.
10. "On the Role of Surface Migration in the Growth and Structure of Graphene Layers," M. Frenklach and J. Ping, *Carbon* (2004), in press.

CHEMICAL DYNAMICS IN THE GAS PHASE: QUANTUM MECHANICS OF CHEMICAL REACTIONS

Stephen K. Gray
Chemistry Division
Argonne National Laboratory
Argonne, IL 60439

E-mail: gray@tcg.anl.gov

PROGRAM SCOPE

This research is in the area of theoretical chemical reaction dynamics. Emphasis is placed on accurate quantum mechanical studies of the spectroscopy and dynamics of experimentally relevant and combustion important chemical systems. Wavepacket or time-dependent quantum methods are most often employed and/or developed, owing both to their simplicity and the intuitive mechanistic pictures they can provide. The quantum results so obtained are also used both to gauge the quality of potential energy surfaces and the validity of more approximate theoretical methods such as quasiclassical trajectories and transition state theory.

RECENT PROGRESS

A six-dimensional quantum (QM) wavepacket study of the $OH + CO \rightarrow H + CO_2$ reaction was carried out with Medvedev, Goldfield, Schatz and co-workers [1]. A four-atom implementation [2] of the real wave packet (RWP) method [3] was employed. The Lakin-Troya-Schatz-Harding (LTSH) ground electronic state potential function [4], which includes the latest *ab initio* extrema, was used. In addition to minima associated with the well-known cis and trans HOCO complexes, the LTSH surface includes minima associated with the more weakly bonded (linear) reactant channel complexes, $OH \cdots CO$, which have been the focus of recent experimental work of Lester and co-workers [5,6]. While the QM calculations were restricted to total angular momentum $J = 0$ and reactants in their ground states, extensive quasiclassical trajectory (QCT) calculations were also carried out both in this limit and for general initial conditions. Both QM and QCT calculations showed that the reactant channel minima can enhance the reactivity at moderate collision energies (e.g., 0.1 eV). However, for moderate and especially lower collision energies we found significant discrepancies in the magnitudes of the QM and QCT reaction probabilities, indicating that zero-point violation can significantly impact the quantitative reliability of the QCT results. Finally, our results still lead to significant differences between experimental and theoretical rate constants in the low temperature regime, which cannot be easily explained by any of the effects noted. This may imply that still more accurate estimates of some features of the global potential energy surface, such as the exit channel barrier, need to be made and incorporated into the LTSH potential function.

Calculations on the unimolecular decay of state-selected unimolecular $OH \cdots CO$ complexes, in order to compare more directly with recent experimental work of Pond and Lester [6], were also carried out [7]. Using methods similar to those we used in a study of resonances in H_2O [8], we obtained estimates of the relevant metastable states corresponding to $OH \cdots CO$ complexes. We considered propagation of such a complex corresponding to two quanta of vibrational excitation in OH and zero-point energy in the remaining modes. This particular complex decay is dominated by simple break-up to form OH and CO as opposed to formation of HOCO and/or $H + CO_2$. Despite some apparent inadequacies of the LTSH potential associated with overall reaction to form $H + CO_2$ noted above, reasonable agreement with the results of Pond and Lester [6], both in terms of OH and CO product distributions and complex lifetimes, was found. We also confirmed that the there are two pathways to the decay of these complexes, one a

direct transfer of one OH quantum to translational/rotational motion (V-T) and the other involving also a near resonant vibrational excitation of the CO (V-V) [6, 7].

FUTURE PLANS

We will extend our study of the decay of reactant channel OH···CO complexes to excited bend states. These states are interesting because of the increased chance of forming HOCO complexes and thus H + CO_2 products. We hope to explicitly answer the question regarding the relative contribution of such processes in the experiments of Pond and Lester [6]. As with our earlier study of OH + CO reaction dynamics [1], these will be computationally challenging calculations, requiring the use of a high performance parallel computing environment. Another interesting unimolecular system we will consider, in collaboration with G. E. Hall (BNL), is NCCN → 2CN. This system has been studied experimentally by North and Hall [9]. An accurate *ab initio* based potential energy surface has been developed recently by Harding (private communication) and we have already initiated wave packet calculations on NCCN unimolecular decay, with the hope of understanding the origins of the experimentally observed velocity-angular momentum vector correlations and rotational product distributions.

The quantum reaction dynamics of CH + H_2 → CH_2 + H, its reverse reaction and the unimolecular decay of CH_3 complexes will be studied with the RWP method [2, 3]. These reactions are important in combustion because they lead to the equilibration of CH and CH_2, and there are interesting experimental results available for comparison [10-13]. Among the fundamental questions quantum dynamics can answer include the nature of the formation and breakup of CH_3^* complexes. Harding has recently developed a high-level potential energy surface for studying this system, and we will extend the existing RWP code, applicable to AB+CD reactants, to the ABC+D case.

References
[1]   D. M. Medvedev, S. K. Gray, E. M. Goldfield, M. J. Lakin, D. Troya, and G. C. Schatz, J. Chem. Phys. **120**, 1231 (2004).
[2]   E. M. Goldfield and S. K. Gray, J. Chem. Phys. **117**, 1604-1612 (2002).
[3]   S. K. Gray and G. G. Balint-Kurti, J. Chem. Phys. **108**, 950 (1998).
[4]   M. J. Lakin, D. Troya, G. C. Schatz, and L. B. Harding, J. Chem. Phys. **119**, 5848 (2003).
[5]   M. I. Lester, B. V. Pond, D. T. Anderson, L. B. Harding, and A. F. Wagner, J. Chem. Phys. **113**, 9889 (2000).
[6]   B. V. Pond and M. I. Lester, J. Chem. Phys. **118**, 2223 (2003).
[7]   Y. He, E. M. Goldfield, and S. K. Gray, J. Chem. Phys., *in press* (2004).
[8]   S. K. Gray and E. M. Goldfield, J. Phys. Chem. A **105**, 2634 (2001).
[9]   S. W. North and G. E. Hall, J. Chem. Phys. **106**, 60 (1997).
[10]   R. G. Macdonald and K. Liu, J. Chem. Phys. **89**, 4443 (1988).
[11]   A. McIlroy and F. P. Tully, J. Chem. Phys. **99**, 3597 (1993).
[12]   R. A. Brownsword, A. Canosa, B. R. Rowe, I. R. Sims, I. W. M. Smith, D. W. A. Stewart, A. C. Symonds and D. Travers, J. Chem. Phys. **106**, 7662 (1997).
[13]   R. A. Eng, G. E. Goos, H. Hippler, and C. Kachiani, Phys. Chem. Chem. Phys. **3**, 2258 (2001).

PUBLICATIONS, S. K. Gray (2002-2004)

1. E. M. Goldfield and S. K. Gray, A quantum dynamics study of H_2 + OH $\rightarrow$ H_2O + H employing the Wu-Schatz-Lendvay-Fang-Harding potential function and a four-atom implementation of the real wave packet method, J. Chem. Phys. **117**, 1604-1612 (2002).

2. S. K. Gray, Chemical reaction dynamics with real wave packets, J. Theor. Comput. Chem. **2**, 373-379 (2002).

3. I. Miquel, M. Gonzalez, R. Sayos, G. G. Balint-Kurti, S. K. Gray, and E. M. Goldfield, Quantum reactive scattering calculations of cross sections and rate constants for the $N(^2D)$ + $O_2(X)$ $\rightarrow$ $O(^3P)$ + $NO(X)$ reaction, J. Chem. Phys. **118**, 3111-3123 (2003).

4. M. Hankel, G. G. Balint-Kurti, and S. K. Gray, Sinc wavepackets: A new form of wavepacket for time-dependent quantum mechanical reactive scattering calculations, Int. J. Quant. Chem., **92**, 205-211 (2003).

5. P. Defazio and S. K. Gray, Quantum dynamics study of the D_2 + OH $\rightarrow$ DOH + D reaction on the WSLFH potential energy function, J. Phys. Chem. A. **107**, 7132-7137 (2003).

6. T. Lu, E. M. Goldfield, and S. K. Gray, The equilibrium constants for molecular hydrogen adsorption in carbon nanotubes based on iteratively determined nano-confined bound states J. Theor. Comp. Chem. **2**, 621-626 (2003).

7. T. Lu, E. M. Goldfield, and S. K. Gray, Quantum states of molecular hydrogen and its isotopes in single-walled carbon nanotubes, J. Phys. Chem. B, **107**, 12989-12995 (2003).

8. D. M. Medvedev, S. K. Gray, E. M. Goldfield, M. J. Lakin, D. Troya, and G. C. Schatz, Quantum wave packet and quasiclassical trajectory studies of OH + CO: Influence of the reactant channel well on thermal rate constants, J. Chem. Phys., **120**, 1231-1238 (2004).

9. D. M. Medvedev and S. K. Gray, A new expression for the direct quantum mechanical evaluation of the thermal rate constant, J. Chem. Phys., *in press* (2004).

10. Y. He, E. M. Goldfield, and S. K. Gray, Quantum dynamics of vibrationally activated OH-CO reactant complexes, J. Chem. Phys., *in press* (2004).

Computer-Aided Construction of Chemical Kinetic Models

William H. Green, Jr., MIT Department of Chemical Engineering,
77 Massachusetts Ave., Cambridge, MA 02139. email: whgreen@mit.edu

Project Scope

The combustion chemistry of even simple fuels can be extremely complex, involving hundreds or thousands of kinetically significant species. The most reasonable way to deal with this complexity is to use a computer not only to numerically solve the kinetic model, but also to construct the kinetic model in the first place. We are developing the methods needed to make computer-construction of accurate combustion models practical, as well as tools to make it feasible to handle and solve the resulting large kinetic models with rigorous error control.

Recent Progress

We have applied the new tools we have developed to several technological problems, including the very complex pyrolysis chemistry of simple fuels, and (with additional support from DOE's Transportation Technologies division) to predict the performance of homogeneous charge compression-ignition (HCCI) engines. We also have begun to address the serious human-interface issues: developing methods to document the large mechanisms constructed using computer-aided modeling software, and to make it feasible for humans to see (and so be able to check) the assumptions underlying the kinetic simulation. (This last IT-oriented effort is financially supported primarily by DOE's MICS division and by NSF, but of course if crucial to make progress on combustion of real fuels.)

The research necessarily spans the range from quantum chemical calculations on individual molecules and elementary-step reactions, through the development of improved rate/thermo estimation procedures based on generalizations, to the creation of algorithms and software for constructing and solving the simulations.

Notable accomplishments during this grant period include:

1) Development of first software able to construct kinetics models with consistent treatment of chemically-activated reactions (including automated $k(T,P)$ calculations). This software allowed us to accurately predict the highly nonlinear and strongly pressure-dependent kinetics of autocatalytic methane and ethane pyrolysis (to form unsaturated cyclics and ultimately coke/soot). [15,16] This work was recognized with the ACS Division of Fuel Chemistry's Glenn Award.

2) Identification of the fundamental cause of HCCI engine knock, development of the best and most numerically efficient predictive HCCI engine simulator, and use of same to design improved HCCI engines.[18]

3) Development of the first rigorous method for controlling the error associated with use of reduced chemistry models in CFD reacting-flow simulations. Also, the first software for determining a range of reaction conditions over which any reduced model is guaranteed to be accurate to any specified tolerance.[9,10,13,14,20]

4)   Development of rate and thermochemical estimates based on quantum chemical calculations for unsaturates, and for many types of oxygen-containing radicals.[17,19,22] We have also developed a very accurate method for predicting the thermochemistry of polycyclic aromatic hydrocarbons, and recently submitted that work for publication in the *Journal of the American Chemical Society*.

Future Plans

We are now preparing a public version of our kinetic modeling software, and a corresponding rate and thermo estimation parameter database, suitable for wide distribution among the combustion chemistry community. In addition to speeding the construction of chemistry models needed for different applications, we believe that the transparency of the assumptions in our approach will facilitate high quality peer reviews, and so improve the quality of large combustion chemistry models. (With existing software and approaches, it is very difficult to check the large models.)

We will apply our new high-accuracy method for predicting PAH thermochemistry to develop a thermodynamically-consistent soot formation model. (Most existing soot-formation models include some irreversible steps. Many of the steps in soot formation are partially equilibrated, so the thermochemistry is crucial.)

We will also compute the thermochemistry and rates for reactions important in combustion of organic nitrogen and organic phosphorus compounds. Preliminary predictions of the high temperature oxidation of methyl phosphonic acid are in very encouraging agreement with experiment.

Publications Resulting from DOE Sponsorship (Since 2002)

1. D.A. Schwer, J.A. Tolsma, W.H. Green, and P.I. Barton, "On Upgrading the Numerics in Combustion Chemistry Codes", *Combust. Flame* **128**, 270-291 (2002).
2. R. Sumathi, H.-H. Carstensen, & W.H. Green, "Reaction Rate Prediction via Group Additivity, Part 3: Effect of Substituents with CH_2 as the Mediator", *J. Phys. Chem. A* **106**(22), 5474-5489 (2002).
3. J. Song, G. Stephanopoulos, and W.H. Green, "Valid Parameter Range Analyses for Chemical Reaction Kinetic Models", *Chem. Eng. Sci.* **57**, 4475 (2002).
4. R. Sumathi and W.H. Green, "Thermodynamic Properties of Ketenes: Group Additivity Values from Quantum Chemical Calculations", *J. Phys. Chem. A* **106**(34), 7937-7949 (2002).
5. R. Sumathi and W.H. Green, "*A priori* Rate Constants for Kinetic Modeling", *Theoretical Chemistry Accounts* **108**, 187-213 (2002).
6. R. Sumathi and W.H. Green, "Missing thermochemical groups for large unsaturated hydrocarbons: Contrasting predictions of G2 and CBS-Q", *J. Phys. Chem. A* **106**(46), 11141-11149 (2002).
7. D.M. Matheu, W.H. Green, and J.M. Grenda, "Capturing Pressure-Dependence in Automated Mechanism Generation: Reactions Through Cycloalkyl Intermediates", *Int. J. Chem. Kinet.* **35**, 95-119 (2003).
8. J.M. Grenda, I.P. Androulakis, A.M. Dean, and W.H. Green, "Application of Computational Kinetic Mechanism Generation to Model the Autocatalytic Pyrolysis of Methane", *Ind. Eng. Chem. Res.* **42**, 1000-1010 (2003).

9. D.A. Schwer, P. Lu, & W.H. Green, "An Adaptive Chemistry approach to modeling Complex Kinetics in Reacting Flows", *Combust. Flame* **133**, 451-465 (2003).

10. B. Bhattacharjee, D.A. Schwer, P.I. Barton, & W.H. Green, "Optimally-Reduced Kinetic Models: Reaction Elimination in Large-Scale Kinetic Mechanisms", *Combust. Flame* **135**, 191-208 (2003).

11. C.D. Wijaya, R. Sumathi, and W.H. Green, "Cyclic Ether Formation from Hydroperoxyalkyl Radicals (QOOH)", *J. Phys. Chem. A* **107**, 4908-4920 (2003).

12. B. Wong, D.M. Matheu, and W.H. Green, "The Temperature and Molecular Size Dependence of the High-Pressure Limit", *J. Phys. Chem. A* **107**, 6206-6211 (2003).

13. D.A. Schwer, P. Lu, W. H. Green, and V. Semiao, "A Consistent-Splitting Approach to Computing Stiff Steady-State Reacting Flows with Adaptive · Chemistry", *Combust. Theory & Modelling* **7**, 383-399 (2003).

14. P. Lu, B. Bhattacharjee, P.I. Barton & W.H. Green, "Reduced Models for Adaptive Chemistry Simulation of Reacting Flows", in *Computational Fluid and Solid Mechanics*, ed. by K.J. Bathe (Elsevier, 2003).

15. D.M. Matheu, J.M. Grenda, M. Saeys, & W.H. Green, "New, computer-discovered pathways for methane and ethane pyrolysis", *Preprints of the ACS Division of Fuel Chemistry* (2003). [awarded Glenn prize by ACS Fuels Division]

16. D.M. Matheu, A.M. Dean, J.M. Grenda, and W.H. Green, "Mechanism Generation with Integrated Pressure-Dependence: A New Model for Methane Pyrolysis", *J. Phys. Chem. A* **107**, 8552-8565 (2003).

17. R. Sumathi and W.H. Green, "Oxygenate, Oxyalkyl, and Alkoxycarbonyl Thermochemistry and Rates for Hydrogen Abstraction from Oxygenates", *Phys. Chem. Chem. Phys.* **5**, 3402-3417 (2003).

18. P.E. Yelvington, M. Bernat i Rollo, S. Liput, J. Yang, J.W. Tester, and W.H. Green, "Predicting Performance Maps for HCCI Engines", *Combust. Sci. & Tech.* (2004).

19. W.H. Green, C.D. Wijaya, P.E. Yelvington, & R. Sumathi, "Predicting Chemical Kinetics with Computational Chemistry: Is QOOH = HOQO Important in Fuel Ignition?", *Mol. Phys.* (2004).

20. B. Bhattacharjee, W.H. Green, and P.I. Barton, "Interval Methods for Semi-Infinite Programs", *Computational Optimization and Applications* (2004).

21. H. Richter, S. Granata, W.H. Green, & J.B. Howard, "Detailed Modeling of PAH and Soot Formation in a Laminar Premixed Benzene/Oxygen/Argon Low-Pressure Flame", *Proc. Combust. Inst.* (accepted).

22. H. Ismail, J. Park, B.M. Wong, W.H. Green, & M.C. Lin, "A Theoretical and Experimental Kinetic Study of Phenyl Radical Addition to Butadiene", *Proc. Combust. Inst.* (accepted).

HIGH-RESOLUTION SPECTROSCOPIC PROBES OF CHEMICAL DYNAMICS[*]

Gregory E. Hall (gehall@bnl.gov)

Chemistry Department, Brookhaven National Laboratory, Upton, NY 11973-5000

PROGRAM SCOPE

This research is carried out as part of the Gas Phase Molecular Dynamics group program in the Chemistry Department at Brookhaven National Laboratory. High-resolution spectroscopic tools are developed and applied to problems in chemical dynamics. Recent topics have included the state-resolved studies of collision-induced electronic energy transfer, dynamics of barrierless unimolecular reactions, and the kinetics and spectroscopy of transient species.

RECENT PROGRESS

Collision-induced singlet-triplet transitions in CH_2

The chemistry of methylene depends dramatically on its electronic spin state, and most realistic combustion models treat singlet and triplet CH_2 as separate chemical species. They have different formation and loss reactions, but also a surprisingly efficient collision-induced interconversion process that can be fast enough to compete with gas kinetic reactive channels. A sparse set of rovibrational levels of "mixed state" character can arise via spin-orbit coupling when singlet and triplet levels of the correct symmetry are nearly degenerate. These special mixed states are thought to act as doorways through which population can transfer from singlet to triplet manifolds by means of collisions that resemble pure rotational energy transfer collisions, and do not require any additional spin mixing during the collision. We have been exploring this process with transient FM spectroscopy to record the time-resolved Doppler absorption spectra of a selection of rotational states of CH_2, starting with nascent photofragments from the well-characterized ketene dissociation at 308 nm, and following the subsequent collisional evolution of populations and Doppler profiles. The observations characterize the translational and rotational thermalization process in competition with reactive and non-reactive quenching, preceding and blending into the time regime of conventionally studied steady-state kinetics. Our measurements show that there are indeed marked differences in the kinetics of the known mixed state levels and others with purely singlet character. A surprise observation is that the two components of several observed pairs of mixed triplet and singlet levels appear to be kinetically coupled more strongly to one another than to nearby levels of pure singlet or triplet character. Figure 1 shows for example, the dominant triplet component of a

Figure 1. Decay kinetics of the two components of a mixed state derived from 8_{18}.

mixed pair is weak initially, but grows within a few hundred nsec to match the shape of the dominant singlet component. The convergence is even faster than the translational thermalization in this sample mixture. At longer times, following translational and rotational relaxation, we observe clear double-exponential decays of singlet methylene, consistent with *reversible* intersystem crossing with vibrationally excited triplet CH_2, as shown in Figure 2. The two nuclear spin modifications of singlet CH_2 show distinct kinetic differences, most significantly in the ratio of fast to slow decay amplitudes. We attribute these kinetic differences to the different set of perturbed levels in the *ortho* and *para* manifolds. Work on this problem is continuing and extensions to other collision partners, as well as new experimental probes are discussed in the following sections.
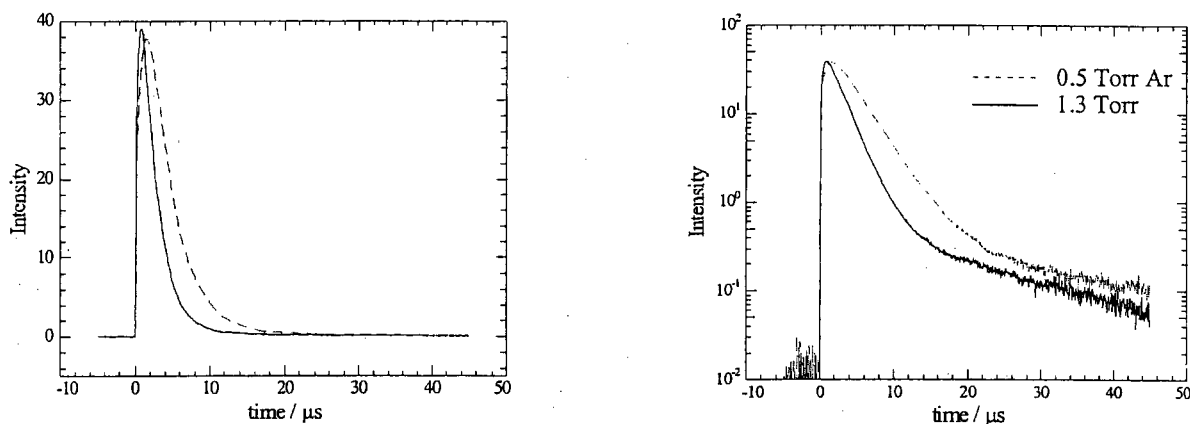
Figure 2. Linear and log plots of CH_2 decay at two different Ar pressures

Dynamical aids to assignment in the spectroscopy of methylene

We have exploited the tools of photodissociation dynamics and nonequilibrium kinetics for the purpose of extending, confirming, and correcting spectroscopic assignments in the notoriously challenging $\tilde{b}^1B_1 \leftarrow \tilde{a}^1A_1$ spectrum of methylene. Following the production of singlet methylene by 308 nm photolysis of ketene (CH_2CO), transient FM absorption spectra in the near-infrared have been collected under stable, low pressure conditions. Nascent line widths vary systematically with the energy of the detected rovibronic state, as do the initial relaxation kinetics prior to establishment of a steady-state rotational distribution near room temperature. Calibrating these properties with a set of assigned lines provides a guide to the identification of previously unassigned lines in the complex spectrum. This information led to new or corrected assignments of many spectral lines, including the assignment of new spectral features involving higher-lying rotational levels than had previously been identified in the radical.

Photochemistry of bromoform

Bromoform, $HCBr_3$ has long been used as a precursor for photolytic production of several species of interest to combustion and atmospheric chemistry, particularly CH in ground and excited electronic states, despite a complex, power-dependent mixture of other fragmentation products including Br, Br_2, CBr_2, CBr, HBr, HCBr, $HCBr_2$ and even bimolecular products such as C_2 and C_2Br. We have used our FM spectrometer to characterize the power-dependent yield of HCBr at

several UV wavelengths, to test the proposition that there is a single-photon channel in the mid-UV leading to Br_2 + HCBr. Our results augment the translational spectroscopy results from the Berkeley ALS experiments (by our collaborator Prof. S. North at Texas A&M), and support the interpretation that Br + $CHBr_2$ is the only important one-photon fragmentation pathway at 248 nm.

Correlated photochemistry: CH_2CO

Velocity-resolved measurements of spectroscopically-selected photofragments from mono-energetically excited precursors permits a determination of the correlated state distribution of products. In the case of ground state dissociation following nonradiative conversion from an optically prepared initial state, such measurements may provide insights into energy randomization in an isolated molecule, and the dynamics of energy flow beyond the transition state. Recent measurements in collaboration with Arthur Suits have provided sliced ion imaging data for the CO fragment of ketene dissociation with remarkable velocity resolution. Preliminary analysis has been devoted to characterizing the resolution and image analysis tools appropriate for the new method of sliced ion imaging. Despite the relatively low and nearly continuous distribution of recoil velocities for the CO fragments, under optimized conditions, multiple rings in the CO images are observed, corresponding to the irregular density of CH_2 rotational states. An effective velocity resolution on the order of 10 m/s for fragments with no more than 800 m/s of recoil velocity will allow a detailed analysis of the product correlations in this prototypical case study of barrierless microcanonical dissociation.

FUTURE WORK

Nonequilibrium kinetics of singlet CH_2

Following clarification of the intersystem crossing kinetics with rare gases, similar measurements in the presence of reactive gases such as H_2O, O_2 and H_2 will be performed. Compared to the rare gases, we will look for differences in the evolution of the state distribution and total singlet survival probability as the nascent CH_2 ensemble relaxes toward a steady-state, exponential decay. Qualitatively, we seek the relative rates of translational and rotational relaxation compared to the total disappearance rates, as well as the relative rates of disappearance before and after thermalization. Contrasting the kinetics of the mixed states with the unperturbed singlet levels may also provide some additional information about the role of triplet CH_2 in these collision systems. Questions regarding an efficient, complex-mediated mechanism for vibrational relaxation of singlet CH_2 (0,1,0) by water should also be directly accessible by dynamical calculations on the singlet CH_3OH potential surface discussed above for the set of related reactions $O(^1D)$ + CH_4, CH_3 + OH and $^1CH_2$ + H_2O. Recent work from the laboratories of Hancock (Oxford) and Pilling (Leeds) on the $^1CH_2$ + O_2 reaction indicating that quenching to $^3CH_2$ is the only significant channel implies that mixed states have little to do with this much more efficient intersystem crossing process. We have the tools in hand to explore these interesting questions.

Double-resonance studies of energy transfer in CH_2

We plan new experiments in which individual CH_2 rotational levels are bleached by a tunable ns dye laser operating in the 590 nm region, while monitoring the populations of the same or nearby rotational levels with near-infrared transient FM spectroscopy. Initial experiments will be required to characterize saturation recovery and saturation transfer as measured by this new technique using "normal" rotational levels. Propensities in state-changing collisions in terms of energy gaps or angular momentum gaps may be observed. Particularly interesting will be the behavior following saturation of single components of a mixed-state pair. The double resonance experiments, combined with the kinetic modeling of pre-steady state kinetics of the multi-state

113

relaxation can provide a uniquely detailed test of the mixed-state model for surface crossing in the small molecule limit.

Correlated photochemistry: NCCN

Doppler-resolved transient FM spectra of CN photoproducts from jet-cooled NCCN photodissociation provide signatures of the dissociation dynamics through correlated state distributions and rotational polarization measurements. Each of these properties differs from a statistical prediction for reasons that are unclear, but potentially revealing. A theoretical collaboration with S. Gray (ANL) is investigating the effect of the ground-state potential beyond the transition state on the product distribution and the rotational polarization. A key question is the rate of energy flow in and out of the torsional coordinate in the energized molecule. Such low frequency modes dominate the density of states and are crucial in statistical theory. In a low total angular momentum system, this motion correlates to product channels with fragment rotation axes parallel to the recoil direction, and these fragment channels appear to be underrepresented in the experimental distributions.

DOE SPONSORED PUBLICATIONS SINCE 2001

Doppler-resolved spectroscopy as an assignment tool in the spectrum of singlet methylene
     G. E. Hall, A. Komissarov and T. J. Sears
     J. Phys. Chem. A, in press (2004)

The photodissociation of bromoform at 248 nm: Single and multiphoton processes
     P. Zou, J. Shu, T. J. Sears, G. E. Hall and S. W. North
     J. Phys. Chem. A, **108,** 1482-8 (2004)

Superexcited state dynamics probed with an extreme-ultraviolet free electron laser
     W. Li, R. Lucchese, A. Doyuran, Z. Wu, H. Loos, G. E. Hall and A. G. Suits
     Phys. Rev. Lett., **92,** 083002 (2004)

Imaging O (^{3}P) + alkane reactions in crossed beams: vertical vs. adiabatic H abstraction dynamics
     X. Liu, R. L. Gross, G. E. Hall, J. T. Muckerman and A. G. Suits
     J. Chem. Phys. **117,** 7947-59 (2002)

Axis-Switching and Coriolis coupling in the *A* (010) - *X* (000) transitions of DCCl and HCCl
     A. Lin, K. Kobayashi, H-G Yu, G. E. Hall, J. T. Muckerman, T. J. Sears and A. J. Merer
     J. Mol. Spectr. **214,** 216-24 (2002)

The E $^3\Pi$ – X $^3\Delta$ transition of jet-cooled TiO observed in absorption
     K. Kobayashi, G. E. Hall, J. T. Muckerman, T. J. Sears and A. J. Merer
     J. Mol. Spectr. **212,** 133-41 (2002)

An ab initio molecular dynamics study of S_0 ketene fragmentation
     K. M. Forsythe, S. K. Gray, S. J. Klippenstein and G. E. Hall
     J. Chem. Phys. **115,** 2134-44 (2001)

SPECTROSCOPY AND KINETICS OF COMBUSTION GASES AT HIGH TEMPERATURES

Ronald K. Hanson and Craig T. Bowman
Department of Mechanical Engineering
Stanford University, Stanford, CA 94305-3032
hanson@me.stanford.edu, bowman@navier.stanford.edu

Program Scope

This program involves two complementary activities: (1) development and application of cw laser absorption methods for the measurement of concentration time-histories and fundamental spectroscopic parameters for species of interest in combustion; and (2) shock tube studies of reaction kinetics relevant to combustion. Species investigated in the spectroscopic portion of the research include OH, CH_3 and NCN using narrow-linewidth ring dye laser absorption. Reactions of interest in the shock tube kinetics portion of the research include: $CH_3 + O_2 \rightarrow$ Products; $C_2H_6 \rightarrow 2CH_3$; $C_3H_8 \rightarrow CH_3 + C_2H_5$; and $CH + N_2 \rightarrow NCN + H$.

Recent Progress: Shock Tube Chemical Kinetics

$CH_3 + O_2 \rightarrow$ Products:

The reaction of methyl radicals (CH_3) with molecular oxygen (O_2) plays a major role in the oxidation of many alkanes. The two well-known bimolecular product channels are the dominant reaction pathways at combustion temperatures:

$$CH_3 + O_2 \quad \rightarrow CH_3O + O \qquad (1a)$$
$$\rightarrow CH_2O + OH \qquad (1b)$$
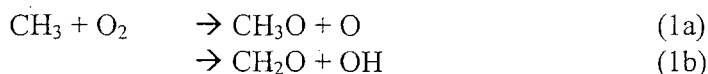
We have investigated the reaction of CH_3 with O_2 in high-temperature shock tube experiments from 1600 to 2700 K. The overall reaction rate coefficient, $k_1 = k_{1a} + k_{1b}$, and individual rate coefficients for the two high-temperature product channels were determined in ultra-lean mixtures of CH_3I and O_2 in Ar/He. Narrow-linewidth UV laser absorption at 306.7 nm was used to measure OH concentrations, for which the normalized rise time is sensitive to the overall rate coefficient k_1 but relatively insensitive to the branching ratio of the individual channels and to secondary reactions. Atomic resonance absorption spectroscopy measurements of O-atoms were used for a direct measurement of channel (1a). Through the combination of measurements using the two different diagnostics, rate coefficient expressions for both channels were determined. Over the temperature range 1600 to 2400 K, $k_{1a} = 6.1 \times 10^7 \, T^{1.5} \exp(-14200/T) \, cm^3 mol^{-1} s^{-1}$ and $k_{1b} = 69 \, T^{2.9} \exp(-4900/T) \, cm^3 mol^{-1} s^{-1}$. The overall rate coefficient is in close agreement with a recent *ab initio* calculation and one other shock tube study, while comparison of k_{1a} and k_{1b} to these and other experimental studies yields mixed results. In contrast to one recent experimental study, reaction (1b) is found to be the dominant channel over the entire experimental temperature range. Final analysis of these data including detailed uncertainty analysis is nearly complete.

Ethane and Propane Decomposition:

The alkane decomposition reactions are important initiation steps in the detailed reaction mechanisms describing alkane oxidation and in describing global combustion phenomena such as ignition times. The decomposition rates of ethane and propane in the fall-off regime at high temperatures were studied in a shock tube using UV narrow-line laser absorption of CH_3 at 216.6 nm. Experimental conditions ranged from 1350 to 2050 K and 0.13 to 8.4 atm with mixtures varying in concentration from 100 to 400 ppm of ethane or propane dilute in argon. Decomposition rate coefficients were determined by monitoring the formation rate of CH_3 immediately behind shock waves and modeling the CH_3 formation with a detailed kinetic model. Calculations were performed using RRKM/master equation analysis with a restricted (hindered) Gorin model for the transition state and fit to the current high temperature dissociation data as well as previous low temperature recombination measurements. The decomposition rate coefficient is in good agreement with the recent calculations of Klippenstein et al. Representative ethane falloff data are presented in Fig. 1.
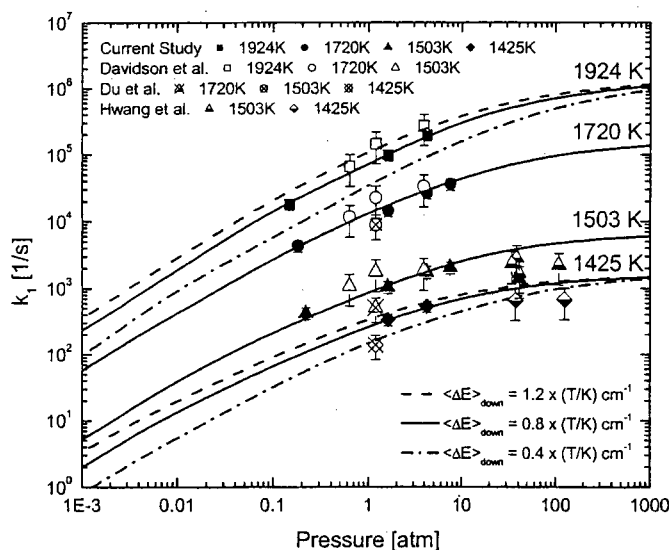
Fig. 1. Falloff plot for $C_2H_6 \rightarrow CH_3 + CH_3$. Solid symbols, current study; open symbols, Davidson et al.; open symbols with x, Du et al.; half-filled symbols, Hwang et al.; solid lines, RRKM/master equation results with $\langle \Delta E \rangle_{down} = 0.8 \times (T [K])$ cm^{-1}; dashed lines, $\langle \Delta E \rangle_{down} = 1.2 \times (T [K])$ cm^{-1}; dot-dashed lines, $\langle \Delta E \rangle_{down} = 0.4 \times (T [K])$ cm^{-1}.

Recent Progress: Spectroscopy

CH$_3$ Absorption Coefficient: We have measured the absorption coefficient (k_v) of CH_3 near 216 nm using external-frequency-doubled laser radiation. The increased power and reduced noise available with this technique, over the previous internal-frequency-doubling technique, has permitted a substantially more accurate measurement of k_v; see Fig. 2. Three precursors were used as sources of methyl radicals: azomethane $CH_3N=NCH_3$ which was used at the lowest temperatures, down to 1200 K, methyl iodide CH_3I which was used at intermediate temperatures between 1600 and 2000 K, and ethane C_2H_6 which was used at the highest temperatures up to 2500 K. Excellent agreement in the measured absorption coefficients was found among the different precursors in the overlapping temperature regions. Measurements of the absorption coefficient over a range of wavelengths 210 to 220 nm were also made and compared to those predicted from a symmetric top model. Accurate expressions for the variation of this absorption coefficient with wavelength and temperature are critical to making accurate, quantitative measurements of CH_3 species concentration in our ongoing studies of hydrocarbon kinetics.
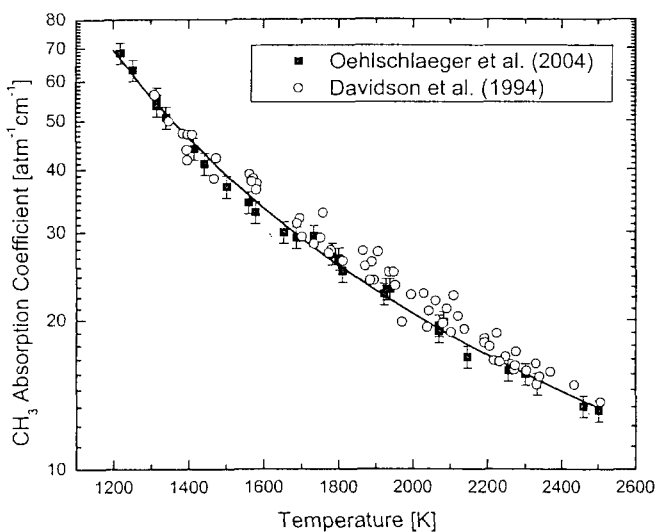
Fig. 2. Absorption coefficient for CH$_3$ at 216.62 nm. Solid symbols, current study; open symbols, earlier work by Davidson et al.

The least-squares-fit expression for the CH$_3$ absorption coefficient at 216.62 nm over the temperature range 1200 to 2500 K is:

$$k_{v,CH3} = 1.475 \times 10^4 \, T^{-1.004} \exp(2109 \, K/T) \, \text{atm}^{-1} \, \text{cm}^{-1} \, (\pm 5\%).$$

Future Plans

1) Continue development of external-cavity frequency-doubling methods for the generation of laser radiation in the deep ultraviolet. Apply these frequency-doubling methods to wavelengths of interest including the detection of CH$_3$ at 216 nm, the detection of NCN at 329 nm, and the detection of HCO at 230 and 258 nm. 2) Develop multi-pass techniques to improve the sensitivity of current OH laser absorption measurements. 3) Develop experimental approaches to measure the overall rate and product branching ratio of the reaction CH+N$_2 \rightarrow$ NCN+H using laser absorption.

Recent Publications of DOE Sponsored Research: 2002-2004

1. J. T. Herbon, R. K. Hanson, C. T. Bowman, and D. M. Golden, "The Reaction of CH_3+O_2: Experimental Determination of the Rate Coefficients for the Product Channels at High Temperatures," accepted for publication, Proceedings of the Combustion Institute (2004).

2. M. A. Oehlschlaeger, D. F. Davidson, and R. K. Hanson, "High Temperature Ethane and Propane Decomposition," accepted for publication, Proceedings of the Combustion Institute (2004); also presented as Paper 03F-56, Western States Section/Combustion Institute Fall Meeting UCLA October (2003).

3. S. Song, D. M. Golden, R. K. Hanson, C. T. Bowman, J. P. Senosiain, C. B. Musgrave, and G. Friedrichs, "A Shock Tube Study of the Reaction $NH_2+CH_4=NH_3+CH_3$ and Comparison with Transition State Theory," International Journal of Chemical Kinetics 35, 304-309 (2003).

4. J. T. Herbon, R. K. Hanson, D. M. Golden, and C. T. Bowman, "A Shock Tube Study of the Enthapy of Formation of OH," Proceedings of the Combustion Institute **29**, 1201-1208 (2002).

5. S. H. Song, R. K. Hanson, C. T. Bowman, and D. M. Golden, "A Shock Tube Study of the NH_2+NO_2 Reaction," Proceedings of the Combustion Institute **29**, 2163-2170 (2002).

6. S. H. Song, R. K. Hanson, D. M. Golden, and C. T. Bowman, "A Shock Tube Study of the Product Branching Ratio of the NH_2+NO Reaction at High Temperatures," Journal of Physical Chemistry A 106, 9233-9235 (2002).

7. S. Song, D. M. Golden, R. K. Hanson, and C. T. Bowman, "A Shock Tube Study of Benzylamine Decomposition: Overall Rate Coefficient and Heat of Formation of the Benzyl Radical," Journal of Physical Chemistry A 106, 6094-6098 (2002).

Theoretical Studies of Potential Energy Surfaces*

Lawrence B. Harding
Chemistry Division
Argonne National Laboratory
Argonne, IL 60439
harding@anl.gov

Program Scope

The goal of this program is to calculate accurate potential energy surfaces for both reactive and non-reactive systems. Our approach is to use state-of-the-art electronic structure methods (MR-CI, CCSD(T), etc.) to characterize multi-dimensional potential energy surfaces. Depending on the nature of the problem, the calculations may focus on local regions of a potential surface (for example, the vicinity of a minimum or transition state), or may cover the surface globally. A second aspect of this program is the development of techniques to fit multi-dimensional potential surfaces to convenient, global, analytic functions that can then be used in dynamics calculations. Finally a third part of this program involves the use of direct dynamics for high dimensional problems to by-pass the need for surface fitting.

Recent Results

Radical-Radical Recombinations: In collaboration with Klippenstein (Sandia-CRF) we have completed a study of oxygen atoms with methyl, ethyl and vinyl radicals. The calculations, focusing on the initial addition, employed MR-CI calculations based on state-averaged CASSCF calculations to allow for the characterization of the three states that correlate with ground state reactants. In each case two of the three states are found to be reactive. VRC-TST calculations were used to calculate high pressure limit recombination rates. For $O+CH_3$, the calculated rate is in excellent agreement with measurements by Micahel et al, Fockenberg et al and Slagle et al. For $O+C_2H_5$ the calculated rate is 20-40% below measurements by Hack et al and Slagle et al, while for $O+C_2H_3$ the calculations are roughly a factor of 2 above a single measurement by Heinemann e al.

Also in collaboration with Klippenstein we have developed a new approach that will allow us to extend these kinds of calculations to much larger systems. The key to the new approach comes from a comparison of radical-radical interaction potentials calculated at the CAS+1+2/aug-cc-pvtz and CAS/cc-pvdz levels. We find that simple, one dimensional, R-dependent but orientation independent corrections for the CAS/cc-pvdz potentials yields potentials in very good agreement with the more accurate but much more costly CAS+1+2/aug-cc-pvtz potentials. This approach has now been tested for $H+CH_3$, $H+CCH$, $H+C_2H_3$, $H+C_2H_5$ and CH_3+CH_3, comparing rates calculated using the corrected CAS/cc-pvdz potentials to rates calculated with the full CAS+1+2/aug-cc-pvtz potentials. The differences between the two predictions are found to be 10% or less in all cases. We have now used this new approach to calculate addition rates for some larger radicals. The results of these calculations are displayed in Figures 1 and 2.
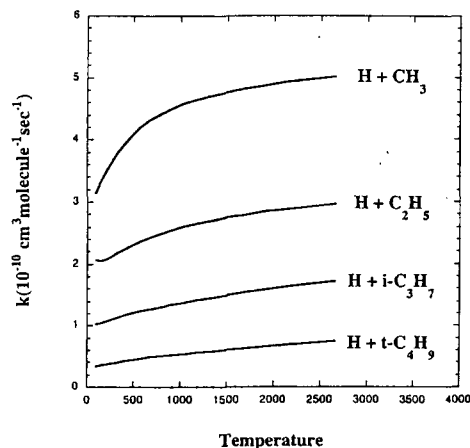
Figure 1. Calculated high pressure limit rate constants for H + R additions
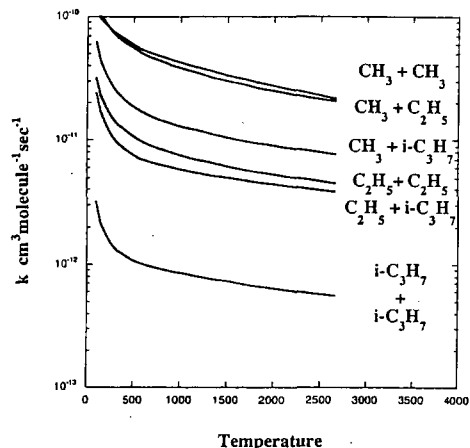
Figure 2. Calculated high pressure limit rate constants for R + R additions.

H$_2$CO: In a collaborative effort with Bowman (Emory University) we have fit a new analytic potential surface for H$_2$CO that gives a realistic description of the molecular decomposition, radical decomposition and isomerization pathways. The fit melds CCSD(T) and MR-CI calculations both done with the aug-cc-pvtz basis set. Approximately 80,000 CCSD(T) calculations where done at Emory to characterize the H$_2$CO minimum, the cis and trans HCOH isomers, the H$_2$+CO asymptote, and the saddle points connecting these minima. An additional 50,000 MR-CI calculations were done at Argonne to characterize the H+HCO and the 2H+CO asymptotes and the H+HCO → H$_2$CO and the H+HCO → H$_2$+CO paths. The CCSD(T) and MR-CI calculations were fit separately to direct product, multinomials in Morse variables. The separate fits were then connected by switching functions. This is the first analytic potential to have realistic characterizations of both the radical and molecular channels. In the near future we plan to use this surface in simulations to examine the question of a possible second molecular channel in the fragmentation of formaldehyde as suggested by Moore et al.[1]

CH$_3$: We have completed a new analytic surface for CH$_3$ which gives a realistic description of the two lowest decomposition pathways,

$$CH_3 \quad \rightarrow \quad CH+H_2$$
$$\rightarrow \quad CH_2+H$$
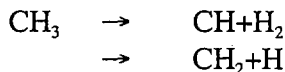
Over 25,000 ab initio (CAS+1+2/aug-cc-pvtz) calculations were done. This expands to a total of over 100,000 points when permutation symmetry is applied. The fit is a full 6th order direct product, multinomial in Morse variables consisting of 924 terms. The points with energies less than 115 kcal/mole above CH$_3$ (the energy of the higher asymptote – CH$_2$+H) are fit with an RMS error of less than 1 kcal/mole. It is planned to use this surface in the near future to study the decomposition of CH$_3$ and the reactions of CH+H$_2$ and CH$_2$+H.

120

H+H₂CCH₂: We have completed high level, CCSD(T)/aug-cc-pvqz calculations on the reaction,

$$H(D) + C_2H_4 \rightarrow C_2H_5 \, (C_2H_4D) \qquad (1)$$
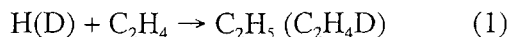
The calculated CCSD(T) barrier height for (1) is 1.9 kcal/mole. The calculated transition state parameters have been used by Wagner to model new high temperature experiments by Michael. The theoretical and experimental results are found to be in excellent agreement.

Future Plans

We plan to extend the approach we developed this year for radical-radical recombination reactions to include resonance stabilized radicals. We will again start by looking at several systems which are small enough to allow high level CAS+1+2/aug-cc-pvtz calculations for purposes of validating the new approach. Two such reaction are,

$$H+NCN \quad \rightarrow \quad HNCN$$
$$H+HCCCH \quad \rightarrow \quad H_2CCCH$$
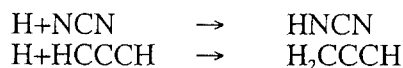
Both of these reactions are also of interest for combustion modeling applications. The ultimate goal of this work will be to treat recombinations, such as propargyl + propargyl, thought to be of importance in soot formation.

References:

(1) R.D. van Zee, M.F. Foltz and C.B. Moore, *J. Chem. Phys.* **99**, 1664 (1993)

PUBLICATIONS (2002 - Present):

On the Enthalpy of Formation of Hydroxyl Radical and Gas-Phase Bond Dissociation Energies of Water and Hydroxyl
B. Ruscic, A.F. Wagner, L.B. Harding, R.L. Asher, D. Feller, D.A. Dixon, K.A. Peterson, Y. Song, X. Qian, C.-Y. Ng, J. Liu and W. Chen
J. Phys. Chem. A **106**, 2727-2747(2002)

Rate Constants, 1100<T<2000 K, for H+NO₂ → OH+NO Using Two Shock Tube Techniques: Comparison of Theory to Experiment
M.-C. Su, S.S. Kumaran, K.P. Lim, J.V. Michael, A.F. Wagner, L.B. Harding and D.-C. Fang
J. Phys. Chem. A **106**, 8261-8270(2002)

A Quasiclassical Trajectory Study of Energy and Angular Distributions for the $H+CO_2 \rightarrow OH+CO$ Reaction
D. Troya, M.J. Lakin, G.C. Schatz, L.B. Harding and M. Gonzalez
Phys, Chem. B **106**, 8148-8160(2002)

Resolving the Mystery of Prompt CO_2: The $HCCO+O_2$ Reaction
S.J. Klippenstein, J.A. Miller, and L.B. Harding
29th Symposium (International) on Combustion **29**, 1209-1218(2002)

A Theoretical Analysis of the CH_3+H Reaction: Isotope Effects, the High Pressure Limit, and Transition State Recrossing
S. J. Klippenstein, Y. Georgievskii and L.B. Harding
29th Symposium (International) on Combustion **29**, 1229-1236(2002)

Implementation of a Fast Analytic Ground State Potential Energy Surface for the $N(^2D)+H_2$ Reaction
T.-S. Ho, H. Rabitz, F. J. Aoiz, L. Banares, S. A. Vazquez, and L. B. Harding
J. Chem. Phys. **119**, 3063-3070 (2003)

A Quasiclassical Trajectory Study of the Reaction $OH + CO \rightarrow H + CO$
M. J. Lakin, D. Troya, G. C. Schatz and L. B. Harding
J. Chem. Phys. **119**, 5848-5849(2003)

Rate Constants for $D + C_2H_2 \rightarrow C_2HD + H$ at High Temperature: Implications to the High Pressure Rate Constant for $H + C_2H_2 \rightarrow C_2H_3$
J. V. Michael, M.-C. Su, J. W. Sutherland, L. B. Harding, and A. F Wagner
J. Phys Chem A 107, 10533-10543(2003)

Speciation of C_6H_6 Isomers by GC-Matrix Isolation FTIR-MS
K.B. Anderson, R.S. Trantor, W. Tang, K. Brezinsky and L.B. Harding
J. Phys. Chem. A (in press)

Reaction of Oxygen Atoms with Hydrocarbon Radicals: A Priori Kinetic Predictions for the CH_3+O, C_2H_5+O and C_2H_3+O Reactions
L.B. Harding, S.J. Klippenstein and Y. Georgievskii
29th Symposium (International) on Combustion (accepted)

Rate Constants for the $D+C_2H_4 \rightarrow C_2H_3D+H$ at High Temperature: Implications to the High Pressure Rate Constant for $H+C_2H_4 \rightarrow C_2H_5$
J.V. Michael, M.-C. Su, J.W. Sutherland, L.B. Harding and A.F. Wagner
29th Symposium (International) on Combustion (accepted)

A Global Analytic Potential Surface for Formaldehyde
X. Zhang, S. Zou, L.B. Harding and J.M. Bowman
J. Phys. Chem A (submitted)

Femtosecond Laser Studies of Ultrafast Intramolecular Processes

Carl Hayden
Combustion Research Facility, MS9055
Sandia National Laboratories
Livermore, CA 94551-0969
CCHAYDE@SANDIA.GOV

Program Scope

The purpose of this research program is to characterize important fundamental chemical processes by probing them directly in time. In this work femtosecond laser pulses are used to initiate chemical processes and follow their progress. The development of new techniques that take advantage of the time resolution provided by femtosecond lasers for studies of chemical processes is an integral part of this research.

Our research focuses on studies of ultrafast energy relaxation and unimolecular reaction processes in highly excited molecules. The goal of these studies is to provide measurements of the time scales for elementary chemical processes that play critical roles in the reaction mechanisms of highly excited reaction intermediates, such as those created in combustion environments by either thermal excitation or exothermic addition reactions. For these studies we have developed the technique of time-resolved photoelectron-photoion coincidence imaging The apparatus constructed for this work measures fragment recoil velocities and photoelectron velocities in coincidence. This approach provides a wealth of new capabilities for femtosecond time-resolved experiments. Using this technique we have made unique measurements of time-resolved energy correlation spectra for the study of complex dissociation processes[1] and also measured time-resolved, molecular frame photoelectron angular distributions from dissociating molecules.[2]

Recent Progress:

Time-resolved studies of CF_3I dissociative ionization

We have collaborated for several years with Dr. Anouk Rijs and Prof. Maurice Janssen at Vrije University, Amsterdam, The Netherlands, on studies of the dissociative multiphoton ionization of CF_3I. In these studies the molecule is two-photon excited with a 264 nm pulse in the region of the $7s$ Rydberg state. The excited molecule is then probed by time-delayed ionization. The lower energy region of the $6s$-$6p$ Rydberg states has been extensively investigated using two-photon excitation with nanosecond lasers.[3,4,5] However, the $7s$ Rydberg state is difficult to access with two photons using nanosecond lasers due to one-photon resonance with the rapidly dissociating A band. Our femtosecond experiments reveal a rapidly evolving neutral state in the region of the $7s$ Rydberg state that upon ionization yields both CF_3^+ and I^+ in conjunction with a substantial contribution from parent ionization.[6] The maximum production of fragment ions occurs when the ionization pulse is delayed by about 100 fs and the fragment ion yield decays with a time constant of approximately 250 fs. Very rapid changes in the vibrational energy distribution in the neutral molecule are observed, resulting in rapid changes in the ionization and fragmentation of the molecule.

The dynamics in the neutral molecule at the two-photon level are difficult to unravel because of the complex ionization dynamics induced by the probe laser pulse in this system.

With the coincidence imaging technique we measure the recoil energy of the electrons and fragment ions from individual ionization events. This energy accounting makes it possible to determine the number of photons involved in different ionization processes and select single photon ionization mechanisms to simplify analysis.

In Figure 1 the energy correlation spectrum is shown for single probe photon dissociative ionization yielding CF_3^+ at a time delay of 300 fs after excitation. The energy correlation spectrum shows the joint probability distribution of the center-of-mass fragment recoil energy (x-axis) and the coincident electron recoil energy (y-axis). The energy correlation spectrum shows three ionization mechanisms. The peak in the lower left corner, corresponding to slowly recoiling CF_3^+ in coincidence with slow electrons, results from near threshold ionization to the barely accessible $CF_3^+ + I(^2P_{1/2})$ limit. A second ionization mechanism results in slowly recoiling CF_3^+ in coincidence with higher energy electrons with an energy distribution peaking around 0.85 eV. These slowly recoiling CF_3^+ fragments come from the direct ionization of the excited neutral molecule to highly vibrationally excited CF_3I^+ that subsequently undergo rapid dissociation to $CF_3^+ + I(^2P_{3/2})$. The predominance of this mechanism suggests the neutral molecule being ionized is vibrationally excited, probably via internal conversion, by the 300 fs delay time. The third dissociative ionization mechanism produces CF_3^+ with a range of energies coincident with electrons that have energies of ~0.5 and ~0.7 eV. This process appears as horizontal stripes on the energy correlation spectrum. We assign this process to electronic autoionization.

Further information to distinguish the two ionization pathways producing higher energy electrons is obtained by extracting molecular frame photoelectron angular distributions (PADs) from the data. These are generated by calculating the angle between the fragment ion recoil vector and the coincident photoelectron velocity vector. The right side of Fig. 1 shows the PADs for the different ionization mechanisms. The strong forward-backward asymmetry in the molecular frame PAD for the process associated with the horizontal stripes in the energy correlation spectrum results from ionization during dissociation of superexcited CF_3I. The close proximity of the I atom when ionization occurs produces a strongly forward-backward asymmetric potential for the departing electron, creating the asymmetric PAD. Both the energy and angular correlations measured with this technique contribute to understanding the ionization mechanisms.

Future Plans
Time-resolved studies of NO dimer photodissociation

We will continue an ongoing collaboration with Prof. James Shaffer at the University of Oklahoma and Dr. Albert Stolow at the Steacie Institute, NRC, Canada, to study the UV photodissociation of NO dimers. In these experiments the NO dimer is excited at ~210 nm then probed with time-delayed ionization. From previous measurements, both in our lab and at the Steacie Institute, we know that the dissociation is relatively slow, occurring on a time scale of ~1 ps. Our current experiments are intended to characterize the excited state of the dimer that undergoes dissociation.

The ionization of the $(NO)_2$ excited state produces very predominantly NO^+. The ionization is unusual because both the photoelectron spectrum and the fragment recoil energy distribution for NO^+ peak at zero energy. We will investigate the dimer excited state using complementary capabilities at the Steacie Institute and Sandia. A magnetic bottle photoelectron spectrometer in Dr. Stolow's lab allows very accurate measurements of electron yields versus

time at many electron energies, while the coincidence imaging method gives simultaneous measurements of electron and fragment recoil energies.

Using the coincidence imaging apparatus we will study the excited state evolution of the ethyl radical. Ethyl radicals can be efficiently produced by photolysis of ethyl iodide at 265 nm. While the radicals will be produced with a range of internal energies we can determine the energy of each radical from its recoil velocity and the C-I bond energy. The first step in the study will be the two-photon ionization of the radicals with a femtosecond pulse at 245 nm following their production with a pulse at 265 nm. Both the measured photoelectron spectrum and the PAD will provide information on the nature of the excited state.

References

1. J.A. Davies, J.E. LeClaire, R.E. Continetti and C.C. Hayden, J. Chem. Phys. **111**, 1 (1999).
2. J.A. Davies, R.E. Continetti, D.W. Chandler and C.C. Hayden, Phys. Rev. Lett. **84**, 5983 (2000).
3. C.A. Taatjes, J.W.G. Mastenbroek, G.v.d. Hoek, J.G. Snijders, and S. Stolte, J. Chem. Phys., **98**, 4355 (1993).
4. N.A. Macleod, S. Wang, J. Hennessy, T. Ridley, K.P. Lawley, and R.J. Donovan, J. Chem. Soc., Faraday Trans., 94, 2689 (1998).
5. F. Aguirre and S.T. Pratt, J. Chem. Phys., 118, 6318 (2003).
6. W.G. Roeterdink and M.H.M. Janssen, Phys. Chem. Chem. Phys., **4**, 601 (2002).

Publications acknowledging BES support, 2002-Present

A.M. Rijs, C.C. Hayden, and M.H.M. Janssen, "Femtosecond Coincidence Imaging Of Dissociative Ionization Dynamics In CF$_3$I," in *Femtochemistry and Femtobiology: Ultrafast Dynamics in Molecular Science*, A. Douhal and J. Santamaria, World Scientific Publishing Co.Pte.Ltd. (Singapore) (2002), 91.

E. A. Wade, J. I. Cline, K. T. Lorenz, C. C. Hayden, and D. W. Chandler, "Direct measurement of the binding energy of the NO dimer," J. Chem. Phys. **116**, 4755 (2002).

A.M. Rijs, C.C. Hayden, and M.H.M. Janssen, "Time-Resolved Coincidence Imaging of the Dissociative Ionization in CF$_3$I," in *XIII Ultrafast Phenomena,* Springer-Verlag, (2003).

J. P. Shaffer, T. Schultz, J. G. Underwood, C. C. Hayden and A. Stolow, "Time-Resolved Photoelectron Spectroscopy: Charge & Energy Flow in Molecules," in *XIII Ultrafast Phenomena,* Springer-Verlag, (2003).

D. W. Chandler and C. C. Hayden, "Ion Imaging Techniques for the Measurement of Ion Velocities," for *Vol. 5 of the Encyclopedia of Mass Spectrometry*, ed. Peter Armentrout, Elsevier Science, in press.

R. E. Continetti and C. C. Hayden, "Coincidence Imaging Techniques," in Advanced Series in Physical Chemistry: Modern Trends in Chemical Reaction Dynamics, ed. K. Liu and X. Yang, World Scientific, Singapore, (2004).

A.M. Rijs, M.H.M. Janssen, E.t.H. Chrysostom, and C.C. Hayden, "Femtosecond Coincidence Imaging of Multichannel Multiphoton Dynamics," Phys. Rev. Lett. **92**, 123002 (2004).

O. Gessner, E.t.H. Chrysostom, A.M.D. Lee, D.M. Wardlaw, M.L. Ho, S.J. Lee, B. M. Cheng, M. Z. Zgierski, I.C. Chen, J.P Shaffer, C.C. Hayden and A. Stolow, "Non-adiabatic intramolecular and photodissociation dynamics studied by femtosecond time-resolved photoelectron and coincidence imaging spectroscopy," Faraday Discuss. **127**, (2004) (accepted).

The forward-backward symmetric MF-PAD indicates dissociation and ionization are not strongly coupled

Strong forward-backward asymmetry in the MF-PAD shows close association of dissociation and ionization
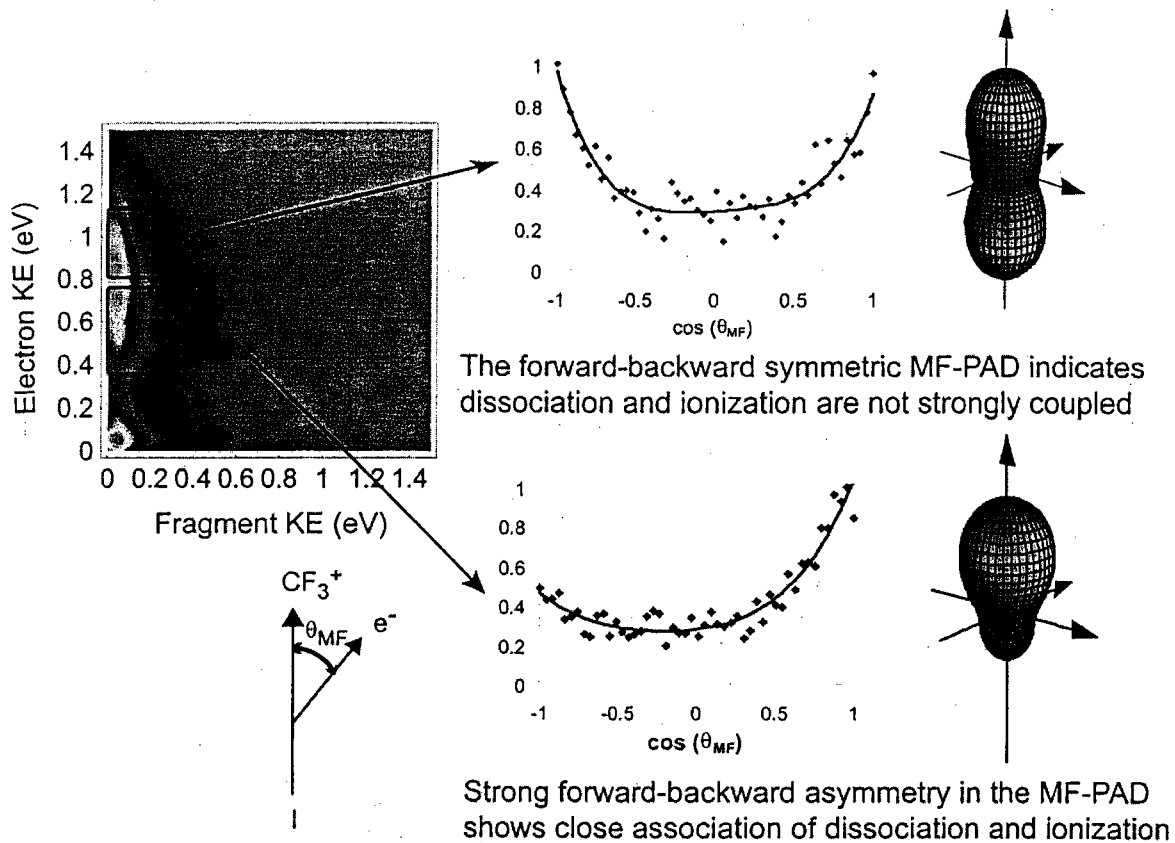
Figure 1. Photoelectron-photoion energy correlation spectrum of (e^-, CF_3^+) at 300 fs time delay. On the right are molecular frame angular distributions from selected regions of the energy correlation spectrum. The PADs are made cylindrically symmetric by selecting events where the fragment recoil is nearly along the laser polarization axis. The graphs are plots of the angular distribution as a function of the cosine of the polar angle. On the far right are three-dimensional fits to the data.

CHEMICAL ACCURACY FROM
AB INITIO MOLECULAR ORBITAL CALCULATIONS

Martin Head-Gordon
Department of Chemistry, University of California, Berkeley, and,
Chemical Sciences Division, Lawrence Berkeley National Laboratory,
Berkeley, CA 94720.
mhg@cchem.berkeley.edu

1. Scope of Project.

Short-lived reactive radicals and intermediate reaction complexes are believed to play central roles in combustion, interstellar and atmospheric chemistry. Due to their transient nature, such molecules are challenging to study experimentally, and our knowledge of their structure, properties and reactivity is consequently quite limited. To expand this knowledge, we develop new theoretical methods for reliable computer-based prediction of the properties of such species. We apply our methods, as well as existing theoretical approaches, to study prototype radical reactions, often in collaboration with experimental efforts. These studies help to deepen understanding of the role of reactive intermediates in diverse areas of chemistry. They also sometimes reveal frontiers where new theoretical developments are needed in order to permit better calculations in the future.

2. Summary of Recent Major Accomplishments.

2.1 Time-dependent density functional theory calculations.

Density functional theory is a simple and effective computational tool for computational studies of the ground and excited states of radicals. For excited states, time-dependent density functional theory (TDDFT) provides an in-principle exact framework for the calculation of excitation energies. Low-lying excited states of radicals can usually be adequately described using TDDFT with existing functionals. This is exciting because such states often involve substantial double excitation character that is tremendously difficult to describe within wavefunction-based approaches. We have recently reported an extension of TDDFT [8] that permits the description of diradicals with good accuracy starting from a triplet ground state and flipping a spin. We are exploring chemical applications of TDDFT, as well as probing its present limitations (see 2.2 below).

The first class of recent chemical applications have been to excited states of polycyclic aromatic hydrocarbon (PAH) cations which are known to be intermediates in sooting flames. They are also of relevance in the interstellar medium, as a likely source of the diffuse interstellar bands (DIB's). We have completed a large series of calculations of most PAH cations for which reliable experimental results are available, and demonstrated that accuracy of about 0.3 eV or better for excited states is attainable via TDDDF [16]. Additionally we have participated in a number of joint theoretical and experimental studies of PAH species [1,10,12], where the main features of the electronic spectra have been assigned to calculated excited states. Trends in oscillator strength in homologous series of PAH's also have interesting astrophysical implications, which we

have explored [9]. Applications such as these [1,9,10,12] are now becoming relatively routine (they are feasible for systems up to about 100 non-hydrogen atoms are feasible on workstations or fast PC's), and yet were completely unfeasible a decade ago.

A second class of chemical applications of TDDFT involves excited states in biological systems. We have characterized the excited states of CO bound to a reduced model of myoglobin [6,14], to probe the origin of the ultrafast photodissociation seen experimentally. We showed that a state which is dissociative in the metal-ligand coordinate crosses the lowest allowed excited state for small stretches of the M-L distance. We have also performed TDDFT calculations on the excited states of models of chlorophyll and associated corotenoids that are found in the photosynthetic light-harvesting complex [18,20,21]. Our calculations [18,21] have possible relevance to the mechanism of non-photochemical quenching (NPQ), the process by which excited chlorophyll molecules are directly relaxed under high-light conditions to prevent damage to the reaction center. We have shown that both direct singlet-singlet excitation energy transfer, and also a novel electron transfer reaction are energetically feasible. If the latter process is operative, we suggest that it may be experimentally probed by seeking the spectral signature of the corotenoid radical cation under high-light conditions.

2.2   Failure of TDDFT for charge-transfer excited states.

While time-dependent density functional theory (TDDFT) calculations are very valuable for broad classes of chemical applications (as exemplified by the studies in Sec. 2.1), it is not yet a complete panacea for the problem of accurate excited state calculations. Today's density functionals are known to yield an incorrect representation of Rydberg excited states, in particular. There are also a number of reports suggesting poor results for charge-transfer excited states. We have recently examined the charge-transfer problem in considerable detail [9,21,26], and, for the first time clarified both the nature of the problem, and its origin. We showed that the long-range Coulomb attraction that should exist between the donor and acceptor is *entirely absent* in TDDFT using local and gradient corrected functionals. A correct description requires 100% non-local exact exchange. Thus the popular B3LYP functional, which includes 20% exact exchange, has 20% of the correct Coulomb attraction! We also suggested a simple work-around which uses a hybrid of single excitation CI (CIS) (which has 100% exact exchange) for charge-transfer excited states, and regular TDDFT for the localized excitations. This approach corrects CIS using ground state DFT calculations at long range, and proved successful in the applications to chlorophyll-corotenoid charge-transfer excited states discussed above.

2.3   New methods for high accuracy electronic structure calculations.

While density functional calculations are extremely valuable, the highest levels of accuracy currently possible come from wavefunction-based electronic structure calculations, such as CCSD(T) (which are also dramatically more expensive). Yet for radicals, CCSD(T) quite often performs more poorly than for closed shell molecules. To try to overcome the deficiencies of (T) corrections for radicals and for the related problem of bond-dissociation to radical fragments, we have developed a new correction to singles and doubles coupled cluster methods [2,3]. These (2) methods have yielded

promising results on highly correlated systems already [2,3]. Additionally we have investigated the origin of the relatively poor results obtained with CCSD(T), and discovered that they can be greatly improved by using different orbitals [15]. The Kohn-Sham orbitals, which are more resistant to symmetry breaking, are the simplest alternative that greatly improves on the usual choice of Hartree-Fock orbitals.

2.4   Characterizing unpaired electrons in radicals.

We have recently proposed a new definition of the unpaired electrons in molecules [11,24], which has a formal advantage over the "distribution of unpaired electrons" that has been explored in recent years. In particular, the latter can in principle yield more unpaired electrons than there are electrons in the molecule, while our new definition does not. We hope to explore practical applications of this property in the future.

3.   Summary of Research Plans.

- Exploration of ways to solve the charge-transfer problem in TDDFT
- Analytical gradients for TDDFT
- Development and testing of simpler coupled cluster methods for radicals
- Joint theoretical-experimental studies on systems that challenge the limits of theory

4.   Publications from DOE Sponsored Work, 2002-present.

[1] "Vibrational and Electronic Spectroscopy of the Fluorene Cation", J. Szczepanski, J. Banisaukas, M. Vala, S. Hirata, R.J. Bartlett, and M. Head-Gordon, J. Phys. Chem. A 106, 63-73 (2002).

[2] "A Perturbative Correction to the Quadratic Coupled Cluster Doubles Method for Higher Excitations", S. R. Gwaltney, E. F. C. Byrd, T. Van Voorhis, and M. Head-Gordon, Chem. Phys. Lett. 353, 359-367 (2002).

[3] "Coupled cluster methods for bond-breaking", M. Head-Gordon, T. Van Voorhis, S.R. Gwaltney and E.F.C. Byrd, in, "Low-Lying Potential Energy Surfaces", edited by M.R. Hoffman, and K.G. Dyall (ACS Symposium Series, volume 828, 2002), pp. 93-108.

[4] "Can coupled cluster singles and doubles be approximated by a valence active space model?", G.J.O. Beran, S.R. Gwaltney, and M. Head-Gordon, J. Chem. Phys. 117, 3040-3048 (2002).

[5] "Quadratic coupled-cluster doubles: implementation and assessment of perfect-pairing optimized geometries", E.F.C. Byrd, T. Van Voorhis, and M. Head-Gordon, J. Phys. Chem. B 106, 8070-8077 (2002).

[6] "Characterization of the relevant excited states in the photodissociation of CO ligated hemoglobin and myoglobin", A. Dreuw, B.D. Dunietz, and M. Head-Gordon, J. Am. Chem. Soc. 124, 12070-12071 (2002).

[7] "Implementation of generalized valence-bond inspired coupled cluster theories", T. Van Voorhis and M. Head-Gordon, J. Chem. Phys. 117, 9190-9201 (2002).

[8] "The spin-flip approach within time-dependent density functional theory: theory and application to diradicals", Y. Shao, M. Head-Gordon, and A.I. Krylov, J. Chem. Phys. 118, 4807-4818 (2003).

[9] "Time Dependent Density Functional Theory Calculations of Large Compact PAH Cations: Implications for the Diffuse Interstellar Bands" J.L. Weisman, T.J. Lee, F. Salama, and M. Head-Gordon, Astrophys. J. 587, 256-261 (2003).

[10] "Vibrational and electronic spectroscopy of acenaphthylene and its cation", J. Banisaukas, J. Szczepanski, J. Eyler, M. Vala, S. Hirata, M. Head-Gordon, J. Oomens, G. Meijer and G. von Helden, J. Phys. Chem A 107, 782-793 (2003)

[11] "Characterizing unpaired electrons from the one-particle density matrix", M. Head-Gordon, Chem. Phys. Lett. 372, 508-511 (2003).

[12] "Electronic Absorption Spectra of Neutral Perylene ($C_{20}H_{12}$), Terrylene ($C_{30}H_{16}$), and Quaterrylene ($C_{40}H_{20}$) and their Positive and Negative Ions: Ne Matrix-Isolation Spectroscopy and Time Dependent Density Functional Theory Calculations", T.M. Halasinski, J.L. Weisman, R. Ruiterkamp, T.J. Lee, F. Salama, and M. Head-Gordon, J. Phys. Chem. A 107, 3660-3669 (2003).

[13] "Local Correlation Models", M. Head-Gordon, T. Van Voorhis, G. Beran and B. Dunietz, in "Computational Science: ICCS 2003", Part IV, Lecture Notes in Computer Science, Vol. 2660, pp. 96-102 (2003).

[14] "Initial steps of the photodissociation of the CO-ligated heme group", B.D. Dunietz, A. Dreuw, and M. Head-Gordon, J. Phys. Chem B 107, 5623-5629 (2003).

[15] "Approaching closed-shell accuracy for radicals using coupled cluster theory with perturbative triple substitutions", G.J.O. Beran, S.R. Gwaltney, and M. Head-Gordon, Phys. Chem. Chem. Phys. 5, 2488-2493 (2003).

[16] "Time-dependent density functional study of the electronic excited states of polycyclic aromatic hydrocarbon radical ions", S. Hirata, M. Head-Gordon, J. Szczepanski and M. Vala J. Phys. Chem. A 107, 4940-4951 (2003).

[17] "Partitioning Techniques in Coupled Cluster Theory", S.R. Gwaltney, G.J.O. Beran, and M. Head-Gordon, in "Fundamental World of Quantum Chemistry: A Tribute to the memory of Per-Olov Lowdin", edited by E. Kryachko and E. Brandas, Kluwer (July, 2003), volume I pp. 433-458.

[18] "Charge-transfer state as possible signature of a zeaxanthin-chlorophyll dimer in the non-photochemical quenching process in green plants", A. Dreuw, G.R. Fleming and M. Head-Gordon, J. Phys. Chem. B 107, 6500-6503 (2003).

[19] "Long-range charge-transfer excited states in time-dependent density functional theory require non-local exchange", A. Dreuw, J.L. Weisman, and M. Head-Gordon, J. Chem. Phys. 119, 2943-2946 (2003).

[20] "Quantum chemical evidence of an intramolecular charge transfer state in the carotenoid peridinin of peridinin-chlorophyll-protein", H.M. Vaswani, C.-P. Hsu, M. Head-Gordon and G.R. Fleming, J. Phys. Chem. B 107, 7940-7946 (2003).

[21] "Chlorophyll fluorescence quenching by xanthophylls", A. Dreuw, G.R. Fleming, and M. Head-Gordon, Phys. Chem. Chem. Phys. 5, 3247-3256 (2003).

[22] "Electro-oxidation of CO on Pt-based electrodes simulated by electronic structure calculations", C. Saravanan, B.D. Dunietz, N.M. Markovic, G.A. Somorjai, M. Head-Gordon and P.N. Ross, J. Electroanal. Chem. 554-555, 459-465 (2003)

[23] "Manifestations of symmetry-breaking in self-consistent field calculations", B.D. Dunietz and M. Head-Gordon, J. Phys. Chem A 107, 9160-9167 (2003).

[24] "Reply to comment on characterizing unpaired electrons in molecules", M. Head-Gordon, Chem. Phys. Lett. 380, 488-489 (2003).

[25] "Are both symmetric and buckled dimers on Si(100) minima? Density functional and multireference perturbation theory calculations", Y. Jung, Y. Shao, M.S. Gordon, D.J. Doren and M. Head-Gordon, J. Chem. Phys 119, 10917-10923 (2003).

[26] "Failure of time-dependent density functional theory for long-range charge-transfer excited states: the zincbacteriochlorin-bateriochlorin and bacteriochlorophyll-spheroidene complexes", A. Dreuw and M. Head-Gordon, J. Am. Chem. Soc. 126, 4007-4016 (2004).

Laser Studies of
Combustion Chemistry

John F. Hershberger

Department of Chemistry
North Dakota State University
Fargo, ND 58105
john.hershberger@ndsu.nodak.edu

Time-resolved infrared diode laser spectroscopy is used in our laboratory to study the kinetics and product channel dynamics of chemical reactions of importance in the gas-phase combustion chemistry of nitrogen-containing radicals. This program is aimed at improving the kinetic database of reactions crucial to the modeling of NO_x control strategies such as Thermal de-NO_x, RAPRENO$_x$, and NO-reburning. The data obtained is also useful in the modeling of propellant chemistry. The emphasis in our study is the quantitative measurement of both total rate constants and product branching ratios.

HCCO+NO Reaction

We have renewed our investigation of the HCCO+NO reaction, which is an important step in NO-reburning mechanisms. Two channels are active:

$$HCCO+NO \quad \rightarrow HCN + CO_2 \qquad\qquad (1a)$$
$$\rightarrow CO + HCNO \qquad\qquad (1b)$$

Previous experimental measurements of the branching ratio have varied from $\phi(CO_2)=0.12$-0.28,[1-3] with the lower number originating from our laboratory. Previous studies have suffered from significant secondary chemistry. Some studies have used the $O+C_2H_2$ reaction to make HCCO, and some have used 193-nm photolysis of CH_2CO. Both of these methods produce substantial yields of CH_2 radicals, which react with NO, producing primarily HCNO+H. Following a suggestion of Richard Bersohn and some mass spectrometric experiments of Laurie Butler, we are using ethyl ethynyl ether, C_2H_5OCCH, as our precursor:

$$C_2H_5OCCH + h\nu \text{ (193 nm)} \rightarrow C_2H_5 + HCCO \qquad\qquad (2)$$
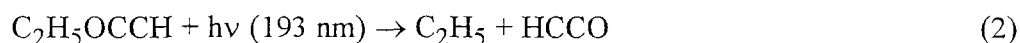
This precursor was recently used by David Osborn in his study of the HCCO+O_2 reaction.[4] It appears to be a cleaner HCCO source than previous methods, but still produces a significant CO background (i.e., CO is produced upon 193-nm photolysis of a C_2H_5OCCH/buffer gas mixture). The mechanism of CO formation is not entirely clear. Some may originate from multiple photon effects, or HCCO photolysis, but we find a nearly linear pulse energy dependence. Some CO may be produced by reactions of HCCO which are suppressed in the presence of an excess of NO. Because of the uncertainties associated with this background, we have chosen to measure the branching ratio of reaction (1) by quantifying the HCNO product rather than CO. This approach presents its own challenges. Quantifying the yields is

straitforward for CO_2, but more difficult for HCNO, for which published infrared absorption linestrengths are not available. We have calibrated the HCNO transient signals in two different ways:

Method 1) Photolysis of ketene at 193 nm in the presence of NO produces HCNO by the pathway:

$$CH_2CO + h\nu \ (193 \ nm) \rightarrow CH_2 + CO \qquad\qquad (3a)$$
$$\rightarrow HCCO + H \qquad\qquad (3b)$$

$$HCCO + NO \qquad \rightarrow HCN + CO_2 \qquad\qquad (1a)$$
$$\rightarrow CO + HCNO \qquad\qquad (1b)$$
$$CH_2 + NO \qquad \rightarrow HCNO + H \qquad\qquad (4)$$

Since the primary ketene photolysis products are $CH_2 + CO$, most of the fulminic acid comes from reaction (4), which has an estimated branching ratio for HCNO production of 84%.[5] By measuring the 193-nm absorption coefficient of our ketene sample, we can estimate the number of radicals produced and therefore the number of HCNO molecules, assuming an excess of NO ensures complete conversion. Comparison of this calculated [HCNO] to the transient signal provides the calibration.

Method 2) The more straitforward way is to synthesize authentic samples of pure HCNO, and measure the static infrared absorption coefficients. After several attempts, we have been able to synthesize and purify small quantities of this reagent, which is sufficiently stable if used the same day.

Using Calibration method #1, we obtain $\phi_{1a} = 0.116$ and $\phi_{1b} = 0.884$. Using method #2, we obtain $\phi_{1a} = 0.114$ and $\phi_{1b} = 0.886$ (in both cases, we assume that no channels other than (1a) and (1b) are active). In summary, both calibration methods are in excellent agreement, and confirm our previous conclusions that the $HCN + CO_2$ channel is only a very minor contribution.

HCNO Kinetics

There is virtually no literature data available on the kinetics of the fulminic acid molecule. With the realization that this molecule plays an important role in NO reburning processes,[6] and the work described above to synthesize pure HCNO, we are in a position to examine reaction kinetics of this species. The HCNO synthesis is slow and inefficient, but our reaction cell geometry is ideally suited to dealing with reagents that are only available in small quantities. As a first effort, we have begun work on the CN + HCNO reaction:

$$CN + HCNO \quad \rightarrow HCN + (NCO) \qquad\qquad (5a)$$
$$\rightarrow NO + HCCN \qquad\qquad (5b)$$
$$\rightarrow HCCO + N_2 \qquad\qquad (5c)$$
$$\rightarrow HCC + N_2O \qquad\qquad (5d)$$

Our initial effort is to measure the total rate constants, with product yield studies to follow later. CN is produced by photolysis of ICN or C_2N_2, and detected by infrared absorption spectroscopy. At present, we have a preliminary 296 K rate constant of $k_5 = 3.1 \times 10^{-11}$ cm^3 molecule^{-1} s^{-1}.

Future plans include kinetic measurements of several other radical species reacting with HCNO, including OH+HCNO, NCO+HCNO, etc.

$C_2H_3 + O_2$ Reaction

In last year's contractor's meeting report, Barry Carpenter reported some calculations on this reaction in an attempt to rationalize a possible minor (~6%) channel for CO_2 production, as reported by some IR emission experiments:[7]

$$C_2H_3 + O_2 \quad \rightarrow CH_2O + HCO \qquad\qquad (6a)$$
$$\rightarrow CH_3 + CO_2 \qquad\qquad (6b)$$

Since our apparatus is ideally suited to quantifying CO_2 yields, we have briefly investigated this reaction to confirm or refute these observations. Upon photolysis of $C_2H_3Br/O_2/SF_6$ mixtures, we find a small but nonzero CO_2 yield. We measured the yield of (6a) by probing CO, assuming rapid conversion of HCO to CO:

$$HCO + O_2 \quad \rightarrow HNO + CO \qquad\qquad (7)$$

Comparison of these product yields gives $\phi_{6a}=0.98$, $\phi_{6b}= 0.02$. Thus the CO_2 is substantially smaller than that reported by the emission experiments. In fact, our CO_2 yield is small enough that we can not entirely rule out the possibility that it originates from some unknown secondary chemistry, possibly involving minor vinyl bromide photolysis channels, or impurities in the C_2H_3Br sample. Therefore our value for ϕ_{6b} should be considered an upper limit.

References

1. Nguyen, M. T.; Boullart, W.; Peeters, J. *J. Phys. Chem.* **1994**, *98*, 8030.
2. Eickhoff, U.; Temps, F. *Phys. Chem. Chem. Phys.* **1999**, *1*, 243.
3. Rim, K. T.; Hershberger, J. F. *J. Phys. Chem. A* **2000**, *104*, 293.
4. Osborn, D. L. *J. Phys. Chem. A* **2003**, *107*, 3728.
5. Grussdorf, J.; Temps, F.; Wagner, H. Gg. *Ber. Bunsenges Phys. Chem.* **1997**, *101*, 134.
6. Miller, J. A.; Klippenstein, S. J.; Glarborg, P. *Combust. Flame* **2003**, *135*, 357.
7. Feng, W.; Wang, B. *Chem. Phys. Lett.* **2002**, *356*, 505.

Publications acknowledging DOE support (2001-present)

"Recent Progress in Infrared Absorption techniques for Elementary Gas Phase Reaction Kinetics", C. Taatjes and J.F. Hershberger, Ann. Rev. Phys. Chem. **52**, 41 (2001).

"Kinetics of HCCl + NO_x Reactions", R.E. Baren, M. Erickson, and J.F. Hershberger, Int. J. Chem. Kinet. **34**, 12 (2002).

"Kinetics of the NCN Radical", R.E. Baren and J.F. Hershberger, J. Phys. Chem. A, **106**, 11093 (2002).

"Kinetics of the SiH_3+O_2 and $SiH_3+H_2O_2$ Reactions", J.P. Meyer and J.F. Hershberger, J. Phys. Chem. A. **107**, 3963 (2003).

"Kinetics of the CCO+NO and $CCO+NO_2$ Reactions", W.D. Thweatt, M.A. Erickson, and J.F. Hershberger, J. Phys. Chem. A **108**, 74 (2004).

Product Imaging of Molecular Dynamics Relevant to Combustion

P. L. Houston
Department of Chemistry
Cornell University
Ithaca, NY 14853-1301
plh2@cornell.edu

Program Scope

Product imaging is being used to investigate several processes important to a fundamental understanding of combustion. The imaging technique produces a "snapshot" of the three-dimensional velocity distribution of a state-selected reaction product. Research in three main areas is planned or underway. First, product imaging will be used to investigate the reactive scattering of radicals or atoms with species important in combustion. These experiments, while more difficult than studies of inelastic scattering or photodissociation, are now becoming feasible. They provide both product distributions of important processes as well as angular information important to the interpretation of reaction mechanisms. Preliminary work on the CN +O_2 reaction has begun. Second, the imaging technique will be used to measure rotationally inelastic energy transfer on collision of closed-shell species with important combustion radicals. Such measurements improve our knowledge of intramolecular potentials and provide important tests of *ab initio* calculations. Work on Ar + SO is underway. Finally, experiments using product imaging will explore the vacuum ultraviolet photodissociation of O_2, N_2O, SO_2, CO_2 and other important species. Little is known about the highly excited electronic states of these molecules and, in particular, how they dissociate. These studies will provide product vibrational energy distributions as well as angular information that can aid in understanding the symmetry and crossings among the excited electronic states

Recent Progress

Photodissociation of O_2

Product imaging has been used to investigate the O_2 ($E\ ^3\Sigma^-_u \leftarrow X\ ^3\Sigma^-_g$) absorption in the 120-130 nm region. The products for dissociation through $v = 0$, and 1 of the E state are exclusively $O(^1D) + O(^3P)$, to within the error limit of our measurement. The quantum yield for $O(^1D)$ formation is unity for dissociation through $v = 1$ and 2,[1,2] but is found both in our work and in that of Lee and Nee[1,2] to be only 0.5 for dissociation through $v = 0$. Since there is no other dissociation channel, this observation suggests that the fluorescence rate and the dissociation rate are comparable following excitation through $v = 0$.

The angular distribution of the $O(^1D_2)$ product shows that the product is aligned in the molecular frame in such a way that J is nearly perpendicular to the axis of recoil between the two oxygen atoms. This finding is consistent with a homogeneous dissociation along the repulsive wall of the B state, as might be expected from the fact that the E state is formed by an avoided crossing between the B state and a $^3\Sigma^-_u$ state leading to $O(^1D) + O(^3P)$. A sketch of the relevant potential energy surfaces in shown in the figure on the next page.

The variation in the anisotropy parameter β with wavelength across the $v = 0$ absorption band of the $E \leftarrow X$ transition is qualitatively in accord with a calculation similar to that used previously for NO,[3] but taking into account the coherent excitation of overlapping lines.

Two-photon Photodissociation of SO₂

In a collaboration with researchers at the University of Puerto Rico, multiphoton excitation and dissociation of SO_2 has been investigated in the wavelength range from 224-232 nm. Strong evidence is found for two-photon excitation to the H Rydberg state, followed by dissociation to SO +

Figure 1. Potential energy curves for O_2 showing the avoided crossing that leads to the $O(^1D_2)$ and $O(^3P)$ products.

O and ionization of the SO product by absorption of a third photon. The two-photon excitation is resonantly enhanced via the $C\,^1B_2$ intermediate state, and the two-photon yield spectrum thus bears a strong resemblance to the spectrum of this intermediate. Product imaging of the $O(^3P_2)$, $S(^1D_2)$ and SO products suggests that following dissociation of SO_2 from the H state, SO is produced in the A and B electronic states. $S(^1D_2)$ is produced both from two-photon dissociation of SO_2 to give S + O_2 and by single-photon dissociation of SO^+. In the former process, the O_2 is likely formed in all of its lowest three electronic states.

Current Projects and Future Plans

Photodissociation of N₂O

The 130.2-nm photodissociation of N_2O has been investigated using four-wave difference frequency mixing in krypton to generate the photons, which both dissociate N_2O and ionize $O(^3P_2)$. Somewhat to our surprise, the 130/212 combination ionized several products. While the dominant signal when the VUV was tuned to the O resonance was O^+, as expected, we also observed N_2^+ and NO^+, whether or not the 130 nm was tuned to the O resonance. Three channels are observed: $O(^1S) + N_2(X)$ (major); $N(^2D) + NO(X)$ (minor); and $O(^3P) + N_2(A,B)$ (minor). We have obtained product images by resonantly ionizing the $O(^3P_0)$ and $N(^2D_{5/2})$ atomic products with vacuum ultraviolet radiation. The NO and N_2 products are imaged by non-resonant vacuum ultraviolet radiation. Analysis of the images shows that the $N_2(X)$ product has a vibrational distribution that is bimodal, with peaks at $v = 2$ and $v = 10$. The NO(X) distribution peaks at $v = 6$. The ratio of $N_2(A)$ to $N_2(B)$ appears to be near unity. Current effort is aimed at measuring the relative quantum yields for these channels and identifying the mechanisms of dissociation.

Vacuum Ultraviolet Photodissociation of CO₂

An unsuccessful attempt was made using the Advanced Light Source to investigate the photodissociation dynamics of CO_2 at 130 nm in End Station One. This was perhaps the first attempt to use the ALS beam as a dissociation source rather than as a detection source. The detection laser, a YAG-pumped dye laser, was tripled using two crystals and

produced light in the 200 nm region used to detect O(^{1}D). Despite two weeks of effort, we found it impossible to obtain product images that clearly depended on the presence of both the ALS beam and the detection beam. A large part of the problem was that the raw ALS beam has a bandwidth so wide that only a small fraction of the VUV energy was absorbed by the CO$_2$; the rest of the light created an large ion background that was difficult to reduce or discriminate against. An obvious solution to this problem would be to use the small monochromator and End Station Three, however, it is currently impossible to place a laser near enough this station to safely accomplish the detection. An alternate approach is now being pursued using the deep ultraviolte free electron laser (FEL) at Brookhaven. Xianghong Liu, a postdoc working at Brookhaven under partial Cornell support, has recently installed a YAG-pumped dye laser at the FEL, and we are planning, with the collaboration of the Suits group, to attempt imaging of CO$_2$ dissociation products following dissociation with the FEL.

The CN + O$_2$ Reaction

The reaction of CN + O$_2$ is important to combustion chemistry in the formation and destruction of NO$_x$ compounds.[4] CN + O$_2$ react to give at least two product channels. NCO + O(^{3}P) is the major product channel and is exothermic by about 13.7 kcal/mole, while the NO + CO product channel is exothermic by 110 kcal/mole and formed in about 6-29% yield,[5-8] with the branching ratio for the minor channel increasing with decreasing temperature.[8] Recent calculations[9] suggest that the major channel is accessed through a linear NCOO (^{2}A″) intermediate that subsequently undergoes O-O bond cleavage. The minor channel is reached by a three-center isomerization reaction. The rate constant for this reaction has been studied by many researchers, including several supported by the DOE chemical dynamics program.[10-13] The recommended rate constant exhibits a mild negative temperature dependence,[14] $k = 1.10 \times 10^{-11} \times \exp(205/T)$ cm^3 molec^{-1} sec^{-1}, consistent with the dominance of attractive forces and a centrifugal barrier in the entrance channel.[15]

Despite many interesting features of the dynamics,[16-23] no differential cross section for the CN + O$_2$ reaction has yet been reported. We have begun to investigate this system by creating rotationally cooled CN from 193-nm photodissociation of C$_2$N$_2$ in one beam and crossing it with a beam of pure O$_2$. In a machine where beams of CN and O$_2$ cross at right angles, we were unable to get sufficient reactive signal for the NCO + O channel to overcome the O background from dissociation and ionization of the O$_2$ reactant. However, a large increase in the intensity of the CN reactant can be achieved by using closely spaced parallel beams. Modifications of our apparatus to pursue this approach are underway

References
1. P. C. Lee and J. B. Nee, Journal of Chemical Physics **112**, 1763-1768 (2000).
2. P. C. Lee and J. B. Nee, Journal of Chemical Physics **114**, 792-797 (2001).
3. B. R. Cosofret, H. M. Lambert, and P. L. Houston, J. Chem. Phys. **117**, 8787-8799 (2002).
4. J. A. Miller and C. T. Bowman, Prog. Energy Coubust. Sci. **15**, 287 (1989).
5. N. Basco, *Proc. Roy. Soc. (London)* **283**, 302-11 (1965).
6. K. J. Schmatjko and J. Wolfrum, *Ber. Bunsenges. Phys. Chem.* **82**, 419-28 (1978).
7. F. Mohammad, V. R. Morris, W. H. Fink, and W. M. Jackson, *J. Phys. Chem.* **97**, 11590 (1993).
8. K. T. Rim and J. F. Hershberger, *Journal of Physical Chemistry A* **103**, 3721-3725 (1999).

9. Z.-w. Qu, H. Zhu, Z.-s. Li, X.-k. Zhang, and Q.-y. Zhang, *Chemical Physics Letters* **353,** 304-309 (2002).

10. J. L. Durant, Jr. and F. P. Tully, *Chemical Physics Letters* **154,** 568-72 (1989).

11. M. Y. Lounge and R. K. Hanson, *Int. J. Chem. Kinet.* **16,** 231 (1984).

12. D. A. Lichtin and M. C. Lin, *Chem. Phys.* **96,** 473 (1985).

13. J. P. Hessler, *Journal of Chemical Physics* **111,** 4068-4076 (1999).

14. Baulch, D. L.; Cobos, C. J.; Cox, R. A.; Esser, C.; Frank, P.; Just, Th.; Kerr, J. A.; Pilling, M. J.; Troe, J.; Walker, R. W.; Warnatz, J.,*J. Phys. Chem. Ref. Data* **21,** 411-429 (1992).

15. I. W. M. Smith, *Advanced Series in Physical Chemistry* **6,** 214-249 (1995).

16. H. Schacke, K. J. Schmatjko, and J. Wolfrum, *Ber. Bunsenges. Phys. Chem.* **77,** 248-53 (1973); K. J. Schmatjko and J. Wolfrum, *Ber. Bunsenges. Phys. Chem.* **82,** 419-28 (1978).

17. D. M. Sonnenfroh, R. G. MacDonald, and K. Liu, *Journal of Chemical Physics* **93,** 1478-9 (1990).

18. D. Patel-Misra, D. G. Sauder, and P. J. Dagdigian, *Journal of Chemical Physics* **93,** 5448-56 (1990).

19. D. G. Sauder, D. Patel-Misra, and P. J. Dagdigian, *Journal of Chemical Physics* **95,** 1696-707 (1991).

20. L. F. Phillips, I. W. M. Smith, R. P. Tuckett, and C. J. Whitham, *Chemical Physics Letters* **183,** 254-63 (1991).

21. D. Patel-Misra, D. G. Sauder, P. J. Dagdigian, and D. R. Crosley, *Journal of Chemical Physics* **95,** 2222 (1991).

22. R. G. Macdonald, K. Liu, D. M. Sonnenfroh, and D. J. Liu, *Canadian Journal of Chemistry* **72,** 660-72 (1994).

23. S. A. Wright and P. J. Dagdigian, *Journal of Chemical Physics* **103,** 6479-89 (1995).

Publications Prepared with DOE Support, 2002 - present

P. L. Houston, "Charged Particle Imaging in Chemical Dynamics: An Historical Perspective," in *Imaging in Molecular Dynamics: Technology and Applications*, B. Whitaker, ed. (Cambridge University Press, Cambridge, 2003).

Bogdan R. Cosofret, H. Mark Lambert, and Paul L. Houston, "N(^{2}D) Product Velocity Mapped Imaging in the VUV Photolysis of Nitrous Oxide at 118.2 nm," Bull. Korean Chem. Soc. **23,** 179-183 (2002). (K.-H. Jung commemorative issue).

Bogdan R. Cosofret, H. Mark Lambert, and Paul L. Houston, "Two-photon Photodissociation of NO through Rydberg Levels in the 265-278 nm region: Spectra and Photofragment Angular Distributions," J. Chem. Phys. **117,** 8787-8799 (2002).

Amitavikram A. Dixit, Yuxiu Lei, Keon Woo Lee, Edward Quinones, and Paul L. Houston, "Dissociation of sulphur dioxide by ultraviolet multiphoton absorption between 224 and 232 nm," in preparation.

H. M. Lambert, A. A. Dixit, E. W. Davis and P. L. Houston, "Quantum Yields for Product formation in the 120-130 nm Photodissociation of O_2," in preparation.

These publications may be accessed at
http://www.ccmr.cornell.edu/~plh2/group/publicat.html

IONIZATION PROBES OF
MOLECULAR STRUCTURE AND CHEMISTRY

Philip M. Johnson
Department of Chemistry
Stony Brook University, Stony Brook, NY 11794
Philip.Johnson@sunysb.edu

PROGRAM SCOPE

Photoionization processes provide very sensitive probes for the detection and understanding of molecules and chemical pathways relevant to combustion processes. Laser based ionization processes can be species-selective by using resonances in the excitation of the neutral molecule under study or by exploiting the fact that different molecules have different sets of ionization potentials. Therefore the structure and dynamics of individual molecules can be studied, or species monitored, even in a mixed sample. We are continuing to develop methods for the selective spectroscopic detection of molecules by ionization, to use these spectra for the greater understanding of molecular structure, and to use these methods for the study of some molecules of interest to combustion science.

RECENT PROGRESS

The exploitation of Rydberg molecules has enabled orders-of-magnitude increases in the resolution available for recording the spectra of molecular ions. These spectra provide information equivalent to photoelectron spectra, but contain much more information by virtue of that resolution and the versatility of laser preparation of the states involved.

We primarily use techniques developed in our laboratory called mass analyzed threshold ionization spectroscopy (MATI) and photoinduced Rydberg ionization spectroscopy (PIRI) to provide high resolution spectra of the various electronic states of ions. MATI and PIRI are multilaser techniques, and the multiresonant nature of the overall process is of great use in sorting out the vibrational structure of some ionic states.

The Jahn-Teller effect in benzene cation: A benchmark study.

Along with H_3, Na_3, and ammonia, benzene cation has been a prototypical system in the study of the Jahn-Teller effect, perhaps the most dramatic type of vibronic coupling. In the development of the modern theory, it has always served as one of the primary examples, having a higher symmetry than the smaller molecules and a richer variety of vibrations to consider. In spite of the interest, it is only recently that detailed experimental vibrational information has begun to emerge, when laser techniques involving Rydberg states provided the means to record cation spectra with adequate resolution to be able to separate out all of the vibrational levels. While these tools have been available for some time, there had been no spectra available that had the combination of resolution, energy breadth, and variety of excitation schemes that would enable definitive analysis of the vibronic structures to be carried out.

There are three low-lying states of benzene cation that are subject to Jahn-Teller interactions, $\tilde{X}\,^2E_{1g}$, $\tilde{B}\,^2E_{2g}$, and $\tilde{D}\,^2E_{1u}$. With the exception of a PIRI study we performed a few years ago on the $\tilde{B}$ state, all previous work has focused on the lower energy part of the ground state spectrum, using only pump-probe spectroscopy through the S_1 state. In a series of papers,

we have used *ab inito* and classical Jahn-Teller calculations to analyze the Jahn-Teller vibronic coupling in benzene cation as a general example of molecules with multiple active modes. These calculations were applied to further the understanding of our previous PIRI spectra of the $\tilde{B}$ state. The present work brings the series to a conclusion by the analysis of new, wider ranging spectra of the cation ground state.

As shown by our theoretical analysis, and by previous studies, one must consider three linearly active vibrational modes in any treatment of the cation ground state. Previous vibrationally resolved spectra had been recorded only using pump-probe techniques through the S_1 state. Over the limited energy range that had been examined, Jahn-Teller calculations could fit the line positions exactly, considering only the linearly active modes v_6, v_8, and v_9. In order to get additional vibrational information that might indicate directions for the improvement of the model, we recorded new $C_6H_6^+$ and $C_6D_6^+$ MATI spectra from different neutral (S_0, S_1, and T_1) states over wide energy ranges and analyzed them using multimode Jahn-Teller calculations. Of particular importance in the analysis was the calculation of Franck-Condon factors from the
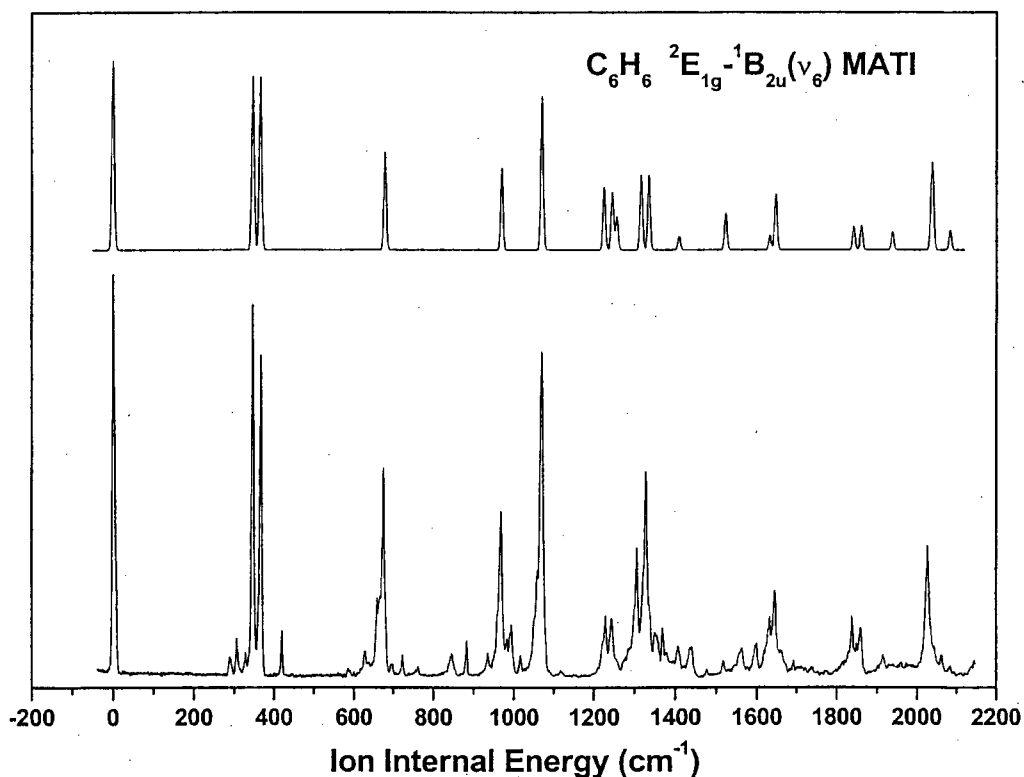
calculated wavefunctions, including effects of geometry change. This enabled a more solid identification of the spectral lines.

The figure above shows one of the new MATI spectra, a pump-probe experiment through the S_1 state. Care was taken to correct the intensities so they could be compared to a spectral simulation (upper trace) derived from the vibrational wavefunctions arising out of the Jahn-Teller calculations (only the three linearly Jahn-Teller active e_{2g} modes and the lower frequency a_{1g} mode are included in the simulation). It is seen that there is a remarkable agreement between

the experiment and a simulation that contained no empirical intensity input, indicating that the classical Jahn-Teller model is working well for the linear interactions.

By virtue of the much larger data set of experimental information, some small but significant discrepancies in the model began to emerge. At higher energies in the spectrum, it would appear to be beneficial to include Fermi interactions between the Jahn-Teller manifolds built upon various totally symmetric vibrational states. The Fermi interactions couple these otherwise isolated manifolds and alter the appearance of the higher energy parts of the spectra. Also, if one is to attain a complete determination of the molecular potential energy surface, all of the quadratically active normal modes should be considered simultaneously. To do this is beyond present technical capabilities, but may become possible as computing technology and quantum chemistry methodology advance.

FUTURE PLANS

We have built a pulsed-amplified CW dye laser system in order to obtain higher resolution electronic spectra of molecular cations using the multiphoton dissociation, and PIRI techniques. This system will enable rotational resolution to be obtained for medium sized molecules and molecular clusters. The pulsed nature of this high resolution source will couple well with our established spectroscopic techniques and with the pulsed coherent vuv generation used to prepare Rydberg states. It will also enable the generation of infrared wavelengths for the measurement of low-lying electronic states and for vibrational spectroscopy. The goal is to develop a general method for cation spectroscopy with orders of magnitude higher optical resolution than current techniques. Initial experiments will be done on substituted benzenes because of our experience with them, but the most promising application of these new methods concerns the determination of the structures of metal containing nanoclusters.

DOE PUBLICATIONS

Philip Johnson, "The Jahn-Teller effect in the lower electronic states of benzene cation: Part I. Calculation of linear parameters for the e_{2g} modes." J. Chem. Phys., 117, 9991-10000 (2002).

Philip Johnson, "The Jahn-Teller effect in the lower electronic states of benzene cation: Part II. Vibrational analysis and coupling constants of the B $^2E_{2g}$ state." J. Chem. Phys. 117, 10001-10007 (2002).

Andrew Burrill, Jia Zhou and Philip Johnson, "The Mass Analyzed Threshold Ionization Spectra of $C_6H_6^+$ and $C_6D_6^+$ obtained via the $^3B_{1u}$ Triplet State," J. Phys. Chem. A, **107**, 4601-4606 (2003).

James Lightstone, Heather Mann, Ming Wu, Philip Johnson and Michael White, "Gas-phase production of molybdenum carbide, nitride, and sulfide clusters and nanocrystallites," J. Phys. Chem. B, **107**, 10359-10366 (2003).

Andrew. B. Burrill, You K. Chung, Heather. A. Mann, and Philip M. Johnson, "The Jahn-Teller effect in the lower electronic states of benzene cation: Part III The ground state vibrations of $C_6H_6^+$ and $C_6D_6^+$," J. Chem. Phys. In Press.

Investigating the chemical dynamics of bimolecular reactions of dicarbon and tricarbon molecules with hydrocarbons in combustion flames

Ralf I. Kaiser
Department of Chemistry
University of Hawai'i at Manoa
Honolulu, HI 96822
kaiser@gold.chem.hawaii.edu

1. Program Scope

The aim of this project is to untangle experimentally the energetics and the dynamics of reactions of dicarbon, $C_2(X^1\Sigma_g^+/a^3\Pi_u)$, and tricarbon molecules, $C_3(X^1\Sigma_g^+)$, with unsaturated hydrocarbons acetylene ($C_2H_2(X^1\Sigma_g^+)$), ethylene ($C_2H_4(X^1A_g)$), methylacetylene (CH_3CCH (X^1A_1)), allene (H_2CCCH_2 (X^1A_1)), and benzene ($C_6H_6(X^1A_{1g})$) on the most fundamental, microscopic level. These reactions are of fundamental importance to understand the formation of carbonaceous nanostructures as well as polycyclic aromatic hydrocarbons and their hydrogen deficient precursors in combustion flames. The closed shell hydrocarbons serve as prototype reaction partners with triple (acetylene), double (ethylene), and aromatic (benzene) bonds; methylacetylene and allene are chosen as the simplest representatives of closed shell hydrocarbon species to investigate how the reaction dynamics change from one structural isomer to the other.

The experiments are carried out under single collision conditions utilizing a crossed molecular beams machine at The University of Hawai'i. The crossed molecular beams technique represents the most versatile approach in the elucidation of the energetics and chemical dynamics of elementary reactions. In contrast to bulk experiments, where reactants are mixed, the main advantage of a crossed beams approach is the capability to form the reactants in separate, supersonic beams. In principle, both reactant beams can be prepared in well-defined quantum states before they cross at a specific collision energy under single collision conditions. The species of each beam are made to collide only with the molecules of the other beam, and the products formed fly undisturbed towards the detector. These features provide an unprecedented approach to observe the consequences of a single collision event, preventing secondary collisions and wall effects.

Projected results of these studies are an identification of the reaction products and the determination of the energetics and entrance barriers of the reaction, the intermediates involved, and of the branching ratios - data which are very much required by the combustion chemistry community. The experiments are pooled together with electronic structure calculations to verify the elucidated reaction mechanisms theoretically. All findings are then incorporated into chemical reaction networks to examine the influence of dicarbon and tricarbon molecules on the growth of carbonaceous nanostructures and of polycyclic aromatic hydrocarbons together with their hydrogen deficient precursors in combustion flames.

2. Recent Progress
2.1. Commission of a hydrocarbon-free crossed molecular beams machine

We finalized the design and commissioned a crossed molecular beams machine; 320 drawings were prepared utilizing Autocad 2D and 3D modeling software. Kurt Lesker Company was contracted to build the main chamber, rotating platform, and detector housings. Smaller items such as supersonic sources (laser ablation source and pulsed valves), cold shields, high voltage insulation units were done by the machine shops of the Department of Chemistry and of the Department of Physics & Astronomy; electronics were build by the chemistry electronics shop.

Briefly, the main chamber of the machine consists of a 304 stainless steel box (70 cm × 60 cm × 30 cm) and can be evacuated by two 2000 ls^{-1} magnetically suspended turbo molecular pump (Osaka Vacuum; TG 2003) backed by a single scroll pump. This arrangement keeps the pressure in the main chamber during an actual experiment to about 10^{-7} mbar. Two source chambers are located inside the main chamber; in its current geometry, both beams cross perpendicularly; optionally, the secondary source can be rotated to vary the intersection angle of the crossing beams to yield collision energies of the reacting particles between 0.3 $kJmol^{-1}$ and 150 $kJmol^{-1}$. Each source chamber is pumped by a 2000 ls^{-1} and a 430 ls^{-1} maglev pump (Osaka Vacuum; TG2003 and TG430) to limit the source pressure during the actual experiment to about 10^{-5} mbar. These pumps require no maintenance and are hydrocarbon free. A dry roots pump RUVAC 510 (Leybold) roughed by two oil-free EcoDry M30 pumps (Leybold) backs the turbo pumps of each source chamber. To minimize the out-gasing of the sealing material, copper gaskets are used preferentially. Whenever O rings are used (detector entrance port, laser entrance window, main door), these are teflon-coated and differentially pumped by an oil-free pumping station at 10^{-6} mbar.

To guarantee an identification of the reaction products, we designed the machine so that two detection schemes can be incorporated: i) a rotatable quadrupole mass spectrometer (QMS) coupled to an electron impact ionizer (with a variable kinetic energy of the electrons) and ii) velocity map ion imaging with one-photon ionization (beyond the current funding period). Angular resolved time-of-flight can be recorded with a triply differentially pumped QMS. The latter is rotatable in the plane of the beams and attached to the lid of the main chamber. Two regions reduce the gas load from the main chamber, whereas the third region contains an electron impact ionizer cooled with liquid nitrogen to reduce the background; to minimize the temperature of the filaments, and hence the background, thoriated iridium is used. The QMS and the scintillation particle detector reside in the second region. Each region is pumped by a maglev turbo pump (430 ls^{-1}); all three pumps are backed by a fourth 430 ls^{-1} pump whose exhaust is connected to a scroll pump. Together with a copper shield, which is attached to a cold head (Sumitomo; 1.5 W at 3.9 K) close to the ionizer, an ultrahigh vacuum of about 8×10^{-13} mbar is achievable; this setup ensures no background counts beyond m/e = 32 except at m/e = 191/193 (Ir^{+}), 95.5/96.5 (Ir^{++}), 63.7/ 64.3 (Ir^{+++}), and 47.75/48.25 (Ir^{++++}).

It is important to address briefly the ionization techniques employed in our experiments. First, electron impact ionization with 200 eV electrons is utilized to identify the 'heavy'

reaction products which are formed via dicarbon and tricarbon versus atomic/molecular hydrogen replacement channel. Secondly, our goal is also to detect the 'light' reaction products which can be formed, for instance, via a potential hydrogen abstraction pathway. However, traditional electron impact ionization at 200 eV electron energy cannot detect the hydrogen abstraction pathways, as the resulting C_xH_{y-1} hydrocarbon products are often generated via dissociative ionization of the parent reactant molecules in the ionizer. However, if we utilize electrons at kinetic energies lower than the ionization potential of the closed shell reactant (the ionization potentials of acetylene, ethylene, methylacetylene, allene, and benzene were determined to be 11.4 eV, 10.5 eV, 10.36 eV, 9.69 eV, 9.2 eV), the dissociative ionization of the reactant molecules and hence the background counts can be eliminated. Tuning the ionization energy lower than the ionization potential of the product allows an investigation how the center-of-mass functions change with an increased fraction of internal energy of the reactant. Also, if the difference of ionization potential of the product isomers is larger than about 0.5 eV, it is in principle also possible to identify the isomer by measuring its ionization efficiency yield as a function of the kinetic energy of the ionizing electrons. Therefore, we record ionization efficiency curves at the center-of-mass angle scanning the electron energy from 7 eV to 15 eV in 0.2 eV steps at and attempt to ascertain whether structural isomers are formed or not. This approach is similar to tunable vacuum ultraviolet (VUV) light generated either by resonant of mixing schemes or at synchrotrons, but does not require extensive laser systems or hardly accessible synchrotrons, but solely high stable power supplies for the electron impact ionizer to generate a stable beam of low energy electrons at currents between 0.1 and 1.0 mA. To compensate for the reduced emission current, we redesigned the ionizer and operate four filaments parallel, i.e. increasing the total emission current by a factor of four. Summarized, the variable electron energy and hence 'tunable' electron impact ionization allows a comprehensive investigation of multi channel reactions involving dicarbon and tricarbon reactant with unsaturated hydrocarbons.

2.2. Supersonic Sources

The generation of supersonic reactant beams of sufficiently high concentration to guarantee a detectable quantity of the final reaction products is essential. We also designed a pulsed, ultra high vacuum compatible laser ablation source to generate dicarbon and tricarbon species; this is supplemented by a high stability chopper wheel motor driver and a dual pulse shape to adjust the rise and fall time of the pulse to the piezo crystal. Here, laser ablation of graphite is applied to generate a highly intense and stable supersonic beam of dicarbon and tricarbon molecules. The output of a 30Hz Nd:YAG laser (GCR-270-30 Spectra Physics) operating at 266 nm is focused onto the rotating graphite rod, and ablated species are seeded in helium carrier gas released by the pulsed piezo valve. The ablation source has been adapted to hydrocarbon-free operation conditions to minimize potential background signal in the product detection. The concentration of ablated $C_2(X^1\Sigma_g^+/a^3\Pi_u)$ and $C_3(X^1\Sigma_g^+)$ can be adjusted and maximized/minimized by carefully adjusting the output power (multiphoton dissociation of carbon molecules), the laser beam profile, the focus size, and the delay time between the laser pulse and the opening of the pulsed valve. This setup provides number densities up to 10^{12} carbon molecules cm^{-3} in the interaction region at velocities of 800 and 3000 ms^{-1}. Note that no ablation source can produce a pure beam of dicarbon or tricarbon molecules. One

reactant can be only minimized/maximized with respect to the other. However, due to conservation of energy and linear momentum, the reaction channels can be determined unambiguously even if dicarbon and tricarbon coexist in the beam. The pulsed primary beam will cross then a second, pulsed hydrocarbon beam in the scattering chamber.

3. Future Plans

The crossed beams machine is currently being calibrated. Hereafter, the scattering experiments are performed with rising complexity at two conceptual levels. For each closed shell hydrocarbon reactant, the energy-dependent dynamics of tricarbon reactions will be investigated first, followed by the reactions of dicarbon molecules in their electronic ground and first excited state. All experiments utilize the QMS/EI detector to record angular resolved time-of-flight spectra. Let us have a closer look at the $C_3(X^1\Sigma_g^+)/C_2H_2(X^1\Sigma_g^+)$ and $C_2(X^1\Sigma_g^+/a^3\Pi_u)/C_2H_2(X^1\Sigma_g^+)$ systems as typical examples to outline the proposed experimental sequence. Two groups of potential reaction products can be identified: products formed via carbon versus atomic hydrogen and molecular hydrogen exchange pathways ('heavy' products C_5H, C_5, C_4H, C_4) and those channels proceeding via hydrogen atom abstraction and/or cleavage of carbon-carbon bonds to form smaller hydrocarbon fragments ('light' products C_4H_x, C_3H_x, C_2H_x, CH_x). The heavy reaction products will be probed via an angular resolved TOF mass spectrometric detection first utilizing the universal detector at 200 eV electron energy. Hereafter, the kinetic energy is reduced to selectively ionize potential low-mass reaction products. After this system has been investigated comprehensively, we intent to incorporate a rotatable, secondary pulsed hydrocarbon beam source. With this experimental configuration we expect to complete our proposed studies.

4. Acknowledgements

5. Publications

X. Guo, E. Kawamura, R.I. Kaiser, *Design and performance of a high repetition rate, dual pulse shaper to operate pulsed, piezo electric valves.* Rev. Sci. Instr. (in progress 2004).

X. Guo, H. Chang, R.I. Kaiser, *Design and characteristics of a high precision chopper wheel motor driver to operate ultrahigh vacuum compatible laser ablation sources with nanosecond time accuracy.* Rev. Sci. Instr. (in progress 2004).

DYNAMICAL ANALYSIS OF HIGHLY EXCITED MOLECULAR SPECTRA

Michael E. Kellman
Department of Chemistry, University of Oregon, Eugene, OR 97403
kellman@oregon.uoregon.edu

PROGRAM SCOPE:

Spectra and internal dynamics of highly excited molecules are essential to understanding processes of fundamental importance for combustion, including intramolecular energy transfer and isomerization reactions. The goal of our program is to develop new theoretical tools to unravel information about intramolecular dynamics encoded in highly excited experimental spectra. We want to understand the formations of "new vibrational modes" when the ordinary normal modes picture breaks down in highly excited vibrations. We use bifurcation analysis of semiclassical versions of the effective Hamiltonians used by spectroscopists to fit complex experimental spectra. Specific molecular systems are of interest for their relevance to combustion and the availability of high-quality experimental data. Because of its immense importance in combustion, the isomerizing acetylene/vinylidene system has been the object of long-standing experimental and theoretical research. We have made significant progress in systematically understanding the bending dynamics of the acetylene system.

We have begun to make progress on extending our methodology to the full bend-stretch vibrational degrees of freedom, including dynamics with multiple wells and above barrier motion, and time-dependent dynamics. For this, development of our previous methods using spectroscopic fitting Hamiltonians is needed, for example, for systems with multiple barriers.

RECENT PROGRESS: DYNAMICS FROM SPECTRA OF HIGHLY EXCITED ACETYLENE APPROACHING ISOMERIZATION.

Bifurcation analysis: Branchings of the normal modes into new anharmonic modes. Our approach to highly excited vibrational spectra uses bifurcation analysis of the classical version of the effective Hamiltonian used to fit spectra. We have applied this to a bifurcation analysis of the bend degrees of freedom of acetylene.

We have had several specific aims in performing the bifurcation analysis of the acetylene bends system. We have succeeded in obtaining a systematic global analysis of the bifurcations that lead to novel modes. We now understand the number and character of the new modes. We have found that there is a unique ``evolutionary tree" of new modes, born in bifurcations of the normal modes. This is in contrast to earlier work on HCP, where multiple bifurcation trees were observed.

The pure bending system is a stepping-stone to inclusion of the stretch degrees of freedom and an attack on the above-barrier isomerization problem for vinylidene-acetylene isomerization, both described below.

Visualization of complex molecular dynamics. One of our primary goals is to translate the abstract dynamical knowledge of the bifurcation analysis into a directly visualizable representation. For this, we are using computer techniques to make animations of the anharmonic modes born in bifurcations. Examples of our animations can be found on a web-site at http://darkwing.uoregon.edu/$\sim$meklab/, which the interested reader is invited to access.

Spectral patterns of isomerizing systems. Earlier work from our group has demonstrated spectral patterns associated with the new modes born in bifurcations. It is of great interest is to extend the bifurcation and spectral analysis to isomerizing systems. We have made a start on this with an investigation [5] of a model of an isomerizing system of coupled stretch and bend, intended to have some of the features of a realistic model of the acetylene-vinylidene isomerization. Below the barrier there are patterns expected from previous work. There are wholly new patterns associated with multiple barriers and above-barrier motion. These patterns are interpreted in terms of nonlinear resonance-type couplings, similar to anharmonic Fermi resonances, between the stretch and bend. There is conventional Fermi resonance below the barrier, and a new type of "cross-barrier" resonance.

Semiclassical quantization of systems of spectral models. Much of our work seeks to assign novel quantum numbers to highly excited spectra, based on the new modes from our bifurcation analysis, when the ordinary normal modes quantum numbers no longer suffice. A fundamental question is whether these quantum numbers can be given a precise meaning. In a series of investigations [1-3] on semiclassical quantization of wavefunctions, we are finding that this can be answered this in the affirmative, even for chaotic systems.

Inclusion of full stretch-bend degrees of freedom. The bifurcation analysis successfully completed so far is for pure bends spectra with vibrational angular momentum $1 = 0$. Obviously, it is of great interest to extend this to systems with $1 > 0$, and to spectra with combinations of stretch and bend excitation, for which fitting Hamiltonians of existing experimental spectra are available. We are completing work on $1 > 0$, and have begun to make headway on the stretch-bend problem, as described below. (Eventually we will want to include rotation degrees of freedom when we have mastered the full vibrational problem.)

147

FUTURE PLANS: FULL STRETCH-BEND DYNAMICS, TIME-DEPENDENT AND REACTIVE DYNAMICS.

Our current goal is to extend our methods to larger systems and systems undergoing intramolecular reactions, i.e. isomerization reactions involving a potential barrier. We are interested in the particular chemical problem of the acetylene-vinylidene isomerization.

The key challenges are: (1) Making current methods practical for more complex systems, with more degrees of freedom. In acetylene, this means inclusion of the stretches in addition to the pure bends previously analyzed; (2) The problem of extending the spectroscopic Hamiltonian to handle qualitatively new physical situations, in particular, motion in multiple potential wells, and very large-amplitude motion above two or more wells.

The challenge of complexity: Analytically scalable bifurcation analysis. Existing spectra of the acetylene system access states in which the stretches and bends are coupled in a highly complex way. As the dimensionality of the problem becomes larger, one of the challenges is whether our analysis can be performed, in a way that is still understandable and useful.

The key to making tractable larger systems such as the full stretch-bend degrees of freedom is use of the polyad quantum number, which is an integral part of the standard spectroscopic fitting Hamiltonian. A fact that has been little-utilized outside our group is that the polyad Hamiltonian affords computation of the mode bifurcation structure by analytic means, i.e. by solution of simple algebraic equations related to the Hamiltonian function, rather than numerical solution of the equations of motion. Specifically, we seek the critical points of the polyad Hamiltonian, defined in a phase space naturally reduced in dimension by means of the conserved polyad numbers. The critical points give periodic orbits or "vibrational modes" when the Hamiltonian is expanded back to the full phase space including polyad numbers and their conjugate angles. Because these modes are obtained analytically, it is not necessary to perform numerical integration of Hamilton's equation and analysis of surfaces of section. This is expected to become extremely advantageous as the number of degrees of freedom and phase space dimensions increases, as in the full stretch-bend system. The solutions for these critical points are solutions of algebraic equations involving polynomials and trigonometric functions.

Spectroscopic Hamiltonians for multiple wells and above barrier spectroscopy. The least-explored theoretical challenge in observing and interpreting isomerization problems in our approach is to be able to handle a future spectroscopy of above-barrier states, incorporating multiple wells in the spectroscopic Hamiltonian; and to develop techniques such as bifurcation analysis to obtain dynamical information. We have made a start on this, using model systems until such time as experimental data become available. We are using some of the ideas developed in our paper [5] on spectral patterns of isomerizing systems.

Time dependent dynamics. Our prior work has focused on extracting information from spectra, i.e. time-independent phenomena such as the new modes that take over from the normal modes after bifurcations. However, dynamics includes time-dependent phenomena, for example intramolecular relaxation, and isomerization reactions. We are currently applying our spectroscopic Hamiltonians to time-dependent vibrational relaxation dynamics. One goal is to understand Coulomb explosion and related studies of the vinylidene/acetylene system. The system is believed to "cycle" between the vinylidene and acetylene forms in a very highly excited condition. This goes on for an extremely long time, up to a microsecond. We hope to model this with the spectroscopic Hamiltonian, and understand it in terms of the knowledge of the molecular phase space. This means understanding the role of the approximate conserved polyad number, breaking of the polyad number, and formation of phase space "zones of stability" described by our bifurcation analysis.

Recent publications (in print or in press since 2002) related to DOE supported research:

1. S. Yang and M.E. Kellman, "Addendum: Direct Trajectory Method for Semiclassical Wavefunctions", Phys. Rev. A. 65, 034103 (2002).

2. S. Yang and M.E. Kellman, "Semiclassical Wave Function Near a Strong Resonance", Phys. Rev. A 65, 064101 (2002).

3. S. Yang and M.E. Kellman, "Perspective on Semiclassical Quantization: How Periodic Orbits Converge to Quantizing Tori", Phys. Rev. A. 66, 052113 (2002).

4. C.Zhou, D. Xie, R.Chen, G.Yan, H.Guo, V. Tyng, and M.E. Kellman, "Highly Excited Vibrational Energy Levels of $CS_2(\tilde{X})$ on a New Empirical Potential Energy Surface and Semiclassical Analysis of the 1:2 Fermi Resonance", Spetrcochimica Acta A 58, 727-746 (2002).

5. S. Yang, V. Tyng, and M.E. Kellman, "Spectral Patterns of Isomerizing Systems", J. Phys. Chem. A. 107, 8345-8354 (2003).

6. M.E. Kellman, M.W. Dow, and Vivian Tyng, "Dressed Basis for Highly Excited Vibrational Spectra", J. Chem. Phys. J. Chem. Phys. 118, 9519-9527 (2003).

High Energy Processes

Alan R. Kerstein
Combustion Research Facility
Sandia National Laboratories
Livermore, CA 94551-0969
Email: arkerst@sandia.gov

PROJECT SCOPE

Turbulent flow involves unsteady motion that typically extends over a much wider range of scales than multi-dimensional simulations can affordably resolve. This necessitates reduced representations encompassing much of the flow behavior. Large-eddy simulations (LES), which resolve the large scales but require modeling of the small scales, are challenged by the need to generalize the small-scale representation from its usual role as an energy dissipation mechanism to a representation of dynamically active couplings between small-scale motions and multiple physical and chemical processes. Empirical parameterization of these couplings is increasingly recognized as insufficient for physically sound predictive extrapolation. Accordingly, the strategy that is adopted to predict and investigate these couplings (and other aspects of turbulent flow phenomenology) is to perform unsteady spatially resolved simulations on a computational domain of reduced dimensionality. A modeling approach developed during this project for simulating these phenomena in one spatial dimension, denoted One-Dimensional Turbulence (ODT), has proven to be particularly suitable for cost-effective computation that provides needed predictive capabilities. Recent efforts have provided initial demonstrations of these capabilities with respect to compressible flow, multi-phase flow, and certain regimes of buoyant stratified flow, and in so doing, have yielded significant physical insights. Planned future efforts fall within three categories: further extension of capabilities, use of demonstrated capabilities to address scientific issues, and adaptation of the approach to achieve the needed subgrid closure capability for LES.

Reduced computational representations of turbulent flow involve one or more of the following simplification strategies: Reducing the range of resolved scales, reducing the flow dimensionality, introducing surrogate physical processes, and evolving statistical properties rather than the flow field itself. For example, conventional LES involves a reduced scale range, supplemented by surrogate physical processes (eddy viscosity and diffusivity) to represent unresolved advection. The diffusion representation of unresolved advection is a particularly prevalent simplification, but its limitations with regard to dynamically active small-scale couplings are becoming increasingly evident.

Ongoing research during this project has demonstrated that, for many turbulent flows of interest, all scales of advection can be reliably and affordably resolved in a 1D unsteady simulation by introducing a surrogate for the $v \cdot grad\ v$ advection operator. (This operator can in fact be specialized to 1D, yielding the Burgers equation, which has been used for turbulence modeling but does not provide quantitative predictions due to its violation of conservation laws.) The elementary operation of the surrogate process is a rearrangement of property profiles along an interval of the 1D domain so as to emulate the effect of a turbulent eddy turnover within that interval. The key physical content of the model is a procedure for random selection of affected intervals in a manner that reflects the processes controlling eddy turnovers in multi-dimensional turbulent flow. A close analogy is obtainable because the 1D domain carries a velocity profile

whose spatial variation (specifically, shear distribution) controls eddy turnovers much as in real flows. The rearrangements representing eddy turnovers affect these velocities as well as other properties. This two-way coupling of velocities and surrogate advection maintains their mutual consistency and leads to velocity profile evolution that captures many important features of turbulent flow. It is noteworthy in this regard that the surrogate process is advective (i.e., it displaces fluid elements) rather than diffusive, and thus preserves fundamental properties of advective motion. On the spatially resolved 1D domain, processes that are truly diffusive (as well as other processes involving transport or state change, such as chemical reactions) are likewise faithfully represented, allowing subtle effects such as differential molecular diffusion to be treated accurately. As illustrated by the work described below, the analogy between this 1D formulation and turbulence phenomenology is broader than this brief explanation can convey, and its uses are diverse, ranging from focused scientific investigations to the development of general-purpose flow simulation tools.

RECENT PROGRESS

Because ODT carries a 1D profile of the velocity vector, it is ostensibly straightforward to advect particles that are coupled to the flow by a drag law. The issue is subtler, however, because rearrangements, rather than the velocity profile, advect fluid in ODT. Accordingly, a mathematical formulation of particle response to rearrangements has been developed that accounts for the finite interaction time of particles with turbulent eddies. (Rearrangements are nominally instantaneous, but an associated eddy time scale governs their occurrences.) Particle motion in turbulent channel flow was simulated, and results were compared to statistics gathered from DNS. The technologically important issue of particle deposition rates was addressed over a wide range of particle response times (normalized by a flow time scale, thus quantifying the influence of particle inertia). ODT reproduces the inertia dependence of deposition seen in DNS and reveals a high-inertia scaling that was not previously recognized. A simple physical explanation of this dependence has been identified.

Single-Column Modeling (SCM) is a widely used 1D representation of vertical transport in the atmospheric boundary layer (ABL). Unlike SCMs, which model turbulent transport using eddy diffusivity, ODT involves unsteady advective motions that give it a character intermediate between conventional SCMs and the LES computations that are considered benchmarks for SCM calibration. To demonstrate this, an ODT simulation of a benchmark case was performed. ODT was run both in high-resolution mode (16000 cells spanning a 400 m domain) to capture near-surface effects not resolved by other methods, and in low-resolution mode (64 and 128 cells) to demonstrate fidelity comparable to other methods implemented at low resolution. For the low-resolution case, a diffusion-type subgrid closure analogous to LES closure was implemented within ODT. Comparison to the high-resolution case highlighted the capabilities and limitations of this approach to closure.

A new scaling law for self-heated turbulent convection has been proposed that accounts for the occurrence of off-center ignition of type 1a (white-dwarf-progenitor) supernova explosions. (Off-center ignition appears to be essential for explaining observed explosion characteristics.) ODT simulations support the proposed scaling and demonstrate the capability to study the parameter dependencies of the number and spatial distribution of ignition points, which will guide the selection of initial conditions for multi-dimensional simulations of the explosion process.

FUTURE PLANS

An initial ODT application to compressible flow involved the introduction of rearrangement events (to represent turbulent eddy motions) in a 1D gas-dynamic simulation of shock-induced mixing, ignition, and subsequent pressure rise in an unconfined propane-air mixture surrounded by ambient air. Finite-rate-chemistry effects were introduced empirically by tuning a chemical delay time to match the measured pressure-rise delay. In future work, a multi-step reduced chemical mechanism will be introduced in the model in order to capture chemical-kinetic effects.

This initial study identified important considerations for physically sound ODT representation of turbulent compressible flow. Foremost is the need to apply rearrangements to the gradient of the dilatational velocity on the ODT domain, rather than to the velocity itself; otherwise rearrangements change the sign of the gradient in some regions, thereby instantly turning local expansion into local compression and *vice versa*. Rearrangement of the gradient, followed by recovery of the transformed velocity profile, changes the total dilatational kinetic energy. This reflects energy exchange between solenoidal and dilatational modes that is a fundamental feature of compressible turbulence. Accordingly, a procedure for enforcing equal-and-opposite changes of the solenoidal kinetic energy during rearrangements will be introduced, analogous to a physically consistent procedure of this type that was previously introduced in a different context.

ODT provides a natural decomposition into solenoidal and dilatational kinetic energy, but it does not capture all the 3D physics of this decomposition. In particular, it has no inherent mechanism for sustaining pressure gradients associated with quasi-steady solenoidal motions. Instead, all pressure fluctuations are radiatively depleted on acoustic time scales. A physically based procedure that prevents this depletion will be essential for sound representation of compressible-flow thermodynamics. A plausible approach has been formulated and will be tested.

A new conceptual picture of extinction-reignition in turbulent nonpremixed combustion was revealed by ODT simulations [1]. The advent of subsequent DNS results provides an opportunity to validate ODT quantitatively for this application by applying ODT to conditions directly corresponding to those of the DNS. The validated formulation will then be used to investigate regimes of higher turbulence intensity than are currently accessible using DNS. This is important for scale-up of DNS-based inferences because extinction is sensitive to rare bursts of intense mixing whose asymptotic scalings become evident only at high turbulence intensity.

In parallel with this effort, which will focus on spatially homogeneous flow, extinction-reignition will be addressed in the context of ongoing experimental study of turbulent jet diffusion flames in the Turbulent Combustion Laboratory (TCL) at the CRF. An early application of ODT to these flames will be revisited, incorporating the substantial subsequent development of ODT methodology, notably a new treatment of variable-density flow, a cylindrical ODT formulation, and a spatially developing implementation of ODT. This upgraded ODT jet diffusion flame methodology will be applied to TCL flames. In addition to the focus on extinction and reignition in those flames, this methodology will be used to generate multiply-conditioned scalar statistics analogous to data being gathered from TCL line-Raman measurements.

A laboratory analog of atmospheric convection involves heavy (salty) water below a lighter fresh-water layer (representing the free atmosphere), with infiltration of fresh water below the salty layer to introduce convective instability. We will coordinate blind ODT predictions with Prof. Harm Jonker (Delft), who is performing the experiment. A key contribution of ODT will be to bridge the gap between the high-Sc (Schmidt number: ratio of viscosity and mass diffusivity) experimental conditions and the order-unity value of Pr (Prandtl number: ratio of viscosity and

thermal diffusivity) in the atmosphere. (Salinity is a surrogate for temperature in this experiment.)

Having recently addressed the constant-property near-wall momentum closure [5], the current focus is momentum and scalar closures for bulk flow. A comprehensive ODT-based closure strategy has recently been formulated [2]. Implementation of bulk momentum closure, with planned generalization to variable-property flows and closure for dynamically active scalars, is underway. This formulation involves a lattice-work of ODT domains, such that the center of each LES cell on a Cartesian mesh is intersected by three orthogonal ODT domains. Couplings among ODT domains, and between ODT and LES as they evolve in tandem during a time-advancement cycle, are currently specialized to the requirements for constant-property momentum closure, but will be generalized in future work to include multi-scalar processes. Prior to addressing reacting flow, simulations of turbulent Rayleigh convection in a rectangular enclosure will be performed because the rich phenomenology of this flow will provide a stringent test of model performance as well as an opportunity to gain further insight into the physics of this canonical flow regime.

Two collaborative efforts involving ODT closure of atmospheric-flow LES are planned. First, the low-resolution ABL implementation of ODT (see Recent Progress) will be used as a near-surface closure of a general circulation model (GCM) of the earth's atmosphere. Advantages of ODT for this application include time-lagged response to upper-atmosphere and surface-level flow and thermal transients, resolution of local shear-buoyancy interactions, and physically based representation of turbulence-induced state fluctuations.

The second atmospheric-flow LES effort is a cloud-scale simulation in which subgrid ODT will be used to evolve cloud droplets as they are vertically advected, grow by collisions and condensation (which is affected by mixing that modulates the local humidity), and eventually precipitate. (LES-resolved horizontal transport will determine the lateral mass transfer between vertical ODT domains.) This study will address the poorly understood influence of turbulence-induced droplet clustering on the various processes that determine the intensity and duration of rainfall.

PUBLICATIONS SINCE 2002

1. J. C. Hewson and A. R. Kerstein, "Local Extinction and Reignition in Nonpremixed Turbulent CO/H2/N2 Jet Flames," Combust. Sci. Tech. **174**, 35 (2002).
2. A. R. Kerstein, "One-Dimensional Turbulence: A New Approach to High-Fidelity Subgrid Closure of Turbulent Flow Simulations," Computer Phys. Commun. **148**, 1 (2002).
3. S. Wunsch and Y. N. Young, "Temperature Statistics in Two-Dimensional Stably Stratified Turbulence, Phys. Rev. E **66**, #016306 (2002).
4. Wm. T. Ashurst, A. R. Kerstein, L. M. Pickett, and J. B. Ghandhi, "Passive Scalar Mixing in a Spatially Developing Shear Layer: Comparison of ODT Simulations with Experimental Results," Phys. Fluids **15**, 579 (2003).
5. R. C. Schmidt, A. R. Kerstein, S. Wunsch, and V. Nilsen, "Near-Wall LES Closure Based on One-Dimensional Turbulence Modeling," J. Comput. Phys. **186**, 317 (2003).
6. A. R. Kerstein, "Turbulence in Combustion Processes: Modeling Challenges," Proc. Combust. Inst. **29**, 1763 (2003).
7. S. Wunsch, "Stochastic Simulations of Buoyancy-Reversal Experiments," Phys. Fluids **15**, 1442 (2003).

KINETICS OF COMBUSTION-RELATED PROCESSES
AT HIGH TEMPERATURES

J. H. Kiefer and R.S. Tranter*

Department of Chemical Engineering
University of Illinois at Chicago
Chicago, IL 60607
(kiefer@uic.edu)

Program Scope

This program involves the use of the shock tube with laser-schlieren, dump-tank GC/MS analysis, and time-of-flight mass spectrometry diagnostics to explore reactions and energy relaxation processes over an extremely wide range of temperatures and pressures. We are interested primarily in energy transfer and the kinetics of unimolecular reactions at combustion temperatures, in particular, the effects of unimolecular falloff. Over the past year we have considerably extended our efforts to include some new results on relaxation, incubation and falloff.

Ethane relaxation, incubation, and dissociation

The C-C bond fission in ethane dissociation, $C_2H_6 \rightarrow 2CH_3$ (1), and its reverse, the recombination of methyl radicals, has long performed the role of prototype for the study of falloff in unimolecular kinetics. It has been examined both experimentally and theoretically in an extraordinarily large number of experimental and theoretical studies. A recent up-to-date and extensive theoretical study using flexible variational transition state theory [1] now seems to have uncovered some indications of non-RRKM behavior in the recombination for high temperatures. Here the high-pressure theoretical rates were too large when compared to available experiment, and the authors suggested the experimental rates might have been reduced by re-crossing of the transition state, a form of non-RRKM behavior. This result certainly needs confirmation, either through improved calculations or additional experiment. Non-RRKM behavior does seem possible here because ethane long been known to show double relaxation at room temperature [2,3], and we have now confirmed this for much higher temperatures (see below). Such double vibrational relaxation is a clear demonstration of slow intra-molecular vibrational relaxation (IVR), at least for low energies, and slow IVR is a most likely cause of non-RRKM behavior.

We have now performed new and improved laser-schlieren (LS) experiments on both relaxation and dissociation over a very wide range of T and P (1000-1467K and P <30 torr for relaxation; and 1500-2200K, 70-550 torr for dissociation). We have then combined the derived rates with higher-pressure UV absorption data from the Stanford group [4] that covered 1400-2000K, 100-5700 torr, and modeled the entire set with the above flexible TST theory of Klippenstein and Harding [1]. Note that use of the shock tube with fast diagnostics is essential if non-RRKM behavior caused by slow IVR is to be

uncovered simply because of the well known speed of IVR processes and the need for reaction rates that compete with these..

An example semilog plot of density gradients arising from vibrational relaxation in an ethane-krypton mixture is presented in the left upper figure. Here the relaxation clearly occurs in two well-defined exponential stages; this is indeed a double relaxation as proposed in refs. 2 and 3. Of course ethane does eventually decompose at the temperatures of experiments like this, but reaction is here far too slow to produce a measurable gradient.

Relaxation times have been estimated from experiments like those of Fig. 1 and are displayed in the right upper figure, where they are seen to be extremely short, a behavior characteristic of hydrocarbons with methyl groups [5].

At higher temperatures dissociation does appear, and incubation times for the onset of steady-state dissociation were obtained. The lowest-pressure LS experiments were then corrected for this incubation before dissociation rates were derived.

A small chain-reaction model was used to fit the entire length of the gradient profiles and this model fit is uniformly of high quality. This mechanism is an excellent description of this reaction, at least for high temperatures, low pressures and short times. Of course the experiments are fairly insensitive to this set of secondary processes at early times, where only the direct dissociation contributes. Thus a good set of initial rates is easily obtained.

The rate data form both the LS and UV experiments is collected and compared to RRKM master-equation calculations in the bottom figure. These calculations use the unscaled theoretical model and master-equation of Klippenstein and Harding [1] with only one minor modification. The model now includes the effect on the molecular partition function and state density of a 1-D hindered rotor treatment of the torsion, and this is the sole anharmonic correction for the molecule. The master-equation calculations assume the usual exponential down model with $<\Delta E>_{down} = 120(T/300)^{0.9}$ cm^{-1}, nearly linear in T. As is quite evident in the figure, the agreement is excellent; this model fits all the data essentially within the experimental scatter.

The above fit suggests there is no non-RRKM behavior in the dissociation of ethane at high temperatures. This would seem to imply that there would also be no non-RRKM behavior in the recombination direction at these temperatures, in apparent disagreement with the earlier application of this theory to the recombination. Perhaps the problem with the fit of the recombination data lies in the data itself.

Time-of-flight mass spectrometer construction

In the last reporting period we stated that a time-of-flight mass spectrometer (TOF-MS) would be added via a nozzle/skimmer interface to the LS shock tube that would provide a real time diagnostic tool capable of measuring species specific concentrations

to compliment the non-specific data acquired in LS experiments. In the intervening period this interface has been constructed. The equipment now includes a custom built XYZ table that supports the interface, the TOF-MS and a set of turbo pumps, and permits accurate alignment of the nozzle and skimmer. The apparatus has been successfully evacuated and its performance is currently been assessed. An initial test study will be performed using the well-defined decomposition of cyclohexene to 1,3-butadiene and ethylene prior to starting work on more interesting reactions, such as the bimolecular acetylene + propargyl radical combination to cyclopentadienyl radical.

Future work

Our main intentions for the forthcoming year or two involve extension of our efforts to detect non-RRKM reaction by continuing the study of relaxation and dissociation in additional species. Among these are the obvious choices CF_2HCH_3 and CF_2HCF_3. Besides these we have confirmed the reported double relaxation in CH_2Cl_2 which shows a most interesting indication of non-linear relaxation in the second stage. We will look at this again and also investigate its dissociation.

References
1. S. J. Klippenstein and L. B. Harding, J. Phys. Chem. **103**, 9388 (1999).
2. R. Holmes, G. R. Jones, and R Lawrence, Trans. Fara. Soc. **62**, 46 (1965).
3. J. D. Lambert and R Salter, Proc. Roy. Soc. (London) **A253**, 277 (1959).
4. M. A. Oehlschlaeger, D. F. Davidson, and R. K. Hanson, Proc. Combust. Inst. **30** (2004).
5. Publication number 4, below.

Publications
1. "Modeling of Nonlinear Vibrational Relaxation of Large Molecules in Shock Waves with a Nonlinear, Temperature-Varying Master Equation, M. J. Davis and J. H. Kiefer, J. Chem. Phys. **116**, 7814 (2002).
2. "Dissociation, Relaxation, and Incubation in the Pyrolysis of Neopentane: Heat of Formation for *tert*-butyl Radical", N. K. Srinivasan, J. H. Kiefer, and R.S. Tranter, J. Phys. Chem. **107**, 1532 (2003).
3. "A Shock-Tube, Laser-Schlieren Study of the Pyrolysis of Isobutene: Relaxation, Incubation, and Dissociation Rates", S. Santhanam, J. H. Kiefer, R.S. Tranter and N. K. Srinivasan, Int. J. Chem. Kinet. **35**, 381 (2003).
4. "Vibrational Relaxation in Methyl Hydrocarbons at High Temperatures: Propane, Isobutene, Isobutane, Neopentane and Toluene", J. H. Kiefer, G. C. Sahukar, S. Santhanam, N. K. Srinivasan., and R.S. Tranter, J. Chem. Phys., 120, 918 (2004).

5. "A Shock-Tube, Laser-Schlieren Study of the Dissociation of 1, 1, 1-trifluoroethane: An Intrinsic non-RRKM Process", J. H. Kiefer, C. Katopodis, S. Santhanam, N. K. Srinivasan, and R. S. Tranter, J. Phys. Chem. **108**, 2443 (2004).

* Now at Argonne National Lab, Argonne, IL 60439 (tranter@anl.gov)
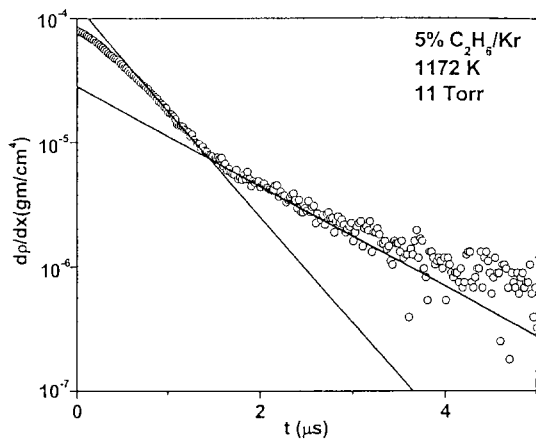
An Example LS experiment showing
double vibrational relaxation
in 5% C_2H_6/Kr.
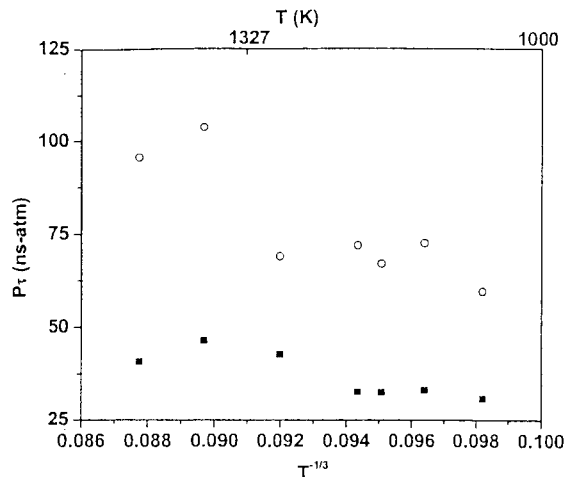
Landau-Teller plot of relaxation times in
C_2H_6/ Kr. Bold symbols are Pτ taken
from the initial fast process, open
symbols are from the later slow step.
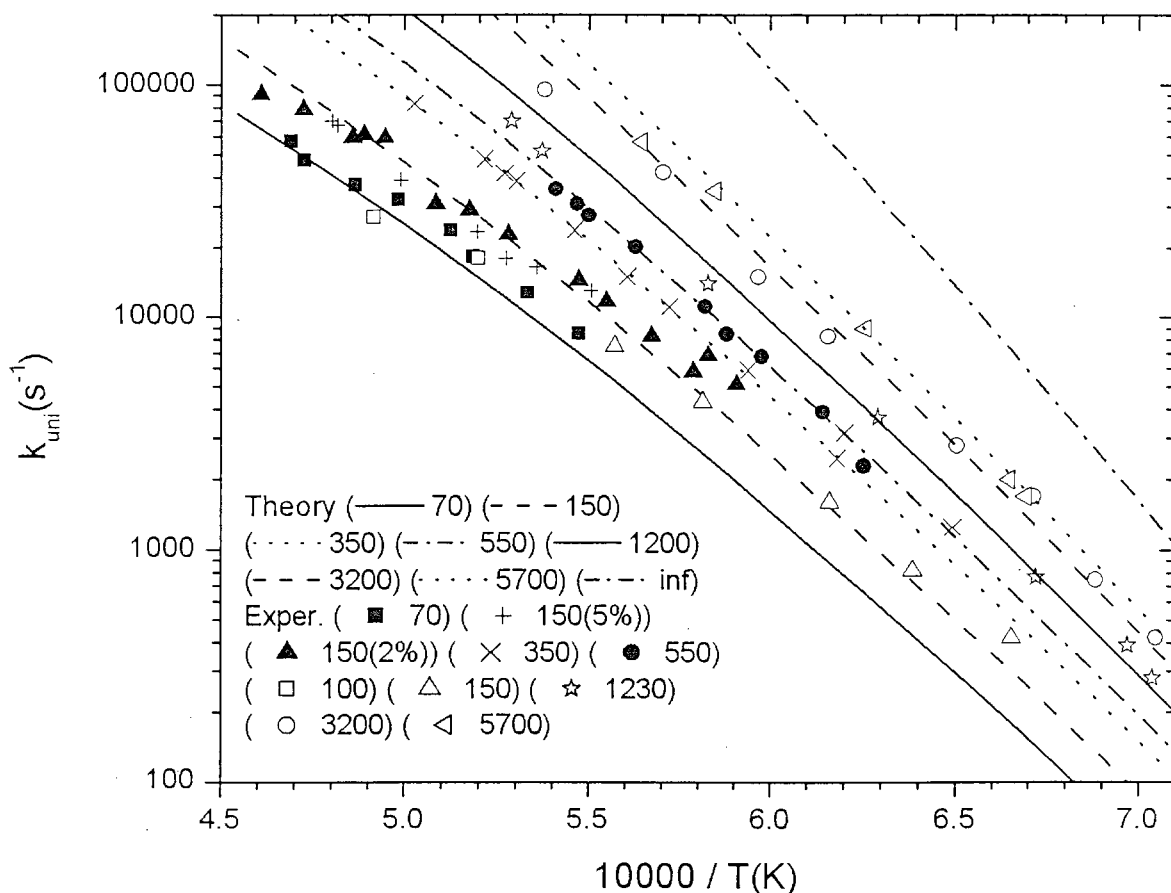
Comparison of RRKM calculations with
both LS and UV rate data. Given pressures are in
Torr. Here the LS data (closed symbols) cover the
first 70-550 Torr in 2% C_2H_6/Kr (unless otherwise noted)
and the UV data (open symbols) cover 100-5700 Torr.

THEORETICAL CHEMICAL KINETICS

Stephen J. Klippenstein
Combustion Research Facility
Sandia National Laboratories
Livermore, CA, 94551-0969
E-mail: sjklipp@sandia.gov

Program Scope

The focus of this program is the theoretical estimation of the kinetics of elementary reaction steps of importance in combustion chemistry. The research involves a combination of *ab initio* quantum chemistry, variational transition state theory, direct dynamics, and master equation simulations. The emphasis of our current applications is on (i) reactions of importance in soot formation, (ii) radical oxidation reactions, and (iii) NO_x chemistry. We are also interested in a detailed understanding of the limits of validity of and, where feasible, improvements in the accuracy of specific implementations of transition state theory. Detailed comparisons with experiments, and with other theoretical methods are used to explore and improve the predictive properties of the transition state theory models. Direct dynamics simulations are being performed as a means for testing the statistical assumptions, for exploring reaction mechanisms, and for generating theoretical estimates where statistical predictions are clearly inadequate. Master equation simulations are used to study the pressure dependence of the kinetics and to produce phenomenological rate coefficients for use in kinetic modeling.

Recent Progress

Soot Formation: The Role of n-C₄H₃ (in collaboration with Jim Miller)

We have performed detailed studies of various aspects of the kinetics of n-C_4H_3 radicals in order to further elucidate the possible role of this radical in aromatic ring formation. We have examined the temperature and pressure dependent kinetics of H addition to diacetylene to form both n- and i-C_4H_3. We have used MRCI calculations to study the heats of formation of n and i-C_4H_3 radicals, and find little difference from related large basis set QCISD(T) calculations. These results are in sharp contrast with those from diffusion Monte Carlo by the Lester group. We have examined the potential energy surface for the n-C_4H_3 + C_2H_2 reaction, discovering in the process numerous important additional channels beyond those considered in the earlier works of Lin and coworkers, of Walch, and of Frenklach and coworkers. We are in the process of implementing this potential energy surface in a master equation based analysis of the kinetics. Preliminary results suggest the predominant formation of linear forms of C_6H_4, at least for the temperatures of significance in combustion.

Radical Oxidation (in collaboration with Larry Harding)

The reactions of oxygen atoms with methyl, ethyl, and vinyl radicals were studied with a combination of *ab initio* quantum chemistry, variational transition state theory, and classical trajectory simulations. The interaction between the two radicals was examined with MRCI calculations employing augmented double zeta and augmented triple zeta basis sets. The implementation of analytic representations of the *ab initio* data within variable reaction coordinate (VRC) transition state theory (TST) yields predictions for the high-pressure limit addition rate coefficients. For the CH_3 + O reaction these predictions are in remarkably good agreement with the extensive experimental data, while for the C_2H_5 + O and C_2H_3 + O reactions

the theoretical predictions appear somewhat lower and higher, respectively, than the rather limited experimental data. VRC-TST analyses also suggest that the abstraction reactions to produce C_2H_4 + OH and C_2H_2 + OH have a rate coefficient that is about 10% of the corresponding addition rate. Experimentally, the abstraction was observed to be about 21 ± 8 % of the total for C_2H_5 + O, but was not observed in C_2H_3 + O.

NOx Chemistry (in collaboration with Craig Taatjes)

The potential energy surface for the C_2H_3 + NO reaction was explored with both quadratic configuration interaction and multi-reference configuration interaction *ab initio* calculations. These *ab initio* predictions were employed in RRKM theory based master equation simulations of the temperature and pressure dependent kinetics, which were compared with related expeirmental observations. The *ab initio* characterizations suggest a significant contribution from HCN + CH_2O formation, with the two isomerization transition states for the pathway leading to this product lying ~15 kcal mol^{-1} below the entrance channel. The master equation analysis provides a reasonably satisfactory reproduction of the experimentally observed kinetic data. At constant pressure the rate constant decreases rapidly with temperature. At higher temperatures, a falloff of the rate constant to lower pressure is observed. The HCN + CH_2O bimolecular channel, which proceeds from the addition complex through tight ring forming and opening transition states, has a negative temperature dependence and is the dominant channel for pressures of about 50 Torr and lower.

Hydrocarbon Reactions

We have investigated the kinetics of the H + C_2H_2 and H + C_2H_4 reactions, as well as their reverse dissociations, in some detail. High level electronic structure calculations were used to characterize the potential energy surfaces. An approximate two-dimensional master equation was used to determine temperature and pressure dependent phenomenological rate coefficients. The effects of angular momentum conservation, tunneling, and the use of variational transition-state theory (as opposed to conventional transition-state theory) to compute microcanonical rate coefficients was investigated in detail. For both reactions, the low-pressure limit is approached very slowly, because reaction just above threshold must occur strictly by tunneling. Assuming a single-exponential-down model for *P(E,E')*, we deduce from experiment values of $\langle \Delta E_d \rangle$, the average energy transferred in a deactivating collision, as a function of temperature for both C_2H_3 and C_2H_5 in baths of He, Ar, and N_2. Our results support the idea that $\langle \Delta E_d \rangle$ increases roughly linearly with temperature, at least for weak colliders. The agreement between theory and experiment is remarkably good for both reactions.

Transition State Theory

We have developed and applied a simple version of variational transition state theory applicable to reactions controlled by long-range interactions. The approach is based on the assumption that the fragment moments of inertia are much smaller than the orbital moment of inertia when the transition state lies at large separations, as it does at low temperature. The predictions from this theory were shown to be in good agreement with related trajectory simulations, generally differing by about 5 to 10% or less. The theoretical predictions are also in remarkably good agreement with experiment for a number of reactions. However, for other reactions, the experimental rate coefficients lie significantly below the theoretical predictions for unknown reasons.

In collaboration with Larry Harding we have developed an efficient implementation of direct variable reaction coordinate transition state theory. A comparison of CASSCF and MRCI interaction energies suggests that the difference between the two methods is nearly orientation independent. This finding allows us to employ small basis set CASSCF energies in the direct sampling over the orientations, coupled with large basis set MRCI evaluations of the minimum energy path. Furthermore, we have observed that the minimum energy path correction from small basis set CASSCF to large basis set MRCI predictions is nearly independent of reaction (at least within a given class of hydrocarbon radical-radical reactions). Thus, we can simply implement a correction evaluated for the $CH_3 + H$ (for C...H additions) and $CH_3 + CH_3$ reactions (C...C reactions). These ideas were tested for the $CH_3 + H$, $C_2H_3 + H$, $C_2H_5 + H$, $CCH + H$, and $CH_3 + CH_3$ via comparisons with calculations implementing the full MRCI/atz interaction energies for all orientations. In every instance, the differences between the two predictions were about 10% or less. We are in the process of applying this methodology to a large series of reactions including such reactions as naphthyl + H and t-butyl + t-butyl.

Master Equation Methodology

We have discussed the kinetics of reversible association/dissociation at great length. We find that late in the reaction, after the characteristic time for internal energy relaxation, phenomenological rate laws will always apply with rate coefficients that satisfy detailed balance. The nonequilibrium factor, f_{ne}, originally introduced by Smith, McEwan, and Gilbert, is not a measure of the degree to which detailed balance is satisfied by the assocation and dissociation rate coefficients. Instead, it is simply the fractional contribution to the "long-time" association rate coefficient of the slowest-relaxing eigenmode of the system. That is, $(1-f_{ne})$ is the fractional contribution to the same rate coefficient of the internal-energy relaxation modes. The standard practice of taking the dissocation rate coefficient to be equal to that for irreversible dissociation is accurate as long as $K_{eq}n_m(1-f_{ne})<<1$, where K_{eq} is the equilibrium constant for the association reaction, and n_m is the concentration of the excess reactant under pseudo first-order conditions for the association reaction.

Future Directions

We will continue our exploration of the reactions leading to the formation of the first aromatic ring with detailed studies of a variety of other possibly important reactions. In particular, we will begin to consider the possible importance of the allyl radical in recombination reactions such as $C_3H_3 + C_3H_5$, $C_3H_5 + C_3H_5$. Our newly developed efficient direct VRC-TST approach should allow us to obtain accurate predictions for the entrance rates in these reactions as well as for the propargyl recombination. We will also explore the possible importance of the i-$C_5H_3 + CH_3$ reaction and the reaction of propargyl radical with allene and/or propyne. The dissociation of C_3H_3 radical may provide an important mechanism for its loss at higher temperatures and so we will also consider this reaction in detail.

As suggested by Lin and coworkers, the reaction of CH with N_2 to form NCN + H is likely an important step in prompt NO formation. The final step in this reaction is barrierless and so a more careful study using our VRC-TST methodology should be useful in providing more quantitative kinetic estimates. This study will be performed in collaboration with Larry Harding.

In collaboration with Craig Taatjes, we will explore D isotope effects in the ethyl + O_2 and propyl + O_2 reactions.

DOE Supported Publications, 2002-Present

1. James A. Miller, Stephen J. Klippenstein, and Christophe Raffy, *Solution Of Some One- And Two-Dimensional Master Equation Models For Thermal Dissociation: The Dissociation Of Methane In The Low-Pressure Limit*, J. Phys. Chem. A, **106**, 4904-4913 (2002).

2. Michael J. Davis and Stephen J. Klippenstein, *Geometric Investigation of Association/Dissociation Kinetics with an Application to the Master Equation for $CH_3 + CH_3 \leftrightarrow C_2H_6$*, J. Phys. Chem. A, **106**, 5860-5879 (2002).

3. Stephen J. Klippenstein and James A. Miller, *From the Time-Dependent, Multiple-Well Master Equation to Phenomenological Rate Coefficients*, J. Phys. Chem. A, **106**, 9267-9277 (2002).

4. Stephen J. Klippenstein, James A. Miller, and Lawrence B. Harding, *Theoretical Kinetic Estimates for the Reaction of HCCO with O_2*, Proc. Comb. Inst., **29**, 1209-1217 (2002).

5. Stephen J. Klippenstein, Yuri Georgievskii, and Lawrence B. Harding, *A Theoretical Analysis of the $CH_3 + H$ Reaction: Isotope Effects, the High Pressure Limit, and Transition State Recrossing*, Proc. Comb. Inst., **29**, 1229-1236 (2002).

6. John D. DeSain, Stephen J. Klippenstein, Craig A. Taatjes, Michael D. Hurley, and Timothy J. Wallington, *Product Formation in the Cl-Initiated Oxidation of Cyclopropane*, J. Phys. Chem. A, **107**, 1992-2002 (2003).

7. Yuri Georgievskii and Stephen J. Klippenstein, *Variable Reaction Coordinate Transition State Theory: Analytic Results and Application to the $C_2H_3 + H \rightarrow C_2H_4$ Reaction*, J. Chem. Phys., **118**, 5442-5455 (2003).

8. John D. DeSain, Stephen J. Klippenstein, and Craig A. Taatjes, *Time-Resolved Measurements of OH and HO_2 Product Formation in Pulsed-Photolytic Chlorine-Atom Initiated Oxidation of Neopentane*, Phys. Chem. Chem. Phys. **5**, 1584-1592 (2003).

9. James A. Miller and Stephen J. Klippenstein, *From the Multiple-Well Master Equation to Phenomenological Rate Coefficients: Reactions on a C_3H_4 Potential Energy Surface*, J. Phys. Chem. A, **107**, 2687-2692, (2003).

10. John D. DeSain, Stephen J. Klippenstein, James A. Miller, and Craig A. Taatjes, *Measurements, Theory, and Modeling of OH Formation in Ethyl + O2 and Propyl + O2 Reactions*, J. Phys. Chem. A, **107**, 4415-4427 (2003).

11. James A. Miller and Stephen J. Klippenstein, *The Recombination of Propargyl Radicals and Other Reactions on a C_6H_6 Potential*, J. Phys. Chem. A, **107**, 7783-7799 (2003).

12. Samuel M. Clegg, Bradley F. Parsons, Stephen J. Klippenstein, and David L. Osborn, *Photodissociation dynamics of Dicyclopropyl Ketone at 193 nm: Isomerization of the Cyclopropyl Ligand*, J. Chem. Phys. **119**, 7222-7236 (2003).

13. Yuri Georgievskii and Stephen J. Klippenstein, *Transition State Theory for Multichannel Addition Reactions: Multifaceted Dividing Surfaces*, J. Phys. Chem. A, **107**, 9776-9781 (2003).

14. James A. Miller, Stephen J. Klippenstein, and Peter Glarborg, *A Kinetic Issue in Reburning: The Fate of HCNO*, Comb. Flame, **135**, 357-362 (2003).

15. Stephen J. Klippenstein, *RRKM Theory and Its Implementation*, in Comprehensive Chemical Kinetics, v. 39, published (2003).

16. James A. Miller and Stephen J. Klippenstein, *The $H + C_2H_2 +(M) \leftrightarrow C_2H_3 (+M)$ and $H + C_2H_4 (+M) \leftrightarrow C_2H_5 (+M)$ Reactions: Electronic Structure, Variational Transition State Theory, and Solutions to a Two-Dimensional Master Equation*, Phys. Chem. Chem. Phys., **6**, 1192-1202 (2004).

17. Frank Striebel, Leonard E. Jusinski, Askar Fahr, Joshua B. Halpern, Stephen J. Klippenstein, and Craig A. Taatjes, *Kinetics of the Reaction of Vinyl Radicals with NO: Ab Initio Theory, Master Equation Predictions, and Laser Absorption Measurements*, Phys. Chem. Chem. Phys., in press (2004).

18. Lawrence B. Harding, Stephen J. Klippenstein, and Yuri Georgievskii, *Reaction of Oxygen Atoms with Hydrocarbon Radicals: A Priori Predictions for the $CH_3 + O$, $C_2H_5 + O$, and $C_2H_3 + O$ Reactions*, Proc. Comb. Symp., **30**, in press (2004).

19. J. H. Kiefer, S. Santhanam, N. K. Srinivasan, R. S. Tranter, S. J. Klippenstein, and M. A. Oehlschlaeger, *Dissociation, Relaxation, and Incubation in the High-Temperature Pyrolysis of Ethane; Experiments and RRKM Modeling*, Proc. Comb. Symp., **30**, *in press* (2004).

20. Juan P. Senosiain, Stephen J. Klippenstein and James A. Miller, *A Complete Statistical Analysis of the Reaction of OH with CO*, Proc. Comb. Symp., **30**, *in press* (2004).

TIME-RESOLVED FTIR EMISSION STUDIES OF
LASER PHOTOFRAGMENTATION AND RADICAL REACTIONS

Stephen R. Leone
Departments of Chemistry and Physics
and Lawrence Berkeley National Laboratory
University of California
Berkeley, California 94720
(510) 643-5467 srl@cchem.berkeley.edu

Scope of the Project

Combustion is a complex process involving short-lived radical species, highly excited states, kinetics, transport processes, fluid dynamics, and energy transfer. Detailed measurements of microscopic reaction pathways, rate coefficients, vibrational and rotational product state distributions, and thermochemistry have resulted in considerable information to aid in the understanding of combustion processes.

Infrared emission provides a method of probing the excited states of species that is complementary to many other techniques, such as laser-induced fluorescence, permitting direct detection of vibration-rotation transitions or low-lying electronic states. The time-resolved FTIR method provides a broad overview of all the emitting species, which is crucial in identifying novel products and transition state mechanisms. This project explores laser-initiated radical reactions, radical-radical reactions, photofragmentation events, energy transfer processes. Vibrationally excited and low-lying electronically excited species generated in chemical dynamics processes are probed by time-resolved Fourier transform infrared (FTIR) emission spectroscopy. Dynamics measurements are obtained by acquiring time-resolved signals after the initiating laser pulse at each mirror position of the spectrometer. These signals are then assembled into interferograms at a series of time delays, to obtain the spectra at each time delay. The current research involves the study a variety of important radical reactions (e.g. $C_2H + O$, $HCCO + O$, $O + C_2H_2$) to determine the nascent product species and states and the mechanisms and kinetic pathways.

The vacuum ultraviolet light at the Chemical Dynamics Beamline of the Advanced Light Source provides a tool to measure the energetics and photoionization spectroscopy of important combustion species. At the Chemical Dynamics Beamline there are new efforts to study photoionization spectroscopy of radical species, such as CH_3 (with Branko Ruscic), propargyl (postdoctoral fellow at the beamline Christophe Nicolas), and ClCO (with Cheuk Ng). Ongoing work at the Chemical Dynamics Beamline also involves interactions with Terry Cool, Andy McIlroy, Craig Tattjes, and Phil Westmoreland in their pursuit of the study of flame chemistry and radical photoionization events using nozzle sampling techniques. Molecular beam photofragmentation studies have been completed by a postdoctoral fellow at the beamline, Jinian Shu, on the dissociation of crotonaldehyde (CH3CHCHCHO), and this type of study is being extended to velocity map imaging using synchrotron radiation for detection. A new laser ablation apparatus has been developed at the beamline with Musa Ahmed to produce and study C_1, through C_5 species in photoionization. The results of the carbon cluster species will be described in more detail. The same source has also been applied to biomolecules by M. Ahmed and to

metal oxide species with Ricardo Metz. A new effort will explore aerosol species and their roles and production in combustion.

C_2H + O Radical-Radical Reaction

The reaction of C_2H with O proceeds with a rate coefficient of 5.6×10^{-11} cm^3 molecule^{-1} s^{-1} and produces primarily CO + CH; the CH can be formed in the ground $X^2\Pi$ state or excited $A^2\Delta$ state. This reaction is investigated to determine the CO(v) vibrational distribution of the two branching pathways, to reveal information about the ratio of the CH(X) and CH(A) state products and details of the reaction mechanism. This reaction is challenging to study because of the many competing processes that also produce CO(v) products when a photolysis mixture of C_2H_2 and SO_2 is used to produce the C_2H and O radicals at 193 nm. The CH + O reaction is an obvious possible competitor, since its rate coefficient is an order of magnitude larger than that for C_2H + O. However, because CH also reacts rapidly with C_2H_2, which is in large excess (the precursor used to produce C_2H by laser photolysis), the contribution of CO(v) from the CH + O reaction is determined to be negligible. Instead, three other reactions, HCCO + O, C_2H + SO_2, and O + C_2H_2 contribute more significantly to the observed CO(v) signals. The absolute rate coefficient for C_2H + SO_2 was measured in this work to model the product signals. The rate coefficient at room temperature is $(1.1\pm0.3) \times 10^{-11}$ cm^3 molecule^{-1} s^{-1}. Under suitable conditions, the CO(v) from the C_2H + O reaction can be studied at early times, with little interference from these other reactions. The overall reaction mixture exhibits vibrational emission from species such as CO, CO_2, CH, SH, SO_2, C_2H, C_4H_2, all of which are characterized under various conditions in this system and by additional studies of other individual reactions.

The vibrational distribution of the CO product from C_2H + O extends to CO(v=12) and is strongly bimodal, suggesting two different distributions that correspond to the CH(X) and CH(A) states. Using a surprisal analysis with back extrapolation to determine the CO(v) vibrational state populations of the CH(X) channel that underlie the CO(v) of the CH(A) channel, a CH(A) branching fraction of 57±30% is suggested. A previously reported CH(A) branching fraction of 20-45%, measured by pulsed laser photolysis/visible chemiluminescence technique by the group of Peeters (Chem. Phys. Lett. **261**, 450 [1996]) was recently revised to 4-12% (J. Chem. Phys. **118**, 10996 [2003]). This significant difference between the surprisal analysis in our work versus the estimates of Peeters may be attributed to several possibilities: (a) The CH(A) fraction may be underestimated in the Peeters' work. (b) The CO(v) vibrational distribution for our measured CH(A) channel could be more inverted with respect to the CO(v=0) channel than predicted by the surprisal extrapolation. (c) The CO(v) vibrational distribution of the CH(X) channel can make a larger contribution to low v levels than predicted by a linear surprisal. The C_2H + O reaction is thought to proceed through the HCCO reactive intermediate. The lifetime of this intermediate and the vibrational distribution of the CO(v) for each branching pathway can shed light on the directness of the process. In this work, the CO(v) products corresponding to both CH(X) and CH(A) channels are close to statistical, suggesting a long-lived HCCO intermediate; however, the pathway that forms the CH(X) state has a somewhat hotter vibrational distribution, suggesting a possible more direct mechanism for that channel. In addition, the pathway to form CH(A) has a remarkable prominence, which was suggested by the Peeters' group to be due to the bent ground state of HCCO coupling into a high electronic angular momentum state. Theoretical investigations and studies of the CH(v) product

distributions may help to answer the question of the HCCO intermediate state lifetime and the mechanism.

O + C$_2$H$_2$ and HCCO Reactions

In recent work, a detailed study was performed on the reactions of the C$_2$H$_2$ + O(^{3}P) and HCCO + O(^{3}P) using Fourier transform infrared spectroscopy (FTIR). The C$_2$H$_2$ + O reaction results in CO, CH$_2$(^{3}B) and HCCO products that subsequently react with O atoms producing additional CO and CO$_2$ products. The analysis of the vibrational states of the vibrationally excited CO(v) reveals the multiple reactions that contribute to the nascent vibrational distribution of the CO(v). By varying the experimental conditions, the nascent vibrational distributions for the CO(v) channels of the C$_2$H$_2$ + O(^{3}P) and the HCCO + O(^{3}P) reactions are extracted. The CO(v) pathways are the only one studied thus far. The nascent vibrational distribution from C$_2$H$_2$ + O(^{3}P) agrees well with the earlier studies obtained by Shaub et al. (Chem. Phys. **45**, 455 [1980]), using a CO laser resonance technique. The nascent vibrational distribution of the HCCO + O(^{3}P) reaction is obtained the first time using two separate precursors. In this reaction, two CO(v) product molecules plus an H atom are produced in each reaction. The nascent vibrational distribution of CO from both the C$_2$H$_2$ + O(^{3}P) and HCCO + O(^{3}P) reactions show noninverted behavior, which is consistent with an intermediate complex mechanism. From the Boltzmann plot the vibrational temperature of the nascent CO distributions are found to be 2400 ± 100 K and 10300 ± 600 K for the C$_2$H$_2$ + O(^{3}P) and the HCCO + O(^{3}P) reactions, respectively. The C$_2$H$_2$ + O reaction may require migration of atoms in the intermediate to form the final CO(v) products. The much hotter vibrational distribution of HCCO + O suggests that this process may proceed through an interesting transition state, in which the CO bond of one or both CO molecules is elongated or is formed in a more direct process.

Photoionization of C$_n$ Species

At the Advanced Light Source, a novel laser vaporization source has been developed to produce carbon cluster species for photoionization spectral studies. Such investigations provide basic thermodynamic and structural information for these fundamental species. The cluster source was used to produce C$_1$, C$_2$, C$_3$, C$_4$, and C$_5$ by vaporization of a graphite rod, and the ionization potentials for each of these species have now been measured (11.26±0.05 eV, 11.4±0.1 eV, 11.5±0.1 eV, 10.5±0.1 eV, and 10.5±0.1 eV, respectively). Comparison with the available literature for these species, the new results suggest that many of the ionization potentials were either not well known or were only bracketed coarsely by experiments. The detailed photoionization efficiency data for species such as C$_3$, coupled with CAS-SCF calculations on the resulting C$_3^+$ ion states, performed by our collaborator M. Hochlaf, suggest that additional intensity maxima in the photoionization efficiency versus energy data can be attributed to identifiable electronically excited states of C$_3^+$. Work is in progress to revise this information and to determine the implications for the basic thermodynamics and structure correlations of carbon cluster species.

Future Plans

New studies will explore radical reactions such as $C_2H + SO_2$, $C_2H + NO$, $CH_3 + N$, and kinetic energy enhanced OH reactions with hydrocarbons. Experiments are also being considered to use the time-resolved FTIR method to examine heterogeneous processes with aerosol or surface reactions. Other investigations are being developed to explore the CH(A) state formed by photodissociation of bromoform with vacuum ultraviolet light at the Advanced Light Source. Upon absorption of a VUV photon in the 10-14 eV regime, a single photon causes the bromoform to undergo a multibody dissociation: $CHBr_3 \rightarrow CH(A) + 3Br$. This reaction can take place as a concerted or as a sequential process, which will be studied with a visible adaptation to the time-resolved FTIR.

Recent Publications

Timothy P. Marcy, Jonathan P. Reid, Charles X. W. Qian, and Stephen R. Leone, "Addition-insertion-elimination reactions of $O(^3P)$ with halogenated iodoalkanes producing HF(v) and HCl(v)," J. Chem. Phys. **114**, 2251 (2001).

Timothy P. Marcy, Robert Richard Díaz, Dwayne Heard, Stephen R. Leone, Lawrence B. Harding, and Stephen J. Klippenstein, "Theoretical and experimental investigation of the dynamics of the production of CO from the $CH_3 + O$ and $CD_3 + O$ reactions," J. Phys, Chem. A **105**, 8361 (2001).

Timothy P. Marcy, Dwayne Heard, Stephen R. Leone, "Product studies of inelastic and reactive collisions of $NH_2 + NO$: Effect of vibrationally and electronically excited NH_2," J. Phys. Chem. A **106**, 8249 (2002).

Viktor Chikan, Boris Nizamov, and Stephen R. Leone, "Product state distributions of vibrationally excited CO(v) for the $CH(X^2\Delta)$ and $CH(A^2\Pi)$ channels of the $C_2H + O(^3P)$ reaction, J. Phys. Chem. A (in preparation).

Viktor Chikan and Stephen R. Leone, "Vibrational distribution of the CO product of the $C_2H_2 + O(^3P)$ and $HCCO + O(^3P)$ reactions studied by Fourier transform infrared spectroscopy," J. Phys. Chem. A (in preparation).

Jinian Shu, Darcy S. Peterka, Stephen R. Leone, and Musahid Ahmed, "Tunable synchrotron vacuum ultraviolet ionization, time-of-flight investigation of the photodissociation of trans-crotonaldehyde at 193 nm," J. Phys. Chem. A (submitted).

Christophe Nicolas, Jinian Shu, Majdi Hochlaf, Lionel Poisson, Darcy S. Peterka, Stephen R. Leone, and Musahid Ahmed, "Vacuum Ultraviolet Photoionization of Small Carbon Clusters," J. Phys. Chem. A (in preparation).

165

INTERMOLECULAR INTERACTIONS OF HYDROXYL RADICALS ON REACTIVE POTENTIAL ENERGY SURFACES

Marsha I. Lester
Department of Chemistry
University of Pennsylvania
Philadelphia, PA 19104-6323
milester@sas.upenn.edu

PROGRAM SCOPE

The primary objective of the DOE-sponsored research in this laboratory is to examine the interaction potentials and reaction dynamics of the hydroxyl radical (OH) with molecular partners of combustion relevance, most recently ethylene and acetylene. For these partners, molecular associations of OH radicals have already been predicted to play a critical role in the reaction mechanism. A hydrogen-bonded complex between OH and the π-bond of C_2H_4 has been suggested as an important precursor in the addition reaction of OH radicals to the double bond of ethylene,[1] and an analogous T-shaped complex has been predicted on the reaction path for OH addition to acetylene (C_2H_2).[2] This laboratory has recently obtained the first experimental evidence of such a hydrogen-bonded complex between the OH and C_2H_2 reactants in the entrance channel to reaction. Infrared action spectra of the OH-C_2H_2 reactant complex have been acquired in the regions of the OH overtone stretch and asymmetric stretch fundamental of acetylene, which reveal the structure and stability of the complex. New spectral analysis procedures are being developed to account for partial quenching of the electronic orbital angular momentum of the OH radical in the T-shaped complex and gain more insight on the nature of the molecular association between the partners. The results of these experiments promise to provide new information on the reaction pathway from the entrance valley to the transition state for these key combustion reactions.

INFRARED ACTION SPECTROSCOPY OF OH-C_2H_2

We have recently stabilized a hydrogen-bonded complex between the OH and C_2H_2 reactants in the entrance channel well leading to the addition reaction. The OH-C_2H_2 complexes are generated by photolyzing HNO_3 at 193 nm to produce OH radicals, which are entrained in a premixed 5-10% C_2H_2 / Ar gas mixture at a total pressure of 60 psi. We have used infrared action spectroscopy to obtain infrared spectra of the OH-C_2H_2 reactant complex in the regions of the $2\nu_{OH}$ OH stretch overtone of the hydroxyl radical and the ν_3 asymmetric stretch fundamental of acetylene. In addition, we have simultaneously identified the principal OH (ν, j_{OH}) product channels that are populated following dissociation of the complex.

The infrared action spectrum of OH-acetylene in the OH overtone region[3] is centered at 6885.5 cm^{-1}, shifted 85.8 cm^{-1} to lower energy of the OH monomer transition. The rotational band structure is characteristic of a parallel (a-type) transition of a near prolate asymmetric top. The transition type indicates that the OH subunit lies along the a-inertial axis, as expected for a T-shaped complex in which OH is hydrogen-bonded to the π-cloud of acetylene. The large spectral shift indicates that the OH subunit is significantly perturbed upon forming a hydrogen bond with the H-side of OH interacting with acetylene. The lines in the P- and R-branches are uniformly spaced by $(B+C)$, but at *odd* multiples of $(B+C)/2$ relative to the Q-branch, rather than

the *even* multiples seen for other acetylene-HX complexes.[4,5] The line positions are fit to obtain a 3.327(5) Å separation between the centers-of-mass of the monomer constituents. The *odd* multiples are a result of half-integral values of the total angular momentum in the complex, arising from the spin of the unpaired electron of OH being coupled to the molecular frame.

By contrast, the infrared spectrum in the asymmetric stretch region of acetylene[6] is centered at 3278.6 cm^{-1}, indicating a much smaller spectral red shift of 10.1 cm^{-1} (relative to the deperturbed monomer v_3 origin). The relatively small spectral shift confirms that the asymmetric acetylenic stretch is remote from the hydrogen bond. This perpendicular (*b*-type) transition exhibits much more complicated rotational band structure consisting of seven peaks of various intensities and widths. This spectrum is very different from those previously reported for similar HF/HCl-acetylene complexes.[7,8] A theoretical model has been developed[9] to examine the origin of this unexpected result as well as more subtle effects seen in the *a*-type band, which we attribute to the partial quenching of the OH orbital angular momentum in the complex.

The theoretical model takes into account the difference potential, the splitting between the $^2A'$ and $^2A''$ potentials in nonlinear configurations, in computing the rotational energy levels and electric dipole transition intensities for the OH-acetylene complex.[9] The model smoothly spans the entire range of the difference potential, which is responsible for the partial quenching of the OH monomer electronic angular momentum. The simulated vibration-rotational spectra are found to be quite sensitive to the magnitude of the difference potential in *a*- and *b*-type transitions. The model has been successfully applied to the analysis of the observed infrared bands of the OH-acetylene complex, and has allowed the determination of the *A* rotational constant (1.217 cm^{-1}) and difference potential (−148 cm^{-1}) from the *b*-type, CH stretching band.[6]

The principal OH (v, j_{OH}) product channels that are populated following dissociation of the complex provide information on the stability of the OH-acetylene complex and the mechanism for inelastic decay. For OH overtone stretch excitation of OH-C$_2$H$_2$,[3] the dominant OH product channel is OH X $^2\Pi_{3/2}$ ($v=1, j_{OH}=23/2$). By constructing an energy cycle, we can estimate an upper limit for the ground state binding energy of OH-C$_2$H$_2$, $D_0 \leq 955$ cm^{-1} (2.7 kcal mol^{-1}), assuming minimal translational energy for the recoiling partners and little excess energy deposited as rotational and/or vibrational excitation of the C$_2$H$_2$ fragment. Other significant product channels, OH ($v=1, j_{OH}=9/2$ and 11/2), likely arise when the correlated C$_2$H$_2$ fragment acquires one quantum of C≡C stretch (v_2) excitation or three quanta of bend ($3v_4, 3v_5,$ or combinations of these modes) in the dissociation event. Thus, it appears that vibrational predissociation of the OH-C$_2$H$_2$ complex proceeds by transfer of the energy released from OH vibration ($v=2\rightarrow1$) to OH rotation or C$_2$H$_2$ vibrations. For asymmetric acetylenic stretch excitation of the OH-C$_2$H$_2$ complex,[6] the OH fragments are observed primarily in low rotational levels of OH ($v=0$). In this case, it appears that vibrational energy transfer within the C$_2$H$_2$ subunit is the dominant decay pathway.

Finally, we have carried out high level *ab initio* calculations of the OH-acetylene potentials with fixed monomer bond lengths to complement the experimental investigation.[3] Calculations at the RCCSD(T) level of theory with extrapolation to the complete basis set limit[10] predict a T-shaped minimum energy structure for the OH-C$_2$H$_2$ complex with well depths of 985 and 1130 cm^{-1} at $R = 3.3$ Å for the reactive $^2A'$ and nonreactive $^2A''$ potential energy surfaces, respectively. The theoretical results are in good accord with the experimental observations. The significant splitting between the $^2A'$ and $^2A''$ surfaces, comparable to the spin-orbit splitting of OH, is also in

good agreement with the value extracted from spectral simulations. This splitting is responsible for the partial quenching of the OH monomer electronic angular momentum, a process that must occur as the system evolves from weakly interacting partners to the addition product.

FUTURE PLANS

In the coming year, we will complete our investigation of the OH-acetylene reactant complex. This primarily involves further development of the theoretical model for interpretation of the spectra. We plan to generalize our results by developing a correlation diagram to illustrate how the OH electronic angular momentum is quenched with progress along the reaction pathway. In addition, we plan to continue our studies of OH reactant complexes with ethylene and acetaldehyde partners. These studies will include infrared spectroscopy, time and/or frequency domain measurements of the lifetime of the vibrationally activated complex, and probes of the inelastic and/or reactive decay processes.

REFERENCES

[1] S. M. Kathmann, M. Dupuis, and B. C. Garrett, personal communication (2001).

[2] C. Sosa and H. B. Schlegel, *J. Am. Chem. Soc.* **109**, 4193 (1987).

[3] J. B. Davey, M. E. Greenslade, M. D. Marshall, M. I. Lester, and M. D. Wheeler, *J. Chem. Phys.*, in press (2004).

[4] P. Carcabal, M. Broquier, M. Chevalier, A. Picard-Bersellini, V. Brenner, and P. Millie, *J. Chem. Phys.* **113**, 4876 (2000).

[5] Z. S. Huang and R. E. Miller, *J. Chem. Phys.* **86**, 6059 (1987).

[6] M. D. Marshall, J. B. Davey, M. E. Greenslade, and M. I. Lester, in preparation (2004).

[7] Z. S. Huang and R. E. Miller, *J. Chem. Phys.* **90**, 1478 (1989).

[8] D. C. Dayton, P. A. Block, and R. E. Miller, *J. Phys. Chem.* **95**, 2881 (1991).

[9] M. D. Marshall and M. I. Lester, J. Chem. Phys., submitted for publication (2004).

[10] P. R. Butler and A. M. Ellis, *Mol. Phys.* **99**, 525 (2001).

DOE SUPPORTED PUBLICATIONS
2002-2004

1. M. Tsiouris, I. B. Pollack, and M. I. Lester, "Infrared Action Spectroscopy and Inelastic Recoil Dynamics of the CH_4-OD Reactant Complex", *J. Phys. Chem. A* **106**, 7722-7727 (2002).

2. J. B. Davey, M. E. Greenslade, M. D. Marshall, M. I. Lester, and M. D. Wheeler, "Infrared Spectrum and Stability of a π-type Hydrogen-Bonded Complex between the OH and C_2H_2 Reactants", *J. Chem. Phys.*, in press (2004).

3. M. D. Marshall and M. I. Lester, "Spectroscopic Implications of the Coupling of Unquenched Angular Momentum to Rotation in OH-Containing Complexes", *J. Chem. Phys.*, submitted for publication (2004).

Theoretical Studies of Molecular Systems

William A. Lester, Jr.
Chemical Sciences Division,
Ernest Orlando Lawrence Berkeley National Laboratory and
Kenneth S. Pitzer Center for Theoretical Chemistry,
Department of Chemistry, University of California, Berkeley
Berkeley, California 94720-1460
walester@lbl.gov

Program Scope

This research program is directed at extending fundamental knowledge of atoms and molecules. The approach combines the use of ab initio basis set methods and the quantum Monte Carlo (QMC) method to describe the electronic structure and energetics of systems of primarily combustion interest.

Recent Progress

Small Hydrocarbons (with A. C. Kollias, D. Domin, and M. Frenklach)
We are pursuing theoretical studies using QMC and various other ab initio as well as density functional theory methods with the objective of predicting enthalpies of formation of chemical species and transition states of reactions of interest for the growth of aromatic precursors to soot. A comparative study is nearing completion of small aliphatic hydrocarbon radicals, C_2 to C_4, for which alternative theoretical methods have provided heats of formation and atomization energies of varying accuracy. For this effort, it is essential that the saturated parents of the radicals are computed to serve as benchmarks for accuracy assessment.

INCITE Project (with M. Frenklac, G. Fleming. A. Aspuru-Guzik, and R. Salomon)
An INCITE (Innovative and Novel Computational Impact on Theory and Experiment) award, received in January 2004, of one million SP hours will enable us to pursue the ground- to triplet-state energy difference of the carotenoids present in light harvesting complexes of bacteria and plants. Specifically, the systems that will be investigated are the light harvesting protein II of *Rs. Molischianum,* and Photosystem I of cyanobacteria. This project is underway using a new QMC computer code, Zori, that complements our code of many years, QuantuMagiC (QmagiC). Zori has the capability of nearly linear scaling with system size.

Future Plans

Future work will continue in the direction of establishing fundamental understanding of mechanisms leading to soot formation as well as other molecular species of combustion interest. For the present and near future, major effort will be on the INCITE project.

DOE Supported Publications 2002-2004

1. W. A. Lester, Jr. and J. C. Grossman, "Quantum Monte Carlo for the Electronic Structure of Combustion Systems," in *Recent Advances in Quantum Monte Carlo – Part II*, eds., W. A. Lester, Jr., S. Rothstein, and S. Tanaka, World Scientific Publishing, Singapore, p. 159 (2002).

2. O. El Akramine, W. A. Lester, Jr., X. Krokidis, C. A. Taft, T. C. Guimaraes, A. C. Pavao, and R. Zhu, "Quantum Monte Carlo Study of the CO Interaction with a Model Surface for Cr(110)" Mol. Phys. **101**, 277 (2003).

3. J. A. W. Harkless, J. H. Rodriguez, L. Mitas, and W. A. Lester, Jr., "Quantum Monte Carlo and Density Functional Theory Study of Peroxynitrite Anion," J. Chem. Phys. **118**, 4987 (2003).

4. A. C. Kollias and W. A. Lester, Jr., "Quantum Monte Carlo Study and Electron Localization Function of CO_2^+," J. Mol. Struct. Theochem **634**, 1 (2003).

5. A. Aspuru-Guzik and W. A. Lester, Jr., "Quantum Monte Carlo for the Solution of the Schroedinger Equation for Molecular Systems", in Special Volume Computational Chemistry, C. Le Bris, ed., of Handbook of Numerical Analysis, P. G. Ciarlet, ed., Elsevier, 2003, p. 485.

6. O. El Akramine, A. C. Kollias, and W. A. Lester, Jr., "Quantum Monte Carlo Study of the Singlet-Triplet Transition in Ethylene", J. Chem. Phys. **119**, 1483 (2003).

7. C. A. Schuetz, M. Frenklach, A. C. Kollias, and W. A. Lester, Jr., "Response Surface Approach to Geometry Optimization in Quantum Monte Carlo: Application to Formaldehyde," J. Chem. Phys. **119**, 9386 (2003).

8. O. El Akramine, A. Aspuru-Guzik, J. C. Grossman, and W. A. Lester, Jr., "Quantum Monte Carlo Study of the Electronic Structure of Free Base Porphyrin," J. Chem. Phys. **120**, 3049 (2004).

9. A. C. Kollias, O. Couronne, and W. A. Lester, Jr., "Quantum Monte Carlo Study of the Reaction: $Cl + CH_3OH \rightarrow CH_2OH + HCl$", accepted by J. Chem. Phys.

Quantum Dynamics of Fast Chemical Reactions

DE-FG02-87ER13679

Progress Report 3/2003 - 3/2004

John C. Light
The James Franck Institute and Department of Chemistry
The University of Chicago
5640 S Ellis, Chicago,Illinois 60637
email: j-light@uchicago.edu

The aims of this research are to develop a theoretical understanding and predictive abiility for a variety of processes occurring in the gas phase. These include bimolecular chemical exchange reactions, photodissociation, predissociation resonances, unimolecular reactions and recombination reactions. Our focus on accurate quantum dynamics of small system is important for reactions involving light atom transfer, role of resonances in dissociation and recombination reactions, and the theoretical spectroscopy and large amplitude dynamics of energetic three and four atom molecules and radical intermediates in reactions.

A major impediment to extension of these techniques to large molecular systems is the poor scaling of quantum methods with number of atoms treated accurately quantum mechanically and with the number of basis functions per atom. The scaling for straightforward quantum solutions is between n^{3d} and n^d where d = 3N -6, N is the number of atoms, and "n" the number of points or basis functions required to describe the motions in *each* dimension accurately – perhaps 10 to 100.

We focus on developing substantially improved approaches and applying them to larger systems of interest. The techniques developed and used are primarily quantum mechanical (sometimes combined with classical mechanics) which permits us to focus on the effects of the internal states of reactants on reactions, and the internal state distributions, isotopic ratios, and branching ratios for products.

I. RECENT PROGRESS

During the past year we have refined computational methods to make the calculation of states of four atom systems more feasible and routine and have applied them to molecular systems relevant to combustion such as CO_2 dimer and hydrogen peroxide, H_2CO, water and ozone. The latter two were investigated near the dissociation limit for bound states and some resonances.

Our theoretical approach to the quantum dynamics of such "floppy" moleculas has utilized three recent important innovations: the generation and use of reduced dimensionality *minimum* PES's to define the basis functions for each subset of the coordinates [1–3]; the combination of these reduced dimensional basis functions to form an *energy selected* non-direct product basis [2–4]; and the use of an iterative (IRLM) solution method for determining eigenvalues, eigenfunctions of the molecule [1,3,4]. Optimized grids for each of the degrees of freedom may also be used. These improvements are synergistic, with the minimum potentials assuring appropriate coordinate ranges for the bases, the energy selected basis reducing both the basis size

and, perhaps more important. the spectral range, and the iterative (IRLM) solution providing excellent scaling as well as eigenfunction evaluation.

Below we report an improved grid approach for problems w several angular degrees of freedom as well as applications to important tetra-atomic and triatomic systems. In all of the calculations reported below the accuracies of the vibrational energies for the given PES's were better than 0.1 cm^{-1} (and usually better than 0.01 cm^{-1}).

A. Direct product angular DVR's:

Most internal coordinate systems used to describe the dynamics of larger molecules contain many angular variables, up to $3N - 4$ for hyperspherical type coordinates. The quantum representations for these angular variables are usually coupled angular momentum bases which may become very large, particularly if the angular motions are restricted. In addition these bases are not direct product type for which fast iterative and sequential solutions are most feasible. This representations of angular functions for large systems is usually difficult or at least not efficient. We have further developed the direct product angular DVR basis for such systems by showing how to do extensive symmetry reduction for high symmetry systems and how to do the solution by sequential reduction much more efficiently than with the coupled angular basis [5].

The sample problem was the carbon dioxide dimer $(CO_2)_2$ on a realistic potential energy surface. The PI group is G_{16} and for the normal isotopic species only the A_g states exist. The use of a direct product of two Legendre DVR's for the θ_1 and θ_2 motions and a Fourier basis for the dihedral angle, ϕ in addition to the dimer distance coordinate gave very accurate results for some 80 vibrational states with a very modest basis. This is somewhat surprising since the direct product DVR does not satisfy the correct boundary conditions required of the wave funcstions due to the angular momentum singularities of the kinetic energy operators. The results were checked against earlier much more difficult calculations using a coupled angular basis [6].

This approach should apply directly to most 4 atom (3 angle) systems and should be able to be extended to larger systems. The only major caveat is for systems where the ground states are linear where convergence may be slower.

B. Tetra-atomic systems with Energy Selected Bases:

Many tetra-atomic systems are important for combustion such as CH_3, HOCO, H_2CO, HOOH, etc. We have looked at the high energy vibrational dynamics of some of these systems. The use of energy selected bases [1] where the reduced dimensionality bases are eigenfunctions of reduced Hamiltonians based on *minimum* potentials in the reduced dimensions was shown to greatly reduce the number of basis functions required while permitting iterative solutions [1–3]. The application to highly excited HOOH was relatively straightforward while the application to the formaldehyde/vinyl system (H_2CO) was more difficult [3]. Some 730 A_1 states (up to 13,600 cm^{-1}) were calculated. This reaches, but does not exceed the barrier to isomerization to vinylidene. At that point the large increase in the density of states made our iterative method very slowly convergent. It is likely that further filtering using an energy

window would be necessary to extend the calculations throughout the isomerization regime.

C. Triatomic molecules near dissociation: Water and Ozone

Although these are triatomic molecules and therefore inherently easier to treat than formaldehyde or hydrogen preoxide, the very highly excited vibrational levels of these systems are of interest for photodissociation and recombination particularly in the atmosphere. In addition the highly excited vibrations and resonance states of ozone for the $(^{16}O)_3$ and $(^{16}O_2\ ^{18}O)$ isotopomers are probably responsible for the observed "isotopic anomaly" of atmospheric ozone in which the isotopic ratios are not in the expected chemical equilibrium.

The vibrational levels of H_2O were computed using the ESB method for the PJT2 potential energy surface of Mussa and Tennyson [7]. Some 1000 even and 800 odd vibrational states were calculated, extending well above the dissociation limit. The identity of the resonance states was determined by examining the stability with respect to the distance parameters of the calculation [3].

In the ozone calculation we determined all the bound states, including the long range van der Waals states, of $^{48}O_3$ and $^{50}O_3$ [8]. We used the accurate PES of Babikov [9]. This calculation was undertaken to resolve a discrepancy between two recently published papers on the same system using the same PES: Grebenshchikov et al and Babikov, J. Chem. Phys **119**, 6512 and 6564 (2003) respectively. In these papers the number of bound van der Waals states reported differed significantly. Since these vdW states are likely to be strongly involved in the anomalous isotope effect in the ozone recombination process, resolution of the discrepancy was important. Our results agreed extremely well with a a subset of the results (corresponding to the proper A_2 vibrational symmetry) of Greabenschikov (within about 0.04 cm−1) [3].

D. Continuing projects: Reactions of ozone and of $H_3^+ + H_2$

Both the recombination of $O_2 + O$ in the atmosphere and the low energy reactions of H_3^+ and H_2 proceed via complexes which have deep attractive wells. In both cases quantum effects will be important, via resonances, tunneling, and nuclear symmetry effects. The understanding of ozone recombination is important for atmospheric chemistry whereas the understanding of the ortho-para exchange processes and rotational relaxation in the low energy H_5^+ collision system is important for interstellar chemistry.

We are continuing calculations on the ozone system in two stages, first to determine the resonance states which might participate in the three body association process; then to calculate the thermal association rates from a master equation. The latter will require the determination of the state specific energy transfer and dissociation rates for collisions of O_3^* with atmospheric gases. This will be a mixed quantum-classical calculation similar to our Ar + HCO calculation done some time ago [10].

The low energy $H_3^+ + H_2$ ion-molecule reaction is one of the only relaxation mechanisms for ortho-para exchange in interstellar space. We will first look at the cross

173

sections from a relatively simple statistical theory approach (Ref [11,12], then look at the long range quantum dynamical effects such as tunneling and anisotropic collision effects on barrier crossing [13]. This five nucleus system is difficult because of the nuclear symmetry and large quantum effects but is fascinating for the same reasons. This calculation also will be a precursor to the more combustion oriented system CH_5^+ which shares the fermion symmetry of the five H nucleii.

Publications supported by this DOE Grant, 2003-2004: References 2,3,5,and 8 below.

REFERENCES

1. H. S. Lee and J. C. Light. Molecular vibrations: Iterative solution with energy selected bases. *J. Chem. Phys.*, 118:3458, 2003.

2. Hee-Seung Lee and J. C. Light. Iterative solutions with energy selected bases for highly excited vibrations of tetra-atomic molecules. *J. Chem. Phys.*, 120:4626, 2004.

3. J. C. Light and H. S. Lee. *Molecular dynamics: energy selected bases.* Kluwer, NATO ASI Series (In Press).

4. X.G. Wang and T.C. Carrington, Jr. The utility of constraining basis function indices when using the lanczos algorithm to calculate vibrational energy levels.

5. Hua Chen H. S. Lee and J. C. Light. Symmetry adapted direct product discrete variable representation for the coupled angular momontum operator: Application to the vibrations of $(CO_2)_2$. *J. Chem. Phys.*, 119:4187, 2003.

6. Hua Chen and J. C. Light. Vibrations of the carbon dioxide dimer. *J. Chem. Phys.*, 112:5070, 2000.

7. H. Y. Mussa and J. Tennyson. Calculation of hte rotation-vibration states of water up to dissociation. *J. Chem. Phys.*, 109:10885, 1998.

8. Hee-Seung Lee and J. C. Light. Vibrational energy levels of ozone up to dissociation revisited. *J. Chem. Phys.*, 120:5862, 2004. Communication.

9. D. Babikov, B. K. Kendrick, R. B. Walker, R. T. Pack P. Fleurat-Lesard and R. Schinke. *J. Chem. Phys.*, 118:6298, 2003.

10. G. S. Whittier and J. C. Light. Quantum/classical time-dependent self-consistent field treatment of Ar-HCO. *J. Chem. Phys.*, 110:4280, 1999.

11. P. Pechukas and J. C. Light. On detailed balancing and statistical theories of chemical kinetics. *J. Chem. Phys.*, 42:3281, 1965.

12. J. C. Light. Statistical theory of bimolecular exchange reactions. *Discuss. Faraday Soc.*, 44:14, 1967.

13. E. J. Rackham, T. Gonzalez-Lezana, and D. E. Manolopoulos. A rigorous test of the statistical model for atom–diatom insertion reactions. *J. Chem. Phys.*, 119:12895, 2003.

Kinetics of Elementary Processes Relevant to Incipient Soot Formation

M. C. Lin
Department of Chemistry
Emory University
Atlanta, GA 30322
chemmcl@emory.edu

I. Program Scope

Soot formation and abatement processes are some of the most important and challenging problems in hydrocarbon combustion. The key reactions involved in the formation of polycyclic aromatic hydrocarbons (PAH's), the precursors to soot, remain elusive. Small aromatic species such as C_5H_5, C_6H_6 and their derivatives are believed to play a pivotal role in incipient soot formation.

The goal of this project is to establish a kinetic database for elementary reactions relevant to soot formation in its incipient stages. In the past year, our major focus has been placed on the experimental studies on the reactions of C_6H_5 with allene, propyne, propene and butadiene; their mechanisms have been elucidated computationally by quantum-chemical calculations. A similar study on the reaction of $C_6H_5C_2H_2$ with O_2 has also been initiated. In addition, several reactions involving CH_3, C_2H_5, and NCN radicals have been calculated at the G2M level of theory.[1] These results are briefly summarized below.

II. Recent Progress

A. Experimental studies

We have developed three complementary methods for determination of the kinetics and mechanisms for C_6H_5 reactions with combustion species, including small alkenes and small aromatics. Combination of these methods: cavity ring-down spectrometry (CRDS), pyrolysis/Fourier transform infrared spectrometry (P/FTIRS) and pulsed laser photolysis/mass spectrometry (PLP/MS), allows us to cover a broad temperature range, 300 - 1000 K

1. C_6H_5 + C_3H_4 Reactions (ref. # 2)

The kinetics for the C_6H_5 reaction with the 2 isomers of C_3H_4, allene and propyne, have been measured by CRDS in the temperature range 297 – 500 K using C_6H_5NO as the C_6H_5 source. Their rate constants can be given by the following expressions in units of cm^3 mol^{-1} s^{-1}:

k(allene) = (2.52 ± 0.47) x 10^{11} exp [(-1324 ± 57)/T]
k(propyne) = (3.92 ±0.84) x 10^{11} exp [(-1704 ±78)/T]

These results are summarized in Fig. 1 for comparison with those of C_6H_5 + C_2H_2 and C_4H_6.
The rate of C_6H_5 + CH_3C_2H is seen to be slightly greater than that of the C_2H_2 reaction, whereas that of the allene reaction is faster than its isomeric reaction by about a factor 2-3 across the temperature range studied. Most significantly, the rate of C_6H_5 + C_4H_6 is about a factor of 50 faster than that of the allene reaction. A computational study on product branching in the two C_3H_4 isomeric reactions is underway.

Fig. 1. Arrhenius plot of the rate constant of the C_6H_5 + C_3H_4 (allene,), C_3H_4 (propyne,), C_2H_4 (solid line) and C_2H_2 (dashed line) data

2. C_6H_5 + C_3H_6 → Products (ref. # 3)

Propene is an important combustion intermediate and fuel. The rate constant for the C_6H_5 with C_3H_6 reaction has been measured by CRDS in the temperature range 296 - 496 K at 40 – 120 Torr Ar pressure.

175

The total second-order rate constant can be represented by the expression, $k = 10^{11.93 \pm 0.10}$ exp[-(1512 ± 51)/T] cm^3 mol^{-1} s^{-1}, which is slightly faster than the analogous C$_6$H$_5$ + C$_2$H$_4$ reaction,[4] $k = 10^{11.86}$ exp(-2250/T) cm^3 mol^{-1} s^{-1}, determined with the same method in the same temperature range. For the title reaction, the result of quantum/TST calculations indicate that the dominant process is the addition to the terminal site of the double bond, although the H-abstraction becomes competitive at high temperatures. The branching rate constants for the addition at the terminal C and the central C and for the C-H abstraction from the CH$_3$ group for 250 – 2500 K under the second-order condition can be given in units of cm^3 mol^{-1} s^{-1} by:[3]

$$k_{R1} = 1.7 \times 10^4 \, T^{2.47} \exp(-370/T)$$
$$k_{R2} = 1.6 \times 10^3 \, T^{2.64} \exp(-847/T)$$
$$k_{R3} = 1.4 \, T^{3.82} \exp(-723/T)$$

3. C$_6$H$_5$ + C$_4$H$_6$ → Products (ref. # 5)

The rate of phenyl radical addition to butadiene has been measured by CRDS in the 298 – 400 K range at 40 Torr pressure using Ar as carrier gas, $k = (3.16 \pm 0.29) \times 10^{12}$ exp [-(870 ± 30)/T] cm^3/mol-sec, see Fig. 1 for comparison with those of C$_6$H$_5$ + C$_3$H$_4$ reactions, and the potential surface of the C$_6$H$_5$ - C$_4$H$_6$ system was explored using quantum chemistry with the B3LYP density functional. Vibrational analysis allowed the determination of thermodynamic data and deduction of high-pressure-limit rate constants via transition state theory. The pressure and temperature dependences of this chemically-activated reaction were computed using a weak collision master equation analysis. The comparison of the prediction for the C$_6$H$_5$ + C$_4$H$_6$ system with experimental data showed good agreement. The dominant product at low temperature is the initial adduct, 4-phenyl-buten-3-yl. Around 1000 K, the dominant product is phenyl butadiene formed from the chemically-activated adduct, even at 10 atm. Above about 1400 K, bimolecular H-abstraction to form benzene is the most important process. Other products such as 1,4-dihydronaphthalene are much less important.

4. C$_6$H$_5$C$_2$H$_2$ + O$_2$ → C$_6$H$_5$C$_2$H$_2$O$_2$ → CHO + C$_6$H$_5$CHO (ref. # 6)

The kinetic data for the formation and decomposition of C$_6$H$_5$C$_2$H$_2$O$_2$ in the C$_6$H$_5$C$_2$H$_2$ + O$_2$ reaction at 298 K has been measured by directly monitoring the C$_6$H$_5$C$_2$H$_2$O$_2$ radical in the visible region with CRDS. The rate of C$_6$H$_5$C$_2$H$_2$ + O$_2$ was found to be (3.71 ± 0.21) × 10^{12} cm^3 mol^{-1} s^{-1} at 298 K and a total pressure of 40 Torr. The decomposition rate of C$_6$H$_5$C$_2$H$_2$O$_2$ was obtained to be (1.36 ± 0.14) × 10^4 s^{-1} (see Fig. 2). The mechanism for this very fast reaction was elucidated quantum-chemically by B3LYP/6-31G(d,p) calculations. The result of the calculations indicated that the reaction effectively occur by two competitive

Scheme 1
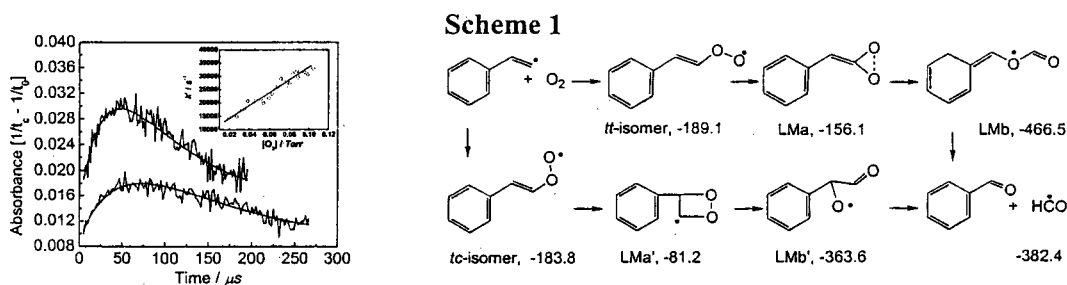
Figure 2. Typical time-resolved absorption plots of C$_6$H$_5$C$_2$H$_2$O$_2$ formed in the C$_6$H$_5$C$_2$H$_2$ + O$_2$ reaction at 298 K with different concentration of O$_2$: Top trace: [O$_2$] = 0.0957 Torr; bottom trace: [O$_2$] = 0.0297 Torr, solid curves are fitted values. Inset: the k' vs. [O$_2$] plot at 298 K.

Association paths giving 3- and 4-member-ring peroxide intermediates which fragment rapidly to $C_6H_5CHO + CHO$ with a predicted 382 kJ/mol exothermicity as shown in Scheme 1.

A more detailed study of the mechanism and associated kinetics will be carried out in the near future for interpretation of measured temperature and pressure dependent data.

B. Computational Studies

1. H + C_2H_5OH (ref. # 7)

The kinetics and mechanism for the H + C_2H_5OH reaction, a key chain-propagation step in the high temperature decomposition and combustion of ethanol, have been investigated with the G2M method using the structures of the reactants, transition states and products optimized at the B3LYP/6-311+G(d, p) level of theory. Four transition states have been identified for the production of $H_2 + CH_3CHOH$ (TS1), $H_2 + CH_2CH_2OH$ (TS2), $H_2 + C_2H_5O$ (TS3) and $H_2O + C_2H_5$ (TS4) with the corresponding barriers, 7.18, 13.30, 14.95 and 27.10 kcal/mol. The predicted rate constants and branching ratios for the three H-abstraction reactions have been calculated over the temperature range 300 - 3000 K using the conventional and variational transition state theory with quantum-mechanical tunneling corrections. The predicted total rate constant, $k_t = 3.15 \times 10^3 \, T^{3.12} \exp(-1508/T) \, cm^3 \, mol^{-1} \, s^{-1}$, agrees satisfactorily with existing experimental data; in particular, the value at 423 K was found to agree quantitatively with an available experimental value.

2. $CH_3 + C_2H_5OH$ (ref. # 8)

The mechanism for the $CH_3 + C_2H_5OH$ reaction has been investigated by the G2M method based on the geometric parameters of the stationary points optimized at the B3LYP/6-311+G(d,p) level of theory. Five transition states have been identified for the production of $CH_4 + CH_3CHOH$ (TS1), $CH_4 + CH_3CH_2O$ (TS2), $CH_4 + CH_2CH_2OH$ (TS3), $CH_3OH + CH_3CH_2$ (TS4) and $CH_3CH_2OCH_3 + H$ (TS5) with the corresponding barriers 12.0, 13.2, 16.0, 44.7, and 49.9 kcal/mol, respectively. The predicted rate constants and branching ratios for the three lower-energy H-abstraction reactions were calculated using the conventional and variational transition state theory with quantum-mechanical tunneling corrections for the temperature range 300–3000 K. The predicted total rate constant, $k_t = 8.36 \times 10^{-76} \, T^{20.00} \exp(5258/T) \, cm^3 \, mol^{-1} \, s^{-1}$ (300–600 K) and $6.10 \times 10^{-25} \, T^{4.10} \exp(-4058/T) \, cm^3 \, mol^{-1} \, s^{-1}$ (600–3000 K), agrees closely with existing experimental data in the temperature range 403–523 K. Similarly, the predicted rate constants for $CH_3 + CH_3CD_2OH$ and $CD_3 + C_2H_5OD$ are also in reasonable agreement with available low temperature kinetic data.

3. NCN + NO

The reaction of NCN and NO along the $^2A'$ and $^2A''$ paths via trans-NCN..NO and cis-NCN..NO complexes have been calculated by the G2M theory. These complexes can further decompose to NNO and CN as well as NCO and N_2 products. The predicted rate constant for the former dominant product channel in the unit of $cm^3 molecule^{-1} s^{-1}$ can be expressed as:

$k(300 \, Torr) = 3.77 \, T^{-4.61} \exp(-395/T)$ (200 – 600 K); $1.08 \times 10^{-40} \, T^{0.64} \exp(4896/T)$ (600 – 1000 K). The predicted rate constants are consistent with the experimental values.[9] The branching ratios at 300 Torr show that the main products are cis-/trans-NCN..NO complexes at the temperature below 600 K and CN + N_2O above 600 K. The yield of NCO and N_2 can be neglected. The predicted rate constants for the reverse reaction, CN + $N_2O \rightarrow$ NCN + NO can be expressed as $k = 2.23 \times 10^{-17} T^{1.98} \exp(-4155/T)$ in the unit of $cm^3 molecule^{-1} s^{-1}$ over the temperature range 200 – 1500 K. It is basically consistent with experimental data reported by Wang et al.[10]

4. NCN + O_2

The potential energy surface of the possible channels of the NCN + O_2 reaction have been investigated at the G2M (CC1) level.

$$NCN + O_2 \rightarrow NCNOO \rightarrow NCO + NO \qquad (1)$$
$$\rightarrow CNO + NO \qquad (2)$$
$$\rightarrow NCNO + {}^{1,3}O \qquad (3)$$

The rate constants for the low-lying channels are calculated in the temperature range of 1000 - 3000 K; the results show that oxidation NCN by O_2 to produce NCO + NO and CNO + NO is rather slow because of the high entrance and exit barriers. The total rate can expressed as:

$k_t = 7.29 \times 10^{-15} T^{0.51} \exp(-12370/T) \text{ cm}^3 \text{ molecule}^{-1} \text{ s}^{-1}$.

III. Future Plans

Currently, we continue the acquisition of kinetic data for C_6H_5 reactions by CRDS and PLP/MS techniques to determine the total rate constants and product branching probabilities in the C_6H_5 reactions with CH_3OH and C_2H_5OH. Computationally, we will carry out high-level *ab initio* MO calculations to improve our predictive capability for the rate constant and product branching ratios of C_6H_5 and $C_6H_5C_2H_2$ reactions with O_2 and other combustion species. We also plan to extend the calculations to include the reaction of C_6H_5 radicals with alkanes to correlate the kinetic data obtained in this laboratory for their abstraction probabilities at *p-*, *s-*, and *t-*CH sites.

IV. References (DOE publications, 2002-present, denoted by *)

1. A. M. Mebel, K. Morokuma and M. C. Lin, J. Chem. Phys., **103**, 7414 (1995).
2*. J. Park, I. V. Tokmakov and M. C. Lin, in preparation.
3*. I. V. Tokmakov, G. J. Nam, J. Park and M. C. Lin, in preparation.
4. T. Yu and M. C. Lin, Combust. Flame, **100**, 169 (1995).
5*. Huzeifa Ismail, Joonbum Park, Bryan M. Wong, W. H. Green, Jr. and M. C. Lin, Proc. Combust. Inst., submitted.
6*. Y. M. Choi, J. Park, L. M. Wang and M. C. Lin, ChemPhysChem, submitted.
7*. J. Park, Z. F. Xu and M. C. Lin, J. Chem., Phys., **118**, 9999 (2003).
8*. Z. F. Xu, J. Park and M. C. Lin, J. Chem. Phys., **120**, 6593 (2004).
9. R. E. Baren and J. F. Hershberger, J. Phy. Chem. A **106**, 11093 (2002).
10. N.S. Wang, D.L. Yang, M.C. Lin, and C. F. Melius, Int.J. Chem. Kinet., **23**, 151 (1991).

Other DOE Publications Not Cited in the Text:
1. L. V. Moskaleva and M. C. Lin, Proc. Combust. Inst., **29**, 1319 (2002).
2   J. Park, R. S. Zhu and M. C. Lin, J. Chem. Phys., **117**, 3224 (2002).
3   J. Park, Y. M. Choi, I. V. Dyakov and M. C. Lin, J. Phys. Chem., A, **106**, 2903 (2002)
4. I. V. Tokmakov and M. C. Lin, J. Phys. Chem., A, **106**, 11309 (2002).
5. B. H. Bui, R. S. Zhu and M. C. Lin, J. Chem. Phys., **117**, 11188 (2002).
6. I. V. Tokmakov, L. V. Moskaleva and M. C. Lin, J. Phys. Chem., A, , **107**, 1066 (2003).
7. I. V. Tokmakov, L. V. Moskaleva, D. V. Paschenko and M. C. Lin, J. Phys. Chem., A, **107**, 1066 (2003).
8. Y. M. Choi and M. C. Lin, J. Phys. Chem., A., **107**, 7755 (2003).
9. I. V. Tokmakov and M. C. Lin, J. Am. Chem. Soc., **125**, 11397 (2003).
10. R. S. Zhu, Z. F. Xu and M. C. Lin, J. Chem. Phys., **120**, 6566 (2004).

INVESTIGATION OF POLARIZATION SPECTROSCOPY AND DEGENERATE FOUR-WAVE MIXING FOR QUANTITATIVE CONCENTRATION MEASUREMENTS

Principal Investigator: Robert P. Lucht
School of Mechanical Engineering, Purdue University, West Lafayette, IN 47907-2088
(Lucht@purdue.edu)

I. PROGRAM SCOPE

Nonlinear optical techniques such as laser-induced polarization spectroscopy (LIPS) and degenerate four-wave mixing (DFWM) are techniques that show great promise for sensitive measurements of transient gas-phase species, and diagnostic applications of these techniques are being pursued actively at laboratories throughout the world. Over the two years we have also begun to explore the use of three-laser electronic-resonance-enhanced (ERE) coherent anti-Stokes Raman scattering (CARS) as a minor species detection method with enhanced selectivity.

The objective of this research program is to develop and test strategies for quantitative concentration measurements using these nonlinear optical techniques in flames and plasmas. We are investigating the physics of these processes by direct numerical integration (DNI) of the time-dependent density matrix equations for the resonant interaction. Significantly fewer restrictive assumptions are required using this DNI approach compared with the assumptions required to obtain analytical solutions. Inclusion of the Zeeman state structure of degenerate levels has enabled us to investigate the physics of LIPS and of polarization effects in DFWM. We have incorporated the effects of hyperfine structure in our numerical calculations of LIPS signal generation. During the last year we have successfully demonstrated injection-seeded optical parametric generation (OPG) systems. The laser radiation produced by these OPG systems is single-frequency-mode and tunable, and the system is an ideal laser source for nonlinear optical diagnostic techniques such as LIPS and ERE CARS. Experimental measurements are performed in well-characterized flames, gas cells, or nonreacting flows for comparison with our theoretical calculations.

II. RECENT PROGRESS

A. Laser-Induced Polarization Spectroscopy Measurements of the Hydrogen Atom

Simultaneous two-color, two-photon laser-induced polarization spectroscopy (LIPS) and laser-induced fluorescence (LIF) of atomic hydrogen was performed using a distributed feedback dye laser system with 60-psec pump and 80-psec probe pulses. These measurements were performed at the picosecond laser facility at Sandia's Combustion Research Facility in collaboration with Tom Settersten and Brian Patterson (Sandia) and Sukesh Roy and Jim Gord (Wright-Patterson Air Force Base). The measurements were performed in an atmospheric-pressure hydrogen/air flame. The two-color LIPS technique is illustrated in Fig. 1. The circularly polarized 243-nm pump beam was tuned to the 1S-2S two-photon resonance and the 486-nm probe beam was in resonance with the $n = 2$ to $n = 4$ single-photon transitions resonances. We have developed a nonperturbative numerical model of this two-photon, two-color H-atom LIPS process. As depicted in Fig. 1, the hyperfine structure of H-atom is incorporated in the DNI calculations. We used this numerical model to study the effects of saturation and Stark shifting on the two-photon process for picosecond laser excitation.

The rates of collisional transfer among the Zeeman states in the 2S and 2P levels and collisional quenching from the 2S and 2P levels were determined by measuring the decay curves for the LIPS and LIF signals as the 486-nm probe beam is delayed relative to the 243-nm pump beam. These curves are shown in Fig. 2. The solid lines in Fig. 2 are the results of a theoretical calculation using the DNI code. The measured temporal shapes of the pump and probe pulses were used as input parameters in the

numerical modeling, and the rates of collisional quenching from and collisional transfer within the 2S and 2P levels were varied to obtain best agreement between the measured and calculated decay curves. The broadening of the spectral lines and the shift in transition frequencies with pump laser power was also investigated. The rates of collisional quenching (Γ_{eg}) and collisional transfer within (Γ_{ee}) the 2S and 2P levels were determined to be 1.2×10^{10} s^{-1} and 9×10^{9} s^{-1}, respectively.

B.   ERE CARS: Measurements of C_2H_2

Electronic-resonance-enhanced (ERE) coherent anti-Stokes Raman scattering (CARS) measurements of acetylene (C_2H_2) were performed using a three-color CARS technique first demonstrated in measurements of NO [1]. The frequency difference between the 532-nm pump beam and the 594-nm Stokes beam was tuned to the 1974 cm^{-1} Raman resonance. The ultraviolet 239-nm probe beam was then scattered from the Raman polarization induced by the pump/Stokes interaction to produce an ERE CARS signal at 229 nm. Measurements were performed on a mixture of 5000 ppm of C_2H_2 in a buffer gas of N_2. The dependence of the ERE CARS signal on pressure and on the probe wavelength was investigated in detail. Significantly, the ERE CARS signal was found to increase as the square the pressure for the 5000 ppm gas mixture. This rapid increase in signal with pressure is quite different from the behavior of the laser-induced fluorescence signal with pressure, for example, and is a major advantage of the ERE CARS technique for measurements of minor species in high-pressure environments. We have also made substantial progress in the last year on the development of a nonperturbative numerical model for the ERE CARS process. This code will be used to model NO ERE CARS data acquired over a range of pressures using our newly developed injection-seeded OPG system described in the next section.

C.   Development of Tunable, Injection-Seeded Optical Parametric Laser Sources

We have developed a pulsed OPG system that is injection-seeded with a distributed feedback (DFB) diode laser. The OPG is injection-seeded at the idler wavelength of 1535 nm without the use of a resonant cavity, eliminating problems associated with the stabilization of the cavity and simplifying greatly the wavelength tuning of the system. The wavelength of the OPG system can be tuned by varying the current and/or the temperature of the DFB laser. Two beta barium borate (β-BBO) crystals are used in the OPG and are pumped by the third harmonic 355-nm output of an injection-seeded Nd:YAG laser. The OPG output is then amplified using an additional two-crystal optical parametric amplifier (OPA) stage. The OPG/OPA system is shown in Fig. 3. A pulse energy of 18 mJ at the signal wavelength of 461 nm has been demonstrated with the system shown in Fig. 3. The frequency spectrum and stability of the OPG/OPA system was monitored using a solid etalon with a 10 GHz free spectral range and a resolution of approximately 500 MHz, confirming the single-mode operation and frequency stability of the system. A high-resolution line shape of low-pressure acetylene obtained by tuning the OPG idler beam across a near-infrared acetylene resonance is shown in Fig. 4. As is evident from Fig. 4, the frequency bandwidth of the OPG laser radiation is less than or equal to 200 MHz (0.007 cm^{-1}), close to the Fourier transform limit for the 5-6 nsec laser pulses from the system.

III. FUTURE WORK

Our investigation of the physics of two-photon, two-color LIPS will continue. We will continue to explore the physics of this process using our direct numerical integration (DNI) code. We plan to use the two-photon, two-color LIPS technique for measurements of the O-atom and of the C-atom, and to compare the detection limits of the LIPS technique with two-photon LIF techniques. Our newly developed OPG laser source will be used for these measurements. The single-mode output, narrow line width, and smooth temporal pulse shape from the OPG system will allow rigorous comparison of theory and experiment. The OPG system will also be used to explore further the potential of infrared LIPS for species measurements

[2]. Further collaborative picosecond LIPS experiments with Tom Settersten at Sandia are planned for the summer of 2004.

We plan to pursue further theoretical and experimental investigations of the ERE CARS process for NO and C_2H_2, especially at higher cell pressures where collisional narrowing may result in significant decreases in the detection limits. The DNI code for ERE CARS has been developed and will be used to explore the physics of the ERE CARS process. As is the case for our LIPS measurements, the OPG system will be used for the ERE CARS measurements and will allow rigorous comparison of theory and experiment.

We will further develop and characterize the injection-seeded OPG/OPA systems. The performance of both the OPG stage and OPA stages will be further optimized, and the wavelength coverage of the system will be investigated. Simultaneous operation of two OPG/OPA systems will be demonstrated and the system will be applied for two-color LIPS and/or three-laser CARS. This OPG/OPA source technology will enhance greatly the potential for quantitative application of pulsed cavity ring-down spectroscopy and nonlinear techniques such as LIPS, DFWM, dual-pump CARS, and ERE CARS spectroscopy.

IV. REFERENCES

1. S. F. Hanna, W. D. Kulatilaka, Z. Arp, T. Opatrný, M. O. Scully, J. P. Kuehner, and R. P. Lucht, *Applied Physics Letters* **83**, 1887-1889 (2003).
2. S. Roy, R. P. Lucht, and A. McIlroy, *Applied Physics B* **75**, 875-882 (2002).

V. BES-SUPPORTED PUBLICATIONS 2002-2004

1. S. Roy, R. P. Lucht, and T. A. Reichardt, "Polarization Spectroscopy Using Short-Pulse Lasers: Theoretical Analysis," *Journal of Chemical Physics* **116 (2)**, 571-580 (2002).
2. S. Roy, R. P. Lucht, and A. McIlroy, "Mid-Infrared Polarization Spectroscopy of Carbon Dioxide: Experimental and Theoretical Investigation," *Applied Physics B* **75**, 875-882 (2002).
3. R. P. Lucht, S. Roy, and T. A. Reichardt, "Calculation of Radiative Transition Rates for Polarized Laser Radiation," *Progress in Energy and Combustion Science* **29**, 115-137 (2003).
4. S. F. Hanna, W. D. Kulatilaka, Z. Arp, T. Opatrný, M. O. Scully, J. P. Kuehner, and R. P. Lucht, "Electronic-Resonance-Enhanced (ERE) Coherent Anti-Stokes Raman Scattering (CARS) Spectroscopy of Nitric Oxide," *Applied Physics Letters* **83**, 1887-1889 (2003).
5. W. D. Kulatilaka, R. P. Lucht, S. F. Hanna, and V. R. Katta, "Two-Color, Two-Photon Laser-Induced Polarization Spectroscopy Measurements of Atomic Hydrogen in Near-Adiabatic, Atmospheric Pressure Hydrogen/Air Flames," *Combustion and Flame*, accepted for publication.
6. W. D. Kulatilaka, T. N. Anderson, T. L. Bougher, and R. P. Lucht "Development of an Injection-Seeded, Pulsed Optical Parametric Generator for High-Resolution Spectroscopy," *Applied Physics B*, submitted for publication (2004).
7. S. Roy, T. B. Settersten, B. D. Patterson, R. P. Lucht, and J. R. Gord, "Two-Color, Two-Photon Laser-Induced Polarization Spectroscopy (LIPS) of Atomic Hydrogen Using Picosecond Lasers," *Physical Review Letters*, submitted for publication (2004).

VI. GRADUATE DISSERTATIONS RESULTING FROM DOE/BES SUPPORT 2002-2004

1. Sukesh Roy, "Laser Diagnostic Investigation of Low-Pressure Diamond-Forming Flames," Ph.D. Thesis, Texas A&M University (2002), supported 50% on BES grant.
2. Waruna D. Kulatilaka, "Investigation of Polarization Spectroscopy for Detecting the Hydrogen Atom in Flames," M.S. Thesis, Texas A&M University (2002).
Graduate Students Supported at Present Time: Waruna Kulatilaka (PhD student at Purdue University)
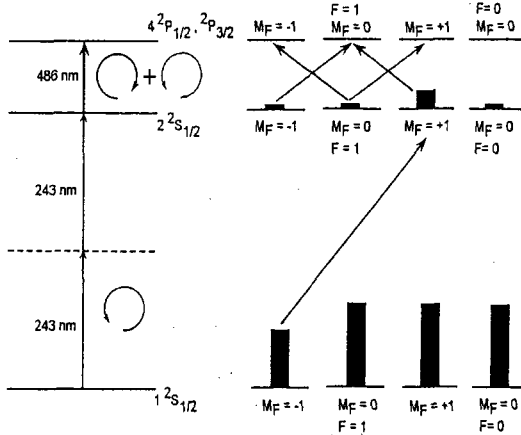
Fig. 1. Energy level schematic diagram for the two-photon, two-color LIPS measurements of the H-atom.
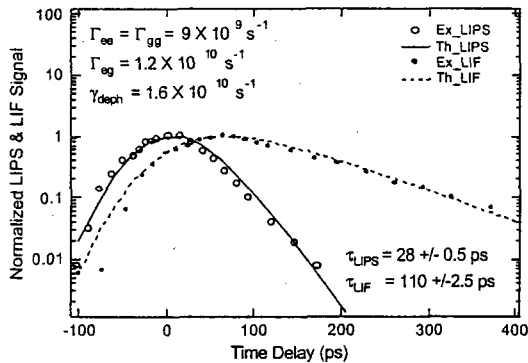
Fig. 2. Two-photon, two-color LIPS and LIF signal intensities as a function of the time delay between the 243-nm pump beam and the 486-nm probe beam.
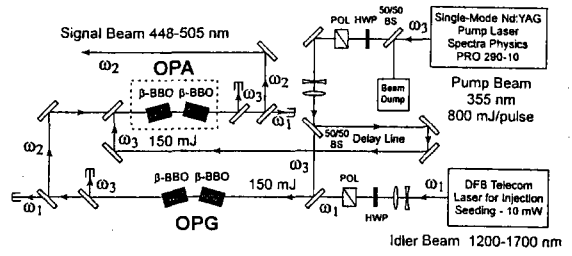
Fig. 3. Injection-seeded OPG/OPA system.
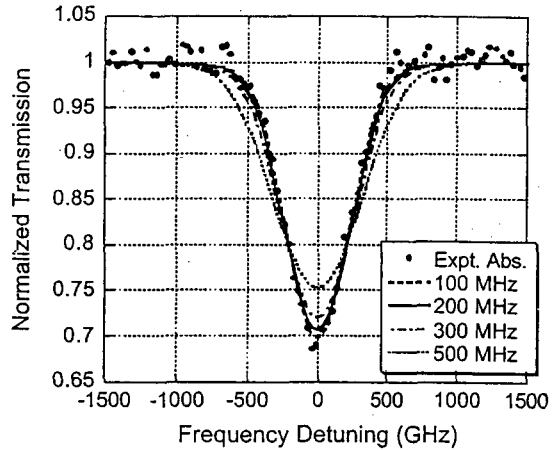
Fig. 4. Absorption spectrum of acetylene at 3 Torr obtained by tuning the idler beam of the OPG/OPA system shown in Fig. 3. The theoretical curves labeled 100 MHz,....500 MHZ are the results of convolutions of the Voigt profile for the C_2H_2 line with a laser frequency spectrum for the specified bandwidth. Both the Doppler width and the collisional width for the line are well known, and at this pressure the collisional width is less than 50 MHz. The results of this comparison indicate that the OPG line width is less than 200 MHz.

Time-Resolved Infrared Absorption Studies of the Dynamics of Radical Reactions

R. G. Macdonald
Chemistry Division
Argonne National Laboratory
Argonne, IL 60439
Email: macdonald@anlchm.chm.anl.gov

Background

There is very little information available about the dynamics of radical-radical reactions. These processes are important in combustion being chain termination steps as well as processes leading to new molecular species. For almost all radical-radical reactions, multiple product channels are possible, and the determination of product channels will be a central focus of this experimental effort. Two approaches will be taken to study radical-radical reactions. In the first, one of the species of interest will be produced in a microwave discharge flow system with a constant known concentration and the second by pulsed-laser photolysis of a suitable photolyte. The rate constant will be determined under pseudo-first order conditions. In the second approach, both transient species will be produced on the same photolysis laser pulse, and followed sequentially or simultaneously using various continuous-wave laser sources. This approach allows for the direct determination of the second-order rate constant under any concentration conditions. In both approaches, the time dependence of individual ro-vibrational states of the reactants and/or products will be followed by frequency- and time-resolved absorption spectroscopy. In order to determine branching ratios and second-order rate constants, it is necessary to measure state-specific absorption coefficients and transition moments of radicals and these measurements will play an important role in this experimental study.

Recent Results

The current series of systems was initiated to investigate the chemistry between $NCO(X^2\Pi)$ and simple alkyl radicals. The NCO radical is an important intermediate in the chemistry of NO_X generation and several NO_X abatement strategies. In general, the chemistry of the NCO radical has not been extensively explored, and in particular, there are few studies of the interaction between NCO and other open shell species.

Not only is it important to determine accurate rate constants for radical-radical interactions, but also it is also important to determine various product channels. Generally, radical-radical reactions are characterized by the possibility of multiple product channels, and it is a difficult experimental challenge to determine these product branching ratios. In the current work, rate constants were determined by computer simulations of numerous species temporal concentration profiles. Rate constants were determined by chi-squared minimization between a computed and measured temporal profile based on the variation of a single rate constant. Rate constants for secondary processes were varied over a limited range of possibilities to investigate the influence of secondary chemistry as well as to infer possible product channels. This strategy was adapted because as many species were monitored as possible, and the temporal profiles

were obtained with high signal-to-noise thus severely constraining the range of possible secondary chemistry.

The NCO and alkyl (R) radicals were generated by the 248 nm photolysis of ClNCO and the subsequent reaction of Cl with RH, where RH was H_2, CH_4 or C_2H_6. In each system NCO and HCl were monitored along with other detectable species.

(a) $NCO(^2\Pi) + Cl(^2P)$

The first reaction studied was the NCO + Cl reaction. There are two possible product channels: recombination to reform NCOCl or $NCl(^3\Sigma^-) + CO$. The following reaction scheme describes the system:

$$NCO + Cl \rightarrow ClNCO \qquad\qquad 1(a)$$
$$\rightarrow NCl(^3\Sigma^-) + CO \qquad\qquad 1(b)$$
$$NCO + NCO \rightarrow 2CO + N_2 \qquad\qquad 2$$
$$NCl + NCl \rightarrow 2Cl + N_2 \qquad\qquad 3$$
$$Cl + ClNCO \rightarrow NCO + Cl_2 \qquad\qquad 4$$
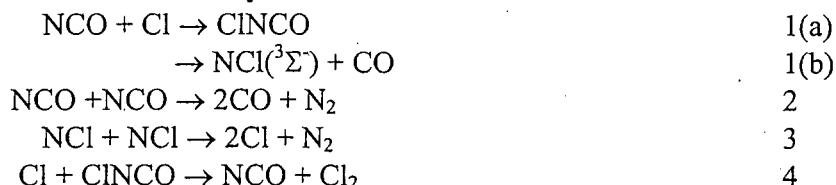
The NCO temporal profiles would be described by the sum of a pure second order and first order decay process if reaction 1(a) were the dominant product channel. Such was not the case and the NCO profiles were analyzed by assuming product channel 1(b) was the only one present followed by reactions 3 and 4. The rate of reaction 1(b) was found to be $7.9 \pm 1.3 \times 10^{-11}$ cm^3 molecule^{-1}s^{-1}, independent of collision partner (Ar or CF_4) or pressure (2 to 6 Torr). The rate of reaction 4 was found to be $2.3 \pm 1.0 \times 10^{-11}$ cm^3 molecule^{-1}s^{-1}.

(b) $NCO(^2\Pi) + H(^2S)$

Preliminary work has been completed on this reaction. The temporal concentration profiles NCO, $NH(^3\Sigma^-)(v=0,1,2)$, and HCl were recorded. Other species probed but not detected were HCN, HNC, NH_2 and HNCO. This system is complicate by the large uncertainty in NH chemistry and the rather small reaction rate constant between Cl and H_2. Work is progressing on studying this reaction at elevated temperatures to accelerate the Cl + H_2 reaction rate, and minimize some of the secondary chemistry. The usefulness of state-to-state detection is illustrated by the observation of vibrationally excited NH. The production of NH(v=1) was found to account for 6.5% of the NH reaction product. The preliminary measurements give the reaction rate constant to be 2.1×10^{-10} cm^3 molecule^{-1}s^{-1}. This is a factor of 10 greater than the only previous measurement for this rate constant[a]

(a) K. H. Becker, R. Kurtenbach, F. Schmidt, and P. Wiesen, Combustion and Flame, **120**, 570, (2000).

(c) $NCO(^2\Pi) + CH_3(^2A_2)$

The temporal concentration profiles for NCO, CH_3, HCl, C_2H_6, HNC, HCN, HNCO, and NH were recorded. The recombination of CH_3 radicals was directly monitored by following the formation of C_2H_6. In order to monitor the concentration of C_2H_6, the absorption cross sections for several Q-K subbranchs of the v_7 vibrational mode were determined. At 293 K, the reaction rate constant for NCO + CH_3 was found to be 1.9×10^{-10} cm^3 molecule^{-1}s^{-1}. Figure 1 shows a typical example of NCO and CH_3 temporal profiles and the resulting determination of the reaction rate constant.

The data has been analyzed assuming that the dominant product channel is recombination yielding the CH_3NCO product. As can be seen from Figure 1, there is excellent agreement between the calculated and experimental profiles for the NCO species, and minor differences between the calculated and experimental CH_3 profiles. However, for the C_2H_6 species (not shown) the differences were significant, with the model predictions 30% to 40% too low. At 294 K and 4.7 Torr, the CH_3 recombination rate constant is close to the high pressure limit and cannot vary too far from the well-established value for Ar as collision partner. This strongly suggests another channel is producing C_2H_6. A possibility is the participation of the energetically accessible $CH_3N(^3A_2)$ + CO channel with the subsequent reaction, $CH_3N + CH_3N \rightarrow C_2H_6 + N_2$, giving C_2H_6.

(d) $NCO(^2\Pi) + C_2H_5(^2A')$

The temporal concentration profiles of NCO, HCl, HNCO, C_2H_4 and HCN were monitored for this system. Unfortunately, the spectral region where the C_2H_5 radical is known to absorb is strongly overlapped by C_2H_6 absorption features, preventing the direct detection of C_2H_5. However, both HNCO and C_2H_4 were observed to be products of the NCO + C_2H_5 reaction so that these two species provide a connection to the C_2H_5 radical temporal dependence. The secondary chemistry is complicated by the reaction of C_2H_5 with ClNCO giving at least HCl and likely HNCO as products. The HNCO molecule was monitored using rotational transitions in the $^qR_0(J)$ rotational manifold of the ν_1 vibrational mode. There is no information available on the strength of this vibrational transition so that experiments are proceeding to measure these line strengths.

Preliminary results indicate that the rate constant for the NCO + C_2H_5 reaction is 2×10^{-10} $cm^3 molecule^{-1}s^{-1}$, similar to that for the other systems. About 50 % of the reaction proceeds through the C_2H_4 + HNCO product channel.

Future Work

Work will proceed to complete the study between NCO and simple alkyl radicals, including the investigation of NCO + H and CH_3 at elevated temperatures.

Work will also begin on the investigation of the $CH_3(^2A_2") + OH(^2\Pi)$, radical – radical reaction. As in the CN + OH work, both species will be interrogated on the same photolysis laser pulse using different laser sources. The product branching ratio into the $^1CH_2 + H_2O$ channel will be probed using time-resolved absorption spectroscopy of $^1CH_2$ using the vibronic transitions of the $^1CH_2$ (b $^1B_1$) $\leftarrow$ (a $^1A_2$) transition in the near infrared. The formation of other product channels will be probed using infrared vibrational spectroscopy.

Publications 2002-2004.

Determination of the rate constant for the $NCO(X^2\Pi) + O(^3P)$ reaction at 292 K.
-Y. Gao and R. G. Macdonald, J. Phys. Chem. 107A, 4625-4635 (2003).

Determination of the rate constant for the radical-radical reaction $CN(X^2\Sigma) + OH(^2\Pi)$ at 292 K.
-B. K. Decker and R. G. Macdonald, J. Phys. Chem. 107A, 9137-9146 (2003).

Model Determination of $k_{NCO+CH3}$ from [NC0] Profile
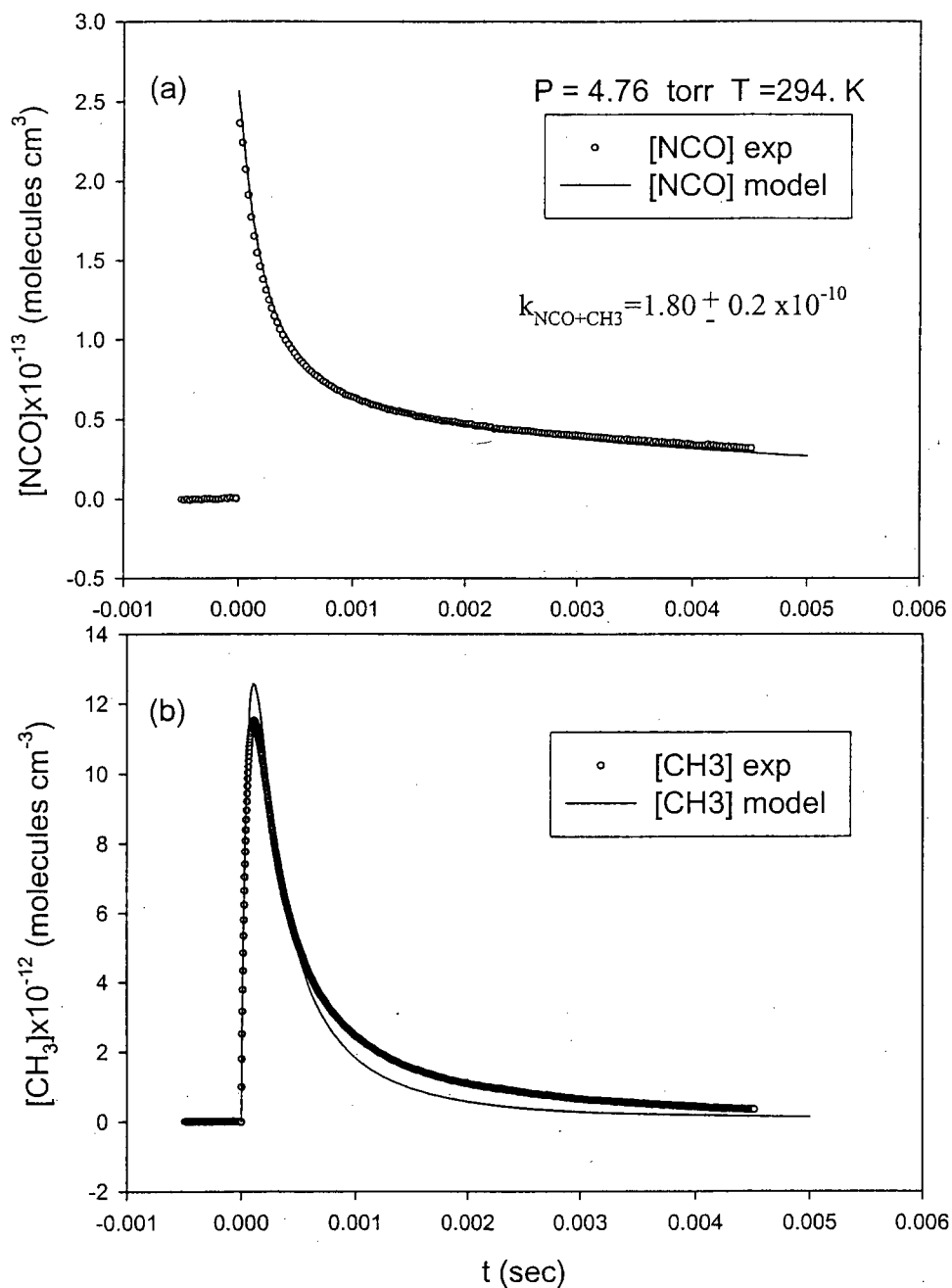
Figure 1. Determination of the rate constant for NCO + CH_3 reaction by minimizing the sum of the squares of the residuals between the experimental and model [NCO] profiles.

FLASH PHOTOLYSIS-SHOCK TUBE STUDIES

Joe V. Michael

Gas Phase Chemical Dynamics Group, Chemistry Division
Argonne National Laboratory, Argonne, IL 60439
e-mail: jmichael@anl.gov

The scope of the program is to measure high-temperature thermal rate constants with shock tube techniques for use in high-temperature combustion. During the past year, we have rebuilt and tested a new multi-pass optical system for use in OH-radical studies. This development is similar to that described in earlier work from this laboratory.[1-3] We have used this detection method to measure rate constants for several bimolecular reactions in reflected shock wave experiments.

The optical configuration consists of an OH resonance lamp, multi-pass reflectors, an interference filter at 308 nm, and a photomultiplier tube (1P28) all mounted external to the shock tube. The microwave discharge was focused onto the reflector on the opposite side of the shock tube through two AR coated windows that were mounted flush to the inside of the shock tube. The reflectors and windows were obtained from the CVI Laser Corporation. These reflectors were attached to adjustable mounts, and the center points of windows and mirrors were all in a coaxial position. With this new configuration, we were able to obtain 32 passes, giving a total path length of 2.8 m, thereby allowing experiments on OH-radicals to be performed at lower concentration than in our previous work.[1-3]

Because this is a new system, we determined the curve-of-growth for OH radicals under similar conditions as the anticipated kinetics experiments. The same method used previously[1] was employed. OH-radicals were generated by the H + NO_2 reaction[3] from controlled H atom formation using C_2H_5I decomposition;[4] i. e.,

$$C_2H_5I\ (+M) \rightarrow C_2H_5 + I\ (+M) \qquad (1)$$
$$C_2H_5I\ (+M) \rightarrow C_2H_4 + HI\ (+M) \qquad (2)$$
$$C_2H_5\ (+M) \rightarrow C_2H_4 + H\ (+M) \qquad (3)$$
$$H + NO_2 \rightarrow NO + OH. \qquad (4)$$
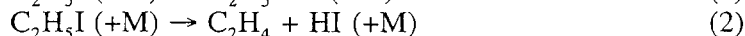
Reaction (3) is fast compared to (1) and (2), and therefore, thermal decomposition of C_2H_5I controls the rate of formation of H. Using relatively high concentrations of NO_2, the rate for (4) can be adjusted to be high, thereby forming a pulse of OH at short times compared to the duration of the experiment. The nearly instantaneous level of absorbance measured was then correlated with $[OH]_0$ as determined from the mechanism, (1) to (4), for known initial concentrations of C_2H_5I and NO_2. Twenty-four experiments were carried out with varying initial reactant concentrations, and the absorption cross section, σ_{OH}, was determined to be $(2.77 \pm 0.15) \times 10^{-17}$ cm². This value agrees with earlier work as discussed in ref. 1.

During the course of this work, we noted that $[OH]_t$ decreased at an apparent rate that was incompatible with the known depletion rates due to OH + OH and OH + C_2H_4. Fig. 1 shows a typical absorbance result for an experiment at 1461 K with $[C_2H_5I] = 3.92 \times 10^{13}$ and $[NO_2] = 5.67 \times 10^{14}$ molecules cm⁻³. In order to relate the absorbance data to concentration for this experiment, a scaling factor of 1.14×10^{14} molecules cm⁻³ was necessary. This implies a value for $\sigma_{OH} = 3.13 \times 10^{-17}$ cm² molecule⁻¹ for this experiment. The experiment was then simulated with a 37 step mechanism where the aforementioned depletion processes are included. The value for OH + OH is from an evaluation[5] that was based on the back reaction, O + H_2O, transformed by using the equilibrium constant adjusted for the new heat of formation for OH.[6] The transformed values are within ±9% of the directly determined values of Wooldridge et al.[7] Values for OH + C_2H_4 are from Tully.[8] The simulation that includes these two noted reactions gives the dashed line in the

figure. In order to recover the depletion rate indicated by the experiment, we had to include a third process that introduced several other secondary reactions into the mechanism. This process is $OH + NO_2 \rightarrow NO + HO_2$. Fig. 2 shows an Arrhenius plot comprised of 17 experiments between 1300-1530 K.

Howard studied both the forward and reverse processes,[9] and the long dashed line in Fig. 2 is an extrapolation of $OH + NO_2$ data obtained between 452 and 1115 K. Howard and others have also directly measured rate constants for the reverse process, $NO + HO_2$, and the combined results gave a heat of formation for HO_2 at 298 K of (2.5 ± 0.6) kcal mole^{-1}. This value has recently been challenged,[10] questioning the accuracy of the $OH + NO_2$ reaction rate data. The data for the reverse process is quite accurate, and therefore, we have compared the present data to transformations of the $NO + HO_2$ data through equilibrium constants in order to test whether the present values are reasonable.

Not only has the heat of formation for HO_2 been questioned, but the heats of formation of both NO and NO_2 have recently been updated.[10] Fig. 3 shows a plot of third-order rate constants for the $O + NO + M$ reaction. This reaction was measured by Yarwood et al.[11] who combined their results with earlier low temperature results to give the evaluation shown as the solid circles. Rohrig et al.[12] studied the thermal decomposition of NO_2, and these data have been transformed with Janaf equilibrium constants to give the solid triangles. Yarwood et al. pointed out that the earlier experimental values for the dissociation were not compatible with their results. However in this more recent study, Rohrig et al. found relatively good agreement between their results and Yarwood (~30%). Using the updates for NO and NO_2, the 30% difference between the two sets of kinetics data remains as seen in Fig. 3 (cf. open circles and solid triangles); however, this spread is well within combined experimental errors. Using the new values for NO, NO_2, and HO_2, new equilibrium constants for the reaction can be calculated.[10] These values have been used to transform the $NO + HO_2$ data from Howard and others, and the results are shown in Fig. 2 as the solid line. Chakraborty et al.[13] have recently carried out theoretical calculations, and transforming their results gives the small dashed line. It is clear that the theory and transformed data for $NO + HO_2$ both agree well with one another. Our conclusion is then that the high-temperature rate constant should taken to be the transformed value from Howard (the solid line in Fig. 2); i. e., $k = 1.53 \times 10^{-11} \exp(-3303 \, K/T)$ cm^3 molecule^{-1} s^{-1} (1000-1600 K). The present experimental results are reasonable and agree with this expression with the maximum deviation being 45%.

In anticipation of a study on the $OH + CH_4$ reaction using the C_2H_5I/NO_2 method for OH generation, we studied the possible secondary reaction, $CH_3 + NO_2 \rightarrow CH_3O + NO$. The methoxy radicals subsequently decompose to give $H + CH_2O$, and H atoms react with excess NO_2 yielding OH. The secondary reactions are fast compared to $CH_3 + NO_2$. In this case, CH_3I served as the source of CH_3. $[OH]_t$ was measured and fitted with a simulations, yielding values for the rate constant between 1360 and 1695 K. Within experimental error, the rate constants were T-independent giving k = (2.4 ± 0.7) to be compared to earlier values from Glaenzer and Troe,[14] Yamada et al.,[15] and Biggs et al.[16] of 2.16 (1100-1400 K), 2.52 (295 K), and 2.31 (298 K), all in units, 10^{-11} cm^3 molecule^{-1} s^{-1}. Fig. 4 shows the data. We also have data on the thermal decomposition of CH_3OH and on the reactions, $OH + OH$, $OH + H_2$, $OH + C_2H_6$, $OH + CH_3$, and $OH + CH_2$.

Additional atom and radical with molecule reaction studies (e. g. Cl + hydrocarbons, OH + hydrocarbons, $CF_2 + O_2$, etc.) and, also, thermal decomposition investigations (e. g. C_2H_5, C_2H_3, etc.) are in the planning stage at the present time. This work was supported by the U. S. Department of Energy, Office of Basic Energy Sciences, Division of Chemical Sciences, Geosciences and Biosciences, under Contract No. W-31-109-ENG-38.

References

1. M.-C. Su, S. S. Kumaran, K. P. Lim, and J. V. Michael, Rev. Sci. Inst. **66**, 4649 (1995).
2. M.-C. Su, S. S. Kumaran, K. P. Lim, J. V. Michael, A. F. Wagner, D. A. Dixon, J. H. Kiefer, and J. DiFelice J. Phys. Chem. **100**, 15827 (1996).

3. M.-C. Su, S. S. Kumaran, K. P. Lim, J. V. Michael, A. F. Wagner, L. B. Harding, and D.-C. Fang, J. Phys. Chem. A **106**, 8261 (2002).

4. S. S. Kumaran, M.-C. Su, K. P. Lim, and J. V. Michael, Proc. Combust. Inst. **26**, 605 (1996).

5. J. V. Michael, Prog. Energy Combust. Sci. **18**, 327 (1992).

6. B. Ruscic, D. Feller, D. A. Dixon, K. A. Peterson, L. B. Harding, R. L. Asher, and A. F. Wagner, J. Phys. Chem. A **105**, 1 (2001).

7. M. S. Wooldridge, R. K. Hanson, and C. T. Bowman, Int. J. Chem. Kinet. **26**, 398 (1994).

8. F. P. Tully, Chem. Phys. Lett. **143**, 510 (1988).

9. C. J. Howard, J. Am. Chem. Soc. **102**, 6937 (1980).

10. B. Ruscic, private communication, Sept., 2003.

11. G. Yarwood, J. W. Sutherland, M. A. Wichramaaratchi, and R. B. Klemm, J. Phys. Chem. **95**, 8771 (1991).

12. M. Rohrig, E. L. Petersen, D. F. Davidson, and R. K. Hanson, Int. J. Chem. Kinet. **29**, 485 (1997).

13. D. Chakraborty, J. Park, and M. C. Lin, Chemical Physics **231**, 39 (1998).

14. K. Glaenzer and J. Troe, Ber. Bunsenges. Phys. Chem. **78**, 182 (1974).

15. F. Yamada, I. R. Slagle, and D. Gutman, Chem. Phys. Lett. **83**, 409 (1981).

16. P. Biggs, C. E. Canosa-Mas, J.-M. Fracheboud, A. D. Parr, D. E. Shallcross, R. P. Wayne, and F. Caralp, J. Chem. Soc. Faraday Trans. **89**, 4163 (1993).

PUBLICATIONS FROM DOE SPONSORED WORK FROM 2002-2004

■ *Rate Constants for H + O_2 + M → HO_2 + M in Seven Bath Gases*, J. V. Michael, M.-C. Su, J. W. Sutherland, J. J. Carroll, and A. F. Wagner, J. Phys. Chem. A **106**, 5297 (2002).

■ *Rate Constants, 1100≤T≤2000 K, H + NO_2 → OH + NO, Using Two Shock Tube Techniques: Comparison of Theory to Experiment*, M.-C. Su, S. S. Kumaran, K. P. Lim, J. V. Michael, A. F. Wagner, L. B. Harding, and D.-C. Fang, J. Phys. Chem. A **106**, 8261 (2002).

■ *C_2D_5I Dissociation and D + CH_3 → CH_2D + H at High Temperature: Implications to the High Pressure Rate Constant for CH_4 Dissociation*, M.-C. Su and J. V. Michael, Proc. Combust. Inst. **29**, 1219 (2002).

■ *H + H_2 Thermal Reaction: A Convergence of Theory and Experiment*, S. L. Mielke, K. A. Peterson, D. W. Schwenke, B. C. Garrett, D. G. Truhlar, J. V. Michael, M.-C. Su, and J. W. Sutherland, Phys. Rev. Lett. **91**, 063201 (2003).

■ *Rate Constants for D + C_2H_2 → C_2HD + H at High Temperature: Implications to the High Pressure Rate Constant for H + C_2H_2*, J. V. Michael, M.-C. Su, J. W. Sutherland, L. B. Harding, and A. F. Wagner, J. Phys. Chem. A **107**, 10533 (2003).

■ *New Rate Constants for D + H_2 and H + D_2 between ~1150 and 2100 K*, J. V. Michael, M.-C. Su, and J. W. Sutherland, J. Phys. Chem. A **108**, 432 (2004).

■ *Rate Constants for D + C_2H_4 → C_2H_3D + H at High Temperature: Implications to the High Pressure Rate Constant for H + C_2H_4 → C_2H_5*, J. V. Michael, M.-C. Su, J. W. Sutherland, L. B. Harding, and A. F. Wagner, Proc. Combust. Inst. **30**, accepted.

■ *Shock Tube Studies using a Novel Multi-pass Absorption Cell: Rate Constant Results for OH + OH, OH + H_2, and OH + C_2H_6*, L. N. Kransnoperov and J. V. Michael, J. Phys. Chem. A, in press.

■ *High Temperature Shock Tube Studies using a Novel Multi-pass Absorption Cell: Rate Constant Results for CH_3OH Decomposition and for OH + CH_3 and OH + CH_2*, L. N. Kransnoperov and J. V. Michael, J. Phys. Chem. A, submitted.

Fig:1

Fig:2

Fig:3

Fig:4
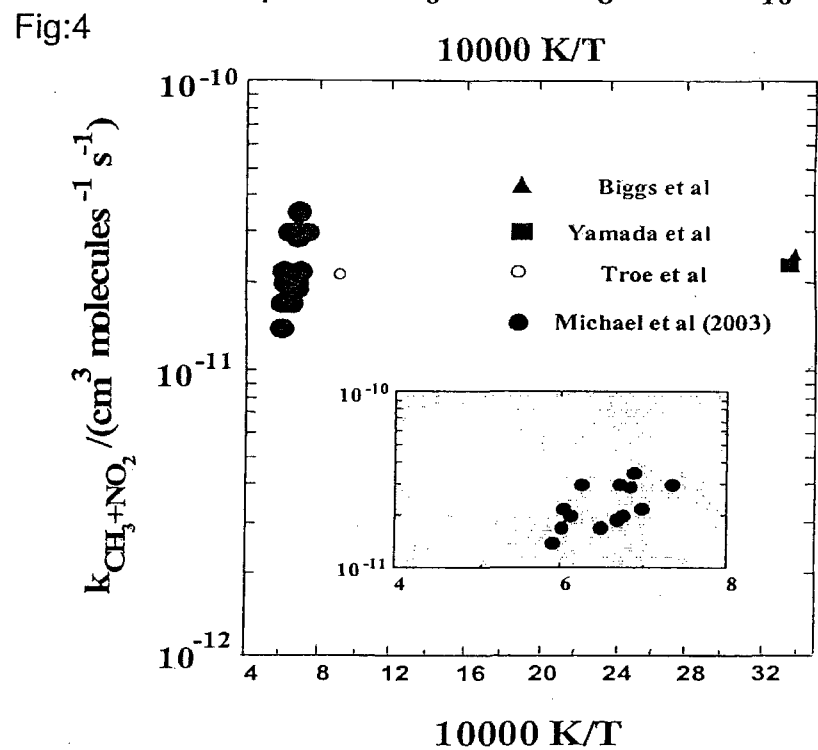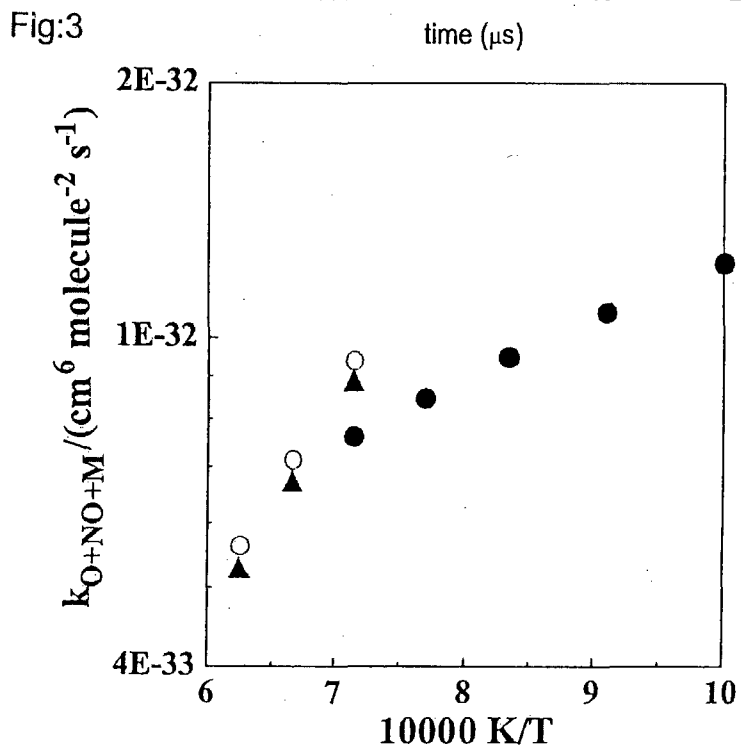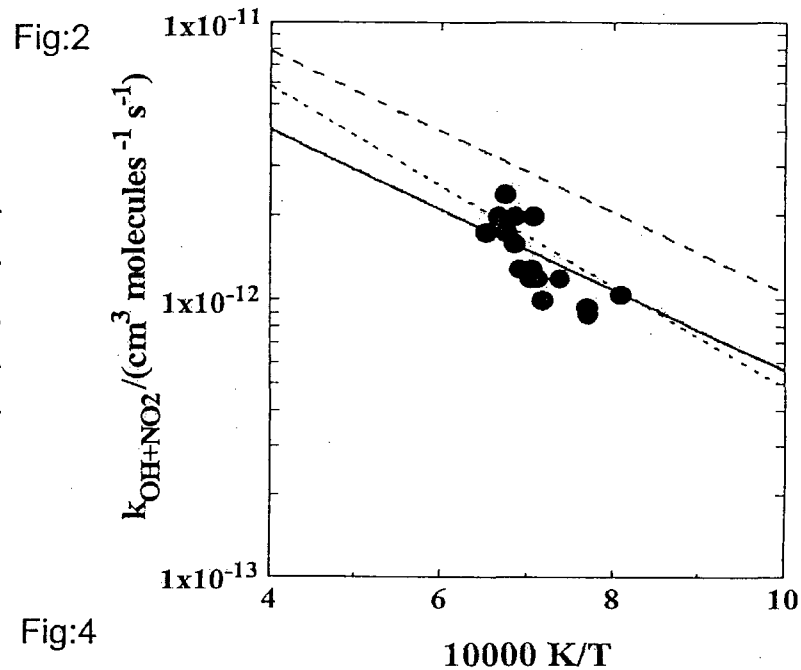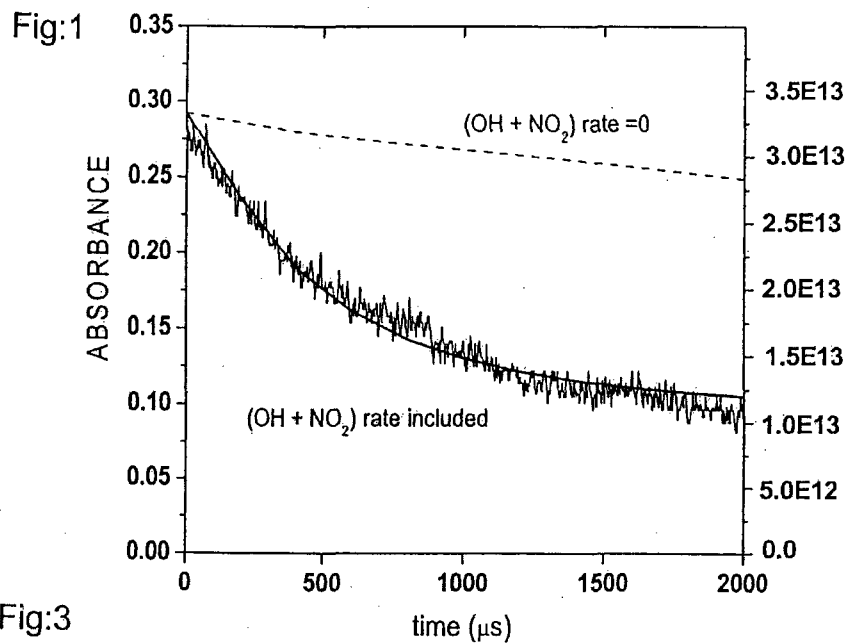
Particle Diagnostics Development

H. A. Michelsen
Sandia National Labs, MS 9055, P. O. Box 969, Livermore, CA 94551
hamiche@ca.sandia.gov

1. Program Scope

Small (sub-micron) particulates are believed to pose a greater health risk than larger soot particles[1] and are expected to have a significant impact on the Earth's climate.[2] A growing concern about adverse health and environmental effects of small particles has prompted strict regulations of fine particulate emissions and has intensified research on the formation and impact of combustion-generated particles.[3] Studies of particle formation and evolution, however, are hindered by a lack of sensitive, accurate, noninvasive measurements of their physical characteristics. The research program described here focuses on the development of optical diagnostics for particles, primarily soot particles, in combustion environments and combustion exhaust plumes. The goal of this work is in situ measurements of volume fraction, size, composition, and morphology of such particles with fast time response and high sensitivity.

2. Recent Progress

To test current models and investigate the influence of experimental conditions on LII behavior, we have measured time-resolved LII signals from soot in a nonsmoking coflow ethylene diffusion flame over a wide range of laser fluences.[4] A Nd:YAG laser was injection seeded to provide a smooth laser temporal profile with a pulse duration of 7 ns, the output was doubled to generate 532-nm light, and the beam was passed through an aperture and relay-imaged into the flame to produce a smooth laser spatial profile. LII temporal profiles were recorded with a fast photodiode with adequate temporal resolution to capture signal evolution during the laser pulse. We used these results to aid in the development of a model that predicts the temporal behavior of LII from soot on a nanosecond time scale. The model accounts for particle heating by laser absorption, oxidation, and annealing and cooling by sublimation, conduction, and radiation. The model also includes mechanisms for convective heat and mass transfer, melting, and nonthermal photodesorption of carbon clusters.[5]

Another set of experiments was performed to investigate the fast photodesorption mechanism in more detail. In these experiments the particles were heated with 532-nm pulses of ~60 ps duration from a regeneratively amplified modelocked Nd:YAG laser. The signal was imaged onto one side of the slit of a streak camera and collected over the wavelength range 590-900 nm. Laser scatter was collected simultaneously on each laser shot on the other side of the slit. Using this arrangement we have collected data to fluences as high as 0.6 J/cm^2 with a temporal resolution of ~15 ps.

The signal depends on the particle diameter ($\propto D^3$) and temperature ($\propto \sim T^5$). As the particle temperature increases during the laser pulse, the signal increases, and, as the particle cools and shrinks (from carbon cluster sublimation and photodesorption), the signal decreases. At laser fluences below ~0.2 J/cm^2, temperatures increase rapidly during the laser pulse and slowly decay (on microsecond timescales) following the laser pulse. This slow decay is predominantly due to conductive cooling.[4-10] At higher fluences particles quickly reach and surpass the sublimation temperature of ~4000 K, becoming superheated, and then cool via sublimation back to the sublimation point.[4-7,9-14] Sublimation also causes particles to decrease in size. At higher fluences, decay rates during and just after the laser pulse are fast, which may be largely attributable to photodesorption of carbon clusters.[4,5] Annealing to more ordered forms of carbon may influence heating, cooling, and mass loss rates at nearly all fluences.[4,5]

Models typically used to describe LII are based on a model initially developed by Melton[10] in which energy- and mass-balance equations are solved to account for particle heating by laser absorption and cooling by conduction to the surrounding atmosphere, radiative emission, and sublimation. Particle

size reduction during sublimation is also calculated. LII signal is derived from calculated temperatures and sizes using the Planck function weighted by the emissivity and the detector's wavelength response. The Melton model[10] uses (1) temperature-independent values for density and specific heat to determine the internal energy of the particle, (2) a Rayleigh approximation to calculate laser absorption and radiative emission rates, (3) the approximation of kinetic control of C_3 only from the surface to calculate sublimation rates, (4) a thermal accommodation coefficient and heat capacity associated with temperatures near room temperature, and (5) a formulation for conductive cooling appropriate for a transition regime between Knudsen and continuum flow.

We have developed a model[4,5] that similarly solves the energy- and mass-balance equations but also includes (1) temperature-dependent thermodynamic parameters for calculating sublimation, conduction, and internal energy storage by the particle, (2) wavelength-dependent optical parameters to describe absorption and emission of radiation based on a Rayleigh-Debye-Gans approximation to account for aggregation, (3) convective heat and mass flow (Stefan flow) during the sublimation of multiple cluster species (C, C_2, C_3, C_4, and C_5) from the surface, (4) a thermal accommodation coefficient appropriate for high temperature conductive cooling, (5) a conductive cooling mechanism assuming free molecular flow at low pressure and a transition regime at high pressure, (6) nonthermal photodesorption resulting in loss of heat and mass by carbon clusters leaving the particle, (7) phase changes (i.e., annealing and melting) and their effects on absorption, radiation, sublimation, and photodesorption, and (8) oxidative heating at the particle surface.

The model descriptions of cooling and mass loss by sublimation and photodesorption are the most important terms for calculating the temporal behavior and magnitude of the LII signal at fluences above 0.2 J/cm^2. This part of the model is also the most complex and, in the case of photodesorption, the most uncertain. Although previous studies have suggested that laser photodesorption of carbon clusters from graphite can proceed by a nonthermal mechanism,[15-20] the nature of this mechanism, including the number of photons required, is not known. Our model includes such a mechanism assuming that it proceeds via a 2-photon process at 532 nm with a cross section and enthalpy of reaction approximated by comparing the results with the data.

Primary particles of mature soot have a microstructure similar to that of polycrystalline graphite.[21] Soot particles anneal into multi-shell carbon onions at temperatures above ~2500 K,[22-24] and graphite surfaces have been shown to melt at atmospheric pressure when heated rapidly with a laser.[25-27] Changes in the phase of soot primary particles are likely to influence heating and cooling rates because of differences in physical properties, such as the index of refraction, enthalpies and entropies of formation of carbon clusters, and thermal accommodation coefficients. Soot annealing rates have not been measured under the conditions encountered during laser heating on sub-second timescales; we infer these rates from annealing rates measured on graphite at lower temperatures on longer timescales. Annealing rates are calculated in the new model using an Arrhenius expression with activation energies for interstitial migration and vacancy/defect formation derived from studies of graphitization.

At low fluences, the differences between the two models are largely due to the thermal accommodation coefficients used to calculate the conductive cooling rate. The Melton model uses a value (0.9) that is appropriate for low-temperature conditions, whereas the new model uses a value (0.3) from measurements made on graphite at temperatures of 700-1400 K. Discrepancies between the models are also partially attributable to differences in the treatment of conductive cooling; the new model assumes free molecular flow conditions when the mean free path exceeds the particle diameter by a factor of ~7, whereas the Melton model assumes that the system is always in the transition regime between Knudsen and continuum flow. Free molecular flow is appropriate when the primary particles are assumed to have minimal contact, i.e., when aggregation is neglected. Both models neglect aggregation for the conduction calculation, which is predicted to decrease conductive cooling rates via the shielding effect. Calculations using quasi-Monte Carlo algorithms indicate that

accounting for aggregation would reduce the conductive cooling rate by ~30% for an aggregate of 500 primary particles and a thermal accommodation coefficient of 0.3.[28]

At higher fluences, the new model gives better agreement with the measurements mainly because (1) at intermediate fluences annealing reduces the rate of cooling by sublimation and (2) at higher fluences photodesorption increases the mass and heat loss rate (and therefore signal decay rate) during the laser pulse. At these fluences, the differences between the two models are also apparent in the predicted fluence dependence of the magnitude of the signal. Including the nonthermal photolysis term allows the new model to reproduce the lack of fluence dependence of the peak signal at fluences above 0.2 J/cm^2, whereas the Melton model predicts that the signal continues to increase with fluence.

3. Future plans

Despite the improved agreement between modeled and measured signals with the new model over previous models, lingering discrepancies at intermediate and high fluences demonstrate an incomplete understanding of the mechanisms for sublimation, photodesorption, and annealing. Uncertainties related to the treatment of sublimation in the models are large and include those associated with (1) neglecting aggregation, which may lower sublimation rates and (2) assuming thermodynamic properties of graphite. In addition, the photodesorption mechanism is speculative, and the uncertainties associated with it are substantial. The annealing process and the influence it has on sublimation and photodesorption are also very poorly understood. Our future work is focused on investigations to narrow the uncertainties associated with these mechanisms.

Our picosecond experiments are designed to isolate mechanisms that take place on short timescales, particularly laser absorption and photolytic desorption, from processes that are expected to evolve over longer (nanosecond) timescales, such as thermal sublimation and annealing. We will refine these measurements and revise the LII model to target the earliest time regime with adequate temporal resolution.

Annealing is another mechanism with large uncertainties. In addition to uncertainties in the rates of annealing, there are large uncertainties associated with the change in optical properties as the particles anneal. Studies of the optical properties of carbon onions (with 10^4 times the number of carbon atoms of C_{60}) have been limited by the inability to generate significant numbers of particles to study. Following a recently published procedure,[29] we have set up an apparatus to generate carbon onions in sufficiently large quantities to measure their optical properties for comparison with those of soot. Transmission Electron Microscopy (TEM) images of the particles generated indicate a mixture of onion-type structures and large amorphous globs up to 10 times larger than the pseudo-onion particles (~40 nm). The technique used to generate these onions thus requires refinement before we can measure their optical properties.

Most of the carbon atoms in mature soot are thought to be included in flat graphite crystallites with sp^2 hybridization. As the particles anneal, defects form, allowing the surfaces to curve. Annealing of fullerenes by formation of 7-member rings leads to greater sp^3 hybridization.[30] Investigations are planned in collaboration with Mary Gilles at the Advanced Light Source at the Lawrence Berkeley National Laboratory using Near-Edge X-ray Absorption Fine Structure (NEXAFS) spectroscopy to study the change in character of the carbon-bond hybridization when the particles are annealed.

We have also initiated experiments designed to test the influence of coatings on particle characteristics and the applicability of optical diagnostics. We have constructed a flow tube system in which we can vary the mean aggregate size of the soot and characterize the size distribution using a scanning mobility particle sizer. Soot is generated by a coflow laminar diffusion flame, which is intercepted by a cross flow of air to extract, dilute, and cool the soot as it travels down a flow tube. We have added a station to this flow tube system in which the particles can be coated with aqueous sulfuric acid, other inorganic species, metallic ash, and heavy and light organic coatings to simulate particles that may be found in exhaust plumes.

4. References

(1) Horvath, H. *J. Environ. Radioact.* **2000**, *51*, 5.

(2) IPCC *Climate Change 2001: The Scientific Basis. Contribution of Working Group I to the Third Assessment Report of the Intergovernmental Panel on Climate Change*; Cambridge University Press: Cambridge, UK and New York, NY, 2001.

(3) NRC *Research Priorities for Airborne Particulate Matter: IV. Continuing Research Progress*; National Academy Press: Washington, DC, 2004.

(4) Michelsen, H. A.; Witze, P. O.; Kayes, D.; Hochgreb, S. *Appl. Opt.* **2003**, *42*, 5577.

(5) Michelsen, H. A. *J. Chem. Phys.* **2003**, *118*, 7012.

(6) Tait, N. P.; Greenhalgh, D. A. *Ber. Bunsenges. Phys. Chem.* **1993**, *97*, 1619.

(7) Mewes, B.; Seitzman, J. M. *Appl. Opt.* **1997**, *36*, 709.

(8) Will, S.; Schraml, S.; Leipertz, A. *Opt. Lett.* **1995**, *20*, 2342.

(9) Schraml, S.; Dankers, S.; Bader, K.; Will, S.; Leipertz, A. *Combust. Flame* **2000**, *120*, 439.

(10) Melton, L. A. *Appl. Opt.* **1984**, *23*, 2201.

(11) Witze, P. O.; Hochgreb, S.; Kayes, D.; Michelsen, H. A.; Shaddix, C. R. *Appl. Opt.* **2001**, *40*, 2443.

(12) Eckbreth, A. C. *J. Appl. Phys.* **1977**, *48*, 4473.

(13) Will, S.; Schraml, S.; Bader, K.; Leipertz, A. *Appl. Opt.* **1998**, *37*, 5647.

(14) Smallwood, G. J.; Snelling, D.; Liu, F.; Gülder, Ö. L. *J. Heat Transfer, Trans. ASME* **2001**, *123*, 814.

(15) Krajnovich, D. J. *J. Chem. Phys.* **1995**, *102*, 726.

(16) Lincoln, K. A.; Covington, M. A. *Int. J. Mass Spectrom. Ion Phys.* **1975**, *16*, 191.

(17) Dreyfus, R. W.; Kelly, R.; Walkup, R. E. *Nucl. Instrum. Methods Phys. Res.* **1987**, *B23*, 557.

(18) Murray, P. T.; Peeler, D. T. *Appl. Surf. Sci* **1993**, *69*, 225.

(19) Kokai, F.; Takahashi, K.; Yudasaka, M.; Iijima, S. *J. Phys. Chem. B* **1999**, *103*, 8686.

(20) Rohlfing, E. A. *J. Chem. Phys.* **1988**, *89*, 6103.

(21) Vander Wal, R. L. *Combust. Sci. Technol.* **1997**, *126*, 333.

(22) Vander Wal, R. L.; Ticich, T. M.; Stephens, A. B. *Appl. Phys. B: Lasers Opt.* **1998**, *67*, 115.

(23) Vander Wal, R. L.; Choi, M. Y. *Carbon* **1999**, *37*, 231.

(24) de Heer, W. A.; Ugarte, D. *Chem. Phys. Lett.* **1993**, *207*, 480.

(25) Venkatesan, T.; Jacobson, D. C.; Gibson, J. M.; Elman, B. S.; Braunstein, G.; Dresselhaus, M. S.; Dresselhaus, G. *Phys. Rev. Lett.* **1984**, *53*, 360.

(26) Malvezzi, A. M. *Int. J. Thermophys.* **1990**, *11*, 797.

(27) Heremans, J.; Olk, C. H.; Eesley, G. L.; Steinbeck, J.; Dresselhaus, G. *Phys. Rev. Lett.* **1988**, *60*, 452.

(28) Filippov, A. V.; Zurita, M.; Rosner, D. E. *J. Colloid Interface Sci.* **2000**, *229*, 261.

(29) Sano, N.; Wang, H.; Chhowalla, M.; Alexandrou, I.; Amaratunga, G. A. J. *Nature* **2001**, *414*, 506.

(30) Murry, R. L.; Strout, D. L.; Odom, G. K.; Scuseria, G. E. *Nature* **1993**, *366*, 665.

5. BES peer-reviewed publications

H. A. Michelsen, P. O. Witze, D. Kayes, and S. Hochgreb, "Time-resolved laser-induced incandescence of soot: The influence of experimental factors and microphysical mechanisms", *Appl. Opt.* **42**, 5577-5590 (2003).

H. A. Michelsen, "Understanding and predicting the temporal response of laser-induced incandescence from carbonaceous particles", *J. Chem. Phys.* **118**, 7012-7045 (2003).

Chemical Kinetics and Combustion Modeling

James A. Miller
Combustion Research Facility
Sandia National Laboratories
Mail Stop 9055
Livermore, CA 94551-0969
Email: jamille@sandia.gov

Program Scope

The goal of this project is to gain qualitative insight into how pollutants are formed in combustion systems and to develop quantitative mathematical models to predict their formation and destruction rates. The approach is an integrated one, combining theory, modeling, and collaboration with experimentalists to gain as clear a picture as possible of the processes in question. My efforts and those of my collaborators are focused on problems involved with the nitrogen chemistry of combustion systems and the formation of soot and PAH in flames, as well as on general problems in hydrocarbon combustion. Current emphasis is on determining phenomenological rate coefficients from the time-dependent, multiple-well master equation for reactions involved in the pre-cyclization and cyclization chemistry of flames burning aliphatic fuels.

Recent Results

A Complete Statistical Analysis of the Reaction Between OH and CO (with Juan Senosiain and Stephen Klippenstein)

This work is a fairly substantial extension of previous work on the same reaction. We have improved the detail of the calculations of Senosiain et al (*Int. J. Chem Kinet.* **35**, 464-474 (2003)) and investigated the impact of variational effects and angular momentum conservation on the overall thermal rate constants. Although the magnitude of these effects is not large, they result in different (adjusted) vibrationally adiabatic reaction barriers and energy transfer parameters. More importantly, they result in nearly temperature-independent rate coefficients below 500 K, in good agreement with low temperature experiments. Reaction barriers obtained by fitting experimental data in a broad temperature and pressure range are in excellent agreement with high level electronic structure calculations (the differences are well below 1 kcal/mole for both transition states involved).

195

The $H+C_2H_2(+M) \rightleftarrows C_2H_3(+M)$ and $H+C_2H_4(+M) \rightleftarrows C_2H_5(+M)$ Reactions: Electronic Structure, Variational Transition-State Theory, and Solutions to a Two-Dimensional Master Equation. (with Stephen Klippenstein)

In this work we investigated the kinetics of the $H+C_2H_2$ and $H+C_2H_4$ reactions, as well as their reverse dissociations, in some detail. High level electronic structure calculations were used to characterize the potential energy surfaces, and these results were *not* adjusted to obtain good agreement with experiment in the subsequent kinetic analysis. An approximate two-dimensional master equation was used to determine phenomenological rate coefficients, $k(T,p)$. The effects of angular momentum conservation, tunneling, and the use of variational transition-state theory (as opposed to conventional transition-state theory) to compute microcanonical rate coefficients were investigated in detail. For both reactions, the low-pressure limit is approached very slowly because reaction just above threshold must occur strictly by tunneling. Assuming a single-exponential-down model for $P(E,E')$, we deduced from experiment values of $<\Delta E_d>$, the average energy transferred in a deactivating collision, as a function of temperature for both C_2H_3 and C_2H_5 in baths of He, Ar and N_2. Our results support the idea that $<\Delta E_d>$ increases roughly linearly with temperature, at least for weak colliders. The agreement between theory and experiment is remarkably good for both reactions. Values of $k(T,p)$ for the two reactions were reduced to the Troe format for use in modeling.

Some Observations Concerning Detailed Balance in Association/Dissociation Reactions (with Stephen Klippenstein)

This investigation was prompted by our earlier work on C_2H_3 and C_2H_5 dissociation. In this article we have considered the chemical kinetics of reversible association/dissociation reactions at great length. We find that, as long as the characteristic time for internal-energy relaxation is faster (not necessarily much faster) than that for chemical reaction, there will always be a period of time, late in the reaction but before equilibrium is reached, during which phenomenological rate laws will apply with rate coefficients that satisfy detailed balance. The nonequilibrium factor, f_{ne}, originally introduced by Smith, McEwan, and Gilbert *(J. Chem. Phys.* **1989**, 90 4265-4273), is *not* a measure of the degree to which detailed balance is satisfied by the association and dissociation rate coefficients. It is simply the fractional contribution to the "long-time" association rate coefficient, k_{add}, of the slowest-relaxing eigenmode of the system. That is, $1- f_{ne}$ is the fractional contribution to the same rate coefficient of the internal-energy relaxation modes. The standard practice of taking the dissociation rate coefficient, k_d, to be equal to that for irreversible dissociation is accurate as long as $\gamma = K_{eq} n_m (1-f_{ne}) \ll 1$, where K_{eq} is the equilibrium constant for the association reaction, and n_m is the concentration of the excess reactant under pseudo first-order conditions for the association reaction.

The Reaction of OH with Acetylene (with Juan Senosiain and Stephen Klippenstein)

The reactions of OH with acetylene and diacetylene play important roles in rich flames. In preparation for a detailed investigation of the latter, and because advancements in the theory of chemical kinetics in quantum chemistry allow more detailed calculations to be done now than in the study of OH + C_2H_2 by Miller and Melius (*Proc. Combust. Inst.* **22**, 1031-1039 (1989)), we have initiated a theoretical study of the former reaction.

The doublet potential energy surface of C_2H_2 and OH was calculated with the RQCISD(T) method and extrapolated to the infinite basis set limit using geometries obtained at the UB3LYP/6-311 ++G(d,p) level. Thermal rate coefficient were obtained by methods we have developed and employed previously. As did Miller and Melius, we found the direct abstraction channel to be the main pathway at high temperatures and low pressures, despite its substantial energy barrier and endothermicity. At low temperatures and high pressures the OH radical adds to acetylene forming hydroxyvinyl radical (CH (OH) CH), which subsequently isomerizes to vinoxy (CHOCH$_2$), COHCH$_2$, and acetyl (COCH$_3$) radicals. Total high temperature rate coefficients are in excellent agreement with experimental determinations, and the rate coefficient of all non-abstraction channels is in agreement with the measurements of Bittner and Howard (*Proc. Combust. Inst.* **19**, 211 (1982)). However, in contrast with Miller and Melius, we find that production of ketene is quite rapid. In fact, ketene is the main product at 1500 K, and its generation is faster than that of hydroxyacetylene at temperatures below 2400 K under 1 atmosphere of pressure.

Future Directions

We shall continue our work on the chemical kinetics of rich flames, particularly that concerned with the formation of the first aromatics containing one or two rings. Currently, we are working on reactions involving $n-C_4H_3$ and $i-C_4H_3$ ($H+C_4H_2 \rightarrow i-C_4H_3$, $H+C_4H_2 \rightarrow n-C_4H_3$, and $n-C_4H_3+C_2H_2$), as well as on reaction of propargyl ($C_3H_3(+M) \rightarrow C_3H_2 + H(+M)$, C_3H_3 + allene, and C_3H_3 + propyne). However, our next major project will be the propargyl + allyl reaction, which could be as important as $C_3H_3+C_3H_3$ as a cyclization step in flames. We shall also continue to maintain our interest in the nitrogen chemistry of combustion, particularly that concerned with NO_x control technologies such as reburning, Thermal De-NO_x, and RAPRENO$_x$.

Publications of James A. Miller
2002-Present

- J.A. Miller and S.J. Klippenstein, "Some Observations Concerning Detailed Balance in Association / Dissociation Reactions," *J. Phys. Chem. A.,* submitted (2004).

- J.P. Senosiain, S.J. Klippenstein, and J.A. Miller, "A Complete Statistical Analysis of the Reaction of OH with CO, " *Proc. Combust. Inst.* **30**, accepted (2003).

- J. Troe, J.A. Miller, and M.J. Pilling, "Unraveling Combustion Mechanisms Through the Quantitative Understanding of Elementary Reactions," *Proc. Combust. Inst.* **30**, in press (2004).

- D.G. Truhlar, A.F. Ramos, S.J. Klippenstein, and J.A. Miller, "Bimolecular Reactions, " Chapter 3 of upcoming volume of *Comprehensive Chemical Kinetics* (Ed. R.W. Carr and M.R. Zachariah), Elsevier Publishing Company, in press (2004).

- J.A. Miller and S.J. Klippenstein, "The $H+C_2H_2(+M) \rightleftarrows C_2H_3(+M)$ and $H+C_2H_4(+M)$ $\rightleftarrows C_2H_5(+M)$ Reactions: Electronic Structure, Variational Transition-State Theory, and Solutions to a Two-Dimensional Master Equation", *Physical Chemistry Chemical Physics,* **6**, 1192-1202 (2004).

- J.A. Miller and S.J. Klippenstein, "The Recombination of Propargyl Radicals and Other Reactions on a C_6H_6 Potential, " *J. Phys. Chem. A* **107**, 7783-7799 (2003).

- J.A. Miller, S.J. Klippenstein, and P. Glarborg, "A Kinetic Issue in Reburning: The Fate of HCNO, " *Combustion and Flame* **135**, 357-362 (2003).

- J.A. Miller and S.J. Klippenstein, "From the Multiple-Well Master Equation to Phenomenological Rate Coefficients: Reactions Occurring on a C_3H_4 Potential Energy Surface," *J. Phys. Chem. A* **107**, 2680-2692 (2003).

- J.D. DeSain, S.J. Klippenstein, J.A. Miller, and C.A. Taatjes, "Measurements, Theory, and Modeling of OH Formation in Ethyl + O_2 and Propyl + O_2 Reactions, " *J. Phys. Chem. A* **107**, 4415-4427 (2003).

- S.J. Klippenstein and J.A. Miller, "From the Time-Dependent, Multiple-Well Master Equation to Phenomenological Rate Coefficients," *J. Phys. Chem. A* **106**, 9267-9277 (2002).

- S.J. Klippenstein, J.A. Miller, and L.B. Harding, "Resolving the Mystery of Prompt CO_2: The HCCO + O_2 Reaction," *Proceedings of the Combustion Institute* **29**, 1209-1217 (2002).

- J.A. Miller, S.J. Klippenstein, and C. Raffy "Solution of Some One- and Two-Dimensional Master Equation Models for Thermal Dissociation: The Dissociation of Methane in the Low-Pressure Limit, " *J. Phys. Chem. A* **106**, 4904-4913 (2002).

Detection and Characterization of Free Radicals Relevant to Combustion Processes

Terry A. Miller

Laser Spectroscopy Facility, Department of Chemistry

The Ohio State University, Columbus OH 43210, email: tamiller+@osu.edu

1 Program Scope

The chemistry of combustion is well-known to be extremely complex. Modern computer codes are now available that employ hundreds of reaction steps and a comparable number of chemical intermediates. Nonetheless the predictions of such models can be no better than the fundamental dynamics and mechanistic data that are their inputs. Spectroscopic identifications and diagnostics for the chemical intermediates in the reaction mechanisms constitute an important experimental verification of the models.

The first phase of our work has been to obtain and analyze the electronic spectra of radicals involved in the oxidation of hydrocarbons, of which some of the most important are the alkoxy, RO, and the peroxy,

Figure 1: Plot of the $\widetilde{B} - \widetilde{X}$ origin frequency of the various alkoxy radicals, $C_nH_{2n+1}O$, vs number of carbon atoms, n. The different structural isomers, 1, 2, 3, and t, clearly fall on different curves.

RO_2, radicals. Once the spectra have been identified and analyzed, we have begun to use them to probe the fundamental dynamics of these radical intermediates.

2 Recent Progress

Figure 2: Survey LIF spectrum of a) 1-butoxy, and b) 1-pentoxy. Labelled bands have been rotationally analyzed.

Recently we have spent the majority of our time studying the alkoxy radicals and so this report will concentrate on those species. Methoxy is the smallest alkoxy radical and we have been collaborating with the group of C. B. Moore to understand the spectra of the partially deuterated isotopomers, CH_2DO and CHD_2O, with the view of investigating their detailed dynamics, especially for the case of CHD_2O. The methoxy work is detailed in the Moore group report, while we concentrate on the larger alkoxy radicals herein.

A while ago, we observed for the first time the laser induced fluorescence (LIF) of

a number of larger alkoxy radicals, $C_nH_{2n+1}O$ $(3 \leq n \leq 12)$ in a supersonic free jet expansion. The larger alkoxy radicals exhibit a great deal more structural complexity than the smallest members of the family, methoxy and ethoxy. In the larger family members multiple structural isomers are present. Fig. 1 shows how the origin frequencies of the LIF spectra clearly fall into subsets based upon primary, secondary, or tertiary substitution, and how even different secondary isomers can be distinguished. In short this plot provides the basis for an isomer specific spectral diagnostic.

Of course these spectra have more structure than just an origin band. Fig. 2 shows this clearly for the spectra of 1-butoxy and 1-pentoxy. Initially it was believed that the higher energy bands corresponded to excited state vibrational structure in the observed $\tilde{B} - \tilde{X}$ electronic transitions. However efforts to assign these bands to vibrational transitions largely failed. The rotational structure of the labelled bands in the butoxy spectrum of Fig. 2 shows why this is the case. This rotational structure clearly "bar-codes" the transitions into three distinct groups (A), (B, D, F), and (C and E).

Figure 3: Lower frequency region of the cyclohexoxy LIF spectrum taken under three different temperature conditions. Lines labelled in the middle have been assigned to "cold" $\tilde{B} - \tilde{X}$ transition (unprimed) and "hot" $\tilde{B} - \tilde{A}$ transition (primed).

The detailed rotational analyses of these spectra is beyond the scope of this report. However the results of these analyses and the subsequent comparison of the resulting spectroscopic parameters (rotational and spin-rotation constants) with quantum chemistry calculations establishes unambiguously that these three groups of lines belong to different conformers of 1-butoxy, with similar conclusions having been reached for the LIF spectra of the other observed $C_nH_{2n+1}O$ radicals.

Of these 5 possible 1-butoxy conformers, the three groups of lines have been uniquely correlated with the $T_1T_2(B,D,F)$ $T_1G_2(C,E)$, and $G_1T_2(A)$ conformers. It may be interesting to note that the two unidentified conformers, G_1G_2 and $G_1'G_2$, both have cyclic structures, more or less reminiscent of the expected transition state structure for the isomerization of the 1-butoxy to the butyl hydroxy radical.

The above discussion has focussed on open-chain alkoxy radicals. Cyclic hydrocarbon compounds give rise to cyclic alkoxy radicals. Cyclohexane, an important cyclic hydrocarbon, is a constituent of automobile fuel and its oxidation produces the cyclohexoxy radical, $C_6H_{11}O$. Fig. 3 shows the LIF spectrum of cyclohexoxy and demonstrates its dramatic dependence upon temperature. Using a variety of spectroscopic techniques, we have assigned all the labelled vibronic bands in the top trace of Fig. 3. The "cold bands", i.e., those retaining significant intensity at the lower temperature (bottom), arise from the $\tilde{B}-\tilde{X}$ electronic transition, terminating on both a' and a'' vibrational levels of the $\tilde{B}$ state with the latter, normally forbid-

Figure 4: Three CRDS spectra of the unbranched butyl peroxy radicals. The top trace (offset=30 ppm) contains both isomers produced by H atom extraction from n-butane by Cl from the photolysis of $(COCl)_2$, followed by O_2 addition. The middle trace (offset=30 ppm) corresponds to n-butyl peroxy produced by direct photolysis of n-butyl bromide followed by O_2 addition. The bottom trace (offset=0 ppm) corresponds to sec-butyl peroxy radical produced by direct photolysis of sec-butyl bromide followed by O_2 addition.

den transitions, being allowed by a pseudo-Jahn-Teller effect in the $\tilde{X}$ state. The "hot bands", which grow in dramatically as the temperature increases are ascribed to $\tilde{B} - \tilde{A}$ electronic transitions terminating solely on a' vibrational levels. The $\tilde{A}$ electronic state is found to be extremely low-lying, with a difference between the vibrationless levels of the $\tilde{A}$ and $\tilde{X}$ states of only 62 cm^{-1}.

2.2 Peroxy Radical Spectroscopy
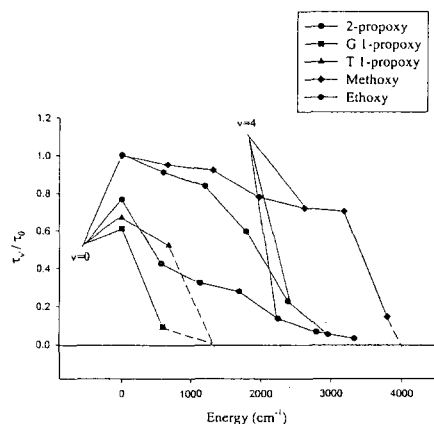
Figure 5: Plot of the measured $\widetilde{B}$ state lifetimes, $\tau_{v'}$ of the various alkoxy radicals, normalized by the lifetime, τ_0 – taken to be 2.57 μsec, of the vibrationless level of methoxy, vs. excess vibrational energy (above the vibrationless level) in the CO stretch in the species. The v=0 and v=4 CO stretch levels are indicated. Dashed lines indicate that the LIF of the next CO stretch was unobserved implying a $(\tau_{v'}/\tau_0) \lesssim 0.05$.

2.3 Radical Dynamics

Once spectral assignments are made that are isomer and, in many cases conformer specific, the identified lines can be used to follow various dynamical processes in exquisite detail. We have pursued this approach in a couple of different ways. In one case we have measured the lifetime of the excited state and found it to be quite dependent upon several factors: 1) degree of vibrational excitation, 2) isomer, and 3) conformer of a given radical. Fig. 5 is a plot for the smallest alkoxy radicals (CH_3O, C_2H_5O, and C_3H_7O) of the $\widetilde{B}$ state lifetime, normalized by its value in the vibrationless level of CH_3O, as a function of excess vibrational energy above the vibrationless level of the $\widetilde{B}$ state.

Interestingly Fig. 5 does not show great variation in lifetime for different radical species in the vibrationless level, but it does show some striking dependence on other parameters. The dramatic decrease in lifetime for v $\approx$ 7 of the CO stretch in methoxy has long

While the majority of our recent efforts have centered on the alkoxy radicals, we have also been exploring the spectroscopy of the peroxy radicals. Our efforts have utilized the cavity ringdown spectroscopy (CRDS) technique to study their weak $\widetilde{A} - \widetilde{X}$ electronic transition in the near infrared (NIR). Using CRDS we approach the sensitivity of peroxy radical detection achieved on the much stronger, and widely utilized, ultraviolet (UV) $\widetilde{B} - \widetilde{X}$ transition. However the UV transition is broad and unstructured making it extremely difficult to discriminate among peroxy radicals, while the NIR transition is intrinsically sharp and its position quite sensitive to peroxy species, making it an excellent diagnostic to distinguish among various propoxy radicals, and follow their reactions and dynamics individually.

We have recently obtained for the first time the spectra of all the isomers of the alkyl propoxy radicals, $C_nH_{2n+1}O_2$ for $n \leq 4$. An example of a CRDS spectrum of the unbranched butyl peroxy radicals is shown in Fig. 4. The spectral lines belonging to individual isomers are indicated in Fig. 4. Note that there is significant structure to the $\widetilde{A} - \widetilde{X}$ origin band and the O-O stretch fundamental excitation. We attribute this structure to various conformers of each butyl peroxy isomer and work is in progress to assign these lines to specific conformers.
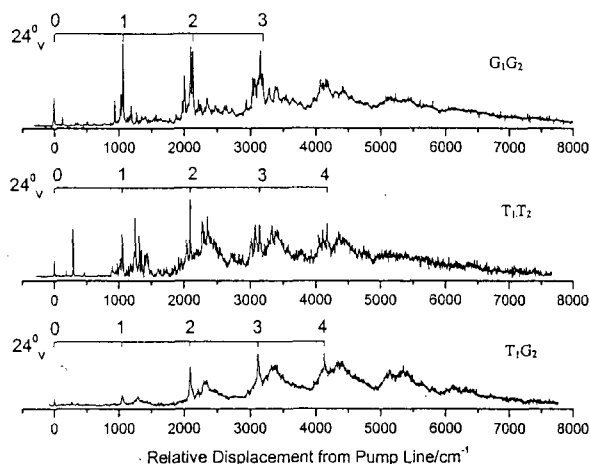
Figure 6: Dispersed fluorescence spectra of three conformers of 1-butoxy, exciting each at its origin. The CO stretch (ν_{24}) progression is indicated.

been attributed to the onset of a predissociation of the $\widetilde{B}$ state by a repulsive level. Because of a lowering of the $\widetilde{B}$ state vibrationless level, it is unlikely that the lifetime decreases for any of the other species shown in Fig. 5 can be similarly attributed to predissociation, although we expect that in all cases they do arise from the onset of a non-radiative decay channel.

We note a rather remarkable difference between the decay behavior of the 1-propoxy and 2-propoxy radicals. As Fig. 5 shows for 2-propoxy the CO stretch progression extends through v = 6, which has over 3000 cm^{-1} of excess vibrational energy. However for both T and G conformers of 1-propoxy, there is no

longer any LIF signal above v = 1 of the CO stretch indicating the molecule effectively decays by non-radiative processes whenever it possesses greater than $\approx$700 cm^{-1} of excess vibrational energy. Furthermore while the lifetimes of the vibrationaless level of the T and G conformers of 1-propoxy are within $\approx$15%, the lifetimes of their v = 1 stretch levels differ by a factor of $\approx$6. Thus we see that the decay dynamics of the $\tilde{B}$ state of the propoxy radical is strongly isomer and conformer dependent. Similar observations have been made for the structural isomers and conformers of butoxy and pentoxy.

Another experiment that illustrates the different behavior of conformers is illustrated by the dispersed fluorescence spectra, shown in Fig. 6 for the three observed conformers of 1-butoxy. The T_1T_2 conformer, which alone has C_s symmetry, shows a strong line at 290 cm^{-1} above the vibrationless level. We tentatively attribute this to the origin of the $\tilde{A}\,^2A''$ state. Interestingly for both the T_1T_2 and T_1G_2 conformer, complex mostly unresolved structure is observed approximately 300 cm^{-1} above each member of the CO stretch (ν_{24}) progression. Such structure is either absent or significantly reduced in the G_1G_2 conformer. These differences likely reflect strongly different vibrational coupling behavior, which is again isomer and conformer significant.

3 Future Plans

The combustion of fossil fuels necessarily involves complicated reaction mechanisms containing numerous reactive intermediates, some of which are relatively large and complex. As the size of organic molecules increase, their structural diversity in terms of isomers and conformers rapidly grows. The complications this diversity presents either for spectroscopic diagnostics or reaction kinetics and dynamics is largely unexplored. We intend both to expand our spectroscopic techniques for probing these intermediates and to explore new classes of intermediates. Once the spectroscopy is well understood, precise dynamics and kinetic studies can be carried out.

We plan to probe the $\tilde{X}$ (and $\tilde{A}$) state using IR/UV double resonance techniques for the alkoxy radicals. By monitoring the LIF as an IR beam is swept, we can obtain ground state vibrational spectra. Such spectra will give us additional "bar-codes" to distinguish among different isomers and conformers. In addition to characterizing the structure of the radicals, the amount of vibronic coupling present at various ground state excitation energies can be evaluated. Alternatively selective vibrational levels of the $\tilde{X}$ state, e.g., a C-H stretch, can be pumped, thereby providing accessible Frank-Condon factors for UV pumping of otherwise unreachable vibrational levels in the $\tilde{B}$ state.

The peroxy radicals are key intermediates in the low-temperature combustion of many organic molecules. To this point we have used CRDS to observe the spectra of a number of peroxy radicals of saturated hydrocarbons. It would be very desirable to obtain CRDS spectra for unsaturated peroxy radicals, either aromatic, e.g., phenyl peroxy, benzoyl peroxy, etc. or not, e.g., vinyl peroxy, propargyl peroxy, etc.

List of Publications

[1] "Rotationally Resolved Electronic Spectra of the $\tilde{B} - \tilde{X}$ Transition in Multiple Conformers of 1-Butoxy and 1-Pentoxy Radicals," S. Gopalakrishnan, L. Zu, and T. A. Miller, *J. Phys. Chem. A*, **107**, 5189 (2003).

[2] "Theoretical Prediction of Spectroscopic Constants of 1-Alkoxy Radicals," G. Tarczay, S. Gopalakrishnan, and T. A. Miller, *J. Mol. Spectros.*, **220**, 276 (2003).

[3] "Radiative and Non-Radiative Decay of Selected Vibronic Levels of the $\tilde{B}$ State of Alkoxy," S. Gopalakrishnan, L. Zu, and T. A. Miller, *Chem. Phys. Lett.*, **380**, 749 (2003).

[4] "Jet-Cooled LIF Spectra of Cyclohexoxy Radical," L. Zu, J. Liu, and T. A. Miller, *J. Chem. Phys.* accepted.

[5] "Dispersed Fluorescence Spectroscopy of Primary and Secondary Alkoxy Radicals," J. Jin, I. Sioutis, G. Tarczay, S. Gopalakrishnan, A. Bezant, and T. A. Miller, *in preparation*.

[6] "Cavity Ringdown Spectra of the Isomers and Conformers of Butyl Peroxy," B. Glover, S. Zalyubovsky, and T. A. Miller, *in preparation*.

Reaction Dynamics in Polyatomic Molecular Systems

William H. Miller

Department of Chemistry, University of California, and
Chemical Sciences Division, Lawrence Berkeley National Laboratory
Berkeley, California 94720-1460
miller@cchem.berkeley.edu

Program Scope or Definition

The goal of this program is the development of theoretical methods and models for describing the dynamics of chemical reactions, with specific interest for application to polyatomic molecular systems of special interest and relevance. There is interest in developing the most rigorous possible theoretical approaches and also in more approximate treatments that are more readily applicable to complex systems.

Recent Progress

The calculation of thermal rate constants for chemical reactions is one of the central tasks of theoretical chemistry. For complex systems, i.e., those with many degrees of freedom, the transition state theory (TST) approximation of no re-crossing flux is usually valid (provided an appropriate 'dividing surface' is used). TST, however, is based inherently on classical mechanics, and a quantum generalization is necessary to obtain accurate results for molecular systems. Quantizing TST, though, is not a unique process, and one is continually searching for a quantum version of TST that is as free as possible from *ad hoc* input, is as general and accurate as possible, and is also simple enough for practical calculations to be carried out for systems with many degrees of freedom.

Within the *semiclassical* approximation to quantum mechanics there actually is a unique quantum TST, developed almost 30 years ago and known nowadays as the *instanton* model or approximation.[1] Though the instanton model has many desirable features--e.g., one does not need to postulate the 'tunneling path' through the barrier region, it being uniquely determined as the periodic orbit on the inverted potential energy surface--and has been widely used in many areas (particularly condensed matter physics), for chemical reaction rates of typical molecular systems it is only of order-of-magnitude accuracy. Though this is actually not too bad, given that tunneling corrections may be many orders of magnitude, it is nevertheless not as accurate as one would typically like. Also, finding the instanton periodic orbit for a complex molecular system with many degrees of freedom would in general be a formidable task.

Quite recently we have developed a fully quantum theory for thermal rate constants that incorporates the qualitative physical content of the semiclassical instanton model, which we refer to as the *quantum instanton* (QI) model or approximation.[2] The QI rate constant is expressed wholly in terms of the quantum Boltzmann operator, $\exp[-\beta \hat{H}]$, which for complex systems can be evaluated by relatively well-established Monte Carlo path integral methods. The derivation of the QI rate expression begins with a formally exact quantum expression for the thermal rate constant, either its time-dependent version[3] in terms of a flux-flux autocorrelation function

$$K(T) = Q_r^{-1} \int_0^\infty dt \ tr \left[e^{-\frac{\beta \hat{H}}{2}} \hat{F} \ e^{-\frac{\beta \hat{H}}{2}} \ e^{i\hat{H}t/\hbar} \ \hat{F} \ e^{-i\hat{H}t/\hbar} \right] \tag{1}$$

or its equivalent time-independent version,[4]

$$K(T) = (2\pi\hbar Q_r)^{-1} \int_{-\infty}^\infty dE \ e^{-\beta E} \frac{1}{2} (2\pi\hbar)^2 \ tr \left[\hat{F}\delta(E - \hat{H}) \ \hat{F}\delta(E - \hat{H}) \right] . \tag{2}$$

In Eqs. (1) and (2) $\hat{F}$ is a flux operator with respect to a dividing surface [defined by $s(\mathbf{q}) = 0$],

$$\hat{F} = \frac{i}{\hbar} \left[\hat{H}, h(s(\mathbf{q})) \right] , \tag{3}$$

$\hat{H}$ is the Hamitonian operator for the molecular system, and Q_r is the reactant partition function (per unit volume for a bimolecular reaction). The derivation of the QI expression for the rate constant involves some semiclassically motivated approximations, but the final result is expressed wholly in terms of the quantum Boltzmann operator,

$$k(T) = Q_r^{-1} \frac{\hbar\sqrt{\pi}}{2} \ C_{ff}(0)/\Delta H \tag{4}$$

where $C_{ff}(0)$ is the zero time value of the flux-flux autocorrelation function

$$C_{ff}(0) = tr \left[e^{-\beta\hat{H}/2} \ \hat{F}_1 \ e^{-\beta\hat{H}/2} \ \hat{F}_2 \right] \tag{5}$$

generalized to the case of two different dividing surfaces (the quantum analog of the ends of the instanton periodic orbit), and ΔH is a particular energy variance (very similar to a thermodynamic specific heat). The two dividing surfaces are chosen so that the rate is stationary with respect to their locations; at high temperature (above the so-called 'cross-over' temperature) the two dividing surfaces merge into one.

Figure 1 shows a contour plot of (the negative logarithm of) $C_{ff}(0)$ as a function of the location for the two dividing surfaces for the 3-d version of the D + H_2 reaction, (a) for 200°K where there are two separate dividing surfaces, and (b) for 300°K where they have merged into one. The QI rate constant[5] agrees with the accurate quantum results to better than 10% for T > 200°K. Similar calculations[6] have been carried out for the H + $CH_4 \rightarrow H_2 + CH_3$ reaction. Calculations for both of these reactions (D + H_2 and H + CH_4) were carried out in full Cartesian space, i.e., using three Cartesian coordinates for each atom. The methodology is thus straight-forwardly applicable to essentially any molecular system.
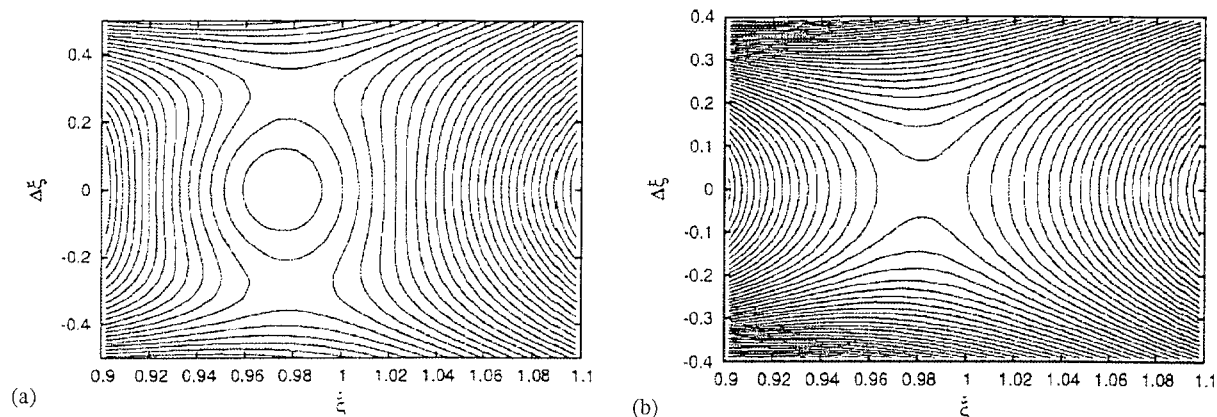
Contour plots of the free energy as a function of two dividing surfaces, for (a) T = 200°K and (b) T = 300°K. The appropriate location of the dividing surface(s) corresponds to a saddle point of this plot.

Future Plans

Further ideas are being explored for improving the quantum instanton approach with regard to its accuracy, generality, and ease of implementation for complex systems. It has already been successfully implemented for the H + CH$_4$ reaction in its full dimensionality, and applications to larger molecular systems are planned.

References

1.   W. H. Miller, J. Chem. Phys. **62**, 1899-1906 (1975).
2.   W. H. Miller, Y. Zhao, M. Ceotto and S. Yang, J. Chem. Phys. **119**, 1329-1342 (2003).
3.   W. H. Miller, J. Chem. Phys. **61**, 1823-1834 (1974).
4.   W. H. Miller, S. D. Schwartz, and J. W. Tromp, J. Chem. Phys. **79**, 4889-4898 (1983).
5.   T. Yamamoto and W. H. Miller, J. Chem. Phys. **120**, 3086-3099 (2004).
6.   Y. Zhao, T. Yamamoto and W. H. Miller, J. Chem. Phys. **120**, 3100-3107 (2004).

2002 - 2004 (to date) DOE Publications

1. W. H. Miller, An Alternate Derivation of the Hermann-Kluk (Coherent State) Semiclassical Initial Value Representation of the Time Evolution Operator, Mol. Phys. **100**, 397-400 (2002). LBNL-47781.

2. V. Guallar, V. S. Batista, W. H. Miller and D. L. Harris, Proton Transfer Dynamics in the Activation of Cytochrome P450eryF, J. Am. Chem. Soc. **124**, 1430-1437 (2002). LBNL-48392.

3. T. Yamamoto, H. Wang, and W. H. Miller, Combining Semiclassical Time Evolution and Quantum Boltzmann Operator to Evaluate Reactive Flux Correlation Function for Thermal Rate Constants of Complex Systems, J. Chem. Phys. **116**, 7335-7349 (2002). LBNL-49465.

4. W. H. Miller, On the Relation between the Semiclassical Initial Value Representation and an Exact Quantum Expansion in Time-Dependent Coherent States, J. Phys. Chem. B **106**, 8132-8135 (2002). LBNL-49606.

5. S. X. Sun and W. H. Miller, Statistical Sampling of Semiclassical Distributions: Calculating Quantum Mechanical Effects Using Metropolis Monte Carlo, J. Chem. Phys. **117**, 5522-5528 (2002). LBNL-51074.

6. Y. Zhao and W. H. Miller, Semiclassical (SC) Initial Value Representation (IVR) for the Boltzmann Operator in Thermal Rate Constants, J. Chem. Phys. **117**, 9605-9610 (2002). LBNL-50669.

7. T. Yamamoto and W. H. Miller, Semiclassical Calculation of Thermal Rate Constants in Full Cartesian Space: The Benchmark Reaction for $D + H_2 \rightarrow DH + H$, J. Chem. Phys. **118**, 2135-2152 (2003). LBNL-51587.

8. V. Guallar, B. F. Gherman, W. H. Miller, S. J. Lippard and R. A. Friesner, "Dynamics of Alkane Hydroxylation at the Non-heme Diiron Center in Methane Monooxygenase," J. Am. Chem. Soc. **124**, 3377-3384 (2002). LBNL-49467

9. W. H. Miller, Y. Zhao, M. Ceotto and S. Yang, "Quantum Instanton Approximation for Thermal Rate Constants of Chemical Reactions," J. Chem. Phys. **119**, 1329-1342 (2003). LBNL-52311.

10. C. Venkataraman and W. H. Miller, "The Quantum Instanton (QI) Model for Chemical Reaction Rates: the 'Simplest' QI with One Dividing Surface," J. Phys. Chem. A (in press). LBNL-53815.

11. T. Yamamoto and W. H. Miller, On the Efficient Path Integral Evaluation of Thermal Rate Constants within the Quantum Instanton Approximation, J. Chem. Phys. **120**, 3086-3099 (2004). LBNL-53821.

12. Y. Zhao, T. Yamamoto and W. H. Miller, Path Integral Calculation of Thermal Rate Constants within the Quantum Instanton Approximation: Application to the $H+CH_4 \rightarrow H_2+CH_3$ Hydrogen Abstraction Reaction in Full Cartesian Space, J. Chem. Phys. **120**, 3100-3107 (2004). LBNL-53881.

13. M. Ceotto and W. H. Miller, Test of the Quantum Instanton Approximation for Thermal Rate Constants for Some Collinear Reactions, J. Chem. Phys. (in press). LBNL-54170.

Unimolecular Reaction Dynamics of Free Radicals

C. Bradley Moore

Department of Chemistry, The Ohio State University

Columbus OH 43210-1106, email: moore.1@osu.edu

1 Program Scope

The fundamental goal of this work is a quantitative understanding of the unimolecular reactions of free radicals. These reactions are of crucial importance in combustion and in atmospheric chemistry. Reliable theoretical models for predicting the rates and products of these reactions are required for modeling combustion and atmospheric chemistry systems. In contrast to the benchmark reactions, $CH_2CO \rightarrow {}^{1,3}CH_2 + CO$, the reactions of free radicals occur over barriers sufficiently low that the hypothesis of rapid energy randomization upon which statistical transition state theories depend is in doubt. A study of the rates and dynamics of methoxy and vinyl radicals in their ground electronic states is in progress:

$$CH_2 = CH \rightarrow HC \equiv CH + H, \qquad \Delta H_0 = 11760 \text{ cm}^{-1} \qquad (1)$$

$$CH_3 - O \rightarrow CH_2 = O + H, \qquad \Delta H_0 = 6950 \text{ cm}^{-1} \qquad (2)$$

These should serve as benchmarks for this important class of reactions. The dissociation of CH_3O has a very low barrier, about 8,400 cm^{-1}. As for many other free radicals, this low barrier results from the simultaneous increase in the bond order of C-O as the C-H bond is broken.

The statistical Transition State Theory (TST), i.e. RRKM and its variants, depends on the basic postulate that complete intramolecular vibrational energy redistribution (IVR) is much faster than the chemical reactions of interest. TSTs give reaction rates that are functions only of total energy and angular momentum. While TSTs are consistent with much experimental data and have gained practical importance for computational modeling of complex reaction systems, some small and moderate size molecular systems, e.g., HCO and HFCO, are observed to decompose at rates that depend systematically on rovibrational quantum numbers. The dissociation of HCO is quantitatively understood in terms of the coupling of modestly perturbed single quantum states to the H+CO continuum. Lower barriers result in limited IVR due to lower vibrational level densities and smaller matrix elements for mode coupling and level mixing at the lower energies.

Methoxy and vinyl will provide benchmark models for unimolecular dynamics in systems that lie between the statistical and single-quantum-state extremes. Other radicals important in combustion and atmospheric chemistry will also be explored.

The experiments use a wide range of time- and wavelength-resolved laser spectroscopies. Radicals are produced by laser flash photolysis of precursors in supersonic jets and then excited to selected rovibronic states by one or more lasers. Products are observed by laser-induced fluorescence and by state-selective, Resonance-Enhanced Multiphoton Ionization (REMPI) with velocity map ion imaging. This allows complete spectroscopic study of the radicals including the intramolecular vibrational couplings revealed in the spectra of highly excited ground electronic state rovibrational energy levels. Decay time and linewidth measurements then give the dissociation rates of well-characterized rovibronic energy levels. Ion imaging and Doppler-resolved REMPI measurements give vector and scalar correlations of the product energy state distributions. Deuterated isotopomers are used in order to excite a single C-H bond along the reaction coordinate.

207

2 Recent Progress

An unambiguous spectroscopic characterization of quantum states, especially in the vicinity of the dissociation threshold, is a prerequisite for the dynamical studies. The rovibrational states of the first excited electronic state of the CHD_2O need to be understood as they will serve as intermediate states from which highly excited rovibrational levels of the ground state will be populated by Stimulated Emission Pumping (SEP). Laser induced fluorescence excitation spectra (LIF), SEP and Dispersed Fluorescence spectra (DF) can then provide an understanding of the levels for dynamical study.

The spectroscopic analysis is quite challenging due to the simultaneous effects of Jahn-Teller and spin-orbit coupling along with breaking of the C_{3v} symmetry in the H/D mixed isotopomers. The spectroscopic studies and analysis are being carried out jointly with Terry Miller's group. A rotational Hamiltonian for fully protonated methoxy, CH_3O, was modified to account for symmetry breaking upon partial deuterium substitution. The asymmetric part of rigid rotor Hamiltonian is accounted for in the (B-C)/2 parameter for both A and E symmetry electronic states. The lifting of vibronic degeneracy (in the absence of spin) was accounted for by the introduction of a ΔE_{xy} constant, which is strictly non-diagonal in the $|\Lambda=+1>$, $\Lambda=-1>$ electronic basis set and reflects the effective splitting caused by the pseudo-Jahn-Teller effect in the CHD_2O/CH_2DO radicals. The adjusted model includes the fully protonated methoxy case for the trivial situation when symmetry perturbation terms (B-C)/2 and ΔE_{xy} are zeros. Despite a very good fit for most of the observed LIF spectra with using this Hamiltonian, the constants generated from fitting the LIF spectrum from the upper spin-orbit component $E_{1/2}$ are considerably different from those used for the description of the LIF transitions from the lower $E_{3/2}$ spin-orbit component. This weakness of the model motivated recording of the pure rotational absorption spectra of the CHD_2O as well as of CH_2DO radicals in the millimeter-wave region to provide a stronger test of the rotational part of the CHD_2O Hamiltonian. The spectra obtained along with the simulated spectra are shown in Figs. 1 and 2. It can be seen, that experimental spectra are reproduced well (Hyperfine splittings are not seen on this scale). Figure 1 shows a large parity splitting for transitions originating from K=0, J=7/2, more than 4 times larger than that observed for K=±1.
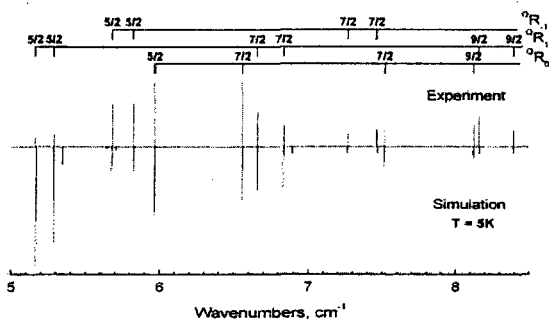
Fig. 1. CHD_2O radical microwave absorption Assignments are in $^{\Delta K}\Delta J_{K''}$ notation.
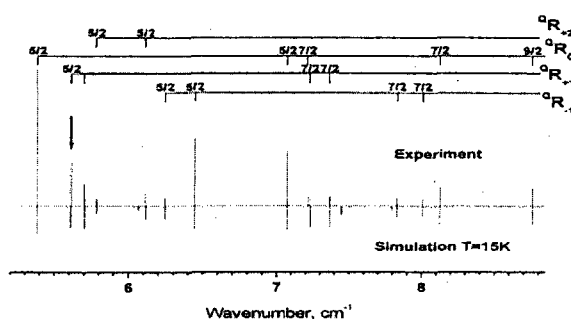
Fig. 2. CH_2DO radical microwave absorption Assignments are in $^{\Delta K}\Delta J_{K''}$ notation.
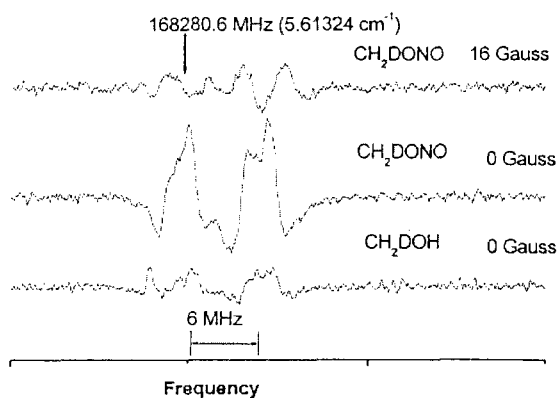
Fig. 3. Hyperfine structure of the CH₂DO line marked by arrow in Fig. 2. Two different precursors and magnetic field were used to discriminate CH₂DO lines from lines of other molecules.
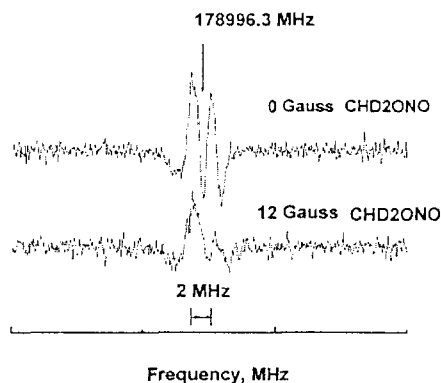
Fig. 4. Hyperfine structure of the CHD₂O line at 178996.3 MHz with and without magnetic field _|_ to detecting microwave beam.

The vibronic structure in the observed DF fluorescence spectra of the CHD_2O radical can not be analyzed in a standard way due to the comparable and large magnitudes of the pseudo-Jahn Teller effect and the spin-orbit interaction. As a first step, the Miller group's[1,2] multimode approach is being applied to DF spectra recorded via excitation of $3^3 5^1$ and $3^3 5^6$ bands of CH_3O; the spectra along with simulated spectra and assignments are shown in Fig. 4 and in Fig. 5, respectively.
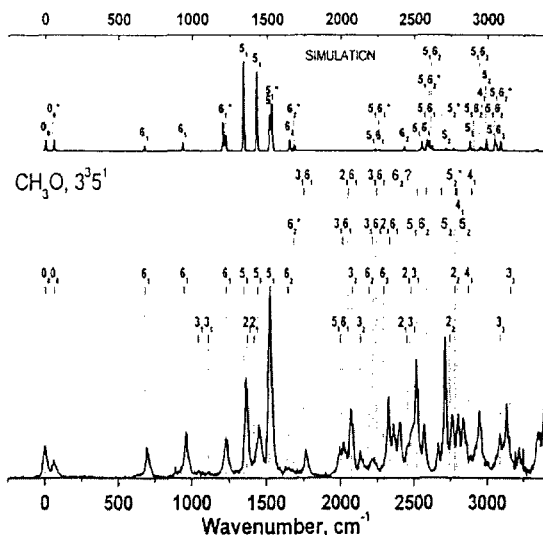
Fig. 4. Dispersed fluorescence spectra obtained via excitation $3^3 5^1$ band of CH_3O.
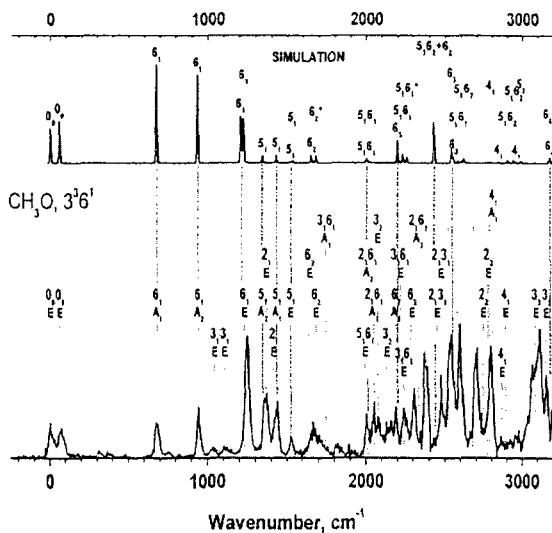
Fig. 5. Dispersed fluorescence spectra obtained via excitation $3^3 6^1$ band of CH_3O.

209

3 Future Plans

The irregular rovibronic level structures evident in spectra of both CHD_2O and CH_2DO methoxy isotopomers will be analyzed using the multimode model. We plan to use both OPO (optical parametric oscillator) and difference frequency laser systems to record fully resolved IR spectra by fluorescence depletion in methoxy isotopomers and by ion imaging vinyl radicals. Levels involving up to three quanta of C-H stretching are of particular interest for dynamical studies as well as for aiding in an analysis of to ground rovibronic state structure. Up to this point, ion imaging in vinyl radical dissociation has been used to reveal the rovibronic structure and dissociation dynamics at energies $6750 - 9150$ cm^{-1} well above the ground state dissociation barrier using the first excited electronic state as an intermediate state from which the electronic energy flows to high vibrational levels of the ground state. Ultimately, infrared excitation schemes should be the most powerful in studying the dissociation dynamics of vinyl radical.

List of Publications

[1] A.M. Mann, X. Chen and V.A. Lozovsky, C.B. Moore, "Dissociation dynamics of the $\tilde{A}\,^2A"$ state of vinyl radical", J. Chem. Phys. <u>118</u>, 4452-4455 (2003).

4 References.

[1]   T. A. Miller, V.E. Bondybey, "The Jahn-Teller Effect in Benzenoid Cations: Theory and experiment" in "Molecular Ions: Spectroscopy, Structure and Chemistry", Ed: T. A. Miller and V. E. Bondybey, North-Holland publishing Company, p. 201, (1983).

[2]   T. A. Barckholtz, T. A. Miller, "Quantitative insights about molecules exhibiting Jahn-Teller and related effects", Int. Rev. Phys. Chem., 17(4), p. 435.

GAS-PHASE MOLECULAR DYNAMICS:
THEORETICAL STUDIES OF REACTION DYNAMICS AND SPECTROSCOPY

James T. Muckerman (muckerma@bnl.gov) and Hua-Gen Yu (hgy@bnl.gov)
Chemistry Department, Brookhaven National Laboratory, Upton, NY 11973-5000

Program Scope

This research is carried out as part of the Gas-Phase Molecular Dynamics group program in the Chemistry Department at Brookhaven National Laboratory. The goal is a theoretical description of the spectroscopy of radical species related to combustion, and the energetics, dynamics and kinetics of elementary chemical reactions in which they are involved.

Recent Progress

Direct dynamics calculations in radical-radical and chemical activation reactions

It is crucial for the success of a direct dynamics method that the electron correlation error in the electronic structure method used be sufficiently constant over the computed potential energy surface to yield accurate energetics. This was a very demanding task in the case of the lowest singlet state of CH_3OH because of the wide variety of possible arrangements of the six atoms. In that study we determined by comparison with features of the accurate potential energy surface for CH_3OH described above that a dual-level direct dynamics method employing a variant of Truhlar *et al.*'s "scaling all correlation" (SAC) method [Gordon & Truhlar, J. Am. Chem. Soc. **108**, 5412 (1986)] is sufficiently accurate for treating the reaction of $O(^1D)$ with CH_4. The method scales the correlation energy from a coupled cluster with double excitations (CCD) calculation by a global constant that also depends on the basis set employed,

$$E_{SAC} = E_{HF} + \frac{E_{CCD} - E_{HF}}{F}$$

where E_{HF} and E_{CCD} are the Hartree-Fock and CCD energies, respectively, obtained using the GAUSSIAN 98 program. The optimum value of the global constant F for the CH_3OH system with the D95(d,p) basis was determined to be 0.78. The RMS deviation of the SAC values from the computed MRCI+Q energies was 0.98 kcal/mol.

The $O(^1D) + CH_4$ reaction at a collision energy of 6.8 kcal/mol was investigated using the SAC method with the CCD/D95(d,p) electronic structure method and basis. A total of 470 trajectories was calculated with a cutoff time of 1 ps, *i.e.*, after 1 ps of simulated time trajectories still trapped in the intermediate CH_3OH complex were stopped and considered to dissociate statistically. The results show that the $O(^1D) + CH_4 \rightarrow OH + CH_3$ reaction occurs both *via* direct and long-lived intermediate reactions. The differential cross section for the direct reaction to form OH is forward peaked with a nearly isotropic background. The branching fractions for OH, H, H_2 and H_2O products (combining direct and complex formation mechanisms) are predicted to be 0.725 : 0.186 : 0.025 : 0.064.

The discovery that an "affordable" electronic structure method, *i.e.*, the SAC/CCD method, can yield sufficiently accurate energies and analytic energy gradients for use in direct dynamics calculations for the $O(^1D) + CH_4$ reaction encourages us to explore its use in other reaction systems of interest. Among these is the allene/propyne system that includes the reactant channels $^1CH_2 + C_2H_2$ and $H + C_3H_3$. Here C_3H_3 is the propargyl radical that is believed to be the precursor of soot in hydrocarbon combustion.

Exploring the multiple reaction pathways for the H + cyc-C_3H_6 reaction

Like the propargyl radical, the allyl radical (C_3H_5) is also an important species in combustion. It can be formed *via* the reaction of H with cyc-C_3H_6. It has long been believed that hydrogen abstraction, H + cyc-

$C_3H_6 \rightarrow H_2 + C_3H_5$, produces allyl through a cyclopropyl ring-opening mechanism, but the Doppler-resolved REMPI experiment of Valentini *et al.* [J. Phys. Chem. A **107**, 8380 (2003)] indicates a surprising channeling of ring-opening energy to the H_2 product that cannot be explained using the hydrogen abstraction mechanism. We plan to search for another possible reaction pathway, and then carry out a direct dynamics study to understand the mysterious behavior of this reaction.

Reaction pathways for the hydrogen atom plus cyclopropane (cyc-C_3H_6) reaction are studied using an extrapolated full coupled-cluster/complete basis set (FCC/CBS) method based on the cc-pVDZ and cc-pVTZ basis sets. For this activated reaction, results reveal two reaction mechanisms, a direct H-abstraction and a H-addition/ring-opening. The hydrogen abstraction reaction yields the H_2 and cyclopropyl (cyc-C_3H_5) radical products. The vibrationally adiabatic ground-state (VAG) barrier height is predicted to be 13.11 kcal/mole. The isomerization barrier height from the product cyclopropyl to allyl radical is 22.53 kcal/mole *via* a cyc-C_3H_5 ring-opening process. In addition, the H-addition and ring-opening mechanism will lead to an n-C_3H_7 radical, which can result in a variety of products such as CH_3 + C_2H_4, H + CH_3CHCH_2 and H_2 + C_3H_5, *etc.* The VAG barrier height of the H-addition reaction is 16.64 kcal/mole, which is slightly higher than that of the direct H-abstraction reaction. Although the H + cyc-$C_3H_6 \rightarrow CH_4 + CH_2CH$ reaction is exoergic by 13.08 kcal/mole, this reaction is unlikely due to a high barrier of 43.2 kcal/mole along the minimum energy path.

Reaction of singlet methylene with H_2

Another carbene reaction of considerable interest is $^1CH_2 + H_2$, which we have found in preliminary CCSD(T)//CCSD calculations to exhibit a conical intersection along the direct C_{2v} reaction path because it is forbidden by orbital symmetry considerations. There does exist, however, a lower symmetry (C_s) reaction path that is energetically favorable.

Future Plans

A direct *ab initio* classical dynamics statistical study of the $^1CH_2 + C_2H_2$ reaction

The $^1CH_2 + C_2H_2 \rightarrow H + C_3H_3$ reaction is one of important combustion reactions because the product propargyl radical (C_3H_3) is believed to be the precursor of soot in hydrocarbon combustion. We plan to carry out a direct *ab initio* molecular dynamics simulation of the reaction using a dual-level SAC approach. In order to avoid propagating a long time trajectory calculation, which results from the long-lived intermediates (cyclopropene, allene and propyne) involved, we will employ a combined dynamics/statistical theory to compute the total reaction probabilities. Such an approach can reveal the dynamics effects on the reaction in contrast to the traditional statistical theory. Generally, the reaction probability from the j channel to the f channel can be expressed as $p_{j \rightarrow f}(E) = p_j^c(E) \frac{p_f^c(E)}{\sum_i p_i^c}$, where the summation runs over all open reactant and product channels. p_j^c is the capture probability in the j channel. This probability can be cheaply calculated for propagating the trajectories for a relatively short time. In addition, the survival probability of the cyclopropene intermediate is going to be investigated as a function of energy.

Theoretical study of the spin-orbital effects on the emission spectrum of HCCl

Recent experiments for the emission spectrum of HCCl from the first excited singlet state show some evidence that several bands belong to the lowest triplet state. Usually, such a transition is not allowed. However, it could happen *via* a spin-orbital interaction between the ground singlet state and the triplet state. In order to explain the observations, we plan to perform an exact variational calculation of the

vibrational states of HCCl including these spin-orbital couplings. The potential energy surfaces and spin-orbital coupling strengths will be calculated using a high level MRCI method.

Converged quantum dynamics calculations of vibrational energies of CH_4 and CH_3D

We have performed exact variational calculations of vibrational energies of CH_4 and CH_3D using a two-layer Lanczos algorithm based on the *ab initio* T8 potential energy surface of Schwenke and Patridge [Spectrochimica Acta **A57**, 887 (2001)]. Well converged vibrational energy levels up to 7000 cm^{-1} from the ground state are reported, together a comparison with experimental results and/or previous theoretical calculations. Our results show that the best previous theoretical calculations have errors as large as 7.5 cm^{-1} for CH_4.

Development of linearly scaled quantum scattering dynamics method

Time-independent quantum scattering theory has the advantage that at a given scattering energy the whole scattering matrix can be obtained directly, *i.e.*, one obtains all state-to-state reaction probabilities in a single calculation. In time-independent scattering calculations, one needs to propagate the wavefunctions from one fixed value of the scattering coordinate to the next (*i.e.*, "sector to sector") from the initial conditions in a set of adiabatic basis functions. Generally, these functions are calculated by directly diagonalizing a matrix in a primitive basis set. Since the direct diagonalization method has a cubic cpu-time scaling with the basis size N, preparing the adiabatic functions becomes the most time-consuming step in the calculations. Also, the matrix needs to be stored in fast memory. These shortcomings severely hamper the extension of the time-independent quantum scattering theory to the study of polyatomic reactions beyond four-atom systems due to the large number (N) of coupled vibrational and rotational states in the problem.

We propose to develop a nearly linearly scaled quantum scattering method by applying the two-layer Lanczos algorithm discussed above to quantum scattering calculations. Basically, the adiabatic functions at each scattering coordinate sector are computed using the two-layer Lanczos algorithm in a DVR or FBR basis set instead of the direct diagonalization method. This is possible because the Hamiltonian matrix in the quantum scattering calculations is similar to that in our spectroscopic studies except for having one fewer degree of freedom that corresponds to the scattering coordinate. As the two-layer Lanczos algorithm consists of the guided spectral transform Lanczos and the standard Lanczos algorithms, it has a nearly linear cpu-time scaling with the basis size N. As a result, the quantum scattering calculations can achieve the same efficiency as the two-layer Lanczos method.

The two-layer Lanczos algorithm will be incorporated with a propagator such as the log-derivative or the smooth variable discretization enhanced renormalized Numerov methods. The $H_2 + CH_3 \rightarrow H + CH_4$ reaction will be employed as the initial example. This is one of the more important radical chain reactions in combustion processes. It has also been the subject of many dynamical studies ranging from the reduced-dimension time-dependent wavepacket and time-independent coupled-channel methods to the 12D multi-configuration time-dependent Hartree approach. Unfortunately, the theoretical thermal rate constants calculated from *ab initio* potential energy surfaces still have large deviations from the experimental results. Consequently, the barrier height for the reverse reaction has been predicted to be about 14.0 kcal/mol but with a relatively large uncertainty of 1.0 kcal/mol. Once the algorithm has been developed and implemented, we can precisely determine the barrier height for this reaction by performing an exact quantum dynamics calculation. Furthermore, as the algorithm is general, it can be applied to other important combustion reactions.

Aside from the calculations of the reaction probability, product distributions, and thermal rate constants of the forward and backward reactions, the vibrational enhancement in the $H + CH_4$ reaction will be

investigated in detail. We will attempt to understand which vibrational mode in methane is the most efficient one for promoting the reaction, and why the effect occurs.

Energetics and dynamics of the reaction of OH with HOCO

In collaboration with J. Francisco (Purdue Univ.), we plan to map out the properties (energies, geometries, vibrational frequencies) of the stationary points on the ground-state singlet potential energy surface for the reaction of OH and HOCO using high-level *ab initio* electronic structure methods. This potential surface includes the product channel $H_2O + CO_2$. Then, in a manner similar to our treatment of the singlet methanol potential surface, we will calibrate the SAC method (probably the SAC/MP2 variant for efficiency in view of the four heavy atoms in the system) to achieve the best fit to the high-level stationary-point calculations. We will then carry out direct dynamics studies of the reaction to elucidate the reaction pathways.

Publications since 2002

1. G. D. Billing, J. T. Muckerman and H.-G. Yu, *Vibrational energy transfer and reactivity in HO + CO collisions.* J. Chem. Phys. **117**, 4755 (2002).
2. K. Kobayashi, G. E. Hall, J. T. Muckerman, T. J. Sears and A. J. Merer, *The $E\,^3\Pi$ - $X\,^3\Delta$ Transition of Jet-Cooled TiO Observed in Absorption.* J. Molec. Spectrosc. **212**, 133 (2002).
3. A. Lin, K. Kobayashi, H.-G. Yu, G. E. Hall, J. T. Muckerman and T. J. Sears, *Axis-Switching and Coriolis Coupling in the A(010) – X(000) Transitions of DCCl and HCCl.* J. Molec. Spectrosc. **214**, 216 (2002).
4. X. Liu, R. L. Gross, G. E. Hall, J. T. Muckerman and A. G. Suits, *Imaging $O(^3P)$ + Alkane Reactions in Crossed Molecular Beams: Vertical vs. Adiabatic H Abstraction Dynamics.* J. Chem. Phys. **117**, 7947 (2002).
5. H.-G. Yu, J. T. Muckerman and T. J. Sears, *A K-dependent Adiabatic Approximation to the Renner-Teller Effect for Triatomic Molecules.* J. Chem. Phys. **116**, 1435 (2002).
6. H.-G. Yu and T. J. Sears, *Vibrational Energy Levels of Methyl Cation.* J. Chem. Phys. **117**, 666 (2002).
7. H.-G. Yu and J. T. Muckerman, *A General Variational Algorithm to Calculate Vibrational Energy Levels of Tetra-atomic Molecules.* J. Molec. Spectrosc. **214**, 11 (2002).
8. H.-G. Yu, *An Exact Variational Method to Calculate Vibrational Energies of Five Atom Molecules Beyond the Normal Mode Approach.* J. Chem. Phys. **117**, 2030 (2002).
9. H.-G. Yu and J. T. Muckerman, *Quantum Dynamics of the Photoinitiated Unimolecular Dissociation of HOCO.* J. Chem. Phys. **117**, 11139 (2002).
10. H.-G. Yu, *Two-Layer Lanczos Iteration Approach to Molecular Spectroscopic Calculation.* J. Chem. Phys. **117**, 8190 (2002).
11. H.-G. Yu, *Accelerating the Calculation of the Rovibrational Energies of Tetraatomic Molecules Using a Two-Layer Lanczos Algorithm.* Chem. Phys. Lett. **365**, 189 (2002).
12. B. Wang, H. Hou, L. Yoder, J. T. Muckerman and C. Fockenberg, *Experimental and Theoretical Investigations on the Methyl-Methyl Recombination Reaction.* J. Phys. Chem. A **107**, 11414 (2003).
13. H.-G. Yu and J. T. Muckerman, *Theoretical Determination of Rovibrational Energies and the Anomalous Isotope Effect of the Weakly Bound Cluster HXeOH.* J. Theor. Comput. Chem. **2**, 573 (2003).
14. H.-G. Yu, *Full-dimensional quantum calculations of vibrational spectra of six-atom molecules. I. Theory and numerical results*, J. Chem. Phys. **120**, 2270 (2004).
15. H. Hou and J. T. Muckerman, *Ab initio Studies of the Metcar Building Blocks TiC_2 and MoC_2.* J. Chem. Phys. (submitted).
16. H.-G. Yu and J.T. Muckerman, *MRCI calculations of the lowest potential energy surface for CH_3OH and direct ab initio dynamics simulations of the $O(^1D)$ + CH_4 reaction*, J. Phys. Chem. A (submitted).
17. H.-G. Yu and J. T. Muckerman, *Exploring the multiple reaction pathways for the H + cyc-C_3H_6 reaction*, J. Phys. Chem. A (submitted).

Acknowledgment

214

Dynamics of Activated Molecules
DE-FG02-03ER15429: September 1, 2003 to October 31, 2006
Amy S. Mullin, Department of Chemistry, Boston University

Introduction

High-energy molecules play important roles in the chemical and physical processes involved in combustion, plasmas and other high temperature non-equilibrium environments, both as reactive species and as energy transporters through collisions. However, understanding the behavior of high-energy molecules poses significant challenges, in part because of their transient nature, the large number of states involved and our lack of knowledge as to how they interact with neighboring species. A highly excited molecule can have several possible fates: decomposition, deactivation or chemical reaction. Each of these processes is influenced by collisions. Molecules with internal energies near the dissociation threshold can be deactivated by collisions, driven to dissociation by collisions or undergo chemical reactions in collisions. Hence, understanding the collisional behavior of high-energy molecules is crucial for understanding and for creating predictive models of high temperature chemical environments. Developing such an understanding is one of the key goals of my research.

The focus of my research program is to investigate the physical and chemical properties of molecules with large amounts of internal energy using novel experimental and theoretical approaches in order to gain new insights into the microscopic details of relatively large, complex molecules. To overcome the inherent difficulties of developing a molecular level understanding of high energy molecules, we employ high resolution transient IR probing to measure energy gain in *small bath molecules* that undergo collisions with highly excited polyatomic molecules, an approach originally developed by George Flynn and coworkers. Using this technique, we have performed in-depth spectroscopic studies that have provided a greater understanding of the behavior of high-energy molecules. Our DOE-funded activities since September 2003 have addressed two outstanding issues regarding the collisional deactivation of highly excited molecules: 1) the role of the energy accepting bath molecule and 2) the role of state density in the hot donor. In the following, I describe our experimental approach and our progress to date.

Transient IR probing of collisional energy transfer

My group has used transient IR absorption probing to investigate the dynamics of strong collisions involving the highly excited azabenzene species shown below. For the studies described here, we have used pulsed 266 nm light to generate highly excited azabenzene molecules with vibrational energies near $E_{vib} \sim 38{,}000$ cm^{-1}, corresponding to vibrational

Pyrazine Pyridine 2-Picoline 2,6-Lutidine
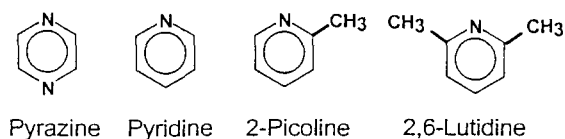
temperatures of 2000-4000 K. This process occurs when azabenzene molecules undergo electronic excitation followed by rapid radiationless decay, to highly vibrationally

215

excited levels of the ground of electronic state. During this funding period, we have investigated collisional energy transfer from the hot molecules to either CO_2 or CH_4 bath molecules using transient high resolution infrared diode laser absorption spectroscopy of the collision products. The remarkable resolution of our IR lasers (0.0003 cm^{-1}) allows us to monitor the vibrational, rotational and translational energies of the scattered CO_2 and CH_4 molecules. IR probing of energy gain in CO_2 was accomplished using CO_2 (00^00, J) $\rightarrow$ CO_2 (00^01, J$\pm$1) transitions at λ=4.3 μm and methane was probed using CH_4 (0000, J) $\rightarrow$ CH_4 (0010, J$\pm$1) transitions at λ=3.1 μm. Experiments were performed at 20 mTorr and the average time between collisions was ~4 μs. Transient absorption signals were collected at t=1 μs following UV excitation, so that population data corresponds to energy transfer essentially from single encounters of the hot donor with CO_2 or CH_4. Information about the nascent translational energy of the scattered molecules was obtained by measuring Doppler-broadened lineprofiles for a number of CO_2 and CH_4 rotational states. In this way, we are able to pluck out state-resolved information about energy transfer of activated molecules, despite the large energy and high state density of the activated molecules.

The role of the energy acceptor in supercollision relaxation

In earlier studies, we have observed in the relaxation of highly excited azabenzene molecules with a series of small bath molecules that some collisions lead to very large releases of energy with ΔE as large as 10,000 cm^{-1}.[1-4] While such supercollision events are rare, they play a significant role in pressure dependent reactive environments and provide insight into the properties of molecules with internal energy near the dissociation limit. The large ΔE values that we observe indicate that supercollision relaxation is often accompanied by vibrational state changes in the hot donor corresponding to multiple quanta transitions. An outstanding question is to what extent the identity of the bath molecule influences supercollision relaxation. To answer this question, we have investigated how strong properties of the energy accepting bath molecule. In previous work, we have used transient IR absorption to monitor energy gain in CO_2, H_2O and DCl following collisions with hot pyrazine (E_{vib}=38,000 cm^{-1}). These studies have revealed a number of important results. For each bath species listed above, donor vibrational energy is transferred into both rotational and translation energy gain of the scattered bath molecules. However, the partitioning of this energy is species dependent. We find the extent to which the transferred energy is partitioned into bath rotation and translation correlates very well with the moment of inertia in the bath molecule, and that mass is a less significant indicator. Furthermore, we find that the recoil velocity of the scattered molecules correlates well with increases in bath rotational angular momentum, as shown here.
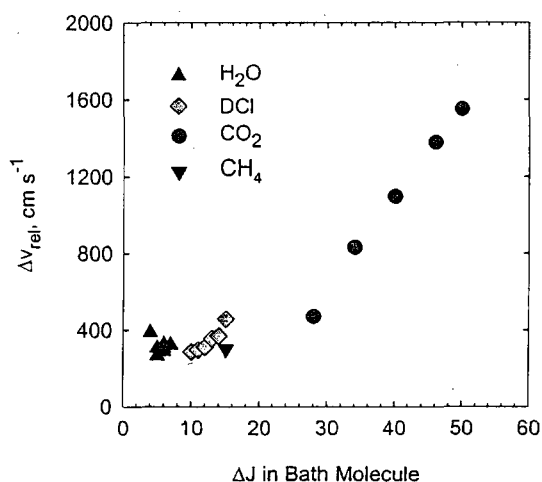
There is evidence from other studies that dipole moments in bath species may lead to enhanced energy transfer. To compare the role of dipole moments and moments of inertia, we are currently studying supercollision relaxation of hot pyrazine with methane. Methane has the same rotational constant as DCl (B=5.43 cm^{-1}), but is nonpolar. Transient Doppler linewidth measurements for CH$_4$ in the J=20 state reveal that CH$_4$ and DCl have very similar kinetic energy distributions in the center of mass frame, supporting the idea that rotational energy spacing in the energy accepting species is key in determining the extent to which the supercollision tail extends to large ΔE values. We are exploring this further by mapping out a more complete distribution of energy transfer profiles.

The role of state density on supercollision relaxation

To investigate what role, if any, state density plays in controlling the shape of the energy transfer distribution function for highly excited molecules, we have investigated the collisional relaxation for a series of highly excited azabenzene molecules of increasing complexity (pyrazine, pyridine, 2-methyl pyridine, 3-methyl pyridine, 4-methyl pyridine and 2,6-dimethyl pyridine) with E$_{vib}$~38600 cm^{-1} in the presence of CO$_2$ or H$_2$O.[5-8] We obtained the high energy component of the nascent energy transfer distribution function P(ΔE) for each hot donor-acceptor pair using state-resolved transient absorption data. The state density ρ(E) for each hot donor molecule and its energy dependence ρ(E-ΔE) were calculated using the Beyer-Swinehart algorithm. We find that both the experimental P(ΔE) curves and the calculated ρ(E-ΔE) curves are well fit using exponential functions. The P(ΔE) data were fit to an exponential function for ΔE=3000-10,000 cm^{-1}, using P(ΔE)=$\alpha_0$exp(-$\beta_0\Delta E$) to obtain an energy transfer shape parameter β_0. The ρ(E-ΔE) data for each hot donor molecule were fit to an exponential function, given by ρ(E-ΔE)=$\alpha_\rho$exp(-$\beta_\rho\Delta E$) to obtain a state density shape parameter β_ρ. The values of β_0 exhibit a linear correlation with β_ρ, as shown here for
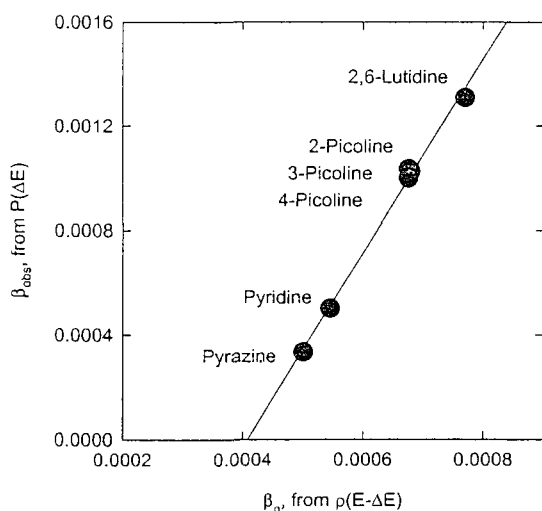
quenching by CO$_2$, revealing how state density influences the shape of the energy transfer distribution function. As the donor complexity increases, its state density becomes a steeper function of ΔE and the probability of energy transfer decreases accordingly. Thus it is the donor state density after a quenching collision has occurred that determines the shape of the energy transfer distribution function. Such a linear correlation between state density and transition probability is evocative of Fermi's Golden Rule which describes transitions between initial states and a continuum (or near continuum) of final states. Typically, collisions cannot be treated by a Golden Rule approach because the interaction energy is large compared to the total energy of the system. However, in the case of highly excited molecules, the internal energy of the hot donor molecules is approximately 100 times greater than the average collision energy and subsequent collisional relaxation may

be well described by a perturbation theory approach. This model also supports earlier results from our lab on the energy-dependence of supercollision relaxation processes.[9-10] We are working to further quantify this correlation using Fermi's Golden Rule and plan to test whether this correlation is valid for molecules with a broader range of donor state densities and molecular structures. In particular, we are interested in exploring how floppiness in the donor molecule influences the relaxation process and its correlation with state density.

References

1. "Supercollision Energy Dependence: State Resolved Energy Transfer in Collisions Between Highly Vibrationally Excited Pyrazine (E_{vib} = 37,900 cm^{-1} and 40,900 cm^{-1}) and CO_2," M. C. Wall and A. S. Mullin, J. Chem. Phys. **108**, 9658-9667 (1998).

2. "State-resolved Studies of Collisional Quenching of Highly Vibrationally Excited Pyrazine by Water: The Case of the Missing V→RT Supercollision Channel," M. Fraelich, M. S. Elioff and A. S. Mullin, J. Phys. Chem. **102**, 9761-9771 (1998).

3. "State-resolved Collisional Relaxation of Highly Vibrationally Excited Pyridine by H_2O: Role of Strong Electrostatic Attraction in V→RT Energy Transfer," M. Fraelich, M. S. Elioff, R L. Sansom and A. S. Mullin, J. Chem. Phys. **111**, 3517-3525 (1999).

4. "Quenching dynamics of highly excited azabenzenes with DCl: The role of the energy acceptor," Z. Li, E. Korobkova, K. Werner,* L. Shum, A. S. Mullin, submitted to Journal of Chemical Physics.

5. "Methylation effects in state resolved quenching of highly vibrationally excited azabenzenes (E_{vib} ~38500 cm^{-1}). I. Collisions with water," Michael S. Elioff, Maosen Fang and Amy S. Mullin, J. Chem. Phys. **115**, 6990-7001 (2001).

6. "Methylation effects in state resolved quenching of highly vibrationally excited azabenzenes (E_{vib} ~38500 cm^{-1}). II. Collisions with carbon dioxide," Jeunghee Park, Lawrence Shum, Andrew Lemoff, Kathryn Werner and Amy S. Mullin, J. Chem. Phys. **117**, 5221-5233 (2002).

7. Erratum: Methylation effects in state resolved quenching of highly vibrationally excited azabenzenes (E_{vib} ~38500 cm^{-1}). I. Collisions with water," Michael S. Elioff, Maosen Fang and Amy S. Mullin, [J. Chem. Phys. **115**, 6990-7001 (2001).] J. Chem. Phys. **117** (2002).

8. "Collisional Quenching of Highly Excited Picoline Isomers with CO_2: Correlations with State Density," Elisa Miller and Amy S. Mullin, manuscript in preparation.*

9. "Observation of an Energy Threshold for Large ΔE Collisional Relaxation of Highly Vibrationally Excited Pyrazine (E_{vib}= 31,000 to 41,000 cm^{-1}) by CO_2," M. S. Elioff, M. C. Wall, A. S. Lemoff and A. S. Mullin, J. Chem. Phys. **110**, 5578-5588 (1999).

10. "Energy dependent quantum state resolved relaxation of highly vibrationally excited pyridine (E_{vib} =36990-40200 cm^{-1}) through collisions with CO_2," Jeunghee Park, Ziman Li, Andrew S. Lemoff, Craig Rossi, Michael S. Elioff and Amy S. Mullin, J. Phys. Chem. A **106**, 3642-3650 (2002).

Reacting Flow Modeling with Detailed Chemical Kinetics

Habib N. Najm

Sandia National Laboratories
7011 East Ave, MS 9051, Livermore, CA 94550
hnnajm@sandia.gov

1 Program Scope

The purpose of this research program is to understand the transient behavior of flames in reacting flow, thereby improving the state of the art in predictive modeling of combustion. The work involves: (1) Using advanced numerics and computational tools to investigate the structure and dynamical behaviour of flames in unsteady vortical laboratory-scale flows; (2) Conducting detailed studies with matched experimental-numerical comparisons to improve understanding of transient flame-flow interaction; (3) Developing advanced techniques for the analysis of, and extraction of information from, multidimensional reacting flow computations; (4) Developing improved numerical methods for discretizing large scale reacting flow systems of equations with detailed kinetics and transport; and (5) Developing efficient massively parallel programming approaches for computing large scale reacting flow with detailed kinetics.

2 Recent Progress

2.1 Uncertainty Quantification (UQ) in Reacting Flow

Our UQ work is motivated by a need to quantify limits of predictability in reacting flow models. Without UQ it is difficult to make rational comparisons between predictions and observations. Particularly, it is not possible to conclude whether disagreements are due to model deficiencies or parametric uncertainties. We have pursued two UQ strategies, one "intrusive", requiring reformulation of the model governing equations, and the other "non-intrusive", allowing the utilization of existing codes as black boxes in a sampling framework. In the following we outline progress in both areas.

2.1.1 Intrusive Spectral Polynomial-Chaos (PC) Reacting Flow UQ

We finalized our implementation of the intrusive Hermite-Gaussian PC-based UQ approach in a one-dimensional (1D) premixed flame model. We demonstrated computations with this approach over short time spans, however the construction exhibited unavoidable instabilities related to the non-linearities in the chemical kinetic model.

We worked on identifying an efficient intrusive UQ construction that would be stable under the non-linearities in chemical system models. These instabilities are a result of fast amplification of uncertainties, and are associated with growth of higher order modes and the development of finite probabilities of unphysical negative temperature and/or concentration values. We evaluated Laguerre polynomials in combination with the (strictly positive) Gamma distribution as the basis for PC expansions, without much success. Both the Hermite-Gaussian and Laguerre-Gamma PC constructions suffer from similar problems with finite probabilities of non-physical values of field variables. In fact, this would be found from any global higher order truncated PC expansion. Instead, we developed a multi-wavelet construction, coupled with an adaptive domain-decomposition approach, that adequately dealt with the chemical non-linearities by using local low order expansions over stochastic space, as opposed to the conventional global expansions. We demonstrated this approach on a homogeneous H_2-O_2 ignition problem at supercritical conditions. This problem could not be stably computed with the global PC expansion approach, but is easily done using the new local construction. Results demonstrated the utility of this new construction for general dynamical systems models, including those with bifurcations, where no global expansion can be used effectively. Moreover, this approach fits easily with the framework we have already established for intrusive UQ.

2.1.2 Non-intrusive Spectral PC Reacting Flow UQ

We used the sampling-based non-intrusive PC approach to conduct further studies of uncertainty quantification in a freely propagating H_2-O_2 flame under supercritical conditions. We investigated UQ predictions based on

higher (3rd) order PC expansions. Results indicated the need for high-order representations in order to capture the solution behavior as the mixture approaches equilibrium in the products region. The convergence of robust integral quantities (e.g. variance) in this region was found to be significantly dependent on incorporating higher-order PC constructions.

2.1.3 Sensitivity Analysis

One key advantage of the spectral polynomial chaos UQ approach is that this representation of uncertainty additionally provides full sensitivity information on the model. We developed a formulation for general high-order stochastic sensitivity analysis, based on the Hermite PC expansions. We applied this to non-intrusive UQ results from both homogeneous ignition and 1D premixed flame computations for H_2-O_2 under supercritical conditions. Results indicate that, in the first-order limit, these coefficients are in agreement with conventional sensitivity coefficients evaluated using the CHEMKIN codes. Including higher order information, however, changes the picture significantly. To begin with, the sensitivity coefficient becomes a stochastic quantity, with a probability distribution from which mean and variance can be easily evaluated. The mean can come close to the first-order results in some cases, although it does exhibit significant ($\sim 50\%$) differences in certain species. This is a result of both high-order information in the dependence of the solution on each parameter, as well as coupling between different parameters. As such, it conveys significant new information about the physics of the problem. Moreover, the variance of the stochastic sensitivity coefficient gives a confidence interval in the sensitivity results. We have observed significant amplitudes of uncertainty in this context, leading to both quantitatively and qualitatively different sensitivity answers. In particular, we have observed such large uncertainties in enthalpic sensitivities in the supercritical H_2-O_2 1D flame context to render the mean sensitivity coefficient prediction practically useless for certain species in the post flame region.

2.2 Computational Reacting Flow Toolkit

We continued to work on the development of a common-component-architecture (CCA) reacting flow code toolkit for enabling multi-D high-order adaptive mesh refinement (AMR) reacting flow computations. We examined the utility of high-order discretizations and interpolants in the AMR context using a reaction-diffusion problem involving H_2-O_2 ignition in 2D. We found clear advantages in terms of net CPU time over low-order discretizations. This is due primarily to the ability to resolve a given flow field with less refined meshes, and hence a shallower refined-mesh hierarchy, with higher-order discretizations. We also examined load balancing and found that the existing load-balancing algorithms in the GrACE AMR mesh framework, based on space-filling-curves, do not adequately balance the spatially-variable per-mesh-cell cost of implicit time integration of the chemical source term. We have identified remedies for this shortfall and are actively pursuing them. We are further in the process of implementing an existing AMR poisson solver from LBNL into the CCA/GrACE framework, which is a necessary step towards a fully-functional momentum solver. We have also formulated a time integration algorithm for the low Mach number momentum equations in the AMR context, and have demonstrated its second-order temporal convergence rate on model problems.

2.3 Computational Singular Perturbation (CSP) Analysis

We have continued to develop CSP analysis tools for multi-D reacting flow analysis. We implemented a singular value decomposition procedure for improving the robustness of the CSP analysis, thereby reducing errors and noise in the analysis results. We used CSP to analyze flame-vortex interactions under large variation in vortex-strength and associated strain-rate disturbances to the flame. Results indicated small changes in the overall features of the analysis results, such as the spatial distribution of exhausted modes and the CSP basis vectors. We have put together a formulation for a CSP-based integrator coupled with an adaptive tabulation strategy (PRISM). The CSP integrator construction follows previous published work, however its coupling with PRISM-tabulation allows its efficient/practical implemenation in realistic computations. The integrator 'filters' the original chemical source term to arrive at a non-stiff source term that can be integrated using an explicit integrator. We demonstrated the use of the stabilized explicit Runge-Kutta-Chebyshev (RKC) integrator operating on the CSP-filtered source term for a model problem with a 10^{15} spectral radius, a substantial stiffness exceeding those in typical atmospheric pressure hydrocarbon kinetics. The construction was shown to maintain accuracy, with substantial gains in efficiency relative to implicit integration of the stiff source term. We also successfully demonstrated non-split time integration

of a reaction-diffusion system using RKC, where the chemical source term was filtered using CSP. This provides a means of using efficient CSP/PRISM integration in a multidimensional reacting flow without operator-splitting.

3 Future Plans

3.1 Flame Studies

We plan to extend our suite of algorithms and codes to allow modeling of low Mach number axisymmetric jet flames. These are useful targets for joint computational-experimental studies for model validation and enhanced understanding of transient flame-flow interactions. In particular, the low speed axisymmetric bunsen flame has been studied extensively, and will be the target of planned experimental measurements under other BES-funded work.

3.2 Uncertainty Quantification

We will move forward with the adaptive domain-decomposition multi-wavelet (ADDMW) construction for UQ. We will complete the evaluation of this technique in the homogeneous ignition context and will proceed towards implementing it in our general intrusive premixed flame code. We will also evaluate the utility of ADDMW in a non-intrusive/sampling context, coupled with a sparse-quadrature, or cubature, approach for evaluation of necessary stochastic integrals. Cubature methods are optimized multi-dimensional quadrature techniques, that have been adequately demonstrated in a range of problems. We expect that coupling ADDMW and cubature will provide a very efficient implementation that will significantly enhance capabilities for sampling-based/non-intrusive UQ studies of flames. We will also begin work on techniques for analysis of experimental data on chemical rate constants in order to arrive at physically-based stochastic representations of uncertain rate constants. We will use Bayesian inference techniques to build suitable prior information in this context, and as a general basis for uncertain model learning and parameter estimation.

3.3 Computational Reacting Flow Toolkit

We will continue development of the CCA AMR low Mach number reacting flow toolkit. We will finalize the implementation of a poisson solver and associated low Mach number momentum solver to enable full reacting flow computations in this framework. We will also pursue a number of developments in load balancing. These will include heuristic predictors of the implicit chemistry time integration costs in each mesh cell, as well as specific redistribution of the (local) chemistry work among processors.

3.4 Computational Singular Perturbation Analysis

We plan to couple CSP analysis/time-integration and PRISM tabulation to arrive at an effective adaptive chemistry tabulation strategy for reacting flow with detailed kinetics. We have already demonstrated explicit RKC time integration of CSP-filtered chemical source terms. To relieve the remaining bottleneck, namely the cost of doing the CSP analysis, the CSP vectors will be tabulated using PRISM. We have seen that the CSP vectors are relatively robust, exhibiting small variability in space outside the primary flame reaction zone. As such, they will enable a somewhat coarse grained discretization of the chemical phase space. Moreover, the effective dimensionality of each hypercube in the table will be the number of active modes, which is much smaller than the full dimensionality of the chemical system over large regions of the flow field. This will reduce the cost of building the necessary response surfaces in each hypercube, and potentially enable efficient tabulation at large dimensionality of the chemical system.

4 DOE-Supported Published/In-Press Publications [2002-2004]

[1] Najm, H.N., and Knio, O.M., Modeling Low Mach Number Reacting Flow with Detailed Chemistry and Transport, *J. Sci. Comp.* (2004) in press.

[2] Pébay, P.P., Najm, H.N., and Pousin, J., A Non-Split Projection Strategy for Low Mach Number Reacting Flows, *Int. J. Multiscale Computational Eng.* (2004) in press.

[3] Debusschere, B.J., Najm, H.N., Pébay, P.P., Knio, O.M., Ghanem, R.G., and Le Maître, O.P., Numerical Challenges in the Use of Polynomial Chaos Representations for Stochastic Processes, *SIAM J. on Sci. Comp.* (2004) in press.

[4] Le Maître, O.P., Ghanem, R.G., Knio, O.M., and Najm, H.N., Uncertainty Propagation using Wiener-Haar Expansions, *J. Comp. Phys.* (2004) in press.

[5] Le Maître, O.P., Najm, H.N., Ghanem, R.G., and Knio, O.M., Multi-Resolution Analysis of Wiener-type Uncertainty Propagation Schemes, *J. Comp. Phys.* (2004) in press.

[6] Matta, A., Knio, O.M., Ghanem, R.G., Chen, C.-H., Santiago, J.G., Debusschere, B., and Najm, H.N., Computational Study of Band Crossing Reactions, *J. MEMS* (2004) in press.

[7] Reagan, M.T., Najm, H.N., Ghanem, R.G., and Knio, O.M., Uncertainty Quantification in Reacting Flow Simulations Through Non-Intrusive Spectral Projection, *Combustion and Flame*, 132:545–555 (2003).

[8] Reagan, M.T., Najm, H.N., Ghanem, R.G., and Knio, O.M., Analysis of Parametric Uncertainty Propagation in Detailed Combustion Chemistry, in *Computational Fluid and Solid Mechanics* (K. Bathe, Ed.), volume 2, Cambridge, MA, (2003), Elsevier Science, , pp. 1501–1505.

[9] Valorani, M., Najm, H.N., and Goussis, D., CSP Analysis of a Transient Flame-Vortex Interaction: Time Scales and Manifolds, *Combustion and Flame*, 134(1-2):35–53 (2003).

[10] Debusschere, B.J., Najm, H.N., Matta, A., Knio, O.M., Ghanem, R.G., and Le Maître, O.P., Protein Labeling Reactions in Electrochemical Microchannel Flow: Numerical Simulation and Uncertainty Propagation, *Phys. Fluids*, 15(8):2238–2250 (2003).

[11] Goussis, D.A., Valorani, M., Creta, F., and Najm, H., Inertial Manifolds with CSP, in *Computational Fluid and Solid Mechanics 2003* (K. Bathe, Ed.), volume 2, Cambridge, MA, (2003), Elsevier Science, , pp. 1951–1954.

[12] Le Maître, O.P., Knio, O.M., Debusschere, B.J., Najm, H.N., and Ghanem, R.G., A Multigrid Solver for Two-Dimensional Stochastic Diffusion Equations, *Comp. Meth. App. Mech. and Eng.*, 192:4723–4744 (2003).

[13] Marzouk, Y.M., Ghoniem, A.F., and Najm, H.N., Toward a Flame Embedding Model for Turbulent Combustion Simulation, *AIAA J.*, 41(4):641–652 (2003).

[14] Najm, H.N., Knio, O.M., and Paul, P.H., Role of Transport Properties in the Transient Response of Premixed Methane-Air Flames, *Proc. Comb. Inst.*, 29:1713–1720 (2002).

[15] Le Maître, O.P., Reagan, M.T., Najm, H.N., Ghanem, R.G., and Knio, O.M., A Stochastic Projection Method for Fluid Flow II. Random Process, *J. Comp. Phys.*, 181:9–44 (2002).

Radical Chemistry and Photochemistry

Daniel M. Neumark
Chemical Sciences Division
Lawrence Berkeley National Laboratory
Berkeley, CA 94720
dan@radon.cchem.berkeley.edu

This research program is aimed at elucidating the photodissociation dynamics and bimolecular chemistry of free radicals and hydrocarbons, with particular emphasis on species that play a role in combustion chemistry. Our experiments yield primary chemistry and photochemistry, bond dissociation energies, heats of formation, and - excited state dynamics. This fundamental information is vital for the development of accurate models of reaction mechanisms in combustion. Although much time and effort has been invested in modeling combustion chemistry, many of the primary processes involved in combustion are poorly understood. As a result, one has a situation where sophisticated kinetics models stand on a weak foundation, because the primary chemistry of the reactions in the models and the thermochemistry of the species involved in these reactions are not known. Examples include the reactions leading to soot formation in flames, and reactions in which NO is produced as a by-product of combustion. Our program is focused on fundamental studies of species and reactions relevant to combustion chemistry. We have developed a state-of-the-art instrument for studying the photodissociation dynamics of free radicals. In addition, a crossed molecular/laser beam instrument is used to investigate the primary chemistry and photochemistry of both closed-shell hydrocarbons and hydrocarbon radicals.

Absolute photoionization cross sections of several hydrocarbon radicals to form $C_3H_5^+$ were measured using tunable VUV synchrotron radiation coupled with photofragment translational spectroscopy. These experiments were carried out on Endstation 1 of the Chemical Dynamics Beamline. At 10 eV, photoionization cross sections for the vinyl and propargyl radicals were determined to be 11.1 ± 2.2 and 8.3 ± 1.6 Mb, respectively. From these values, the photoionization efficiency curves from 7.8-10.8 eV for these radicals were placed on an absolute scale. Similar experiments on allyl and 2-propenyl yielded cross sections of 6.2 ± 1.2 and 5.1 ± 1.0 Mb, respectively, at 10 eV. These results will be very useful when coupled to the flame diagnostics experiments currently in progress at the Beamline.

The photodissociation dynamics of bare I_2^- and $I_2^- \cdot Ar$ at 413 and 390 nm were investigated using our fast beam instrument coupled with a new photofragment coincidence imaging detector. The experiments yielded the dissociation energy of I_2^- ($D_0(I_2^-) = 1.012 \pm 0.008$ eV) and the I_2^--Ar binding energy ($D_0(I_2^-\text{-Ar}) = 45 \pm 8$ meV). The experiments show that $I_2^- \cdot Ar$ undergoes three-body dissociation to $I^- + I^* + Ar$, with very low momentum in the Ar atom and unequal momentum partitioning between the two I atoms.

This instrument was also used to investigate the photodissociation dynamics of I_3^- from 390-290 nm (3.18-4.28 eV) have been investigated using fast beam photofragment translational spectroscopy in which the products are detected and analyzed with coincidence imaging. At photon energies ≤ 3.87 eV, two-body dissociation that generates $I^- + I_2$ (A $^3\Pi_{1u}$) and vibrationally excited I_2^- (X $^2\Sigma_u^+$) + I ($^2P_{3/2}$) is observed, while at energies ≥ 3.87 eV, I* ($^2P_{1/2}$) + I_2^- (X $^2\Sigma_u^+$) is the primary two-body dissociation channel. In addition, three-body dissociation yielding $I^- + 2I$ ($^2P_{3/2}$) photofragments is seen throughout the energy range probed; this is the dominant channel at all but the lowest photon energy. Analysis of the three-body dissociation events indicates that this channel results primarily from a synchronous concerted decay mechanism.

Finally, the photodissociation spectroscopy and dynamics resulting from excitation of the $\tilde{B}$ $^2A''$ $\leftarrow$ $\tilde{X}$ $^2A''$ transition of CH_2CFO have been examined using fast beam photofragment translational spectroscopy. The photofragment yield spectrum revealed vibrationally resolved structure between 29 870 cm^{-1} and 38 800 cm^{-1}, extending ~6000 cm^{-1} higher in energy than previously reported in a laser-induced fluorescence excitation spectrum. At all photon energies investigated, only the CH_2F + CO and HCCO + HF fragment channels are observed. Both product channels yield photofragment translational energy distributions that are characteristic of a decay mechanism with a barrier to dissociation.

The new detection scheme on our fast radical beam photodissociation instrument enables the study of three-body dissociation events and offers enhanced sensitivity to photofragments formed with low translational energy. This latter capability will be exploited in planned studies of the ethoxy and HCNN radical. Preliminary indications are that our previously published claim that ethoxy photodissociates to $C_2H_3 + H_2O$ was incorrect, and that instead OH + C_2H_4 and CH_3 + CH_2O are primary products (another channel, H + CH_3CHO) cannot be detected on this instrument. Studies are currently underway to re-examine the issue of whether dissociation occurs when the $B \leftarrow X$ transition in ethoxy is excited.

Radical photoionization cross section measurements on Endstation 1 will continue, with particular emphasis on measuring cross sections for CH_3 and C_6H_5 radicals produced from the photodissociation at 193 nm of CH_3Cl and C_6H_5Cl. In these experiments, tunable VUV synchrotron radiation is used to photoionize both photofragments, and if the photoionization cross section of one is known, the cross section for the other can be determined by momentum-matching considerations. Once the CH_3 cross section is determined, we plan to measure the HCO cross section via photodissociation of CH_3CO at 308 nm.

Finally, radical photodissociation and crossed beam experiments will be carried out on a crossed molecular beams instrument utilizing electron impact ionization of the scattered products. As part of this program, we will develop molecular beam radical sources via laser photolysis of stable precursor molecules. The bimolecular reaction dynamics experiments will include oxidation reactions of the C_2H_3 and CH radicals. The

CH + N$_2$ reaction is also of particular interest because of its role in the mechanism for prompt NO formation in flames; one of the unifying themes of our program is to characterize of the potential energy surface for this reaction by photodissociation of the HNCN and HCNN radicals and by reactive scattering of CH + N$_2$. While rate constants for many of these reactions have been determined, identification of the primary products and their branching ratios has been challenging, and the proposed dynamics experiments will address this issue directly.

Publications:

R. T. Bise, A. A. Hoops, D.M. Neumark, "Photodissociation and photoisomerization pathways of the HNCN free radical". Chem. Phys. Lett. 114, 9000, (2001).

A. A. Hoops, R. T. Bise, J. R. Gascooke, D. M. Neumark, "State-resolved translation energy distributions for NCO photodissociation". J. Phys. Chem. 114, 9020, (2001).

J. C. Robinson, W. Sun, S. Harris, F. Qi, D. M. Neumark, "Photofragment translational spectroscopy of 1,2-butadiene at 193 nm" J. Chem. Phys. 115, 8359, (2001).
LBNL-49510

J. C. Robinson, S. A. Harris, W. Sun, D. M. Neumark, "Photofragment translational spectroscopy of 1,3-butadiene and 1,3-butadiene-1,1,4,4-d$_4$ at 193nm" Journal of American Chemical Society 124, 1021, (2002).

J. C. Robinson, N. E. Sveum, and D. M. Neumark "Determination of absolute photoionization cross sections for vinyl and propargyl radicals," J. Chem. Phys. 119, 5311 (2003).

A. A. Hoops, J. R. Gascooke, A. E. Faulhaber, K. E. Kautzman, and D. M. Neumark, "Fast beam studies of I$_2^-$ and I$_2^-$·Ar photodissociation," Chem. Phys. Lett. 374, 235 (2003).

J. C. Robinson, N. E. Sveum, and D. M. Neumark "Determination of absolute photoionization cross sections for isomers of C$_3$H$_5$: allyl and 2-propenyl radicals," Chem. Phys. Lett. 383, 601 (2004).

A.A. Hoops, J. R. Gascooke, A. E. Faulhaber, K. E. Kautzman, and D.M.Neumark,"Two- and three-body photodissociation of gas phase I$_3^-$," J. Chem Phys. 120, 7901 (2004).

A. A. Hoops, J. R. Gascooke, K. E. Kautzman, and D. M. Neumark, "Photodissociation spectroscopy and dynamics of the CH$_2$CFO radical," J. Chem. Phys. (in press).

High-Resolution Photoionization and Photoelectron Studies: Determination of Accurate Energetic Database for Combustion Chemistry

C. Y. Ng

Department of Chemistry, University of California at Davis
One Shields Avenue, Davis, California 95616
E-mail Address: cyng@chem.ucdavis.edu

Program Scope: The main goal of this project is to obtain accurate thermochemical data, such as ionization energies (IEs), dissociative photoionization thresholds, bond dissociation energies, and 0 K heats of formation ($\Delta H°_{f0}$'s) for small and medium sizes molecular species and their ions of relevance to combustion chemistry. Accurate thermochemical data determined by high-resolution photoionization and photoelectron studies for selected polyatomic neutrals and their ions are also useful for the development of the next generation of *ab initio* quantum computational procedures.

Recent Progress:

1   J. Liu, M. Hochlaf, and C. Y. Ng, "Pulsed Field Ionization-Photoelectron Bands for CS_2^+ in the Energy Range of 13.2 –17.6 eV: An Experimental and Theoretical Study", *J. Chem. Phys.* **118**, 4487 (2003).

The VUV pulsed field ionization-photoelectron (PFI-PE) spectra for CS_2 have been obtained in the energy range that covers the formation of the $CS_2^+(B^2\Sigma_u^+$ and $C^2\Sigma_g^+)$ states. The simulation of the origin PFI-PE bands yields accurate IE values of 14.4742±0.0005 eV and 16.1883 ± 0.0005 eV for the formation of $CS_2^+(B^2\Sigma_u^+$ and $C^2\Sigma_g^+)$ states, respectively. The PFI-PE bands for $^2\Sigma_u^+(3_0^2$ and $3_0^3)$ that are in near energy resonance with the 0 K thresholds for the formation of $S^+(^4S) + CS(X^1\Sigma^+; v''=0$ and 1) are found to be enhanced. These enhancements are attributed to the prompt dissociation of excited CS_2 in high-n ($n\geq100$) Rydberg states prior to PFI.

2.   W. Chen, J. Liu, and C. Y. Ng, "Vacuum Ultraviolet Pulsed Field Ionization-Photoelectron Study for N_2O^+ in the Energy Range of 16.3-21.0 eV", *J. Phys. Chem.* A**107**, 8086-8091 (2003).

The VUV-PFI-PE spectra for N_2O have been measured in the VUV range that covers the formation of $N_2O^+(A^2\Sigma^+$, $B^2\Pi$, and $C^2\Sigma^+)$. Many vibronic bands, which were not resolved in previous photoelectron studies, are identified. The simulation of the rotational contours resolved in the PFI-PE bands associated with excitation to $N_2O^+(A^2\Sigma^+$, $v_1^+ = 0$-1, $v_2^+ = 0$, and $v_3^+ = 0$-1) has revealed the orbital angular momentum of the outgoing photoelectrons, and yielded IEs for these states.

3.   X.M. Qian, T. Zhang, C. Y. Ng, A. H. Kung, and M. Ahmed, "Two-Color Photoionization Spectroscopy Using Vacuum Ultraviolet Synchrotron Radiation and Infrared Optical Parametric Oscillator Laser Source, *Rev. Sci. Instrum.***74**, 2784-2890 (2003).

The first two-color VUV)-IR photoionization study using high-resolution VUV synchrotron radiation and high-repetition rate IR optical parametric oscillator (OPO) laser source has been demonstrated. The VUV-IR ionization spectrum of Ar has been recorded in the energy region between the ionization thresholds for $Ar^+(^2P_{3/2})$ and $Ar^+(^2P_{1/2})$ to illustrate the feasibility of this scheme as a general approach for high-resolution two-color photoionization studies. The optical resolution of 0.3 cm^{-1} achieved in this study is shown to be limited by the bandwidth of the IR OPO laser and the Doppler width due to the random motion of the Ar sample.

4.   H. K. Woo, K.-C. Lau, J.-P. Zhan, C. Y. Ng, Y.-S. Cheung, and W. K. Li, and P. M. Johnson, "Vacuum Ultraviolet Laser Pulsed Field Ionization-Photoelectron Study of *trans*-Butene", *J. Chem. Phys.***119**, 7789 (2003).

The VUV-PFI-PE spectrum of *trans*-2-butene in the energy range of 73,500-75,850 cm^{-1} has been measured using VUV lasers. The semi-empirical simulation of fine structures resolved in the original PFI-PE band yields a value of 73,624.7±2.0 cm^{-1} for the IE(*trans*-2-butene). The vibrational bands for *trans*-2-butene ion resolved in the PFI-PE spectrum are assigned based on *ab initio* calculations of the vibrational frequencies and Franck-Condon factors (FCFs) for ionization transitions. The PFI-PE spectrum is compared to the recently reported PFI-photoion (PFI-PI) spectrum for *trans*-2-butene. The major difference observed between the PFI-PE and PFI-PI spectra is that the intensities for excited vibrational bands were significantly suppressed or indiscernible in the PFI-PI spectrum, suggesting that the lifetimes for high-*n* Rydberg states associated with these excited vibrational bands were greatly reduced under the conditions used in the PFI-PI study. The conditions used in the PFI-PI study also led to an IE value of about 20 cm^{-1} lower than that obtained in the PFI-PE measurement.

5. X.-M. Qian, A. H. Kung, T. Zhang , K. C. Lau, and C. Y. Ng , "Rovibrational-state selected photoionization of acetylene by the two-color IR + VUV scheme: observation of rotationally resolved Rydberg transitions", *Phys. Rev. Lett.* **91**, 233001 (2003).

We have demonstrated a rovibrational-state-selected photoionization experiment using an IR laser and high-resolution VUV synchrotron radiation. The VUV-photoionization of acetylene [$C_2H_2(X^1\Sigma_g^+;$ $v_3=1$, J' = 8 or 10)] prepared by IR-excitation reveals three strong autoionizing Rydberg series converging to $C_2H_2^+(X^2\Pi_u; v_3^+=1)$ with little ion background interference. Rotational transitions resolved for the Rydberg states provide an estimate of ≈1.8 ps for their lifetimes. This experiment opens the way for state-selective photoionization studies of polyatomic molecules.

6. M. Hochlaf, K.-M. Weitzel, and C. Y. Ng, "Vacuum ultraviolet pulsed field ionization-photoelectron studies of H_2S in the range of 10-17 eV", *J. Chem. Phys.*, accepted.

The VUV-PFI-PE spectra of H_2S have been recorded in the VUV range of 10–17 eV that covers the formation of the $H_2S^+(X^2B_1$, A^2A_1 and B^2B_2) states. This experiment provides evidence that the IE[$H_2S^+(A^2A_1)$] may be 0.12 eV lower than that reported in the previous study. The simulation of rotational structures resolved in PFI-PE bands shows that the formation of $H_2S^+(X^2B_1)$ and $H_2S^+(A^2A_1)$ from photoionization of $H_2S(X^1A_1)$ is dominated by type-C and type-B transitions, respectively. This observation is consistent with predictions of the multichannel quantum defect theory. The PFI-PE measurement has revealed perturbations of the (0,6,0) K^+=3 and (0,6,0) K^+=4 states of $H_2S^+(A^2A_1)$. Interpreting that these perturbations arise from Renner-Teller interactions at energies close to the common barriers to linearity of the $H_2S^+(X^2B_1$ and $A^2A_1)$ states, we have deduced a barrier of 23,209 cm^{-1} for $H_2S^+(X^2B_1)$ and 5,668 cm^{-1} for $H_2S^+(A^2A_1)$.

7. X.-M. Qian, K.-C. Lau, G.-Z. He, C. Y. Ng, and M. Hochlaf, "Vacuum Ultraviolet Pulsed Field Ionization Study of ND_3: Accurate Thermochemistry of the ND_2/ND_2^+ and ND_3/ND_3^+ Systems", *J. Chem. Phys.*, accepted.

The dissociation of energy-selected ND_3^+ to form ND_2^+ + D near its threshold has been investigated using the PFI-PE-photoion coincidence (PFI-PEPICO) method. The breakdown curves for ND_3^+ and ND_2^+ give a value of 15.891±0.001 eV for the 0 K dissociation threshold or appearance energy (AE) for ND_2^+ from ND_3. We have also measured the PFI-PE vibrational bands for ND_3^+(X; v_2^+=0, 1, 2 and 3), revealing partially resolved rotational structures. The simulation of these bands yields precise ionization energies (IEs) for ND_3^+ X(0,v_2^+=0-3,0,0) ← ND_3 X(0,0,0,0). Using the 0 K AE (ND_2^+) and IE(ND_3)=10.200±0.001 eV determined in the present study, together with the known 0 K bond dissociation energy for ND_3 [D_0(D-ND_2) = 4.7126±0.0025 eV], we have determined the $D_0(ND_2^+$-D), IE(ND_2), and 0 K heat of formation for ND_2^+ to be 5.691±0.001 eV, 11.1784±0.0025 eV and 1261.82±0.4 kJ/mol, respectively. The PFI-PE spectrum is found to exhibit a step-like feature near the AE(ND_2^+), indicating that the dissociation of excited ND_3^+ at energies slightly above the dissociation threshold occurs in ≤ 10^{-7} s, as observed for the NH_3 system. The available energetic data for the NH_2/NH_2^+ and NH_3/NH_3^+ system are found to be in excellent accord with those for the

ND_2/ND_2^+ and ND_3/ND_3^+ system after taking into account the zero point vibrational energy corrections. This finding indicates that the energetic data for these two systems are reliable with well-founded error limits.

8. H. K. Woo, P. Wang, K.-C. Lau, X. Xing, and C. Y. Ng, "Single-photon VUV laser pulsed field ionization-photoelectron studies of *trans-* and *cis*-1-bromopropenes", J. Chem. Phys., accepted.

The VUV-PFI-PE spectra of *trans-/cis*-1-bromopropenes have been measured in the VUV region of 74,720–76,840 cm^{-1}. The simulation of fine structures observed in the origin PFI-PE vibrational bands of these molecules has provided the IE(*trans*-1-bromopropene)= 9.2715±0.0002 eV and IE(*cis*-1-bromopropene)=9.3162±0.0002 eV. The vibrational bands resolved in these VUV-PFI-PE spectra of *trans-/cis*-1-bromopropenes have been assigned based on theoretical vibrational frequencies and calculated Franck-Condon factors for the ionization transitions.

Future Plans:

In collaboration with the group of Branco Russic at Argonne, we are making excellent progress in the photoionization studies of radicals at the Chemical Dynamics Beamline of the Advanced Light Source (ALS). Using an excimer laser photodissociation radical source, we have produced and successfully obtained the PIE spectra for a series of radicals, including methyl radicals (CH_3), vinyl radicals (C_2H_3), propargyl radicals (C_3H_3), and chlorocarbonyl radicals (ClCO), and phenyl radicals (C_6H_5). Reliable IEs have been obtained for these radicals. The measured PIE spectra for photofragments also provide valuable information on their internal energy contents acquired in the photodissociation processes. We are currently learning how to perform PFI-PE measurements on these radicals using the VUV laser PFI apparatus established in our laboratory. The PFI-PEPICO scheme established at the ALS is unique in the World for accurate 0 K AE measurements. We plan to continue with the PFI-PECO experiments at the ALS on combustion relevant molecular species.

Publications of DOE sponsored research (2002-present)

1. X.-M. Qian, Y. Song, K.-C. Lau, C. Y. Ng, J. Liu, W. Chen, and G.-Z. He, "A Pulsed Field Ionization Study of the Reaction $D_2O + h\nu \rightarrow OD^+ + D + e^-$", *Chem. Phys. Lett.* **353**, 19-26 (2002).

2. Branko Ruscic, Albert F. Wagner, Lawrence B. Harding, Robert L. Asher, David Feller, Kirk A. Peterson, Y. Song, X.-M. Qian, C.Y. Ng, J. Liu, and W. Chen, "On the Enthalpy of Formation of Hydroxyl Radical and Gas-Phase Dissociation energies of Water and Hydroxyl", *J. Phys. Chem.* **A106**, 2727-2747 (2002).

3. C. Y. Ng, "Vacuum Ultraviolet Spectroscopy and Chemistry Using Photoionization and Photoelectron Methods", *Ann. Rev. Phys. Chem.* **53**, 101-140 (2002).

4. W. Chen, M. Hochlaf, P. Rosmus, G.-Z. He, and C. Y. Ng, "Vacuum Ultraviolet Pulsed Field Ionization Photoelectron Study of OCS in the Energy range of 15.0-19.0 eV", *J. Chem. Phys.* **116**, 5612 (2002).

5. H. K. Woo, J.-P. Zhan, K.-C. Lau, C. Y. Ng, and Y.-S. Cheung, "Vacuum Ultraviolet Laser Pulsed Field Ionization Photoelectron Study of cis-2-Butene", *J. Chem. Phys.* **116**, 8803 (2002).

6. C. Y. Ng, "State-Selected and State-to-State Ion-Molecule Reaction Dynamics", *J. Phys. Chem. (Invited Feature Article)*, **A106**, 5952-5966 (2002).

7. Y.-J. Chen, P. T. Fenn, K.-C. Lau, C. Y. Ng, C.-K. Law, and W.-K. Li, "A Study of the Dissociation of $CH_3SCH_3^+$ by Collisional Activation: Evidence of Non-Statistical Behavior", *J. Phys. Chem.* **A106**, 9729 (2002).

8. Y.-S. Cheung, C. Y. Ng, S.-W. Chiu, and W.-K. Li, "Application of Three-Center-Four-Electron Bonding for Structural and Stability Predictions of Main Group Hypervalent Molecules: The Fulfillment of Octet Shell Rule", *J. Mol. Struct., Theochem.* **623**, 1-10 (2003).

9. J. Liu, W. Chen, M. Hochlaf, X.-M. Qian, C. Chang, and C. Y. Ng, "Unimolecular Decay Pathways of State-Selected CO_2^+ in the Internal Energy Range of 5.2-6.2 eV: An Experimental and Theoretical Study", *J. Chem. Phys.* **118**, 149 (2003).

10. X. M. Qian, T. Zhang, Y. Chiu, D. J. Levandier, J. S, Miller, R. A. Dressler, and C. Y. Ng,, "Rovibrational State-Selected Study of $H_2^+(X, v^+=0-17, N^+=1)+Ar$ Using the Pulsed Field Ionization-Photoelectron-Secondary Ion Coincidence Scheme", *J. Chem. Phys. (communication)*, **118**, 2455 (2003).

11. J. Liu, M. Hochlaf, and C. Y. Ng, "Pulsed Field Ionization-Photoelectron Bands for CS_2^+ in the Energy Range of 13.2 −17.6 eV: An Experimental and Theoretical Study", *J. Chem. Phys.* **118**, 4487 (2003).

12. Wenwu Chen, Jianbo Liu, and C. Y. Ng, "Vacuum Ultraviolet Pulsed Field Ionization-Photoelectron Study for N_2O^+ in the Energy Range of 16.3-21.0 eV", *J. Phys. Chem.* A**107**, 8086-8091 (2003).

13. X.M. Qian, T. Zhang, C. Y. Ng, A. H. Kung, and M. Ahmed, "Two-Color Photoionization Spectroscopy Using Vacuum Ultraviolet Synchrotron Radiation and Infrared Optical Parametric Oscillator Laser Source, *Rev. Sci. Instrum.* **74**, 2784-2890 (2003).

14. X.-M. Qian, T. Zhang, C. Chang, P. Wang, C. Y. Ng, Y.-H. Chiu, D. J. Levandier, J. S. Miller, R. A. Dressler, T. Baer, and D. S. Peterka, "High-Resolution State-Selected Ion-Molecule Reaction Studies Using Pulsed Field Ionization Photoelectron-Secondary Ion Coincidence Method", *Rev. Sci. Instrum.* **74**, 4096-4109 (2003).

15. H. K. Woo, K.-C. Lau, J.-P. Zhan, C. Y. Ng, Y.-S. Cheung, and W. K. Li, and P. M. Johnson, "Vacuum Ultraviolet Laser Pulsed Field Ionization-Photoelectron Study of *trans*-Butene", *J. Chem. Phys.* **119**, 7789 (2003).

16. X.-M. Qian, A. H. Kung, T. Zhang , K. C. Lau, and C. Y. Ng , "Rovibrational-state selected photoionization of acetylene by the two-color IR + VUV scheme: observation of rotationally resolved Rydberg transitions", *Phys. Rev. Lett.* **91**, 233001 (2003).

17. X.-M. Qian, T. Zhang, X. N. Tang, C. Y. Ng, Y. Chiu, D. J. Levandier, J. S. Miller, and R. A. Dressler, "A state-selected study of the $H_2^+(X, v^+=0-17)$ + Ne proton transfer reaction using the pulsed field ionization-photoelectron-secondary ion coincidence scheme", *J. Chem. Phys.* **119**, 10175-10184 (2003).

18. H. K. Woo, P. Wang, K.-C. Lau, X. Xing, C. Chang, and C. Y. Ng, "State-selected and State-to-State Photoionization Study of trichloroethene Using the two-Color Infrared-Vacuum Ultraviolet Scheme", *J. Chem. Phys. (communication)*, **119**, 9333-9336 (2003).

19. H. K. Woo, P. Wang, K. C. Lau, X. Xing, and C. Y. Ng, "Vacuum Ultraviolet-Infrared Photo-Induced Rydberg Ionization Spectroscopy: C-H stretching frequencies for trans-2-butene and trichloroethene cations", *J. Chem. Phys.* **120**, 1756 (2004).

20. M. Hochlaf, K.-M. Weitzel and C. Y. Ng, "Vacuum ultraviolet pulsed field ionization-photoelectron studies of H_2S in the range of 10-17 eV", *J. Chem. Phys.*, accepted.

21. X.-M. Qian, K.-C. Lau, G.-Z. He, C. Y. Ng, and M. Hochlaf, "Vacuum Ultraviolet Pulsed Field Ionization Study of ND_3: Accurate Thermochemistry of the ND_2/ND_2^+ and ND_3/ND_3^+ Systems", *J. Chem. Phys.*, accepted.

22. H. K. Woo, P. Wang, K.-C. Lau, X. Xing, and C. Y. Ng, "Single-photon vacuum ultraviolet laser pulsed field ionization-photoelectron studies of *trans*- and *cis*-1-bromopropenes", *J. Chem. Phys.*, accepted.

KINETICS AND DYNAMICS OF COMBUSTION CHEMISTRY

David L. Osborn
Combustion Research Facility, Mail Stop 9055
Sandia National Laboratories
Livermore, CA 94551-0969
Telephone: (925) 294-4622
Email: dlosbor@sandia.gov

PROGRAM SCOPE

The goal of this program is to elucidate mechanisms of elementary combustion reactions through the use of broadband and ultrasensitive spectroscopy. Several techniques are employed. First, time-resolved Fourier transform spectroscopy (TR-FTS) is used to probe multiple reactants and products with broad spectral coverage (> 1000 cm^{-1}), moderate spectral resolution (0.1 cm^{-1}) and a wide range of temporal resolution (ns – ms). The inherently multiplexed nature of TR-FTS makes it possible to simultaneously measure product branching ratios, internal energy distributions, energy transfer, and spectroscopy of radical intermediates. Together with total rate coefficients, this additional information provides further constraints upon and insights into the potential energy surfaces that control chemical reactivity. Because of its broadband nature, the TR-FTS technique provides a global view of chemical reactions and energy transfer processes that would be difficult to achieve with narrow-band laser-based detection techniques.

Second, cavity-enhanced frequency modulation spectroscopy (a.k.a. NICE-OHMS) is used to provide an ultrasensitive, differential absorption spectroscopic probe. We have measured a time-resolved, transient absorption spectrum of the NH_2 radical using this technique, which opens the door to measurements of chemical kinetics in flow cells and monitoring of species in flames. This cavity-enhanced FM spectroscopy technique provides very high sensitivity, the generality of absorption spectroscopy, and insensitivity to background absorptions that vary slowly with frequency. These advantages allow the suppression of secondary chemistry by increased dilution of reactive species while still retaining sufficient detection sensitivity.

Finally, a new apparatus utilizing photoionization mass spectroscopy for the study of chemical kinetics is under construction at the Advanced Light Source. The asset of widely-tunable VUV photons for photoionization promises isomer-specific product detection.

RECENT PROGRESS

The mechanism of the HCCO + O$_2$ reaction: Probing multiple pathways to a single product channel

Acetylene is a ubiquitous species present in the combustion of aliphatic and aromatic hydrocarbons.[1] Acetylene is oxidized in flames exclusively by oxygen atoms:

$$O + C_2H_2 \quad \rightarrow \quad {}^3CH_2 + CO \qquad \Delta H_{rxn} = -47.9 \text{ kcal/mol} \qquad (1a)$$
$$\rightarrow \quad HCCO + H \qquad \Delta H_{rxn} = -19.6 \text{ kcal/mol} \qquad (1b),$$
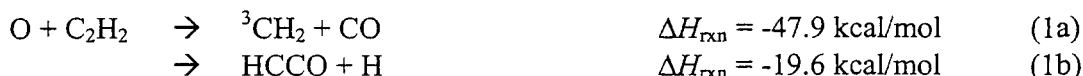
where reaction (1b), producing HCCO, is the dominant product channel. In lean flames, the ketenyl radical (HCCO) reacts primarily with O$_2$, leading to the following possible channels:

$$\text{HCCO} + \text{O}_2 \rightarrow \quad \text{H} + \text{CO} + \text{CO}_2 \qquad \Delta H_{\text{rxn}} = -110.4 \text{ kcal/mol} \qquad (3\text{a})$$
$$\rightarrow \quad \text{OH} + \text{CO} + \text{CO} \qquad \Delta H_{\text{rxn}} = -86.0 \text{ kcal/mol} \qquad (3\text{b})$$
$$\rightarrow \quad \text{OCHCO} + \text{O} \qquad \Delta H_{\text{rxn}} = -1.3 \text{ kcal/mol} \qquad (3\text{c}).$$

In 2002, we applied emission-based TR-FTS to measure the branching ratio and state distributions of reaction (3). These experiments demonstrated that channel (3a), yielding H + CO + CO_2, represents at least 90% of the products at 300K, in agreement with theoretical predictions.[2] This work provides experimental evidence that the genesis of prompt CO_2[3] lies in the single reaction HCCO + O_2. Recently we have delved further into this reaction's mechanism.

In a chemical reaction, each product branching ratio is typically interpreted as a measurement of the flux through one exit channel of that reaction. However, it is possible that two energetically feasible paths on the potential energy surface (PES) lead to a single product channel. The potential energy surface for HCCO + O_2 provides several distinct, energetically feasible pathways leading to H + CO + CO_2, as shown in Fig. 1. Following the addition of O_2 to ketenyl at the methylidyne carbon, formation of a 4-membered or 3-membered ring intermediate is possible. The direct dynamics classical trajectory calculations of Klippenstein, Miller, and

Figure 1: Potential energy diagram (including zero-point energy) of HCCO + $^{18}\text{O}_2$

231

Harding predict flux through both pathways. Experimentally, it is not easy to make such a determination, since the products are H + CO + CO_2 in either case. We have used isotopic labeling combined with state-specific product detection to answer this question.

In the $HCC^{16}O$ + $^{18}O_2$ reaction, all the possible isotopomers of the products are distinguishable using rotationally-resolved infrared spectroscopy. The dominant isotopic products are $C^{18}O$ and $^{16}OC^{18}O$. Combined with data from the corresponding reaction in natural isotopic abundance, these results show that at least 85% of the reactive flux passes through the four-membered OCCO ring intermediate. The three-membered COO ring intermediate represents less than 15% of the total reactive flux. Furthermore, H atom transfer during decomposition of the four-membered ring intermediate is at most a minor process. These results demonstrate the possible dangers in the common assumption that each observed product channel in a reaction arises from a single pathway on the potential energy surface.

The time-resolved FTIR spectra also show that CO and CO_2 are formed highly vibrationally excited, and can be roughly described by vibrational temperatures of 9050 ± 1400 K and 6100 ± 700 K respectively. The average vibrational energy deposited in CO and CO_2 is reasonably well predicted by the Separate Statistical Ensembles method, implying that statistical rather than dynamical effects dominate this reaction mechanism.

Time-resolved, ultrasensitive cavity-enhanced frequency modulation spectroscopy

We have built an ultra-sensitive laser absorption spectrometer based on the Noise Immune Cavity Enhanced Optical Heterodyne Molecular Spectroscopy technique (NICE-OHMS) developed by Ye, Hall and coworkers.[4] This technique utilizes frequency modulation (FM) spectroscopy to reduce sources of technical noise, coupled with a high-finesse sample cavity to provide long absorption pathlengths. An amplitude and frequency-stabilized cw laser (Ti:Sapphire) is locked to a stable high finesse cavity and frequency modulated at 541 MHz, a value equal to the free spectral range (FSR) of the cavity. The carrier and sidebands are detected in transmission, and the heterodyne signal arising from molecular absorption is demodulated at 541 MHz to give the NICE-OHMS signal.

We have made the first observation of the extremely weak (7 ← 0) vibrational overtone of NO near 796 nm. Although NICE-OHMS is a differential technique, we can calibrate the spectrometer response to enable measurement of absolute absorption cross sections. For this overtone we measure a transition dipole moment $|\mu_{70}| = 4.5$ x 10^{-6} Debye and the associated Herman-Wallis factor. The minimum detectable absorption is currently 8 x 10^{-11} cm^{-1} $Hz^{-1/2}$.

We have recently observed a time-resolved, transient absorption of the NH_2 radical on the $\tilde{X}$ ($^2B_1$) (170 ← 000) overtone. NH_2 is produced from photolysis of NH_3. While the results are preliminary, this experiment shows that the abrupt change in optical path length caused by photolysis does not disturb the lock between the laser and the high-finesse cavity. The robustness of this lock loop is critical to the study of chemical kinetics using this technique.

Future Directions

Using TR-FTS, we will investigate reactions of the vinyl (C_2H_3) and propargyl (C_3H_3) radicals to determine product channel identities and energy disposal. We will continue development of transient NICE-OHMS measurements for chemical kinetics. In addition, we hope to apply this cavity enhanced FM technique to measurements in low-pressure flames, which display low-level, broad background absorption of ~ 1 ppm. Because NICE-OHMS is a

differential technique, it will be insensitive to absorptions that change negligibly on the scale of the modulation frequency.

A major new effort involves construction of a photoionization mass spectrometry (PIMS) apparatus coupled to a flow tube reactor for chemical kinetics measurements. This experiment will operate at the Chemical Dynamics Beamline of the Advanced Light Source (ALS) at Lawrence Berkeley National Laboratory. While the study of chemical kinetics using PIMS is well-established,[5] this apparatus will have two unique features that should make it especially powerful for chemical kinetics. First, the widely tunable, intense VUV radiation from the ALS will allow isomer-specific ionization of product species. For example, the ability to distinguish allene from propyne (C_3H_4 isomers) and vinyl alcohol from acetaldehyde (C_2H_4O isomers) has already been demonstrated in the ALS low-pressure flame chamber.[6]

The second unusual feature of this experiment is the mass spectrometer. We will employ a small magnetic sector instrument coupled to a time- and position-sensitive, single-ion counting detector. The exit slit of the magnetic sector will be removed so that a range of masses may be detected simultaneously. This approach creates a mass spectrometer with 100% duty cycle (like a quadrupole instrument) and the multiplex advantage of measuring a broad range of masses simultaneously (as in time-of-flight spectroscopy), while retaining the sensitivity to count single ions at very high count rates.

One interesting problem to explore using this instrument is the reaction $C_3H_3 + C_2H_2$. Previous work by Knyazev and Slagle[7] has shown that the initial product (C_5H_5) can react with excess acetylene to form C_7H_7. This process continues to form C_9H_8 and perhaps larger species. Measuring the isomeric forms of these products using the ALS-PIMS apparatus will provide critical information to the reaction mechanism for this molecular weight growth process.

BES sponsored publications, 2002 - present

"On the mechanism of the HCCO + O_2 reaction: Probing multiple pathways to a single product channel," P. Zou and D. L. Osborn, Physical Chemistry Chemical Physics **6**, 1697 (2004).

"Photodissociation dynamics of dicyclopropyl ketone at 193 nm: isomerization of the cyclopropyl ligand," S. M. Clegg, B. F. Parsons, S. J. Klippenstein, and D. L. Osborn, Journal of Chemical Physics **119**, 7222 (2003).

"Cavity-enhanced Frequency Modulation Absorption Spectroscopy of the Sixth Overtone Band of Nitric Oxide," J. Bood, A. McIlroy, and D. L. Osborn, *Proc. SPIE* **4962,** 89 (2003).

"The reaction of HCCO + O_2: experimental evidence of prompt CO_2 by time-resolved Fourier transform spectroscopy," D. L. Osborn, Journal of Physical Chemistry A **107**, 3728 (2003).

References

[1] H. Gg. Wagner, *Proc. Comb. Inst.* **17**, 3 (1979).
[2] S. J. Klippenstein, J. A. Miller, and L. B. Harding, *Proc. Comb. Inst.* **29**, 1209 (2002).
[3] G.P. Glass, G.B. Kistiakowsky, J.V. Michael and H. Niki, *Proc. Combust. Inst.* **10**, 513 (1964).
[4] J. Ye, L. S. Ma, and J. L. Hall, *J. Opt. Soc. Am. B* **15**, 6 (1998).
[5] I. R. Slagle and D. Gutman, J. Am. Chem. Soc. **107**, 5342 (1985).
[6] T. A. Cool, K. Nakajima, T. A. Mostefaoui, F. Qi, A. McIlroy, P. R. Westmoreland, M. E. Law, L. Poisson, D. S. Peterka, and M. Ahmed *J. Chem. Phys.* **22**, 8356 (2003).
[7] V. D. Knyazev and I. R. Slagle, *J. Phys. Chem. A* **106**, 5613 (2002).

The Effect of Large Amplitude Motion on the Vibrational Level Structure and Dynamics of Internal Rotor Molecules

David S. Perry, Principal Investigator
Department of Chemistry, University of Akron,
Akron OH 44325-3601
DPerry@UAkron.edu

Introduction

In the presence of large amplitude motion, a molecular system no longer remains close to a well-defined reference geometry, which challenges the concepts of the traditional theory of molecular vibrations. Among the challenged concepts are normal modes and point group symmetry. The large amplitude coordinate may take on the character of a reaction coordinate along which one must continuously redefine the remaining "normal" coordinates. The consequences are that large amplitude motion can result in novel energy level structures and it can promote coupling between vibrations and hence accelerate IVR.

In this project, we examine the vibrational level structure of molecules with a single internal rotor including methanol, nitromethane, and methylamine. Vibrational fundamental and overtone spectra of the jet-cooled molecules are examined by cavity ringdown, FTIR spectroscopy, and photodissociation spectroscopy (IRLAPS). The ringdown experiments are done in our lab in Akron; the jet-FTIR is done in collaboration with Robert Sams at Pacific Northwest Labs (PNNL); the IRLAPS experiments are done in Thomas Rizzo's lab at the EPFL in Switzerland. To understand the level structures and vibrational mode coupling taking place, we analyze high resolution spectra, develop quantum mechanical models of the nuclear motion, and probe the potential surface with *ab initio* calculations. Recent progress on several activities under this project is outlined below.

A. Inverted Torsional Tunneling in Methanol and Tests of the Vibrational Born-Oppenheimer Approximation

In previous work under this project,[1] we discovered the inverted torsional tunneling splitting in the asymmetric CH stretch vibrational states ($v_2=1$ and $v_9=1$). These results were successfully explained by our 4-dimensional model calculation that included the three CH stretch coordinates and the torsion.[2] Torsional motion interchanges the identities of the CH bonds *anti* and *gauche* to the OH, and the CH bonds in these positions have different force constants. A single lowest-order coupling term with the required symmetry (A_1 in G_6) was sufficient to reproduce the observed torsional structure. We concluded from that study, that the inverted torsional structure was a general phenomenon that derives from molecular symmetry and that the single coupling term results in a myriad of mixed vibrational states throughout the CH stretch-torsion manifold.

Subsequent spectroscopic reports[3] of other asymmetric vibrations have confirmed the generality of the effect, and a number of theoretical studies[4] have contributed to our understanding. Most recently, Fehrensen, Luckhaus, Quack, Willeke, and Rizzo[5] have used *ab*

initio calculations, an adiabatic (Born-Oppenheimer-like) separation of the torsion from the other vibrations, and the concept of geometric phase to account for the torsional structure of excited methanol vibrational states. This insightful treatment gives an appealing conceptual unity with electronic spectroscopy and provides a criterion for when such inverted torsional structure should be expected.

It is difficult to test the range of applicability and accuracy of the Born Oppenheimer approximation because the relevant full-dimensional calculations needed as a reference are often intractable. In this vibrational case, our 4-dimensional model calculation is the reference calculation needed and therefore we have the opportunity to evaluate the Born-Oppenheimer separation of the torsion from the three CH stretches.

In addition to testing the validity of the adiabatic separation of the torsion from the other vibrations, we are exploring the role of geometric phase and the extent of nonadiabatic effects. We find that the adiabatic approach provides a qualitatively correct but not exact level structure. Nonadiabatic effects are found to be substantial as evidenced by large off-diagonal matrix elements in the adiabatic representation and eigenfunctions that are substantially mixed relative to the adiabatic basis. Furthermore, the exact treatment shows a transition from a pair of C_s-like vibrations, ν_2 and ν_9, at low torsional excitation to a level structure characteristic of a single C_{3v}-like degenerate asymmetric CH stretch at high torsional excitation. This change in the nature of the vibrational motion is not captured in the adiabatic treatment. The scaling of IVR coupling matrix elements in this large amplitude system is revealed by the calculation and can be compared to the prediction by Pearman and Gruebele.

B. Slit-Jet Cavity-Ringdown Spectra of Methanol and Propyne

The rotationally resolved overtone spectrum of the OH (ν_1) + CH (ν_3) stretch combination band of methanol between 6510 and 6550 cm^{-1} has been recorded at sub-Doppler resolution using continuous-wave cavity ringdown spectroscopy (CW-CRDS). The experimental sensitivity has been shown to be close to the theoretical shot noise limit. Of 572 recorded lines, 358 lines have been assigned by ground state combination differences, including the 21 subbands with J' up to 8 and K' up to 3. Perturbations of A K' =2 and E K' = -1, -2, and -3 levels have been observed and deperturbations carried out. The torsion-rotation constants in the upper state have been obtained by fitting the observed spectrum to the Herbst Hamiltonian and they are found to be in a reasonable agreement with the extrapolated values based on the fundamental bands, ν_1 and ν_3. This combination band has fewer perturbations than the ν_1 fundamental and the coupling matrix elements are smaller, 0.02 to 0.66 cm^{-1} as compared to 0.35 to 1.6 cm^{-1}. Consistent with our previous results on the $2\nu_1$ and $3\nu_1$ overtones, we find that these low overtones and combinations of methanol are relatively less perturbed than the relevant fundamentals and much less perturbed than the higher overtones. A *J. Mol. Spectrosc.* article [5] is in press. The tuning range of the external cavity diode laser has been extended to reach the $\nu_1+\nu_9$ band, which is expected to have inverted torsional structure, and the data collection has begun.

The exceptionally weak $\nu_1+\nu_6$ band of propyne has been recorded and assigned. The initial fits to a symmetric rotor Hamiltonian have been accomplished.

C. Higher Symmetry Systems: Nitromethane and Methyl Amine

Nitromethane (CH_3NO_2) and methyl amine (CH_3NH_2) are internal rotor molecules with one more atom than methanol. Each has two equivalent atoms attached to the nitrogen, which increases the molecular symmetry group from G_6 to G_{12}. These molecules provide the opportunity to test and extend the concepts that are being developed for methanol in section A.

In nitromethane, the planarity of the heavy atoms results in a low 6-fold torsional barrier. We have slit-jet FTIR spectra from PNNL of the asymmetric NO stretch. Analogous to the asymmetric methanol vibrations discussed above, we should expect an anomalous ordering of the torsional levels in this nitromethane band. The rotational levels of the lowest two torsional states have been assigned including a perturbation at $K_a = 5$ in the lowest torsional state. We are collaborating with Georg Soerensen at the University of Copenhagen on fitting the data to a large-amplitude Hamiltonian.

In methyl amine, the amine group is non-planar which results in two large amplitude degrees of freedom, internal rotation with a 3-fold barrier and inversion at the nitrogen. The two degrees of freedom have comparable tunneling frequencies (0.2 to 0.3 cm^{-1}). We have assigned jet spectra of the asymmetric CH stretch and more work on the interpretation is required.

Plans for the Next Year

1. Work on the Born-Oppenheimer approximation described in section A. above will continue. This work is opening up new questions, such as, "How are new kinds of vibrational motion born as the excitation of different degrees of freedom is increased?" and, "What limiting forms of adiabatic separation are most appropriate in different regions of quantum number space?"

2. Experimental work on methanol will include additional cavity ringdown spectra in the OH + CH combination region and IRLAPS experiments on torsionally excited states built on the CH stretches. Both kinds of experiments will focus on the asymmetric CH stretches to further test the concepts outlined in section A. above. Our present laser head can reach the $v_1 + v_9$ band, but an additional laser head will be required to reach the $v_1 + v_2$ band. Since these bands are even weaker than the $v_1 + v_3$ band that we have completed, sensitivity enhancements to the cavity ringdown experiment are being implemented.

3. The nitromethane analysis is now focused on testing the suitability of Soerensen's Hamiltonian, and if necessary adapting it to include the effects of geometric phase. An attempt will be made to extend the assignments to higher torsional states because these will provide the most rigorous test of the Hamiltonian.

4. Ringdown spectra of several propyne combination bands have been recorded and one band has been fully assigned. More analysis and interpretation is required to prepare this work for publication.

5. IRLAPS experiments, intended to probe the effect of torsional conformation on IVR dynamics, are planned.

Cited References

[1] L.-H. Xu, X. Wang, T. J. Cronin, D. S. Perry, G. T. Fraser, and A. S. Pine, *J. Mol. Spectrosc.* **185**, 158 (1997).

[2] X. Wang and D. S. Perry, *J. Chem. Phys.* **109**, 10795 (1998).

[3] R. M. Lees and L.-H. Xu, *Phys. Rev. Let.* **84**, 3815 (2000).

[4] J. T. Hougen, *J. Mol. Spectrosc.* **181**, 287 (1997); J. T. Hougen, *J. Mol. Spectrosc.* **207**, 60 (2001); M. A. Temsamani, L.-H. Xu, and D. S. Perry, *Can. J. Phys.* **79**, 467 (2001).

[5] B. Fehrensen, D. Luckhaus, M. Quack, M. Willike, and T. R. Rizzo, *J. Chem. Phys,* **119**, 5534 (2003).

Publications, 2002-2004

[1] David Rueda, Oleg V. Boyarkin, Thomas R. Rizzo, Indranath Mukhopadhyay, and David S. Perry, Torsion-rotation analysis of OH stretch overtone-torsion combination bands in methanol, *J. Chem. Phys.* **116**, 91-100 (2002).

[2] A. Chirokolava, David S. Perry, O.V. Boyarkin, M. Schmidt, and T.R. Rizzo, Rotational and torsional analysis of the OH-stretch third overtone in $^{13}CH_3OH$, *J. Mol. Spectrosc.* **211**, 221-227 (2002).

[3] Indranath Mukhopadhyay, David S. Perry, Yun-Bo Duan, John C. Pearson, S. Albert, Rebecca A.H. Butler, Eric Herbst, and Frank C. De Lucia, Observation and analysis of high-*J* inter-species transitions in CH_2DOH, *J. Chem. Phys.* **116**, 3710-3717 (2002).

[4] L. Wang, Y.-B. Duan, R. Wang, G. Duan, I. Mukhopadhyay, D.S. Perry, K. Takagi, Determination of reduced Hamiltonian parameters for the CD_3OH isotopomers of methanol, *Chem. Phys.*, **292**, 23-29, (2003).

[5] Shucheng Xu, Jeffrey J. Kay, and David S. Perry, Doppler-limited CW infrared cavity ringdown spectroscopy of the v_1+v_3 OH+CH stretch combination band of jet-cooled methanol, *J. Mol. Spectrosc., in press.* (Available on line at www.sciencedirect.com.)

INVESTIGATION OF NON-PREMIXED TURBULENT COMBUSTION

Principal Investigator: Stephen B. Pope
                           Sibley School of Mechanical &
                           Aerospace Engineering
                           Cornell University
                           Ithaca, NY 14853
                           pope@mae.cornell.edu

Scope of the Research Program

In transportation, process industry and power generation, vast amounts of fossil fuel are consumed, and significant amounts of pollutants are emitted. More advanced combustion technologies are required to address the national goals of energy conservation and environmental protection. The overall goal of this research project is to contribute to the development of predictive capabilities for combustion processes in order to facilitate the development of improved combustion technologies.

In most of the industries that manufacture combustion devices, turbulent combustion models are employed as a primary design tool. These are computer models that predict the combustion performance by solving a set of equations that model the fundamental physical and chemical processes involved. The turbulent combustion models considered in this project are PDF methods, in which a modeled transport equation is solved for the joint probability density function of velocity, turbulence frequency, and the thermochemical composition of the fluid (species mass fractions and enthalpy).

One of the two themes of this research project is the development of methodologies for the computationally-efficient implementation of combustion chemistry in PDF methods and other modeling approaches. This is an important issue because, as more efficient algorithms are developed, more detailed and accurate descriptions of combustion chemistry can be used at an affordable computational cost. The second theme of the research project is to make PDF calculations of non-premixed turbulent flames and to compare the results to detailed measurements obtained at Sandia.

Recent Progress

We briefly summarize here the principal finding of the six publications stemming from this research program over the past year.

The problem of chemistry reduction can be viewed from several different perspectives. A useful perspective is that of *species reconstruction*. The problem of species reconstruction is: given partial information about a reactive gas mixture (e.g., temperature, pressure, and certain major species mass fractions) estimate the full composition (i.e., the mass fractions of the remaining

species). Existing methods such as QSSA (quasi-steady state approximation) and RCCE (rate-controlled constrained equilibrium) provide different approaches to species reconstruction. Ren & Pope (2004c) describe a much more accurate method based on "pre-image curves." For a methane-air test case (with 27 degrees of freedom in the full chemistry) the pre-image curve method with 6 degrees of freedom is shown to be two orders of magnitude more accurate than RCCE (with the same degrees of freedom), and more accurate than QSSA with 12 degrees of freedom.

In methane combustion, of order 50 chemical species are involved. At a given point and time in a methane flame, the composition can therefore be represented as a point in a 50-dimensional composition space. The union of all such points for all positions and times is defined to be the *accessed region* in the composition space. Important questions addressed by Pope (2004b) are: what is the dimensionality and geometry of this accessed region? Simple turbulent combustion models (e.g., the steady flamelet model) assume that the accessed region is a low-dimensional manifold of dimension one or two. In contrast, in PDF methods, no assumption is made and the accessed region may be 50-dimensional. It is shown in this paper that the combination of fluctuations in turbulent mixing rates and the curvature of reaction trajectories indeed leads to a high-dimensional accessed region; although this may be close to a lower-dimensional (e.g., 5D) attracting manifold.

An important issue in PDF models of turbulent combustion is the modeling of turbulent mixing. Ren & Pope (2004a) applied three existing mixing models to the test case of a partially-stirred reactor. The models considered are IEM (interaction by exchange with the mean), modified Curl, and EMST (Euclidean minimum spanning tree). The results show that, when the mixing timescale is not much smaller than the residence time, the three models yields qualitatively different results, and quantitatively different extinction residence times.

The oldest and most widely used technique for reducing combustion chemistry is the quasi-steady state approximation (QSSA). Recently, there has been some controversy concerning the fundamental issues of element conservation and the satisfaction of the laws of thermodynamics in QSSA systems. Ren & Pope (2004b) show that all of these basic principals are satisfied by QSSA systems if they are viewed as consisting only of the major (i.e., non-steady-state) species.

In several chemistry reduction methods (e.g., RCCE) it is necessary to calculate the chemical equilibrium composition of an ideal gas mixture subject to linear constraints on the species. A new method of *Gibbs function continuation* has been developed which overcomes two difficulties encountered in previous methods (Pope 2004c). First, the number of "constraint potentials" to be determined is not increased by the number of constrained species; and, second, the ill-conditioned equation system to determine the constraint potentials is replaced by a stable continuation method which is guaranteed to converge.

The ISAT algorithm has proved extremely successful in accelerating PDF computations of turbulent combustion by up to three orders of magnitude. It is natural, therefore, to attempt to extend these benefits to other areas, in particular to the computation of laminar or turbulent flames by direct numerical simulation (DNS). This is a non-trivial extension, because the coupling between reaction and mixing is much tighter in DNS than it is in PDF methods. Singer & Pope (2004) develop and demonstrate an ISAT implementation based on Strang splitting for a simple one-dimensional premixed flame. It is shown that second-order accuracy in space and time is achieved, together with modest gains in computational performance. Greater gains are to be expected for more complex flows and chemistry.

Future Plans

Current and future work is in three areas. First, research on the pre-image curve method will seek to: devise improved methods of generating pre-image curves; determine optimal reduced representations; increase the computational efficiency of the method; and combine it with ISAT. Second, the research on using ISAT for DNS of flames continues in a collaboration with Dr. Habib Najm (Sandia). The ISAT algorithm is being implemented in the Sandia code *dflame* and will be tested in hydrogen and methane flames in 1D and then 2D. Third, with the improved modeling, chemistry and numerical algorithms that have been developed over the past few years, we will make PDF computations of the Sandia piloted jet flames in order to quantify the performance of different submodels (for mixing, chemistry and turbulence).

Publications from DOE Research 2002-2004

1. R. Cao and S.B. Pope (2003) "Numerical integration of stochastic differential equations: weak second-order mid-point scheme for applications in the composition PDF method," J. Comput. Phys. **185**, 194–212.

2. M. Muradoglu, K. Liu and S.B. Pope (2003) "PDF Modeling of a Bluff-Body Stabilized Turbulent Flame," Combust. Flame **132**, 115-137.

3. M. Muradoglu and S.B. Pope (2002) " Local time-stepping algorithm for solving the probability density function turbulence model equations," AIAA Journal, **40**, 1755-1763.

4. S.B. Pope (2004a) "Ten questions concerning the large-eddy simulation of turbulent flows," New Journal of Physics **6**, 35.

5. S. B. Pope (2004b) "Accessed Compositions in Turbulent Reactive Flows", Flow, Turbulence and Combustion (to be published).

6. S.B. Pope (2004c) "Gibbs function continuation for the stable computation of chemical equilibrium," Combustion and Flame (submitted).

7. Z. Ren and S.B. Pope (2004a) "An investigation of the performance of turbulent mixing models." Combustion and Flame **136**, 208–216.

8. Z. Ren and S.B. Pope (2004b) "Entropy production and element conservation in the quasi-steady-state approximation." Combustion and Flame (to be published).

9. Z. Ren and S.B. Pope (2004c) "Species reconstruction using pre-image curves" Proceeding of the Combustion Institute, **30**, (to be published).

10. M.A. Singer and S.B. Pope (2004) "Exploiting ISAT to solve the equations of reacting flow," Combustion Theory and Modelling **8**, 361–383.

OPTICAL PROBES OF ATOMIC AND MOLECULAR DECAY PROCESSES

S.T. Pratt
Building 200, B-125
Argonne National Laboratory
9700 South Cass Avenue
Argonne, Illinois 60439

Telephone: (630) 252-4199
E-mail: stpratt@anl.gov

PROJECT SCOPE

Molecular photoionization and photodissociation dynamics can provide considerable insight into how energy and angular momentum flow among the electronic, vibrational, and rotational degrees of freedom in isolated, highly energized molecules. This project involves the study of these dynamics in small polyatomic molecules, with an emphasis on understanding the mechanisms of intramolecular energy flow and determining how these mechanisms influence decay rates and product branching ratios. The experimental approach combines double-resonance laser techniques, which are used to prepare selected highly excited species, with mass spectrometry, ion-imaging, and high-resolution photoelectron spectroscopy, which are used to characterize the decay of the selected species. Additional techniques, including excited-state absorption spectroscopy by fluorescence-dip techniques and zero-kinetic energy-photoelectron spectroscopy are used also as necessary. Photoelectron imaging capabilities are currently being developed to allow the determination of photoelectron angular distributions.

RECENT PROGRESS

In the past year, we have continued to work on the vibrational-mode dependence of vibrational autoionization in small polyatomic molecules. In collaboration with Ed Grant, of Purdue University, we have extended our comparison of the symmetric stretch and bending vibrations as promoters of vibrational autoionization in NO_2. In particular, we have used photoelectron spectroscopy to study the decay of Rydberg series converging to the (110) level of the ground electronic state of NO_2^+. [Here we use the notation (v_1,v_2,v_3), where v_1, v_2, and v_3 label the symmetric stretch, bend, and asymmetric stretch, respectively.] Determination of the vibrational level of NO_2^+ produced upon autoionization provides a direct comparison of the autoionization rates for the two modes. Photoelectron spectra of the selected levels show that autoionization strongly favors the loss of one quantum from the symmetric stretch, as opposed to loss of a quantum from the bending vibration. These results are consistent with our earlier, less direct, comparison of these two modes through the study of the autoionization of the (100) and (020) Rydberg series. As discussed below, we are working with Christian Jungen of the Laboratoire Aime Cotton in Orsay, France to develop models for understanding these results. Because the rate for vibrational autoionization with the symmetric stretch is so fast, we sought to confirm that the process really was vibrational autoionization by examining the photoelectron spectra of autoionizing resonances converging to the (200) level of the of the NO_2^+ ground state. Photoelectron spectra of these resonances were entirely consistent with the standard model for vibrational autoionization, i.e., the $\Delta v_1 = -1$ process was much faster than the $\Delta v_1 = -2$ process. Unfortunately, although we can conclude that the results are consistent with vibrational

autoionization, we cannot confirm that vibrational autoionization is the only possible mechanism. Theoretical work is currently underway to address this question.

Patrice Bell, a graduate student of Ed's, spent a year and a half at Argonne performing this work, and she received her Ph.D. in December, 2003. As an off-shoot of this work, we used double-resonance spectroscopy and photoelectron spectroscopy to explore the ability to make vibrationally state selected NO_2^+ by photoionizing selected vibrational levels of the $3p\sigma$ Rydberg state. This work was motivated by a request from Scott Anderson at the University of Utah, who wished to use such schemes to study the vibrational mode dependence of ion-molecule reactions of NO_2^+. We demonstrated that the double-resonance approach could be used to prepare samples of ground-state NO_2^+ in the (000), (100), (010), or (001) levels with greater than 95% purity, and this approach has now been incorporated into Anderson's experiments.

In collaboration with Wally Glab of Texas Tech University, we completed a series of experiments on the rotational state distributions following vibrational autoionization of water. These results provide insight into the detailed mechanism of vibrational autoionization, and provide a significant challenge to state of the art theory. In addition to providing information on the coupling between vibrational and rotational degrees of freedom, the rotational distributions also contain information on the partial wave character of the ejected photoelectron. These studies required us to address a number of experimental issues that are relevant to a number of future experiments, particularly with respect to generating vacuum ultraviolet (vuv) light and using it in the electron spectrometer. This work has already paid dividends in our most recent ion-imaging experiments discussed below.

In a second series of experiments, we continued to explore the use of imaging techniques to study the photodissociation dynamics of neutral and ionic species. We completed our first two-color study of the photodissociation of state-selected ions. In these experiments, the vibrationless ground state of CF_3I^+ was prepared by two-photon resonant, three photon ionization, and the state-selected ions were photodissociated by a second laser via the A ← X transition. The images show that the preferred dissociation process leads to the production of I* + CF_3^+ with the maximum amount of energy in the v_2 umbrella vibration. This is consistent with the Franck-Condon factors between the pyramidal geometry of the CF_3 moiety in CF_3I^+ and the planar geometry of CF_3^+. Future studies may involve preparing selected vibrationally excited levels of CF_3I^+ to characterize other regions of the ionic potential surfaces.

We have also used ion imaging to study the photoionization and photodissociation dynamics of the $B^1\Sigma_u^+$ and $C^1\Pi_u$ states of H_2 and D_2. Photoionization of selected vibrational levels of these states leads to $H_2^+ X^1\Sigma_g^+$, which is photodissociated by absorption of an additional photon. The images allow the determination of the asymmetry parameters for the photodissociation of $H_2^+ X^1\Sigma_g^+$ as a function of the ion's vibrational state. The observations are consistent with theoretical expectations for this process. Photodissociation of the $B^1\Sigma_u^+$ and $C^1\Pi_u$ states results in a ground state H(D) atom and an excited H(D) atom in an n = 2, 3, or 4 level. These excited atoms are photoionized by the absorption of an additional photon, providing images of the neutral photodissociation process. The results provide new information on the doubly excited neutral states with gerade symmetry, and appear to confirm an earlier suggestion [C. R. Scheper et al., J. Chem. Phys. 109, 8319 (1998)] that singly excited Rydberg states converging to highly vibrationally excited levels of $H_2^+ X^1\Sigma_g^+$ play an

important role in the process. Preliminary studies of HD appear to show evidence for interesting interference phenomena that we are currently investigating.

Finally, we have initiated a study of the internal energy dependence of the relative photoionization cross sections of selected free radicals by using ion imaging to characterize the internal energy and vuv photoionization to detect the radicals. This work is important because vuv photoionization is increasingly being used to detect products of photodissociation and reactive scattering, as well as to characterize species in flames. Initial work involves a comparison of the internal energy dependence of the relative photoionization efficiency of CH_3 and CF_3. Because the ground states of CH_3 and CH_3^+ have similar geometries, the photoionization cross sections near threshold are not expected to depend too strongly on internal energy. However, the ground state of CF_3 is pyramidal and the ground state of CF_3^+ is planar, and in this case a strong dependence on internal energy is expected. Preliminary experiments have also been performed to characterize the photodissociation dynamics of propargyl chloride at 193 nm. Work is planned to characterize the relative photoionization efficiency of the propargyl radical as a function of internal energy.

FUTURE PLANS

Our immediate plans are to pursue our imaging studies of the internal energy dependence of relative photoionization cross sections of selected free radicals. While initial work can be performed with relatively simple vuv sources, if the experiments are successful we will ultimately need to separate the vuv light from the beams used to generate it. This capability will be incorporated into a new imaging machine, which will be constructed in the coming year. This machine will also allow "slicing" experiments to eliminate the need for image reconstruction and the use of a variety of different sample sources (discharges, photodissociation, pyrolysis, etc.). In addition, this machine will allow both ion and photoelectron imaging. Photoelectron imaging of autoionizing states of polyatomic molecules will allow the determination of photoelectron angular distributions, which provide information on the partial wave composition of the photoelectron. Such studies will provide an important perspective on the sources of the mode dependence of autoionization in NO_2 and NH_3. The imaging electron spectrometer will also provide an important complement to the magnetic bottle electron spectrometer currently in use. Imaging studies of superexcited states that undergo both autoionization and predissociation are planned, and the ability to examine both the ionization and dissociation processes in a complementary manner should be particularly revealing.

I will continue to collaborate with Christian Jungen on theoretical models of vibrational autoionization in polyatomic molecules. We are currently working on a paper that shows how to extract information about autoionization rates from quantum chemical calculations of low-lying Rydberg states. We are also working to extend our earlier study of simple polyatomic molecules to situations involving degenerate electronic states. In this situation, the Renner-Teller and Jahn-Teller interactions can play an important role. In the past year, I also spent three weeks working at the ETH Zurich with Professor Frederic Merkt on the very high resolution pulsed field ionization spectroscopy of some weak bands in HCl. These results are currently being analyzed. Attempts to observe steps at the dissociative ionization threshold, such as those observed in other molecules by C. Y. Ng and coworkers were unsuccessful. This visit was also extremely useful for developing ideas for incorporating laser-based vuv techniques in my lab at Argonne.

DOE-SPONSORED PUBLICATIONS SINCE 2002

1. C. Ramos, P. R. Winter, T. S. Zwier, and S. T. Pratt
    PHOTOELECTRON SPECTROSCOPY VIA THE 1 $^1\Delta_u$ STATE OF DIACETYLENE
    J. Chem. Phys., **116**, 4011-4022 (2002).

2. S. T. Pratt
    PHOTOIONIZATION DYNAMICS OF THE B^{1}E" STATE OF AMMONIA
    J. Chem. Phys. **117**, 1055-1067 (2002).

3. S. T. Pratt
    PHOTOIONIZATION OF DABCO VIA HIGH VIBRATIONAL LEVELS OF THE S_1 STATE
    Chem. Phys. Lett. **360**, 406-413 (2002).

4. F. Aguirre and S. T. Pratt
    VELOCITY MAP IMAGING OF THE PHOTODISSOCIATION OF CF_3I: VIBRATIONAL ENERGY DEPENDENCE OF THE RECOIL ANISOTROPY
    J. Chem. Phys., **118**, 1175-1183 (2003).

5. S. T. Pratt, J. A. Bacon, and C. A. Raptis
    VIBRATIONAL AUTOIONIZATION IN POLYATOMIC MOLECULES
    in *Dissociative Recombination*, Edited by S. Guberman, Kluwer, New York, 2003, p. 309-319.

6. F. Aguirre and S. T. Pratt
    ION-IMAGING OF THE PHOTODISSOCIATION OF CF_3I^+
    J. Chem. Phys., **118**, 6318-6326 (2003).

7. P. Bell, F. Aguirre, E. R. Grant, and S. T. Pratt
    MODE-DEPENDENT VIBRATIONAL AUTOIONIZATION OF NO_2
    J. Chem. Phys., **119**, 10146-10157 (2003).

8. F. Aguirre and S. T. Pratt
    VELOCITY MAP IMAGING OF THE PHOTODISSOCIATION OF CF_3I^+ IN THE A ← X BAND
    J. Chem. Phys., **119**, 9476-9485 (2003).

9. S. T. Pratt
    PHOTOIONIZATION OF EXCITED STATES OF MOLECULES
    Radiation Physics and Chemistry, in press.

10. P. Bell, F. Aguirre, E.R. Grant, and S.T. Pratt
    MODE-DEPENDENT VIBRATIONAL AUTOIONIZATION OF RYDBERG STATES OF NO_2. II. COMPARING THE SYMMETRIC STRETCHING AND THE BENDING VIBRATIONS
    J. Chem. Phys. 120, 2667-2676 (2004)

11. W. L. Glab and S. T. Pratt
    ION ROTATIONAL DISTRIBUTIONS FOLLOWING VIBRATIONAL AUTOIONIZATION OF RYDBERG STATES OF WATER
    J. Chem. Phys., in press.

Reactions of Atoms and Radicals in Pulsed Molecular Beams
Hanna Reisler
Department of Chemistry, University of Southern California
Los Angeles, CA 90089-0482
reisler@usc.edu

Program Scope

We study photoinitiated reactions of molecules and free radicals that involve competitive pathways and/or isomerization by exploiting multiple-resonance excitation schemes, state-selected product detection, and photofragment translational spectroscopy and ion imaging for generation of correlated distributions. Reaction thresholds are reached either via radiationless transitions from electronically excited states, or by vibrational excitation in the ground state.

Rotationally resolved infrared spectroscopy of the hydroxymethyl radical (CH$_2$OH)

The hydroxymethyl radical (CH$_2$OH) and its isomer, the methoxy radical (CH$_3$O), are important intermediates in hydrocarbon combustion and atmospheric processes. Insights into intramolecular vibrational redistribution (IVR), isomerization, and unimolecular dissociation on the ground potential energy surface (PES) of CH$_2$OH can be obtained from spectroscopic investigations of its fundamental and overtone vibrational transitions. According to *ab initio* calculations, CH$_2$OH requires ~16,000 cm^{-1} to surmount the barrier to H + CH$_2$O(^{1}A$_1$) on the ground state, while the barrier to CH$_3$O decomposition has been determined experimentally to be only ~ 11,000 cm^{-1} relative to the energy of CH$_2$OH. The height of the isomerization barrier (calculated at ~ 14,000 cm^{-1}) will therefore dictate whether the CH$_2$OH radical can decompose via the isomerization route. It is expected that the low barriers to isomerization and dissociation would result in increased anharmonicity, thereby promoting IVR.

Knowledge of the vibrational spectroscopy of the radical is prerequisite to understanding the competition between CH$_2$OH/CH$_3$O isomerization and direct O-H bond fission on the ground PES. Early experiments on CH$_2$OH infrared (IR) spectroscopy were carried out in argon and nitrogen matrices,[1] and vibrational bands involving the OH (v_1) and CO (v_6) stretches, CH$_2$ scissors (v_4), in- (v_5) and out-of-phase (v_7) HCOH bends, and torsion (v_8) were observed. In flow reactor (300 K) studies of REMPI spectroscopy via the $3p_z$ state,[2] transitions from vibrational "hot bands" of CH$_2$OH on the ground state were identified, and v_6, v_8, and the CH$_2$ wag (v_9) frequencies were determined. The two CH stretch vibrations, v_2 and v_3, were not observed and no rotationally resolved spectra were reported. Despite its small size, the vibrational spectroscopy of CH$_2$OH can be rather complex. Both OH- and CH-stretches serve as chromophores for vibrational excitation and irregular vibrational energy patterns have been calculated for the coupled v_8 and v_9 modes.[3] Spectral patterns observed in high-overtone excitation can shed light on IVR, isomerization, and unimolecular dissociation mechanisms.

We report the first observations of rotationally-resolved OH- and CH-stretch vibrational transitions in CH$_2$OH, obtained in a molecular beam by using double resonance ionization detected IR (DRID-IR) spectroscopy. The radical is produced by the reaction of Cl atoms with CH$_3$OH carried out in a quartz tube attached to a piezoelectrically-driven pulsed nozzle. A 355 nm pulsed laser beam crosses the edge of the tube and dissociates Cl$_2$. The Cl atoms react rapidly with CH$_3$OH, producing CH$_2$OH, which undergoes cooling during the supersonic expansion before reaching the detection region.

In depletion spectroscopy experiments, the probe laser beam frequency is fixed at 41,062 cm^{-1} to access the peak of the CH$_2$OH 2^{2}A''(3p_z) $\leftarrow$ 1^{2}A'' origin band.[3] The population of the ground state is depleted whenever IR absorption to a vibrationally excited state takes place, thereby attenuating the CH$_2$OH$^+$ ion signal obtained by 1+1 REMPI. It is used here to pinpoint spectral locations of the vibrational transitions in the ground state. However, the large CH$_2$OH$^+$ ion signal generated by the probe laser beam reduces the signal-to-noise (S/N) ratio.

In DRID-IR spectroscopy, the UV frequency is adjusted to excite CH_2OH in a selected rovibrational state in the ground state to a Franck-Condon favorable vibronic level in the $3p_z$ Rydberg state and then further ionize it. Rovibrational spectra are recorded by tuning simultaneously the IR and UV laser frequencies and fixing their total energy at the peak of the transition to the selected vibronic level in $3p_z$. This scheme takes advantage of the broad homogeneous linewidth of the rotational lines of the transition to the $3p_z$ state (>10 cm^{-1}).[2,3] The UV beam (probe) frequency is not resonant with any of the vibronic transitions from ground state CH_2OH, and hence no ion signal is detected in the absence of IR radiation. The major advantage of DRID-IR over depletion spectroscopy is that it is largely background free. A prerequisite for its successful application is the existence of a vibronic transition with a good Franck-Condon factor (FCF) from the vibrationally excited state to the $3p_z$ Rydberg state. Furthermore, the observed spectra are species-selective, since only cations of a specific mass are detected.

Figure 1 displays infrared spectra of CH_2OH in the region of the (a) CH symmetric stretch (v_3), (b) CH asymmetric stretch (v_2), and (c) OH stretch (v_1). The spectra are recorded using DRID-IR, and spectral fits are shown along with symmetric top assignments. The intensities in the DRID-IR traces are given as CH_2OH^+ ion signal intensities, which are roughly proportional to the absorption cross section.

We also carried out REMPI experiments, in which following IR excitation the UV laser wavelength was scanned. The goal of these experiments was to locate vibronic resonances with large FCFs in the $3p_z$ state for DRID-IR spectroscopy. The IR laser beam frequency was fixed at the position of maximum absorption in the depletion spectra, while the UV frequency was scanned in the energy region around 41,062 cm^{-1} – the peak of the origin band of the $2^2A''(3p_z) \leftarrow 1^2A''$ transition.

The open circles in Fig. 2 depict the 1+1 REMPI spectrum of CH_2OH obtained with the IR laser off, while the solid line marks the IR+UV REMPI spectrum. Two features are prominent in the "IR-on" spectra. The first is a decrease in the intensity of the origin band at 41,062 cm^{-1} as a result of depletion of ground state population by IR absorption. This is most prominent in the v_1 spectrum, and is barely discernible for the v_2 and v_3 fundamentals whose oscillator strengths are much lower.

New vibronic bands associated with UV excitation of the IR-excited vibrational state to Franck-Condon favored levels in the $3p_z$ state are also seen in Fig. 2. The appearance of these bands suggests that the ion signal can be significantly enhanced by choosing specific resonances in $3p_z$, as required by DRID-IR. This method also allows assignment of new vibronic levels in the $3p_z$ state that are inaccessible by REMPI from the ground vibrational state.

The DRID-IR vibrational spectra shown in Fig. 1 exhibit well-resolved rotational bands. The fundamental OH stretch (v_1) and CH symmetric stretch (v_3) transitions have similar rotational structures, while the CH asymmetric stretch (v_2) is different. In order to assign the spectra, rotational constants and orientations of the vibrational transition dipole moments were determined by *ab initio* calculations, and rotational spectra were modeled as asymmetric rotors. Infrared intensities and orientations of the vibrational transition dipole moments were computed for displacements from equilibrium along each normal coordinate. The results show that the transition dipole moments of v_1, v_2, and v_3 lie in the a/b-plane. The v_1 and v_3 fundamental transitions are hybrid bands of a/b-type, while the spectrum of v_2 is a pure b-type transition. The calculated infrared intensity of the v_1 fundamental is significantly larger than that of v_2 and v_3. The calculated infrared intensities and the I_b/I_a ratios are summarized in Table 1. The experimental intensities obtained by DRID-IR spectroscopy are not directly proportional to IR absorption cross sections, but the much weaker depletion of ground state population observed following v_2 and v_3 excitations compared to v_1 (Fig. 1) is in agreement with the calculated relative intensities. Aided by the *ab initio* calculations, the rotational structures of the OH stretch and CH asymmetric and symmetric stretch fundamentals have been modeled by using the asymmetric rotor program ASYTOP. The fitted I_b/I_a ratios are in good agreement with the calculated values. The measured vibrational frequencies and types of transitions of the OH and CH fundamentals are in excellent agreement with *ab initio* calculations. The two CH transitions are different in frequency and transition type, corresponding to CH bonds of different equilibrium bond-length.

Table 1: Theoretical and experimental constants for the v_1, v_2 and v_3 fundamentals.

Mode	Harmonic Frequency (cm^{-1})		Infrared Intensity (km/mol)	$R = I_b/I_a$		Rotational constants $(cm^{-1})_{obs}$ [b]		
	v_{calc} [a]	v_{obs}	I_{calc}	R_{calc}	R_{obs}	A_1	B_1	C_1
v_3 CH sym str	3013.6	3043.4	18.4	0.1	0.6 ± 0.4	6.48	0.98	0.88
v_2 CH asym str	3128.2	3161.5	11.2	Pure b	Pure b	6.41	0.97	0.88
v_1 OH stretch	3686.7	3674.9	54.9	1.2	0.8 ± 0.4	6.41	0.96	0.88

[a] The calculated frequencies are scaled by 0.95.
[b] The calculated zeroth-level rotational constants are: $A_0 = 6.51$, $B_0 = 1.00$, $C_0 = 0.88$.

Rotational structure is still present in the spectrum of the first overtone transition of the OH stretch ($2v_1$) whose center is at 7158 cm^{-1}, but the linewidth has increased to 0.8 cm^{-1}. This linewidth was independent of IR laser energy in the range 3-5 mJ. The regularity of the rotational structure indicates that IVR is not extensive at this energy region even though the internal energy of the radical is almost half of the barrier heights to isomerization ($\sim$ 14,000 cm^{-1}) and O-H bond dissociation ($\sim$ 16000 cm^{-1}). The $2v_1$ spectrum is modeled by a similar procedure to that used for the fundamental transitions. The only difference is that a Lorentzian linewidth is varied to obtain a best fit to the data (0.8 ± 0.1 cm^{-1}) instead of fixing it at the IR laser bandwidth (0.4 cm^{-1}). The OH stretch anharmonicity for CH_2OH obtained in this work is 95.9 cm^{-1}.

Referring to the observed increase in rotational linewidth, we note that because of the large bandwidth of our IR laser beam we cannot distinguish between a homogeneous linewidth and the spectral overlap of a few sharp transitions involving mixed states that borrow oscillator strength from the "bright" OH overtone. A calculation of the vibrational density of states using the Beyer-Swinehart algorithm and neglecting anharmonicity, gives a density of $\sim$ 5 states per cm^{-1} in the region of $2v_1$, but restricting the coupling to low-order resonances (i.e., combination levels with a total number of quanta less than 6) reduces the density of effectively coupled states to less than one state per cm^{-1}. By comparing this spectrum to those of similar molecules, we conclude that the increase in rotational linewidth is probably due to spectral overlap of a few transitions around each rotational level of $2v_1$ borrowing intensity from the "bright" OH chromophore. The OH stretch anharmonicity estimated in this work, 95.9 cm^{-1}, is comparable to but slightly higher than the corresponding values in methanol and hydroxylamine.

Future Work

Experimental work is in progress on the spectroscopy of higher vibrational overtones of the OH stretch, and product formation via direct dissociation and/or isomerization pathways. We also plan to extend this work to the electronic and vibrational spectroscopy of higher hydroxyalkyl radicals.

References

1. Jacox, M.; DE.Milligan. *J. Mol. Spectrosc.* **1973**, *47*, 148.; Jacox, M. *Chem. Phys.* **1981**, *59*, 213.

2. Johnson, R. D.; Hudgens, J. W. *J. Phys. Chem.* **1996**, *100*, 19874.

3. Aristov, V.; Conroy, D.; Reisler, H. *Chem. Phys. Lett.* **2000**, *318*, 393.

Publications, 2002-

Photodissociative spectroscopy of the hydroxymethyl readical (CH$_2$OH) in the 3s and 3p$_x$ states, L. Feng, X. Huang and H. Reisler, J. Chem. Phys. **117**, 4820-4824 (2002).

O-D bond dissociation from the 3s state of deuterated hydroxymethyl radical (CH$_2$OD), L. Feng, A.V. Demyanenko, and H. Reisler, J. Chem. Phys. **118**(21), 9623-9628 (2003).

Competitive C–H and O–D bond fission channels in the UV photodissociation of the deuterated hydroxymethyl radical CH₂OD, Lin Feng, Andrey V. Demyanenko, and Hanna Reisler, J. Chem. Phys.**120**(14), 6524-6530 (2004).

Rotationally resolved infrared spectroscopy of the hydroxymethyl radical (CH₂OH), Lin Feng, Jie Wei, and Hanna Reisler, J. Phys. Chem., in press, April 2004.
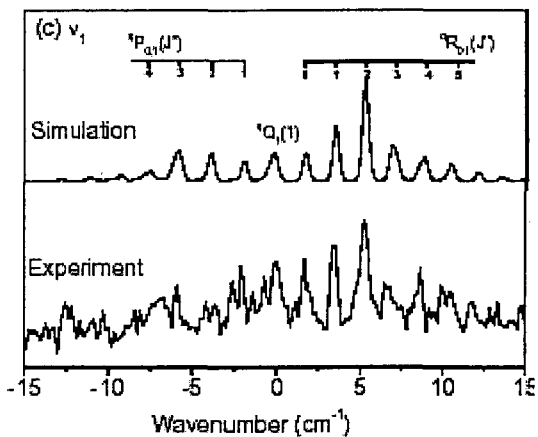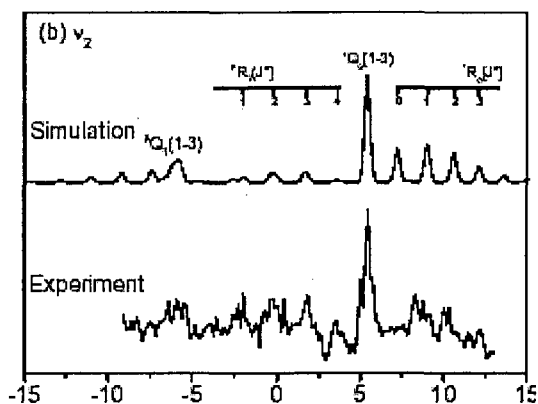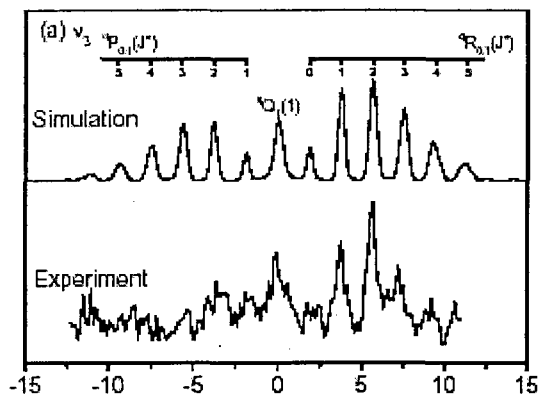
Fig. 1 [left]. Comparisons of experimental spectra of (a) v_3; (b) v_2, and (c) v_1 obtained by DRID-IR spectroscopy with spectral fits. The spectra in (a), (b) and (c) are shifted by 3043.4, 3161.5 and 3674.9 cm⁻¹, respectively.

Fig. 2 [bottom] IR+UV REMPI spectrum of CH₂OH obtained via the $3p_z$ state with IR off (open circles), and IR frequency tuned to (solid line) (a) the CH symmetric stretch; (b) the CH asymmetric stretch; (c) the OH stretch; and (d) its first overtone.
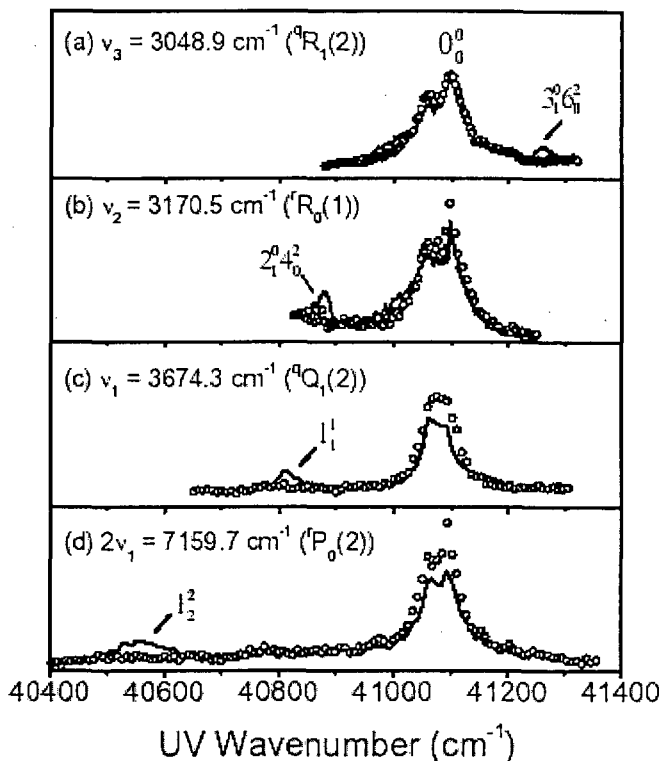
Electronic Structure, Molecular Bonding and Potential Energy Surfaces

Klaus Ruedenberg

Ames Laboratory USDOE, Iowa State University, Ames, Iowa, 50011

ruedenberg@iastate.edu

Scope

Essential for the theoretical untangling of the reaction mechanism occurring in combustion processes is the identification of transition states and reaction paths on potential energy surfaces. The first stage of the quantum mechanical solutions of such problems necessarily consists of solving them in the context of the full valence space model, which has proven useful and effective for elucidating many reactions while, at the same time, providing chemical insights. It is furthermore indispensable when, for the sake of accuracy, dynamic correlation refinements must be added. Even with the orbital restrictions defining full orbital valence spaces, however, the dimensions of the corresponding full configurational valence spaces exceed the available computational capabilities for many molecules of interest in combustion chemistry. Fortunately, large parts of the full configurational valence spaces are ineffective deadwood and this percentage increases with the size of the molecule. The challenge is, to identify, *ahead of time*, the "configurational live wood" whose energy agrees with the full-space energy within chemical accuracy. This is manifestly a relevant problem in the quantum chemistry of combustion.

Recent Results

We have developed a method for solving the outlined problem within the variational context. We have identified the optimal molecular orbital orbitals, the split-localized orbitals: They yield stronger CI convergence than natural orbitals, they yield linear scaling with molecular size, and they are determined and ordered *a-priori*. On the basis of these orbitals, a systematic *a-priori* procedure has been devised that identifies the configurational live wood successively in the doubly, triply, quadruply, quintuply , sextuply, etc excited configurations (with respect to the dominant configurations). The method reduces full valence space-type multi-configurational expansions by orders of magnitude and the reduction fraction increases with the size of the molecule, so that larger systems become accessible.

The first of the two figures illustrates, for a number of molecules, that split-localized orbitals typically yield superior CI convergence as compared to natural orbitals. The second figure illustrates, for the same molecules, that the CI expansion ordered by our *a-priori* procedure converges just as fast as the CI expansion ordered *a posteriori* according to the magnitudes of the coefficients of the exact full wavefunction.

Future work

The described methods will be extended for the efficient use with multi-configurational dominant reference functions, in particular with a view to applications to transition states.

Orbital Dependence of Deadwood as Exhibited by Truncations of SDTQ CI Expansions based on

O : Natural Orbitals   ● : Split-Localized MO's

CI TRUNCATION ERRORS FOR SDTQ ENERGIES, mh

HNO SDTQ[12/12]

1 mh accuracy

HNO SDTQ[12/9]

1 mh accuracy

OCO SDTQ[16/16]

1 mh accuracy

OCO SDTQ[16/12]

1 mh accuracy

NCCN SDTQ[18/18]

1 mh accuracy

NCCN SDTQ[18/16]

1 mh accuracy
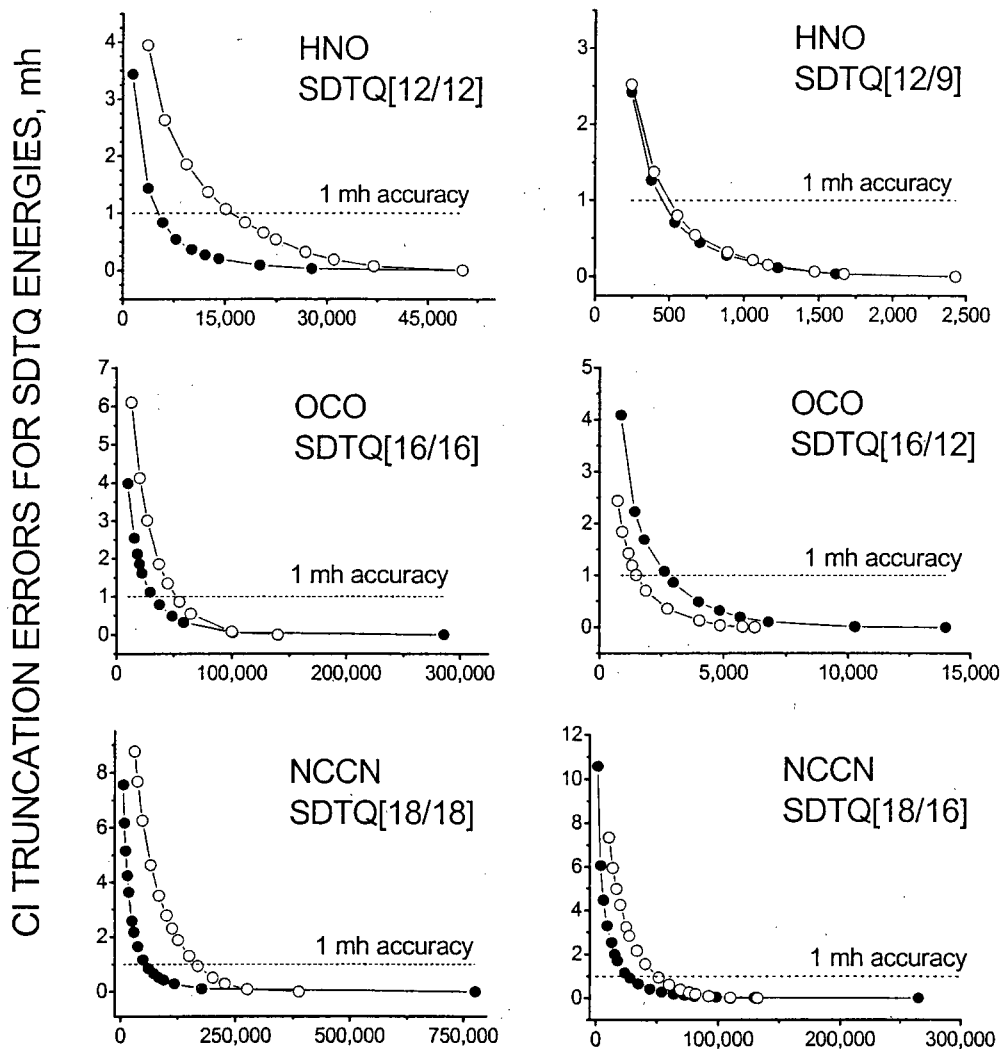
NUMBER OF DETERMINANTS IN TRUNCATED CI EXPANSIONS

Elimination of Deadwood from SDTQ CI Expansions
by Means of Truncations determined
O : A posteriori from exact SDTQ wavefunctions
● : By a priori estimates from SD wavefunctions

CI TRUNCATION ERRORS FOR SDTQ ENERGIES, mh

HNO
SDTQ[12/12]
50,254 detmnts

1 mh; 5,905 det's

HNO
SDTQ[12/9]
2,428 detmnts

1 mh; 643 det's

OCO
SDTQ[16/16]
285,577 detmnts

1 mh; 31,150 det's

OCO
SDTQ[16/12]
13,977 detmnts

1 mh; 2,798 det's

NCCN
SDTQ[18/18]
776,316 detmnts

1 mh; 49,033 det's

NCCN
SDTQ[18/16]
264,788 detmnts

1 mh; 25,776 det's

NUMBER OF DETERMINANTS IN TRUNCATED CI EXPANSIONS

251
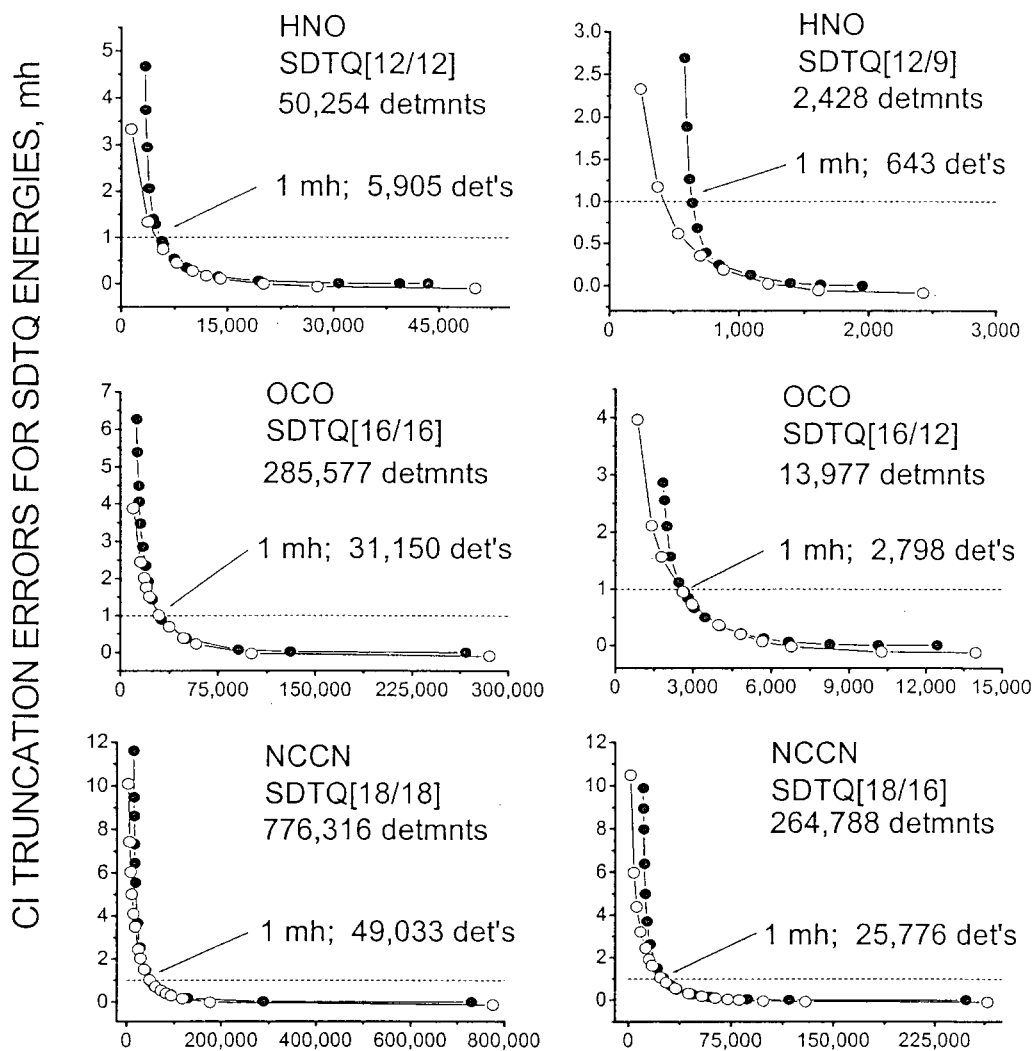
Publications 2002, 2003, 2004

Deadwood in Configuration Spaces. II. SD and SDTQ Spaces,
   Joseph Ivanic and Klaus Ruedenberg
   Theor. Chem. Accounts, 107, 220-228 (2002)

Electron Pairs, Localized Orbitals and Electron Correlation
   Laimutis Bytautas and Klaus Ruedenberg
   Molecular Physics, 100, 757-781 (2002)

A MCSCF Method for Ground and Excited States Based on Full Optimizations of Successive Jacobi Rotations
   Joseph Ivanic and Klaus Ruedenberg
   J. Computational Chemistry 24, 1250-1262 (2003)

Split-Localized Orbitals Can Yield Stronger Configuration Interaction Convergence than Natural Orbitals
   L. Bytautas, J. Ivanic and K. Ruedenberg
   J. Chem. Phys. 119, 8217 (2003)

Molecule Intrinsic Minimal Basis Sets. I. Exact Resolution of Ab-Initio Optimized Molecular Orbitals in terms of Deformed Atomic Minimal-Basis Orbitals
   W. C. Lu, C. Z. Wang, M. W. Schmidt, L. Bytautas, K. M. Ho, K. Ruedenberg
   J. Chem. Phys. 120, 2629-2637 (2004)

Molecule Intrinsic Minimal Basis Sets. II. Bonding Analyses for Si_4H_6 and Si_2 to Si_{10}
   W. C. Lu, C. Z. Wang, M. W. Schmidt, L. Bytautas, K. M. Ho, K. Ruedenberg
   J. Chem. Phys., J. Chem. Phys. 120, 2638-2651 (2004)

Correlation Energy Extrapolation Through Intrinsic Scaling
   I., Laimutis Bytautas and Klaus Ruedenberg
   J. Chem. Phys., accepted

Correlation Energy Extrapolation Through Intrinsic Scaling. II
   Laimutis Bytautas and Klaus Ruedenberg
   J. Chem. Phys., accepted

Active Thermochemical Tables

Branko Ruscic

Chemistry Division, Argonne National Laboratory, 9700 South Cass Avenue, Argonne, IL 60439

ruscic@anl.gov

Program Scope

The *spiritus movens* of this program is the need to provide the chemical community with accurate and reliable thermochemical, spectroscopic and structural information on chemical species that are intimately connected to energy-producing processes, such as combustion, or play prominent roles in the associated environmental issues, thus contributing to the global comprehension of the underlying chemical reactions and/or providing benchmark values for test and development of advanced theoretical approaches. The experimental portion of this effort uses photoionization mass spectrometry and related methods to study transient and metastable species that are produced *in situ* using various suitable techniques. Recently, the program has been focused on developing a novel approach (described below in more detail) that aims to extract the maximum data content from thermochemically relevant measurements and hence produce not only the *best currently available* thermochemical values for the species of interest, but also provide critical tests of new data and pointers to the most efficient future experimental and theoretical developments. The effort of this program is coordinated with related experimental and theoretical efforts within the Argonne Chemical Dynamics Group to provide a broad perspective on this area of science.

Recent Progress

Development of Active Thermochemical Tables and of the underlying Thermochemical Network

Active Thermochemical Tables (ATcT) are a new paradigm of how to derive accurate, reliable, and internally consistent thermochemical values, and are rapidly becoming the archetypal approach to thermochemistry for the 21st century. At the core of ATcT is the explicit utilization and statistical treatment of underlying interdependences between thermochemical quantities, conveniently expressed through a network of relationships. The current development of ATcT has several related components: The conceptual advances in the underlying methodology, together with the construction and evaluation of the Thermochemical Network and the resulting practical advances in thermochemistry of stable and ephemeral species, are a direct product of this project (funded by DOE BES), while the accompanying software development involved in bringing to life a practical instance of ATcT as a web-service is highly leveraged by an additional funding source (DOE MICS).

The thermochemical properties for any chemical species are derived from basic determinations that generally fall into two categories: *species-specific* and *species interrelating*. A subset of properties (heat capacity, entropy, enthalpy increment) can be derived directly from *species-specific* information, such as spectroscopic measurements for gas-phase species or direct measurements of selected properties (e.g. heat capacity) for condensed-phase species. However, the enthalpy and/or Gibbs energy of formation are always obtained from determinations (such as bond dissociation energies, kinetic equilibria, electrode potentials, solubility data, etc.) that express these quantities *relative* to other chemical species. This leads to intricacies, which traditional thermochemistry approaches via a *sequential process*. During each step, a new chemical species is adopted. The "best" information linking it to previously determined species is utilized to obtain its enthalpy of formation. The selected value is then frozen, and used subsequently as a constant. The end result is a static tabulation that has a number of problems, the largest being hidden progenitor-progeny dependencies across the tabulation, which frustrate any serious attempt to update the compilation with new knowledge. New data can be used, at best, to update the properties of one species (tantamount to revising a step in the middle of the original sequence). While this may improve things locally, it introduces new inconsistencies across the tabulation, since there will be other species in the table that are pegged directly or indirectly to the old value of the revised species and also need to be updated. Which those may be, is not explicit. Other difficulties, such as cumulative errors, are caused by lack of corrective feedback to the thermochemistry of species that have been determined in previous steps and frozen. The traditional process also produces uncertainties that are not necessarily properly quantified and tend not to reflect the information content that is being used in other parts of the tabulation. It can be argued that, even under the best of circumstances, the available information is exploited only partially in the sequential approach.

In reality, the measurable species-interconnecting thermochemical quantities form a Thermochemical Network (TN). Figure 1 provides a graphical representation of a small Thermochemical Network, related to our recent

revision of the bond dissociation energy in water by ~2 kJ/mol. The primary vertices of the graph (squares) represent the enthalpies of formation which need to be determined, while the secondary vertices (ovals) represent
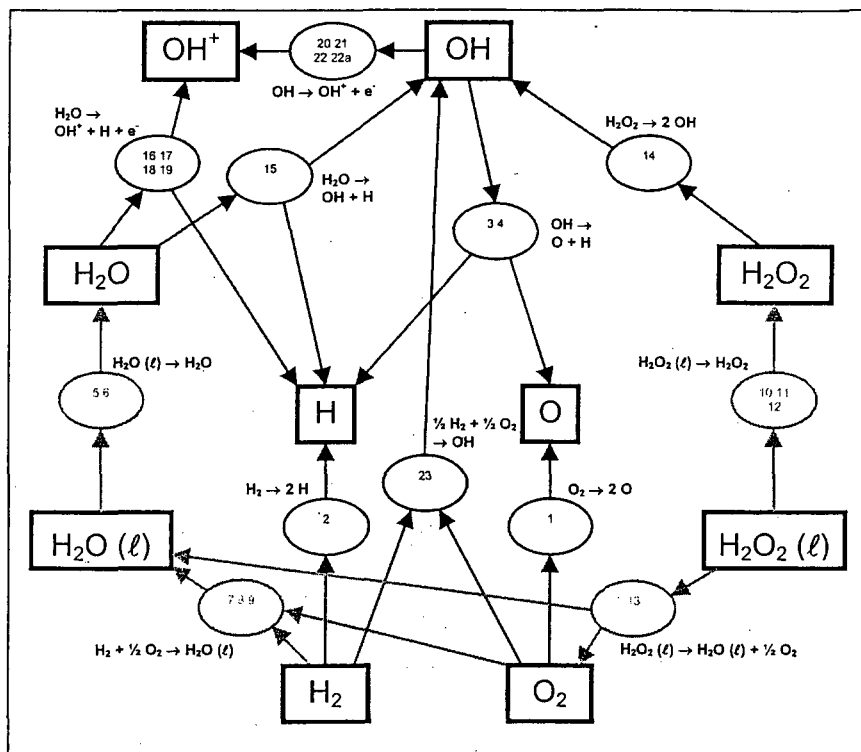
Figure 1. A graphical representation of a small Thermochemical Network.

chemical reactions. The directed edges (arrows) and their weights define participation in the chemical reactions. In general, secondary vertices have multiple degeneracies (competing measurements, denoted by reference numbers in the ovals). Clearly, there are many allowed paths through the graph between two arbitrarily selected primary vertices. The traditional sequential approach uses only a very small subset of possible paths. However, the best solution of the TN is obtained not by selecting a particular path, but by considering and evaluating all paths. This can be accomplished by finding the simultaneous solution of the whole system via minimization of a suitable statistical measure (such as χ^2), provided that the adjunct uncertainties are an honest and realiastic representation of the underlying confidence in the determinations present in the TN. If the latter is not fulfilled, "optimistic" uncertainties will tend to skew the results. Hence, the optimization needs to be preceded by a statistical analysis that will detect and correct possible "optimistic" uncertainties. ATcT currently uses an iterative "*worst offender*" analysis, which has proven to be very successful. The isolation of "offenders" is made possible by the presence of alternative paths in the graph. During each iteration the uncertainty of the current "worst offender" is adjusted by a few percent, and the procedure is repeated until the TN is self-consistent, at which point the final solutions for all primary vertices can be computed. These are then coupled to species-specific information to develop the full complement of thermochemical information.

The current developmental version of ATcT kernel (1.19) has nearly 50,000 lines of code and many user-selectable options. An earlier stable ("production") version is currently running as a web service and is accessible for testing and exploration via the Collaboratory for Multi-Scale Chemical Science (http://cmcs.org).

The development of the Core TN is an ongoing project, which requires a significant effort and utmost care. The Core TN has now been expanded considerably from its initial role of simply providing a test example for ATcT software development. A substantial portion of the underlying data has been critically evaluated, producing revised values for a number of "key" thermochemical quantities. The Core TN is currently encompassing well over 200 thermochemically-distinct species containing H, O, C, N, and halogens, and is growing almost daily.

The development strategy of the Core TN is, to the extent possible, driven by several immediate goals. The first goal, which was to provide definitive ATcT values for the O/H system and to demonstrate the new hypothesis-testing capability, has now been successfully completed. The relevant part of the TN is complete (now including HO_2 thermochemistry, which involved NO_x and halogen thermochemistry, in turn involving the expansion of ATcT such that it can handle correctly aqueous thermochemistry) and has produced new and definitive values (based on current knowledge) for all H/O species. As one of the consequences, the thermochemistry of OH is now so firmly established that it approaches spectroscopic-type of accuracy (effectively removing the OH thermochemistry from the list of possible uncertainties in modeling). The new results involving HO_2 and NO_x have now been successfully used (and verified) by J. Michael (ANL, see accompanying report in this compendium) in explaining new kinetic measurements.

Another initial goal was to improve on the enthalpy of formation (and particularly, on its uncertainty) of C atom in gas phase (equivalent to the vaporization enthalpy of graphite, a 50-year old quandary). This quantity is one of the CODATA "key" thermochemical quantities. *Inter alia*, it acts as a reference value for theoretical calculations that derive thermochemistry via atomization energies. The generally used CODATA value has a surprisingly large uncertainty given its very fundamental nature (± 0.45 kJ/mol, currently the most uncertain atomic species relevant in combustion, albeit a few others that we have also improved on are not much behind). We now have a new value (slightly *outside* the original uncertainty of the CODATA value), but with less than half of the original uncertainty. The improvement was achieved by using all available information in the TN, further amplified by new data arising from the reinterpretation of the spectroscopic data on the dissociation of CO, coupled to targeted state-of-the art computations (in collaboration with A. Csaszar, Eötvös U. Budapest, and J. Stanton, U. Texas Austin), both of which converged to a similar new value for $D_0(CO)$, slightly higher than the previously accepted value, and, by convergence, exerting a synergistic action within the TN. The interesting aspect is that the thermochemistry of C in gas phase has a potential of further steadily improving as the TN is growing. Another interesting aspect is that this a species where one can demonstrate how state-of-the-art theoretical electronic structure calculations can be happily commingled with experimental data to produce improved thermochemistry. This commingling of theory and experiment is one of the salient features of ATcT, leveraging on the high fidelity of modern electronic structure theory, and reflecting the continuing need for experimental validation.

Related to the above topic of reference values for the enthalpies of formation of atoms, as used by theoretical computations, we have new values for several atoms, including an improved value for O (with an uncertainty lower by a factor of 50), halogens, and N (with an uncertainty lower by a factor of almost 9). The latter was achieved by performing targeted photoionization experiments at the ALS/Berkeley, in collaboration with C.-Y. Ng (U. C. Davis) and incorporating the results in the Core TN. The ability to point to new experiments and/or calculations that will most efficiently improve the thermochemical knowledge is another salient feature of ATcT, and is, in fact, by itself a new paradigm leading toward science that will make efficient use of available resources. We are currently conceptually developing automated methods to uncover "weakest links" in TN, which will make use of statistical analyses of the topology of the underlying TN graph.

The Core TN has now been expanded with the relevant C_1 and C_2 chemistry to the point where we are able to start improving on the best available values for the sequential bond energies in methane, ethane, and others. We are also currently in the process of implementing evaluated data from two different IUPAC Task Groups.

Other progress

As part of the IUPAC Task Group on Thermochemistry of Radicals (where the Argonne effort is central to the project success), we are in the process of performing critical and meticulous evaluations of the thermochemistry of a number of small radicals important in combustion and atmospheric chemistry. The resulting "IUPAC recommended values" will be published in a series of papers; Part I as in press.

We have entered into collaboration with C.-Y. Ng (U. C. Davis) to perform a number of thermochemically relevant photoionization measurements at the Chemical Dynamics Beamline at ALS Berkeley, which are driven by deficiencies or inconsistencies in some basic thermochemical quantities that are being uncovered as we are compiling the core Thermochemical Network for ATcT.

In collaboration with R. Botto and T. Kupka (ANL) we have performed a theoretical study of NMR shifts. The effort aims to thoroughly evaluate various computational approaches that may be suitable for routine predictions of NMR shifts by bench chemists and used in the interpretation of spectra.

In our laboratory, we are currently installing and developing a source of radicals for photoionization studies based on laser dissociation. The setup will allow us to explore radicals that are not easily accessible by the in situ chemical reaction method and will also allow thorough pre-testing of complex cases that are best measured at synchrotron facilities.

We have an ongoing collaboration with the group of T. Turany (Eötvös U. Budapest) on extending the Active Table approach to Monte Carlo analysis of reaction mechanisms. We also have an ongoing collaboration with A. Csaszar (Eötvös U. Budapest) and J. Stanton (U. Texas Austin) on computing via state-of-the art theoretical approaches critical thermochemistry of several small radicals (where the choice of targets is driven via Active Tables).

Future Plans

Future plans of this program pivot around further developments of Active Thermochemical Tables, coupled to experimental investigation of radicals and transient species that are intimately related to combustion processes, such as those that potentially define the initial attack of O_2 on hydrocarbon moieties during combustion, as well as other ephemeral species that are implicated in subsequent atmospheric chemistry (particularly hydrocarbon moieties that contain oxygen and/or nitrogen). In collaboration with theorists in the Argonne Chemical Dynamics Group, we also plan on determining in quantitative ways the effect of hindered rotations on thermochemical quantities of both transient and stable species. We also intend to further test and enhance our fitting methods for accurate determination of fragment appearance potentials.

Publications resulting from DOE sponsored research (2002 -)

- *Theoretical Investigation of the Transition States Leading to HCl Elimination in 2-Chloropropene,* B. Parsons, L. Butler, and B. Ruscic, *Mol. Phys.* **100**, 865-874 (2002)
- *On the Enthalpy of Formation of Hydroxyl Radical and Gas-Phase Bond-Dissociation Energies of Water and Hydroxyl,* B. Ruscic, A. F. Wagner, L. B. Harding, R. L. Asher, D. Feller, D. A. Dixon, K. A. Peterson, Y. Song, X. Qian, C. Y. Ng, J. Liu, W. Chen, and D. W. Schwenke, *J. Phys. Chem. A* **106**, 2727-2747 (2002).
- *Toward Hartree-Fock and Density Functional Complete Basis-Set-Predicted NMR Parameters,* T. Kupka, B. Ruscic, and R. E. Botto, *J. Phys. Chem. A.* **106**, 10396-10407 (2002)
- *A Grid Service-Based Active Thermochemical Table Framework,* G. von Laszewski, B. Ruscic, P. Wagstrom, S. Krishnan, K. Amin, S. Nijsure, S. Bittner, R. Pinzon, J. C. Hewson, M. L. Morton, M. Minkoff, and A. F. Wagner, *Lecture Notes in Computer Science* **2536**, Springer, Berlin-Heidelberg (2002), pp 25-38
- *Hartree-Fock and Density Functional Complete Basis Set (CBS) Predicted Nuclear Shielding Anisotropy and Shielding Tensor Components,* T. Kupka, B. Ruscic, and R. E. Botto, *Solid State Nucl. Mag. Res.* **23**, 145-167 (2003)
- *A Framework for Building Scientific Knowledge Grids Applied to Thermochemical Tables,* G. von Laszevski, B. Ruscic, K. Amin, P. Wagstrom, S. Krishnan, and S. Nijsure, *Int. J. High Perform. Comp. Applicat.* **17**, 431-447 (2003)
- *A Divertimento in Thermochemistry: From Photoionization Spectroscopy of Radicals to Active Tables,* B. Ruscic, *Abstr. Pap. 225th ACS National Meeting,* March 23-27, 2003, New Orleans, LA, PHYS-058 (2003)
- *Radical Photoionization Studies with VUV Synchrotron Radiation,* C. Nicolas, M. L. Morton, D. S. Peterka, M. Ahmed, L. Poisson, B. Ruscic, C.-Y. Ng, X. Tang, and T. Zhang, *Abstr. Pap. 225th ACS National Meeting,* March 23-27, 2003, New Orleans, LA, PHYS-269 (2003)
- *Further Refinements of the Bond Dissociation Energy in Water and Hydroxyl Radical Using the Active Thermochemical Table Approach,* B. Ruscic, R. E. Pinzon, M. L. Morton, B. Wang, A. F. Wagner, G. von Laszewski, S. G. Nijsure, K. A. Amin, S. J. Bittner, and M. Minkoff, *Proc. 58th Int. Symp. Mol. Spectrosc.,* June 16-20, 2003, Columbus, OH, WG09 (2003)
- *Metadata in the Collaboratory for Multi-Scale Chemical Science,* C. Pancerella, J. D. Myers, T. C. Allison, K. Amin, S. Bittner, B. Didier, M. Frenklach, W. H. Green, Jr., Y.-L. Ho, J. Hewson, W. Koegler, C. Lansing, D. Leahy, M. Lee, R. McCoy, M. Minkoff, S. Nijsure, G. von Laszewski, D. Montoya, R. Pinzon, W. Pitz, L. Rahn, B. Ruscic, K. Schuchardt, E. Stephan, A. Wagner, B. Wang, T. Windus, L. Xu, C. Yang (full peer reviewed paper for Dublin Core Conf. DC-2003, Sept 28 - Oct. 2, Seattle, WA, published electronically at http://www.siderean.com/dc2003/401_Paper67.pdf)
- *Refinements of the Bond Dissociation Energy of Carbon Monoxide and of the Enthalpy of Formation of Carbon Atom in Gas Phase Using the Active Thermochemical Tables Approach,* B. Ruscic, R. E. Pinzon, M. L. Morton. A. G. Csaszar, J. F. Stanton, M. Kallay, and G. von Laszewski, *Proc. 59th Int. Symp. Mol. Spectrosc.,* June 21-25, 2004, Columbus, OH (2004) *(in press)*
- *IUPAC Critical Evaluation of Thermochemical Properties of Selected Radicals: Part I,* B. Ruscic, J. E. Boggs, A. Burcat, A. G. Csaszar, J. Demaison, R. Janoschek, J. M. L. Martin, M. L. Morton, M. J. Rossi, J. F. Stanton, P. G. Szalay, P. R. Westmoreland, F. Zabel, and T. Berces, *J. Phys. Chem. Ref. Data* **33**, 000-000 (2004) *(in press)*
- *Comparing Optimized vs. Experimental Geometries in GIAO NMR Calculations Employing the Complete Basis Set (CBS) Limit Approach,* T. Kupka, B. Ruscic, and R. Botto, *J. Comp. Chem.* **25**, 0000-0000 (2004) (submitted)
- *Active Thermochemical Tables,* B. Ruscic, in: *2005 Yearbook of Science and Technology* (yearly update to *Encyclopedia of Science and Technology*), McGraw-Hill, New York (2004) (submitted)

Toward Subchemical Accuracy in Computational Thermochemistry: Focal Point Analysis of the Heat of Formation of NCO and [H,N,C,O] Isomers

Henry F. Schaefer III

Center for Computational Chemistry, University of Georgia

Athens, GA, 30602-2525

Email: hfs@uga.edu

(706)542-2067

The role of isocyanic acid (HNCO) in the reduction of nitrogenous by-products of combustion processes has been the subject of intense study for some time. In large measure this interest has been driven by the role HNCO plays in the RAPRENOx process, by which NO_x in effluent streams is reduced to more innocuous species such as N_2, H_2O and CO_2. In addition, the cyanato radical (NCO) is a key intermediate in RAPRENOx and other combustion processes and has itself been the subject of extensive investigation.

In continuing pursuit of thermochemical accuracy to the level of 0.1 kcal mol^{-1}, the heats of formation of NCO, HNCO, HOCN, HCNO, and HONC have been rigorously determined using state-of-the-art *ab initio* electronic structure theory, including conventional coupled cluster methods [CCSD, CCSD(T), CCSDT] with large basis sets, conjoined in cases with explicitly-correlated MP2-R12/A computations. Limits of valence and all-electron correlation energies were extrapolated via focal point analysis using correlation consistent basis sets of the form cc-pVXZ (X = 2-6) and cc-pCVXZ (X = 2-5), respectively. In order to reach subchemical accuracy targets, core correlation, spin-orbit coupling, special relativity, the diagonal Born-Oppenheimer correction (DBOC), and anharmonicity in zero-point vibrational energies (ZPVEs) were accounted for. Various coupled-cluster schemes for partially including connected quadruple excitations were also explored, although none of these approaches gave reliable improvements over CCSDT theory. Based on numerous, independent thermochemical paths, each designed to balance residual *ab initio* errors, our final proposals are made.

For the cyanato radical and isocyanic acid, we determine $\Delta H^{\circ}_{f,0}$(NCO) = +30.5 kcal mol^{-1} and $\Delta H^{\circ}_{f,0}$(HNCO) = −27.6 kcal mol^{-1}. The considerable breadth and remarkable internal consistency of our data suggests errors bars of ±0.2 kcal mol^{-1} for these quantities. Among the numerous experimental determinations of these heats of formation, our conclusions best compare with the 1996 spectroscopic results of Zyrianov, Droz-Georget, Sanov, and Reisler, $\Delta H^{\circ}_{f,0}$(NCO) = +30.3 ± 0.4 kcal mol^{-1} and $\Delta H^{\circ}_{f,0}$(HNCO) = −27.8 ± 0.4 kcal mol^{-1}. Such accord between theory and experiment would be virtually unparalleled for species with more than 20 electrons. Based on our heat of formation of isocyanic acid, we ascertain $\Delta H^{\circ}_{f,0}$(HOCN) = −3.1, $\Delta H^{\circ}_{f,0}$(HCNO) = +40.9, and $\Delta H^{\circ}_{f,0}$(HONC) = +56.3 kcal mol^{-1}, with uncertainties of only a few tenths of a kcal mol^{-1} in the first and last cases. For fulminic acid (HCNO) the uncertainty is

somewhat larger, owing to poorer correlation convergence in the computed isomerization energy and an enormous anharmonicity in the zero-point vibrational energy of this quasilinear molecule.

Enthusiasm for the apparent near-achievement of subchemical accuracy in this study for the target heats of formation must be tempered by admission of possible sources of significant systematic error. First, the adopted empirical reference enthalpies may have errors considerably larger than the stated uncertainties, as demonstrated by the recent work of numerous collaborators which revised the heat of formation of the hydroxyl radical by 0.5 kcal mol^{-1}. Second, our calibrations on dissociation energies of multiple bonds indicate that several available schemes for partially including connected quadruple excitations within the coupled-cluster formalism not only fail to provide reliable improvements over CCSDT theory but often significantly deteriorate the excellent bond-energy predictions already given by this established method. Therefore, we have based our conclusions on energies for our error-balanced reactions discerned from CCSDT theory in the complete basis set limit, even though scattered quadruples increments of several tenths of a kcal mol^{-1} were often observed. With the advent of correlation-consistent basis set extrapolations and the development of explicitly correlated methods, the practical determination of accurate post-CCSDT corrections is now perhaps the chief obstacle to the achievement of true subchemical accuracy in computational thermochemistry. It is encouraging that meaningful full CCSDTQ computations may become possible for systems with 3-4 heavy atoms in the near future. However, highlighting the problem of post-CCSDT effects in numerous computational applications should promote further research in this area and perhaps spawn novel ideas applicable to larger systems.

Publications Supported by DOE: 2002, 2003, 2004

1. F. Stahl, P. R. Schleyer, H. F. Schaefer, and R. I. Kaiser, "The Reactions of Ethynyl Radicals as a Source C_4 and C_5 Hydrocarbons in Titan's Atmosphere," *Planetary and Space Sciences* **50**, 685 (2002).

2. B. G. Rocque, J. M. Gonzales, and H. F. Schaefer, "An Analysis of the Conformers of 1,5-Hexadiene," *Ernest R. Davidson Issue, Mol. Phys.* **100**, 441 (2002).

3. I. Hahndorf, Y. T. Lee, R. I. Kaiser, L. Vereecken, J. Peeters, H. F. Bettinger, P. R. Schreiner, P. R. Schleyer, W. D. Allen, and H. F. Schaefer, "A Combined Crossed-Beam, *Ab Initio*, and Rice-Ramsperger-Kassel-Marcus Investigation of the Reaction of Carbon Atoms $C(^3P_j)$ with Benzene, $C_6H_6(\tilde{X}\,^1A_{1g})$ and d_6-Benzene, $C_6D_6(\tilde{X}\,^1A_{1g})$," *J. Chem. Phys.* **116**, 3248 (2002).

4. L. Vereecken, J. Peeters, H. F. Bettinger, R. I. Kaiser, P. R. Schleyer, and H. F. Schaefer, "Reaction of Phenyl Radicals with Propyne," *J. Amer. Chem. Soc.* **124**, 2781 (2002).

5. J. C. Reinstra-Kiracofe, G. S. Tschumper, H. F. Schaefer, S. Nandi, and G. B. Ellison, "Atomic and Molecular Electron Affinities: Photoelectron Experiments and Theoretical Computations," *Chem. Revs.* **102**, 231 (2002).

6. N. R. Brinkmann, N. A. Richardson, S. S. Wesolowski, Y. Yamaguchi, and H. F. Schaefer, "Characterization of the $\tilde{X}^2A_1$ and $\tilde{a}\,^4A_2$ Electronic States of CH_2^+," *Chem. Phys. Lett.* **352**, 505 (2002).

7. R. I. Kaiser, I. Hahndorf, O. Asvany, Y. T. Lee, L. Vereecken, J. Peeters, H. F. Bettinger, P. R. Schleyer, and H. F. Schaefer, "Neutral-Neutral Reactions in the Interstellar Medium: Elementary Reactions of C_6H_5 and C_6H_6," *Astronomy and Astrophysics*, **406**, 385 (2003).

8. R. I. Kaiser, F. Stahl, P. R. Schleyer, O. Asvany, Y. T. Lee, and H. F. Schaefer, "Atomic and Molecular Hydrogen Elimination in the Crossed Beam Reaction of d_1-Ethynyl Radicals $C_2D(\tilde{X}\,^2\Sigma^+)$ with Acetylene, $C_2H_2(\tilde{X}\,^1\Sigma_g^+)$: Dynamics of d_1-Diacetylene (HCCCCD) and d_1-Butadiynyl (DCCCC) Formation," *Phys. Chem. Chem. Phys.* **4**, 2950 (2002).

9. N. D. K. Petraco, W. D. Allen, and H. F. Schaefer, "The Fragmentation Path for Hydrogen Atom Dissociation from Methoxy Radical," *J. Chem. Phys.* **116**, 10229 (2002).

10. L. Horny, N. D. K. Petraco, C. Pak, and H. F. Schaefer, "What Is the Nature of Polyacetylene Neutral and Anionic Chains $HC_{2n}H$ and $HC_{2n}H^+$ (n = 6-12) that Have Been Recently Observed in Neon Matrices?" *J. Amer. Chem. Soc.* **124**, 5861 (2002).

11. P. Jensen, S. S. Wesolowski, N. R. Brinkmann, N. A. Richardson, Y. Yamaguchi, H. F. Schaefer, and P. R. Bunker, "A Theoretical Study of $\tilde{a}\,^4A_2$ CH_2^+," *J. Mol. Spectrosc.* **116**, 10229 (2002).

12. D. Moran, F. Stahl, E. D. Jemmis, H. F. Schaefer, and P. R. Schleyer, "Structures, Stabilities and Ionization Potentials of Dodecahedane Endohedral Complexes," *J. Phys. Chem. A* **106**, 5144 (2002).

13. Q. Li, J. F. Zhao, Y. Xie, and H. F. Schaefer, "Electron Affinities, Molecular Structures, and Thermochemistry of the Fluorine, Chlorine, and Bromine Substituted Methyl Radicals," Invited Article, *Mol. Phys.* **100**, 3615 (2002).

14. F. Stahl, P. R. Schleyer, H. Jiao, H. F. Schaefer, K.-H. Cheu, and N. L. Allinger, "The Resurrection of Neutral Tris-Homoaromaticity," *J. Org. Chem.* **67**, 6599 (2002).

15. K. W. Sattelmeyer and H. F. Schaefer, "The v_5 Vibrational Frequency of the Vinyl Radical: Conflict Between Theory and Experiment," *J. Chem. Phys.* **117**, 7914 (2002).

16. Y. Xie, W. Wang, K. Fan, and H. F. Schaefer, "The Ring Structure of the NO Dimer Radical Cation: A Possible New Assignment of the Mysterious IR Absorption at 1424 cm^{-1}," *J. Chem. Phys.* **117**, 9727 (2002).

17. L. Horny, N. D. K. Petraco, and H. F. Schaefer, "Odd Carbon Long Linear Chains $HC_{2n+1}H$ (n = 4-11): Properties of the Neutrals and Radical Anions," *J. Amer. Chem. Soc.* **124**, 14716 (2002).

18. P. R. Schreiner, A. A. Fokin, P. R. Schleyer, and H. F. Schaefer, "Model Studies on the Electrophilic Substitution of Methane with Various Electrophiles E (E = NO_2^+, F^+, Cl^+, Cl_3^+, HBr_2^+, HCO^+, OH^+, H_2O-OH^+, and Li^+)," *Fundamental World of Quantum Chemistry; A Tribute Volume to the Memory of Per-Olov Löwdin,* Editors E. J. Brändas and E. S. Kryachko (Kluwar, Dordrecht, Holland, 2003), Volume 2, pages 359-386.

19. J. P. Kenny, W. D. Allen, and H. F. Schaefer, "Complete Basis Set Limit Studies of Conventional and R12 Correlation Methods: The Silicon Dicarbide (SiC_2) Barrier to Linearity", *J. Chem. Phys.* **118**, 7353 (2003).

20. A. A. Fokin, P. R. Schreiner, S. I. Kozhushkov, K. Sattelmeyer, H. F. Schaefer, and A. de Meijere, "Delocalization in Sigma Radical Cations: The Intriguing Structures of Ionized [n] Rotanes", *Organic Letters* **5**, 697 (2003).

21. E. F. Valeev, W. D. Allen, R. Hernandez, C. D. Sherrill, and H. F. Schaefer, "On the Accuracy of Atomic Orbital Expansion Methods: Explicit Effects of k Functions on Atomic and Molecular Energies", *J. Chem. Phys.* **118**, 8594 (2003).

22. B. Papas, S. Wang, N. DeYonker, and H. F. Schaefer, "The Naphthalenyl, Anthracenyl, Tetracenyl, and Pentacenyl Radicals, and their Anions", *J. Phys. Chem. A.* **107**, 6311 (2003).

23. K. Sattelmeyer, H. F. Schaefer, and J. F. Stanton, "Use of 2h and 3h-p- like Coupled-Cluster Tamm-Dancoff Approaches for the Equilibrium Properties of Ozone", *Chem. Phys. Lett.* **378**, 42 (2003).

24. N. R. Brinkmann, G. S. Tschumper, G. Yan, and H. F. Schaefer, "An Alternate Mechanism for the Dimerization of Formic Acid", *J. Phys. Chem.* **107**, 10208 (2003).

25. K. W. Sattelmeyer, Y. Yamaguchi, and H. F. Schaefer, "Energetics of the Low-Lying Isomers of HCCO", *Chem. Phys. Lett.* **383**, 266 (2004).

26. L. D. Speakman, B. N. Papas, H. L. Woodcock, and H. F. Schaefer, "A Reinterpretation of Microwave and Infrared Spectroscopic Studies of Benzaldehyde", *J. Chem. Phys.* **120**, 4247 (2004).

27. R. D. DeKock, M. J. McGuire, P. Piecuch, W. D. Allen, H. F. Schaefer, K. Kowalski, S. A. Spronk, D. B. Lawson, and S. L. Laursen, "The Electronic Structure and Vibrational Spectrum of *trans*-HNOO", *J. Phys. Chem. A* **108**, 2893 (2004).

28. M. Schuurman, S. Muir, W. D. Allen, and H. F. Schaefer, "Toward Subchemical Accuracy in Computational Thermochemistry: Focal Point Analysis of the Heat of Formation of NCO and [H, N, C, O] Isomers", *J. Chem. Phys.*

29. Y. Yamaguchi and H. F. Schaefer, "The Diazocarbene (CNN) Molecule: Characterization of the $\tilde{X}\,^3\Sigma^-$ and $\tilde{A}\,^3\Pi$ Electronic States", *J. Chem. Phys.*

Spectroscopy and Dynamics of Transient Species

Trevor J. Sears, *Department of Chemistry, Brookhaven National Laboratory, Upton, NY 11973-5000*
(*sears@bnl.gov*)

Program Scope

High resolution spectroscopy, augmented by theoretical and computational methods, is used to investigate the structure and reactivity of chemical intermediates in the elementary gas phase reactions involved in combustion chemistry and in chemical processes occurring at or near surfaces of heterogeneous catalysts. Techniques to improve the sensitivity of laser absorption spectroscopy are developed as are models of intra-and inter-molecular interactions in molecular free radicals and other reactive species. The results lead to improved understanding and modeling of processes involving these species and are applicable to a wide variety of practical problems.

Recent Progress

Dynamical aids to assignment in the spectroscopy of methylene

We have exploited the tools of photodissociation dynamics and nonequilibrium kinetics for the purpose of extending, confirming, and correcting spectroscopic assignments in the notoriously challenging $\tilde{b}^1B_1 \leftarrow \tilde{a}^1A_1$ spectrum of methylene. Following the production of singlet methylene by 308 nm photolysis of ketene (CH_2CO), transient FM absorption spectra in the near-infrared have been collected under stable, low pressure conditions. Nascent line widths vary systematically with the energy of the detected rovibronic state, as do the initial relaxation kinetics prior to establishment of a steady-state rotational distribution near room temperature. Calibrating these properties with a set of assigned lines provides a guide to the identification of previously unassigned lines in the complex spectrum. This information led to new or corrected assignments of many spectral lines, including the assignment of new spectral features involving higher-lying rotational levels than had previously been identified in the radical. A statistical analysis of the distribution of observed absorption line intensities compared to that calculated for the Renner-Teller mixed singlet states in the absence of triplet perturbation results in compelling evidence for a lack of frequent, strong, triplet perturbations in the $\tilde{b}^1B_1$ state. Additional measurements of the time dependent populations of individual CH_2 $\tilde{a}^1A_1$ state rotational levels has led to new insights into the rate of collisional ISC in methylene. This is discussed in Greg. Hall's abstract.

Technical improvements to FM spectrometer

We have modified one of our spectrometers to operate at radio sideband frequencies of close to 1 GHz, compared to the 190 MHz we have used in the past. The increase in sideband frequency has provided, as expected, an increase in absorption sensitivity. A disadvantage is the more complex line shape functions observed, due to the greater dispersion contribution at the larger sideband frequencies. Practically, the limitation to a further increase in operating frequency (and a theoretical further increase in sensitivity) is the unavailability of high-speed photodiodes with adequate optical power handling capacity for our requirements. Reducing the optical power on the detector to remain inside the linear and safe operating regime for a higher speed diode reduces the ultimate detection limits simply because of the statistics associated with the smaller number of photons incident on the detector per detection time interval.

Hot band transitions in HCCl

In order to measure and characterize the fundamental vibrational intervals in the ground state of the HCCl radical, we have recorded bands to the red of the band origin of the $\tilde{A}^1A'' \leftarrow \tilde{X}^1A'$ spectrum. Surprisingly, only the ν_3 (C-Cl stretching) vibration in HCCl has previously been measured at high resolution. We have recorded and are analyzing the (000) – (010) band and should also be able to record the, weaker, (000)-(011) band at longer wavelengths. These bands include axis switching-induced

rotational sub-bands (see below) which will give additional information on the structural changes occurring on excitation of ground state vibrational modes. We are also extending our previous *ab initio* calculations to calculate the position of the low-lying triplet excited state as an aid to interpretation of fluorescence spectra recently obtained by B.-C. Chang in Taiwan.

Axis-switching in floppy molecules
Axis-switching is a phenomenon that occurs in electronic spectra of polyatomic molecules when there is a large difference between the equilibrium geometries of the connected states. It leads to the appearance of new rotational sub-bands in the spectrum, and modifies the rotational line intensities in the normal sub-bands. We recorded have spectra of both HCCl and HCBr in which the upper states exhibits large amplitude bending motion (LAM). The standard spectroscopic model, which we have successfully used to interpret the observed structure in other bands in the spectra of these species, underestimates the effect compared to what is observed. This was not unexpected since this model is based on the concepts of small, harmonic, displacements from a rigid equilibrium structure. We developed an extension of our K-dependent adiabatic model for the rovibronic levels of this type of radical, but its predictions also depart from the observations for the observed levels exhibiting LAM. Further work directed towards understanding this problem and resolving the remaining disagreements between experiment and theory is planned.

Future Plans
Coordinatively unsaturated metal-containing species
Using various high resolution ion spectroscopic methods and in collaboration with Prof. P. Johnson and student H. Mann at Stony Brook University, we are recording spectra of small niobium metal and niobium carbide clusters. These met-car precursors are theoretically predicted to possess electronic configurations that are similar in many ways to those of the equivalent sub-structures in large met-car clusters that have been shown to be exceptionally chemically interesting. This work relates to other experimental and theoretical work in the area of nano-catalysis in the chemistry department at BNL.

Spectroscopy of other combustion-related free radicals
Cyano-formyl radical (OCCN) is related to the well-known HCO radical which is ubiquitous in hydrocarbon flames. Surprisingly, there is almost no spectroscopic information on this species. H.-L. Dai (Penn) has recently reported low resolution IR emission spectra in which the strongest vibrational fundamental was identified, however there is no other experimental work reported in the literature. Computational work by J. Francisco (Purdue) suggests that the electronic structure is (as expected) analogous to HCO, and one therefore expects an extended electronic band system in the near-IR and visible part of the spectrum. We plan to search for the high resolution electronic spectrum of this species using FM laser absorption or LIF in the near-IR making use of a newly acquired near-IR phototube. The radical will be made from carbonyl cyanide ($CO(CN)_2$), or methyl cyanoformate($CO(CN)(OCH_3)$), both of which have been shown to produce the radical on UV photolysis.

In collaboration with J. Francisco (Purdue) and R. Buenker (Wuppertal), we are planning to revisit the spectrum of CCBr. Rotational structure in a band recorded in our laboratory and tentatively attributed to CCBr, was assigned several years ago. However, the nature of the electronic transition involved was not clear and existing quantum chemical calculations did not address states above the lowest excited state, which was predicted to lie at an energy of less than 4000 cm^{-1}. With rapidly increasing access to larger levels of computer power, accurate predictions of the positions and character of higher states should be possible, as should the energies of high vibrational levels in the lowest excited state, that may also be contributing to our observed spectrum.

Improved detectors for FM laser absorption experiment

The ultimate sensitivity of our FM laser absorption experiment is governed by the statistics of the number of photons incident on the detector. With the very small area detectors required for a response speed appropriate to sideband spacings of the order of 1GHz, the optical power handling capacity of the photodiode becomes a serious limitation. In collaboration with scientists in the Instrumentation Division at BNL, we are planning to investigate modified silicon-based devices that will permit higher d.c. power levels, while maintaining the necessary response speed. Potentially, this could lead to a dramatic increase in the absolute sensitivity of the experiment.

Nano-crystal precursors: Spectroscopy of metal-centered radicals

Recent computational work in the group has shown that the nano-crystalline met-car material Ti_8C_{12}, and possibly higher members such as $Ti_{14}C_{13}$, can be thought of as built up from several isomeric modifications of the TiC_2 moiety. In order to test the accuracy of the state-of-the-art computational work, experimental information on this important building block is most desirable. One would like to get this from accurate spectroscopic measurements that probe the structure and electronic character of the species. However, it is still true that the existing high resolution spectroscopic work on metal containing radicals is mostly limited to diatomic species that have been studied by laser induced fluorescence (LIF) during the past 30 years. Some new approaches to attack the problem are evidently required. We plan a multi-pronged attack directed towards observing high resolution spectra of this type of species.

Initial efforts have begun in collaboration with P. Johnson (USB). It is predicted that the carbides should have relatively low ionization potentials, and this has been demonstrated by others to be true in (for example) Nb_xC_y for many small clusters ($x + y < \sim 10$). In fact, the IP's are accessible to doubled dye or OPO/OPA lasers since they correspond to wavelengths longer than 200 nm. This observation opens up the possibility for high resolution ionization-based spectroscopies such as ZEKE/PFI or MATI. Since the ionization can be carried out resonantly, it is likely to be considerably more sensitive than MPI-based spectroscopic experiments that have, in the past, failed to detect small early transition metal-carbide species.

New near-IR dispersed laser induced fluorescence experiment

In order to extend our experimental capabilities, and improve the detection efficiency of the LIF experiment at BNL, we propose to combine a 1 meter monochromator with a recently acquired near-IR phototube. In this way, dispersed laser fluorescence may be collected following excitation using pulsed red or near-IR dye, OPO/OPA, or our Ti:sapphire ring lasers. The metal-containing species possess many low-lying electronic states due to multiple unoccupied low-lying molecular orbitals, derived form the incompletely filled metal d-orbitals. For the smaller species that fluoresce, dispersed fluorescence at near-IR wavelengths will provide an overview of the optically accessible low-lying electronic states for comparison to computational results and a road map for future high resolution work.

Publications 2001-

Absorption spectroscopy of singlet CH_2 near 11200 cm^{-1}
K. Kobayashi and T. J. Sears, *Can J. Phys.* **79**, 347-358 (2001).
Experimental and theoretical studies of the near-IR spectrum of bromomethylene
H. –G. Yu, T. Gonzalez-Lezana, A.J. Marr, J. T. Muckerman, and T. J. Sears, *J. Chem. Phys.* **115**, 5433-5444 (2001).
A theoretical study of the potential energy surface for the reaction $OH+CO=H+CO_2$
H. –G. Yu, J. T. Muckerman, and T. J. Sears, *Chem. Phys. Letts.* **349**, 547-554. (2001).
A K-dependent adiabatic approximation to the Renner-Teller effect for triatomic molecules
H. –G. Yu, J. T. Muckerman, and T. J. Sears, *J. Chem. Phys.* **116**, 1435-1442 (2002).
Rovibronic energies of CH_3^+
H. –G. Yu and T. J. Sears, *J. Chem. Phys.* **117**, 666-669 (2002).

The E-X spectrum of jet-cooled TiO observed in absorption

K. Kobayashi, G. E. Hall, J. T. Muckerman, T. J. Sears, and A. J. Merer, *J. Molec. Spectrosc,* **212**, 133-141 (2002).

Axis-switching and Coriolis coupling in the A (010)-X (000) transitions of HCCl and DCCl

A. Lin, K. Kobayashi, H.-G. Yu, G. E. Hall, J. T. Muckerman, T. J. Sears, and A. J. Merer, *J. Molec. Spectrosc.* **214**, 216-224 (2002).

Hot bands in the *A-X* spectrum of HCBr

B. –C. Chang, J. Guss and T. J. Sears, *J. Molec. Spectrosc.* **219**, 136-144 (2003).

The photodissociation of bromoform at 248 nm: Single and multiphoton processes

P. Zou, J. Shu, T. J. Sears, G. E. Hall and S. W. North, *J. Phys. Chem A* **108**, 1482-1488 (2004).

Doppler-resolved spectroscopy as an assignment tool in the spectrum of singlet methylene

G. E. Hall, A. Komissarov and T. J. Sears, *J. Phys Chem A.* (in press, 2004)

The vibrational dependence of axis-switching in triatomic spectra

H. G. Yu, G. E. Hall, J. T. Muckerman and T. J. Sears, *J. Chem. Phys.* (submitted, 2004)

Picosecond Nonlinear Optical Diagnostics

Thomas B. Settersten
Combustion Research Facility, Sandia National Laboratories
P.O. Box 969, MS 9056
Livermore, CA 94551-0969
tbsette@sandia.gov

Program Scope

This program focuses on the development of innovative laser-based detection strategies for important combustion radicals and the investigation of the fundamental physical and chemical processes that directly affect quantitative application of these techniques. These investigations include the study of fundamental spectroscopy, energy transfer, and photochemical processes. This aspect of the research is essential to the correct interpretation of diagnostic signals, enabling reliable comparisons of experimental data and detailed combustion models. These investigations use custom-built tunable picosecond (ps) lasers, which enable efficient nonlinear excitation, provide high temporal resolution for pump/probe studies of collisional processes, and are amenable to detailed physical models of laser-molecule interactions.

Recent Progress

Imaging of atomic oxygen. Atomic oxygen is a critical combustion intermediate that can be detected using two-photon excitation near 226 nm and fluorescence detection at 845 nm. Its detection in flames, however, is hindered by photolytic production of atomic oxygen. While it is commonly assumed that O_2 photolysis via Schumann-Runge transitions is a significant interference to LIF detection of atomic oxygen in flames, our pump-probe experiments demonstrated that this process contributed negligibly. We identified CO_2 as the important photolytic precursor in diffusion and premixed flames using methane as the fuel. Because the rate for photolytic production of atomic oxygen from vibrationally excited CO_2 scales linearly with laser intensity and the two-photon excitation rate scales quadratically with intensity, the use of ps lasers, as opposed to nanosecond (ns) lasers, significantly reduces the pulse energy required for nonlinear excitation and can reduce concomitant photochemistry that often corrupts measurements obtained with ns excitation. In collaboration with Jonathan Frank, we directly compared ps and ns excitation for interference-free imaging applications, and we demonstrated approximately 10 times more sensitive detection of atomic oxygen using ps excitation. Recently, we successfully extended this work to produce interference-free 2-D images of atomic oxygen in flow-flame interaction experiment (for details, see abstract by J.H. Frank in this volume).

Atomic hydrogen detection. In collaboration with Robert Lucht (Purdue) and Sukesh Roy (ISSI), we launched a joint experimental and theoretical investigation of the detection of atomic hydrogen in flames with a two-color polarization spectroscopy technique that used a single ps laser. The use of ps excitation may substantially reduce sensitivity to changes in the collisional environment and may reduce photolytic interference in combustion applications. For the initial

1

experiments, we built a Distributed Feedback Dye Laser (DFDL) producing 75-ps pulses at 486 nm. We used a small fraction of the 486-nm output to probe the $4p\,^2P_{1/2,3/2} \leftarrow 2s\,^2S_{1/2}$ transition, and frequency-doubled the remaining output to produce a 243-nm pump beam that pumped the two-photon $2s\,^2S_{1/2} \leftarrow\leftarrow 1s\,^2S_{1/2}$ transition. In a substantial parallel effort, a multi-state formalism of the time-dependent density matrix equations (including the Zeeman-state structure and hyperfine splitting of the energy levels) is being developed to simulate the experiment. The time-dependent, density-matrix equations are solved by direct numerical integration (DNI). Comparison of model prediction and experimentally measured power broadening and shifting of the two-photon resonance has been used for model validation, and we are analyzing data currently to extract population relaxation and coherence dephasing rates.

Ground-state population dynamics. We initiated investigations of OH ground-state RET using single-mode ps laser pulses ($\sim$50 ps) that provide adequate temporal resolution for time-resolved studies of RET in atmospheric-pressure flames and sufficient spectral resolution for state-resolved excitation. In this work, we used ps two-color polarization spectroscopy (TC-PS), in which a ps UV pulse probed the spatial anisotropy in the distribution of m_J levels in $X\,^2\Pi_{3/2}(v = 1, N)$ induced by a ps IR pulse. The m_J state distribution can be described in terms of three tensor density matrix elements (multipole moments), which correspond to population, orientation and alignment, respectively. A linearly-polarized IR laser generates an aligned m_J distribution, while a circularly-polarized IR laser generates an oriented m_J distribution. Collisions occurring after the IR pulse randomize the induced anisotropy, and in general, the multipole moments decay with different rates that depend on the experimental conditions. By time delaying the probe pulse we observed the rate of alignment or orientation decay depending on the IR laser polarization. Previous studies have used single-color PS, which is sensitive to anisotropy in both the excited and ground state. This ambiguity is removed in our two-color experiment. We also probed states not directly coupled by the IR transition, and it was possible to observe TC-PS signal resulting from inelastic collisions (RET) that preserved some degree of anisotropy. Our results demonstrated the high sensitivity of TC-PS and its immunity to the thermal background that hinders the use of LIF-based detection for ground-state RET studies in flames.

Future Plans

Fluorescence quenching. We propose a substantial effort in the next review period to develop accurate predictive models for the quenching of fluorescence from CO $B\,^1\Sigma^+(v = 0)$ and NO $A\,^2\Sigma^+(v = 0)$. This research builds on our previous success using time-resolved ps-LIF to measure temperature- and species-dependent cross sections for these species. We will also develop quenching models for O $(3p\,^3P)$ and H (n=3) in support of our continuing and proposed work on two-photon ps-LIF detection of these species. We propose to extend our measurements to temperatures approaching 2000 K using premixed, low-pressure flames. Using our time-resolved ps-LIF apparatus, we can very accurately measure fluorescence lifetimes, which will be on the order of 2 ns or longer under low-pressure flame conditions. We will infer quenching cross sections from the measured lifetimes in a series of engineered flames using the computed species concentrations and measured temperature in each flame. The higher-temperature data will enable the development and validation of comprehensive quenching models. Initial work will focus on the design, construction, and characterization of a low-pressure flame facility. A variety of premixed low-pressure flames, using various fuels, oxidizers, diluents, and flow rates will be utilized to achieve the desired conditions.

2

Photolytic interferences. We have shown compelling evidence for the photolytic production of atomic oxygen from vibrationally excited CO_2 in flames and demonstrated the significance of this interference to two-photon LIF detection of atomic oxygen using excitation at 226 nm. This process also interferes with two-photon detection of CO using excitation at 230 or 217 nm. Continuing to collaborate with Jonathan Frank, we will measure the temperature- and wavelength-dependent photolysis yields of $O(2p\,^3P)$ and $CO(X\,^1\Sigma)$ from CO_2. The experiment will employ either an excimer laser at 193 nm or a tunable ns laser to photodissociate CO_2 in a high-temperature fluorescence cell. A delayed ps laser will probe the products with two-photon LIF detection of CO and O. Time-resolved fluorescence detection will be employed to correct for the effect of fluorescence quenching. Absolute calibration of the CO LIF detection will be determined by seeding the flow with a known concentration of CO. Because the photodissociation of CO_2 results in equal concentration of CO and O, this absolute calibration can be used to calibrate the O LIF detection scheme. Saturation with increasing laser energy of the photolysis processes will be characterized. We will compile these results in the form of a model that can be incorporated in comprehensive two-photon LIF models for the detection of CO and O. The results of this proposed work will be used in the development of an absolute in situ calibration technique for two-photon LIF detection of atomic oxygen using facile photolysis of CO_2 that is either naturally present in the flame or seeded for the purpose of the calibration. Similar pump-probe experiments will be conducted to characterize the photolytic production of atomic hydrogen that occurs when two-photon excitation at 205 nm is employed in flames.

Hydroxyl ground-state population dynamics. In the previous review period, we made significant progress on the development of ps TC-PS for the study of collisional dynamics in the ground state. The time resolution afforded by ps laser pulses and the quantum state selectivity of TC-PS enabled measurement of the relaxation times of alignment and orientation for the ground state of OH. In the coming year, we propose to measure the individual decay rates for population, orientation, and alignment in OH $X\,^2\Pi_{3/2}(v = 1, N)$. For this work, we will use ps two-color resonant four-wave mixing (TC-RFWM) in the grating geometry, which allows control over the polarization of all four fields that take part in the four-wave mixing process. Our initial model development, using the spherical tensor formalism, identifies polarization schemes that isolate signals arising solely from alignment or orientation gratings in the ground state. Furthermore, we identify other polarization schemes that give rise to signals that are primarily due to population gratings ($> 98\%$). This experimental effort will require substantial model development, which is also proposed. We initiated collaboration with Robert Lucht and Sukesh Roy to model ps TC-PS. The theoretical derivations are now complete, and we propose to implement this formalism in a numerical model. This model will solve the density matrix equations in terms of all m_J levels, and it will include a large relaxation matrix containing all state-to-state and coherence dephasing rates. We will be able to explicitly calculate the time evolution of the multipole moments and determine their relaxation rates as a function of the collision model used in formulation. This will guide our proposed development of a model of far fewer dimensions that will track the time evolution of the multipole moments using the spherical tensor formalism.

Nitric oxide ground-state population dynamics. Laser-induced fluorescence is commonly used for measurement of nitric oxide in combustion systems. For high-pressure applications, it is not clear whether population cycling is important. Population cycling refers to the process by which a molecule is excited multiple times by the same laser pulse. This occurs when collisions rapidly quench laser-excited molecules to the ground state and subsequent rapid RET in the ground

state refills the laser-pumped level during a saturating laser pulse. The fate of quenched NO molecules is not known currently, and the effects of ground-state refilling are uncertain. We propose collaborative experiments (Volker Sick, U. Mich.; John Daily, U. Colorado; Helmut Kronemayer and Christof Schulz, U. Heidelberg) to investigate potential cycling of NO population during a saturating ns laser pulse used for LIF measurements. A rate-equation-based model is being used to identify operating conditions for the experiment and to evaluate experimental measurements. Dilute samples (<10 ppm) of NO in a bath gas of N_2 and O_2, CO_2, or H_2O will be prepared in a low-pressure flow cell. An intense ns laser will saturate a transition in the NO $A - X$ (0,0) band, and a weak ps pulse will probe the pumped level via LIF excited by a single rotational line in the NO $A - X$ (1,0) band. A grating monochromator will be used to detect the probe fluorescence at 215 nm; we have demonstrated sufficient rejection of Rayleigh scattering and ns-LIF using this experimental arrangement. The pump-probe delay will be scanned to measure the evolution of the population in the pumped state during and after the saturating laser pulse. We will measure room-temperature ground-state refilling rates due to N_2 collisions using a gas stream only containing NO in N_2. Nitrogen is a very weak quencher of NO A, and we do not expect to observe measurable signal recovery due to quenched NO molecules. The addition of O_2, CO_2, or H_2O to the gas stream, however, will rapidly quench NO A, and based on model predictions, signal recovery will be observed if there is significant branching of the quenching product state distribution to NO $X\,^2\Pi(v = 0)$. The experiment will be refined and optimized using the room-temperature flow cell prior to measurements in an atmospheric-pressure flame. Using these results, we will implement the appropriate representation of the quenching mechanism in the computational model.

BES-Supported Publications (2002-present)

T. B. Settersten, M. A. Linne, "Modeling short-pulse excitation for gas-phase laser diagnostics," *J. Opt. Soc. Am. B* **19**, 954 (2002).

T. B. Settersten, M. A. Linne, "Picosecond pump-probe absorption spectroscopy in gases: models and experimental validation," *Appl. Opt.* **41**, 2869 (2002).

T. B. Settersten, A. Dreizler, R. L. Farrow, "Temperature- and species-dependent quenching of CO $B\,^1\Sigma^+(v = 0)$ probed by two-photon laser-induced fluorescence using a picosecond laser," *J. Chem. Phys.* **117**, 3173 (2002).

T. B. Settersten, R. L. Farrow, J. A. Gray, "IR-UV double-resonance spectroscopy of OH in a flame," *Chem. Phys. Lett.* **369**, 584 (2003).

T. B. Settersten, R. L. Farrow, J. A. Gray, "IR-UV double-resonance spectroscopy of CH_3 in a flame," *Chem. Phys. Lett.* **370**, 204 (2003).

T. B. Settersten, A. Dreizler, B. D. Patterson, P. E. Schrader, R. L. Farrow, "Photolytic interference affecting two-photon laser-induced fluorescence detection of atomic oxygen in hydrocarbon flames," *Appl. Phys. B* **76**, 479 (2003).

A. N. Karpetis, T. B. Settersten, R. W. Schefer, and R. S. Barlow, "Laser imaging system for determination of three-dimensional scalar gradients in turbulent flames," *Opt. Lett.* **29**, 355 (2004).

X. Chen, B. D. Patterson, T. B. Settersten, "Time-domain investigation of OH ground-state energy transfer using picosecond two-color polarization spectroscopy," *Chem. Phys. Lett.* **388**, 358 (2004).

J. H. Frank, B. D. Patterson, X. Chen, T. B. Settersten, "Comparison of nanosecond and picosecond excitation for two-photon LIF imaging of atomic oxygen in flames," *Appl. Opt.*, in press (2004).

4

Theoretical Studies of Potential Energy Surfaces and Computational Methods

Ron Shepard
Chemistry Division
Argonne National Laboratory
Argonne, IL 60439
[email: shepard@tcg.anl.gov]

Program Scope: This project involves the development, implementation, and application of theoretical methods for the calculation and characterization of potential energy surfaces (PES) involving molecular species that occur in hydrocarbon combustion. These potential energy surfaces require an accurate and balanced treatment of reactants, intermediates, and products. This difficult challenge is met with general multiconfiguration self-consistent-field (MCSCF) and multireference single- and double-excitation configuration interaction (MRSDCI) methods. In contrast to the more common single-reference electronic structure methods, this approach is capable of describing accurately molecular systems that are highly distorted away from their equilibrium geometries, including reactant, fragment, and transition-state geometries, and of describing regions of the potential surface that are associated with electronic wave functions of widely varying nature. The MCSCF reference wave functions are designed to be sufficiently flexible to describe qualitatively the changes in the electronic structure over the broad range of molecular geometries of interest. The necessary mixing of ionic, covalent, and Rydberg contributions, along with the appropriate treatment of the different electron-spin components (e.g. closed shell, high-spin open-shell, low-spin open shell, radical, diradical, etc.) of the wave functions are treated correctly at this level. Further treatment of electron correlation effects is included using large scale multireference CI wave functions, particularly including the single and double excitations relative to the MCSCF reference space. This leads to the most flexible and accurate large-scale MRSDCI wave functions that have been used to date in global PES studies.

Electronic Structure Code Maintenance, Development, and Applications: A major component of this project is the development and maintenance of the COLUMBUS Program System. The COLUMBUS Program System computes MCSCF and MRSDCI wave functions, MR-ACPF (averaged coupled-pair functional) energies, MR-AQCC (averaged quadratic coupled cluster) energies, spin-orbit CI energies, and analytic energy gradients. Geometry optimizations to equilibrium and saddle-point structures can be done automatically for both ground and excited electronic states. The COLUMBUS Program System is maintained and developed collaboratively with several researchers including Isaiah Shavitt (University of Illinois), Russell M. Pitzer (Ohio State University), and Hans Lischka (University of Vienna, Austria). The COLUMBUS Program System of electronic structure codes is maintained on the various machines used for production calculations by the Argonne Theoretical Chemistry Group, including IBM RS6000 workstations, DEC/COMPAC ALPHA workstations, the parallel IBM SP at NERSC, and the Group's 64-CPU Linux cluster. Most recently, the codes have been ported to the 512-CPU Linux cluster, Chiba City, and to the new 320-CPU JAZZ Teraflop facility at Argonne. The COLUMBUS codes also have been ported recently to the Macintosh personal computer, allowing sophisticated production-level electronic structure calculations on desktop and laptop computers. These computer codes are used in the production-level molecular applications by members and visitors of the Argonne Theoretical Chemistry Group. The next major release of the COLUMBUS codes will begin to incorporate the newer language features of F90/F95. This will facilitate future development and maintenance effort.

In collaboration with Hans Lischka (University of Vienna, Austria), Robert Harrison (Oak Ridge National Laboratory), and Thomas Mueller (Central Institute for Applied Mathematics, Juelich, Germany), the parallel version of the CI diagonalization program CIUDG and the parallel CI density code CIDEN have been developed and ported to several large parallel machines. We use the widely available TCGMSG and MPI libraries to support internode communication, and we use the Global Array library for distribution of large datasets across the nodes of the machine, thereby providing our parallel code a high degree of portability. These programs run on networks of workstations, small-scale shared-memory parallel machines (e.g. Cray and IBM SMP nodes), and small-scale distributed memory machines (e.g. Linux clusters). The current versions of the parallel CI and CI density codes allow for molecular geometry optimizations through a sequence of single-point calculations with analytic energy gradients. The controlling scripts have been modified and tested to allow for automatic geometry optimization in the same way as that done for the sequential versions of these codes.

Fig. 1 shows the parallel performance of the CI code on the Argonne JAZZ cluster. The timings displayed are for a single CI iteration for various numbers of nodes. The reference space is a direct-product wave function that allows for the qualitatively correct fragment products resulting from dissociation of any molecular bond in the molecule (i.e. C_2H_3 ($^2A'$), H (^1S), and $CH_2(^1B_1)$). Timings for both Myranet and 100Mbs ethernet communications are given. These timings are preliminary (as of 2-Apr-2004, cc-pVQZ ethernet timings are not available), and future program optimizations may improve the performance significantly, especially for larger node calculations an for the slower ethernet-based results. A single CI optimization requires 10 to 15 of these iterations to achieve convergence. A geometry optimization requires typically 5 to 10 CI wave function optimization steps, or about 100 times the effort shown in Figure 1. A global potential energy surface determination would require 10^3 to 10^4 CI calculations, or 10^4 to 10^5 times the effort shown in Fig. 1.
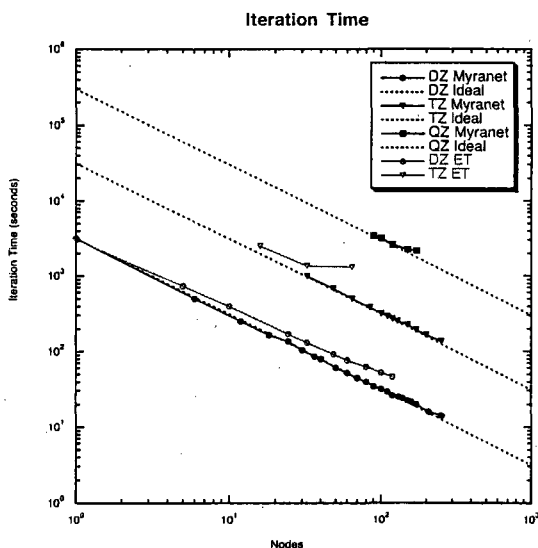
Fig. 1. Iteration times for a single MRCI iteration for C_2H_4 (^1A_g). The reference wave function is a direct-product expansion consisting of 3012 CSFs. Three basis sets are used, cc-pVDZ, cc-pVTZ, and cc-pVQZ, and the corresponding CI wave function expansion lengths are N=24,098,072, N=197,655,128, and N=857,810,264 respectively. These timings are preliminary.

In collaboration with David Yarkony (Johns Hopkins University) and Hans Lischka (University of Vienna), the ability to compute nonadiabatic coupling between different electronic states of molecules has been incorporated into the COLUMBUS Program System. This results in the ability to compute branching ratios of chemical reactions that

involve PES cusps and crossings. It will also allow for the automatic location of cusp and crossing conformations and of the noncrossing conformations of the PES that maximize the nonadiabatic coupling.

Iterative Matrix Diagonalization: A new iterative subspace diagonalization approach, called the Subspace Projected Approximate Matrix (SPAM) method, has been developed over the past few years. In a subspace method, a new trial vector is added to an existing vector subspace each iteration. The choice of expansion vectors determines the convergence rate. The traditional Davidson and Lanczos methods are examples of iterative subspace methods. In the SPAM approach, an approximate matrix is constructed each iteration using a projection operator approach, and the eigenvector of this approximate matrix is used to define the new expansion vector. The convergence rate is improved in the SPAM method over the Davidson and Lanczos approaches because of these improved expansion vectors. The efficiency of the procedure depends on the relative expense of forming approximate and exact matrix-vector products. The SPAM method allows for the simultaneous optimization of several roots and it allows for an arbitrary number of levels of matrix approximations. This results in a multiroot-multilevel SPAM algorithm that has a wide range of possible applications. This matrix diagonalization method has been applied to a wide range of eigenvalue problems, including optimization of the lowest eigenpairs, the highest eigenpairs, and interior eigenpairs using both root-homing and vector-following.

The SPAM method is being applied to the molecular vibration eigenvalue problem. This is based on the TetraVib program of Yu and Muckerman (*J. Molec. Spec.* **214**, 11-20 (2002)) that was described at the 2002 Combustion Contractor Meeting. This code is based on a combination of spherical harmonic basis functions for the angular degrees of freedom and discrete variable representation (DVR) of the radial degrees of freedom. One feature of the new program is that the vibrational wave functions are available explicitly. This allows expectation values to be computed routinely. Table 1 shows some vibrationally averaged expectation value properties for the lowest few vibrational states of even and odd parity of the H_2CO molecule.

Table 1. Expectation value properties for the lowest few vibrational states for H_2CO.

root	p	λ/eV	$\langle r_1 \rangle = \langle r_2 \rangle$	$\langle r_3 \rangle$	$\langle \theta_1 \rangle = \langle \theta_2 \rangle$	$\sigma(r_1)$	$\sigma(r_3)$	$\sigma(\theta_1)$	$\sigma(\phi)$
1	0	0.744823	2.0835	2.4549	119.81	0.1449	0.0744	7.69	11.93
1	1	0.907577	2.0865	2.4554	119.19	0.1453	0.0742	8.08	21.12
2	0	0.936336	2.0867	2.4580	119.56	0.1457	0.0756	11.92	18.21
3	0	0.949337	2.0840	2.4681	119.70	0.1450	0.0820	8.07	12.50
4	0	1.005487	2.0872	2.4603	119.22	0.1460	0.0768	11.36	17.55
2	1	1.112430	2.0865	2.4700	119.11	0.1454	0.0826	8.24	21.25
3	1	1.131556	2.0889	2.4605	119.30	0.1462	0.0766	12.48	25.24
4	1	1.199842	2.0901	2.4609	118.66	0.1467	0.0767	12.11	25.19
PES			2.0426	2.4443	119.94				

The SPAM method is being incorporated into the COLUMBUS MRSDCI code. Work is also in progress to extend the SPAM method to include application to the generalized symmetric eigenvalue problem, the complex hermitian eigenvalue problem, the complex hermitian generalized eigenvalue problem, and the general (nonhermitian) eigenvalue problem. The application to other linear and nonlinear problems (including the coupled-cluster equation solution) is also being considered.

Computation of Eigenvalue Bounds: During the development of the SPAM method, it was necessary to compute bounds of approximate eigenvalues and eigenvectors. This work resulted in the development of a general computational procedure to compute rigorous eigenvalue bounds for general subspace eigenvalue methods. This method consists of the recursive application of a combination of the Ritz bound, the Residual norm bound, the Gap bound, and the Spread bound. In addition to application within the SPAM method, this method may also be applied to the Davidson method as used in CI calculations and to the Lanczos method as used in the computation of vibrational eigenvalues. This software will be distributed using anonymous ftp.

Public Distribution of Software: The COLUMBUS Program System is available using the *anonymous ftp* facility of the internet. The codes and online documentation are available from the web address http://www.itc.univie.ac.at/~hans/Columbus/columbus.html. In addition to the source code, the complete online documentation, installation scripts, sample calculations, and numerous other utilities are included in the distribution. A partial implementation of an IEEE POSIX 1009.3 library has been developed and is also available from ftp://ftp.tcg.anl.gov/pub/libpxf. This library simplifies the porting effort required for the COLUMBUS codes, and also may be used independently for other Fortran programming applications. The SPAM code described above is available from ftp://ftp.tcg.anl.gov/pub/spam.

Publications:

"An Ab Initio Study of the Ionization Potentials and the f-f Spectroscopy of Europium Atoms and Ions," C. Naleway, M. Seth, R. Shepard, A. F. Wagner, J. L. Tilson, W. C. Ermler, and S. R. Brozell, *J. Chem. Phys.* **116**, 5481-5493 (2002).

"An Ab Initio Study of the f-f Spectroscopy of Americium^{+3}," J. L. Tilson, C. Naleway, M. Seth, R. Shepard, A. F. Wagner, and W. C. Ermler, *J. Chem. Phys.* **116**, 5494-5502 (2002).

"Reducing I/O Costs For The Eigenvalue Procedure In Large-Scale CI Calculations," R. Shepard, I. Shavitt, and H. Lischka, *J. Computational Chem.* **23**, 1121-1125 (2002).

"Analytic MRCI Gradient for Excited States: Formalism and Application to the n-π^* valence- and n-(3s,3p) Rydberg States of Formaldehyde," H. Lischka, M. Dallos, and R. Shepard, *Mol. Phys.* **100**, 1647-1658 (2002).

"The Analytic Evaluation of Nonadiabatic Coupling Terms at the MR-CI Level. I: Formalism," H. Lischka, M. Dallos, P. G. Szalay, D. R. Yarkony, and R. Shepard, *J. Chem. Phys. (in press).*

"Analytic Evaluation of Nonadiabatic Coupling Terms at the MR-CI level. II. Determination of Minima on the Crossing Seam: the $1^1B_1/2^1A_1$ and $2^1A_1/3^1A_1$ Crossings for Formaldehyde and the Photodimerization of Ethylene," M. Dallos, H. Lischka, P. G. Szalay, R. Shepard, and D. R. Yarkony, *J. Chem. Phys. (in press).*

"An Ab Initio Study of AmCl$^+$: f-f Spectroscopy and Chemical Binding," Jeffrey L. Tilson, Conrad Naleway, Michael Seth, Ron Shepard, Albert F. Wagner, and Walter C. Ermler, *J. Chem. Phys. (in press).*

COMPUTATIONAL AND EXPERIMENTAL STUDY OF LAMINAR FLAMES

M. D. Smooke and M. B. Long
Department of Mechanical Engineering
Yale University
New Haven, CT 06520
mitchell.smooke@yale.edu

Program Scope

Our research has centered on an investigation of the effects of complex chemistry and detailed transport on the structure and extinction of hydrocarbon flames in coflowing axisymmetric configurations. We have pursued both computational and experimental aspects of the research in parallel. The computational work has focused on the application of accurate and efficient numerical methods for the solution of the boundary value problems describing the various reacting systems. Detailed experimental measurements were performed on axisymmetric coflow flames using two-dimensional imaging techniques. Spontaneous Raman scattering and laser-induced fluorescence were used to measure the temperature, major and minor species profiles. Laser-induced incandescence has been used to measure soot volume fractions. Our goal has been to obtain a more fundamental understanding of the important fluid dynamic and chemical interactions in these flames so that this information can be used effectively in combustion modeling.

Recent Progress

The major portion of our work during the past year has focused on a combined computational and experimental study of time varying, axisymmetric, laminar unconfined methane-air diffusion flames and on a combined computational and experimental study of the formation of soot in axisymmetric, laminar ethylene-air diffusion flames. Additional research was begun on partially premixed laminar flames. The time varying systems can bridge the gap between laminar and fully turbulent systems. In addition, time varying flames offer a much wider range of interactions between chemistry and fluid dynamics than do steady-state configurations. The sooting flames can enable the investigator to understand the detailed inception, oxidation and surface growth processes by which soot is formed in hydrocarbon flames. The partially premixed work interfaces with scalar dissipation and mixture fraction measurements at Sandia National Laboratories.

Time-Varying Flames: Atmospheric pressure, overventilated, axisymmetric, coflowing, nonpremixed laminar flames were generated with a burner in which the fuel flows from an uncooled 4.0 mm inner diameter vertical brass tube (wall thickness 0.038 mm) and the oxidizer flows from the annular region between this tube and a 50 mm diameter concentric tube. The oxidizer is air while the fuel is a mixture containing methane and nitrogen 65%/35% by volume, to eliminate soot. The burner includes a small loudspeaker in the plenum of the fuel jet, which allows a periodic perturbation to be imposed on the exit parabolic velocity profile. Perturbations of 30% and 50% of the average velocity have been investigated. Because the flame is slightly lifted, there is no appreciable heat loss to the burner.

Two-dimensional profiles of temperature, mixture fraction, and mole fractions of N2, CO2, CH4, H2, CO, and H2O as well as CH* emission have been measured in the time-varying flame. Although the velocity field is of fundamental importance in determining the flame structure, there has been less extensive comparison of measured and computed velocity fields than for various scalar quantities. This is due in part to practical difficulties in measuring accurate velocities in

these relatively low-speed flames. In previous work, we have used particle image velocimetry (PIV) to measure the velocity profile at the exit of the forced-flow burner. However, that measurement did not require the use of particles that would survive flame temperatures. For measurements in the flame, refractory particles must be used, which are more difficult to seed into the flow effectively. To provide consistent and accurate flow conditions, all gases are metered using mass flow controllers. Particle seeding for velocity measurements must be introduced downstream of the mass flow controllers and, particularly for the small volume flow rate from the fuel jet, it is difficult to provide uniform seeding of a sufficient seeding density to provide accurate single-shot velocity measurements. In a recent set of experiments, preliminary velocity measurements were made in one of our steady flames. In order to obtain sufficient seeding density for the PIV measurements, an ensemble of image pairs were accumulated and used for the processing. This approach works well in the steady flame, and by locking the measurements to a given phase, should be applicable to our time-varying flames as well.

Limited information is currently available in the literature on velocity fields in forced time-varying flames, and we are not aware of any detailed comparisons with computations. One recent study by Papadopoulos, et al. [1] used PIV to measure velocity profiles in a forced flickering flame. In that work, no correction was made for thermophoretic effects on the velocity. Our estimates indicate that, particularly for the radial velocity component, this effect can be significant. The effects of thermophoretic drift can be corrected if temperature field measurements are also available, as they are for the flames we have been studying.

Soot Modeling: Soot kinetics are modeled as coalescing, solid carbon spheroids undergoing surface growth in the free molecule limit. The particle mass range of interest is divided into sections and an equation is written for each section including coalescence, surface growth, and oxidation. For the smallest section, an inception source term is included. The transport conservation equation for each section includes thermophoresis, an effective bin diffusion rate, and source terms for gas-phase scrubbing. The gas and soot equations are additionally coupled through non-adiabatic radiative loss in the optically-thin approximation. The inception model employed here is based on an estimate of the formation rate of two- and three-ringed aromatic species (naphthalene and phenanthrene), and is a function of local acetylene, benzene, phenyl and molecular hydrogen concentrations. Oxidation of soot is by O_2 and OH. The surface growth rate is based upon that of Harris and Weiner [2] with an activation energy as suggested by Hura and Glassman [3]. Using planar laser imaging, we obtain two-dimensional fields of temperature, fuel concentration, and soot volume fraction in the C_2H_4/N_2 flame. The temperature field is determined using the two scalar approach of Starner et al. [4]. The soot volume fraction field is determined by laser-induced incandescence (LII). Probe measurements of the soot volume fraction are used for calibration.

Two chemical kinetic mechanisms were utilized in the modeling work. They included a 65 species mechanism based upon the work of Sun et al. [5] and a 101 species reaction set from Appel, Bockhorn and Frenklach [6]. Fuel and nitrogen are introduced through the center tube (4mm id) and air through the outer coflow with plug flow velocity profiles. Both velocity profiles were those employed in the experiments. Flames containing 40% (60%), 60% (40%) and 80% (20%) mole fractions of ethylene (nitrogen) with a bulk-averaged velocity of 35 cm/sec were studied. The coflow air velocity was 35 cm/sec. Reactant temperatures were assumed to be 298 K. Calculations were performed on an IBM Winterhawk II computer with 20 soot sections.

The results indicate two principal deficiencies of the soot model. First, centerline soot is always substantially under predicted and second, the computed wings of the flame are extended much beyond those determined experimentally. Our model allows particles to grow by coalescence and

274

surface growth without any size limit contrary to experimental data (20-30 nm). In addition, large diameter soot particles slow the oxidation process and are the direct cause of the extended wings. In effect, the model does not treat primary particle aggregation (and hence underestimates surface area for larger volume fractions) and ageing. In an attempt to remedy these deficiencies, we turned off coalescence and surface growth at a pre-selected particle size of 25nm. These modifications made a significant improvement in the computed soot volume fraction distributions.

Lastly, we examined the effects of radiation reabsorption in the model. In principle, some re-absorption of thermal emissions can occur. This optical thickness effect reduces the net rate of thermal radiation energy loss. Utilizing the discrete transfer method of Lockwood and Shah [7], we directed a number of rays from the boundaries through the body of the flame. We then determined path-integrated radiative fluxes along rays using the program RADCAL [8]. This energy source rate was then employed as a fixed correction term in the energy equation and the process iterated. The small changes to the temperature profiles made 10-20% changes in the ratio of the peak soot along the centerline to the peak overall soot – more in line with the experiments.

Partially Premixed Flames: We have recently begun to study rich partially premixed laminar methane/air flames in conjunction with Adonios Karpetis and Robert Barlow of Sandia's Combustion Research Facility. From their preliminary measurements, Karpetis and Barlow can derive the full three-dimensional scalar dissipation rate as a function of a conserved scalar. They have compared their values with published values obtained using a nonpremixed counterflow flame model. The lack of agreement between the measurements and the counterflow results motivates our study, in which we hope to predict the scalar dissipation rate more accurately. The work focuses on three flames, all in an axisymmetric coflow configuration; each of these flames has the same overall equivalence ratio ($\Phi = 3.19$), but the three flames have different inner jet flow rates. Comparison with experimental results will occur along each flame's centerline and also via radial profiles measured at various axial positions. In the experiment, the inner tube extends 2.54 cm above the burner surface, requiring that the tube be present within the computational domain as well. Thus, computational temperatures along the tube surface will be set equal to experimental measurements obtained using thermocouples embedded in the tube wall. Use of an adaptive gridding technique is dictated by the fact that flame front thicknesses, particularly in partially premixed flames, can be as small as one-hundredth of the overall flame height, and use of a standard tensor-product gridding technique would require so many grid points (and computer memory) as to be computationally infeasible.

Future Plans

During the next year we hope to expand our research in several main areas. We will continue our study of sooting hydrocarbon flames with the goal of understanding the differences in soot distribution between the computational and experimental results. A significant portion of this work will address radiation reabsorption, soot aggregation and ageing. The goal will be to include a detailed soot model into the gas phase system so as to predict soot volume fractions as a function of time. Laser induced incandescence (LII) will be used to measure soot volume fractions. Work will also continue on the rich partially premixed flames.

References

1. G. Papadopoulos, R.A. Bryant, and W.M. Pitts, *Experiments in Fluids*, **33**, p. 472, (2002).

2. Harris, S.J., and Weiner, A.M., *Combust. Sci. Tech.*, **31**, p. 155, (1983).

3. Hura, H.S. and Glassman, I., *Proceedings of the Combustion Institute*, 22, p. 371, (1988).

4. Starner, S., Bilger, R. W., Dibble, R. W., Barlow, R. S., *Combust. Sci. Tech.*, 86, p. 223, (1992).

5. Sun, C. J., Sung, C. J., Wang, H., and Law, C. K., *Comb and Flame*, 107, p. 321, (1996).

6. Appel, J., Bockhorn, H. and Frenklach, M., *Comb. and Flame*, 121, p. 122, (2000).

7. F.C. Lockwood and N.G. Shah, *Proceedings of the Combustion Institute, 18*, p. 1405, (1981).

8. Grosshandler, W.L., *RADCAL: A Narrow-Band Model for Radiation Calculations in a Combustion Environment*, NIST Technical Note 1402 (1993).

DOE Sponsored Publications since 2002

1. J. Fielding. J. H. Frank, S. A. Kaiser, M. D. Smooke, and M. B. Long, "Polarized/Depolarized Rayleigh Scattering for Determining Fuel Concentration in Flames," *Proceedings of the Combustion Institute*, 29, (2002).

2. C.F. Kaminski and M.B. Long, "Multi-dimensional Diagnostics in Space and Time," in *Applied Combustion Diagnostics,* K. Kohse-Hoinghaus and J.B. Jeffries, ed., (Taylor and Francis, New York) 2002.

3. J.H. Frank, S.A. Kaiser, and M.B. Long, "Reaction-Rate, Mixture Fraction, and Temperature Imaging in Turbulent Methane/Air Jet Flames," *Proceedings of the Combustion Institue., 29,* (2002).

4. S. V. Naik, N. M. Laurendeau, J. A. Cooke and M. D. Smooke, "A Soot Map for Methane-Oxygen Counterflow Diffusion Flames," *Combust. Sci. and Tech., 175,* (2003).

5. S. V. Naik, N. M. Laurendeau, J. A. Cooke, and M. D. Smooke, "Effect of Radiation on Nitric Oxide Concentrations Under Sooting Oxy-Fuel Conditions," *Comb. and Flame, 134,* (2003).

6. M. D. Smooke, R. J. Hall and M. B. Colket, "Modeling the Transition from Non-Sooting to Sooting Coflow Ethylene Diffusion Flames," to be published *Comb. Theory and Modeling,* (2004).

7. J. A. Cooke, M. D. Smooke, M. Bellucci, A. Gomez, A. Violi, T. Faravelli and E. Ranzi, "Computational and Experimental Study of a JP-8 Counterflow Diffusion Flame," to be published *Proceedings of the Combustion Institute,* 30, (2004).

8. V. V. Toro, A. V. Mokhov, H. B. Levinsky and M. D. Smooke, "Combined Experimental and Computational Study of Laminar, Axisymmetric Hydrogen-Air Diffusion Flames," to be published *Proceedings of the Combustion Institute,* 30, (2004).

9. K.T. Walsh, J. Fielding, M.D. Smooke, A. Linan and M.B. Long, "A Comparison of Computational and Experimental Lift-Off Heights of Coflow Laminar Diffusion Flames," to be published *Proceedings of the Combustion Institute,* 30, (2004).

Universal/Imaging Studies of Chemical Dynamics

Arthur G. Suits*

Chemistry Department, Brookhaven National Laboratory, Upton, NY 11973
and
Department of Chemistry, Stony Brook University, Stony Brook, NY 11794
asuits@chem.wayne.edu

Program Scope

The focus of this program is on combining universal ion imaging probes, providing global insight, with state-resolved probes providing quantum mechanical detail, to develop a molecular-level understanding of chemical phenomena. Particular emphasis is placed upon elementary reactions important in understanding and predicting combustion chemistry. This research is conducted using state-of-the-art molecular beam machines, reactive scattering, and vacuum ultraviolet lasers in conjunction with ion imaging technqiues. An ongoing parallel effort is made to develop new tools and experimental methods with which to achieve these goals.

Recent Progress

Direct imaging of hydrogen abstraction dynamics: energy dependence of the dynamics. We have obtained the first direct differential cross sections for reaction of ground state oxygen with alkanes, via single-photon VUV probe of the hydrocarbon radical product in these reactions. Crossed-beam reaction of O(^{3}P) with the a variety of hydrocarbon target molecules show direct back scattering and a large fraction of energy in internal modes of the hydrocarbon radical – on the order of 60% of the available energy – clearly showing the inadequacy of the quasi-triatomic model often invoked to understand these reactions. We have augmented these studies with ab initio calculations and Monte Carlo simulations of Doppler spectra performed by Jim Muckerman and Greg Hall. Virtually all that is known about these systems comes from laser-induced fluorescence spectra of the OH product. Only one previous study described differential cross sections for these systems, and that was obtained only for the OH (v=1) product. The current effort along these lines is directed to extending measurements of the detailed energy dependence of the dynamics, to include other atomic reactants such as Cl (^{2}P$_{3/2}$) and O(^{1}D) and to investigate the relative importance of potential surface topology and dimensionality and reaction kinematics in determining energy and angular momentum disposal. Recent work involves application of our DC slicing technique, discussed further below, to record the contour map for these reactions directly.

One recent study represents a direct comparison of ground state and electronically excited oxygen atom reactions with hydrocarbons. The results we have obtained for O(^{1}D) and O(^{3}P) reaction with n-pentane yield some anticipated results as well as some surprises. Ten years ago, Park and Wiesenfeld reported OH internal state distributions for reaction of O(^{1}D) with a range of target hydrocarbons. They found inverted vibrational distributions for reaction with methane, but the level of OH vibrational excitation decreased with increasing target complexity. In addition, the OH rotational distributions also became colder with increasing target complexity, in stark contrast to the case for the ground state reaction. Our results for the ground state reaction are consistent with our previous studies and our proposed picture of "vertical" H abstraction. However, for the singlet reaction, we clearly see two components in the translational energy release and considerable coupling of the energy release and differential cross sections. We can associate the faster forward scattered component with formation of a transient insertion intermediate (which

paradoxically is associated with vibrationally excited OH) while the slower isotropic component is associated with the statistical decay of an activated alcohol, in effect supporting the picture outlined by Park and Wiesenfeld, albeit with simultaneous insight into the hydrocarbon radical internal energy distribution.

Application of DC slice imaging to orbital polarization. We have recently adapted the DC slice imaging approach, described below, to obtain the absolute speed-dependent angular momentum polarization anisotropy parameters as well as the alignment-free angular and translational energy distributions in photodissociation experiments. Our interest in particular has been in probing atomic orbital alignment and orientation, although the same techniques and analysis apply to rotational angular momentum polarization. In recent years these studies have evolved from being novelties of interest in themselves, to becoming a new window into photoexcitation dynamics and nonadiabatic processes. Recent results for ozone photodissociation show some surprising phenomena. The $O(^1D)$ produced in ozone photodissociation at 266nm is strongly aligned, with the angular momentum vector preferentially perpendicular to the recoil direction. This is consistent with earlier results from the Houston group. This alignment is largely incoherent in origin, and likely results from adiabatic dissociation on the initially excited surface. We have also measured the orientation of the $O(^1D)$ atom throughout the Hartley band, and we see a strong coupling of this orientation with the recoil speed of the atom, with the coherent parallel/perpendicular term actually changing sign with the vibrational level of the O_2 cofragment, as shown in Fig. 1.
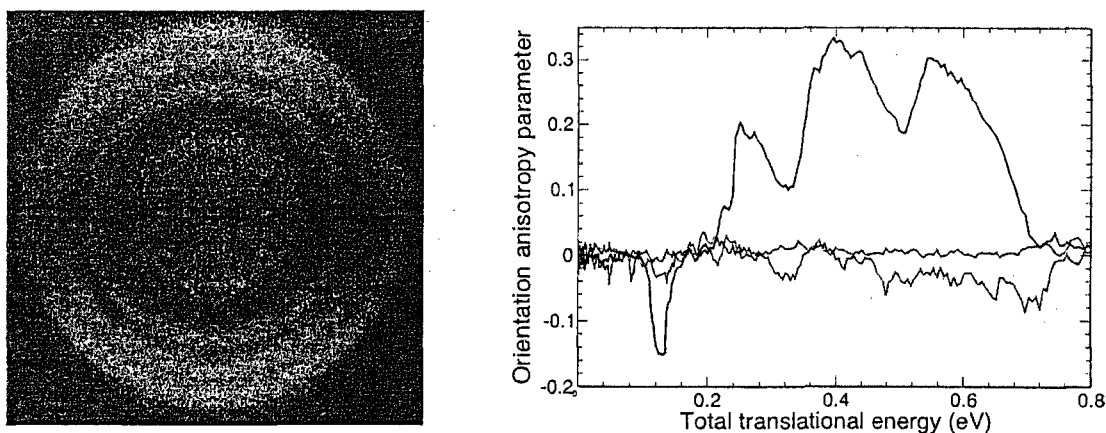

Figure 1. (left) Orientation image of $O(^1D)$ from 266nm dissociation of ozone obtained with linear photolysis 45 to image plane, with right-left circular probe polarization. The signal for the innermost ring is negative, while the outer rings are positive. (right) Speed-dependent orientation anisotropy parameters obtained from images. The heavy line is the γ_1' parameter associated with coherent dissociation via linearly polarized light.

These striking results likely provide evidence of a crossing between the initially prepared "B" surface and the "A" surface. We are currently measuring the dependence of this on the dissociation wavelength, to understand whether it is indeed an interference effect arising from interaction between adiabatic and nonadiabatic dissociation pathways.

DC slice imaging of ketene photodissociation. We have recently developed a slicing approach to velocity map imaging that obviates the need for reconstruction techniques that can introduce noise and artifacts into the results, leading to greatly enhanced S/N and improved resolution. We have applied this technique to achieve improved velocity resolution and S/N for photochemistry and, recently, reactive scattering studies. In collaboration with G. Hall, we have applied this to the study of ketene photodissociation from 300-330 nm. The slice imaging technique, applied to

detection of specific CO rotational levels, provides simultaneously the rovibrational distribution of the methylene cofragment. We have recorded images for many CO rotational levels at several photolysis wavelengths, and achieve a velocity resolution on the order of 10 m/s. For a number of CO rotational levels we have seen partial rovibrational resolution of the methylene product. Preliminary results for CO (v=0, J=4 and 20) show significant deviation from the statistical phase space theory (PST) limit, and can be well fitted by a model that suppresses both high and low rotational states of CH_2 in coincidence with low energy CO states. The suppression of high rotational states is an effect reproduced in the dynamically corrected statistical theory, while the suppression of low rotational states remains unexplained at this level of theory.

Selected Future Plans

DC slice imaging of O(1D) + HCl reaction dynamics. The dynamics of the reaction of O(^{1}D) with HCl have been shown, in QCT calculations, to manifest both features of the shallow long-range van der Waals well and the deep insertion well. This is a fascinating system for which a fairly high quality potential surface exists and on which extensive dynamics studies have been performed. There are two product channels in the reaction: OH+Cl and OCl + H. The latter channel has been studied using the venerable universal crossed molecular beam method, but, owing to unfavorable kinematics, the dominant former channel is not amenable to study using that approach. The agreement with the QCT calculations is poor, and one possible explanation is the importance of reaction on the electronically excited surfaces that are not included in the QCT calculations. Alternatively, the properties of the single detected product state may not be representative of the global reaction dynamics. This is clearly a system where imaging could provide key insight. We plan to use VUV generated by four-wave mixing in mercury to effect sensitive 1+1' resonant ionization of Cl atoms. In addition, we will continue our studies of H abstraction dynamics in polyatomic systems, using the Hg cell to obtain higher probe photon energies, allowing us to study C1, C2 and C3 systems that are now out of our reach.

State-correlated photochemistry of HCCO. A new system of interest for our high-resolution photochemistry studies, building upon our success with ketene itself, is the ketenyl radical, HCCO. There is a marvelous body of work on the spectroscopy and dynamics of this system. However, the dynamics measurements were obtained at fairly low translational energy resolution. Nevertheless, they provide a roadmap for rich correlated state imaging measurements of the CO. This radical system has the great advantage that metastable levels of the state may be excited state-specifically, so that even employing a photolyic radical source we need not worry about contamination by dissociation of excited radicals. Small changes in photolysis energy are seen to change the branching between dissociation on the doublet and quartet surfaces quite dramatically. Again, quantum state specific probing of the CO product will provide correlated internal state information on the rovibrational levels of both ground state (X $^2\Pi$) and electronically excited (a $^4\Sigma^-$) CH product, allowing detailed investigation of ground state dissociation and intersystem crossing dynamics in this system.

DOE Publications 2002-present

R. L. Gross, X. Liu and A. G. Suits, "The ultraviolet photodissociation of 2-chlorobutane: an imaging study comparing universal and state-resolved probe techniques," *Chem. Phys. Lett.* **362**, 229 (2002).

X. Liu, R. L. Gross and A. G. Suits, "Differential Cross Sections for O(3P)+alkane reactions by direct imaging," *J. Chem. Phys.* **116**, 5341 (2002)

X. Liu, R. L. Gross, G. E. Hall, J. T. Muckerman and A. G. Suits, "Imaging O(^{3}P) + alkane reaction dynamics in crossed molecular beams: Vertical versus adiabatic H abstraction dynamics," *J. Chem. Phys.* **117**, 7947 (2002).

F. Qi and A. G. Suits, "Photodissociation of propylene sulfide at 193 nm: A photofragment translational spectroscopy study with VUV synchrotron radiation," *J. Phys. Chem. A.* **106** 11017 (2002).

J. K. C. Lau, W. K. Li, F. Qi and A. G. Suits, "A Gaussian-3 study of the photodissociation channels of propylene sulfide," *J. Phys. Chem. A.* **106** 11025 (2002).

W. Li, L. Poisson, D. S. Peterka, M. Ahmed, R. Lucchese and A. G. Suits, "Dissociative photoionization dynamics in ethane studied by velocity map imaging," *Chem. Phys. Lett.* **374**, 334 (2003).

R. L. Gross, X. Liu and A. G. Suits, "O(^{3}P) versus O(^{1}D) Reaction Dynamics with n-Pentane: A Crossed-Beam Imaging Study," *Chem. Phys. Lett.* **376**, 710 (2003).

W. Li, R. Lucchese, A. Doyuran, Z. Wu, H. Loos, G. E. Hall and A. G. Suits, "Superexcited state dynamics probed with an extreme ultraviolet free electron laser," *Phys. Rev. Lett.*, **92** 083002 (2004).

X. Liu and A. G. Suits, "The dynamics of hydrogen abstraction in polyatomic molecules," in **Modern Trends in Chemical Reaction Dynamics**, X. M. Yang and K. Liu, eds. (World Scientific, Singapore: 2004)

280

Elementary Reaction Kinetics of Combustion Species

Craig A. Taatjes

Combustion Research Facility, Mail Stop 9055, Sandia National Laboratories, Livermore, CA 94551-0969

cataatj@sandia.gov   www.ca.sandia.gov/CRF/staff/taatjes.html

SCOPE OF THE PROGRAM

This program aims to develop new optical methods for studying chemical kinetics and to apply these methods to the investigation of fundamental chemistry relevant to combustion science. The central goal is to perform accurate measurements of the rates at which important free radicals react with stable molecules. Understanding the reactions in as much detail as possible under accessible experimental conditions increases the confidence with which modelers can treat the inevitable extrapolation to the conditions of real-world devices. Another area of research is the investigation and application of new detection methods for precise and accurate kinetics measurements. Absorption-based techniques are emphasized, since many radicals critical to combustion are not amenable to fluorescence detection.

An important part of our strategy is using experimental data to test and refine detailed calculations (working in close cooperation with Stephen Klippenstein and Jim Miller), drawing on the calculational results to gain insight into the interpretation of our results and to guide experiments that will probe key aspects of potential energy surfaces. This strategy has been very successful in our investigations of the reactions of alkyl radicals with O_2, where the combination of rigorous theory and validation by detailed experiments has made great strides toward a general quantitative model for alkyl oxidation. Reactions of unsaturated hydrocarbon radicals that may play a role in soot formation chemistry are also targets of investigation.

PROGRESS REPORT

The current efforts of the laboratory center on developing high-sensitivity absorption-based techniques for kinetics measurements, and on applying these techniques to investigate important combustion reactions. A major focus in the last year has been the continuing application of cw infrared frequency-modulation (FM) spectroscopy to measurements of product formation in reactions of alkyl radicals with O_2.

Measurements of Product Formation in Alkyl + O_2 Reactions

C_2D_5, C_3D_7 + O_2 Investigations of the formation of DO_2 from the Cl-initiated oxidation reactions of completely deuterated ethane and propane have continued. The comparison of the measured DO_2 reactions with master-equation predictions show good agreement for the oxidation of deuterated ethane, but the predicted DO_2 production from

281

propane oxidation displays systematically smaller prompt yields and slightly slower secondary production rates than observed experimentally. Further measurements using photolysis of deuterated alkyl iodides are planned to complement the Cl-initiated oxidation measurements and better determine the source of the discrepancy with the calculations. Kinetic isotope effects for much of the secondary chemistry in Cl-initiated ethane and propane oxidation are unknown; measurement of DO_2 production in an alternative system will add confidence to modeling of the results.

i-propyl and *n*-propyl + O_2 To enable better refinement of models for R + O_2 reactions, measurements of reactions of individual isomers are desirable. The reactions of *n*-propyl and *i*-propyl radicals with O_2 have been measured by using 266 nm photolysis of 1-propyl and 2-propyl iodides. The Cl-initiated oxidation experiments derive an HO_2/Cl_0 calibration by comparison with Cl-initiated methanol oxidation. In the present method, such a calibration is lacking; however, the initial alkyl radical density is inferred from a simultaneous measurement of the absorption on the spin-orbit transition of the I atom photolysis co-product. Transient HO_2 FM signals taken under similar conditions in different experiments can also be compared by scaling to the observed I atom absorption. The results show clearly the differences between HO_2 formation in *i*- and *n*- propyl oxidation. The *n*-propyl reaction produces smaller prompt HO_2 yields and exhibits a slower secondary rise in HO_2 from RO_2 dissociation. This is in excellent agreement with the qualitative predictions of master equation simulations based on ab initio characterization of the stationary points on the $C_3H_7O_2$ surfaces. Quantitative comparisons and possible refinement of the theoretical models are currently underway.

In the course of the present study, measurements of the I^* branching fraction in the alkyl iodide photolysis are easily performed using the absorption-vs.-gain method of Leone and coworkers. The measured values, $\Phi_{1\text{-iodopropane}} = 0.68$, $\Phi_{2\text{-iodopropane}} = 0.25$, and $\Phi_{\text{iodoethane}} = 0.68$, are in good agreement with literature measurements. Observation of the I atom decay in the present experiments suggests a significant RO_2 + I reaction rate coefficient.

Cl-initiated oxidation of partially deuterated methanols The reaction of CH_2OH with O_2 produces HO_2 + CH_2O with 100% yield. The reaction of Cl with CH_3OH forms almost exclusively CH_2OH, so Cl-initiated methanol oxidation converts Cl to HO_2 essentially quantitatively, and thus has been used as a reference system in the investigations of HO_2 formation in Cl-initiated oxidation of alkanes. It is expected *a priori* that the HO_2 produced in the reaction of CH_2OH + O_2 should originate from transfer of the OH hydrogen to the O_2 and that the formaldehyde product is the remaining O-CH_2 group. Therefore, reaction of CH_2OD with O_2 should produce only CH_2O + DO_2, with no HO_2 produced. This would permit measurements of HCl absorptions in Cl-initiated CH_3OD oxidation to be associated with the DO_2 concentration, and hence give the relative absorption cross sections of DO_2 and HCl, for example. Measurements of HO_2 formation in Cl-initiated CH_3OD oxidation (and DO_2 formation in CD_3OH oxidation) have been undertaken to confirm this postulate.

Surprisingly, transient DO_2 FM signals from Cl-initiated CD_3OH oxidation at 700 K are ~15% of the amplitude of DO_2 signals from Cl-initiated CD_3OD oxidation under the same conditions. Analogous experiments comparing HO_2 signals from CH_3OD and CH_3OH oxidation give similar yields. Measurements at 295 K show far smaller "wrong" isotopomer yields of a few percent. HCl absorption measurements demonstrate that the initial step in the oxidation, the reaction of Cl with CD_3OH, produces less than 3% HCl at 700 K. Some of the "wrong" HO_2 isotopomer could be produced by rapid oxidation of the formaldehyde product; kinetic simulations suggest that this could provide a yield of at most 3-5% under the conditions of our experiments (or about the measured room temperature yield). Further experiments are underway to determine whether assumptions in the modeling of the formaldehyde oxidation are incorrect or whether unexpected chemistry in the $CH_2OH + O_2$ reaction is indicated. The goal is to characterize this system so that HCl absorption can be used to calibrate DO_2 FM signals.

Laser Photolysis/cwLPA Measurements of C_2H_3 Reactions

Long-path absorption spectroscopy in the (A-X) band of C_2H_3 has been applied to investigations of the $C_2H_3 + NO$ reaction. In the past year measurements on this reaction have been extended to lower pressures at elevated temperature, to investigate a discrepancy between predicted addition rates and the observed pressure dependence. At room temperature, the overall rate constant for removal of vinyl radical by NO is measured to be $1.6 \pm 0.4 \times 10^{-11}$ cm^3 molecule^{-1} s^{-1}, with negligible pressure dependence from 10 Torr to 160 Torr of helium. At constant pressure the rate constant decreases rapidly with temperature. At higher temperatures, a falloff of the rate constant to lower pressure is observed. However, the data display a clear departure from simple falloff at low pressure and elevated temperature, indicating a significant zero-pressure rate coefficient. The body of results, from 295 to 700 K and pressures from 10 to 320 Torr, have been compared to RRKM theory based master equation simulations of the temperature and pressure dependent kinetics. These simulations are carried out by Stephen Klippenstein, using his new QCISD(T) and MRCI calculations of key stationary points on the C_2H_3NO surface. The *ab initio* characterizations suggest a significant contribution from $HCN + CH_2O$ formation, with both isomerization transition states for the pathway leading to this product lying ~15 kcal mol^{-1} below the entrance channel. The master equation analysis provides a satisfactory reproduction of the observed kinetic data.

FUTURE DIRECTIONS

Characterization of $R + O_2$ reactions will continue. The ability to simultaneously probe various reactants and products will play a key role in extending these measurements. One important extension of the deuterated alkane oxidation work will be to probe OD formation. Because the reaction coordinate for the internal isomerization to QOOH (the precursor to OH formation) involves a large degree of H-atom motion, the deuterium kinetic isotope effect may be larger for OH formation than for HO_2 formation. Further in the future, oxidation of selectively deuterated alkanes may make it possible to distinguish among different internal abstraction pathways in $R + O_2$ reactions.

Interpretation of isotopic labeling experiments will require detection of both HO_2 and DO_2 and an understanding of the kinetic isotope effects on the overall reaction. In the long term, detection of the hydroperoxy radical intermediate in the $R + O_2 \rightarrow RO_2 \rightarrow QOOH \rightarrow QO + OH$ mechanism might be possible in the infrared. In addition to characterizing saturated alkyl radical reactions with O_2 at a higher level of detail, the present methodology will be extended to reactions of unsaturated radicals with O_2.

In collaboration with Stephen Leone and Musa Ahmed at Lawrence Berkeley National Laboratory and David Osborn at Sandia, a new apparatus is being constructed at the Advanced Light Source (ALS) at LBNL that will apply synchrotron photoionization mass spectrometry to chemical kinetics. This machine will employ new technologies in magnetic sector mass spectrometers and position-sensitive detectors to enable simultaneous multiple-mass detection. The ready tunability of the ALS photon energy should permit isotopic discrimination similar to that enjoyed in the current ALS flame experiments. Formation of and reactions of ethenol will be one possible target of kinetic investigations when the apparatus is completed.

Publications acknowledging BES support 2002-present

1. Milena Shahu, Chun-Hui Yang, Charles D. Pibel, Andrew McIlroy, Craig A. Taatjes, and Joshua B. Halpern, "Vinyl Radical Visible Spectroscopy and Excited State Dynamics," *J. Chem. Phys.* 116, 8343-8352 (2002).

2. Jared D. Smith, John D. DeSain, and Craig A. Taatjes, "Infrared Laser Absorption Measurements of HCl(v=1) Production in Reactions of Cl Atoms with Isobutane, Methanol, Acetaldehyde, and Toluene," *Chem. Phys Lett* 366, 417-425 (2002).

3. John D. DeSain, Stephen J. Klippenstein, Craig A. Taatjes, Michael D. Hurley, and Timothy J. Wallington, "Product Formation in the Cl-Initiated Oxidation of Cyclopropane" *J. Phys. Chem. A* 107, 1992-2002 (2003).

4. Michael D. Hurley, William F. Schneider, Timothy J. Wallington, David Mann, John D. DeSain, and Craig A. Taatjes, "Kinetics of Elementary Reactions in the Chain Chlorination of Cyclopropane," *J. Phys. Chem. A* 107, 2003-2010 (2003).

5. John D. DeSain, Stephen J. Klippenstein, and Craig A. Taatjes, "Time-resolved Measurements of OH and HO_2 Formation in Pulsed-Photolytic Chlorine Atom Initiated Oxidation of Neopentane," *Phys. Chem. Chem. Phys.* 5, 1584-1592 (2003).

6. John D. DeSain, Andrew D. Ho, and Craig A. Taatjes, "High Resolution Diode Laser Absorption Spectroscopy of the O-H stretch overtone band $(2,0,0) \leftarrow (0,0,0)$ of the HO_2 Radical," *J. Mol. Spectrosc.*, 219, 163-169 (2003).

7. John D. DeSain, Stephen J. Klippenstein, James A. Miller and Craig A. Taatjes, "Measurement, Theory, and Modeling of OH Formation From the Reactions of Ethyl and Propyl Radicals with O_2," *J. Phys. Chem. A* 107, 4415-4427 (2003).

8. John D. DeSain and Craig A. Taatjes, "Infrared Laser Absorption Measurements of the Kinetics of Propargyl Radical Self-Reaction and the 193 nm Photolysis of Propyne," *J. Phys .Chem. A*, 107, 4843-4850 (2003).

9. Frank Striebel, Leonard E. Jusinski, Askar Fahr, Joshua B. Halpern, Stephen J. Klippenstein and Craig A. Taatjes, "Kinetics of the Reaction of Vinyl Radicals with NO: Ab Initio Theory, Master Equation Predictions, and Laser Absorption Measurements," *Phys. Chem. Chem. Phys.*, in press.

Flame Chemistry and Diagnostics

Craig A. Taatjes, Nils Hansen, Andrew McIlroy

Combustion Research Facility, Mail Stop 9055, Sandia National Laboratories,
Livermore, CA 94551-0969
cataatj@sandia.gov   amcilr@sandia.gov

SCOPE OF THE PROGRAM

The goal of this program is to provide a rigorous basis for the elucidation of chemical mechanisms of combustion, combining experimental measurements employing state of the art combustion diagnostics with detailed kinetic modeling. The experimental program concentrates on the development and application of combustion diagnostics for measurements of key chemical species concentrations. These measurements are carried out in low-pressure, one-dimensional laminar flames and are designed to serve as benchmarks for the validation of combustion chemistry models. Comparison of experimental data to models employing detailed chemical kinetics is critical to determining important chemical pathways in combustion and in pollutant formation in combustion systems. As turbulent combustion models become increasingly sophisticated, accurate chemical mechanisms will play a larger role in computations of realistic combustion systems. Verification of detailed chemistry models against a range of precise measurements under thoroughly-characterized steady conditions is necessary before such flame models can be applied with confidence in turbulent combustion calculations.

PROGRESS REPORT

Molecular Beam Mass Spectrometry at the Advanced Light Source

In collaboration with Terrill Cool of Cornell University and Phillip Westmoreland of the University of Massachusetts, great progress has been made measuring low pressure flames using molecular beam mass spectrometry with synchrotron photoionization at the Advanced Light Source at Lawrence Berkeley National Laboratory. The molecular-beam, photoionization mass spectrometer (PIMS), developed in cooperation with Musa Ahmed at LBNL, is now in full operation. In the past year, the flames using the following fuels have been characterized, and the data is currently being reduced for comparison to detailed models: benzene, 1,3-butadiene, ethane, propane, ethene, propene, ethanol, 1-propanol, and 2-propanol.

Vinyl alcohol as a combustion intermediate The presence of ethenol (vinyl alcohol) has been unambiguously determined in rich low-pressure flames of several fuels. Ethenol, the simplest enol, had never been observed in any flame until its measurement at the ALS in a rich ($\Phi = 1.9$) ethene flame. It can be readily separated from its acetaldehyde tautomer by the difference in ionization threshold. In the last year further

measurements have demonstrated that ethenol is a significant intermediate in combustion of many alkenes and alcohols. Ethenol has been identified unmistakably in ethanol, 1-propanol, 2-propanol, ethene, and 1,3-butadiene flames, and possibly in propene flames. The ethenol concentration relative to acetaldehyde is considerably larger than would be expected from equilibration of the two tautomers. However, ethenol is not evident in the alkane flames that have been measured in the ALS apparatus (ethane, propane). The profiles for ethenol in ethene flames are clearly different from those of acetaldehyde, with acetaldehyde peaking closer to the burner. Several reactions may be responsible for ethenol production, including the reaction of ethene with OH, and sequential H atom loss from ethanol.

Measurements of Species Profiles in Propane Flames Concentration profiles for 25 species have been measured in a rich ($\Phi = 1.8$) low-pressure propane flame. Several isomeric determinations have been made based on differences in ionization energy. The ratio of allene to propyne at m/e = 40 has been measured as 42:58, the same as that determined in a rich ethene flame in previous work at the ALS. The contributions of acetone, propanal, and butane isomers at m/e = 58 have also been determined, different butene isomers have been discriminated, and cyclopentadiene identified.

Measurements of Ethanol Flames Measurement of concentration profiles for ~ 25 stable and radical species in $\Phi = 1$ and $\Phi = 1.97$ low-pressure ethanol flames have been carried out at the ALS. These measurements can be compared with electron-impact MBMS measurements taken at the University of Bielefeld in Katharina Kohse-Höinghaus's group. Kohse-Höinghaus and Tina Kasper, a graduate student in her group, are collaborating with us on the investigation of alcohol flames at the ALS. Although quantitative analysis is ongoing, several qualitative features can be noted. The PIMS data show clear evidence of ethenol in both flames, peaking near the bottom of the luminous zone. A clear threshold is seen at 10.85 eV for m/e = 43, allowing identification of the vinoxy radical (CH2C(O)H).

Measurements of 1- and 2-Propanol Flames Concentration profiles have been measured for flames of both propanol isomers. Discrimination of the isomeric composition of the m/e = 58 peak in the preheat zone shows acetone in the 2-propanol flames and propanal in the 1-propanol flame. Both allene and propyne are observed in the rich propanol flames. Ethenol is seen in these flames, peaking near the bottom of the luminous zone. Reduction and final analysis of the data is continuing.

Determination of Photoionization Cross Sections

Reliable determination of concentration profiles in the VUV PIMS flame experiments requires knowledge of ionization cross sections for flame species. Absolute cross sections have been measured for over 20 key stable combustion intermediates. Photoionization spectra are taken of mixtures of propene and the species of interest,

yielding the unknown absolute cross section by reference to the known cross section of propene. Comparison of derived cross sections (where possible) with independently measured cross sections gives good agreement, providing some confidence in the method. In addition, fragmentation measurements have been performed for 12 species as a function of photon energy. Several of the fuels investigated at the ALS (especially alkanes and propanols) exhibit fragmentation within 1 eV of the ionization threshold; this fragmentation must be understood to reliably extract profiles.

Photoionization Spectra of Flame Species

The identification of chemical species in a flame with VUV PIMS involves measurement of the photoionization efficiency spectra. It is thereby sometimes possible to provide new ionization potential data from flame-sampled MBMS experiments. These determinations do not approach state-of-the-art precision, but are useful in cases where no other experimental measurements are yet available.

The HONO molecule has recently been observed in ALS experiments on low-pressure hydrogen-oxygen flames doped with NO_2. The HONO photoionization efficiency spectrum has been measured between 10.83 eV and 11.63 eV. A Franck-Condon simulation, using calculated geometries and force constants of the cation and neutral, has been constructed to describe the gradual onset of ionization. This simulated photoionization efficiency is then used as a fitting function to estimate the ionization energy from the experimental data. The apparent ionization threshold of (10.97 ± 0.03) eV is in excellent agreement with calculated values and is consistent with published bracketing determinations of the proton affinity of NO_2.

The HCCO radical has been identified in laser VUV photoionization experiments on 1,3-butadiene/H_2/O_2/Ar flames in the flame chemistry laboratory at Sandia. The only literature value for the ionization potential is 9.5 eV, with no estimate of precision. Analysis of the flame-sampled MBMS data, including a field ionization correction, gives an improved IP value of (9.60 ± 0.03) eV. It may prove possible to use flames as a source for measurement of ionization potentials of novel species where little data is currently available.

FUTURE DIRECTIONS

One key immediate task is the analysis of the large body of ALS data accumulated in the past year, which may compel further or confirmatory measurements during subsequent beam cycles. Several new areas of investigation are planned for the ALS flame experiments. Studies of oxygenated fuel chemistry will continue with investigations of aldehydes (ethanal, propanal) and ketones. Doping these fuels in a well-characterized H_2/O_2 flame may be an attractive alternative or complement to pure-fuel studies. For cyclic aliphatic fuels (e.g., cyclohexane, cyclopentene), dehydrogenation of

the cycloalkanes will compete with fragmentation and ring-opening; the isomeric selectivity of the ALS photoionization will have a large impact in unraveling chemical pathways.

Efforts to apply cavity-enhanced frequency-modulation spectroscopy ("NICE-OHMS") as a flame diagnostic will continue, in collaboration with David Osborn. Recent advances in the application of NICE-OHMS are detailed in David Osborn's abstract. A stable cavity has been constructed that is compatible with our low-pressure flame chamber, and will be ready to test soon. Using a $Ti:Al_2O_3$ laser with <100 kHz of frequency noise, this should produce outstanding sensitivity. With a ~0.75 m cavity, we will use 99.8% reflectivity mirrors to give a cavity mode width of 130 kHz. Initial experiments will probe acetylene, NO, and O_2 using well known transitions within the $Ti:Al_2O_3$ tuning range. With the success of these experiments, we plan to frequency double the laser with an external cavity doubler in order to probe CH, C_2, and CH_2O.

Publications acknowledging BES support 2002-present

1. A. McIlroy and J. B. Jeffries, "Cavity ring-down spectroscopy for concentration measurements," in *Applied Combustion Diagnostics*, K. Kohse-Höinghaus and J. B. Jeffries, editors; Taylor and Francis: London, 2002.

2. M. Shahu, C.-H. Yang, C. D. Pibel, A. McIlroy, C. A. Taatjes, and J. B. Halpern, "Vinyl Radical Visible Spectroscopy and Excited State Dynamics," *J. Chem. Phys.* 116, 8343-8352 (2002).

3. S. Roy, R. P. Lucht, A. McIlroy, "Mid-infrared polarization spectroscopy of carbon dioxide," *Appl. Phys. B* 75, 875-882 (2002).

4. M. Kamphus, N. N. Liu, B. Atakan; F. Qi, and A. McIlroy, "REMPI temperature measurement in molecular beam sampled low-pressure flames," *Proc. Combust. Inst.* 29, 2627-2633 (2002).

5. P. Wilcox, E. t. H. Chrysostom, A. McIlroy, J.W. Daily, I. M. Kennedy, "Measurement of CrO in flames by cavity ringdown spectroscopy," *Appl. Phys. B* 77, 535-540 (2003).

6. T. A. Cool, K. Nakajima, T. A. Mostefaoui, F. Qi, A. McIlroy, P. R. Westmoreland, M. E. Law, L. Poisson, D. S. Peterka, M. Ahmed, "Selective detection of isomers with photoionization mass spectrometry for studies of hydrocarbon flame chemistry," *J. Chem. Phys.* 119, 8356-8365 (2003).

7. J. Bood, A. McIlroy, and D. L. Osborn, "Cavity-enhanced frequency modulation absorption spectroscopy of the sixth overtone band of nitric oxide," *Proc. SPIE* 4962, 89-100 (2003).

8. A. McIlroy, A. H. Steeves and J. W. Thoman, Jr. "Chemical Intermediates in Low-Pressure Dimethyl Ether/Oxygen/Argon Flames," *Combustion and Flame*, accepted.

9. A. McIlroy and Fei Qi, "Identifying Combustion Intermediates via Tunable Vacuum Ultraviolet Photoionization Mass Spectrometry," *Combust. Sci. Technol.*, accepted.

10. T. A. Cool, K. Nakajima, C. A. Taatjes, A. McIlroy, P. R. Westmoreland, M. E. Law and A Morel, "Studies of a Fuel-Rich Propane Flame with Photoionization Mass Spectrometry," *Proc. Combust. Inst.* 30, accepted.

THE EXTRACTION OF UNDERLYING MOLECULAR VIBRATIONAL DYNAMICS FROM COMPLEX SPECTRAL REGIONS

H.S. Taylor, Principal Investigator
Department of Chemistry, SSC 704
University of Southern California
Los Angeles, CA 90089-0482
E-mail: taylor@usc.edu
Phone: (213) 740-4112; Fax: (213) 740-3972

The purpose of our research program is to extract information from the results of experimental FTIR and dispersed florescence experiments that probe the high vibrational levels of molecules.

The referred to results came to us in the form of what is known as the spectroscopic Hamiltonian (Hsp). Along with Hsp comes the simple to obtain (all algebraic) eigenvalues (E_j) and eigenfunctions $| E_j >$. They are obtained as the final set in an iterative fitting in which the parameters in Hsp are adjusted to produce the eigenvalues of the experimental spectrum. The eigenfunctions represented on the abstract non-interacting mode number representation basis $\{|\bar{n}>\}$ ie $| E_j > = \sum_j c_{\bar{n}}^s |\bar{n}>$; the $c_{\bar{n}}^j$ are therefore known. Hsp depends on zero order mode oscillator creation $\{a_k^+\}$ and destruction $\{a_k\}$ operators. It involves oscillator, single and interacting mode anharmonic terms and in the cases we treat, multiple resonance terms (as Fermi, Dennison-Darling etc.) The mode frequencies and linear parameters that weight the interaction operators appear as adjustable parameters. The interactions included in Hsp are suggested by the near rational ratio of the fundamental frequencies (eg 2:1$\Rightarrow$Fermi; 1:1, or 2:2$\Rightarrow$ Dennison-Darling etc.) and also include interaction operators which are higher order and enable a better fit of the experimental data.

Fundamentally what we add to this existing picture, that has determined via Hsp the nature of the interactions underlying the spectra, is first a state-by-state assignment of each observed level. The assignment is made in terms of non-obvious, quantized quasiconstants of the motion in number equal to the degrees of freedom. Second, the complex spectrum (in the sense that no one could assign it or extract information from it before) can be sorted into ladders of interleaved states. Each ladder is a simpler spectrum in that it is based on the quantization of a now revealed classical internal molecular motion. It is the intertwining that has made the spectrum complex and unassignable. These achievements, for systems as the bending modes of acetylene[1,2], the high vibrations of DCO[3], N_2O[4] and the proton in CHBrClF[5], were done by using Heisenberg's semiclassical correspondence rules, to convert the basis $|\bar{n}>$ into action-angle variables $(\bar{I}, \bar{\phi})$. This immediately showed that the $|\bar{n}>$ basis functions in $|E_j>$ could be replaced by exp $(-i\bar{I}, \bar{\phi})$ yielding semiclassical eigenfunctions in the variables $\bar{\phi}$. Use of the available constants of the motion, of which the polyad (P) is one, then relates in standard canonical transformation fashion, the actions $\bar{I}$ to P and two new actions J_a, J_b and the angles $\bar{\phi}$ to a cyclic angle θ [it disappears from Hsp and only appears in an ignorable phase in $| E_j >$] and to new angle variables $\psi_\square, \psi_\square$. Since P is a constant of the motion, working Polyad by Polyad, the

problem is now reduced to a two degree of freedom in the angles $\psi_\square, \psi_\square$. The manifestly complex (as opposed to real) semiclassical wave functions in the two angles are obtained by new substituting in the expression for $|E_j\rangle$ the semiclassical correspondence $|\bar{n}\rangle \to \exp[i(n_a\psi_\square + n_b\psi_\square)]$. It is therefore trivially obtained (no calculation; just variable transformation and substitution). Next the wave function <u>density</u> and <u>phase</u> are reach separately plotted on the two angle, toroidal angle space. At this point based on the topology of these simple but unfamiliar plots the ladders can be sorted. Different ladders have visually different topology. Based on a count of nodes and phase advances (eg $2\pi l$; l integer), quantum numbers in addition to P can be assigned. Based on the observed localization of density the particular interaction in the Hsp that underlies the ladder can be recognized. In the past two years a similar effort has been made for the hydrogen CDBrClF[6] and CF3CHBrClF[7]. These problems only reduced to 3 dimensions in the most reduced toroidal angle space, making inspection of the wave function a "tour de force" as slices had to be inspected. The real problem was to choose the most revealing directions in which to slice. 3D graphics are of no visible use. Of course viewing full dimensional eigenstates densities, sliced or projected (no phases exist) in original mode or even transformed coordinates almost never are of any use. Except for an occasional extreme (lowest) on the ladder state nothing is revealed. Problems as HCP[7] and HOCl[8] which have been analyzed in full dimension space are one resonance (i.e. regular - non chaotic) problems with only two coupled modes and are two dimension in bond or normal coordinates and become with our methods trivial 1D type problems in reduced semiclassical representations.

The reader will note that so far all the assignment is obtained by <u>analysis</u>; there are <u>no computations at all</u>. All we need is a good graphics ability so as to view the density and phase of ψ on the reduced dimension wave functions toroidal configuration space in the variables $\bar{\psi}$. We do not need periodic orbits or a study of phase space which required laborious classical calculations in our earlier papers. Moreover it is shown in the papers that the density and phase picture clearly indicate to the eye, organizing lines about which their particular topology is organized. These organizing lines or planes are idealizations of the governing periodic orbits of our previous work. Without serious calculation we show[6] how to transform these idealize orbits or motions in $\bar{\psi}$ space back to initial mode space thereby giving a qualitative picture of the internal motions underlying any ladder. Since the method requires no computation, hopefully in the future spectroscopists who create Hsp's will not, as in the past two decades have to stop their efforts after determining the interactions only. Neither will they or cooperating computational chemists in order to understand the dynamics need to calculate, first the PES and second full dimensions wave packet dynamics or eigenfunctions associated with the PES.

Besides the analysis for the two molecules mentioned above this years progress was the development of the analysis methods that replace extensive computation by analytic thinking. The latter in turn is based on the ideas that emerged in the field of classical non-linear dynamics[10]. To our view the newly developed analytic methodology is an equal contribution to the progress as is the actual analysis of the molecular systems themselves.

In the future we will be analyzing the $SCCl_2$ system. We are working collaboratively to obtain Hsp from the experiments of M. Gruebele[11]; from the theory of E.L. Sibert[12] for constructing Hsp from Gruebele's part fitted, part calculated PES. We will do the analysis. We are always searching for new experiments which supply an Hsp to analyze. We are studying the possibility of finding reliable PEDs for other molecules of interest for which experiments do not exist. We will use the method of reference 12 to construct an Hsp and then do the analysis.

REFERENCES

1. M.P. Jacobson, C. Jung and R.W. Field, J. Chem. Phys., $\underline{111}$, 600-618 (1999).

2. C. Jung, M. Jacobson, H.S. Taylor, J. Phys. Chem. A, $\underline{105}$, 681-693 (2001).

3. C. Jung, H.S. Taylor and E. Atilgan, J. Phys. Chem. A, $\underline{106}$, 3092-3101 (2002).

4. H. Waalkens, C. Jung and H.S. Taylor, $\underline{106}$, 911-924 (2002).

5. C. Jung, E. Ziemniak and H.S. Taylor, J. Chem. Phys., $\underline{115}$, 2449 (2001).

6. C. Jung, C. Mejia-Monasterio and H.S. Taylor, J. Phys. Chem., $\underline{120}$, 4194 (2004).

7. C.Jung, C. Mejia-Monasterio and H.S. Taylor, PCCP, Accepted (2004).

8. H. Ishikawa, R.W. Field, S.C. Farantos, M. Joyeux, J. Koput, C. Beck and R. Schinke, Annu. Rev. Phys. Chem., $\underline{50}$, 443-484, (1999).

9. M. Joyeux, S.C. Farantos and R. Schinke, J. Phys. Chem. A, $\underline{106}$, 5407-5421 (2002).

10. A.J. Lichtenberg and M.A. Lieberman, Springer-Verlag, New York, (1983).

11. R. Bigwood, B. Milam and M. Gruebele, Chem. Phys. Lett., $\underline{287}$, 333 (1998).

12. E.L. Sibert III, J. Chem. Phys., $\underline{88}$, 4378 (1988).

Theoretical Chemical Dynamics Studies of Elementary Combustion Reactions

Donald L. Thompson

Department of Chemistry, University of Missouri, Columbia, MO 65211
thompsondon@missouri.edu

Program Scope

The focus of our research is the development and application of theoretical/computational methods for accurate predictions of the rates of reactions in many-atom systems. The specific objectives of the research are: (1) Develop improved methods that take advantage of modern high-performance computing capabilities for using *ab initio* potential energy surfaces (PESs) in many-atom chemical dynamics simulations and rate calculations. (2) Develop better methods for simulating chemical reactions using classical molecular dynamics (with particular emphasis on developing a better understanding of the validity of the classical approximation and correcting for it where appropriate). (3) Develop a better understanding of the fundamental dynamics and predict rates for important hydrocarbon combustion chemistry reactions. The first of these is the core of the project. Our goal is to develop an automatic PES generation algorithms. Specifically, we are developing interpolative moving least-squares (IMLS) methods for accurately fitting *ab initio* energies to provide global PESs and for use in direct dynamics simulations. The chemical focus is on reactions resulting from the radicals: H, CH_2, CH_3, C_2H_3, C_2H_5, C_3H_3, and C_3H_5.

Recent Progress

Formulating accurate PESs based on *ab initio* calculations is tedious and not readily "generalizable." Relatively straightforward general fitting methods would find ready use in many reaction dynamics simulations. Potential viable approaches are the modified Shepard interpolation and interpolating moving least-squares (IMLS) methods. We are developing practical methods for using IMLS to fit many-atom PESs.[i-iii] The modified Shepard methods, which are currently being widely used, have the disadvantage that gradients and Hessians are required at every point. Hessians are generally not readily available in high-level *ab initio* calculations. The IMLS methods do not require first and second derivatives. We have been testing IMLS methods by fitting PESs for which there are analytical surfaces available so that we can do much more extensive testing than would be feasible if we directly fit *ab initio* points. Our studies include IMLS fitting of a model 1D Morse oscillator,[ii] a 3D N_2H PES,[i] and a 6D HOOH PES.[iii]

The qualities of IMLS fits that emerge from our studies are: (1) They are *broadly applicable*: 1D, 3D, and 6D PESs are fit with basis functions that are straightforward and with weights that are broadly similar and need few if any preliminary calculations to set. The fits are smooth with generally well-behaved derivatives (2) The methods are *extensible*: As soon as the number of calculated points available to be fit exceeds the number of basis functions chosen, a global IMLS fit of the PES can be constructed. Such a fit will have a large rms fitting error. Each additional point made refines the fit; regular or random selections of points can be used with equal facility. (3) The approach offers the *capability of automatic PES generation*: An IMLS fit of any degree highly accurately reproduces the *ab initio* value; however, far from *ab initio* points fits of different degrees differ. The obvious basis for automatic point selection is to calculate additional *ab initio* values where the difference between IMLS degrees is maximal. The results for 6D HOOH demonstrate substantial reductions in the required number of *ab initio* points using this approach.[ii] (4) The methods are *compact*: A terse summary of our results is that, over a 100 kcal/mol range in PES values, ten or so *ab initio* points are needed for 1D, a few hundred for 3D,

and a few thousand for 6D. Key discoveries, illustrated for 6D HOOH, are: (a) IMLS can be applied to not only a PES but to the difference of a PES from a zeroth-order reference PES, which we can readily generate using methods we have developed for constructing approximate PESs for complex reactions. With a relatively small number of *ab initio* points to characterize critical points, we can design a zeroth-order potential V^0 that is a good approximation to V. The difference $\Delta V = V - V^0$ is less variable and much easier to fit than V itself with far fewer *ab initio* points. Introducing V^0 adds negligible cpu time to the overall cost of computing an interpolated surface but the reduction in *ab initio* points is substantial. In the IMLS fitting of the 6D HOOH PES,[iii] the rms fitting errors are reduced 50% by fitting ΔV rather than V and the number of *ab initio* points needed for a given accuracy is reduced by a factor of ~5. In general, the method works better for the IMLS than for the modified Shepard. (b) When the purpose of an IMLS fit is the prediction of dynamical observables, e.g., rates, then the number of *ab initio* calculations required can be much lower than that needed for a general PES. In trajectory studies of ·HOOH→2OH converged rates were obtained with only a few hundred *ab initio* points with a mixed degree (up to fourth degree) IMLS fit.[iv]

As a part of our efforts to find better ways of representing PESs, we have explored the feasibility of using the empirical valence-bond (EVB)[v] method for "linking" existing analytical PESs as "components" in the construction of PESs for larger systems. We began with the EVB formalism of Chang and Miller.[vi] We applied it to the *cis-trans* isomerization of HONO and computed the rates in the low-energy tunneling regime using our semiclassical approach.[vii] Our conclusion is that the EVB approach may be useful in some applications, but does not provide a general, reliable method for constructing PESs.

Most of our efforts during the past year were devoted to the development of efficient PES fitting methods; however, we carried out a study to investigate the accuracy of the quasiclassical approximation for simple bond-fission reactions; more specifically the effects of aphysical flow of ZPE on reaction rates. We chose HOOH and HONO, two somewhat similar molecules, for this study.[viii] We calculated dissociation rates for the O-N bond in *trans*-HONO and the O-O bond in HOOH for selected O-H excitations. The quasiclassical trajectory method seems to work well for HONO. For the $v_{OH} = 5$ state where the energy is about 100 cm^{-1} below the reaction threshold, the computed dissociation rate is quite small, indicating that aphysical flow of ZPE is not a serious problem here. The rate for the $v_{OH} = 5$ state is also about an order of magnitude smaller than that for the $v_{OH} = 6$ state, thus the error introduced by the ZPE flow should not have significant effect on the calculated rates for the $v_{OH} = 6$ and 7 states. Both calculated lifetimes for the $v_{OH} = 6$ and 7 states are well above the experimental lower limits derived from spectral linewidths, suggesting that line broadening due to dissociation is not a dominant contributor to the observed linewidths. We have also performed calculations for the same energies classically distributed among the modes, and the computed rates are much slower than that for the local-mode sampling, showing that IVR is not fast enough for the system to be statistical. These results are consistent with the conclusions of Reiche *et al.*[ix] based on their spectral analysis that the IVR is the major source of the linewidths and the state mixing is not complete on the time scale of the reaction. On the other hand, the quasiclassical trajectory approximation breaks down for HOOH near the threshold region because of the aphysical flow of the ZPE. However, the method seems to work better for higher energy states. The reason that the quasiclassical trajectory approach works for HONO and not for HOOH near the threshold region is because of differences in their intramolecular couplings. The couplings are relatively weak in HONO and the calculated rates are non-statistical while the couplings are strong in HOOH, except the coupling between the two OH modes is relatively weak, and the rates are statistical. One way to check for aphysical behavior of the ZPE is to compute rates near the reaction threshold. However, even if the computed rates for low-energy states are not accurate due to aphysical energy flow, the rates for high-energy states may still be valid.

Future Plans

We will focus on ways to extend IMLS methods to larger systems. The scalability of IMLS methods can be improved by (1) reducing the total number of *ab initio* points required, (2) reducing the number of ab initio points that must be explicitly used in an evaluation of an IMLS fit, and (3) reducing the number of basis functions used in the IMLS fit. The total number of *ab initio* points needed can be reduced by combining an automatic point selection scheme with a fit of a difference PES, incorporating previously developed PESs that are a part of the larger PES of interest, and incorporating gradient information. We will investigate ways to reduce the number of *ab initio* points needed for an IMLS evaluation. The cost of an IMLS evaluation depends linearly on how many of the *ab initio* points must be explicitly included in the least-squares solutions. Since weights associated with each *ab initio* point can vary by tens of orders of magnitude, weights can be used to screen out only the most important *ab initio* points in an IMLS evaluation. How to do weight-based screening efficiently will be investigated. Reducing the basis could greatly increase the scalability. The cost of an IMLS evaluation depends on the square of the number of basis functions. Several approaches for basis set reduction will be explored.

Of particular interest to us is how to automate PES generation by using dynamics or kinetics codes. The long-term goal is methods in which the PES is generated by the dynamics during the course of simulations. By contrasting different degree IMLS fits, the demands of a classical trajectory for PES information to advance to the next time step can be satisfied by either a new *ab initio* calculation or by an IMLS fit evaluation with the current set of *ab initio* points. The magnitude of the difference between IMLS fits tolerated before triggering a new *ab initio* calculation can be adjusted to converge the dynamical observables being calculated. Modified Shepard studies have shown the efficacy of related versions of this kind of approach. We will examine an approach based on a hierarchy of IMLS degrees in which very high degree IMLS fits too expensive for routine use but of near comparable accuracy to *ab initio* calculations can be used to generate pseudo *ab initio* values. The magnitude of the difference between IMLS fits triggers first a pseudo *ab initio* calculation and then at a higher value an actual *ab initio* calculation.

We plan to focus on reactions involving saturated and unsaturated polyatomic hydrocarbon radicals, particularly barrier-less reactions between radicals. We will explore the detailed reaction dynamics and compute rates for recombination and its reverse of unimolecular decomposition. These studies will be done as we develop *ab initio* PESs using the IMLS methods. Some of the studies will be done in collaboration with the Chemical Dynamics Group at ANL; they have in hand extensive collections of *ab initio* points for radical-radical recombinations. We plan to study a representative set of four reactions for which *ab initio* data is already available: $H + CH_3$, $H + C_2H_5$, $H + C_3H_3$, and $CH_3 + CH_3$. These studies will initially be designed to test the IMLS PES fitting for recombination kinetics. Both direct IMLS fits and fits based on zeroth-order potentials will be investigated. Preliminary results suggest that pairwise-additive potentials modified by switching functions can qualitatively represent the *ab initio* results with *transferable* parameters. If so, zeroth-order potentials could be produced for whole families of recombination reactions (e.g., H+alkyl) and used to accelerate IMLS PES generation. Time permitting we will also begin studies of the rather complex isomerization and decomposition reactions of the allene-propyne (C_3H_4) system.

Publications

• Yin Guo and Donald L. Thompson, *"Semiclassical Calculations of Tunneling Splitting in Hydrogen Peroxide and Its Deuterated Isotopomers,"* J. Phys. Chem. A **106**, 8374-8377 (2002). (Part of Don W. Setser Festschrift)

- Yin Guo and Donald L. Thompson, "*A Theoretical Study of Cis-Trans Isomerization in HONO Using an Empirical Valence Bond Potential*," J. Chem. Phys. **118**, 1673-1678 (2003).
- Gia G. Maisuradze and Donald L. Thompson, "*Interpolating Moving Least-Squares Method for Fitting Potential Energy Surfaces: Illustrative Approaches and Applications*,"
J. Phys. Chem. A **107**, 7118-7124 (2003). (Part of Donald J. Kouri Festschrift)
- Gia G. Maisuradze, Donald L. Thompson, Albert F. Wagner, and Michael Minkoff, "*Interpolating Moving Least-Squares Method for Fitting Potential Energy Surfaces: Detailed Analysis of One Dimensional Applications*," J. Chem. Phys. **119**, 10002-10014 (2003).
- Yin Guo and Donald L. Thompson, "*A Classical Trajectory Study of Bond Dissociation in HONO and HOOH*" Chem. Phys. Letters 382, 654-660 (2003).
- Akio Kawano, Yin Guo, Donald L. Thompson, Albert F. Wagner, and Michael Minkoff, "*Improving the Accuracy of Interpolated Potential Energy Surfaces by Using an Analytical Zeroth-Order Potential Function*," J. Chem. Phys., in press.
- Yin Guo, Akio Kawano, Donald L. Thompson, Albert F. Wagner, and Michael Minkoff, "*Generating Potential Energy Surfaces by an Interpolating Moving Least-Squares Approach for Classical Dynamics Calculations*," J. Chem. Phys., submitted.
- Gia G. Maisuradze, Donald L. Thompson, Albert F. Wagner, and Michael Minkoff, "*Interpolating Moving Least-Squares Methods for Fitting Potential Energy Surfaces: Analysis of Application to a Six-Dimensional System*" J. Chem. Phys., to be submitted.

Reference

[i] G. G. Maisuradze and D. L. Thompson, J. Phys. Chem. A **107**, 7118 (2003)

[ii] G. G. Maisuradze, D. L. Thompson, A. F. Wagner, and M. Minkoff, J. Chem. Phys. **119**, 10002 (2003).

[iii] A. Kawano, Y. Guo, D. L. Thompson, A. F. Wagner, and M. Minkoff, J. Chem. Phys., in press.

[iv] Y. Guo, A. Kawano, D. L. Thompson, A. F. Wagner, and M. Minkoff, J. Chem. Phys., in press.

[v] A. Warshel, Accts. Chem. Res. **14**, 284 (1981).

[vi] Y. T. Chang and W. H. Miller, J. Phys. Chem. **94**, 5884 (1990).

[vii] Y. Guo and D. L. Thompson, J. Chem. Phys. **118**, 1673 (2003).

[viii] Y. Guo and D. L. Thompson, Chem. Phys. Lett. **382**, 654 (2003).

[ix] F. Reiche, B. Abel, R. D. Beck, and T. R. Rizzo, J. Chem. Phys. **112**, 8885 (2000).

Terascale High-Fidelity Simulations of Turbulent Combustion with Detailed Chemistry
http://scidac.psc.edu/

SciDAC: Computational Chemistry
(DOE Office of Science, BES: Chemical Sciences, Program Manager: R. Hilderbrandt)

Work-in-progress Report – *Period from 03/31/03 to 03/31/04*

List of Principal Investigators

- Arnaud Trouvé (University of Maryland, UMD, *atrouve@eng.umd.edu*)
- Jacqueline Chen (Sandia National Laboratories, SNL, *jhchen@ca.sandia.gov*)
- Hong G. Im (University of Michigan, UMI, *hgim@umich.edu*)
- Christopher J. Rutland (University of Wisconsin, UWI, *rutland@engr.wisc.edu*)
- Raghurama Reddy, Sergiu Sanielevici (Pittsburgh Supercomputing Center, PSC, Carnegie Mellon Univ., *rreddy@psc.edu, sergiu@psc.edu*)

Project Summary

The present project is a multi-institution collaborative effort aimed at adapting a high-fidelity turbulent reacting flow solver called S3D to terascale, massively parallel, computer technology. S3D adopts the direct numerical simulation (DNS) approach: DNS is a unique tool in combustion science proposed to produce both high-fidelity observations of the micro-physics found in turbulent reacting flows as well as the reduced model descriptions needed in macro-scale simulations of engineering-level systems. The new S3D software is enhanced with new numerical and physical modeling capabilities; it is also modified to become object-oriented and fit into an advanced software environment based on an adaptive mesh refinement framework called GrACE and the Common Component Architecture (CCA).

Program Scope

Direct numerical simulation (DNS) is a mature and productive research tool in combustion science that is based on first principles of continuum mechanics. Because of its high demand for computational power, current state-of-the-art DNS remains limited to small computational domains (*i.e.* weakly turbulent flows) and to simplified problems corresponding to adiabatic, non-sooting, gaseous flames in simple geometries. The objective of this research project is to use terascale technology to overcome many of the current DNS limitations and allow for first-principles simulations of pollutant emissions (NO_x, soot) from turbulent combustion systems.

The effort leverages an existing DNS capability, named S3D, developed at Sandia National Laboratories. S3D is a compressible Navier-Stokes solver coupled with an integrator for detailed chemistry (CHEMKIN-compatible), and is based on high-order finite differencing, high-order explicit time integration, conventional structured meshing, and MPI-based parallel computing implementation. The objective here is to both re-design S3D for effective use on terascale high-performance computing platforms, and to enhance the code with new numerical and physical modeling capabilities.

The list of new numerical developments includes: an implicit/explicit operator-splitting technique for efficient time integration; a modified inflow boundary scheme for acoustically-smooth turbulence forcing; and a pseudo-compressibility method for more efficient computation of slow flow problems. The list of new physical modeling developments includes: a thermal radiation capability; a soot formation capability; and a Lagrangian particles capability to simulate dilute liquid fuel sprays.

The new S3D software has also been modified to fit into GrACE, an advanced parallel computing framework targeted for adaptive mesh refinement applications. Our project has developed a library of wrappers to fit the S3D Fortran 90 environment into the C++ GrACE framework. Our effort is now focused in making S3D compliant to a software interoperability standard, the Common Component Architecture (CCA) developed by the SciDAC ISIC in Ref. [1]. The CCA environment will allow exchanging software components developed by different teams working on complementary tasks. It will allow in particular the re-use of components developed by a separate Sandia-led research project called CFRFS [2]. This exchange of software components between different projects is a unique feature allowed by the SciDAC structure that promotes interactions between different teams of application scientists (our project and CFRFS [2]) and between application scientists and computer scientists (our project, CFRFS and the CCA ISIC [1]).

Recent Progress

As explained above, the present developments for S3D include a complete software re-design, new numerical methods and new physical modeling capabilities. We present here a summary of progress made during the past 12 months work period of this project extending from 03/31/02 to 03/31/03.

Software design developments:

- S3D has been modified to fit into GrACE. The developments include a new library of wrappers to fit the S3D Fortran 90 environment into the C++ GrACE framework (PSC/Roberto Gomez, Raghurama Reddy, Junwoo Lim).

- S3D is currently being adapted to the CCA framework (PSC/Raghurama Reddy)

Numerical developments:

- A new pseudo-compressibility method has been developed and implemented into S3D (UMD/Arnaud Trouvé, [3-5]). This method allows for more efficient computations of slow flow problems while still using a fully compressible formulation.

- The S3D inflow boundary scheme (using a characteristic-based analysis) has been modified to allow for injection of laminar/turbulent flow perturbations while minimizing spurious acoustic wave reflections (UMI/Hong Im, [6-8]).

Physical model developments:

- A new thermal radiation solver (discrete ordinate method, DOM, grey and non-scattering medium) has been implemented into S3D (UMI/Hong Im, [9]). A second separate solver based on the discrete transfer method (DTM) has been implemented into S3D (UMD/Arnaud Trouvé).

297

• A phenomenological soot model based on transport equations for the soot volume fraction and particle number density has been implemented into S3D (UMD/Arnaud Trouvé [9]).

• A Lagrangian particle model to describe dilute liquid sprays has been developed and coupled to the gas-phase Eulerian solver in S3D (UWI/Christopher Rutland, [10-12]).

New combustion science:

The new DNS solver is currently used in a series of demonstration studies selected for both their technical challenge and scientific value. The list of ongoing pilot studies includes: the simulation of turbulent ethylene-air counter-flow diffusion flames (to study flame extinction phenomena and edge-flame dynamics) [6,9,13]; the simulation of a turbulent ethylene-air jet diffusion flame near a solid wall (to study flame-wall interactions and the associated wall heat transfer) (see Fig. 1); the simulation of turbulent auto-ignition for a population of vaporizing liquid fuel (n-heptane) droplets (to study spray auto-ignition in homogeneous charge compression ignition – HCCI – engines) [10-12,14-15]. Additional S3D-based studies may be found in Refs. [16-19].

Future Plans

The main focus of the coming work period will be to: (1) release a CCA/GrACE-based version of S3D; (2) and exchange software components with the CFRFS project [2], and thereby initiate developments to adapt S3D to AMR.
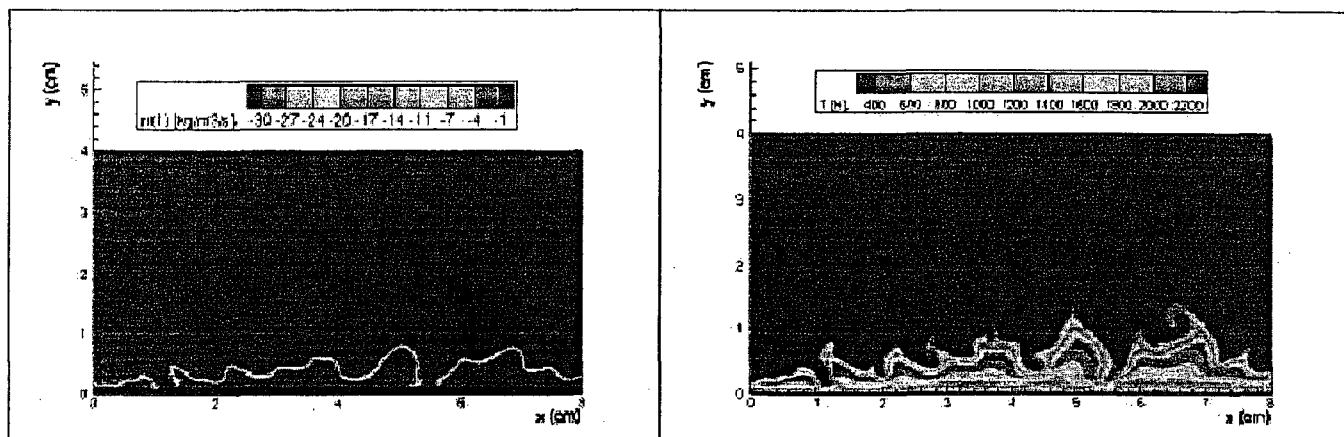
Figure 1. Instantaneous variations of fuel mass reaction rate (left) and temperature (right) during the simulation of a turbulent reacting wall boundary layer. The flow is from left to right; the flame develops at the interface of the fuel stream (bottom left) and the air stream (top left). The wall boundary (bottom) remains at 300 K. Two wall-induced flame extinction events are observed in these snapshots, near $x = 1.2$ cm and $x = 5.4$ cm.

References

[1] Armstrong, R. C., *et al.* "Center for Component Technology for Terascale Simulation Software", SciDAC Integrated Software Infrastructure Center (ISIC), http://www.cca-forum.org/ccttss/

[2] Najm, H., *et al.* "A Computational Facility for Reacting Flow Science", SciDAC project, http://cfrfs.ca.sandia.gov/

[3] Wang, Y. & Trouvé, A. (2003) "Artificial Acoustic Stiffness Reduction in Fully Compressible, Direct Numerical Simulation of Combustion", *3rd Joint Meeting US Sections of Combustion Institute*, Chicago, IL.

[4] Wang, Y. & Trouvé, A. (2003) "Artificial acoustic stiffness reduction in fully compressible, direct numerical simulation of combustion", *submitted to Combust. Theory Modelling.*

[5] Trouvé A., Wang Y., Im H. G., Yoo C. S., Rutland C. J., Wang Y., Chen J. H., Sutherland J. C., and Mason S. D. (2004), 'Direct numerical simulation of turbulent combustion using a fully compressible flow formulation," *10th SIAM Intl. Conf. on Numerical Combustion*, Sedona, AZ.

[6] Yoo, C. & Im, H. G. (2003) "A Computational Study on the Dynamics of Counterflow Hydrogen-Air Edge Flames", *3rd Joint Meeting US Sections of Combustion Institute*, Chicago, IL.

[7] Yoo, C. S. and Im, H. G. (2004), "Soft inflow boundary conditions for direct numerical simulations of compressible reacting flows," *10th SIAM Intl. Conf. on Numerical Combustion*, Sedona, AZ.

[8] Yoo, C. S. and Im, H. G. (2004), "Soft inflow boundary conditions for direct numerical simulations of compressible reacting flows," *submitted to J. Comp. Phys.*

[9] Yoo, C. S., Im, H. G. Trouvé, A., and Wang, Y. (2004), "Direct numerical simulation of turbulent nonpremixed counterflow ethylene-air flame with soot and radiation models," *10th SIAM Intl. Conf. on Numerical Combustion*, Sedona, AZ.

[10] Wang, Y. and Rutland, C. J. (2003), "Direct numerical simulation of turbulent droplets flow with evaporation," *The 41st AIAA Aerospace Sciences Meeting and Exhibit*, AIAA Paper 2003-1281, 6-9 January 2003, Reno, Nevada, USA.

[11] Wang, Y. and Rutland, C. J. (2003), "On the combustion of normal heptane fuel droplets in isotropic turbulence with DNS," *3rd Joint Meeting of the US Sections of the Combustion Institute*, Chicago, IL.

[12] Wang, Y. and Rutland, C. J. (2004), "Effects of temperature and equivalence ratio on the ignition of n-heptane fuel droplets in turbulent flow," *submitted to 31st Intl. Symp. Combustion.*

[13] Yoo, C. S. and Im, H (2004), "Transient dynamics of edge flames in a laminar nonpremixed hydrogen-air counterflow," *submitted to 31st Intl. Symp. Combustion.*

[14] Sankaran, R., Im, H. G., Hawkes, E. R. & Chen, J. H. (2004), 'The effects of nonuniform temperature distribution on the ignition of a lean homogeneous hydrogen-air mixture," *submitted to 31st Intl. Symp. Combustion.*

[15] Chen, J. H., Hawkes, E. Hewson, J. C., Sankaran, R., Im, H. G., Mason, S. D. (2004), "Ignition front propagation in a constant volume with temperature inhomogeneities," *submitted to 31st Intl. Symp. Combustion.*

[16] Chen, J. H., Mason, S. D. & Hewson, J. C. (2003) "The Effect of Temperature Inhomogeneity on Low-Temperature Autoignition of Fuel-Lean Premixed Hydrogen/Air Mixtures", *3rd Joint Meeting US Sections of Combustion Institute*, Chicago, IL.

[17] Hawkes, E. R. & Chen, J. H. (2003) "Turbulent Stretch Effects on Hydrogen Enriched Lean Premixed Methane-Air Flames", *3rd Joint Meeting US Sections of Combustion Institute*, Chicago, IL.

[18] Liu, S. & & Chen, J. H. (2003) "The Effect of Product Gas Enrichment on the Chemical Response of Premixed Diluted Methane/Air Flames", *3rd Joint Meeting US Sections of Combustion Institute*, Chicago, IL.

[19] Sutherland, J. C., Smith, P. J. & Chen, J. H. (2003) "DNS of a Nonpremixed CO-H2 Jet using Detailed Chemistry – Toward Improved LES Models", *3rd Joint Meeting US Sections of Combustion Institute*, Chicago, IL.

VARIATIONAL TRANSITION STATE THEORY

Principal investigator, mailing address, and electronic mail

Donald G. Truhlar

Department of Chemistry, University of Minnesota, 207 Pleasant Street SE,
   Minneapolis, Minnesota 55455

truhlar@umn.edu

Program scope

This project involves the development of variational transition state theory (VTST) with multidimensional tunneling (MT) contributions and its application to gas-phase reactions. The further development of VTST as a useful tool for combustion kinetics also involves multidimensional tunneling calculations for the transmission coefficient, electronic structure calculations for the input potential energy surfaces, and methods to interface the electronic structure calculations to the dynamics calculations. Our current work is especially focused on developing and applying new methods for electronic structure theory and dynamics and for interfacing reaction-path and reaction-swath dynamics calculations with electronic structure theory. The work involves development of new theory, development and implementation of practical techniques for applying the theory to various classes of reactions and transition states, and applications to specific reactions, with special emphasis on combustion reactions and reactions that provide good test cases for methods needed to study combustion reactions. A theme that runs through our current work is the development of consistently and generally defined electronic structure methods with empirical elements, including molecular mechanics, density functionals, and scaled-electron-correlation components and the use of these methods in direct dynamics calculations of chemical reaction rates.

Recent progress

Aiming at generating reactive PES with minimal computational effort, we have introduced an efficient algorithm called multiconfiguration molecular mechanics (MCMM). MCMM describes polyatomic potential energy surfaces through several interacting MM configurations and can thus be viewed as an extension of standard MM to chemical reactions. Such a goal is achieved by combining molecular mechanics potentials for the reactant and product wells with electronic structure data (energy, gradient, and Hessian) at the saddle point and a small number of non-stationary points. We developed a general strategy for placement of the non-stationary points for fitting potential energy surfaces in the kinetically important regions and for calculating rate constants for atom transfer reactions by variational transition state theory with multidimensional tunneling. Then we improved the efficiency of the MCMM method by using electronic structure calculations only for certain critical elements of the Hessians at the non-stationary points and by using interpolation for the other elements at the non-stationary points. We tested this new MCMM strategy for a diverse test suite of six reactions involving hydrogen-atom transfer. The new method yields quite accurate rate constants as compared with the standard MCMM strategy employing full electronic structure Hessians and also as compared with direct dynamics calculations using an uninterpolated full potential energy surface at the same electronic structure level. In comparison with the standard MCMM strategy, this new procedure reduces the computational effort associated with the non-stationary points by a factor of up to 3 for the test reactions and up to 11 for even larger reactive systems.

We have carried out benchmark high-level calculations for the barrier heights of five degenerate and nearly degenerate rearrangements (CH_3 + CH_4 or C_2H_6, C_2H_5 + CH_4 or C_2H_6, and n-C_3H_7 + n-C_3H_8) involving hydrogen transfer between hydrocarbon fragments. The performance of eleven existing and five new semiempirical methods based on neglect of diatomic differential overlap (NDDO) and intermediate neglect of differential overlap (INDO) was evaluated. Two new NDDO methods were developed to provide both accurate barrier heights and transition state geometries.

We tested many new-generation hybrid DFT (HDFT) methods against our AE6 and BH6 databases. According to our resent assessment, some HDFT methods such as B3LYP, mPWPW91, B1B95, and B97-2 are successful for thermochemistry but unsatisfactory for kinetics. Our assessments showed that MPW1K is an HDFT model with excellent performance for kinetics. We optimized a Becke88–Becke95 1-parameter model for kinetics (BB1K) against a representative benchmark kinetics database. We also developed two doubly HDFT methods MC3BB and MC3MPW by mixing the scaling all correlation (SAC) method with HDFT methods using a multi-coefficient approach. We also optimized three methods, namely, MPW1B95, MPWB1K, and MC3MPWB methods, based on the modified Perdew and Wang' exchange functional (mPW) and Becke's 1995 non-local kinetic energy correlation functional (B95). MPW1B95 is suitable for general applications in thermochemistry, and its performance for atomization energy, ionization potential, and electron affinity calculations is better than the popular methods B3LYP, mPW1PW91 and PBE1PBE. MPWB1K is n HDFT model for kinetics. MC3MPWB, as well as MC3BB and MC3MPW, gives good performance on atomization energy and barrier height calculations.

Another project involves hydrogen abstraction from dimethyl sulfide by OH. This has branched into research on sulfur-containing compounds and research on hydrogen abstraction of similar reactants, such as DMSe and DME. We found that MPW1K does an excellent job of reproducing MC-QCISD and MCG3 results for the S-O and S-H bonds of H_2S-OH and H_2S-HO. Reaction rates have been calculated using MPW1K and MC-QCISD and have shown that MCG3///MPW1K reproduces MCG3///MC-QCISD, which means much computer time will be saved by using the adequate MPW1K paths when determining reaction rates.

Software distribution

We have developed several software packages for applying variational transition state theory with optimized multidimensional tunneling coefficients to chemical reactions and for carrying out MCCM calculations, hybrid Hartree-Fock density functional theory calculations, and direct dynamics and MCMM applications. The URL for our software distribution site is http://comp.chem.umn.edu/Truhlar. The number of license requests that we fulfilled during the period Jan. 1, 2002–Apr. 2, 2004 for selected software packages developed wholly or partially under DOE support is as follows:

	Total	academic	government/DoD	industry
GAMESSPLUS*	60	56	1	3
GAUSSRATE	72	67	4	1
HONDOPLUS**	55	46	6	3
MOPAC-mn	146	122	8	16
POLYRATE	175	162	10	3
6 OTHERS	72	65	4	4

Future plans

Our work includes several specific objectives for the upcoming three-year period. (1) It will be useful, especially for the treatment of small-barrier association reactions, to create a hybrid theory incorporating quantization and multidimensional tunneling into the multifaced-dividing-surface generalization of the variable reaction coordinate approach to VTST, and research aimed at this objective will be initiated. (2) Projects will be undertaken to develop improved density functional methods and improved multi-coefficient correlation methods for using electronic structure theory to calculate potential energy surfaces. (3) We will extend our barrier-height database, currently consisting mainly of hydrogen-atom reactions, to encompass a broader selection of the reaction types that are important for combustion research. (4) We will further develop the multi-configuration molecular mechanics approach as an efficient tool for the semiautomatic fitting of potential energy surfaces for large systems. (5) We will attempt to develop more reliable methods for including anharmonicity at variational transition states, especially for torsions. (6) We will develop new methods for the calculation of substituent

effects. Reactions to be considered as test cases include: reactions of hydrogen atoms with hydrogen peroxide, methanol, ethanol, acetaldehyde, acetone, 2-butanone, acetylene, methylformate, fluoromethyl formate, and polycyclic aromatic hydrocarbon anions; reactions of $C(^3P)$ with allene; hydrogen atom abstraction from fluoroformaldehyde by NO_3; reaction of hydroxyl radical with hydrogen sulfide, dimethyl sulfide, ethylene, benzene, and toluene; reactions of CF_3 with various hydrocarbons; and rearrangement of unsymmetrically substituted o-tolylcarbenes. In addition to developing the methods, we are putting them into user-friendly packages that will allow more researchers to carry out calculations conveniently by the new methods.

Publications, 2002-present

Journal articles

1. "POTLIB 2001: A Potential Energy Surface Library for Chemical Systems," R. J. Duchovic, Y. L. Volobuev, G. C. Lynch, T. C. Allison, J. C. Corchado, D. G. Truhlar, A. F. Wagner, and B. C. Garrett, Computer Physics Communications **144**, 169-187 (2002).
2. "Parameterized Direct Dynamics Study of Rate Constants of H with CH_4 from 250 to 2400 K," J. Pu and D. G. Truhlar, Journal of Chemical Physics **116**, 1468-1478 (2002).
9. "What are the Best Affordable Multi-Coefficient Strategies for Calculating Transition State Geometries and Barrier Heights?" B. J. Lynch and D. G. Truhlar, Journal of Physical Chemistry A **106**, 842-846 (2002).
10. "Interpolated Algorithms for Large-Curvature Tunneling Calculations," A. Fernandez-Ramos, D. G. Truhlar, J. C. Corchado, and J. Espinosa-Garcia, Journal of Physical Chemistry A **106**, 4957-4960 (2002).
11. "Tests of Potential Energy Surfaces for H + CH_4 ↔ CH_3 + H_2: Deuterium and Muonium Kinetic Isotope effects for the Forward and Reverse Reaction," J. Pu and D. G. Truhlar, Journal of Chemical Physics **117**, 10675-10687 (2002).
12. "Obtaining the Right Orbitals is the Key to Calculating Accurate Binding Energies for Cu+ Ion," B. J. Lynch and D. G. Truhlar, Chemical Physics Letters **361**, 251-258 (2002).
13. "Validation of Variational Transition State Theory with Multidimensional Tunneling Contributions Against Accurate Quantum Mechanical Dynamics for H + CH_4 -> H_2+ CH3 in an Extended Temperature Interval," J. Pu and D. G. Truhlar, Journal of Chemical Physics **117**, 1479-1481 (2002).
14. "Reply to Comment on Molecular Mechanics for Chemical Reactions," D. G. Truhlar, Journal of Physical Chemistry A **106**, 5048-5051 (2002).
15. "Reduced Mass in the One-Dimensional Treatment of Tunneling," D. G. Truhlar and B. C. Garrett, Journal of Physical Chemistry A **107**, 4006-4007 (2003).
16. "The Effectiveness of Diffuse Basis Functions for Calculating Relative Energies by Density Functional Theory," B. J. Lynch, Y. Zhao, and D. G. Truhlar, Journal of Physical Chemistry A **107**, 1384-1388 (2003).
17. "Robust and Affordable Multi-Coefficient Methods for Thermochemistry and Thermochemical Kinetics: The MCCM/3 Suite and SAC/3," B. J. Lynch and D. G. Truhlar, Journal of Physical Chemistry A **107**, 3898-3906 (2003).
18. "Generalized Transition State Theory in Terms of the Potential of Mean Force," G. K. Schenter, B. C. Garrett, and D. G. Truhlar, Journal of Chemical Physics **119**, 5828-5833 (2003).
19. "Force Field Variations along the Torsional Coordinates of CH_3OH and CH_3CHO," T. V. Albu and D. G. Truhlar, Journal of Molecular Spectroscopy **219**, 129-131 (2003).
20. "H + H_2 Thermal Reaction: Another Solved Problem of Quantum Mechanics, " S. L. Mielke, K. A. Peterson, D. W. Schwenke, B. C. Garrett, D. G. Truhlar, J. V. Michael, M.-C. Su, and J. W. Sutherland, Physical Review Letters **91**, 063201/1-4 (2003).

21. "Small Representative Benchmarks for Thermochemical Calculations," B. J. Lynch and D. G. Truhlar, Journal of Physical Chemistry **107**, 8996-8999 (2003).
22. "Small Basis Sets for Calculations of Barrier Heights, Energies of Reaction, Electron Affinities, Geometries, and Dipole Moments," B. J. Lynch and D. G. Truhlar, Theoretical Chemistry Accounts, in press.
23. "Small Representative Benchmarks for Thermochemical Calculations," B. J. Lynch and D. G. Truhlar, Journal of Physical Chemistry A **107**, 8996-8999 (2003); erratum: **108**, 1460 (2003).
24. "Benchmark Results for Hydrogen Atom Transfer Between Carbon Centers and Validation of Electronic Structure Methods for Bond Energies and Barrier Heights," A. Dybala-Defratyka, P. Paneth, J. Pu, and D. G. Truhlar, Journal of Physical Chemistry B, in press.
25. "Tests of Second-Generation and Third-Generation Density Functionals for Thermochemical Kinetics, " Y. Zhao, J. Pu, B. J. Lynch and D. G. Truhlar, Phys. Chem. Chem. Phys. **6**, 673-676 (2004).
26. "Development and Assessment of a New Hybrid Density Functional Method for Thermochemical Kinetics," Y. Zhao, B. J. Lynch and D. G. Truhlar, J. Phys. Chem., in press.
27. "Efficient Molecular Mechanics for Chemical Reactions: Multiconfiguration Molecular Mechanics using Partial Electronic Structure Hessians," H. Lin, J. Pu, T. V. Albu, and D. G. Truhlar, Journal of Physical Chemistry A, in press.
28. "Doubly Hybrid DFT: New Multi-Coefficient Correlation and Density Functional Methods for Thermochemistry and Thermochemical Kinetics, Y. Zhao, B. J. Lynch, and D. G. Truhlar. Journal of Physical Chemistry A, in press.

Book chapters

1. "Multilevel Methods for Thermochemistry and Thermochemical Kinetics," B. J. Lynch and D. G. Truhlar, American Chemical Society Symposium Series, edited by A. K. Wilson, American Chemical Society, Washington, in press.
2. "Variational Transition State Theory and Multidimensional Tunneling for Simple and omplex Reactions in the Gas Phase, Solids, Liquids, and Enzymes," D. G. Truhlar, in *Isotope Effects in Chemistry and Biology*, edited by H. Limbach and A. Kohen (Marcel Dekker, Inc., New York, 2004), to be published.

Computer programs

"POLYRATE–version 9.3," J. C. Corchado, Y.-Y. Chuang, P. L. Fast, J. Villà, W.-P. Hu, Y.-P. Liu, G. C. Lynch, K. A. Nguyen, C. F. Jackels, V. S. Melissas, B. Lynch, I. Rossi, E. L. Coitiño, A. Fernandez-Ramos, J. Pu, T. V. Albu, R. Steckler, B. C. Garrett, A. D. Isaacson, and D. G. Truhlar, University of Minnesota, Minneapolis, Nov. 2003.

"GAUSSRATE–version 9.1," J. C. Corchado, Y.-Y. Chuang, E. L. Coitiño, and D. G. Truhlar, University of Minnesota, Minneapolis, July 2003.

"HONDOPLUS–version 4.5," H. Nakamura, J. Xidos, J. Thompson, J. Li, G. D. Hawkins, T. Zhu, B. J. Lynch, Y. Volobuev, D. Rinaldi, D. A. Liotard, C. J. Cramer, and D. G. Truhlar, University of Minnesota, Minneapolis, Mar. 2004.

"MULTILEVEL–version 3.1," J. M. Rodgers, B. J. Lynch, P. L. Fast, Y. Zhao, J. Pu, Y.-Y. Chuang, and D. G. Truhlar, University of Minnesota, Minneapolis, Sept. 2003.

"MULTILEVELRATE–version 9.3," J. Pu, J. C. Corchado, B. J. Lynch, P. L. Fast, and D. G. Truhlar, University of Minnesota, Minneapolis, Jan. 2004.

"MC-TINKER," T. V. Albu, J. C. Corchado, Y. Kim, J. Villà, J. Xing, H. Lin, and D. G. Truhlar, University of Minnesota, Minneapolis, Dec. 2003.

"MC-TINKERATE–version 9.1," T. V. Albu, J. C. Corchado, Y. Kim, J. Villa, J. Xing, H. Lin, and D. G. Truhlar, University of Minnesota, Minneapolis, Dec. 2003.

KINETIC DATABASE FOR COMBUSTION MODELING

Wing Tsang
National Institute of Standards and Technology
Gaithersburg, MD 20899
wing.tsang@nist.gov

Program Scope or Definition: The aim of this project is to develop chemical kinetic databases for use in the simulation of combustion processes. The essential ingredients for the work are the rate expressions for the chemical reactions that convert reactants into products through a variety of reaction intermediates and the thermodynamic properties of all relevant species. Such information represents essential elements in the quantitative understanding of combustion phenomena. This work has particular relevance at the present time due to the increasing capability of computational fluid dynamics codes to handle detailed chemistry. The proper description of combustion requires an understanding of both fluid dynamics and chemistry. We are approaching the time that realistic systems can be simulated. This leads to the possibility of powerful design tools that will increasingly take the place of empirical physical testing. The information in the databases represents transferable elements that can be used in a large variety of scenarios. For kinetics, they begin with the thermal rate constants for unimolecular and bimolecular processes. However, with the higher temperatures, the Boltzmann distribution of the molecules becomes increasingly distorted. Rate expressions are no longer solely dependent on temperature. The focus of current work has been to determine the consequences of such effects for increasingly larger molecules with low reaction thresholds.

Recent Progress: Unimolecular reactions in the most general sense are processes that describe the breakdown (fuels) as well as the formation (PAH) of larger molecular entities. As such they play a particularly important role in combustion chemistry. The physical phenomenon is well understood[1]. However, as is often the case, the application to real systems leads to many problems. This discussion will be concerned with the solution of one particular problem. It has opened the way for attacking a number of related issues.

Traditionally, the building of kinetic databases has involved the collection of experimental data, the evaluation of the experimental procedure and tests using rate expressions for analogous reactions as a basis [2]. Such procedures are particularly straightforward for truly thermal reactions since they are solely dependent on temperature. The introduction of pressure as a variable complicates the situation. It will now be necessary, first to extract from the experimental measurements the high pressure rate expression and then to project it to pressures and temperatures of interest. We have developed a program CHEMRATE with the aim of systematizing the process[3,4]. However, it opened a whole range of system specific problems. The following will contain a brief discussion of these issues.

The treatment of unimolecular reactions is a reflection of how experiments are carried out [5]. For thermal decomposition processes a compound is placed in a vessel, concentration decreases are measured as a function of time and rate constants are then extracted. Physically there is usually a short period, the incubation time, where the distribution function adjusts to the environment prior to the establishment of a new steady state distribution that is reflected in the rate constant. This is a closed system and is appropriate for slower processes.

304
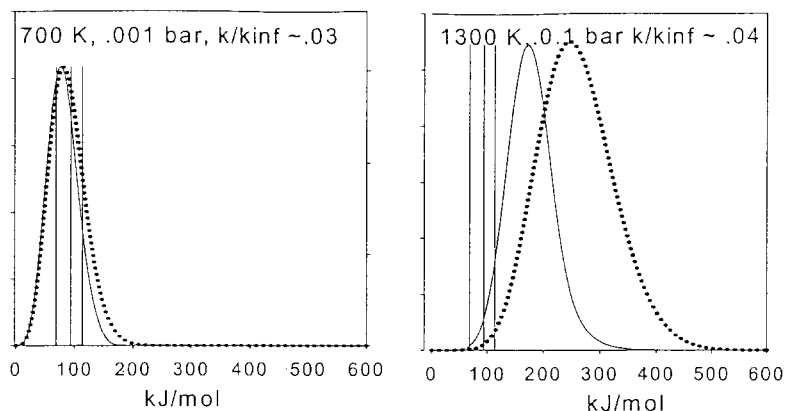
Figure 1: Distribution functions for 1-hexyl radicals during decomposition at specified conditions. Y-axis is arbitrary and set to match peaks for comparative purposes. Dotted line is Boltzmann distribution. Solid line is final distribution. Vertical lines are reaction thresholds. The highest is for C-C bond cleavage. Others are for isomerizations.

In chemical activation experiments active radicals are continuously generated. For example H-atoms may be made from steady state photolysis of a precursor and reacted with an olefin to make a chemically activated alkyl radical. Stabilization and decomposition rate constants are then determined from product ratios. Here again there is an initial period where the distribution functions are adjusting to values above the threshold and the final results are appropriate to the steady state distribution that is ultimately achieved.

For the thermal decomposition of radicals, the initial work followed the traditional closed system approach. However an open system approach is in retrospect the more natural, since radicals are continually being created. In the following we use the decomposition of 1-hexyl radical as an example. It involves isomerization to form the other hexyl radicals as well as beta bond scissions. The physical situation is summarized can be seen in Figures 1 and 2. The former is a plot of the distribution functions at 700 K and 1300 K for 1-hexyl radicals. It can be seen that for 700 K the peak of the distribution function is slightly behind the bond cleavage threshold. This is close to the usual picture for thermal decomposition processes. There is a dramatic change for the situation at 1300 K. Now the peak is in front of the reaction threshold. For such a
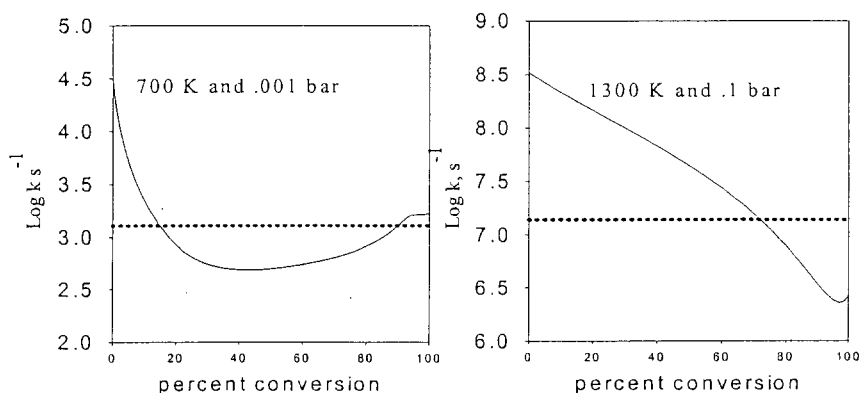

Figure 2. Rate constant versus conversion for closed system (solid line) at 1300 K, 0.1 bar and 700 K, 0.001 bar. The dotted line is the rate constant derived from an open system. Based on results from Figure 1.

305

situation reactions are now so rapid that for a closed system all of the molecule will have disappeared before the onset of a steady state distribution. Hence it is not possible to talk about rate constants. The general situation can be seen in Figure 2 where the rate constants are changing with the extent of decomposition. In earlier work we have attempted to describe the system in terms of an average rate constant. Since variations in apparent rate constants can be as much as a factor of 100, and we are concerned with 8 reactions. this is unsatisfactory. With the peak of the distribution function in front of the reaction threshold and the in situ creation of the radical, the situation is very similar to that for chemical activation. Continuous generation guarantees that a steady state distribution will ultimately occur. It then becomes possible to describe the system in terms of rate constants. The physical picture can be seen in Figure 3. We see after an initial incubation period, where the rate constants are varying as a consequence of the variation in the energy distribution functions, leading ultimately to invariant rate constants.

This new feature has now been incorporated into CHEMRATE and opens up the entire range of reactions involving larger molecules with low reaction thresholds. We have now applied it to all normal alkyl (heptyl) and 1-olefinyl radicals with 7 carbon atoms or less and for a variety of unsaturated species. Particularly important are the decomposition of the 1-olefinyl radicals, since they lead to the unsaturated compounds; ethylene, propene, 1,3 butadiene that represent inputs to existing soot models as well as allyl and other dienes that should have important influence on PAH formation. Rate constants in established databases appear to be serious underestimates.

There remain problems on the effective use of this information. Typical Arrhenius plots of the results can be seen in Figure 4. Rate constants as a function of temperature is plotted for various pressures. The shape of the curve is peculiar. For a single step unimolecular decomposition, the general shape involves continual departures from high pressure values. In the present case after the initial fall off there is a gradual turn up of the rate constants. This is a reflection of the reaction being so fast that it has retained a memory of its initial configuration. It is obvious that it will not be possible to fit such information on the basis of the generalized Troe form [6] that was developed for a single channel irreversible reaction. We prefer the use of look up tables. Even for fitting data for particular pressures requires 5 parameters for 10% accuracy
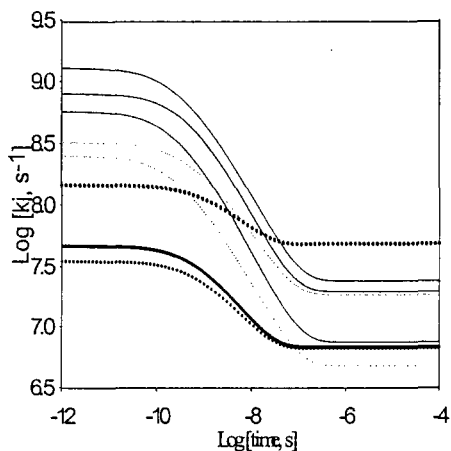

Figure 3: Rate constants versus time for 1-hexyl radical decomposition at 1100K, 1 bar. Dark line refer to 1-hexyl decomposition Dark dotted lines are isomerization channels from 1-hexyl. Light lines are for decomposition of other hexyl radicals. Light dotted lines are for their isomerization channels.
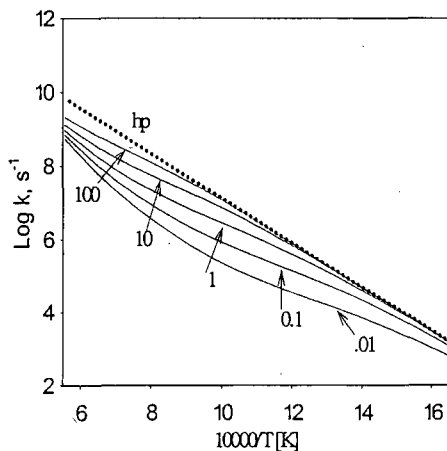
Figure 4; Rate constants as a function of temperature for the reaction $1\text{-}C_6H_{13}=C_2H_4+1\text{-}C_4H_9$ at various pressures (bar).

Another problem is the proliferation of species. It will be necessary to differentiate between radicals created by different pathways. This must be treated on a case by case basis. In the present case, neglecting such effects will lead to errors of no more than 25%. Combustion is practically always carried out above 1 bar. Non-equilibrium effects will not be as large as in low pressure systems. Note from Figure 4 that between 1 and 100 bar the difference in rate constants is about a factor 5. Parameterization over such small ranges may be less difficult.. We have shown that for reactions from the same initial precursor an arbitrary cutoff where the unimolecular reactions become exactly second order can lead to constants for the generalized Troe fits [6]. Extensions to this approach will be useful. For sufficiently fast reactions only the branching ratio for product formation is important. Little error is introduced by the use of high pressure values. At the lower temperature end rate constants are at the high pressure limit. Energy transfer effects will be of concern only in the 750-1200 K and 1-100 bar range.

Future Plans: We will extend the application of unimolecular rate theory to cover oxidation processes. These reaction are competitive with the cracking processes described earlier. Here again, there are many processes where energy transfer can seriously perturb the high pressure values that are generally recommended in combustion kinetics databases. Thus for example after the creation of the initial fuel radical oxygen can add. This can then undergo a whole series of isomerization and decomposition processes similar to those that have been discussed earlier .

Publications: 2002-2004

Roy, K. Awan, I. A., Manion, J. A.., "Thermal Decomposition of 2-chloropropene and 2-bromopropene", Phys. Chem., Chem. Phys., 2003, 5, 1806-1810

Tsang, W., "Energy Transfer Effects During Multichannel Decomposition of Ethanol", Int. J. Chem. Kin., (in press)

Babushok, V. and Tsang, W., "Gas Phase Mechanism for Dioxin Formation", Chemosphere 2003, 51, 1023-1029

Babushok, V. , Tsang, W., McNesby K. L., "Additive Influence on Polycyclic Aromatic Hydrocarbon Formation", P. Combust. Inst., 2003, 29, 2315,-2323

Babushok V. Tsang, W., Kinetic Modeling of Heptane Combustion and PAH Formation, J. Prop. and Power", (in press)

Tsang, W., "Progress in the Development of Combustion Kinetic Databases for Liquid Fuels" Data Science Journal (in press)

References:

1. Gilbert.. R.S. and Smith S. C.,"Theory of Unimolecular and Recombination Reactions", Blackwell Scientific, London, 1990

2. Curran, H. J., Gaffuri, P., Pitz, W. J., Westbrook, C. K., Comb. and Flame., 114, 149, 1998

3. Tsang, W., "A Pre-processor for the Generation of Chemical Kinetics Data for Simulations" AAIA-2001-0359, 39th AIAA Aerospace Sciences Meeting and Exhibit, Jammary 8-11, 2001 Reno. NV

4. Tsang, W. , Bedanov., V and Zachariah, M. R.,Berichte der Busen-Gesellshaft fur Physikalische Chemie, 1997,101, 491.

5. Robinson , P. J. Holbrook, K. A., "Unimolecular Reactions", Wiley Interscience, New York, 1972

6. Troe, J., J. Chem. Phys., 66, 458, 1977

SINGLE-COLLISION STUDIES OF
ENERGY TRANSFER AND CHEMICAL REACTION

James J. Valentini
Department of Chemistry
Columbia University
3000 Broadway, MC 3120
New York, NY 10027
jjv1@columbia.edu

PROGRAM SCOPE

This research program aims to develop an understanding of the dynamics of bimolecular reactions. We are interested in many reactions—ones that are actually important in combustion, those that are prototypes of such reactions, and those that illustrate fundamental dynamical principles that govern combustion reactions. The principal question that we pose in our current work is how "many body" effects influence bimolecular reactions. By many-body effects we mean anything that results from having a reaction with a potential energy surface of more than three mathematical dimensions. For the reactions that we study now there are actually many more than three dimensions, at least 12 and usually many more, and part of our effort is to determine how many of them actually participate in the important dynamics of the reactions. These are polyatomic reactions, that is, reactions in which one or both the reactants and one or both of the products are molecules with from 4 to 20 atoms. Our major current interest is in reactions for which the reactants offer multiple, identical reaction sites. Though sometimes we are interested in the intimate details particular to one specific reaction, our approach is more commonly to study an entire class of reactions to develop a general understanding of how the factors of energetics, kinematics, and reactant/product structure control the dynamics in a series of analogous systems. As part of developing that understanding we devise and test models that explicate the interplay of these different influences.

Our experiments are measurements of quantum-state-resolved partial cross sections under single-collision conditions. We use pulsed uv lasers to produce reactive radical species and thereby initiate chemical reactions. The reaction products are detected and characterized by resonant multi-photon ionization (REMPI) and time-of-flight mass spectroscopy. We have up to now had the capability to determine reactive cross sections resolved by product quantum state of one of the products. However, we are in the process of implementing the ability to measure partial cross sections resolved by scattering angle as well, and to determine the correlation of the quantum state of one product with the quantum state of the other.

In a new collaborative effort with David Chandler we are studying ways to produce molecules at ultra-low temperatures, and study collisions at the low energies associated with these temperatures.

By studying an extensive series of homologous reactions, $H + RH \rightarrow H_2 + R$, where RH is an alkane or a substituted alkane, we have developed a local reaction model of atom + polyatom abstraction reaction dynamics. The model is based on the idea of a local impact parameter, defined as the distance between the relative velocity vector and a line parallel to it that passes through a particular reactive atom in a polyatomic molecule. This local impact parameter replaces the ordinary impact parameter as the organizing principle of the reactive collision. Associated with this local impact parameter is a local opacity function and a local orbital angular momentum. In effect, the model portrays reaction in molecules with several different reaction sites as several separate reactions happening at the same time, and competing with one another.

We have carried out these studies with alkanes from methane to n-hexane to neopentane as well as several fluorocarbons and chlorocarbons. The experimental measurements in this effort were completed this year, and we are now analyzing the last results for isobutane, neopentane, and two different fluoroalkanes. We expect to submit manuscripts on these results in the next couple of months.

Much of our laboratory effort this year has been in the construction of an ion imaging apparatus for our bimolecular studies. This is designed to allow measurement of quantum-state-resolved differential cross sections for the reactions of H with RH that we have just completed. The resolution of the apparatus should allow us to make some measurements of correlations of the quantum states of the two reaction products, or, when the density of states is too great, the correlation of the internal energy of the radical product with the quantum state of the H_2 product.

This year we showed that we can extend these experiments to the investigation of radical-radical reactions, by photolytic generation of an H atom and an R• radical in the same photolysis pulse. We have studied the reaction of H atoms with vinyl radicals to make molecular hydrogen plus acetylene. The energy release in this reaction is very large. It produces H_2 with rovibrational energies higher than we have seen in any other H-by-H abstraction reaction. We are doing a complete analysis of these results and expect to submit our first manuscript on them in the next two months.

We have continued the collaboration with David Chandler that we began last year, to produce ultra-cold molecules by velocity cancellation in molecular collisions. The experiment takes advantage of the fact that in some molecular collisions the velocity vector of a scattered product in the center-of-mass frame is exactly the negative of the velocity vector of the center-of-mass, yielding a lab-frame product velocity that is identically zero. We have succeeded in making NO in selected rotational states with a velocity spread that represents a temperature of less than 1K, in collisions of NO with Ar, and reduction in that temperature seems readily achievable. The cold NO is produced in sufficient densities for trapping and subsequent spectroscopic and collision dynamics studies. A publication describing our first results appeared in Science this past year. Another longer manuscript is in preparation.

FUTURE PLANS

We will begin to use the new ion imaging capability to try to obtain state-to-state differential cross sections, starting with the prototype $H + CH_4 \rightarrow H_2 + CH_3$ reaction. We believe that we will have enough velocity resolution to observe the population of individual vibrational states of the CH_3 product in the translational energy distribution of the $H_2(v',j')$. We have just begun to characterize the imaging capabilities of our new apparatus, and the results are encouraging.

We will continue our cold molecule studies with David Chandler, exploring different collisional systems. Simple analysis of the kinematics and energetics of the scattering in a crossed beam arrangement indicates that there are particular combinations of scattering partners and collision energies that are very favorable for production of zero-lab-velocity products. One such favorable combination is D_2 scattering from He, and we plan to try that experiment soon. We also expect to attempt to trap the cold NO molecules that we have already shown we can produce.

PUBLICATIONS

1.   A. Srivastava, C.A. Picconatto, and J.J. Valentini, "State-to-State Dynamics of $H + c\text{-}RH \rightarrow H_2(v',j') + c\text{-}R$ Reactions: The Influence of Reactant Stereochemistry, Chem. Phys. Lett. 354, 25-30 (2002).

2.   J.J. Valentini, " Mapping Reaction Dynamics via State-to-State Measurements: Rotations Tell the Tale," J. Phys. Chem. 106, 5745-5759 (2002).

3.   N. S. Shuman, A. Srivastava, C.A. Picconatto, D.S. Danese, P.C. Ray, and J.J. Valentini, " Evidence of a Surprising Channeling of Ring-Opening Energy to the H_2 Product in the $H + c\text{-}C_3H_6 \rightarrow H_2 + C_3H_5$ Abstraction Reaction," J. Phys. Chem. 107, 8380-8382 (2003).

4.   M.S. Elioff, J.J. Valentini, and D.W. Chandler, "Subkelvin Cooling NO Molecules via "Billiard-Like" Collisions with Argon," Science 302, 1940-1943 (2003).

Time-Resolved Structural Dynamics:

The Ring-Opening Reaction of 1,3-Cyclohexadiene

Peter M. Weber
Department of Chemistry
Brown University, Providence, Rhode Island 02912
Peter_Weber@brown.edu

1. Program Scope

The ring-opening reaction of 1,3-cyclohexadiene to form 1,3,5-hexatriene is a textbook example of electrocyclic reactions and the Woodward - Hoffmann rules. In spite of this reaction's importance, many questions regarding the reaction mechanism in the gas phase remain unanswered. Using this reaction as a model system, our program develops, refines, and tests two new experimental techniques that are designed to explore the structural dynamics of reactions leading to isomeric product mixtures. The two techniques provide complementary time-resolved views of the molecular structures.

In the first technique, high-energy electrons from a pulsed electron beam are scattered off the time-evolving structures. The resulting electron diffraction patterns can be inverted to give the structure at the time when the electron pulse interacts with the molecule. Current technical developments focus on the optimization of the pump-probe electron diffractometer, theoretical simulations, and the development of data analysis routines.

In the second technique, a 3- or 4-photon ionization scheme provides multiplex spectra of Rydberg levels. We have shown that such Rydberg spectra can be quite sensitive to the isomeric form of the ionized molecules, and can therefore serve to fingerprint the molecular structure. The technique is now extended to probe time-dependent dynamics by measuring the Rydberg spectra at variable delay times after a photolysis pulse.

Both the time-resolved electron diffraction and the time-resolved Rydberg fingerprint spectroscopy method are applied to explore the ultrafast dynamics of 1,3-cyclohexadiene upon irradiation with 260 nm photons.

2. Recent Progress

Time-resolved Rydberg fingerprint spectroscopy

The basic idea of the Rydberg fingerprint spectroscopy is that while electrons in Rydberg states spend much of their time far away from the ion core, they occasionally pass through the ion core. The passing of the electron through the ion core is associated with a scattering event, which induces a phase shift in the wave function. Since the interference of the electron wave function before and after a round trip has to be

constructive, the phase shift is mirrored by a shift of the energy of the orbit. This suggests that the energy of a Rydberg level depends on the geometrical structure of the molecular ion core. In contrast to electron diffraction, where an unbound electron is scattered, the energies of Rydberg levels relate to the scattering of a bound electron. The electron diffraction signal can be inverted to provide structures. While the Rydberg spectra would be difficult to invert, they can provide a fingerprint for a structure, which can then be compared to separately measured spectra.

In our experiments, Rydberg levels are accessed by multiphoton excitation via a superexcited valence state, and internal conversion to the set of Rydberg levels.[i] The spectrum of Rydberg levels is observed by ionizing with a further photon, recording the kinetic energy spectrum of the photoelectrons, and analyzing for the binding energy.

Applying the idea to the ring-opening problem of cyclohexadiene, we recorded the Rydberg fingerprints of different isomeric structures. Figure 1 shows the Rydberg fingerprint spectra of 1,3-cyclohexadiene, 1,4-cyclohexadiene, and of a mix of hexatrienes.[ii] The observed peaks are labeled by their quantum defects δ, which are calculated according to

$$E_B = \frac{Ry}{(n-\delta)^2}$$

Here, Ry is the Rydberg constant, and n is the principal quantum number.

In order to explore the time-dependence of the Rydberg spectra, we have now applied a time-resolved two-color photoionization scheme. 1,3-cyclohexdiene is excited with a 4.5 eV photon to the 1^1B_2 state, from where it reacts via internal conversion to the 2^1A_1 state. The Rydberg spectra are obtained by ionizing out of the transient excited states via a two-photon process. The Rydberg fingerprint spectrum so obtained is almost identical to the one-color spectrum shown in figure 1, suggesting that the molecule is captured before it crosses a conical intersection to the ground state surface. Preliminary time-resolved measurements show an exponential decay of the excited state with a time constant of 93 fs.
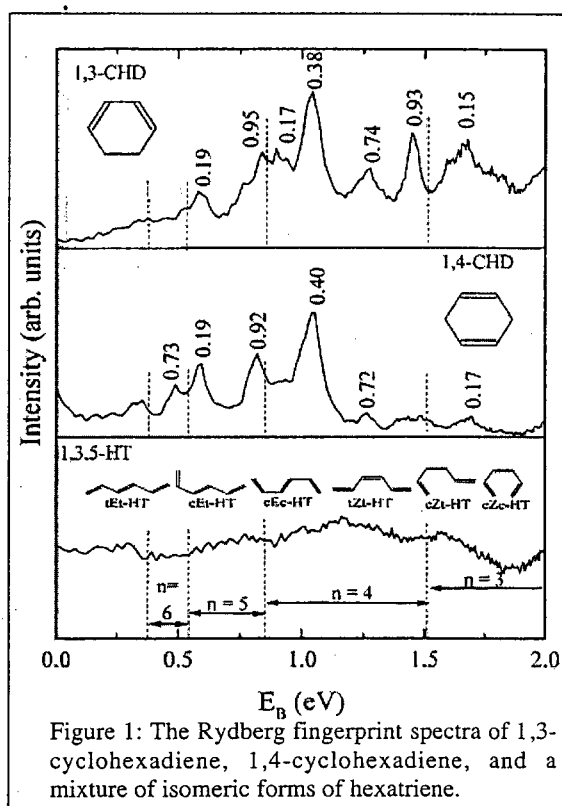

Figure 1: The Rydberg fingerprint spectra of 1,3-cyclohexadiene, 1,4-cyclohexadiene, and a mixture of isomeric forms of hexatriene.

312

The goal of the pump-probe electron diffraction experiment is to observe structural dynamics by scattering a short electron pulse from a molecule in a transient state. Pump-probe electron diffraction has been successfully applied toward the elucidation of structural dynamics in small and medium sized molecules.[iii] Limitations to the technique arise from the small number of molecules available in effusive beams or free jet expansions, from the small fraction of molecules excited to the electronic state of interest, and from space-charge interactions between the electrons within a pulse.[iv] Constrained by such boundary conditions, the magnitude of the pump-probe electron diffraction signal is by necessity only a small fraction of the total observed signal, typically on the order of 1% or less. As a result, experimental artifacts can make the observation of the pump-probe diffraction signals difficult, or may adversely affect the analysis and interpretation of the data.

The electron diffraction signal depends on the inverse fourth power of the scattering vector, which causes the electron diffraction signal to be extremely spiked about the forward direction of the electron beam. Because of this extremely spiked nature of the electron diffraction signal, the pump-probe electron diffraction experiment is very sensitive toward pointing instabilities of the electron beam. Depending on the energy of the electron beam, and the scattering angle of the electrons, deflections in the micro-radian regime suffice to cause undesired artifacts.

During 2003 we have developed a data reduction algorithm that can largely correct for the pointing instability artifacts. The individual diffraction patterns (pump-laser on, and pump-laser off) are separately centered using a cross correlation of the symmetrically equivalent, modulated parts of the diffraction patterns.[3] The precision of the centering procedure is found to be ± 0.003 Å^{-1}. This corresponds, for the 20 keV electron energy used in our experiment, to 40 μrad. Application of the algorithm to the pump-probe diffraction signal of 1,3-cyclohexadiene shows that the centering artifacts are, indeed, almost completely eliminated.

3. Future Plans

Ongoing research continues to develop both structural dynamics techniques. The Rydberg fingerprint spectroscopy will be enhanced by the availability of a new laser system that produces shorter pulses. The electron diffraction experiment will benefit from the continued development of the experimental technique, as well as from the higher pulse energy available from the new laser system. Both techniques will be applied to further explore the reaction dynamics of 1,3-cyclohexadiene, and map the excited state dynamics of this interesting molecule.

References cited:

i. "Ultrafast dynamics in superexcited states of phenol," C. P. Schick and P. M. Weber; *J. Phys. Chem. A*, **105**, 3725-3734 (2001). "Ultrafast dynamics in the 3-photon double resonance ionization of phenol via the S_2 electronic state," C. P. Schick and P. M. Weber; *J. Phys. Chem. A*, **105**, 3735-3740 (2001).

ii. "Rydberg states: sensitive probes of molecular structure," N. Kuthirummal and P. M. Weber, Chemical Physics Letters, **378**, 647 – 653 (2003).

iii. "Ultrafast diffraction imaging of the electrocyclic ring-opening reaction of 1,3-cyclohexadiene," R. C. Dudek and P. M. Weber, Journal of Physical Chemistry A, **105**, 4167 (2001).

iv. "Pump-Probe Low Energy Electron Diffraction," J. Thompson, P. M. Weber, and P. J. Estrup. SPIE conference on Time Resolved Electron and X-ray Diffraction, July 1995, San Diego, Vol. 2521, 113.

4. Publications resulting from DOE sponsored research

1. "Experimental and theoretical studies of pump-probe electron diffraction: time-dependent and state-specific signatures in small cyclic molecules," Peter M. Weber, Ray C. Dudek, Seol Ryu, and Richard M. Stratt, in *"Femtochemistry and Femtobiology: Ultrafast Events in Molecular Science,"* Eds. M. Martin and J. T. Hynes, Elsevier, (2004). (In press)

2. "Probing reaction dynamics with Rydberg states: The ring opening reaction of 1, 3-cyclohexadiene," N. Kuthirummal and P. M. Weber, in *"Femtochemistry and Femtobiology: Ultrafast Events in Molecular Science,"* Eds. M. Martin and J. T. Hynes, Elsevier, (2004). (In press)

3. "Centering of ultrafast time-resolved pump-probe electron diffraction patterns" J. D. Cardoza, R. C. Dudek, R. J. Mawhorter, and P. M. Weber. *Chemical Physics*, **299**, 307 – 312 (2004).

4. "Electron diffraction of molecules in specific quantum states: a theoretical study of vibronically excited s-tetrazine" S. Ryu, R. M. Stratt, K. K. Baeck and P. M. Weber, *Journal of Physical Chemistry A*, **108**, 1189 – 1199 (2004).

Kinetic Modeling of Combustion Chemistry

Charles K. Westbrook and William J. Pitz
Lawrence Livermore National Laboratory

This program is focused on the use of chemical kinetic models for combustion of hydrocarbon and other fuels, and it is coordinated with other programs dealing specifically with applications of kinetic models to practical combustion systems, such as automobile engines and flame suppression. It therefore involves several interconnected activities, beginning with development of detailed chemical kinetic reaction mechanisms for selected fuels, followed by application of those mechanisms to laboratory experiments to refine and validate the mechanisms, and finally to application of the mechanisms to applied problems of industrial and other interest. During these activities, individual and groups of reactions and thermochemical data which are most in need of further study are identified and communicated to other contractors who could address those needs.

During the past year, several rather distinct types of activities were pursued. The first consisted of kinetic model development for conventional hydrocarbon species, including toluene and methyl cyclohexane. Both are important species for study because they illustrate the role that fuel molecular size and structure play in determining many combustion properties. They are also intended to represent large classes of fuel components that are present in practical liquid fuels such as gasoline and diesel fuels. The second class of fuels studied in the past year consisted of large oxygenated hydrocarbons which are of interest because such oxygenates have been shown to be effective in reducing soot emissions when used as diesel engine fuels. Specific studies were carried out this year for dimethyl ether and dimethyl carbonate. Finally, the third class of fuels studied this year consist of a variety of organophosphate species which are interesting as flame suppressants but are also important because they include chemical warfare (CW) nerve agents such as Sarin, VX and others. For all of these fuels, reaction mechanisms have been developed and the work has been published in refereed papers.

Combustion of organophosphorus compounds

An important class of organophosphorus compounds (OPC's) are closely related to many hydrocarbons for which we already have detailed kinetic reaction mechanisms. Building on past experience with phosphate species thermochemistry and kinetics, and on fluorine chemistry models, we have developed models for a wide range of non-toxic OPC's, including dimethyl methyl phosphonate (DMMP), di-isopropy methyl phosphonate (DIMP), trimethyl phosphate (TMP), triethyl phosphate (TEP) and others. These models have been tested extensively through comparison between computed model results and experimental data from seeded hydrocarbon flames. These models can then be adapted to describe CW agent kinetics by including the features that are unique to such toxic species as Sarin, VX, and others.

315

In previous years, we used these kinetic models to study incineration of toxic OPC species [1]. During the past year, we investigated chemical inhibition of propane/air flames [2] by the addition of small amounts of selected OPC's, including trimethyl phosphate, dimethyl methyl phosphonate, and others, as well as more conventional flame inhibitors such as CF_3Br and iron pentacarbonyl. As noted in the accompanying figure, the OPC's appear to be roughly intermediate in inhibition effectiveness between the more inhibiting $Fe(CO)_5$ and the less inhibiting Halon 1301 (CF_3Br). Application of theoretical kinetic analysis tools to the OPC's led to our identification of several catalytic reaction pathways that lead to radical recombination along with regeneration of the basic OPC unit, which appears to consist of HOPO (in fuel-rich flames) and $HOPO_2$ (in lean flames). This work also showed that the same basic OPC unit (i.e., HOPO and $HOPO_2$) produces most of the flame inhibition for hydrocarbon flames, regardless of the initial OPC molecule used as the inhibitor. Therefore, all of the different OPC inhibitors in the accompanying figure are nearly identical in their effectiveness at inhibiting the stoichiometric propane/air flame, since the core OPC catalytic reaction pathways are the same. The kinetic insights provided by this analysis suggest several possible explanations for the unusually strong inhibition provided by $Fe(CO)_5$ which we hope to address in the coming year.
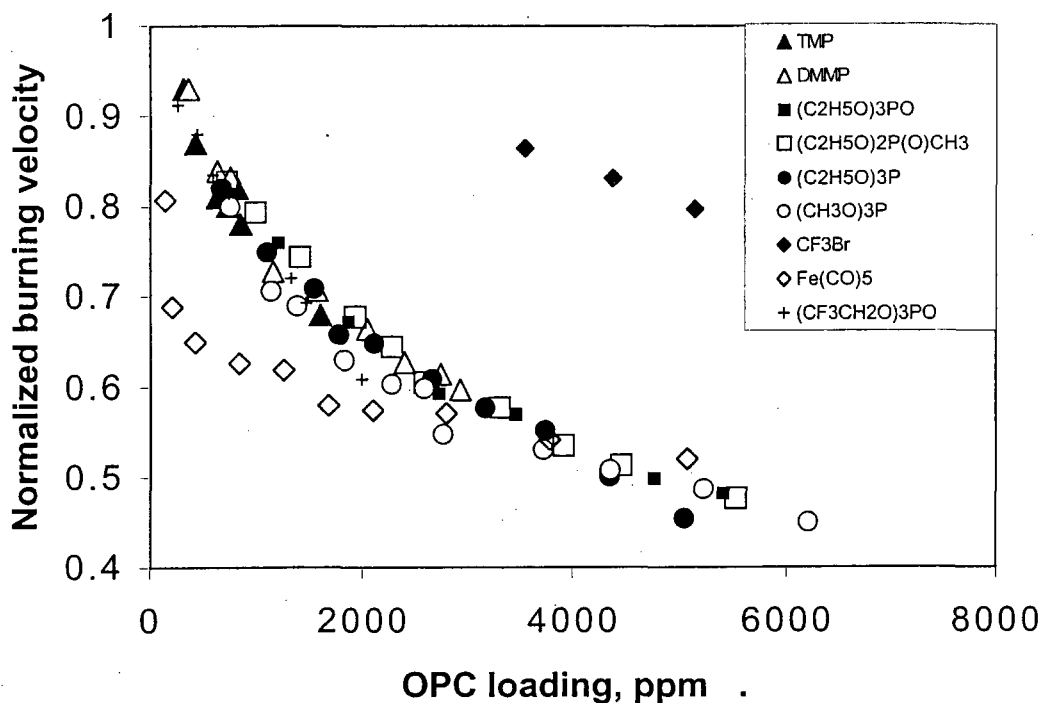
Experimental laminar burning velocity of inhibited, stoichiometric propane/air flames with various levels of inhibitor.

Combustion of oxygenated hydrocarbons and soot production

Recent engine experiments have shown that addition of oxygenates species to diesel fuel can reduce soot emissions, but there was no fundamental explanation of the reasons for these effects, and no way to extrapolate the phenomenon to other oxygenated additive species. We found [3] that it was possible to simulate ignition under fuel-rich diesel conditions at elevated pressures and relate the compositions of the rich ignition to species which lead to soot production. When oxygenated species such as methanol, ethanol, dimethyl ether, and dimethoxy methane were added to a typical diesel fuel, the levels of soot precursors were reduced. During the past year, we developed a reaction mechanism for a new oxygenated species dimethyl carbonate. This species, together with tri-propylene glycol monomethyl ether (TPGME) and dibutyl maleate (DBM) from prior studies, are much closer to realistic diesel fuel in their physical properties than simpler fuels such as methanol or dimethoxy methane. The new study [4] is consistent with previous modeling studies that the differences in soot reducing potential of each oxygenate are linked to structural factors of the oxygenated additives that can be predicted. Additional experimental and kinetic modeling of oxygenated species, both in engines and in diffusion flames, continued to improve our modeling capabilities for this class of fuels [4-6].

Other kinetic modeling

We continued our examination of mechanisms by which fuel structure and size affect ignition and other combustion properties, focusing on isomers of heptane and octane [7-9]. We also continued our modeling applications to actual internal combustion engines, especially on those operated in Homogeneous Charge, Compression Ignition (HCCI) mode [10]. In another study [11], we collaborated with Professor John Lee of McGill University to show that low temperature, cool-flame hydrocarbon kinetics, in addition to considerable relevance for knock tendency in spark-ignition engines, could also alter the detonation properties of hydrocarbon/air mixtures.

westbrook1@llnl.gov, 925-422-4108
pitz1@llnl.gov, 925-422-7730

References and publications in the past two years

1.   Glaude, P.-A., Melius, C., Pitz, W. J., and Westbrook, C. K., "Detailed Chemical Kinetic Reaction Mechanisms for Incineration of Organophosphorus and Fluoro-Organophosphorus Compounds", **Proc. Combust. Inst. 29**, 2469-2476 (2003).

2.   Korobeinichev, O.P., Shvartsberg, V.M., Shmakov, A.G., Bolshova, T.A., Jayaweera, T.M., Melius, C.F., Pitz, W.J., Westbrook, C.K., and Curran, H.J., "Flame Inhibition by Phosphorus-Containing Compounds in Lean and Rich Propane Flames", **Proc. Combust. Inst. 30**, accepted for publication (2004).

3. Curran, H. J., Fisher, E. M., Glaude, P.-A., Marinov, N. M., Pitz, W. J., Westbrook, C. K., Layton, D. W., Flynn, P. F., Durrett, R. P., zur Loye, A. O., Akinyemi, O. C., and Dryer, F. L., "Detailed Chemical Kinetic Modeling of Diesel Combustion with Oxygenated Fuels," SAE Transactions, Section 3, Volume 110, pp. 1019-1029 (2001).

4. Glaude, P.-A., Pitz, W.J., and Thomson, M.J., "Chemical kinetic model of dimethyl carbonate in an opposed flow diffusion flame", **Proc. Combust. Inst. 30,** accepted for publication (2004).

5. Kaiser, E. W., Wallington, T. J., Hurley, M. D., Platz, J., Curran, H. J., Pitz, W. J., and Westbrook, C. K., "Experimental and Modeling Study of Premixed Atmospheric-Pressure Dimethyl Ether-Air Flames", **J. Phys. Chem. A 104,** No. 35, 8194-8206 (2000).

6. Zhang, X.L., Lu, T., Law, C.K., and Westbrook, C.K., "Experimental and Computational Study of Nonpremixed Ignition of Dimethyl Ether in Counterflow", **Proc. Combust. Inst. 30,** accepted for publication (2004).

7. Westbrook, C.K., Pitz, W.J., Curran, H.C., Boercker, J., and Kunrath, E., "A Detailed Chemical Kinetic Modeling Study of the Shock Tube Ignition of Isomers of Heptane", **Int. J. Chem. Kinetics 33,** 868-877 (2001).

8. Westbrook, C. K., Pitz, W. J., Boercker, J. E., Curran, H. J., Griffiths, J. F., Mohamed, C., and Ribaucour, M., "Detailed Chemical Kinetic Reaction Mechanisms for Autoignition of Isomers of Heptane Under Rapid Compression", **Proc. Comb. Inst. 29,** 1311-1318 (2003).

9. Curran, H.J., Gaffuri, P., Pitz, W.J. and Westbrook, C.K., "A Comprehensive Modeling Study of iso-Octane Oxidation", **Combustion and Flame 129,** 253-280 (2002).

10. Aceves, S.M., Flowers, D., Martinez-Frias, J., Espinosa-Loza, F., and Pitz, W.J., "Additive characteristics for HCCI Combustion", Society of Automotive Engineers paper SAE2003-01-1814 (2003).

11. Romano, M. P., Radulescu, M.I., Higgins, A.J., Lee, J.H.S., Pitz, W. J., and Westbrook, C. K., "Sensitization of Hydrocarbon-Oxygen Mixtures to Detonation Via Cool Flame Oxidation", **Proc. Combust. Inst. 29,** 2833-2838 (2003).

12. Violi, A., Kubota, A., Pitz, W.J., Westbrook, C.K. and Sarofim, A. "A Fully-Integrated Molecular Dynamics - Kinetic Monte Carlo Approach for the Simulation of the Growth of Soot Precursors, **Proc. Comb. Inst. 29,** 2343-2349 (2003).

PROBING FLAME CHEMISTRY WITH MBMS, THEORY, AND MODELING

Phillip R. Westmoreland

Department of Chemical Engineering
University of Massachusetts Amherst
159 Goessmann Laboratory, 686 N. Pleasant
Amherst, MA 01003-9303

Phone 413-545-1750
FAX 413-545-1647
westm@ecs.umass.edu
http://www.ecs.umass.edu/che/westmoreland.html

Program Scope

The objective is to establish kinetics of combustion and molecular-weight growth in hydrocarbon flames as part of an ongoing study of flame chemistry. Our approach combines molecular-beam mass spectrometry (MBMS) experiments on low-pressure flat flames; *ab initio* thermochemistry and transition-state structures; rate constants predicted by transition-state and chemical activation theories; and whole-flame modeling using mechanisms of elementary reactions. The MBMS technique is powerful because it can be used to measure a wide range of species, including radicals, quantitatively with high sensitivity and low probe perturbation.

Recent Progress

In the past year, we have focused on three thrusts. First, we have probed an allene-doped fuel-lean C_2H_4 flame and a cyclohexane flame in our MBMS experiments at UMass. Second, we have examined these and other flames in a complementary MBMS at the LBNL Advanced Light Source. Third, we have used flame models to examine heat generation and the most relevant reactions in model and experimental flames.

Ethylene flame mapping at UMass. Flame chemistry of olefins is the key link between alkane combustion and formation of aromatic pollutants. Fuel-lean ethylene flames ($\phi = 0.70$) were mapped, similar to that of Bhargava and Westmoreland,[1] but one is doped with allene. The list of species with measured profiles is presented in Table 1. Combination of these data with the ALS measurements is discussed below.

Table 1. Species with profiles measured in the present lean flames of ethylene and allene-doped ethylene, listed by molecular weight.

H	OH	CHO	C_3H_3	C_3H_6	C_6H_5 **
H_2	H_2O	C_2H_6	C_3H_4 allene*	C_2H_3O	C_6H_6 benzene **
CH	C_2H_2	CH_2O	C_3H_4 propyne*	CO_2	1,5-hexadiyne **
CH_2	C_2H_3	O_2	Ar	Ethenol	Fulvene **
CH_3	C_2H_4	HO_2	HCCO	Acetaldehyde	
CH_4	CO	H_2O_2	C_3H_5	C_5H_5 **	
O	C_2H_5	C_3H_2	CH_2CO	C_5H_6 **	

* Resolved only in allene-doped flame.
** Detected and/or in allene-doped flame but below limits of detection in undoped flame.

Combining UMass EI MBMS with Photoionization MBMS at LBNL. During the past two years, we have complemented the UMass MBMS data capability by building, testing, and developing a new flame-MBMS system at Lawrence Berkeley National Laboratory's Advanced Light Source (ALS) to identify and measure key isomers. This work has been in collaboration with Terry Cool of Cornell and Andy McIlroy and Craig Taatjes of the Sandia Combustion Research Facility, initially encouraged by Tom Baer. The apparatus has been constructed on the Chemical Dynamics Beamline at (http://www.chemicaldynamics.lbl.gov/es3/flamediagnostic.htm). With its intense, finely tuned VUV photons, we can discriminate many isomeric species by their photoionization thresholds and measure their absolute concentrations using photoionization cross-sections. Significant findings include the first detection of vinyl alcohol in flames [DOE Publ. 4]

---

[1] A. Bhargava and P. R. Westmoreland, *Combustion and Flame* 115, 456-467 (1998).

and the first resolution of C_3H_4 and C_6H_6 isomers in flame MBMS measurements [DOE Publ. 6,8]. Other joint work includes propane [DOE Publ. 9] and ethanol flames.

Molecules and radicals are ionized at electron energies of 8 to 18 eV, set slightly above the ionization thresholds of the species to avert fragmentation. Signal is obtained as a function of molecular weight, more accurately of mass-to-charge ratio m/z. Comparing the apparata:

In the UMass system, the molecular beam sampled from the flame is chopped with a toothed wheel and introduced into an electron-impact ionizer. The EI ionizer has an energy spread of about 0.7 eV, adequate for distinguishing isomers with threshold ionization energies different by 2 eV or more. Our quadrupole mass spectrometer (Extrel) can resolve masses in three different ranges: m/z = 1-50 daltons (ultra-high resolution of $m/\Delta m$=1000), 1-500, and 4-2000. Positive and negative ions can be measured from radicals and molecules with analog (continuous) or pulse-counting detection. Its advantages are greater sensitivity for weak signals, sufficient mass resolution to resolve oxygenates from hydrocarbons by mass, and established, successful methods for mapping and calibrating flame species.

In the ALS system, the unchopped molecular beam is ionized by 10^{14} photons/sec ranging from 5.0 to 24 eV but resolvable to $E/\Delta E$ = 1200 with a monochromator. This resolution corresponds to ±0.005 eV at 12.00 eV, so resolution of isomers is limited only by their photoionization (PI) cross-sections, not the source. A 1.3-m time-of-flight mass spectrometer separates the ions, which are detected by a multichannel plate. Advantages are the low photon energies necessary for single-photon ionization, the wide range of electron energies relative to tunable lasers, and the precise PI energy resolution relative to EI. Disadvantages include present inability to eliminate background signal, limitation to relatively nontoxic fuels, and quite limited beam time.

Our emphasis in the past year was resolution of C_3H_4 and C_6H_6 isomers. The first-ever resolution of C_6H_6 isomers by flame MBMS is shown in Fig. 1. In a fuel-rich C_2H_2 flame,[2] microprobe/GC-MS analyses had shown four C_6H_6 isomers split 17/17/3.5/61% in order of elution times. Because no standards were available for the other isomers, only the elution time of benzene (61%) could be identified. PIE curves at particular points in the two allene-doped flames resolved their principal isomers: benzene (84%), 1,5-hexadiyne (15%), and possibly fulvene (< 0.4%) in the fuel-rich flame and benzene (45%), 1,5-hexadiyne (35%), and fulvene (20%) in the fuel-lean flame.
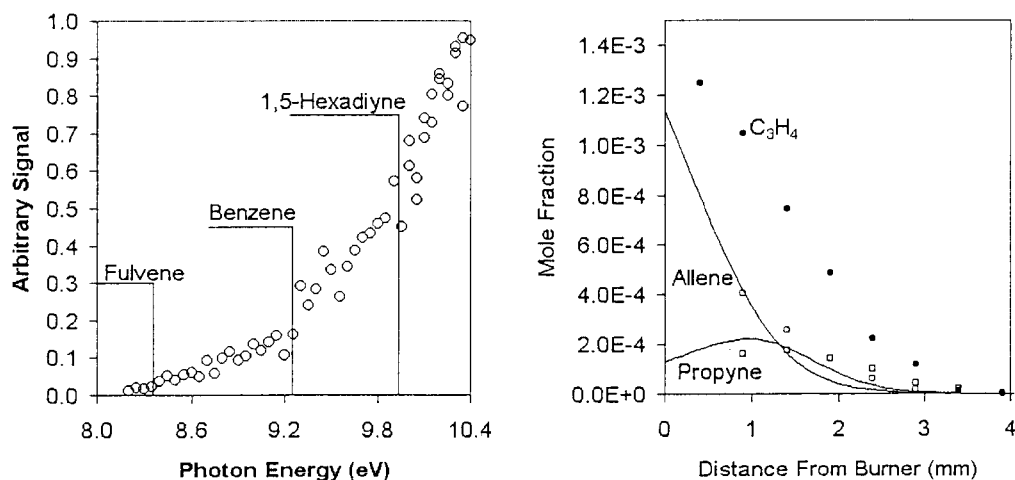

Figure 1 (left). Resolution of C_6H_6 isomers at 5.0 mm in an allene-doped fuel-lean flame.
Figure 2 (right). C_3H_4 isomers in an allene-doped fuel-lean flame: data points and model curves.

[2] Westmoreland, P.R., "Experimental and Theoretical Analysis of Oxidation and Growth Chemistry in a Fuel-Rich Acetylene Flame," Ph.D. dissertation, Chemical Engineering, Massachusetts Institute of Technology (1986).

From the literature, five C_6H_6 isomers have thresholds of 8.3 to 8.9 eV, where fulvene is the lowest. The limitations on resolving them appear to be uncertainties about the shapes of their PIE curves and the noise levels that are present. PIE curves for standards and proposed new data-collection techniques could help identify more of the isomers.

Even when allene (propadiene) is doped into the ethylene flame, C_3H_4 cannot be assumed to be all allene. Thermal isomerization to propyne (methylacetylene) is possible, and chemically activated isomerization by H addition may be much faster. Figure 2 shows the resolved profiles. The fractional split was obtained using the ALS using estimated cross sections for the two isomers. Total mole fraction of C_3H_4 from the UMass EI instrument was then split to give the points shown. Agreement of the predicted curves with these data is generally good.

In modeling this flame [DOE Publ. 8] using the rate constants of Miller and Klippenstein,[3] the model predicted C_3H_3 self-combination reactions to be the major benzene formation route through direct formation as well as through formation of thermal fulvene and linear C_6H_6, which can then isomerize to benzene. Benzene is destroyed mainly through hydrogen abstraction to form phenyl and through O attack to form phenoxy. A major phenyl destruction path is to benzene, thus producing an equilibrium cycle between benzene and phenyl. Phenoxy and phenol have a similar cycle. In another cycle, benzene and phenyl both produce phenoxy, which then produces phenol, which then can produce benzene. The ultimate destruction of benzene goes through phenyl and phenoxy. Both species undergo CO elimination by O addition to phenyl and decomposition of phenoxy to form cyclopentadienyl, which undergoes further oxidation to form CO, CO_2 and H_2O.

Cyclohexane mapping. Early measurements in cyclohexane have revealed a significant amount of dehydrogenation early in the flame. This result is somewhat surprising because alkane models suggest that the initial reaction should be abstraction of H, followed by rapid unzipping of the ring to $2C_2H_4+C_2H_2+H$ by beta scissions. The latter sequence occurs, but formation of burner deposits, cycloolefins, and benzene point to interesting dehydrogenation chemistry.

We have begun experiments on both apparata. The initial measurements at the ALS were broken off because of effects on the burner, which later proved to be deposits on the burner. Fuel condensation was ruled out; total pressure was 20 Torr but the vapor pressure of cyclohexane is 150 Torr at 34°C, the controlled burner temperature. Low-pressure flat flames of cyclohexane also proved surprisingly difficult to stabilize. The flame must be rather close to the burner to be visibly flat and to avoid changes in the flame due to probe perturbation. At the same conditions, an *n*-hexane flame is much easier to stabilize. Heavier species measured at 2 mm from the burner include masses 66 (1,3-cyclopentadiene), 78 (mostly benzene with some 1,5-hexadiyne and very little fulvene), 80 (probably 1,3- and 1,4-cyclohexadiene), 81 (C_6H_9 radicals), 82 (cyclohexene), 83 (cyclohexyl), 84 (cyclohexane), and 98 (possibly cyclohexanone).

We have adopted the conditions of $\phi = 1.0$, 20 torr, and 40 cm/s (at 298). Major species profiles have now been measured successfully at UMass, as well as several minor species. The deposits have also been examined. They dissolve in acetone and contain mostly two and three-ring methylated polycyclics.

Developing a new flame modeling method. Earlier, we developed a solution method for solving the nonadiabatic energy equation in a flat flame [DOE Publ. 2]. This work was originally motivated when we found that the experimental maximum temperature in the lean ethylene flame was higher than the kinetically computed adiabatic flame temperature T_{adia}. This indicates a serious problem in the model, as T must be less than or equal to the true, thermodynamic T_{adia}. A similar problem is seen in modeling H_2/O_2 flame data. At the same time, H, O, and OH predictions with the experimental profile were too high, while predictions for major species were not greatly in error. Using a measured temperature profile instead of an energy balance for flat-flame modeling (the conventional approach) captures the true radiative losses. On the other hand, it does not force the conservation of energy.

---

[3] Miller, J.A., Klippenstein, S.J., *J. Phys. Chem. A* **107**(39), 7783 (2003).

We incorporated radiative losses, burner losses, and new boundary conditions into the Sandia Premix code in order to solve the nonadiabatic energy equation. In lightly sooting rich flames, the resulting predicted temperatures are in excellent agreement with the data. In the lean flames, the predictions bear out kinetics as being the source of the underpredicted heat release. A new post-processing technique, Net Heat Flux Analysis, evaluates the contributions of convection, diffusion, radiation, and different reactions. Initial use of this method points to O-atom chemistry as the best explanation.

Future Plans

Mapping cyclohexane flames is the present experimental emphasis. A suitable vaporizer has been developed, and the fuel-lean cyclohexane flame should be fully mapped before the end of June. During the July and December allocations of ALS beamtime, we will resolve isomers detected in the UMass apparatus.

We have proposed to extend this work to *n*-hexane flames, to rich cyclohexane flames, and to toluene flames. Hexane will provide new high-temperature kinetics of H abstraction, rich cyclohexane will allow study of the competition between dehydrogenation chemistry and aromatics growth from small radicals, and toluene will provide oxidation and growth kinetics. These studies will benefit from the powerful combination of thorough measurements with the UMass EI apparatus and resolution of isomers with the ALS MBMS.

Publications of DOE-sponsored Research, 2001-2004

1. M. E. Law, T. Carrière, and P.R. Westmoreland, "New Insights into Fuel-Lean Ethylene Flames," *Chem. Phys. Prop. Combustion*, 194-197 (2001).
2. T. Carrière and P.R. Westmoreland, "Complete Solution of the Flat-Flame Equations in the Non-Adiabatic Case," *Chem. Phys. Prop. Combustion*, 241-244 (2001).
3. T. Carrière, P.R. Westmoreland, A. Kazakov, Y.S. Stein, and F.L. Dryer, "Modeling Ethylene Combustion from Low to High Pressure," *Proc. Combust. Inst.*, 29, 1257-1266 (2002).
4. T. A. Cool, K. Nakajima, T. A. Mostefaoui, F. Qi, A. McIlroy, P. R. Westmoreland, M. E. Law, L. Poisson, D. S. Peterka, and M. Ahmed, "Selective Detection of Isomers with Photoionization Mass Spectrometry for Studies of Hydrocarbon Flame Chemistry," *J. Chem. Phys.* **119**(16), 8356-8365 (2003).
5. A. Morel, M. E. Law, P. R. Westmoreland, T. A. Cool, K. Nakajima, T. A. Mostefaoui, F. Qi, A. McIlroy, L. Poisson, D. S. Peterka, M. Ahmed, " Selective detection of isomers using a new photoionization MBMS apparatus," *Chem. Phys. Prop. Combustion*, 281-284 (2003).
6. M. E. Law, A. Morel, P. R. Westmoreland, T. A. Cool, C. Taatjes, "Selective Detection of C_3H_4 and C_6H_6 Isomers in Flames," *Chem. Phys. Prop. Combustion*, 285-288 (2003).
7. B. Ruscic et al., "IUPAC critical evaluation of thermochemical properties of selected radicals - Part I," *J. Phys. Chem. Ref. Data* (in press).
8. M. E. Law, T. Carrière, and P.R. Westmoreland, "Allene Addition to a Fuel-Lean Ethylene Flat Flame," *Proc. Comb. Institute* **30**, accepted.
9. T.A. Cool, K. Nakajima, C.A. Taatjes, A. McIlroy, P.R. Westmoreland, M.E. Law, A. Morel, "Studies of a Fuel-Rich Propane Flame with Photoionization Mass Spectrometry" *Proc. Combustion Inst.* **30**, accepted.

322

Photoinitiated Processes in Small Hydrides

Curt Wittig
Department of Chemistry
University of Southern California
Los Angeles, CA 90089
U. S. A.
wittig@usc.edu

During the past year our work has been ongoing in two directions. We have continued our studies of nonadiabatic interactions with work on the $\tilde{B}/\tilde{X}$ conical intersection in water. We recently published the results of experiments in which intramolecular dynamics are examined following excitation of the H_2O $\tilde{B} \leftarrow \tilde{X}$ system.[1] A brief synopsis of these results and the current state of the proposed experiments on H_2O is presented below.

We have also continued our studies of relativistic effects (spin-orbit splittings and effects that arise from the increased mass of electrons accelerated by a heavy nucleus), studying both the H_2Te and SbH_3 systems. Recent theoretical work has confirmed our earlier explanation of the structured long wavelength tail of the H_2Te absorption spectrum.[2-4] The signal-to-noise ratio (S/N) in the H_2Te experiments was sufficient to permit us to analyze the secondary photolysis of the TeH product. A more detailed analysis of the H_2Te results and a paper are in progress and a brief summary is presented below.[5]

The SbH_3 experiments are progressing slowly but well. We have to both synthesize SbH_3 and keep the sample around long enough to carry out experiments. We learned much about working with unstable molecules in the course of the H_2Te experiments, but each new molecule presents new challenges. We have obtained an absorption spectrum of room temperature SbH_3, as discussed below, and the HRTOF experiments are underway.

I. Photodissociation of H_2O via the $\tilde{B}$ state

Dynamics on the $\tilde{B}$ state of water involve major changes in geometry and nonadiabatic effects. The dynamics following excitation to $\tilde{B}$ have been examined at a limited number of wavelengths, and the $\tilde{B}/\tilde{X}$ conical intersection in water has been characterized theoretically.[6-8] The $\tilde{B}/\tilde{X}$ intersection has a dramatic effect on the dynamics of photoinitiated dissociation, leading primarily to $OH(X^2\Pi) + H$. Dissociation on $\tilde{B}$ $(2A')$ leads to $OH(A^2\Sigma^+) + H$, and dissociation on $\tilde{X}(1A')$ and $\tilde{A}(1A'')$ both lead to $OH(X^2\Pi) + H$. We have studied the H_2O $\tilde{B} \leftarrow \tilde{X}$ system by using two-photon 266 nm absorption. Following dissociation, the H-atom product is probed via high-n Rydberg time-of-flight spectroscopy (HRTOF). The HRTOF method gives accurate values for relative H-atom yields. The time-of-flight and center-of-mass ($c.m.$) translational energy distributions are shown in Figure 1.

To obtain adequate S/N required a short flight tube (~ 14 cm), which led to a loss of resolution. Despite the low resolution, several conclusions could be drawn. The weakly structured broad distribution centered around 7000 cm^{-1} indicates that OH products are produced with

significant internal energy. The observed structure is consistent with highly rotationally excited OH($X^2\Pi$) in $v = 0$ superimposed on rotationally excited OH in higher vibrational levels. When compared to excitation of the $\tilde{B} \leftarrow \tilde{X}$ system at 121.6 nm,[9] it is clear that, as the excitation energy decreases, the bias towards highly rotationally excited OH(X) decreases. No OH(A) products were detected (figure 1a). The measured OH($A\ ^2\Sigma^+$)/OH($X\ ^2\Pi$) branching ratio is < 0.1%, demonstrating the high efficiency of the $\tilde{B}/\tilde{X}$ conical intersection. The branching ratio is two orders of magnitude less than predicted by theory.[8]
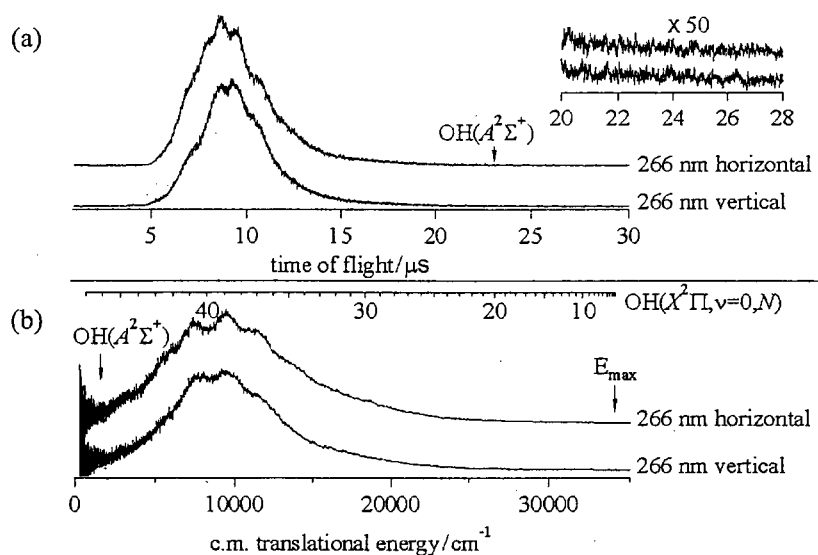
Figure 1. (a) Time-of-flight distributions. No OH($A^2\Sigma^+$) is detected at $\times$ 50 magnification. (b) Translational energy distributions. The broad peak is attributed to highly rotationally excited OH($X^2\Pi$,$v = 0$) with structure due to $v > 0$.

We are continuing our study of dynamics in the $\tilde{B} \leftarrow \tilde{X}$ system of water. To that end, we are implementing a tunable VUV radiation source using sum-frequency difference mixing (SFDM). This method is more technically challenging then other available methods, but it has the advantage of significantly higher conversion efficiencies. An additional dye laser necessary for the SFDM has been purchased and received. When the HRTOF experiments on SbH$_3$ are completed (see below), tunable VUV radiation will be integrated into the experiments.

II. Near UV absorption spectrum and photodissociation dynamics of H$_2$Te

The room temperature UV absorption spectrum, photodissociation of H$_2$Te at two wavelengths in its first absorption band, and preliminary analysis have been published.[3] The c.m. translational energy distributions for photolysis at 355 nm are shown in figure 2. The primary photolysis signal has led to two important results: (i) At 355 nm, the TeH($^2\Pi_{1/2}$) excited electronic state is preferentially populated; (ii) The H-atoms from the TeH($^2\Pi_{1/2}$) + H channel at 355 nm have $\langle E_{rot} \rangle \sim 60$ cm^{-1} and $\langle E_{trans} \rangle \sim 1600$ cm^{-1}. Thus, H$_2$Te may prove to be a good source of tunable H

atoms with modest translational energy. To explain the long wavelength structure in the UV absorption spectrum we proposed that the HTe–H coordinate would have a potential energy surface (PES) leading to TeH($^2\Pi_{1/2}$) +H that is analogous to the weakly bound $^3\Pi_{0+}$ state in the isoelectronic HI system. Alekseyev *et al.* recently calculated cuts on the PES's in the HTe–H coordinate.[2] The shapes of the potentials and the structure in the calculated absorption spectrum show uncanny agreement.
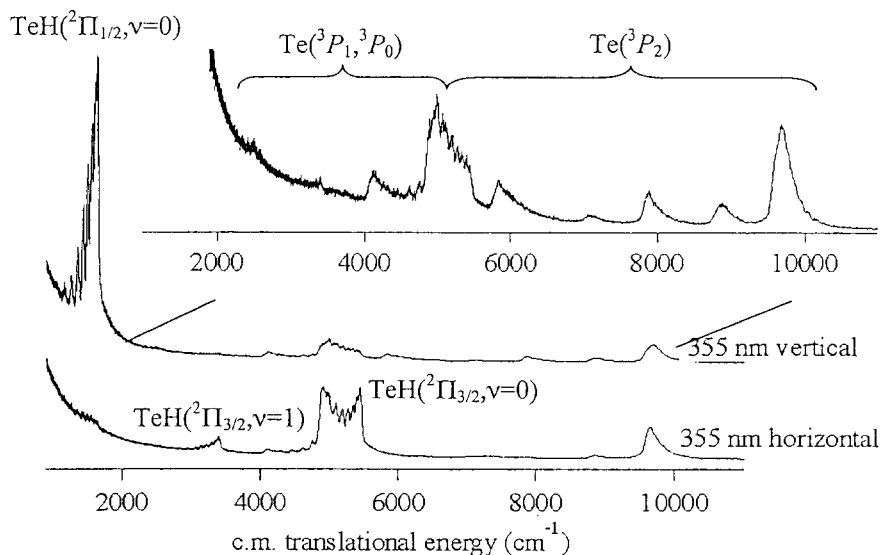

Figure 2. Center-of-mass translational energy distribution for 355 nm photodissociation of H$_2$Te. Labels indicate TeH product states from primary photolysis and Te states produced from secondary photolysis.

Secondary photolysis peaks (figure 2) indicate both the sensitivity of the apparatus and the large absorption cross section of the TeH product. We observe secondary photolysis distributions from 355 nm photolysis of H$_2$Te followed by both 355 nm and 364.5 nm (radiation from Lyman-α generation) photolysis of the TeH product. The H-atom product is then probed by HRTOF. All three energetically allowed Te states ($^3P_{0,1,2}$) are populated. Preliminary analysis of the secondary photolysis signal yields the dissociation energy of TeH, which has not been previously measured: D_0(TeH) = 22,300 ± 150 cm^{-1}, in good agreement with theoretical predictions.[10] Detailed analyses of primary and secondary photolysis results at 266 nm and 355 nm are progressing.

III. Another heavy system for studying relativistic effects: SbH$_3$

HRTOF experiments are underway on SbH$_3$. We have synthesized SbH$_3$ and obtained a room temperature UV absorption spectrum (figure 3). Note that, as in H$_2$Te, a long wavelength tail is observed, this time extending to ~ 280 nm. Although low in yield, the synthesis is relatively simple, cheap, and safe.[11] Sb$_2$O$_3$ and LiAl$_4$ are heated to ~ 160 °C yielding SbH$_3$. The gas is captured with a liquid nitrogen trap and immediately used in experiments. As with H$_2$Te there are a number of sample stability issues. Unlike H$_2$Te, SbH$_3$ is not light sensitive, as can be seen

by the UV absorption spectrum. SbH$_3$ is thermally unstable at room temperature. We have found that it decomposes at room temperature to give a white/silver layer on the collection vessel, which is most likely atomic antimony and/or its oxide. To form a molecular beam, a carrier gas (Ar or He) is bubbled through an SbH$_3$ sample kept below its boiling temperature (−18 °C).
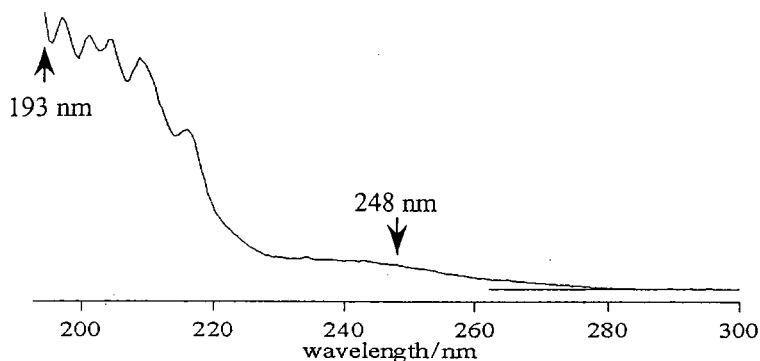

Figure 3. Absorption spectrum of room temperature SbH$_3$ taken with a Cary Series 50 spectrophotometer. Line indicates baseline.

Experiments are underway to photolyze SbH$_3$ with 193 nm radiation and probe the H atoms products using the HRTOF method. This energy is sufficient to break two of the SbH bonds. None of bond energies are known; theoretical calculations predict D_e values of 63.3, 55.8, and 53.9 kcal/mole for each of the successive SbH bonds.[12] A bimodal distribution in the products at 193 nm would allow us to determine D_0 for two of the SbH bonds. Photolysis at 248 nm may prove to be interesting as well. At this wavelength not only will the long wavelength tail of the absorption spectrum be accessed, the energy in the system will be near the dissociation energy of the second SbH bond. Photodissociation dynamics in this region may be quite different than those observed at higher energies.

References (1-5 were supported on this grant)

1. J. Underwood, C. Wittig, Chem. Phys. Lett. **386**, 190 (2004).
2. A.B. Alexseyev, H.-P. Liebermann, and C. Wittig, unpublished, manuscript available (2004).
3. J. Underwood, D. Chastaing, S. Lee, P. Boothe, T. Flood, C. Wittig, Chem. Phys. Lett. **362** 483 (2002).
4. D. Chastaing, J. Underwood, C. Wittig, J. Chem. Phys. **119**, 928 (2003).
5. J. Underwood, C. Wittig, unpublished (2004).
6. D. Yarkony, Mol. Phys. **93**, 971 (1998).
7. R. van Harrevelt, M.C. van Hemert, J. Chem. Phys. **112**, 5777 (2000).
8. R. van Harrevelt, M.C. van Hemert, J. Chem. Phys. **112**, 5787 (2000).
9. S.A. Harrich, D.W. Hwang, X. Yang, J. Lin, X. Yang, R.N. Dixon, J. Chem. Phys. **113**, 10073 (2000).
10. K.D. Setzer, E.H. Fink, A.B. Alekseyev, H.P. Liebermann, R.J. Bunker, J. Mol. Spect. **206** 181 (2001).
11. J.M. Bellama, A. G. MacDiarmid, Inorg. Chem. **7**, 2070 (1968).
12. D. Dai, K. Balasubramanian, J. Chem. Phys. **93**, 1837 (1990).

Theoretical Studies of the Reactions and Spectroscopy of Radical Species Relevant to Combustion Reactions and Diagnostics

David R. Yarkony

Department of Chemistry, The Johns Hopkins University, Baltimore, MD 21218

yarkony@jhu.edu

Our research employs computational techniques to study electronically nonadiabatic processes involving radical species. relevant to combustion reactions and combustion diagnostics.

Photodissociation of H_2NH

The demonstration by Fleming Crim's group[1] of profound mode specific effects, in the photodissociation of the $\tilde{A}^1A_2{}''$ state of NH_3 led us to initiate a study of this process in which conical intersections play a key role.

The analysis of Crim's and previous experiments is based on a 1987 study[2] which reported portions of the $1^1A - 2^1A$ seam of conical intersection with C_{2v} symmetry. The figures below, illustrative of the results obtained to date, showadditional portions of the seam of conical intersection, portions without C_{2v} symmetry, relevant to Crim's experiments. The structures forming the outer loop represent a linear synchronous transit path from an approximate transition state to a point of conical intersection of the 1^1A-2^1A state. The conical intersection point for the loop on the right, denoted $\mathbf{R}^{x,C2v}$ has C_{2v} symmetry and is typical of the previous *ab initio* results. The conical intersection point on the left denoted $\mathbf{R}^{x,Cs}$ has C_s symmetry and has not been reported previously. Note that $E_2(\mathbf{R}^{x,Cs}) < E_2(\mathbf{R}^{x,C2v})$ when the longest R(N-H) is in the range [3.0, 3.1] a_0 and that the lowest energy C_{2v} conical intersections occur for R(N-H) ~ 3.7 a_0. Since for ground state NH_3 R(N-H) ~ 2.1a_0 these C_s conical intersections which energetically accessible in Crim's experiments, may be sampled before the system has a chance to reach the energetically accessible C_{2v} symmetry intersections!
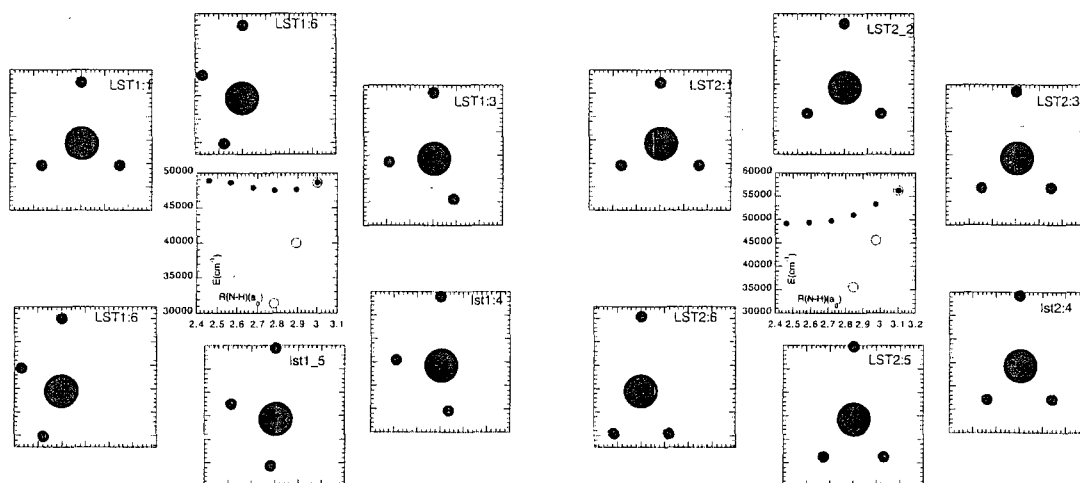
Linear synchronous transit path from approximate transition state on S_1 to a point of conical intersection. Energies of the 1^1A (2^1A) state open (filled) circles along the path are in the center of the plate. Left hand plate general C_s symmetry conical intersection while for the right hand plate the terminus is a C_{2v} conical intersection.

The present results evince the need for more detailed calculations on this system. We will be particularly interested in factors, pitch, tilt and asymmetry parameters,[3] that affect the efficiency of conical intersections in inducing nonadiabatic transitions. These electronic structure calculations

are expected to be only part of the story. We will also consider the role of nuclear dynamics, including the possibility of dynamical bottlenecks or preferred routings, in producing the enormous selectivity observed by Crim. This will be done in collaboration with Michael Collins using his GROW[4] technology to guide the selection of points on the potential energy surfaces.

Photodissociation of H_2COD

Hanna Reisler's group at the University of Southern California observed that the spectrum of the H_2COD 2^2A state, which begins at ~ 3.2 eV, is quite diffuse.[5] This result was somewhat surprising in view of the fact that in this region the excited state has 3s Rydberg character and the core of 3s Rydberg wave function is the <u>bound</u> cation H_2COH^+. We showed that Reisler's observations are a consequence of conical intersections of the 2^2A and 1^2A states.[6] The relevant region of the 2^2A -1^2A seam of conical intersections occurs for R(O-D) long and can lead to ground state H_2CO + D.

Of current concern is whether the origin of the diffuse spectrum is an intrinsic property of the 2^2A potential energy surface or a consequence of Franck-Condon factor limitations (the O-H bond is significantly stretched at the conical intersection). Further Reisler's group also observed that at higher energies both H and D are produced when H_2COD is photodissociated through the 2^2A state. This too appears to be a consequence of 2^2A -1^2A conical intersections, although in this case R(C-H) is large. To confirm this hypothesis more reliable energetics are required.

Thus we anticipate the 1^2A-2^2A seam of conical intersections is mechanistically significant in two distinctly different regions of nuclear coordinate space. A quantitative treatment of radiationless decay of the 2^2A state requires a more complete and accurate characterization of this seam in the region between these two extremes. Further at the points of conical intersection located to date the electronic states have $^2A''$ and $^2A'$ symmetry. Thus as shown in our DoE funded study of conical intersections in HNCO in these regions intersecting branches of the same seam of conical intersections, confluences, may exist. The existence of confluences which would have important consequences for nuclear dynamics. We are currently investigating whether energetically accessible confluencex exist for the H_2COH conical intersection.

Locating Conical Intersections

Points of conical intersection are not isolated but are continuously connected forming seams. The seams are N^{int} –2 dimensional subspaces in the N^{int} dimensional space of internal nuclear coordinates. For general polyatomic molecules N^{int} –2 is a large number and it is desirable to determine sections of these seams for which the energy has been minimized. While it is relatively straightforward to locate points of conical intersection, energy optimization is more costly to achieve. We attribute this difficulty to the erratic behaviour of the algorithmic parameters along the search path which precludes extrapolation. This erratic behaviour might seem intrinsic to the problem since it is a consequence of the singular character of the conical intersection which is the object of the search. Fortunately this is not the case. We have recently introduced extrapolatable functions, a set of functions that are well-behaved along the search path.[7] These functions form the basis for a simple, virtually no-additional cost, algorithm that uses hessian updating to significantly improve convergence to an energy minimized point of conical intersection.

The figure below illustrates the improvement measured relative to a unit hessian, denoted M = I, of the method M=Uab which updates the entire hessian provided $\Delta E_{IJ} < a.10^{-b}$ and otherwise updates the part corresponding to the average energy. This figure illustrates the importance of at least some approximation to the hessian since the solid circles, which indicate M=I, approach their updated counterparts slowly at best. The data for NRM clearly shows how updating the entire hessian – (a,b) ≠ (0,0) improves convergence relative to the minimal updating U00.

Plot of NRN(M) for M = I, Uab, where NRM → 0 at convergence.

COLUMBUS

We have continued our collaborative effort[8] with Ron Shepard (Argonne) and Hans Lischka(Vienna) to incorporate into the COLUMBUS[9] suite of electronic structure codes our algorithms for locating and analyzing conical intersections. During the captioned performance period we enhanced the capability to locate energy minimized two and three state conical intersection with the introduction of our extrapolatable function techniques described above. During the current performance period we will continue to fine tune these procedures.

References

1   A. Bach, J. M. Hutchison, R. J. Holiday, and F. F. Crim, J. Chem. Phys. **116**, 4955 (2002); A. Bach, J. M. Hutchison, R. J. Holiday, and F. F. Crim, J. Chem. Phys. **118**, 7144 (2003).
2   M. I. McCarthy, P. Rosmus, H.-J. Werner, P. Botschwina, and V. Vaida, J. Chem. Phys. **86**, 6693 (1987).
3   D. R. Yarkony, J. Chem. Phys. **114**, 2601 (2001).
4   K. C. Thompson, M. J. T. Jordan, and M. A. Collins, J. Chem. Phys. **108**, 8302 (1998).
5   L. Feng, X. Huang, and H. Reisler, J. Chem. Phys. **117**, 4820 (2002); L. Feng, A. V. Demyanenko, and H. Reisler, J. Chem. Phys. **118**, 9623 (2003).
6   B. C. Hoffman and D. R. Yarkony, J. Chem. Phys. **116**, 8300 (2002).
7   D. R. Yarkony, Faraday DIscussions 127 (2004).
8   H. Lischka, M. Dallos, P. Szalay, D. R. Yarkony, and R. Shepard, J. Chem. Phys. (2004); M. Dallos, H. Lischka, P. Szalay, R. Shepard, and D. R. Yarkony, J. Chem. Phys. (2004).
9   H. Lischka, R. Shepard, I. Shavitt, R. Pitzer, M. Dallos, T. Müller, P.G.Szalay, F. B. Brown, R. Alhrichs, H. J. Böhm, A. Chang, D. C. Comeau, R. Gdanitz, H. Dachsel, C. ERhard, M. Ernzerhof, P. Höchtl, S. Irle, G. Kedziora, T. Kovar, V. Parasuk, M. Pepper, P. Scharf, H. Schiffer, M. Schindler, M. Schüler, and J.-G. Zhao, COLUMBUS, An ab initio Electronic Structure Program (2003).

PUBLICATIONS SUPPORTED BY DE-FG02-91ER14189: 2002 - present

1   *Conical Intersections and the Spin-Orbit Interaction,*Spiridoula Matsika and David R. Yarkony, in **The Role of Degenerate States in Chemistry**, Advances in Chemical Physics, Michael Baer and Gert. D. Billing, eds, J. Wiley, New York, 2002, pp. 557-583

2   *Conical Intersections: Their description and consequences,* David. R. Yarkony, in **Conical Intersections: Electronic Structure,Dynamics and Spectroscopy**, *Wolfgang Domcke, David R. Yarkony and Horst Köppel, eds. World Scientific Publishing, Singapore, (2004).*

3   *Determination of potential energy surface intersections and derivative couplings in the adiabatic representation* David. R. Yarkony, in **Conical Intersections: Electronic Structure,Dynamics and Spectroscopy**, *Wolfgang Domcke, David R. Yarkony and Horst Köppel, eds. World Scientific Publishing, Singapore, (2004)*

4   *Photodissociation of the Hydroxymethyl Radical I. The Role of Conical Intersections in LineBroadening and Decomposition Pathways*
Brian C. Hoffman and David R. Yarkony, J. Chem. Phys. **116** 8300-8306, (2002).

5   *Spin-orbit Coupling and Conical Intersections. IV: A perturbative determination of the electronic energies,derivative couplings and a rigorous diabatic representation near a conical intersection. The general case*
S. Matsika and D. R. Yarkony, *J. Phys. Chem* B. **106** 8108-8116 (2002)

6   *Photdissociation of the vinoxy radical through conical and avoided intensections*
S. Matsika and D. R. Yarkony, J. Chem. Phys. **117**, 7198 (2002)

7*   *Accidental Conical Intersections of three states of the same symmetry: Location and Relevance*
S. Matsika and D. R. Yarkony, J. Chem. Phys.117,6907-6910(2002)

8   *Beyond two-state conical intersections. Three-state conical intersections in low symmetry molecules: The allyl radical*
S. Matsika and D. R. Yarkony, J. Amer. Chem. Soc. 125, 10672-10676 (2003)

9   The analytic evaluation of nonadiabatic coupling terms at the MR-CI level I; Determination of minima on the crossing seam
Dallos, M.; Lischka, H.; Szalay, P.; Shepard, R.; Yarkony, D. R. *J. Chem. Phys.* 2004).

10   Marching along ridges. Efficient location of energy minimized conical intersections of two states using extrapolatable functions
D. R. Yarkony, *J. Phys. Chem. A* (2004).

The Chemistry and Spectroscopy of Combustion Species: Isomer-Specific Excitation and Detection

Timothy S. Zwier

Department of Chemistry, Purdue University, West Lafayette, IN 47907-2084

zwier@purdue.edu

Program Definition and Scope

Combustion models necessarily face a daunting task as they seek to describe the complex array of reactions that produce and destroy aromatics and polyaromatic hydrocarbons in flames. Many of these reactions involve species with several isomers, only some of which are efficiently transformed into aromatics. The objectives of this research program are to develop and utilize laser-based methods to characterize the spectroscopy and isomerization dynamics of structural and conformational isomers of aromatic derivatives that play a role in soot formation.

Recent Progress

A. Spectroscopy and dynamics of *ortho-*, *meta-*, and *para-*ethynylstyrene

We are nearing completion of a thorough study of the spectroscopy and dynamics of *ortho-*, *meta-*, and *para-* ethynylstyrene, a series of $C_{10}H_8$ isomers with the same mass as naphthalene. We have synthesized all three isomers. In the case of the ethynylstyrenes, the asymmetry of the vinyl substituent makes

*ortho-*ethynylstyrene   *meta*-ethynylstyrene (2 isomers)   *para-*ethynylstyrene
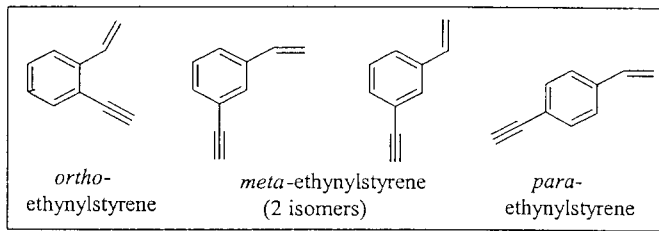
it possible to have two conformational isomers of the *ortho-* and *meta-* structural isomers. In practice, we only observe one conformational isomer of *ortho-*ethynylstyrene, but *meta* has two conformers of nearly equal population. Interestingly, the *ortho* isomer that is missing is the one that would be poised to cyclize to naphthalene. UV-UV hole-burning spectroscopy has been used to separate the transitions due to the two conformational isomers, which have $S_1 \leftarrow S_0$ origin transitions separated by about 270 cm^{-1}. We also have recorded resonant ion-dip infrared spectra of all four ethynylstyrene species in both S_0 and S_1 states. This isomer-specific spectroscopy serves as a foundation for studies of isomerization dynamics (Sec. D).

### B. Spectroscopic characterization of C_6H_6 isomers

In keeping with our interest in studying the spectroscopy and dynamics of combustion processes in an isomer-specific fashion, we have built and characterized a high-temperature flow system for making and handling several C_6H_6 isomers which are intermediates along the pathway from two propargyl radicals to benzene. Several groups have recently studied the kinetics and product state distributions of this reaction over a range of temperatures. Our goal has been to study the isomerization processes on the C_6H_6 surface beginning from the intermediates on that surface rather than from two propargyl radicals. We are presently exploring the primary photodissociation products following UV photoexcitation of 1,5-hexadiyne, DMCB, and fulvene, detecting the products using single-photon VUV ionization at 118 nm. An ongoing challenge of studying the isomerization of these isomers is the broad, unstructured ultraviolet absorptions of most of the intermediates, which make isomer specific detection difficult by our methods, whether in the ultraviolet or in IR-UV double resonance. We are particularly interested in studying the fulvene→benzene isomerization. The barrier separating fulvene from benzene is calculated to be at about 74 kcal/mol, but this is some 7-11

kcal/mol above the best experimental value, motivating the need for further experimental work. As a lead-in to that study, we have searched for LIF signal from jet-cooled fulvene in the region of its S_0-S_1 origin, where absorption spectra show reasonably sharp transitions. Our first attempt at this search was unsuccessful, but we have since built an improved fluorescence collection system which will collect about 30% of the emitted fluorescence with better spatial discrimination against scattered light. We will soon test this new system and search again for fulvene fluorescence under jet-cooled conditions. This will open the way for UV-UV hole-burning, photoacoustic, and hole-filling studies aimed at determining the barrier to isomerization with improved accuracy.

C. Preliminary results on 3-benzyl 1,5-hexadiyne and diphenylmethane

In light of the difficulties in real-time, isomer-specific detection of the C_6H_6 intermediates in the ultraviolet, we have recently initiated a parallel set of studies in which an ultraviolet 'tag' is attached to the C_6H_6 intermediates. Since 1,5-hexadiyne is a (reasonably) stable C_6H_6 intermediate that is positioned early in the C_6H_6 isomerization pathway to benzene, we have recently synthesized 3-benzyl-1,5-hexadiyne (IA, shown below), and have studied its R2PI, UV-UV hole-burning and RIDIR spectroscopy. We have shown that there are five conformational isomers involving different configurations for the 1,5-hexadiyne side-chain, and have made tentative assignments of these conformations based on an analysis of the electronic frequency shifts, acetylenic and alkyl CH stretch fundamentals, and vibronic structure. We hope soon to record SEP spectra of each isomer, and record their rotational band contours to provide further evidence for our assignments. Using the SEP-hole filling techniques (Sec. D) we will study its conformational isomerization dynamics.

The 3-benzyl-1,5-hexadiyne 'starting material' then has analogs involving the other C_6H_6 intermediates, which are also shown below. Of these, diphenylmethane (VIIA) is commercially available, and we have already obtained preliminary results on its R2PI and RIDIR spectroscopy. This molecule is fascinating because it has two phenyl ring torsional coordinates with low barriers. This leads to a good deal of low frequency vibronic structure in the R2PI spectrum, which we are presently puzzling over. We suspect that the degree of localization or delocalization of the excited states in this bichromophore will depend strongly on the shape of

| 3-benzyl 1,5-hexadiyne | 1-benzyl 3,4-dimethylene | 3-benzyl fulvene | Diphenylmethane |
| IA | cyclobutene, IIIA | IVA | VIIA |
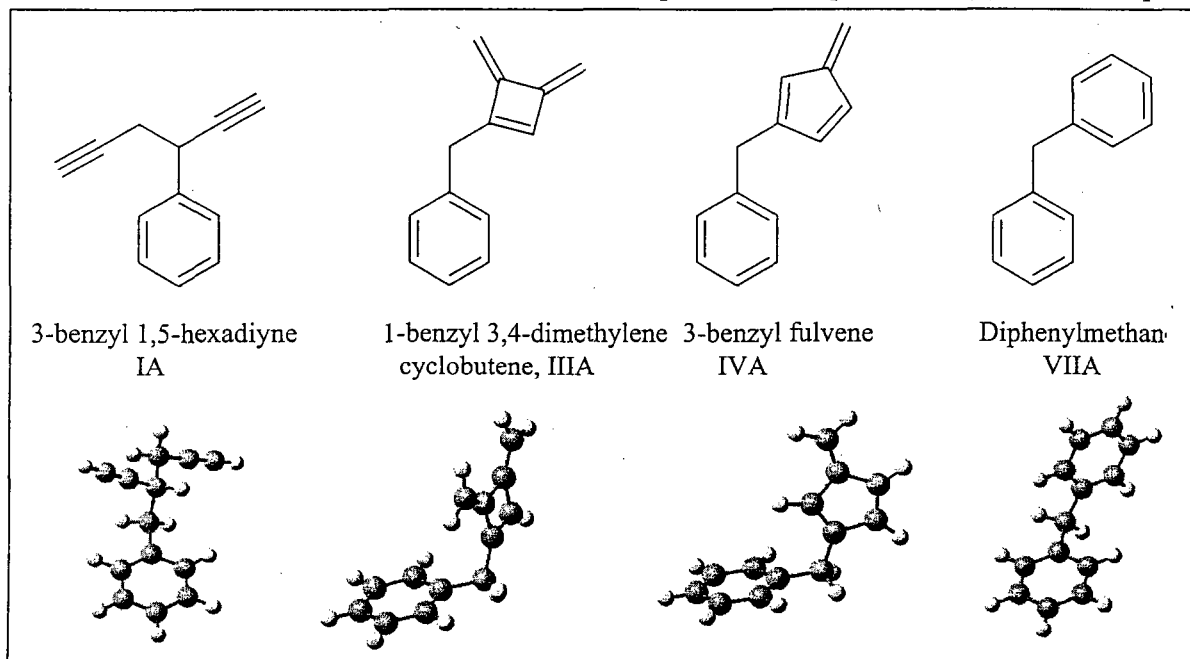
the excited state surfaces along the two phenyl ring torsional coordinates. At the C_{2v} geometry, the excited states will be completely delocalized over the two rings, but at the computed ground state geometry (shown on the preceding page), vertical excitation should produce excited states partially or entirely localized on the two rings. We need yet to characterize the ground state torsional surface for diphenylmethane using dispersed fluorescene and/or stimulated emission pumping.

3-benzyl-1,5-hexadiyne (IA) can be used to synthesize the other two C_6H_5-CH_2-C_6H_5 intermediates shown above by thermal rearrangement. The heater/flow cell we have built to thermally isomerize 1,5-hexadiyne can also be used to convert 3-benzyl-1,5-hexadiyne (IA) to 1-benzyl-3,4-dimethylenecyclobutene (IIIA, 300-400°C) or 3-benzyl-fulvene (IVA, 500-600°C). We plan to flow the products directly into the heated nozzle for expansion into vacuum, using helium as the buffer gas, for spectroscopic characterization.

D. Conformational isomerization dynamics of a series of phenylalkynes

Gasoline and diesel fuels are complicated mixtures containing about 30% aromatics, including alkylbenzene, alkenylbenzene, and alkynylbenzenes of various chain lengths. The combustion of these molecules is influenced by their structural and conformational make-up, and by the rates of isomerization between them. We have recently demonstrated a new experimental method that will enable us to study the isomerization dynamics in new ways. Stimulated emission pumping (SEP) is being used to selectively excite a single conformation to a well-defined vibrational energy early in the supersonic expansion. The excited molecules are re-cooled in the supersonic expansion before isomer-specific detection in LIF or R2PI. By tuning the SEP dump laser in a 20-10-20 Hz laser configuration, we can directly measure the energy thresholds for isomerization of individual A→B reactant-product isomer pairs (B.C. Dian, J.R. Clarkson, and T.S. Zwier, Science 303, 1169 (2004)). We hope soon to apply this powerful new method, called SEP hole-filling spectroscopy, to the study of the conformational isomerization in substituted benzenes capable of isomerization. As a first step towards this goal, we are presently studying the conformation-specific UV and IR spectroscopy of a series of phenylalkynes: C_6H_5-$(CH_2)_n$-$C\equiv C$-H, with n=2-4. From such studies, we will determine the energy thresholds for isomerization in specific X→Y reactant-product isomer pairs, the relative energies of the minima, and, in cases where there are several flexible sites, the efficient isomerization pathways on the multidimensional surface. The competition between cooling and isomerization can be used to provide new tests of the application of RRKM theory to large molecules with low barriers and many flexible degrees of freedom.
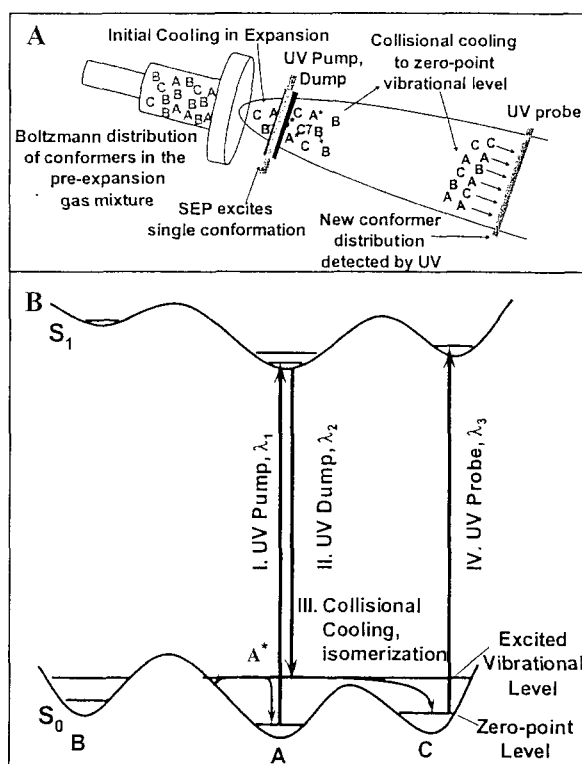
Publications acknowledging DOE support, 2002-present

Christopher Ramos, Paul R. Winter, Timothy S. Zwier, and Stephen T. Pratt, "Photoelectron Spectroscopy via the $1\,^1\Delta_u$ state of Diacetylene", J. Chem. Phys. **116**, 4011 (2002).

Allison G. Robinson, Paul R. Winter, and Timothy S. Zwier, "The singlet-triplet spectroscopy of 1,3-butadiene using cavity ring-down spectroscopy", J Chem. Phys. 116 (18): 7918-7925 (2002).

Allison G. Robinson, Paul R. Winter, and Timothy S. Zwier, "The Ultraviolet Photochemistry of Diacetylene with Styrene", J. Phys. Chem. A **106** (24): 4789-4796 (2002).

Jaime A. Stearns and Timothy S. Zwier, "The infrared and ultraviolet spectroscopy of jet-cooled *ortho-*, *meta-*, and *para*-diethynylbenzene", J. Phys. Chem. A 107, 10717-10724 (2003).

Participants

Dr. Musahid Ahmed
Lawrence Berkeley Laboratory
One Cyclotron Road
Berkeley, CA 94720
Phone: (510)486-6355
mahmed@lbl.gov

Prof. Wesley D. Allen
The Center for Computational
Quantum Chemistry
The University of Georgia
Athens, GA 30602-2525
Phone: (706)542-7729
wdallen@ccqc.uga.edu

Dr. Sarah W. Allendorf
Combustion Research Facility
Mail Stop 9055
Sandia National Laboratories
PO Box 969
Livermore, California 94551-0969
Phone: (925)294-3379
swallen@sandia.gov

Prof. George H. Atkinson
Science and Technology Adviser to
   the Secretary of State
Room 3240, Department of State
2201 C Street NW,
Washington, DC 20520
Phone: (202)647-8725
atkinsongh@state.gov

Prof. Tomas Baer
Department of Chemistry
University of North Carolina
Chapel Hill, North Carolina 27599
Phone: (919)962-1580
baer@unc.edu

Dr. Robert S. Barlow
Combustion Research Facility
MS9051
Sandia National Laboratories
Livermore, California 94551-0969
Phone: (925)294-2688
barlow@ca.sandia.gov

Prof. Joel M. Bowman
Department of Chemistry
Emory University
1515 Pierce Drive
Atlanta, Georgia 30322
Phone: (404)727-6590
bowman@euch4e.chem.emory.edu

Dr. Bastiaan Braams
Math and Computer Sciences
Emory University
Atlanta, GA 30322
Phone: (404)727-1980
breams@mathcs.emory.edu

Professor Kenneth Brezinsky
Chemical Engineering Dept.
810 S. Clinton
The University of Illinois at Chicago
Chicago, Illinois 60607-7022
Phone: (312)996-9430
kenbrez@uic.edu

Dr. Nancy Brown
Environmental Technologies
Division
Advanced Energy Technology
Lawrence Berkeley National
Laboratory MS 51-208
One Cyclotron Road
Berkeley, California 94720
Phone: (510)486-4241
njbrown@lbl.gov

Prof. Laurie J. Butler
The James Franck Institute
The University of Chicago
5640 S. Ellis Avenue
Chicago, Illinois 60637
Phone: (773)702-7206
ljb4@midway.uchicago.edu

Dr. Robert W. Carling
MS 9054
Combustion Research Facility
Sandia National Laboratories
Livermore, California 94551-0969
Phone: (925)294-2206
rwcarli@sandia.gov

Prof. Barry K. Carpenter
Department of Chemistry &
Chemical Biology
Cornell University
Ithaca, NY 14853-1301
Phone: (607)255-3826
bkc1@cornell.edu

Dr. David W. Chandler
Combustion Research Facility
MS 9054
Sandia National Laboratories
Livermore, California 94551-0969
Phone: (925)294-3132
chandler@ca.sandia.gov

Dr Jacqueline H. Chen
Combustion Research Facility
MS 9051
Sandia National Laboratories
Livermore, California 94551-0969
Phone: (925)294-2586
jhchen@sandia.gov

Dr. Robert K. Cheng
Energy and Environment Division
University of California
Lawrence Berkeley National
Laboratory
One Cyclotron Road
Berkeley, California 94720
Phone: (510)486-5438
rkcheng@lbl.gov

Prof. Robert E. Continetti
Department of Chemistry and
Biochemistry, 0340
University of California, San Diego
9500 Gilman Drive
La Jolla, CA 92093-0340
Phone: (858)534-5559
rcontinetti@ucsd.edu

Prof. Terrill A. Cool
College of Engineering
School of Applied & Engineering
Physics
Cornell University
Ithaca, New York 14853-1301
Phone: (607)255-4191
tac13@cornell.edu

Prof. F. Fleming Crim
Department of Chemistry
University of Wisconsin
1101 University Avenue
Madison, Wisconsin 53706
Phone: (608)263-7364
fcrim@chem.wisc.edu

Prof. Robert F. Curl, Jr.
Department of Chemistry
Rice University
P.O. Box 1892
Houston, Texas 77005
Phone: (713)348-4816
rfcurl@rice.edu

Prof. Hai-Lung Dai
Department of Chemistry
University of Pennsylvania
Philadelphia, Pennsylvania 19104-
6323
Phone: (215)898-5077
dai@sas.upenn.edu

Prof. H. Floyd Davis
Department of Chemistry &
Chemical Biology
Baker Laboratory
Cornell University
Ithaca, New York 14853-1301
Phone: (607)255-0014
hfd1@cornell.edu

Dr. Michael J. Davis
Chemistry Division
Argonne National Laboratory
9700 South Cass Avenue
Argonne, Illinois 60439
Phone: (630)252-4802
davis@tcg.anl.gov

Prof. Frederick L. Dryer
Department of Mechanical &
Aerospace Engineering
Princeton University
Princeton, New Jersey 08544
Phone: (609)258-5206
fldryer@princeton.edu

Prof. G. Barney Ellison
Department of Chemistry
University of Colorado
Boulder, Colorado 80309-0215
Phone: (303)492-8603
barney@jila.colorado.edu

Prof. Kent M. Ervin
Department of Chemistry/216
College of Arts and Sciences
University of Nevada, Reno
Reno, Nevada 89557-0020
Phone: (775)784-6676
ervin@chem.unr.edu

Dr. Askar Fahr
Chemical Kinetics and Thermo-
Dynamics Division
National Institutes of Standards and
Technology
Gaithersburg, MS 20899
Phone: (301)975-2511
askar.fahr@nist.gov

Prof. Robert W. Field
Department of Chemistry
Room 6-219
Massachusetts Institute of
Technology
77 Massachusetts Ave.
Cambridge, Massachusetts 02139
Phone: (617)253-1489
rwfield@mit.edu

Prof. George Flynn
Department of Chemistry
Mail Stop 3109
Columbia University
3000 Broadway
New York, New York 10027
Phone: (212)854-4162
Flynn@chem.columbia.edu

Prof. Michael Frenklach
Department of Mechanical
Engineering
Lawrence Berkeley National
Laboratory
University of California at Berkeley
Berkeley, California 94720-1740
Phone: (510)643-1676
myf@me.berkeley.edu

Prof. Graham P. Glass
Department of Chemistry
Rice University
P.O. Box 1892
Houston, Texas 77251
Phone: (713)348-3285
gglass@rice.edu

Dr. Stephen K. Gray
Chemistry Division
Argonne National Laboratory
9700 South Cass Ave.
Argonne, Illinois 60439
Phone: (630)252-3594
gray@tcg.anl.gov

Prof. William H. Green, Jr.
Department of Chemical
Engineering, 66-448
Massachusetts Institute of
Technology
77 Massachusetts Ave.
Cambridge, Massachusetts 02139
Phone: (617)253-4580
whgreen@mit.edu

Dr. Gregory E. Hall
Chemistry Department
Brookhaven National Laboratory
Upton, New York 11973
Phone: (631)344-4376
gehall@bnl.gov

Dr. Nils Hansen
Combustion Research Facility
MS9055
Sandia National Laboratories
Livermore, California 94551-0969
Phone: (925)294-6272
nhansen@sandia.gov

Prof. Ronald K. Hanson
Department of Mechanical
Engineering
Stanford University
Stanford, California 94305
Phone: (650)723-4023
hanson@me.stanford.edu

Dr. Lawrence Harding
Chemistry Division
Argonne National Laboratory
9700 South Cass Avenue
Argonne, Illinois 60439
Phone: (630)252-3591
harding@anl.gov

Prof. Martin Head-Gordon
Department of Chemistry
University of California at Berkeley
Berkeley, California 94720
Phone: (510)642-5957
mhg@cchem.berkeley.edu

Prof. John Hershberger
Department of Chemistry
North Dakota State University
Fargo, ND 58105-5516
Phone: (701)231-8225
john.hershberger@ndsu.nodak.edu

Dr. Jan P. Hessler
Chemistry Division
Argonne National Laboratory
9700 South Cass Avenue
Argonne, Illinois 60439
Phone: (630)252-3717
hessler@anl.gov

Dr. Richard L. Hilderbrandt
Chemical Sciences, Geosciences and
Biosciences Division, SC-14
U.S. Department of Energy
1000 Independence Avenue, SW
Washington, DC 20585-1290
Phone: (301)903-0035
richard.hilderbrandt@science.doe.gov

Prof. Paul L. Houston
Department of Chemistry
122 Baker Laboratory
Cornell University
Ithaca, New York 14853-1301
Phone: (607)255-4303
plh2@cornell.edu

Prof. Philip M. Johnson
Department of Chemistry
State University of New York
at Stony Brook
Stony Brook, New York 11794
Phone: (631)632-7912
philip.Johnson@sunysb.edu

Prof. Ralf I. Kaiser
Department of Chemistry
The University of Hawaii at Manoa
2445 The Mall
Honolulu, HI 96822
Phone: (808)956-5731
kaiser@gold.chem.hawaii.edu

Dr. Andrei Kazakov
Department of Mechanical &
Aerospace Engineering
Princeton University
Princeton, New Jersey 08544
Phone: (609)258-5280
andrei@princeton.edu

Prof. Michael E. Kellman
Department of Chemistry
University of Oregon
Eugene, Oregon 97403
Phone: (541)346-4196
kellman@oregon.uoregon.edu

Prof. John Kiefer
Department of Chemical
Engineering
810 S. Clinton
University of Illinois at Chicago
Chicago, Illinois 60607
Phone: (312)996-5711
john.h.kiefer@uic.edu

Dr. William H. Kirchhoff
14511 Woodcrest Drive
Rockville, MD 20853-2371
Phone: (301)460-5580
william.kirchhoff@worldnet.att.net

Dr. Stephen J. Klippenstein
Combustion Research Facility
MS 9055
Sandia National Laboratories
Livermore, California 94551-0969
Phone: (925)294-2289
SJKLIPP@sandia.gov

Prof. Stephen R. Leone
Department of Chemistry
University of California
Berkeley, CA 94720-1460
Phone: (510)643-5467
srl@cchem.berkeley.edu

Prof. Marsha I. Lester
Department of Chemistry
University of Pennsylvania
231 South 34th Street
Philadelphia, Pennsylvania 19104-6323
Phone: (215)898-4640
milester@sas.upenn.edu

Prof. John C. Light
The James Franck Institute
The University of Chicago
5640 S. Ellis Avenue
Chicago, Illinois 60637
Phone: (773)702-7197
j-light@uchicago.edu

Prof. Ming-Chang Lin
Department of Chemistry
Emory University
1515 Pierce Drive
Atlanta, Georgia 30322
Phone: (404)727-2825
chemmcl@emory.edu

Prof. Robert P. Lucht
School of Mechanical Engineering
Purdue University
West Lafayette, IN 47907-2088
Phone: (765)494-0539
lucht@purdue.edu

Dr. R. Glen Macdonald
Chemistry Division
Argonne National Laboratory
9700 South Cass Avenue
Argonne, Illinois 60439
Phone: (630)252-7742
rgmacdonald@anl.gov

Dr. Andrew McIlroy
Combustion Research Facility
MS 9055
Sandia National Laboratories
Livermore, California 94551-0969
Phone: (925)294-3054
amcilr@sandia.gov

Dr. William J. McLean
Combustion Research Facility
MS9054
Sandia National Laboratories
Livermore, California 94551-0969
Phone: (925)294-2687
wjmclea@sandia.gov

Dr. Joe V. Michael
Chemistry Division
Argonne National Laboratory
9700 South Cass Avenue
Argonne, Illinois 60439
Phone: (630)252-3171
michael@anlchm.chm.anl.gov

Dr. Hope A. Michelsen
Combustion Research Facility
M/S 9054
Sandia National Laboratories
Livermore, CA 94551
Phone: (925)294-2335
hamiche@sandia.gov

Dr. James A. Miller
Combustion Research Facility
MS-9055
Sandia National Laboratories
Livermore, California 94551-0969
Phone: (925)294-2759
jamille@ca.sandia.gov

Prof. Terry A. Miller
Department of Chemistry
Ohio State University
140 West 18th Avenue
Columbus, Ohio 43210
Phone: (614)292-2569
tamiller+@osu.edu

Prof. William H. Miller
Department of Chemistry
University of California at Berkeley
Berkeley, California 94720
Phone: (510)642-0653
miller@cchem.berkeley.edu

Prof. C. Bradley Moore
Office of Research
208 Bricker Hall
Ohio State University
190 N. Oval Mall
Columbus, Ohio 43210
Phone: (614)292-1582
moore.1@osu.edu

Prof. Amy S. Mullin
Department of Chemistry
Boston University
590 Commonwealth Avenue
Boston, Massachusetts 02215-2507
Phone: (617)353-8477
mullin@chem.bu.edu

Prof. Daniel M. Neumark
Department of Chemistry
University of California at Berkeley
Berkeley, California 94720
Phone: (510)642-3502
neumark@cchem.berkeley.edu

Prof. Cheuk-Yiu Ng
Department of Chemistry
One Shields Avenue
University of California at Davis
Davis, CA 95616
Phone: (530)754-9645
cyng@chem.ucdavis.edu

Dr. David L. Osborn
Combustion Research Facility
MS 9055
Sandia National Laboratories
Livermore, California 94551-0969
Phone: (925)294-4622
dlosbor@sandia.gov

Prof. David S. Perry
Department of Chemistry
University of Akron
Akron, Ohio 44325
Phone: (330)972-6825
dperry@uakron.edu

Prof. Stephen B. Pope
Department of Mechanical and
    Aerospace Engineering
Cornell University
106 Upson Hall
Ithaca, New York 14853
Phone: (607)255-4314
pope@mae.cornell.edu

Dr. Stephen Pratt
Chemistry Division
Argonne National Laboratory
9700 South Cass Avenue
Argonne, Illinois 60439
Phone: (630)252-4199
stpratt@anl.gov

Dr. Larry A. Rahn
Combustion Research Facility
MS 9056
Sandia National Laboratories
Livermore, California 94551-0969
Phone: (925)294-2091
rahn@sandia.gov

Prof. Hanna Reisler
Department of Chemistry
University of Southern California
Los Angeles, California 90089-0482
Phone: (213)740-7071
reisler@usc.edu

Prof. Thomas R. Rizzo
Institut de Chimie Physique I
Departement de Chimie
EPFL - Ecubiens
1015 Lausanne
SWITZERLAND
Phone: 41021693 3073
thomas.rizzo@epfl.ch

Dr. Eric A. Rohlfing
Chemical Sciences, Geosciences and
  Biosciences Division, SC-14
U.S. Department of Energy
1000 Independence Avenue, SW
Washington, DC 20585-1290
Phone: (301)903-8165
eric.rohlfing@science.doe.gov

Prof. Klaus Ruedenberg
Department of Chemistry
Iowa State University of Science and
Technology
Ames, Iowa 50011
Phone: (515)294-5253
ruedenberg@iastate.edu

Dr. Branko Ruscic
Chemistry Division
Argonne National Laboratory
9700 South Cass Avenue
Argonne, Illinois 60439
Phone: (630)252-4079
ruscic@anl.gov

Prof. Henry Frederick Schaefer III
Department of Chemistry
University of Georgia
Athens, Georgia 30602
Phone: (706)542-2067
hfs@uga.edu

Dr. Trevor Sears
Chemistry Department
Brookhaven National Laboratory
Upton, New York 11973
Phone: (631)344-4374
sears@bnl.gov

Dr. Thomas B. Settersten
Combustion Research Facility
MS 9056
Sandia National Laboratories
Livermore, California 94551-0969
Phone: (925)294-4701
tbsette@sandia.gov

Dr. Ron Shepard
Chemistry Division
Argonne National Laboratory
9700 South Cass Avenue
Argonne, Illinois 60439
Phone: (630)252-3584
shepard@tcg.anl.gov

Prof. Mitchell Smooke
Department of Mechanical
Engineering
Yale University
P.O. Box 208284
New Haven, Connecticut 06520-
8284
Phone: (203)432-4344
mitchell.smooke@yale.edu

Prof. Arthur G. Suits
Department of Chemistry
5101 Cass Avenue
Wayne State University
Detroit, MI 48202
Phone: (313)577-9008
asuits@chem.wayne.edu

Dr. Craig Taatjes
Combustion Research Facility
MS 9055
Sandia National Laboratories
Livermore, California 94551-0969
Phone: (925)294-2764
cataatj@sandia.gov

Prof. Howard S. Taylor
Department of Chemistry
University of Southern California
Los Angeles, California
Phone: (213)740-4112
taylor@usc.edu

Professor Donald L. Thompson
Department of Chemistry
University of Missouri
Columbia, MO 65211
Phone: (573)882-8374
thompsondon@missouri.edu

Dr. Robert Tranter
Chemistry Division
Argonne National Laboratory
9700 South Cass Avenue
Argonne, Illinois 60439
Phone: (630)252-6505
tranter@anl.gov

Prof. Donald G. Truhlar
Department of Chemistry
139 Smith Hall
University of Minnesota
207 Pleasant St. SE
Minneapolis, Minnesota 55455
Phone: (612)624-7555
truhlar@umn.edu

Dr. Wing Tsang
Chemical Kinetics Division
Center for Chemical Technology
A147 Chemistry Building
Natl. Inst. of Standards and
Technology
Gaithersburg, Maryland 20899
Phone: (301)975-2507
wing.tsang@nist.gov

Dr. Frank P. Tully
Division of Chemical Sciences,
Geosciences and Biosciences SC-14
U.S. Department of Energy
1000 Independence Avenue, SW
Washington, DC 20585-1290
Phone: (301)903-5998
frank.tully@science.doe.gov

Prof. James J. Valentini
Department of Chemistry
Columbia University
3000 Broadway, MC 3120
New York, New York 10027
Phone: (212)854-7590
jjv1@columbia.edu

Dr. Albert F. Wagner
Chemistry Division
Argonne National Laboratory
9700 South Cass Avenue
Argonne, Illinois 60439
Phone: (630)252-3597
wagner@tcg.anl.gov

Prof. Peter M. Weber
Department of Chemistry
Brown University
Box H
Providence, Rhode Island 02912
Phone: (401)863-2594
Peter_Weber@brown.edu

Dr. Charles K. Westbrook
Division of Computational Physics
Lawrence Livermore National
Laboratory
P. O. Box 808, L-091
Livermore, California 94550
Phone: (925)422-4108
westbrook1@llnl.gov

Prof. Phillip R. Westmoreland
Department of Chemical
Engineering
University of Massachusetts
Amherst, Massachusetts 01003
Phone: (413)545-1750
westm@ecs.umass.edu

Prof. Curt Wittig
Department of Chemistry
University of Southern California
Los Angeles, California 90089-0484
Phone: (213)740-7368
wittig@usc.edu

Prof. David R. Yarkony
Department of Chemistry
Johns Hopkins University
3400 N. Charles Street
Baltimore, Maryland 21218
Phone: (410)516-4663
yarkony@jhu.edu

Prof. Timothy S. Zwier
Department of Chemistry
Purdue University
West Lafayette, Indiana 47907
Phone: (765)494-5278
zwier@purdue.edu

Author Index